Digitized by the Internet Archive
in 2023 with funding from
Kahle/Austin Foundation

https://archive.org/details/contributionsfro0009unse_x2f0

Carnegie Institution of Washington

CONTRIBUTIONS

FROM THE

MOUNT WILSON OBSERVATORY

VOLUME IX

NOS. 169–199

WITH TWENTY-ONE PLATES

MARCH, 1919—OCTOBER, 1920

UNIVERSITY OF ARIZONA
LIBRARY

V. 9

CONTENTS

NO. PAGE

169. THE STARK EFFECT FOR METALS. *T. Takamine* 1

170. NOTE ON THE RELATIONSHIP OF MEAN PARALLAX TO MEAN PROPER MOTION. *Gustaf Strömberg* 21

171. NOTE ON THE POLARIZATION OF THE NIGHT SKY. *Harold D. Babcock* 33

172. THE ORBIT OF THE SPECTROSCOPIC BINARY BOSS 2285. *Alfred H. Joy and Giorgio Abetti* 37

173. ON THE BRIGHTNESS OF THE SKY AT NIGHT AND THE TOTAL AMOUNT OF STARLIGHT. *P. J. van Rhijn* 41

174. THE CHARACTERISTICS OF ABSORPTION SPECTRA PRODUCED BY THE ELECTRIC FURNACE. *Arthur S. King* 61

175. STUDIES BASED ON THE COLORS AND MAGNITUDES IN STELLAR CLUSTERS. FIFTEENTH PAPER: A PHOTOMETRIC ANALYSIS OF THE GLOBULAR SYSTEM MESSIER 68. *Harlow Shapley* . 71

176. STUDIES BASED ON THE COLORS AND MAGNITUDES IN STELLAR CLUSTERS. SIXTEENTH PAPER: PHOTOMETRIC CATALOGUE OF 848 STARS IN MESSIER 3. *Harlow Shapley and Helen N. Davis* 85

177. BRIGHT NEBULAE AND STAR CLUSTERS IN SAGITTARIUS AND SCUTUM. *John C. Duncan* 125

178. THE SPECTRUM OF ELECTRICALLY EXPLODED WIRES. *J. A. Anderson* 135

179. THE SPECTRUM OF NOVA OPHIUCHI 1919. *Walter S. Adams and Cora G. Burwell* 147

180. PRELIMINARY OBSERVATIONS OF THE ZEEMAN EFFECT FOR ELECTRIC FURNACE SPECTRA. *Arthur S. King* 153

181. OBSERVATIONS OF THE ELECTRIC FURNACE SPECTRA OF COBALT, NICKEL, BARIUM, STRONTIUM, AND CALCIUM IN THE REGION OF GREATER WAVE-LENGTH. *Arthur S. King* 167

182. THE PHOTOGRAPHIC DETERMINATION OF STELLAR PARALLAXES WITH THE 60-INCH RELFECTOR. FOURTH SERIES. *Adriaan van Maanen* 175

183. NOTE ON THE AIR LINES IN SPARK SPECTRA FROM λ 5927 TO λ 8719. *Paul W. Merrill* 211

184. ON THE APPLICATION OF INTERFERENCE METHODS TO ASTRONOMICAL MEASUREMENTS. *A. A. Michelson* 219

CONTENTS

NO. PAGE

185. Application of Michelson's Interferometer Method to the Measurement of Close Double Stars. *J. A. Anderson* 225

186. Photographs of Nebulae with the 60-Inch Reflector, 1917–1919. *Francis G. Pease* 239

187. The Color of the Nebulous Stars. *Frederick H. Seares and Edwin P. Hubble* 273

188. On the Distribution of the Stars in Space, Especially in the High Galactic Latitudes. *J. C. Kapteyn and P. J. van Rhijn* 289

189. On the Systematic Differences in Trigonometrically Determined Parallaxes. *Adriaan van Maanen and Coral Wolfe* 305

190. Studies Based on the Colors and Magnitudes in Stellar Clusters. Seventeenth Paper: Miscellaneous Results. *Harlow Shapley* 323

191. The Surface Brightness of the Galatic System as Seen from a Distant External Point and a Comparison with Spiral Nebulae. *Frederick H. Seares* 337

192. Magnitudes of Faint Comparison Stars for Nova Persei, No. 2. *Frederick H. Seares* 359

193. Experiments on the Possible Influence of Potential Difference on the Radiation of the Tube Resistance Furnace. *Arthur S. King* 363

194. Intensity Differences in Furnace and Arc among the Component Series in Band Spectra. *Arthur S. King* 375

195. Studies Based on the Colors and Magnitudes in Stellar Clusters. Eighteenth Paper: The Periods and Light-Curves of 26 Cepheid Variables in Messier 72. *Harlow Shapley and Mary Ritchie* 379

196. The Spectroscopic Orbit of the Cepheid Variable X Cygni. *John C. Duncan* 395

197. An Examination of the Infra-Red Spectrum of the Sun, λ 8900–λ 9900. *Frederick S. Brackett* 399

198. The Variation with Temperature of the Electric Furnace Spectrum of Manganese. *Arthur S. King* 411

199. The Parallaxes of 1646 Stars Derived by the Spectroscopic Method. *W. S. Adams, A. H. Joy, G. Strömberg, and Cora G. Burwell* 423

LIST OF PLATES

NO FACING PAGE

I. The Stark Effect for Metals; (*a*), (*b*), (*c*), (*d*) Silver; (*e*) Cobalt; (*f*), (*g*) Copper 3

II. The Stark Effect for Metals; (*a*), (*b*) Iron; (*c*), (*f*) Nickel; (*d*), (*e*) Molybdenum 7

III. Messier 8, Consisting of Nebula N.G.C. 6523 and Star Cluster N.G.C. 6530 126

IV. Nebula and Star Cluster N.G.C. 6611 = M 16 128

V. Swan Nebula N.G.C. 6618 = M 17 130

VI. Central Part of the Swan Nebula 130

VII. Globular Star Cluster N.G.C. 6656 = M 22 132

VIII. Photographs of Electrically Exploded Wires . . . 138

IX. Spectra of Electrically Exploded Iron Wires with Iron Arc Comparison 141

X. Effect of a Magnetic Field on the Electric Furnace Spectrum of Iron 165

XI. Effect of a Magnetic Field on the Electric Furnace Spectrum of Iron 165

XII. Appearance of Interference System from Artificial Stars in the Laboratory 235

XIII. (*a*) N.G.C. 2288, 2289, 2290, 2291, 2294; (*b*) N.G.C. 3786, 3788; (*c*) N.G.C. 1491; (*d*) N.G.C. 1186; (*e*) N.G.C. 3367; (*f*) N.G.C. 2146 243

XIV. (*a*) N.G.C 2245, 2247; (*b*) N.G.C. 2359 243

XV. (*a*) N.G.C. 3379, 3384, 3389; (*b*) N.G.C. 4395, 4399, 4400, 4401 243

XVI. (*a*) N.G.C. 3395–96; (*b*) N.G.C. 4656–57 243

XVII. (*a*) N.G.C. 5278–79; (*b*) N.G.C. 5257, 5258; (*c*) I.C. II 5146 243

XVIII. (*a*) I.C. I 1470; (*b*) N.G.C. 5544, 5545; (*c*) N.G.C. 6888 . 243

XIX. Variable Stars in Clusters; (*a*) N.G.C. 6779 = Messier 56; (*b*) N.G.C. 5024 = Messier 53; (*c*) N.G.C. 6864 = Messier 75, (*d*) N.G.C. 7492, (*e*) N.G.C. 6981 = Messier 72 325

XX. Section of λ 3883 Band in Furnace (*b*) and Arc (*a*, *c*) . 376

XXI. Infra-Red Spectrum of the Sun, λ 8900–λ 9900 401

Contributions from the Mount Wilson Observatory, No. 169
Reprinted from the *Astrophysical Journal*, Vol. L, pp. 23–41, 1919

THE STARK EFFECT FOR METALS

By T. TAKAMINE

In 1917 J. A. Anderson[1] developed a method suitable for examining the Stark effect for metals having a relatively high melting-point. The apparatus and methods used in the present investigation are essentially the same as employed by him, excepting a slight modification in the construction of the cathode and the grating spectrograph.

APPARATUS AND METHODS

In his experiments Anderson used a cathode having a diameter of about 13 mm. In order to attain a much stronger electric field, the diameter of the cathode, in the present work, was decreased to 2 to 5 mm.

In Fig. 1, *A*, a cylinder of the metal which is to be studied, is put into the iron frame *C*. *B* is a disk of fused silica having a hole in the center. The upper end of the cathode *A* extends about 0.3 mm above the upper surface of *B*. *D* and *E* are silica tubes ground to fit tightly together. *D* has a vertical slot, about 1 mm in width, which extends down to the level of the upper surface of *B*. The upper end of the slot was covered by a small piece of metal. *F* is the platinum wire leading down to the electrode below.

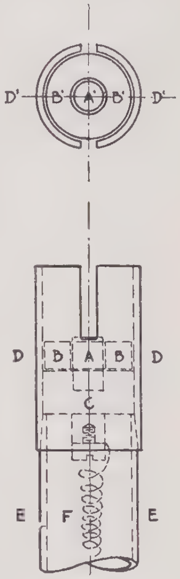

Fig. 1

The grating spectrograph is essentially the same as described by Anderson, excepting that a telescope objective of 5-foot focus, made by Brashear, was used as the collimator lens, and a Bausch & Lomb Tessar of F/4.5 aperture and 40-cm focus as the camera lens. A Voigtländer Heliar lens of 15-cm focus and a double-image prism were placed between the source and the slit of the spectrograph, so that two images of the uncovered portion of the slot appear one above the other on the slit. The bell jar containing the cathode and the anode is pumped out until the Crookes dark space has a length of 1 or 2 mm. Direct current to produce the discharge is supplied by a set of high-potential generators, each giving about 800 volts, connected in series. The number of dynamos used varied from 16 to 24. A milliammeter and a water-resistance were connected in series with the discharge tube, the current being in general between 20 and 40 milliamperes. The exposures varied considerably according to the cathode metal, ranging from a few minutes up to 2 hours. In order to avoid excessive heating of the cathode, the discharge was passed intermittently, the bell jar being kept cool by means of an electric fan.

---

[1] *Mt. Wilson Contr.* No. 134; *Astrophysical Journal*, **46**, 104, 1917.

The intensity of the electric field was determined by using Stark's data for the "Grobzerlegung" of the Balmer lines Hβ, Hγ, and Hδ;[1] its maximum value at the cathode ($E_{\text{max.}}$) varied from 28,000 volt/cm to 75,000 volt/cm.

With the cathode of smaller diameter used in the present work the distribution of the electric field in the Crookes dark space was found to be parabolic, as noted by Yoshida and the author.[2]

It has already been noticed by Anderson that the spectra of metals used as the cathode are excited to greater brightness when the residual gas is either air or oxygen than when it is hydrogen. In the present work air proved to be preferable to either oxygen or hydrogen. It would seem that the presence of nitrogen acts favorably in producing bright metallic spectra.

RESULTS

The spectra of the following ten metals were examined: Ag, Au, Co, Cu, Fe, Mg, Mn, Mo, Ni, W.

Of these, no affected lines were observed in the spectra of Mn and W. In the course of the experiments a few lines of Na, N, and O were also found to be affected by an electric field. The spectra of Co, Fe, Mn, Mo, and Ni were fairly rich in lines, while the rest of them showed a rather small number of lines. The color of the

---

[1] *Elektrische Spektralanalyse chemischer Atome*, 1914.

[2] *Memoirs of the College of Science* (Kyoto Imperial University), **2**, 137, 1917.

PLATE I

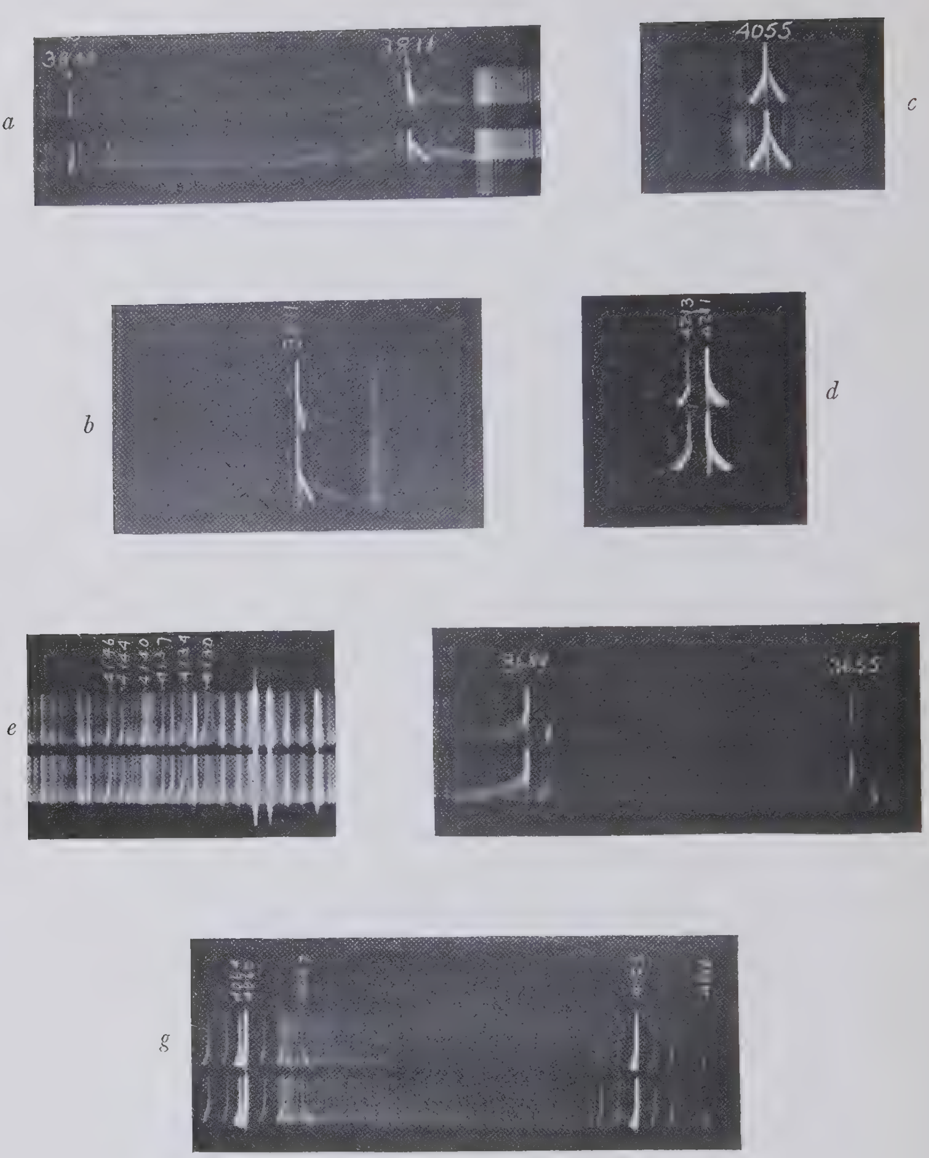

TAKAMINE—THE STARK EFFECT FOR METALS

In each illustration the *n*-components are above, the *p*-components below

a Silver $E_{\text{max.}} = 48{,}000$ volt/cm
b Silver $E_{\text{max.}} = 31{,}300$ "
c Silver $E_{\text{max.}} = 26{,}700$ "
d Silver $E_{\text{max.}} = 26{,}700$ "
e Cobalt $E_{\text{max.}} = 33{,}300$ "
f Copper $E_{\text{max.}} = 75{,}200$ "
g Copper $E_{\text{max.}} = 33{,}000$ "

glow in the Crookes dark space was a very bright green in the case of Ag, Cu, and Mg; fairly bright for Fe and Ni; and yellowish for Au, Co, Na, and Mo.

In the tables the first column contains the wave-lengths, the second the series numbers whenever known; the third and fourth give the displacements of the *p*- and *n*-components, respectively, with relative intensities on a scale of 1–10. The displacements were measured at the maximum electric field, $E_{\text{max.}}$, which is given in the fourth column. For some lines special remarks are given below the table.

Silver.—With silver as the cathode the brilliancy of the greenish glow in the Crookes dark space was extraordinary, and strong lines came out with a few seconds' exposure. The Stark effect for silver lines is remarkably similar to that for helium lines. Excepting the green lines, the rest of the first subordinate-series lines are spread out very widely on both sides, while those belonging to the second subordinate series are displaced in one direction only. Moreover, the former show a number of detached components just as in the case of helium. This is illustrated for the line λ 3810.85, in Plate I*a*, *b*. The only difference we notice between helium and silver is that in the case of helium all the detached components appear invariably on the violet side, while in silver they usually appear on the red side.

With respect to these detached components, it is important to note that Merton[1] has found that those belonging to helium can be arranged in a combination series. It seems very likely that the detached components of silver may have similar properties.

These detached components are not of sufficient intensity to appear in the negative glow if, indeed, they exist there at all; they appear with sufficient intensity for observation only in the electric field.

It is important to notice that there is another class of lines, first observed by Koch[2] in the helium spectrum, which shows this feature still more markedly. Their approximate wave-lengths are 4519, 4046, and 3930 A, and they begin to appear with an

---

[1] *Proc. Royal Soc.*, **95A,** 30, 1918.

[2] *Annalen der Physik,* **48,** 98, 1915.

TABLE I

SILVER

λ	SERIES	*p*-COMPONENT		*n*-COMPONENT		$E_{\text{max.}}$ IN VOLT/CM
		Δλ	Int.	Δλ	Int.	
3682.45.....	IN, II6	$v_3-5.00$ $v_2-1.59$ $v_1-0.69$ 0 $r_1+4.35$ $r_2+13.00$	2 6 1 4 2 1	.... $v_2-1.84$ $v_1-0.84$ 0 $r_1+4.90$	.... 1 5 2 1	48,000
3810.85.....	IN, I6	$v_3-7.15$ $v_2-1.77$ $v_1-0.41$ 0 $r_1+5.21$ $r_2+11.04$	6 10 2 5 3 3	$v_3-4.78$ $v_2-1.40$ $v_1-0.43$ 0 $r_1+5.36$	3 3 10 5 4	48,000
3840.74.....	IIN, II5	+ 0.15	2	+0.08	2	48,000
3981.87.....	IIN, I5	+ 0.13	3	+0.14	3	48,000
4055.44.....	....	.... $v_1-5.20$ 0 $r_1+3.33$	...... 8 4 10	$v_2-4.49$ $v_1-3.21$ 0 $r_1+3.29$	2 6 3 10	56,000
4081.7.....	....	+ 0.88	3	+0.86	3	55,000
4206.8.....	....	+ 1.46	2	+1.28	2	55,000
4210.87.....	IN, II5	.... $v_1-3.80$ 0 $r_2+4.23$	...... 10 6 5	$v_2-3.54$ $v_1-1.91$ 0 $r_1+3.99$	3 10 6 5	56,000
4212.76.....	IN, I5	$v-3.47$ 0 $r+2.53$	3 5 3	−2.98 0 +2.70	3 5 3	56,000
4226.55.....	....	+ 2.33	3	+2.14	3	56,000
4476.31.....	....	+ 0.04	10	+0.02	10	48,000
4668.58.....	....	+ 0.03	10	+0.03	10	48,000

REMARKS

λ 3810.85 The behavior of v_2 in the *p*-component and v_1 in the *n*-component are anomalous. A companion line at +0.86 A has a violet component.

4055.44 In both the *p*- and *n*-components v_1 is detached from the main line by 0.2 A.

4081.7 The line appears only in a strong electric field.

4226.55 The line appears only in a strong electric field.

electric field considerably stronger than is required in the case of the detached components discussed above, and gain in intensity very rapidly as the field-strength is increased. According to Koch these new types of lines, which, for convenience, we may call lines of Koch's type, can be arranged in a combination series. The silver lines at λλ 4081.7 and 4206.8 are evidently of Koch's type.

The line λ 3682.45, which forms a doublet with λ 3810.85, is quite similar to the latter in its mode of decomposition. In both the *p*- and *n*-components of these two lines the violet components v_1 and v_2 show an anomalous behavior. In a weak field they are displaced approximately in proportion to the field-strength; as the field increases this law ceases to hold, and in a strong field the displacement becomes practically constant. As will be seen in Plate I*b*, the phenomenon is especially marked for v_1 of the *n*-component. The intensity of these *p*- and *n*-components is, so to speak, complementary. In fact v_1 is weak and v_2 strong in the *p*-component, while in the *n*-component exactly the opposite holds. As shown in Plate I*a*, *b*, the line λ 3810.85 is accompanied by a weaker line λ 3811.7, which has a violet component only.

The electric effect for the two neighboring lines λλ 4210.87 and 4212.76 is shown in Plate I*d*. These two lines, together with the line λ 4055.44 shown in Plate I*c*, form a doublet of the first subordinate series. The line λ 4212.76 behaves quite like λ 4055.44, while the line λ 4210.87 has its red component detached and at a considerable distance.

Gold.—As shown in Table II, only three affected lines of this element were observed.

TABLE II

GOLD

λ	*p*-COMPONENT		*n*-COMPONENT		$E_{\text{max.}}$ IN VOLT/CM
	Δλ	Int.	Δλ	Int.	
3796.15.......	−1.61	6	$v_2-1.57$ $v_1-0.52$	3 5	21,000
4084.31.......	+0.05	7	+0.04	7	30,000
4128.80.......	+0.32	4	+0.25	4	30,000

TABLE III

COBALT

λ	*p*-COMPONENT		*n*-COMPONENT		$E_{max.}$ IN VOLT/CM
	Δλ	Int.	Δλ	Int.	
3664.7	+0.11	1	....	....	33,300
3702.4	+0.04	5	....	....	33,300
3704.17	+0.05	4	....	....	33,300
3732.52	+0.05	6	+0.05	6	33,300
4045.54	+0.11	6	+0.20	5	33,300
4072.43	+0.44	5	+0.35	4	33,300
4096.11	+0.71	5	+0.47	4	33,300
4126.1	−0.84	2	−0.74	1	33,300
4128.3	+1.11	1	....	....	33,300
4129.86	−1.75	3	−1.76	2	33,300
	+1.18	2	+0.98	1	33,300
4130.62	+1.36	4	+1.11	4	33,300
4132.41	+0.20	7	+0.20	7	33,300
4133.94	+1.20	4	+0.96	4	33,300
4135.85	+1.65	5	+1.33	2	33,300
4137.52	+0.52	3	+0.41	2	33,300
4139.60	+0.64	5	+0.49	5	33,300
4140.50	+0.70	4	+0.71	3	33,300
4141.35	+1.08	1	....	....	33,300
4143.98	+0.63	5	+0.52	4	33,300
4144.52	+0.88	5	+0.65	4	33,300
4158.59	+2.06	2	....	....	33,300
4164.7	+0.87	2	....	....	33,300
4177.77	+0.53	3	+0.41	2	33,300
4198.62	−1.71	3	+1.10	2	33,300
4200.0	+1.27	2	+1.00	1	33,300
4201.6	+1.53	4	+1.37	3	33,300
4212.2	+0.78	3	+0.78	2	33,300
4215.70	+0.15	1	+0.08	1	33,300
4220.59	+0.12	2	+0.26	2	33,300
4221.21	−0.06	2	−0.05	2	33,300
4223.93	+1.25	2	+1.25	2	33,300
4307.57	−0.53	3	−0.40	2	33,300
4459.8	−0.40	4	−0.27	3	33,300
4489.1	+0.46	4	+0.60	3	33,300
4512.8	+0.70	2	+0.82	2	33,300
4514.3	−0.06	4	−0.05	4	33,300
4517.24	+0.65	2	+0.10	2	33,300
4550.8	−0.77	2	−1.02	2	33,300
4557.2	+1.23	2	+1.25	2	33,300
4591.8	−0.08	8	−0.10	8	33,300
4660.2	+0.42	2	+0.44	2	33,300
4704.57	−0.24	2	−0.25	2	33,300
5336.36	−0.10	2	−0.15	2	25,200
5418.0	−1.06	1	−0.65	1	25,200
5546.1	−0.45	5	−0.18	5	25,200
5616.5	0	4	0	4	25,200
	+0.37	1	+0.50	1	25,200
5636.15	−0.22	6	−0.17	6	25,200
5637.6	−0.68	6	−0.76	6	25,200

REMARKS

λ 4130.62 Complex?
4133.94 Complex?
4198.62 *p*- and *n*-component displaced in different directions.

PLATE II

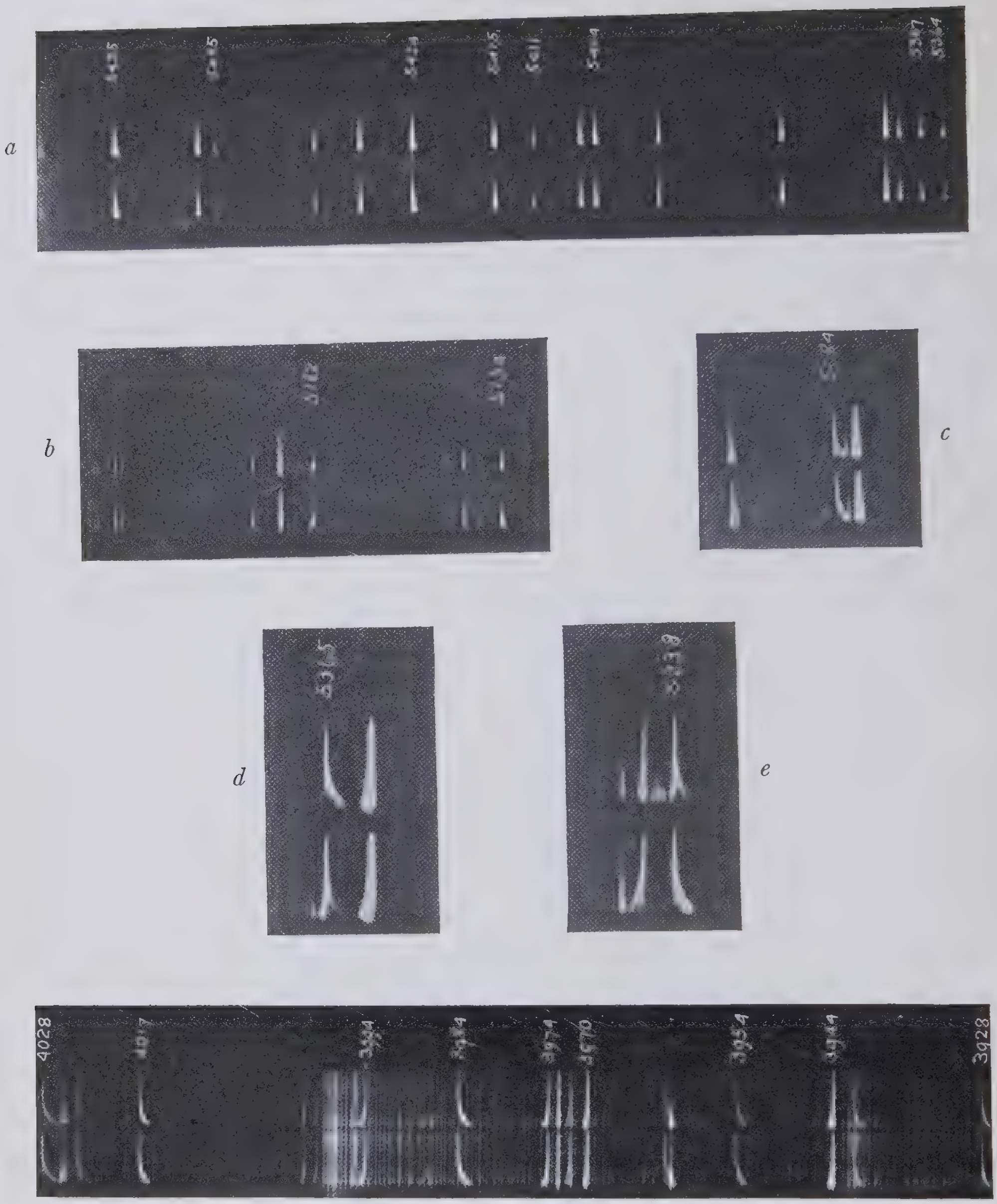

Takamine—The Stark Effect for Metals

In each illustration the *n*-components are above, the *p*-components below

a	Iron	$E_{\text{max.}} = 29{,}800$	volt/cm
b	Iron	$E_{\text{max.}} = 29{,}800$	"
c	Nickel	$E_{\text{max.}} = 38{,}500$	"
d	Molybdenum	$E_{\text{max.}} = 38{,}600$	"
e	Molybdenum	$E_{\text{max.}} = 38{,}600$	"
f	Nickel	$E_{\text{max.}} = 39{,}000$	"

The line λ 3796.15 has a very faint detached component on the violet side, thus showing similarity to the copper lines λλ 3654.59 and 3688.60.

The series relation in the spectrum of gold is not known, but judging from their Stark effect the lines λλ 3796.15 and 4128.80 behave like diffuse series lines, while the line λ 4084.31 behaves like a sharp series line.

Cobalt.—Like nickel, cobalt shows a considerable number of affected lines. In the case of chromium, Anderson found that many of the affected lines were not given in the ordinary wave-length tables. For several lines in the cobalt spectrum this is also the case, but for reasons similar to those given by Anderson in his paper they are included in Table III. A group of affected lines near λ 4100 is shown in Plate I*e*.

Copper.—The Stark effect for copper lines is in many respects similar to that for silver. Although too faint to be seen in Plate I*f*, the diffuse series lines λλ 3654.59 and 3688.60 are accompanied by detached components on the violet side. A series of lines, evidently of Koch's type, was also observed in the copper spectrum. Their approximate wave-lengths are 3652.6, 3686.7, 4015.8, and 4056.8 A, the last two being superposed on the detached components of the diffuse series lines λλ 3654.59 and 3688.60.

The lines which form the term $n=4$ of diffuse series, namely λλ 4022.83, 4062.14, and 4063.50, are all displaced toward the red, as shown in Plate I*g*. On account of the great intensity, a number of ghosts appear on either side in the reproduction.

Iron.—As will be seen in Table V and Plate II*a*, *b*, the Stark effect for iron lines is exceedingly small compared with other elements, but the fact that it can be observed seems to be of no small importance, especially in connection with the pole effect, which will be discussed later.

In the present investigation, which is of a preliminary character, only the green portion of the iron spectrum was studied.

Magnesium.—In a previous investigation, carried out by N. Kokubu and the author,[1] four magnesium lines, λλ 3093.1, 3097.1,

---

[1] *Memoirs of the College of Science* (Kyoto Imperial University), **3**, 173, 1918.

TABLE IV

COPPER

λ	SERIES	*p*-COMPONENT		*n*-COMPONENT		$E_{\text{max.}}$ IN VOLT/CM
		Δλ	Int.	Δλ	Int.	
3654.59.....	IN, II6	v − 2.51 r + 4.80	2 3	v −2.49 r +3.45	2 3	44,000
3686.67.....	....	+ 1.26	4	+1.40	4	44,000
3688.60.....	IN, I6	v_2−10.30 v_1 0 r + 6.72	1 3 2 5	.... 0 r +5.36	.... .. 2 5	44,000
3825.13.....	IIN, II5	− 0.16	3	−0.10	3	44,000
3830.........	....	+ 1.79	2	+0.61	2	44,000
3861.88.....	IIN, I5	− 0.11	3	−0.12	3	44,000
3894.64.....	....	+ 0.27	1	+0.23	1	44,000
4015.8.......	....	− 0.47	2	−0.43	2	33,000
4022.83.....	IN, II5	+ 0.46	7	+0.33	7	33,000
4056.8.......	P2	− 0.62	3	−0.65	3	33,000
4062.14.....	IN, I5	+ 0.60	10	+0.44	10	33,000
4063.50.....	IN, I5	+ 0.37	4	+0.33	4	33,000
4480.59.....	IIN, II4	+ 0.09	6	+0.11	6	44,000
4531.04.....	IIN, I4	+ 0.04	6	+0.03	6	44,000
5153.33.....	IN, II4	− 0.10	6	−0.05	6	25,300
5218.45.....	IN, I4	− 0.09	10	−0.07	10	25,300
5220.25.....	IN, I4	....	4	−0.06	4	....

REMARKS

λ 3654.59	The violet component is detached from the main line in both the *p*- and *n*-components. Superposed on the end of this violet component is another line which appears only in strong electric field, having the wave-length 3652.0.
3688.60	In the *p*-components v_1 approaches the main line as the field-strength is increased.
4015.8	The line appears only in strong electric field, and may be regarded as a detached component of 4022.83.
4056.8	The line appears only in strong electric field and may be regarded as a detached component of 4062.14.

4352.2, and 4703.3, were found to be displaced toward the red, and the line λ 4571.3 toward the violet in an electric field. Besides these lines the strong triplet λλ 3829.5, 3832.5, and 3838.4 showed a tendency to shift toward the violet, but as the dispersion was very small (30 A per mm), the fact was stated with reserve at that

TABLE V

IRON

λ	p-COMPONENT		n-COMPONENT		$E_{\text{max.}}$ IN VOLT/CM
	Δλ	Int.	Δλ	Int.	
5133.675	−0.14	5	−0.15	5	29,800
5162.312	+0.73	4	+0.28	4	29,800
5324.196	+0.05	2	+0.05	2	29,800
5364.859	−0.06	2	....	....	29,800
5367.455	−0.13	3	−0.05	3	29,800
5404.131	−0.05	5	−0.05	3	29,800
5410.900	−0.02	3	−0.04	3	29,800
5415.189	−0.11	6	−0.06	6	29,800
5424.057	−0.13	10	−0.12	10	29,800
5445.040	−0.06	2	−0.06	2	29,800
5455.435	−0.35	8	−0.38	8	29,800

REMARKS

λ 5455.435 This line was not resolved from the neighboring line 5455.614.

time. In the present work, using a dispersion of about 5.3 A per mm, the results in Table VI were obtained.

TABLE VI

MAGNESIUM

λ	p-COMPONENT		n-COMPONENT		$E_{\text{max.}}$ IN VOLT/CM
	Δλ	Int.	Δλ	Int.	
3529.501	−0.08	3	−0.07	3	30,000
3832.450	−0.11	7	−0.06	7	30,000
3838.435	−0.12	10	−0.05	10	30,000

Molybdenum.—The spectrum of molybdenum shows many affected lines, especially in the green and violet regions. In the p- and n-components of the lines λλ 5238.41 and 5364.50 we notice the same complementary phenomenon in relative intensity which was noted in the case of the silver line λ 3810.85. In addition we have the curious feature that the p-component of λ 5238.41 behaves exactly like the n-component of λ 5364.50, while the n-component of the former behaves just like the p-component of the latter. This remarkable feature is illustrated in Plate II*d*, *e*.

TABLE VII
MOLYBDENUM

λ	*p*-COMPONENT		*n*-COMPONENT		$E_{\text{max.}}$ IN VOLT/CM
	Δλ	Int.	Δλ	Int.	
4017.50	−0.44	2	−0.18	2	38,600
4025.64	+0.41	1	+0.39	1	38,600
4028.85	−1.49	4	−1.06	4	38,600
4032.65	−1.51	3	−1.07	3	38,600
4060.4	−1.01	3	−0.62	3	38,600
4071.54	−1.17	1	−1.09	1	38,600
4157.58	0 +0.92 −0.47	2 4 3	0 +0.81	2 2	38,600
4284.79	$v_2-1.78$ $v_1-0.13$ 0 $r_1+1.45$	3 2 2 4	$v-1.76$ $0+0.18$ $r+1.86$	3 3 2	38,600
4290.40	+0.47	3	+0.36	3	38,600
4529.53	$r_1+0.41$ $r_2+2.09$	2 1	$v-0.34$ 0 $r+1.53$	1 2 2	38,600
4535.09	+0.53	3	+0.58	3	38,600
4567.87	+0.20	1	+0.22	1	38,600
4582.69	−0.89 0	3 2	−0.49	2	38,600
4652.49	+0.42	4	+0.33	3	38,600
4688.41	−0.20	3	−0.20	3	38,600
4758.71	−0.13	2	....	....	38,600
4764.64	+0.25	3	+0.25	3	38,600
5171.33	+0.49	4	+0.94	2	38,600
5173.14	−0.13	5	−0.04	5	38,600
5174.35	−0.33	6	−0.33	6	38,600
5238.41	−1.48	10	−1.41 +0.34	3 4	38,600
5241.09	....	....	−0.50 0 +0.47	2 1 1	38,600
5243.01	0 +1.07	2 3	+0.32	3	38,600
5245.71	−0.10	4	....	....	38,600
5260.76	+0.81	10	+0.64	10	38,600
5264.50	−1.22 +0.43	2 4	−1.40 +0.43	5 1	38,600
5367.30	−1.22 0 −0.48	2 1 1	+0.48 −0.60 0 +0.57	1 1 1 1	38,600
5406.64	+0.49	1	+0.35	1	38,600
5544.78	+0.34	1	+0.49	1	38,600

REMARKS

λ 5241.09	This line may be regarded as a detached component of 5238.41. The *p*-component is too faint for measurement.
5367.30	This line may be regarded as a detached component of 5364.50. The *n*-component is very weak.

Nickel.—In 1917 Anderson[1] observed a number of affected nickel lines near λ 4000 A. In the present work, using a stronger electric field, the effect was much enhanced, as shown in Plate II*f*. Many affected lines were also found in the green and yellow regions. Plate II*c* shows the effect for λ 5084.20.

The Stark effect for a few lines of nitrogen, sodium, and oxygen was observed rather accidentally in the course of the present work.

Nitrogen.—In our previous paper dealing with the Stark effect of calcium and magnesium[2] it was reported that certain lines of unknown origin came out quite frequently when Al, Ca, Mg, and Ta were used as the cathode, the residual gas being air or hydrogen. Two of these lines, namely λλ 4100.7 and 4110.3, were found to be displaced toward the violet and were marked by the letters *C* and *D* in our paper. Later, Yoshida noticed that these lines had been recorded by Moissan and Deslandres[3] in their investigation of the nitrogen spectrum.

In his study of the Doppler effect in canal rays, Hermann[4] mentions that the two nitrogen lines λλ 4100 and 4110 behave differently from other lines. Since the discharge in pure nitrogen was not tried in the present work, the origin of these two lines may still be open to question. Table IX gives the displacement of these two lines.

Sodium.—The cobalt cubes used contained a small quantity of sodium as impurity, which brought out the sodium lines λλ 5682.90 and 5688.26 fairly strongly. They belong to the first subordinate series of sodium and were found to be displaced toward the red, as shown in Table X.

---

[1] *Physical Review*, **9**, 575, 1917.

[2] T. Takamine and N. Kokubu, *Memoirs of the College of Science* (Kyoto Imperial University), **3**, 173, 1918.

[3] *Comptes Rendus*, **126**, 1689, 1898.

[4] *Physikalische Zeitschrift*, **7**, 567, 1906.

TABLE VIII

NICKEL

λ	*p*-COMPONENT		*n*-COMPONENT		$E_{\text{max.}}$ IN VOLT/CM
	Δλ	Int.	Δλ	Int.	
3826	+0.69	3	+0.57	3	....
3831.89	+0.27	1	+0.17	1	....
3893	−0.96	2	−0.83	2	....
3896	−0.82	2	−0.82	2	....
3909.10	+0.17	3	+0.18	3	....
3918.7	−0.17	1	−0.23	1	39,000
3921.7	−0.93	4	−0.93	4	39,000
3939.3	+0.49	3	+0.57	3	39,000
3941	−1.01	3	−1.02	3	39,000
3944.3	0	2	0	2	39,000
	+0.39	7	+0.40	7	39,000
3953.0	+0.65	1	+0.64	1	39,000
3954	−1.21	4	−1.21	4	39,000
3955.2	+0.57	1	+0.47	1	39,000
3957.8	+0.62	1	+0.57	1	39,000
3960.7	−1.36	1	....	1	39,000
3962.25	−1.16	4	−1.22	4	39,000
3964.4	+0.54	3	+0.42	3	39,000
3968.3	−0.65	1	−0.51	1	39,000
3970.65	+0.19	8	+0.25	8	39,000
3972.0	+0.40	3	+0.40	3	39,000
3974.83	+0.48	6	+0.44	6	39,000
3984.18	−1.46	7	−1.31	7	39,000
3987.2	+1.12	2	+1.06	2	39,000
3994.1	+0.50	5	+0.57	5	39,000
3998.5	+0.36	2	+0.36	2	39,000
3999.8	+0.18	2	+0.18	2	39,000
4007.8	−0.77	1	−0.73	1	39,000
4017.67	−1.04	8	−0.91	8	39,000
4022.5	−1.00	2	−1.00	2	39,000
4024.1	−0.48	3	0	2	39,000
	0	....	....	....	39,000
4024.9	+0.99	2	+0.59	2	39,000
4025.1	+0.42	4	+0.41	4	39,000
4025.8	−0.70	3	−0.52	3	39,000
4027.8	−1.54	5	−1.44	5	39,000
4029.9	+0.70	2	....	....	39,000
4034	+0.27	2	+0.24	2	39,000
4037.7	+0.96	3	+0.70	3	39,000
4410.66	−0.18	6	−0.08	6	39,000
4937.45	−1.21	1	−1.34	1	38,500
5018.48	+0.70	2	....	....	....
5082.55	+0.44	3	+0.25	3	38,500
5084.20	V −1.29	7	−1.40	4	38,500
	0	1	0	......	
	r_1	....	r_1+1.92	......	
	r_2 +4.70	1	r_2+4.62	1	

TABLE VIII—*Continued*

λ	*p*-Component		*n*-Component		$E_{\text{max.}}$ in Volt/cm
	Δλ	Int.	Δλ	Int.	
5100.12	+0.30	8	+0.15	8	38,500
5142.91	−0.09	4	−0.07	4	21,800
5146.61	−0.13	3	−0.07	3	21,800
5155.90	−0.79	5	−0.79	5	21,800
5176.72	−0.15	4	−0.09	4	21,800
5184.78	+0.29	3	+0.30	3	21,800
5462.69	−0.86	1	−0.56	1	21,800
5588.09	−0.15	2	−0.11	2	21,800

REMARKS

λ 3893	Band superposed on this line.
3909.10	Band superposed on this line.
3939.3	Koch's type.
3957.8	Koch's type.
3962.25	Koch's type. Detached component of 3962.25?
3987.2	Koch's type.
4024.9	Detached component of 4024.1?
5084.20	In both *p*- and *n*-components r_1 and r_2 are detached.

TABLE IX

Nitrogen

λ	*p*-Component		*n*-Component		$E_{\text{max.}}$ in Volt/cm
	Δλ	Int.	Δλ	Int.	
4100.7	−0.15	5	−0.27	5	56,000
4110.3	−0.50	5	−0.40	5	56,000

TABLE X

Sodium

λ	Series	*p*-Component		*n*-Component		$E_{\text{max.}}$ in Volt/cm
		Δλ	Int.	Δλ	Int.	
5682.90	IN, II4	+1.82	2	+1.72	2	25,200
5688.26	IN, I4	+2.21	2	+2.08	2	25,200

Oxygen.—The red oxygen lines λλ 6156.198, 6156.993, and 6158.415, which form a triplet in the first subordinate series, were all found to be displaced toward the red, as shown in Table XI. It may be remarked here that in the discussion given by Schönrock[1] on the width of lines the data for this triplet show considerable discrepancy, which may perhaps be accounted for by the Stark effect.

TABLE XI

OXYGEN

λ	SERIES	*p*-COMPONENT		*n*-COMPONENT		$E_{max.}$ IN VOLT/CM
		Δλ	Int.	Δλ	Int.	
6156.198......	TNI	+0.37	1	+0.48	1	18,200
6156.993......	TNI	+0.51	2	+0.39	2	18,200
6158.415......	TNI	+0.60	3	+0.39	3	18,200

In connection with this it may be mentioned that the Stark effect for a number of green oxygen lines was first observed by Yoshida.

THE STARK EFFECT AND THE POLE EFFECT

One of the interesting features revealed by the present investigation is that there seems to be an unmistakable connection between the pole effect and the Stark effect. The pole effect for different elements has been studied by various investigators, an elaborate study of the phenomenon having been specially made for iron by St. John and Babcock.[2] Table XII gives the comparison of these two effects for iron lines.

As will be seen from the table, the two effects are in complete agreement as to the direction of displacement. Quantitatively, also, the agreement is fairly good except for the three lines λλ 5162.312, 5424.057, and 5455.435. The last line is a blend, made up of λ 5455.614, which is an "*a*" line in the classification of St. John and Babcock, and λ 5455.435, which is an "*e*" line, and

---

[1] *Annalen der Physik*, **20**, 995, 1906.

[2] *Mt. Wilson Contr.* Nos. 106, 137; *Astrophysical Journal*, **42**, 231, 1915; **46**, 138, 1917.

TABLE XII

IRON

λ	POLE EFFECT	STARK EFFECT ($E_{max.}$: 29,800 VOLT/CM)	
		p-Component	n-Component
5133.675	−0.045	−0.14	−0.15
5162.312	+0.030	+0.73	+0.28
5324.196	+0.015	+0.05	+0.05
5364.859	−0.028	−0.06	
5367.455	−0.025	−0.13	−0.05
5404.131	−0.025	−0.05	−0.05
5410.900	−0.026	−0.02	−0.04
5415.189	−0.030	−0.11	−0.06
5424.057	−0.027	−0.13	−0.12
5445.040	−0.020	−0.06	−0.06
5455.435	−0.016	−0.35	−0.38

hence shifted to the violet in the pole effect. In my spectrograms the dispersion was insufficient to separate the two, and consequently the displacement given is subject to considerable error.

The pole effect for nickel lines was recently examined by Babcock and Merrill (unpublished), and a comparison of pole and Stark effect was also made for this element. In the green part of the spectrum very close agreement was found, as shown in Table XIII; but in the violet part those lines which show Stark effect are so diffuse in the pole effect spectrograms, especially at the negative pole, as to render the measurement almost impossible. An inspection of these diffuse lines, however, indicates that most of them are widened toward the same side as in the case of the Stark effect.

TABLE XIII

NICKEL

λ	POLE EFFECT	STARK EFFECT		$E_{max.}$ IN VOLT/CM
		p-Component	n-Component	
4937.45	−0.006	−1.21	−1.34	38,500
5018.48	+0.006	+0.70		38,500
5082.55	+0.009	+0.44	+0.25	38,500
5084.20	−0.009	−1.29	−1.40	38,500
5100.12	+0.015	+0.30	+0.15	38,500
5155.90	−0.007	−0.79	−0.79	21,800
5176.72	−0.008	−0.15	−0.09	21,800
5184.78	+0.011	+0.29	+0.30	21,800

It should be remarked that in discussing the various causes of the broadening of spectrum lines Stark[1] suggested that the pole effect may be due to intermolecular electric fields. On comparing the results for the Stark effect with those obtained by King[2] for furnace spectra, it was found that the lines which are affected in an electric field belong to high-temperature lines in King's classification.

A preliminary search for the possible relations between the Stark effect and the pressure effect on spectrum lines was made also. For this purpose a series of investigations on the pressure effect of the lines of Ag, Au, Cu, Fe, and Ni carried out by Duffield[3] was referred to. Although it is difficult to make any definite statement, still in many cases there seem to be some indications that the Stark effect is involved as one of the causes affecting the pressure shift. For example, in the case of copper, Duffield classifies the lines in his Table VI in two groups, the one being strengthened as the pressure increases, while the other is weakened. On referring to the Stark effect we find that the lines which are affected by an electric field are all included in the latter class. In comparing the pressure effect with the Stark effect, however, we see many lines which are broadened on one side with high pressure, but remain unaffected by an electric field, so that the relation is not so simple as in the case of pole and Stark effect.

The relation between the Stark effect and the broadening of lines in arc and spark spectra was studied by Stark and Kirschbaum,[4] Stark,[5] Wendt,[6] Merton,[7] and others. In the course of the present work the following features were noticed:

1. In the ordinary arc spectrum of copper the lines λλ 4022.83 and 4063.50 are usually very diffuse toward the red. In the Stark effect these two lines are also displaced toward the red.

2. Striking similarity was noticed in the appearance of the silver lines λλ 4210.87 and 4212.76 as they appear in the arc and in a

---

[1] *Jahrbuch der Radioaktivität*, **12**, 349, 1915.

[2] *Mt. Wilson Contr.* Nos. 66, 108; *Astrophysical Journal*, **37**, 239, 1913.

[3] *Trans. Royal Soc.*, **208A**, 111, 1908; **209A**, 205, 1908; **211A**, 33, 1909; **215A**, 205, 1915.

[4] *Annalen der Physik*, **43**, 1017, 1914.

[5] *Jahrbuch der Radioaktivität*, **12**, 349, 1915.

[6] *Annalen der Physik*, **45**, 1257, 1914.

[7] *Loc. cit.*

strong electric field. (Compare Fig. 1, Plate I, in Duffield's paper, *Phil. Trans.*, **211A,** 33, 1909, with Plate I*c*.)

3. Generally speaking, those diffuse lines which are marked by the letters *u* and *U* in tables of wave-length given in Kayser's *Handbuch der Spectroscopie* were found to be affected by an electric field.

4. In the green part of the spectrum of a condensed spark discharge between iron poles those lines which are affected by an electric field invariably appear very hazy.

STARK EFFECT AND SERIES RELATIONS

Unfortunately the series relations in the spectra of the elements investigated here are not yet known except for silver and copper.

In Table XIV the affected lines of silver and copper are arranged according to their series relation, the + and − signs showing the direction of displacement in an electric field.

TABLE XIV

	Silver		Copper	
	I.N.S.	II.N.S.	I.N.S.	II.N.S.
$n=4$..........	5471.72? 65.66? 5209.25?	4668.70+ 4476.29+	5220.25− 18.45− 5153.33−	4531.04+ 4480.59+ ....
$n=5$..........	4212.76 (complex) 4210.87 (complex) 4055.46 (complex)	3981.87+ 3840.74+	4063.50+ 62.14+ 22.83+	3861.88− 25.13− ....
$n=6$..........	3810.85 (complex) 3682.45 (complex)	3710.1 + ...	3688.60 (complex, main line+) 54.59 (complex, main line+)	

In general, the diffuse series lines (I.N.S.) show more or less complex decompositions, while the sharp series lines (II.N.S.) are simply displaced in one direction, a feature which is very pronounced in the Stark effect for helium lines.[1]

---

[1] The fact that some of the sharp series lines of helium are not merely shifted in an electric field, but are resolved into a number of components, is stated in a previous paper (*Proceedings Tokyo Math. Phys. Soc.*, II, **9**, 394, 1918).

With respect to the direction toward which the lines are displaced, silver shows all its sharp series lines displaced toward the red, while in the case of copper the lines of both sharp and diffuse series change sign of displacement as we go from the term number $n=4$ to $n=5$. It is remarkable that exactly the same feature was observed for the diffuse-series lines of magnesium in our previous work,[1] in that the lines λλ 3829.5, 3832.5, and 3838.4 corresponding to $n=4$ are displaced toward the violet, while the members of the next term λλ 3093.1 and 3097.1 are displaced toward the red.

In general the relation of the Stark effect to the series law seems to be less simple than that of the Zeeman effect. An extension of our study of the Stark effect to the ultra-violet region seems to be highly desirable.

For those elements whose series relations are not yet established it appears that the Stark effect may be utilized as a powerful means of finding the relationships.

It may be worth mentioning that, of the elements studied in the present work, Na, Cu, Ag, and Au are all in the first column of the periodic table, while O and Mo together with Cr, which was studied by Anderson, are in the sixth column. The similarity of the electric decomposition of the lines of the elements in any one column of the periodic table is very striking when we compare, for example, the lines of Ag, Au, and Cu; also those of Mo and Cr as well as those of Fe, Co, and Ni.

In conclusion I wish to express to the members of the Observatory staff my very deep appreciation of the opportunity for my work at the Observatory. I am under particular obligation to Dr. J. A. Anderson for his kind guidance throughout the experiments, and to Miss M. O. Burns of the Computing Division for her careful measurements and reductions.

SUMMARY

1. Adopting the method employed by Anderson, the Stark effect on the spectra of the following metals was investigated: Ag, Au, Co, Cu, Fe, Mg, Mo, Ni. In addition to this a few lines of Na, O, and N were found to be affected by an electric field.

---

[1] T. Takamine and N. Kokubu, *loc. cit.*

2. Close relations were found between the pole effect and Stark effect in the spectra of iron and nickel.

3. Several instances showing the close relation between the Stark effect and the broadening of lines in the arc and spark spectra were noticed.

4. The connection between the series relationship and the Stark effect seems to be somewhat more complicated than in the case of the Zeeman effect. In some cases the side toward which the line is displaced in an electric field is different for different term numbers.

5. As in the case of helium, detached components and isolated lines, having the peculiar property of showing themselves only in strong electric fields, were observed in the spectra of silver and copper.

6. In the spectrum of molybdenum a curious complementary feature between p- and n-components of the two lines, λλ 5238.41 and 5364.50, was observed in that the p-component of the former was exactly the same as the n-component of the latter, and vice versa.

Mount Wilson Observatory
March 1919

Contributions from the Mount Wilson Observatory, No. 170

NOTE ON THE RELATIONSHIP OF MEAN PARALLAX TO MEAN PROPER MOTION

By GUSTAF STRÖMBERG

Recent correspondence with Professor Kapteyn has directed attention to an apparent contradiction in the results for parallaxes determined by the spectroscopic method which were published in *Contribution* No. 142 and used in deriving the formula for mean parallax given in *Contribution* No. 144. When arranged in the order of proper motion and grouped into means, the spectroscopic parallaxes for stars of very small proper motion are systematically larger than the corresponding mean trigonometric values. Since the initial values of the reduction constants for the spectroscopic method were necessarily calculated from trigonometric parallaxes, one might thus be led to infer that the spectroscopic results are not in harmony with the data upon which they are based. Such a conclusion would not, however, be justified, for two reasons: first, the constants used in deriving the spectroscopic parallaxes in *Contribution* No. 142 depend not only on the trigonometric results for stars in this list but also on data for other stars published elsewhere;[1] and second, in the comparison described, the group of small proper motions does not include all the distant objects, even of the list in *Contribution* No. 142, which were used in deriving reduction constants for the highly luminous stars. A considerable number of stars of small parallax have relatively large proper motions, and these naturally appear in the group of rapidly moving stars which as a class are relatively near and not highly luminous.

As a whole the spectroscopic results are, in fact, in harmony with the trigonometric parallaxes upon which they were based, as may be seen from Tables II and III in *Contribution* No. 142. It is only when the stars are arranged according to proper motion that the systematic difference appears, and it is then important only for the stars of small proper motion.

---

[1] *Proc. Nat. Acad. Sci.*, **2**, 152, 1916.

The discrepancy in question, which had already revealed itself in another manner during the continued development of the spectroscopic method, is not therefore a contradiction in the sense suggested above, but instead an indication of systematic errors which were to be expected in the early results for distant stars arising from the very scanty data available for small parallaxes when the method was first introduced. As additional data became available, it was soon found that the absolute magnitudes of highly luminous stars derived with the original reduction constants were systematically too faint. The corrections required for the brightest stars ranged from −0.5 to −1.5 mags. The results for the less luminous stars, on the other hand, appeared to be substantially correct.

A final reduction system could, however, be approached only through a series of successive approximations; and later, when even more complete material had become available, an extensive investigation of the whole question was undertaken, based on all known trigonometric parallaxes of high weight and also upon the parallactic motions of the stars whose parallaxes had been spectroscopically determined. Inasmuch as the latter now number more than a thousand, they afford an invaluable aid in establishing a final system, especially for the case of the distant stars. Since it is proposed during the course of the year to revise again the entire calculation with the aid of still more extensive data, the publication of details will be deferred until later. Certain general statements, however, can profitably be made at present.

The general method has been to divide the stars according to five spectral classes and then, within each division, arrange the results according to the absolute magnitudes calculated from the line-intensities. Systematic corrections to these absolute magnitudes were then computed for each of the groups, the respective values of ΔM being derived from both trigonometric parallaxes and parallactic motions. The resulting corrections found by the two methods are in general small and in close agreement with each other. When applied to the provisional absolute magnitudes determined spectroscopically, they lead to parallaxes which are in excellent agreement with the trigonometric results, even when the data are grouped according to proper motion.

After the completion of the calculation, through the kindness of Schlesinger and Mitchell we received extensive manuscript lists of directly measured parallaxes of bright stars, and these too are in close agreement with the revised spectroscopic values.

One very important result of the investigation is the light thrown upon the sensitiveness of the spectroscopic method as applied to stars of different luminosity. If for any given luminosity the change in the absolute brightness should be large as compared with the change in the line-intensity, it would be impossible to determine the corresponding absolute magnitude accurately from observed line-intensities. By grouping the data in such a way as to give for the various spectral classes a series of corresponding values of mean line-intensity and mean absolute magnitude, we derive at once upon plotting the results a series of curves which show the change of $\overline{M}$ with line-intensity throughout the whole range of observed luminosity. The behavior for different spectral lines is different, but in no case, even among the most luminous stars, does the rate of change in $\overline{M}$ attain values which would render the calculated value of the absolute magnitude seriously uncertain. In most cases the curves are approximately straight lines, so that the uncertainty seems to be practically independent of the luminosity.

Another consequence of the rapidly increasing number of spectroscopic parallaxes is that it has been possible to make a closer study of the nature of the relationship between mean parallax and mean proper motion for certain apparent magnitudes, and especially to test Kapteyn's formula for stars of very small proper motion. In particular it was important to find whether or not the mean parallax tends toward a finite lower limit when the proper motion approaches zero, as was indicated in my previous paper.[1]

Since the spectroscopic criterion is found to be valid for the most luminous stars, it is evident that spectroscopic parallaxes are much more suitable for such a study than those derived trigonometrically, for the percentage errors in the former are approximately constant. The absolute errors thus decrease with the parallax, and for small parallaxes should be very small, whereas the absolute errors in the trigonometric parallaxes are about the same for all values of the parallax.

---

[1] *Mt. Wilson Contr.* No. 144; *Astrophysical Journal*, **47**, 7, 1918.

All the stars between apparent magnitudes 3.5 and 6.5 having proper motions smaller than 0ʺ5, for which either spectroscopic or trignometric parallaxes were available (February 1919), have been used in this preliminary investigation. After applying corrections to the spectroscopic results to reduce them to the revised system of absolute magnitudes referred to above, the data were grouped according to apparent magnitude and proper motion. Stars of apparent magnitudes 4.5 and 5.5 have been included with both the adjacent groups. All spectral classes from A7 to Md have been taken together. Only the best trigonometric parallaxes have been used, and those of larger probable error appear only in combination with other determinations for the same star. The resulting mean values are in Table I, π_s indicating the spectroscopic parallaxes and π_t those obtained trigonometrically.

The values $\overline{\pi}_k$ are mean parallaxes computed from Kapteyn's formula[1]

$$\log \overline{\pi}_k = -0.789 + 0.649 \log \overline{\mu} - 0.0434 \, \overline{m},$$

using for $\overline{\mu}$ the mean of the proper motions for the corresponding groups of spectroscopic and trigonometric parallaxes, and for $\overline{m}$, 4.0, 5.0, and 6.0, respectively. The differences between the three series of parallaxes are in the last three columns of the table.

In spite of the fact that both the spectroscopic and trigonometric results have been greatly increased in number since the systematic corrections were calculated last summer, and the further fact that these corrections were based upon parallactic motions as well as trigonometric parallaxes, the agreement between the spectroscopic (π_s) and the trigonometric (π_t) results is as good as can be expected especially when we bear in mind that the relation between parallax and proper motion is a statistical one and for the two classes of parallaxes refers partly to different groups of stars.

---

[1] *Groningen* 8, p. 24. The constants in this formula are partly based on parallactic motions calculated with a solar velocity of 16.7 km per sec. To reduce the results to the solar velocity at present accepted they should be decreased by about 16 per cent. Since the parallaxes with which we are concerned are very small, the correction has been disregarded in the comparison.

TABLE I

μ	Spectroscopic Parallaxes					Trigonometric Parallaxes				$\bar{\pi}_k$	$\pi_s-\pi_t$	$\pi_s-\pi_k$	$\pi_t-\pi_k$
	No.	$\bar{\mu}$	$\bar{m}$	$\bar{M}$	$\bar{\pi}_s$	No.	$\bar{\mu}$	$\bar{m}$	$\bar{\pi}_t$				
	Apparent Magnitudes 3.5 to 4.5												
≦0″.020	15	0″.012	4.03	−0.68	0″.013	9	0″.009	3.92	+0″.012	0″.005	+0″.001	+0″.008	+0″.007
0.021 to 0.040	11	.030	4.06	−0.32	.014	10	.029	4.01	+ .009	.011	+ .005	+ .003	− .002
.041 " .070	13	.060	3.99	+0.20	.018	11	.059	4.03	+ .016	.018	+ .002	.000	− .002
.071 " .100	17	.088	4.14	+0.16	.016	6	.085	4.13	+ .014	.022	+ .002	− .006	− .008
.101 " .150	26	.123	3.95	+0.38	.022	21	.124	3.93	+ .026	.028	− .004	− .006	− .002
.151 " .200	20	.169	3.98	+0.92	.028	10	.169	3.92	+ .026	.034	+ .002	− .006	− .008
.201 " .300	17	.234	4.12	+0.69	.026	15	.240	4.29	+ .058	.043	− .012	− .017	− .005
.301 " .500	21	.397	4.08	+1.84	.048	16	.398	4.05	+ .051	.060	− .003	− .012	− .009
	Apparent Magnitudes 4.5 to 5.5												
≦0.020	50	0.010	5.18	−0.03	+0.010	8	0.014	4.95	+0.011	0.006	− .001	+0.004	+0.005
0.021 to 0.040	25	.028	5.01	+0.04	+ .011	15	.028	4.85	+ .011	.010	.000	+ .001	+ .001
.041 " .070	22	.055	5.06	+0.34	+ .013	14	.056	4.97	+ .017	.015	− .004	− .002	+ .002
.071 " .100	17	.084	5.01	+0.76	+ .018	10	.084	4.81	+ .026	.020	− .008	− .002	+ .006
.101 " .150	18	.122	5.02	+0.46	+ .016	15	.125	4.89	+ .020	.025	− .004	− .009	− .005
.151 " .200	18	.171	4.85	+1.56	+ .034	12	.175	4.79	+ .045	.032	− .011	+ .002	+ .013
.201 " .300	13	.240	4.95	+3.05	+ .050	18	.242	5.00	+ .042	.039	+ .008	+ .011	+ .003
.301 " .500	22	.369	5.00	+2.52	+ .039	16	.378	4.98	+ .042	.052	− .003	− .013	− .010
	Apparent Magnitudes 5.5 to 6.5												
≦0.020	144	0.012	5.94	+0.19	0.008	13	0.015	5.94	+0.007	0.006	+0.001	+0.002	+0.001
0.021 to 0.040	49	.027	6.05	+0.17	.007	5	.028	5.92	+ .004	.009	+ .003	− .002	− .005
.041 " .070	36	.054	6.02	+0.41	.008	18	.056	5.90	+ .022	.014	− .014	− .006	+ .008
.071 " .100	30	.084	5.97	+0.86	.013	17	.084	5.93	+ .017	.018	− .004	− .005	− .001
.101 " .150	15	.124	5.95	+1.33	.016	11	.123	5.95	+ .024	.023	− .008	− .007	+ .001
.151 " .200	12	.180	5.96	+3.07	.033	10	.179	5.93	+ .041	.029	− .008	+ .004	+ .012
.201 " .300	20	.246	6.01	+3.33	.037	21	.251	5.92	+ .041	.036	− .004	+ .001	+ .005
.301 " .500	37	.381	6.02	+4.43	.053	23	.370	5.98	+ .054	.047	− .001	+ .006	+ .007

The agreement of the results with the mean parallaxes derived from Kapteyn's formula (for the various comparisons see also Fig. 1) is also as good as could have been anticipated, and shows that his results in *Groningen* No. 8, which were based on the proper motions of the Bradley stars and a comparatively small number of directly measured parallaxes, are in good accordance with recent determinations of proper motion and parallax.

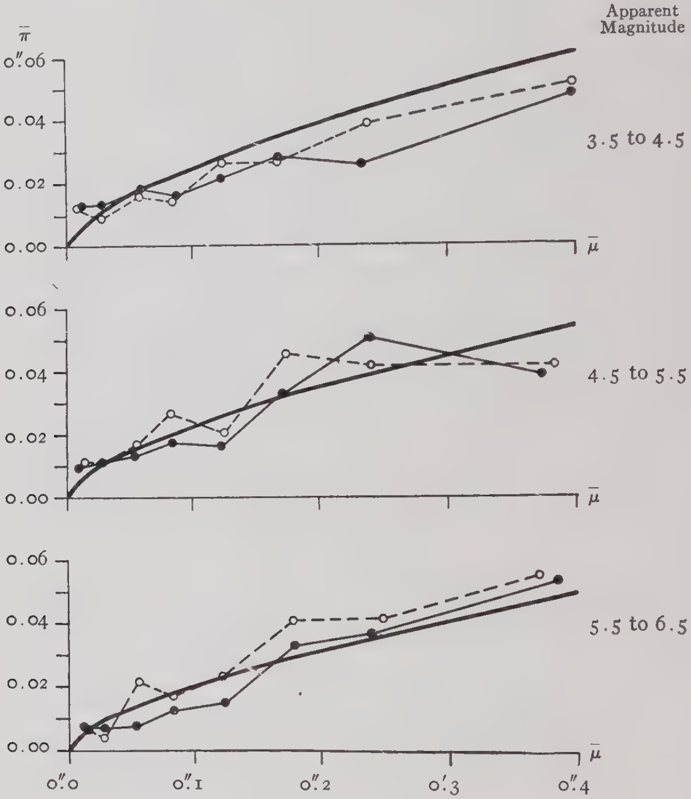

FIG. 1

Relationship between mean parallax $\bar{\pi}$ and mean proper motion $\bar{\mu}$. The dots indicate spectroscopically determined parallaxes, the open circles trigonometric parallaxes, both for groups of stars within certain intervals of proper motion. The smooth curve indicates Kapteyn's relation between $\bar{\pi}$ and $\bar{\mu}$ for the apparent magnitudes 4.0, 5.0, and 6.0.

It should be noted that the formula which summarizes Kapteyn's results claims to be nothing more than an interpolation formula, namely, the simplest of several tried which satisfactorily represent the observed data then available, and that the smallest observed *mean* motion used in its derivation is about 0″.04 with a corresponding mean parallax of 0″.01.[1] Kapteyn himself points out as an objection to the formula that its analytical form requires a zero value of the parallax for stars having zero proper motion, but immediately remarks.[2] "for proper motions sensibly below 0″.01, the parallaxes derived from our [Kapteyn's] formulae cannot be accepted with any great confidence. The harm done, however, is not great, because it is doubtful whether we can affirm the reality of any computed proper motion of such an amount."

Meanwhile it has become important to know something of the analytical character of the formula for very small values of the proper motion because of its bearing on the frequency of highly luminous stars. Apparently some modification of the simple form proposed by Kapteyn will be required for the representation of parallaxes corresponding to very small proper motions, for as it stands it implies that stars of vanishingly small motions are of enormous luminosity. The difficulty is also revealed by the remark that for any given m the expression

$$5 \log \pi = M - m - 5$$

defines a lower limit to the parallax, whose numerical value, independently, of the proper motion, is determined by the upper limit of the luminosity. Practically the luminosity is not infinite; in fact, M is probably very seldom less than -5. Hence the mean parallax cannot be zero no matter how small the proper motion. It may be noted, however, that, as m increases, the minimum value of π decreases, and in consequence we should expect the representation afforded by Kapteyn's formula in the region of extrapolated values to be more satisfactory for the fainter apparent magnitudes than in the case of the brighter stars. In fact, something of the kind seems to be indicated by the data now available.

---

[1] On page 2 of *Contribution* No. 144 a reference was made to extrapolated values of the mean parallax derived with the aid of this formula. It should be stated that here as elsewhere in that contribution the deviation of the mean parallaxes computed with the formula of Kapteyn from those derived spectroscopically is appreciable only for proper motions less than 0″.03. This remark is made in justice to Professor Kapteyn, inasmuch as certain passages in the article might be interpreted as implying that the validity of the formula is much more restricted than it really is.

[2] *Publications of the Astronomical Laboratory at Groningen*, **8**, p. 20.

When the spectroscopic method of determining stellar parallaxes was first applied to stars of small proper motion it was found that the line-intensities of stars of proper motion up to about $0\rlap{.}''03$ or $0\rlap{.}''04$ were nearly the same,[1] which indicated that the corresponding absolute magnitudes were nearly constant. The spectroscopic parallaxes thus appeared to have a lower limit, depending on the apparent magnitude and on the upper limit of luminosity. The sensitiveness of the method was then tested in the manner described above for the stars in question by grouping them according to line-intensity and comparing the results with the absolute magnitudes which were calculated from parallactic motions derived by considering all the stars of the same line-intensity, without restriction as to the amount of proper motion.

In other words the distant stars showed scarcely any correlation between amount of proper motion and line-intensity, whereas there was a strong correlation between line-intensity and mean parallactic motion.

It thus seemed desirable to modify Kapteyn's formula in such a way as to obtain a finite parallax for vanishing proper motion. The following mean parallax formula was accordingly proposed:[2]

$$\log \overline{\pi} = \log A + b \log (\overline{\mu} + c) + \overline{m} \log \epsilon$$

or

$$\overline{\pi} = A\ (\overline{\mu} + c)^b \epsilon^{\overline{m}}.$$

The constant b was found difficult of determination; but fortunately it could be assumed equal to 1, the resulting error affecting only the parallaxes of stars of very large proper motion. Hence the simpler relation was used:

---

[1] Attention was called to this fact in the sentence preceding equation (5), *Contribution* No. 144: "For values of μ smaller than about $0\rlap{.}''03$ the parallax is almost independent of the proper motion." The meaning here is that if we consider the parallaxes for $\mu < 0\rlap{.}''03$ *by themselves* (see Fig. 1, *Contribution* No. 144) the values of $\log \pi$ can be as well represented by a line parallel to the $\log \mu$-axis as they are by the curve adopted. The latter refers to the results as a whole, and, being the equivalent of a linear relation between π and μ, would indicate that the variation of π with μ is just as great below $\mu = 0\rlap{.}''03$ as it is above this limit.

[2] *Mt. Wilson Contr.* No. 144; *Astrophysical Journal*, **47**, 7, 1918.

$$\bar{\pi}=A\ (\bar{\mu}+c)\ \epsilon^{\bar{m}}$$

or

$$\log \pi=\log A+\log\ (\bar{\mu}+c)+\bar{m}\ \log \epsilon,$$

i.e., a linear relationship between $\bar{\pi}$ and $\bar{\mu}$. The divergence between this formula and that of Kapteyn is clearly seen if we plot[1] the logarithms of π and μ.

Since the above formula was proposed, the spectroscopic parallaxes have been revised and corrected for systematic error and a large amount of additional data has been collected. But in spite of this, the present results, as shown by Figs. 1, 2, and 3, do not indicate that any change in the analytical form of the equation is required. The constants have of course been modified, but the evidence still points strongly toward the conclusion that for very small mean proper motions, below the limit to which Kapteyn's formula strictly applies, the mean parallax approaches a finite limit whose value in turn approaches zero as the apparent magnitude m of the stars considered becomes very large.

Consider first the trigonometric parallaxes. Here we must bear in mind that the parallaxes of stars having small proper motions are very small. In consequence their percentage errors are large. The most reliable comparison is afforded by the stars of brightest apparent magnitude, since their parallaxes on the average are larger than those of fainter stars. For apparent magnitudes 3.5 to 4.5 there is a close linear relationship between π and μ, the parallax for vanishing proper motion being about 0."01. In the case of apparent magnitudes 4.5 to 5.5 the relationship is perhaps not strictly linear (i.e., $b<1$), but there is here also a clearly marked lower limit for the trigonometric parallaxes equal to 0."01, the same as for stars of mean magnitude 4.0. For the stars of magnitude 5.5 to 6.5 the trigonometric parallaxes can be reconciled with a curve through the origin, but the errors are here of nearly the same magnitude as the parallaxes themselves.

Turning to the spectroscopic parallaxes, we find that they similarly show lower limits for the mean parallaxes corresponding to vanishing proper motion, whose values are 0″.011, 0″.009, and 0″.006, respectively, for the magnitudes 4.0, 5.0, and 6.0. These limiting values of π correspond to the following minima of *mean* absolute magnitude: −0.8, −0.2, and −0.1, respectively.

---

[1] *Loc. cit.*

We may summarize the result thus: The spectroscopic method of determining absolute magnitudes, when applied to stars of proper motion below 0″.03 or 0″.04 and of apparent magnitude brighter than 6.5, indicates a maximum luminosity corresponding to a *mean* absolute magnitude of about −0.5, which defines the lower limit of parallax for ordinary stars of types F, G, K, and M. There are of course absolutely brighter stars of these types, but they cannot be distinguished by the amount of proper motion alone. In classing the stars according to line-intensity, however, we find groups of stars of luminosity up to about −2, and in individual cases an even higher luminosity up to absolute magnitude −4 or −5. The lower limit of the mean parallax thus defined for stars of small proper motion is not in conflict with the trigonometric parallaxes, at least not for stars brighter than 5.5. For apparently fainter stars the trigonometric parallaxes are too small to indicate the limiting value, at least with the present amount of data.

The number of stars having extremely small proper motions is not very large, but the mean parallax formula should be valid for all proper motions. Table II, derived from Boss's catalogue, will give some idea of the number of stars of small proper motion of spectral types F, G, K, and M.

TABLE II

PERCENTAGES OF STARS OF DIFFERENT PROPER MOTIONS

	μ		
Apparent Magnitude	$\lesseqgtr 0''.050$	$\lesseqgtr 0''.024$	$\lesseqgtr 0''.012$
<3.0	35	11	8
3.0 to 4.0.......	26	12	8
4.0 " 4.5.......	34	16	5
4.5 " 5.0.......	40	19	8
5.0 " 5.5.......	43	20	8
5.5 " 6.0.......	43	20	7

The percentage errors in the motions are of course very large for small proper motions, but fortunately these are less serious in their effect upon the mean parallax than formerly appeared to be the case, for the modified formula, which seems to be required by the observed data, indicates that for small proper motion the percentage change in π with changes in μ is small. Consequently a considerable uncertainty in μ means only a small uncertainty in the corresponding mean parallax.

For vanishing proper motions the modified mean parallax formula goes asymptotically over into

$$\log \pi = \log A' + \dot{\overline{m}} \log \epsilon,$$

which is of the same form as Kapteyn's second parallax formula. The meaning of the two formulae is somewhat different, however, for the asymptotic limit holds only for zero proper motions, while Kapteyn's relation between mean parallax and apparent magnitude refers to the mean proper motion of the stars of the apparent magnitude considered.

In this connection attention should be called to the fact that the mean of a group of observed proper motions is always too large, owing to the effect of the squares of the errors. If the errors in the measurements of the two components of proper motion, $\mu_\alpha \cos \delta$ and μ_δ, have a normal distribution, it can be proved that, even when the proper motions are all actually zero, the *mean* of the measured values of proper motion will be

$$\sqrt{\frac{\pi}{2}}\,\epsilon = 1.25\ \epsilon = 1.86\ r,$$

where ϵ and r are the absolute values of the mean and probable errors in the two measured components. The lower limit of the mean of the observed proper motions is thus equal to this amount. For $r = \pm 0''.005$ (Boss's catalogue) the limit is $0''.0093$. Any grouping of stars according to proper motion smaller than about $0''.015$ is to a large extent a grouping according to accidental errors. Further, the number of stars of proper motion smaller than $0''.012$ as given in Table II would be somewhat increased if the mean proper motions had been corrected for the effect of the squares of the errors.

Finally it may be remarked that the functional relationship between $\bar{\pi}$ and $\bar{\mu}$ given above does not apply if we group the stars on another basis than the amount of proper motion itself. For example, let us classify the stars of a given apparent magnitude according to some characteristic correlated with absolute magnitude (line-intensity, Cepheid variation, etc.) and compute the mean parallax and mean proper motion for each of the groups thus derived. Passing from group to group in the order of increasing luminosity, $\bar{\pi}$ and $\bar{\mu}$ both decrease and *simultaneously* approach zero as the luminosity becomes infinitely great.

This is clearly seen if we start from the relation between proper motion and linear tangential velocity, t, relative to the sun. For a single star this relation is

$$\mu=\frac{\pi t}{k}, \qquad k=4.738.$$

For a constant m and increasing luminosity, π gradually decreases and produces a corresponding decrease in μ; but $\bar{\mu}$ cannot become zero unless $\bar{\pi}$ also vanishes, for the *mean* tangential velocity of a group of stars of any given luminosity can in no case be equal to zero. A similar result follows when we classify the stars according to apparent magnitude and form for each group the mean proper motion and mean parallax. In this case also the functional relationship between $\bar{\mu}$ and $\bar{\pi}$ must be such that they approach zero simultaneously as we consider larger and larger values of m.

These cases are to be distinguished sharply from that with which we have been concerned in the above discussion. There we have grouped the stars directly according to proper motion. For any given apparent magnitude the parallax cannot fall below a certain limit; but, by virtue of the basis of grouping, there is no finite lower limit to the average linear velocity t. With such an arrangement of the data, therefore, the mean proper motion approaches zero as we pass from group to group; $\bar{\pi}$ also decreases, but, in this case, converges toward a finite limit for zero proper motion.

MOUNT WILSON OBSERVATORY
March 1919

Contributions from the Mount Wilson Observatory, No. 171
Reprinted from the *Astrophysical Journal*, Vol. L, No. 3, pp. 228–31, 1919

NOTE ON THE POLARIZATION OF THE NIGHT SKY

By HAROLD D. BABCOCK

At the suggestion of Lord Rayleigh (then Professor Strutt), attempts were begun at Mount Wilson during the past spring to detect the presence of polarization in the background of the night sky. During the preceding year he himself had made some observations in England for this purpose, and very kindly loaned to us the large Nicol prism and pair of quartz plates which he had used. When combined with a short-focus lens of large relative aperture, these form a photographic Savart polariscope well adapted to the problem. It was found, however, that the weight of the assembled apparatus and the losses of light therein were undesirably large, and a simplified arrangement was developed (after Cornu) which has proved very satisfactory.

For monochromatic light the variation of intensity across the field of a Savart polariscope takes the form of a smooth curve, i.e., the maxima and minima are separated by regions of intermediate intensity. Furthermore, when a considerable range of wavelengths is employed, there is a flattening of the scale of contrasts, due to the change of spacing of the bands with the wave-length. This effect must tend to diminish the sensitivity of the Savart polariscope, especially when it is used photographically to detect a small percentage of polarized light in a large amount of ordinary light. In the polariscopes described below, areas of maximum and minimum intensity are placed side by side in the field of view, unseparated by regions of intermediate intensity, and they suffer no loss of sharpness when white light is used, so that advantage is taken of the well-known apparent enhancement of contrast due to juxtaposition of areas of different blackness upon the photographic plate. Furthermore, the number of air surfaces in the optical system may be reduced to four and the total thickness of solid media may be kept down to a couple of centimeters or even less, so that the losses of light may be made very small.

The first instrument which was designed to fulfil these conditions consisted of a Nicol prism of the Glan-Thompson type, having a compound half-wave plate of mica attached to one side. The Nicol was selected on account of the uniformity of its polarization over the angular field, and the half-wave plate was made of mica strips 2×8 mm with axes alternately at 0° and 45° to the principal plane of the Nicol. The mica was of such a thickness as to introduce a relative retardation of $\lambda/2$ for the region of the spectrum to which ordinary photographic plates are most sensitive. The alternate strips of mica appear light and dark, their contrast depending upon the amount of polarized light in the incident beam, as well as upon the orientation of the Nicol with respect to the plane of polarization. This polariscope was found to be highly sensitive and readily adaptable to such problems as the one at hand.

Upon consultation with Dr. Anderson, however, he offered a suggestion as to a still simpler method of constructing a polariscope which would fulfil the conditions discussed above. He then very kindly prepared the two essential elements required, which are described below, and most of the observations have been made with this apparatus. It is a pleasure to acknowledge here my indebtedness to him.

In its simplest form this polariscope consists of a small plate of calcite 5 or 6 mm thick, having cemented to one side a glass screen containing a series of equal opaque and transparent strips. The width of strip is made equal to the separation of the two images of a point seen through the calcite plate, and the glass screen is so oriented upon the calcite as to bring the two images of each transparent strip just into contact side by side.

It is evident that if the incident light is wholly or partially polarized the strips will in general appear alternately light and dark. When the plane of polarization is at 45° to the principal directions in the calcite the illumination will be uniform, but if the angle is 0° or 90° there will be maximum contrast between the two sets of images, dependent upon the percentage of polarized light in the incident beam.

The glass screen was made by photographic reduction from a model having dimensions about 8 by 10 inches. Upon a glass plate of this size were mounted a row of pieces of rolled-metal strip, the alternate ones being afterward removed, so as to leave a grid having equal black and white spaces when viewed by transmitted light.

The calcite plate and attached screen were mounted in one end of a tube about ten inches long, at the other end of which was an aplanatic hand magnifier lens of 37 mm focal length. A simple metallic screw-cap held a photographic plate in the proper position behind the lens to receive a sharp image of the strips of the screen as seen through the calcite plate. Diaphragms were used to prevent undesirable light from reaching the plate.

This arrangement proved an exceedingly delicate detector of polarized light, but its sensitivity was still further increased by the addition of a narrow strip of mica at right angles to the strips of the glass screen. The thickness of the mica was such that it introduced a relative retardation of one-half a wave-length for blue light, and its axis was at 45° to the principal directions in the calcite. As a result the portion of the field covered by the mica has the relative intensity of the alternate strips reversed as compared to the rest of the field. This is found to be of material assistance when the difference between alternate images is very small.

The polariscope was provided with an index and a graduated circle by means of which the principal planes of the calcite plate could be oriented with respect to the position of the sun. The most satisfactory method of adjusting was to mount the polariscope upon the tube of a small telescope having an equatorial mounting. The polariscope was set for the neutral position (where sensitiveness of setting is a maximum) by daylight in a direction at 90° from the sun. A rotation of 45° then brings one of the principal planes of the calcite through the sun, and a reading of the hour circle of the telescope and the time makes it possible to set the polariscope correctly for the subsequent exposure.

All the plates were taken in the northern sky in a direction very nearly 90° from the position of the sun. All were made within a day or two of the time of new moon and nearly all of the exposures were of two hours' duration, symmetrical about the time of true midnight. Fast plates were used and a contrast developer. Upon one of the nights the atmosphere was clear enough so that three observers agreed in their separate locations of the *Gegenschein.* It must be said, however, that for some weeks past, probably including the last two periods of observation, the transparency of the atmosphere on Mount Wilson has been below its best. Sunset colors have been brighter than usual and there has been a slight milkiness apparent in the daylight sky. Visual measures of the daylight polarization of the sky by Anderson in Pasadena have shown a decrease in the percentage of polarization during the past few weeks.

The photographs suitable for discussion number eight. There is evidence upon two or three of them of a very slight difference between adjacent strips, but considering the marked sensitiveness of the instrument, it must be said that the total amount of polarized light shown is extremely small.

Quantitative measures of the sensitiveness have not been made, but it is probably safe to say that we have not found more than 1 per cent of polarization in the background of the night sky.

Mount Wilson Observatory
August, 1919

Contributions from the Mount Wilson Observatory, No. 172
Reprinted from the *Astrophysical Journal*, Vol. L, No. 5, pp. 391–93, 1919

THE ORBIT OF THE SPECTROSCOPIC BINARY BOSS 2285

By ALFRED H. JOY and GIORGIO ABETTI

The variable velocity of the star Boss 2285=Pi $8^{h}108$ ($\alpha=8^{h}30^{m}.5$, $\delta=+6°58'$; 1900.0) was discovered at this observatory from plates taken in 1918.[1] With Boss 2286=Lal. 16895 it forms the physical system β G.C. 4677=Σ 1245. The measures of position angle and distance show no change since the time of the observations by Dembowski. The lack of relative motion is confirmed by van Maanen from measures of the two components on his parallax plates which give: 1916.23, P.A. 25°.0, dist. 10″.49. The Harvard apparent magnitudes, the proper motions by Boss, the Mount Wilson spectral types, and the absolute parallaxes with corresponding absolute magnitudes by van Maanen are:

	Harvard m	μ	Spec.	π	M
Boss 2285 . . .	6.04	0″.195	F7	+0″.022	+2.8
Boss 2286 . . .	7.15	0.201	G3	0.026	4.2

The absolute magnitudes determined by Adams and Joy from the spectra are 4.5 and 5.5, which would give a mean parallax of 0″.048. Measures of the four plates of Boss 2286 give radial velocities ranging from +23.4 km to +31.0 km with a mean of +27.9 km which may be compared with the velocity of +25.2 km found in this investigation for the center of mass of the system Boss 2285. The spectrum of the secondary star is not visible on any of the plates.

Table I gives a list of the photographs. The Greenwich mean time refers to the middle of the exposure; the phase is derived from the period 14.296 days and refers to the epoch J.D. 2421598.0. The plates have been taken with the 60-inch reflector and the 18-inch single-prism spectrograph. The various plates have been measured by Adams, Joy, Abetti, Strömberg, and Miss Burwell, and the number in the table indicates the number of measures of each plate. No systematic difference between the measures was found, so that the mean result has been used in the table.

---

[1] *Publ. Astr. Soc. of the Pacific*, 31, 41, 1919.

TABLE I

Plate No.	Date	G.M.T.	Phase	Velocity	No. of Meas.	O−C	Remarks
				km		km	
7853.....	1919, Feb. 8	18^h40^m	$0\overset{d}{.}490$	− 0.4	3	+0.1	
5770.....	1917, May 6	15 42	0.686	− 2.0	4	+1.8	
6818.....	1918, Mar. 31	17 41	0.961	− 3.3	4	−2.1	
6876.....	1918, Apr. 29	16 51	1.334	+ 3.3	3	+1.6	
7936.....	1919, Mar. 10	18 26	1.888	+ 6.5	3	−2.6	
6886.....	1918, Apr. 30	17 22	2.356	+16.5	3	−0.1	
7943.....	1919, Mar. 11	17 25	2.846	+25.9	3	+1.6	
7944.....	1919, Mar. 11	17 52	2.864	+25.0	3	+0.5	
6575.....	1918, Jan. 21	21 22	3.594	+35.4	3	+2.0	
6589.....	1918, Jan. 22	20 41	4.565	+38.5	3	−1.7	
7864.....	1919, Feb. 12	20 55	4.584	+40.7	3	+0.4	
7772.....	1919, Jan. 15	21 29	5.199	+47.9	4	....	Weak
6597.....	1918, Jan. 23	21 16	5.590	+41.7	5	−1.3	
7786.....	1919, Jan. 17	22 28	7.240	+44.5	4	+2.6	
6504.....	1917, Dec. 29	21 40	9.199	+32.8	4	−2.5	
6615.....	1918, Jan. 27	20 17	9.549	+35.4	3	+1.8	
7975.....	1919, Mar. 18	16 03	9.789	+29.9	3	−2.5	
6515.....	1917, Dec. 30	23 47	10.287	+32.2	4	+2.5	
6925.....	1918, May 23	15 59	11.002	+16.9	3	....	7-in. camera
7914.....	1919, Feb. 19	20 17	11.557	+20.3	4	−1.0	
6659.....	1918, Jan. 30	19 10	12.503	+15.2	3	+1.5	
6799.....	1918, Mar. 29	17 29	13.248	+ 6.7	4	−0.6	
6744.....	1918, Mar. 15	19 30	13.628	+ 2.9	4	−1.1	

The velocity-curve was first drawn through all the observations with the aid of a preliminary period determined from a comparison of the times of recurrence of approximately equal velocities. Since the eccentricity was shown to be considerable, the method of Lehmann-Filhés was used for determining the approximate elements of the orbit, which were then slightly adjusted so as to make the residuals as small as possible. Plate 7772, which was very weak, and 6925, which was taken with the 7-inch camera, showed rather large differences and were omitted in the final solution and are not shown in the figure. A least-squares solution, with twenty-one equations of condition of the form given by Lehmann-Filhés and Schlesinger, was used for improving the approximate elements. The following corrections were found:

$$\delta P = +0.005 \text{ days}$$
$$\delta K = -0.26 \text{ km}$$
$$\delta\omega = -13^\circ.00$$
$$\delta e = +0.006$$
$$\delta T = -0.526 \text{ days}$$
$$\delta\gamma = +0.03 \text{ km}$$

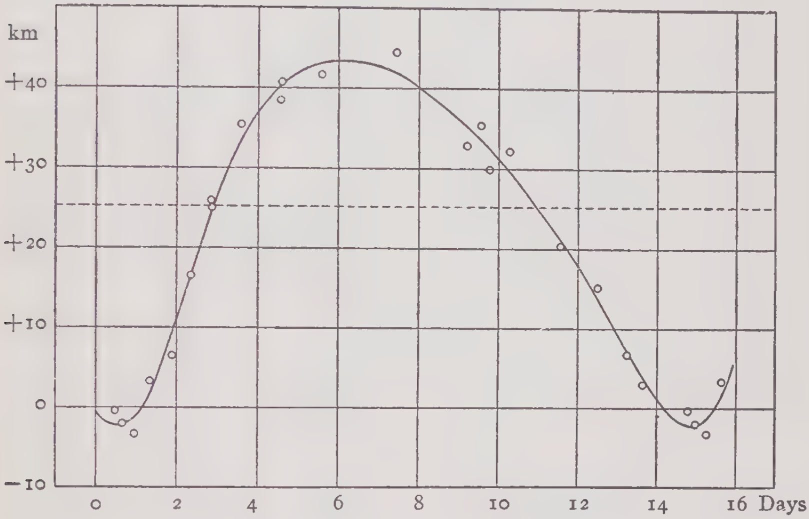

FIG. 1.—Velocity-curve of Boss 2285

After applying these corrections, we have for the final elements:

$P = 14.296 \pm 0.003$ days
$K = 22.74 \pm 1.20$ km
$\omega = 220^\circ.80 \pm 1^\circ.98$
$e = 0.276 \pm 0.021$
$T =$ J.D. $2421599.474 \pm 0.157 =$ 1918, Jan. 5, $11^h 22^m$ G.M.T.
$\gamma = +24.23 \pm 0.62$ km
$a \sin i = 4{,}300{,}000$ km
$\dfrac{m_1^3 \sin^3 i}{(m+m_1)^2} = 0.015 \odot$

The residuals O−C given in Table I were computed with these elements. The computed curve and the observed velocities are shown in Fig. 1.

MOUNT WILSON OBSERVATORY
April 1919

Contributions from the Mount Wilson Observatory, No. 173
Reprinted from the *Astrophysical Journal*, Vol. L, No. 5, pp. 356–75, 1919

ON THE BRIGHTNESS OF THE SKY AT NIGHT AND THE TOTAL AMOUNT OF STARLIGHT

By P. J. VAN RHIJN

1. INTRODUCTION

The following is an abstract of the results of an investigation which will appear in the "Papers from the Mount Wilson Observatory." It contains a discussion of observations of the brightness of the sky made at Mount Wilson during the summer and autumn of 1913. The main points investigated are the total amount of starlight per square degree for each galactic latitude and the distribution over the sphere of the illumination of the sky which is not due to the stars. The latter appears to vary with the latitude and longitude of the area observed; the evidence indicates that at least part of the light of the sky proceeds from a source probably identical with that of the zodiacal light.

2. THE OBSERVATIONS

The instrument used is that described by Yntema.[1] For details as to the method of measurement, reference may be made to the extended account of the investigation. Here it need only be remarked that the determination of the brightness of the sky has been made in two steps: (*a*) comparison of the light of various regions of the sky with that of an area at the North Pole; (*b*) comparison of the light at the pole with that of a star of known magnitude.

The first step has been made by varying the illumination of an annular screen in a measurable way until it disappeared against the background of the sky. The amount of light per square degree at the pole has been determined in terms of starlight by first comparing the surface brightness of the sky near the pole with that of an artificially illuminated disk of opal glass, and then estimating the stellar magnitude of the disk by observing it from a distance such that it had the appearance of a star.

---

[1] *Groningen Publications*, No. 22, pp. 9–11, 1909.

The small electric lamps used in the photometers were fed by a two-cell storage battery. The constancy of the current was carefully controlled. The only photometric principle used in the measurements is the law of inverse squares.

The areas measured were identified by means of a map showing all the stars visible to the naked eye. The time of observation was noted in all cases.

The observations made in series are as follows: (1) measures of the brightness at the North Pole, which was determined several times each night; (2) measures of areas on a circle parallel to the horizon; (3) measures on a circle perpendicular to the horizon.

3. GENERAL PLAN OF THE INVESTIGATION

The observations have been used to investigate the following questions: (*a*) Yntema found that the brightness of the sky is not due exclusively to the stars,[1] a result confirmed by the present data. What is the distribution of this additional light over the sphere and what is its cause? (*b*) Is it possible to eliminate the additional light and thus discuss the distribution of starlight alone?

The first of these questions may be answered by investigating the skylight for galactic latitudes higher than 40°. Above this limit the light due to the stars is a relatively small percentage of the total brightness and can be computed with sufficient accuracy from the counts of stars given in *Groningen Publications*, No. 27, Table V. We thus find for all stars fainter than magnitude 5.5 the results shown in Table I. These may be considered as the quantities of starlight actually measured with our photometer.

TABLE I

LIGHT PER SQUARE DEGREE OF ALL STARS FAINTER THAN MAG. 5.5

(Unit=a star of mag. 1.00, Harvard Visual Scale)

Gal. Lat.	Amount of Light
40°	0.012
50	.011
60	.009
70	.009
80	.008
90	0.008

---

[1] L. Yntema, *op. cit.*, p. 35.

Yntema found that the so-called earthlight, i.e., the brightness not due to the stars,[1] changes with the zenith distance of the area observed, but that it is approximately independent of the azimuth. I first investigated, by means of measures on a circle parallel to the horizon, whether the earthlight is really the same for all points on such a circle. Only those areas were used whose galactic latitudes exceed 40°. The earthlight was found by subtracting the direct and scattered starlight from the total brightness. The differences vary clearly with the azimuth, being always larger in the eastern part of the sky. It will be shown that these variations are caused by a kind of zodiacal light extending over the whole sky. The observed brightness corrected for starlight depends distinctly on the latitude and longitude relative to the sun. The excess of this zodiacal brightness over its mean value will be found for each latitude and longitude,[2] and a correction equal to this excess with opposite sign has been applied to all measures. The values of the earthlight thus corrected are independent of the azimuth; in any series of measures parallel to the horizon we can thus find the starlight for areas in the Milky Way by taking the difference between the total observed brightness and the corrected[3] value of the earthlight, the amount of which has been found from areas in higher galactic latitudes. This gives the solution of the second problem stated above.

I next considered the dependence of the corrected earthlight on the zenith distance by means of the series of measures in high galactic latitudes along circles perpendicular to the horizon. The values increase with increasing zenith distance. This is partly due to earthlight scattered by the atmosphere, the scattering being greatest near the horizon. The amount of scattered earthlight was found by means of Abbot's determination of the ratio of direct and scattered sunlight.[4] After subtraction of the scattered earthlight, the residuals, corrected for the absorption of the atmosphere, still increase toward the horizon. An empirical formula which represents these residuals was found and used to determine the earthlight for areas near the Galaxy. Subtraction of the values thus found from the observed brightness then gave the starlight in the lower galactic latitudes. This is another solution of the second question.

---

[1] The starlight scattered by the atmosphere is *not* contained in the earthlight. The determination of its amount will be described below.

[2] Longitude means always longitude relative to the sun.

[3] That is, corrected for the excess of zodiacal light over its mean value.

[4] *Astronomical Journal*, **28**, 130, 1914.

From the preceding lines it appears that I have based my conclusions as much as possible on a comparison of measures included in the *same* series of observations, which were always finished within one hour. This has been done in order to eliminate any variation of the earthlight with the time.[1]

4. CHANGE OF THE SKY-BRIGHTNESS NEAR THE NORTH POLE

The brightness at the North Pole has been measured repeatedly every night. Its value appears to be subject to large variations. Even during the same night the light near the pole may change as much as 20 per cent. These fluctuations are due to a variation of the earthlight. I have not, however, been able to find any systematic tendency in these variations. The mean brightness is practically the same before and after midnight, and the changes from one night to another are rather capricious.

5. DEPENDENCE OF THE EARTHLIGHT ON THE AZIMUTH. ZODIACAL LIGHT EXTENDING OVER THE WHOLE SKY

All series of observations parallel to the horizon have been treated in the way indicated in Table II, which serves only as an example.

The first six columns of Table II give the number, the galactic latitude (b), the latitude (β), the longitude relative to the sun (λ), the zenith distance (z), and the azimuth (A). The co-ordinates have been computed from the right ascension, the declination, and the time of observation. B denotes the observed amount of light per square degree expressed in terms of that of a star of magnitude 1.00 (Harvard Scale). The earthlight for areas whose galactic latitudes exceed 40° is given under the heading $B_{s',s}$. This has been formed by subtracting the direct starlight (s) and the scattered

---

[1] See section 4.

TABLE II

REDUCTION OF A SERIES OF OBSERVATIONS PARALLEL TO THE HORIZON

(Unit=a star of mag. 1.00, Harvard Visual Scale)

No. (1)	b (2)	β (3)	λ (4)	z (5)	A (6)	B (7)	$B_{s'}$ (8)	$B_{s',s}$ for $b>40°$ Uncorr. (9)	Corr.* (10)	$B_{s'}$ Corr.* $b<40°$ (11)	Corr. Zod. L. (12)	$B^z_{s',s}$ $b>40°$ (13)	$B^z_{s'}$ $b<40°$ (14)	Starlight $b<40°$ (15)
240....	North Pole	......	......	......	......	0.118	......	......	......	......	......	......	......	......
241....	+56°	+47°	+ 82°	56°	108°	.108	0.101	0.092	0.103	......	+0.004	0.107	......	......
242....	+53	+65	+ 54	53	137	.104	.097	.088	.097	......	+ .016	.113	......	......
243....	+49	+69	+ 42	53	144	.100	.093	.083	.091	......	+ .019	.110	......	......
244....	− 1	+47	− 84	57	214	.156	.149	......	......	0.168	+ .004	......	0.172	+0.061
245....	+ 5	+54	− 79	55	207	.132	.125	......	......	.140	+ .010	......	.150	+ .039
246....	+11	+58	− 72	54	199	.118	.111	......	......	.123	+ .012	......	.135	+ .024
247....	−12	+40	− 93	57	228	.140	.133	......	......	.150	+ .002	......	.152	+ .041
248....	−55	+ 5	−136	57	291	.122	.115	.106	.120	......	− .010	.110	......	......
249....	−61	− 2	−145	58	307	.128	.120	.112	.128	......	− .011	.117	......	......
250....	+25	+29	+122	55	72	.130	.123	......	......	.138	+ .001	......	.139	+ .028
251....	North Pole	......	......	......	......	.119	......	......	......	......	......		......	......
Mean..	......	......	......	......	......	......	......	......	......	......	......	0.111	......	......

* Corrected for atmospheric absorption to the zenith.

starlight (s') from the measured brightness B. As has been explained already, the direct starlight per square degree has been derived from counts of stars (see Table I). The scattered starlight has been computed by means of Abbot's observations already quoted.

For the same zenith distance the earthlight, in nearly all cases, is larger for areas near azimuth 270° than for those near azimuth 110°. This is also true of the series of Table II. The difference is to be explained by a dependence of the earthlight on the position of the measured area relative to the ecliptic. That this is really the case is shown in Table III, which contains the differences in the earthlight for the smallest and the largest latitudes occurring in each series, β_1 and β_2, respectively. Excepting one case, for which the difference in β is only 12°, the lower latitude corresponds always to a higher illumination.

TABLE III

DIFFERENCES IN EARTHLIGHT, SMALLEST AND LARGEST LATITUDES IN EACH SERIES PARALLEL TO THE HORIZON

β_1	β_2	Diff.	β_1	β_2	Diff.
22°	64°	+0.019	0°	70°	+0.032
21	69	+ .022	11	59	+ .041
27	69	+ .033	2	69	+ .037
58	70	− .005	9	67	+ .043
14	73	+ .025	2	23	+ .009
1	63	+0.037	7	19	+ .006
			10	63	+0.031

If now the brightness of the sky depends on the latitude, it is probably connected with the illumination usually called the zodiacal light, and must then also vary with the longitude relative to the sun. We have therefore to find the dependence of the earthlight on the latitude and longitude. It is impossible, however, to derive directly the absolute amount of the light which is related to the ecliptic and which for convenience will be called zodiacal light. For, as will be shown presently, it is very probable that the brightness of the sky is produced in part by other causes, whose contribution to the general illumination varies with the zenith distance in a manner which is unknown. We therefore derive, first of all, *not* the absolute amount of zodiacal light, but the excess of zodiacal light over its mean value for each latitude and longitude. This has been done on the supposition that the zodiacal light is the same north and south of the ecliptic; the sign of the longitude relative to the sun has also been disregarded.[1] The difference in the intensity of zodiacal light for various latitudes and longitudes can be found by subtracting any two values of the earthlight $B_{s',s}$ in the same series parallel to the horizon; for it can be shown that the variation of the earthlight with the azimuth is due to the zodiacal light alone. It follows, for instance, from the comparison of the mean $B_{s',s}$ for observations Nos. 241 to 243 with that for Nos. 248 and 249 that the zodiacal glow at $\beta=3°$, $\lambda=140°$, is $0.124-0.097=+0.027$ larger than at $\beta=60°$, $\lambda=59°$. By combining the differences thus found it is possible to compute for any latitude and longitude the excess of zodiacal light over a certain mean value.

The method used for the combination of the various differences has been described at length in the detailed investigation. It need only be stated here that the values of the excess of zodiacal light over its mean value were distributed among four groups having latitudes near $\beta=0°$, 20°, 55°, and 70°, respectively. A small correction was applied in order to reduce the figures to the exact values of these latitudes. The corrected light intensities were then plotted as a function of the longitude. Finally, in order to find the absolute amount of zodiacal light, the values of the excess were increased by +0.069. The quantity +0.069, to be derived in a later section, is somewhat hypothetical and the absolute values are less trustworthy than their differences for any two values of the latitude and longitude.

The graphically interpolated values of the zodiacal light thus found are given in Table IV. It may be remarked that Fessenhoff's[2] observations have been used for the smaller longitudes near the ecliptic and that in my measures special attention has been given to the brightness of the counterglow at $\beta=0°$, $\lambda=180°$.

---

[1] The longitude relative to the sun has been counted from 0° to +180° and 0° to −180°; the longitude of the sun itself is, of course, zero.

[2] *La Lumière Zodiacale.* Thèse de doctorat, 1914.

We have now to derive an interpolation formula for the zodiacal light as a function of the latitude and the longitude. This formula will be used mainly to compute the excess of zodiacal light at any point (β, λ) over the mean value. After the application of this excess with the reversed sign to the observed brightness the quantity of zodiacal light is the same for all areas.

TABLE IV

VALUES OF THE ZODIACAL LIGHT

(Unit=a star of mag. 1.00, Harvard Visual Scale)

Lat.	Long. from Sun	Zodiacal Light	Wt.	O−C	Lat.	Long. from Sun	Zodiacal Light	Wt.	O−C
0°......	40°	0.329	1^5	+0.007	20°....	40°	0.183	1^5	−0.016
0	60	.184	1^5	− .001	20	70	.125	1^5	+ .012
0	70	.149	2	− .001	20	100	.081	7	.000
0	80	.127	5	.000	20	130	.069	9	− .002
0	100	.098	12	+ .001	20	160	.072	12	− .001
0	130	.084	11	+ .005	55	40	.069	5	+ .007
0	160	.083	13	+ .001	55	100	.058	10	+ .004
0	170	.083	15	− .005	70	40	.047	7	− .004
0	180	0.097	4	+0.001	70	100	0.047	3	−0.002

It is, of course, desirable to use a formula which has a physical basis. We shall, therefore, try the function resulting from Seeliger's theory of the zodiacal glow,[1] which supposes the zodiacal light to be due to a reflection of sunlight by small particles of meteoric matter. The cloud of particles is symmetrical relatively to a plane which contains the axis of the zodiacal light and extends equally far in all directions in this plane. Seeliger found that on this hypothesis the intensity of zodiacal light depends in the following way on the density D of the meteoric matter and the law of phases $f(\alpha)$:

$$\frac{H}{J}=\frac{C}{\sin\psi}\int_{\tau}^{\psi} D(x,y)\, f(\alpha)d\alpha \tag{1}$$

---

[1] "Ueber kosmische Staubmassen und das Zodiacallicht," *Sitzungsberichte der math. phys. Classe der kgl. bayer. Akademie der Wissenschaften*, 31, Heft 3, 1901.

where

H = surface brightness of the zodiacal light
J = surface brightness of the sun
α = angle at the reflecting particle formed by the lines toward the sun and the earth. (See Fig. 1, where S represents the sun, O the observer, P a reflecting particle, and the plane SOP' the ecliptic. PP' is perpendicular to this plane)
ψ = Angle SOQ in Fig. 1 = supplement of the angle at the observer between the lines toward the sun and the particle
τ = value of α at the exterior limit of the cloud
x and y = co-ordinates of the particle relative to the sun in a plane perpendicular to the ecliptic
$D(x, y)$ = density of the cloud as a function of the co-ordinates x and y
$f(\alpha)$ = function representing the dependence of the quantity of reflected light on the phase angle α
C = a constant

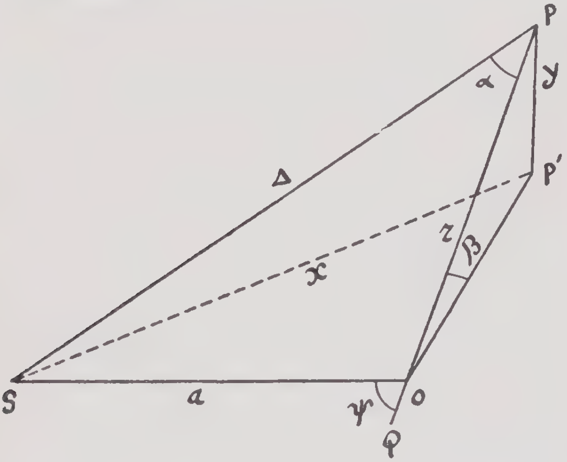

Fig. 1

If the function $f(\alpha)$ were known from terrestrial experiments, we might find the distribution of the density D by means of equations of the form (1), where the left-hand member is the observed quantity. This, however, is not the case; various laws have been proposed,[1] but it is at present impossible to decide which of these is the right one.

Our observations, however, afford the material for a determination of the law of phases for small values of α, for in the neighborhood of the counterglow the variation of the zodiacal light with the position of the area depends almost exclusively on the law of phases, whereas the adopted density distribution is of little importance. This is clear a priori and has, moreover, been demonstrated by Searle.[2] The law of phases for small values of α can, therefore, be determined from the observed brightness of the zodiacal light near the counterglow. After some trials I found the fractions given in the third column of Table V. For large values of α the law of phases was made to agree approximately with the form of Lommel and Seeliger.[3] Table V shows that my data yield a larger decrease of the brightness with the phase angle for small values of α than does Seeliger's formula. This is in agreement with the investigations made on the asteroids.[4] The adopted values of $f(\alpha)$ in the third column of Table V can be represented by the formula:

$$f(\alpha)=+0.655-0.711\sin\alpha+0.345\cos\alpha+0.406\sin^2\alpha \qquad (2)$$

TABLE V

THE LAW OF PHASES

α	Lommel and Seeliger	Adopted	α	Lommel and Seeliger	Adopted
0°......	1.00	1.00	70°.....	0.54	0.46
10	.98	.88	90	.38	.35
20	.93	.78	110	.24	.23
30	.86	.70	130	.12	.13
50	0.70	0.57	140*.....	0.08	0.10

* Phase angles larger than 140° do not occur in the present investigation.

---

[1] Müller, *Die Photometrie der Gestirne*, pp. 58–62, 1897. See also Otto Frh. v.u.z. Aufsess, "Experimentelle Untersuchungen über den Einfluss der Phase und der Rotation auf die Helligkeit von Kugeln und beliebig gestaltenen Körpern," *Astronomische Abhandlungen als Ergänzungshefte zu den Astronomischen Nachrichten*, No. 17, 1910.

[2] *Harvard Annals*, **19**, 233, 1893.

[3] Müller, *op. cit.*, p. 62.

[4] *Ibid.*, p. 378.

Various formulae have been tried for the density, which is to be determined from the condition that the zodiacal brightness, computed by means of (1), should agree with the observations. I first considered only the measures in the ecliptic for various longitudes, but later the higher latitudes were also taken into account. It was found that the formula

$$\text{Density} = D_0(1 - 0.176\, x^2 - 1.406\, y^2) \tag{3}$$

satisfies the observations.

The brightness computed by means of formulae (1), (2), and (3) has been compared with the observed values in Table IV. The residuals O − C are all small. These considerations show that the present material at least does not contradict Seeliger's theory of the zodiacal light, although our lack of knowledge of the law of phases makes it impossible to put the theory to a severe test.

Formulae (1), (2), and (3), however, have been derived mainly for another purpose, viz., the computation of the zodiacal light at points of the sky for which no direct observations are available. The results of this computation have been given in Table VI, which represents the total amount of zodiacal light for different values of the latitude and longitude relative to the sun. It will be remembered that the values on which the table is based have been derived by increasing the excess of zodiacal light over a certain mean value by +0.069, and that this latter figure is somewhat uncertain on account of the hypothesis underlying its derivation. The same holds for the data of Table VI, the difference between any two values of the zodiacal light being more trustworthy than the values themselves. Fortunately it is the differences, in the main, which are needed for the reduction.

6. DETERMINATION OF THE STARLIGHT FOR GALACTIC LATITUDES LESS THAN 40° FROM THE OBSERVATIONS ALONG CIRCLES PARALLEL TO THE HORIZON

The method used to determine the starlight from series of measures parallel to the horizon is also illustrated by Table II. The first ten columns have already been explained. In the twelfth column is given a correction for the excess of zodiacal light over a certain mean value. This has been derived by subtracting 0.069 from the figures of Table VI and reversing the sign of the difference

TABLE VI

Computed Values of the Zodiacal Light

(Unit=a star of mag. 1.00, Harvard Visual Scale)

Long. from Sun	Latitude (β)									
	0°	10°	20°	30°	40°	50°	60°	70°	80°	90°
0°	......	......	......	......	0.112	0.077	0.060	0.050	0.046	0.045
10	......	......	......	......	.110	.076	.060	.050	.046	.045
20	......	......	......	......	.103	.076	.060	.050	.046	.045
30	......	......	......	......	.097	.073	.059	.049	.046	.045
40	0.325	0.258	0.191	0.132	.090	.072	.059	.049	.046	.045
50	.247	.206	.161	.113	.086	.071	.058	.049	.046	.045
60	.184	.168	.138	.105	.084	.069	.057	.049	.046	.045
70	.149	.139	.119	.097	.079	.066	.055	.049	.046	.045
80	.127	.119	.103	.087	.073	.063	.053	.048	.046	.045
90	.109	.102	.090	.079	.068	.061	.053	.047	.046	.045
100	.098	.090	.081	.075	.065	.060	.052	.047	.046	.045
110	.090	.084	.076	.071	.064	.059	.052	.047	.046	.045
120	.086	.080	.073	.068	.061	.057	.052	.047	.046	.045
130	.082	.077	.070	.066	.060	.057	.052	.047	.046	.045
140	.081	.078	.070	.066	.060	.056	.051	.047	.046	.045
150	.081	.078	.071	.066	.060	.056	.051	.046	.045	.045
160	.082	.079	.072	.066	.060	.056	.051	.046	.045	.045
170	.085	.082	.074	.067	.060	.056	.050	.046	.045	.045
180	0.097	0.090	0.075	0.067	0.060	0.055	0.050	0.046	0.045	0.045

thus found. These corrections *a* have been applied to the figures of the tenth and eleventh columns, thus giving the results in the thirteenth and fourteenth columns, respectively. The areas in small and large galactic latitudes have been treated separately, because for the former the amount of the starlight is unknown.

The thirteenth column thus contains the observed brightness corrected for direct starlight (s), scattered starlight (s'), and excess of zodiacal light (z), whereas the figures in the fourteenth column have been corrected for the last two quantities only. The values of $B^z_{s',s}$ and $B^z_{s'}$ include an amount of zodiacal light which is the same for all areas. The quantities $B^z_{s',s}$ appear to be independent of the azimuth. We therefore form their mean and subtract the result from each value of $B^z_{s'}$ in the fourteenth column for which the galactic latitude is less than 40°. The differences inserted in the fifteenth column represent the starlight per square degree, reduced for atmospheric absorption to the zenith.

Most of the series were treated in this way. In only a few cases was the number of observations in galactic latitudes greater than 40° too small to apply this method. In such cases I computed the mean value of $B^{z}_{s',s}$ from the measures whose galactic latitudes exceed 20°. The starlight between 20° and 40° required for the reduction of these cases was obtained from all other series parallel to the horizon which include a sufficiently large number of observations in the higher galactic latitudes. The results are averaged in Table VII, the probable errors being derived from the internal agreement of the observations.

TABLE VII

TOTAL LIGHT PER SQUARE DEGREE OF ALL STARS FAINTER THAN MAG. 5.5 DERIVED FROM SERIES PARALLEL TO THE HORIZON

(Unit=a star of mag. 1.00, Harvard Visual Scale)

Gal. Lat.		Starlight	Prob. Error
Limits	Mean		
0° to 9°.....	4°.2	0.068	±0.003
10 to 19	14.1	.042	.002
20 to 29	25.8	.032	.002
30 to 39	35.5	0.013	±0.002

7. DEPENDENCE OF THE EARTHLIGHT, CORRECTED FOR ZODIACAL GLOW, ON THE ZENITH DISTANCE. PROBABILITY OF A PERPETUAL AURORA

We pass to the consideration of the series of observations perpendicular to the horizon. The variation of the earthlight with the zenith distance will be investigated first. This can be done only for areas whose galactic latitudes exceed 40°, where the starlight is supposed to be known. An example of the method employed is given in Table VIII.

The first nine columns of Table VIII contain the same quantities as the corresponding columns in Table II. The tenth column

TABLE VIII

REDUCTION OF A SERIES OF OBSERVATIONS PERPENDICULAR TO THE HORIZON

No. (1)	b (2)	β (3)	λ (4)	z (5)	A (6)	B (7)	$B_{s'}$ (8)	$B_{s',s}$ $b>40°$ (9)	Corr.* Zod. L. (10)	$B^z_{s',s}$ $b>40°$ (11)	$B^z_{s'}$ $b<40°$ (12)	Corr. Sc.E.L. (13)	$B^{z,e}_{s',s}$ $b>40°$ (14)	$B^{z,e}_{s'}$ $b<40°$ (15)	STARLIGHT Uncorr. (16)	STARLIGHT Corr. (17)
194	+72°	+41°	+ 30°	73°	132°	0.158	0.147	0.141	−0.018	0.123	....	−0.041	0.082	....	....	....
195	+66	+46	+ 24	71	138	.139	.129	.122	− .012	.110	....	− .039	.071	....	....	....
196	+62	+56	+ 39	59	136	.133	.125	.117	+ .004	.121	....	− .028	.093	....	....	....
197	+55	+63	+ 49	51	137	.115	.108	.099	+ .013	.112	....	− .024	.088	....	....	....
198	+45	+70	+ 76	39	135	.115	.109	0.098	+ .020	0.118	....	− .020	0.098	....	....	....
199	+36	+71	+108	29	134	.115	.109	....	+ .022	....	0.131	− .018	....	0.113	0.020	0.020
200	+25	+70	+141	19	138	.124	.119	....	+ .022	....	.141	− .016	....	.125	.032	.032
201	+18	+68	+165	16	155	0.138	0.133	....	+0.022	....	0.155	−0.016	....	0.139	0.046	0.046

* This correction has been reduced to the zenith distance z for atmospheric absorption.

gives the correction for the excess of zodiacal light derived in the same way as in section 6. The corrected values in the eleventh column thus contain a constant quantity of zodiacal light, the scattered earthlight, and, in addition, any light of unknown origin. In the thirteenth column is given a correction for scattered earthlight, derived by means of Abbot's observations already referred to and the total amount of earthlight known from the present investigation. The fourteenth column, in which the scattered earthlight is subtracted from the data in the eleventh column, thus contains a quantity of zodiacal light constant over the whole sky and perhaps some light produced by unknown sources of illumination. In order to find whether there are such sources, I have investigated the variation of the values of $B^{z,e}_{s',s}$ with the zenith distance. The data are collected in Table IX; all measures similar to those of Table VIII, for which the galactic latitude exceeds 40°, have been used.

TABLE IX

MEAN BRIGHTNESS CORRECTED FOR STARLIGHT, EXCESS OF ZODIACAL LIGHT, AND SCATTERED EARTHLIGHT $\left(B^{z,e}_{s',s}\right)$ AS A FUNCTION OF THE ZENITH DISTANCE

Limits z	Mean z	$B^{z,e}_{s',s}$	Prob. Error	No.	Weight	$B^{z,e}_{s',s}$ in Zenith	Comp.
10° to 29°	24°	0.085	±0.004	8	1.6	0.087	0.087
30 to 39	36	.084	.003	11	2.2	.087	.089
40 to 49	45	.090	.003	14	1.4	.095	.092
50 to 59	54	.086	.003	20	2.0	.096	.096
60 to 69	64	.086	.003	21	2.1	.104	.103
70 to 77	73	0.077	±0.005	13	0.6	0.111	0.116

The seventh column of Table IX gives the values of $B^{z,e}_{s',s}$ corrected for atmospheric absorption. If these values included nothing but a constant quantity of zodiacal light for the whole sky, they would be independent of the zenith distance. Since they increase with increasing zenith distance, there must exist some other source of illumination whose intensity is greatest near the horizon. This conclusion is strengthened by the fact that Slipher has photographed the green auroral line in the spectrum of the background of the sky.[1] A study by Störmer of the auroras occurring in 1913 showed that they originated in a comparatively shallow layer at a great height above the earth,[1] whence we conclude that the sky light due to this source should vary directly as the thickness of the auroral layer in the direction of the line of sight, i.e., as the secant of the zenith distance. This holds only for zenith distances smaller than say 70°.

---

[1] *Popular Astronomy*, **25**, 274, 1916.

We may therefore write

$$B_{S',s}^{z,e}=a+p\ \sec z,$$

where a represents the constant quantity of zodiacal light and $p\ \sec z$ the auroral brightness. A least-squares solution of the data of Table IX gives

$$a=+0.076 \qquad p=+0.0113.$$

The values computed with these constants are given in the last column of Table IX.

Other solutions were also made, which allow for the deviation of the thickness of the auroral layer from the secant law. Taking these into consideration the final value is $a=+0.072$. This differs little from the value +0.069, adopted in section 5 in accordance with a provisional solution. It is to be noted that the constant quantity of zodiacal light thus determined, which is the remainder after applying the correction indicated in section 6 by α, has been computed on the hypothesis that the only source of light, except the zodiacal glow, is the aurora borealis, and that the illumination contributed by the aurora varies as the secant of the zenith distance.

8. DETERMINATION OF THE STARLIGHT FOR GALACTIC LATITUDES LESS THAN 40° FROM OBSERVATIONS ALONG CIRCLES PERPENDICULAR TO THE HORIZON

From the third column of Table IX it appears that the observed brightness corrected for starlight, excess of zodiacal light, and scattered earthlight is independent of the zenith distance down to $z=70°$. This fact has been used as follows to determine the starlight near the galaxy.

---

[1] *Astrophysical Journal*, **43**, 243, 1916.

The fifteenth column of Table VIII gives the observed brightness at low galactic latitudes, corrected for scattered starlight, excess of zodiacal light, and scattered earthlight,[1] and thus includes exactly the same sources of illumination as the values in the fourteenth column, plus the direct starlight. It has been stated already that the quantities in this column are independent of the zenith distance down to $z=70°$. In order to find the starlight at lower galactic latitudes, we therefore need only diminish the figures in the fifteenth column by the average value of the fourteenth column for $z<70°$. This has been done in the case of Table VIII. The values of the starlight inserted in the sixteenth column have been corrected for atmospheric absorption and appear in the seventeenth column.

All series of measures perpendicular to the horizon have been treated in this way, except that in a certain number of cases the mean value of $B^{z,e}_{s',s}$ has been computed from all areas whose galactic latitudes exceed 30°, or even 15°, because the series in question do not include a sufficient number of observations in galactic latitudes greater than 40° to afford a reliable result. The starlight for galactic latitudes 15° to 40° thus required for the derivation of the values of $B^{z,e}_{s',s}$ was found from the series perpendicular to the horizon which do contain a sufficient number of observations between 15° and 40° as well as above 40°. The results are given in Table X.

TABLE X

TOTAL LIGHT PER SQUARE DEGREE OF ALL STARS FAINTER THAN MAG. 5.5 DERIVED FROM THE SERIES OF OBSERVATIONS PERPENDICULAR TO THE HORIZON

(Unit=a star of mag. 1.00, Harvard Visual Scale)

Limits *b*	Mean *b*	Starlight	Prob. Error
0° to 9°.....	4°5	0.081	±0.003
10 to 19	14	.056	.002
20 to 29	24	.030	.001
30 to 39	35	0.016	±0.001

---

[1] The seventh column gives the observed brightness; in the eighth column this brightness has been corrected for scattered starlight; in the twelfth column the excess of zodiacal light has been subtracted, and in the fifteenth a correction for scattered earthlight has been applied.

9. FINAL RESULT FOR THE AMOUNT OF STARLIGHT AS A FUNCTION OF THE GALACTIC LATITUDE. COMPARISON WITH OTHER AUTHORITIES. TOTAL AMOUNT OF STARLIGHT OVER THE WHOLE SKY

Comparing Tables VII and X we see that the values of the starlight derived from the series parallel and perpendicular to the horizon agree pretty well. The difference between the two series of results for the region of the Milky Way is at least partially real, as is easily demonstrated by means of Eaton's observations[1] of the galactic light.

The results of Tables VII and X have been combined with equal weight in Table XI. The light of the stars brighter than magnitude 5.5, which is not included in my measures, has also been added. In addition Yntema's values[2] and those computed by means of the number of stars in *Groningen Publications*, No. 27, Table V, and *Groningen Publications*, No. 18, are also given. The agreement with Yntema's values is good; but the enormous difference between Yntema and myself, on the one hand, and *Groningen Publications*, No. 18, on the other, shows that the magnitude scale

TABLE XI

TOTAL AMOUNT OF STARLIGHT PER SQUARE DEGREE

(Unit=a star of mag. 1.00, Harvard Visual Scale)

Gal. Lat.	This Paper	Yntema	*Gron.*, 27	*Gron.*, 18
0°	0.080	0.088	0.055	0.186
10	.065	.055	.043	.118
20	.044	.033	.027	.055
30	.026	.024	.020	.032
40	.015	.020	.015	.022
50	.014	.018	.014	.018
60	.012	.015	.012	.015
70	.011	.013	.011	.013
80	.010	.013	.010	.012
90	0.010	0.012	0.010	0.012

---

[1] *Verhandelingen der Koninklyke Akademie van Wetenschappen te Amsterdam*, Eerste sectie, deel VIII, No. 3, 1903.

[2] *Groningen Publications*, No. 22, p. 31, 1909.

used for the latter is probably in error. The same conclusion was arrived at from other evidence in *Groningen Publications*, No. 27.

The total amount of light received from all the stars in both hemispheres as computed from the present material is equal to 1440 stars of magnitude $1^{m}.00$, Harvard Visual Scale.

10. ACCIDENTAL AND SYSTEMATIC ERRORS

The mean of two measures of the brightness of the sky, made by moving the lamp in opposite directions, may be considered as a single observation. Its probable error, computed from the differences between the values found for the same area, is found to be 0.7 per cent of the amount. This does not contain the uncertainty due to errors in the magnitude of the artificial star. Including these, the probable error of a complete measure is about 2 per cent of the amount.

It is practically certain that the relative brightness of different areas, as measured in the present paper, is free from systematic error. In addition I have taken all possible precautions to obtain the correct value for the absolute amount of light received from one square degree at the North Pole. Nevertheless my value differs considerably from that found by Newcomb and Burns, which is as follows:

TABLE XII

Values of the Extra Galactic Sky Brightness Found by Different Observers

Authority	Brightness per Square Degree
Newcomb, *Astrophysical Journal*, **14**, 297	0.029
Burns, *ibid.*, **16**, 166	0.050
Abbot, *Astronomical Journal*, **27**, 20	0.075
Yntema, *Groningen Publications*, No. 22	0.140
Van Rhijn, present paper	0.130

Burns does not give all the details necessary to check his method of measurement and reduction. I do not feel sure that his results are free from objection. He compares the brightness of the sky with the extra-focal image of a star of known magnitude, the sky being observed with one eye and the extra-focal image, as seen through the telescope, with the other. I do not think that accurate results can be expected if, as in this case, the sources of brightness compared are not in contact. The internal agreement of Burns's observations is, moreover, rather poor.[1] This method seems, therefore, inferior to that used in the present paper.

Abbot and Yntema used the same instrument and method as I myself have used. In view of the difficulties affecting all kinds of photometric measurements, further determinations of the absolute amount of the sky-brightness are very desirable. I have thought of various methods which may be used, and hope in the near future to give some of them a trial.

GRONINGEN ASTRONOMICAL LABORATORY
September 1919

---

[1] *Op. cit.*

Contributions from the Mount Wilson Observatory, No. 174
Reprinted from the *Astrophysical Journal*, Vol. LI, No. 1, pp. 13–22, 1920

THE CHARACTERISTICS OF ABSORPTION SPECTRA PRODUCED BY THE ELECTRIC FURNACE

By ARTHUR S. KING

ABSTRACT

Absorption spectra of metallic vapors, produced by the electric furnace.—By placing a short plug of graphite in the middle of a tube furnace, a continuous spectrum corresponding to the temperature of the plug was obtained as a background for a pure absorption spectrum due to the hot metallic vapor. *Barium, calcium, cobalt, iron, nickel,* and *titanium* were investigated. The furnace demonstrates, more clearly than is possible with the arc, the fact that lines of the same intensity in the emission spectrum may differ greatly in absorptive power. This variation was found to be closely related to the behavior of the lines at different furnace temperatures. The lines relatively strong at low temperature are strongest in the absorption spectrum, these lines often being faint in the arc. As the temperature of the plug rises, lines appear in absorption which are given faintly in emission at lower temperature. The result is that the relative intensities in absorption correspond with those in the emission spectrum several hundred degrees lower.

Mixed absorption and emission spectra of metallic vapors.—By placing the graphite plug beyond the middle of the furnace tube, mixed spectra were obtained; for whether the heated vapor emits or absorbs more light of a given wave-length depends on the relative temperatures of the plug and the vapor. Thus the lines of either the low temperature or the higher temperature could be obtained in emission or in absorption or suppressed at will. Striking effects were obtained with *calcium* and *iron.* By adjusting the background, the author secured on the same spectrogram the high-temperature lines in emission, the low-temperature lines in absorption, and intermediate lines suppressed. These experiments may help to *explain stellar spectra containing both bright and dark lines.* Experiments are also described in which the incandescent vapor in the tube, without a plug, gave an absorption spectrum consisting only of those lines which in the emission spectrum at lower temperature are self-reversed.

Kirchhoff's law; application to the absorption spectra of metallic vapors in the electric furnace.—This is briefly discussed.

In former experiments with the electric furnace the writer has occasionally made use of the column of vapor inclosed in a graphite tube to produce absorption spectra, the incandescent background being given by the terminal of a carbon arc burning outside the furnace chamber. In this way the pressure-shifts[1] of absorption lines and the phenomena of anomalous dispersion[2] have been observed.

---

[1] *Mt. Wilson Contr.*, No. 60; *Astrophysical Journal*, **35**, 183, 1912.

[2] *Mt. Wilson Contr.*, No. 79; *Astrophysical Journal*, **45**, 254, 1917.

In the work here described the furnace was made to supply its own continuous spectrum by placing in the middle of the tube, the heated portion of which was 20 cm long and 12.5 mm internal diameter, a short plug of graphite. The light from the plug passing through a metallic vapor filling the tube produces an absorption spectrum. The arrangement gives a close approach to black-body conditions, and is similar to that of Liveing and Dewar,[1] who studied the reversals of spectrum lines by passing a carbon rod into a carbon tube heated by an external arc.

1. *Relation of emissive and absorptive power.*—It was of special interest to see how the effects obtained may be interpreted as following from Kirchhoff's law, and also how the absorption spectrum compares with the emission spectrum of the furnace at the same temperature, obtained by simply removing the plug, thus leaving all conditions unchanged except the length of the column of vapor.

Kayser, discussing the application of Kirchhoff's law to absorbing vapors,[2] lays stress on the fact that lines in the same spectrum may differ in absorbing power, so that a given relation between the background and the absorbing vapor need not be expected to reverse all of the lines emitted by the latter. If for any given wave-length the emission of the plugged tube, practically that of a black body, be denoted by e, and that of a black body having the same temperature as the vapor in the tube by e', then the emissive power of the vapor will be $e'A$, where A is its absorption coefficient for the given wave-length. The total emission from the tube filled with vapor will then be

$$e+e'A-eA=e-(e-e')A.$$

If an absorption line is to appear, $(e-e')A$ must be above a minimum positive value, the darkness of the line increasing as this product becomes larger. Hence the emission of the vapor for the given wave-length must be less than that of the plug. If $e-e'$ becomes 0, only the continuous spectrum of the plug will appear, a condition frequently obtained in my experiments, usually by locating the plug in a cooler portion of the tube and thus reducing the value of e. The vapor may then absorb a given wave-length strongly and still no trace of the line will be seen, the large value of A being rendered ineffective by the zero value of the factor $e-e'$.

---

[1] *Proceedings of the Cambridge Philosophical Society*, **4**, 256, 1882.

[2] *Handbuch der Spectroscopie*, **2**, p. 53.

Assuming, however, a considerable difference in the emissive powers of the plug and the metallic vapor, the value of A determines whether a line will appear strong in absorption or be invisible as a result of A approaching 0. Kayser notes the well-known difference in reversibility of lines in the arc as evidence that the value of A is not the same for all lines. There is, however, a question as to whether the vapor producing a certain line is present in an appreciable quantity in the outer envelope of the arc, for the method of long and short lines shows that lines difficult to reverse are likely to be confined to the core. The furnace, on the other hand, supplies definite data. A photograph with no plug in the tube shows what lines are being emitted by the vapor. If under these conditions two of the lines are of about the same intensity, and if, when the plug is replaced, one of the lines appears strong in absorption and the other is weak or absent, a real difference in their absorptive powers is evident. Phenomena of this kind have regularly appeared in the absorption spectra to be described. There is a close connection between the absorptive effects and the class of a line as determined by the changes in its intensity at various furnace temperatures, and this relationship has been specially noted.

2. *Probable temperature differences.*—The difference of temperature between the graphite plug and the absorbing vapor is difficult to determine. Pyrometric measurements were made on a thin plug placed at intervals along the tube from near the open end to the middle. Close to the end, where the tube is cooled by the massive contact block, there is evidently a considerable drop in temperature, but for points more than 2.5 cm away from the block the temperature thus measured was surprisingly uniform. For a central temperature of 1800° C. the drop within this limit amounted to about 100°, but at 2400° the difference seemed to be not more than 25°. There is a question, however, as to how fully the inclosed vapor takes up the temperature of the wall of the tube, and as to

the influence, when the tube is very highly heated, of the rapid drop close to the end. There is also the consideration that if the radiation of metallic vapors in the furnace is due to temperature, the emission of a black body should be stronger than that of the vapor at the same temperature. This would give a virtual difference between e and e' at all times when the plug is in the hottest portion of the tube. Evidence in support of this latter point has been given in a previous paper,[1] in which it was noted that the continuous spectrum from a plugged tube extended at least 300 A farther into the ultra-violet than the spectrum of iron vapor when the tube was excited to the same temperature. In any case, the emissive power of the vapor is less than that of the plug and the term $e-e'$ will be greater than 0.

3. *General character of the absorption spectra.*—For the examination of absorption spectra several elements were selected whose emission spectra have previously been studied in detail with regard to temperature variations. These were iron, titanium, nickel, cobalt, calcium, and barium, the first two receiving the larger share of attention. It was evident at once that the absorption spectra differed greatly from those shown at the same temperature in emission. With titanium, no absorption lines showed at 2000°, though a large number of lines, listed in a former paper,[2] appeared at this temperature when there was no plug in the tube. When the temperature of the plugged tube was raised to 2400°, an absorption spectrum was brought out consisting of the same lines as are shown in emission at 2000°. These are the low-temperature lines, belonging to classes I and II, the difference between the classes being in the rate at which the lines strengthen with increasing temperature. Similar results with the other elements showed that the absorption spectrum corresponds with the emission spectrum at a temperature several hundred degrees lower. As a means of picking out low-temperature lines the absorption spectrum, obtained quickly at high temperature, is almost as reliable as the emission spectrum corresponding to the temperature at which the vapor begins to radiate and which often requires a

---

[1] *Mt. Wilson Contr.*, No. 66; *Astrophysical Journal*, **37**, 239, 1913.

[2] *Mt. Wilson Contr.*, No. 76; *Astrophysical Journal*, **39**, 139, 1914.

very long exposure to photograph. A different condition prevails in the ultra-violet, however, since in this region the emission spectrum ceases rather abruptly at a certain limit, depending on the temperature, while the easy reversal of ultra-violet lines causes a strong absorption spectrum which extends almost as far as the continuous ground given by the plug.

4. *Relation of absorptive power to temperature class.*—We may now take up the variation of *A* for different lines and its connection with the temperature classification. The difference in absorptive power of lines belonging to different temperature classes was very distinctly brought out. The strongest absorption lines are those of class I. The stronger lines of class II also show considerable intensity in absorption, but if two lines belonging respectively to classes I and II are of about the same intensity in emission (for example, λλ 4415 and 4427 of iron) that of class I will be stronger in absorption. Such lines of class III as appear faintly in emission at low temperatures can be obtained in absorption, but only with difficulty. For instance, in the iron spectrum at 2000°, λ 4260 (class III) is stronger in emission than λ 4258 (class I A), but in absorption, with the tube at the same temperature, λ 4258 becomes the stronger. Numerous other contrasting pairs of the same kind might be noted. The absorption spectrum of iron at 2000° is very similar in the blue and violet to the emission spectrum at 1650°, which is about the lower limit for the appearance of lines of class III. This results simply from the fact that at 1650° the lines of class I dominate the spectrum and, because of their higher absorptive power, they again dominate when a temperature stage is reached at which an absorption spectrum first appears. Lines of classes II and III, which are certainly being emitted by the vapor at this higher temperature, are deficient in absorbing power and either appear faintly or are quenched by the continuous spectrum. The same reasoning explains the absence in absorption, for the temperatures used in these experiments, of lines of classes IV and V and of all but the stronger lines of class III. On account of their relatively small absorbing power, a background of higher temperature would be required to show them in absorption.

It seems unnecessary to list the lines which have thus been obtained in absorption for iron and titanium, since they can at once be selected from the tables[1] of the furnace classification for these spectra. For lines of the same class the relative intensities in absorption are the same as for the furnace in emission, the differences between the two kinds of spectra showing a consistent connection with the class of the lines concerned.

The absorption spectrum of calcium is of interest on account of the variety of types of lines represented. λ 4227 may have great width, depending on the amount of vapor present. H and K are narrow absorption lines, strengthening with the temperature, with little dependence on vapor density. The other calcium lines appearing in absorption within the range λ 3500 to λ 5000 correspond in strength with their furnace classes; the strong lines as usual are of class I, some lines of class II show faintly, while the lines of class III, usually of diffuse structure, are absent. The spectra of the other elements photographed showed a repetition of the conditions noted.

The difference between the arc spectrum and that of the absorption furnace is accentuated by the fact that, in the latter, lines of class I A are very strong and those of class III are weak or absent. In the arc, the reverse condition holds, I A lines being very faint while those of class III are among the strongest. The fact that the strong lines of class III, which fade out at lower temperature, are difficult to produce in absorption is in harmony with the observation of Liveing and Dewar that "it is by no means always the strongest lines which are most easily reversed, but those which are both persistent and strong."

5. *Variation of absorption effects with wave-length.*—The iron spectrum, which was examined in absorption and emission from λ 3000 to λ 8200, furnishes an illustration of the change in the absorption spectrum with wave-length. A plug temperature of 2600° gave no iron lines in absorption beyond λ 5507. Iron lines of class I are few and relatively faint in the red. In the case of other elements, however, there is no difficulty in obtaining lines

---

[1] King, *Mt. Wilson Contr.*, Nos. 66, 76; *Astrophysical Journal*, **37**, 239, 1913; **39**, 139, 1914.

of high absorptive power in this region, the potassium pair λλ 7765–99, for example, appearing readily in absorption. In the yellow and green the iron lines of class I absorb strongly, and a few of class II faintly. The strong lines of class III near λ 4900 were absent in absorption, though they appear in emission at much lower temperatures. In the blue, besides a fairly complete spectrum of lines in classes I and II, a few of the strongest lines of class III appeared faintly in absorption. This condition extends into the ultra-violet, where in the emission furnace many lines reverse readily. As would be expected, their strength in absorption corresponds closely with the width of the self-reversal in emission. Presumably higher temperatures would bring out absorption lines of successively higher classes and show lines in the red which appear in emission at low and medium temperatures.

6. *Production of mixed absorption and emission spectra.*—By placing the graphite plug beyond the center of the tube away from the spectrograph, so that some of the metallic vapor is hotter than the plug, it is possible to obtain emission and absorption lines at the same time. The lines then showing in absorption are those of the low-temperature class. When the plug was not quite in the hottest portion of the tube, the pure absorption spectrum was replaced by one in which some of the lines, usually those of class II, appeared in emission on a continuous ground. Moving the plug to a still cooler portion caused a relative strengthening of the emission spectrum, and a position could be found such that the regular emission spectrum appeared, complete with the exception of the most easily absorbed lines of class I, which still appeared in absorption. Owing doubtless to the higher vaporization point of titanium, a mixture with iron showed the iron lines to be more easily absorbed. It is thus simply a matter of adjusting the intensity of the incandescent background to obtain in emission the higher temperature lines (including the enhanced lines when these are given by the furnace) while the low-temperature lines appear in absorption, a difference clearly due to the different absorbing power of lines belonging to different classes.

7. *Effects due to balancing of emission and absorption.*—I have experimented further in this way by placing the plug only 2 or 3 cm

from the farther end of the heated tube, thus causing its emission to be of about the same strength as that of the metallic vapor in the hottest portion. Some lines then appear in emission and others in absorption, according to their temperature class, while others, often among the strongest in the spectrum, are absent, being neutralized by the incipient absorption which they are undergoing. With calcium in the tube under these conditions, H and K appear in emission, and λ 4227 in absorption, with no trace of any other lines from λ 3500 to λ 5000. Some of the high-temperature lines are doubtless quenched by the continuous background on account of their weak emission by the vapor, but many strong low-temperature lines, such as the group of six near λ 4300 and the series triplet λλ 4425–55, disappear because they are beginning to reverse and are in the state where emission and absorption are nearly equal. With iron the effects were very striking. A condition was obtained such that the strongest lines in the blue region, λλ 4271.9, 4308, 4326, 4384, were invisible, while most lines of classes II and III, weaker than these, showed in emission and many of the easily absorbed lines of class I in absorption. The absent line λ 4384 is a member of a triplet of which the lines are always affected alike by changes in the source, but in this case its weaker companions λλ 4404 and 4415 show as emission lines. A change in the position of the plug evidently can be used to eliminate from the spectrum any set of lines having about the same absorbing power. In the case of stellar spectra, especially those containing both bright and dark lines, the principle here involved can hardly fail to be active in causing an apparent lack of certain lines whose absence is not easily explained by the temperature conditions of the star in question.

8. *Production of absorption spectra without the use of a plug.*—In connection with the results obtained with the plugged tube, a class of furnace spectra may be considered, numerous examples of which have been accumulated but which have been of no use in the regular comparison of spectra produced at various temperatures. These spectra appear when the temperature used is so high that the tube filled with vapor (without any plug) gives a strong continuous spectrum. This occurs with some vapors more

strongly than with others and is doubtless due in large measure to the long column of mixed metallic and carbon vapor, although probably the vapor particles reflecting light from the wall of the tube also contribute. The intensity of the continuous spectrum can be increased by operating the furnace at atmospheric pressure, but with high temperature it appears at the usual working pressure of a few millimeters, so that the well-known effect of high pressure in producing a continuous spectrum cannot be operative here. The presence of such a spectrum prevents any comparison of line-intensities with those corresponding to lower temperatures, for which the continuous background is less in evidence. For usable spectrograms, the continuous spectrum must be kept down, so that no faint lines may be quenched by it, and so that when lines reverse we have the normal self-reversal. Any increase in temperature which is accompanied by strong continuous emission brings about a radical change and a more or less complete transition to the absorption spectrum obtained with a plug at the center of the tube. The absorption lines are those of the low-temperature emission spectrum, and, at the highest stage used for temperature comparisons, are for the most part self-reversed. The lines of higher classes and low absorbing power are blotted out by the continuous ground. The result is that at a very high temperature only low-temperature lines are visible, though at a lower stage, before the continuous emission sets in, a spectrum of richness comparable with the arc is seen. The transition between the two is equivalent to an obliteration of the whole emission spectrum; what were formerly the centers of reversals then remain as absorption lines.

SUMMARY

1. By using a furnace tube obstructed by a graphite plug in its hottest portion, pure absorption spectra have been obtained.

2. The types of lines which in an absorption spectrum under given conditions may be expected to be the strongest have been identified. They are not necessarily those which are strongest in the emission spectrum. Instead, the selection is determined by the temperature class, low-temperature lines being most strongly absorbed, with successively higher classes appearing in absorption

as the temperature of the source of the continuous background rises. As a result, the absorption at each stage of temperature corresponds closely with the emission spectrum several hundred degrees lower.

3. Lines of the same temperature class follow the recognized rule for reversed lines, the lines of shorter wave-length appearing more readily in absorption.

4. When the plug is in a cooler portion of the tube, the spectrum consists of both bright and dark lines according to their temperature class; strong lines are then often neutralized through a balancing of emission and absorption.

5. Absorption spectra similar to those given by a plugged tube may be produced without a plug if the furnace contains vapor at very high temperature. The lines then showing are of the low-temperature classes, whose absorptive power is high, while those of smaller absorptive power are obliterated.

6. The phenomena studied in these experiments are those likely to appear when an extended mass of vapor containing temperature gradients is under examination. It is believed that their main characteristics may account for many conditions of line-intensity observed for such masses of vapor.

Mount Wilson Observatory
November 1919

Contributions from the Mount Wilson Observatory, No. 175
Reprinted from the *Astrophysical Journal*, Vol. LI, No. 1, pp. 49–61, 1920

STUDIES BASED ON THE COLORS AND MAGNITUDES IN STELLAR CLUSTERS

FIFTEENTH PAPER: A PHOTOMETRIC ANALYSIS OF THE GLOBULAR SYSTEM MESSIER 68

By HARLOW SHAPLEY

ABSTRACT

Globular star cluster Messier 68.—The paper contains the results of a characteristic *photometric analysis* of this hitherto unexplored typical cluster, based on fifteen photographs made at the primary focus of the 60-inch reflector. Twenty-eight *variable stars* were discovered, all but one of which appear to be typical, short-period, cluster variables. This cluster is poorer in *giant stars* than some others, as only 250 are brighter than the absolute magnitude zero. The magnitudes and colors of 56 of the brightest of these are tabulated. Most of them are red or yellow. The *distance* of the cluster as computed by three methods which give concordant results is about 55,000 light-years. The *form* is quite accurately circular as far as the two thousand brightest stars are concerned.

Stellar clusters.—Further evidence in support of the following general conclusions is supplied by the analysis of M 68: (1) Cluster type *variables* are bluer at maximum than at minimum brightness. (2) Their mean brightness appears to be an astrophysical constant which is a little more than one magnitude fainter than the mean brightness of the 25 brightest stars of the cluster. (3) The fainter the *giant star*, the bluer is its color, on the average. (4) The brightest giant stars are always very red and have absolute photo-visual magnitudes between −4 and −3. (5) The general *luminosity curve* for the stars of the cluster differs widely from a symmetrical probability curve. (6) The *distance* of such clusters can be computed from the diameter of the image of the cluster, or from the mean magnitude of the 25 brightest stars, or from the mean magnitude of the short-period variables.

The present paper reports on a characteristic photometric analysis of a typical globular cluster. The intention of the report, in addition to presenting explicit results that come out of the study of Messier 68, is to examine numerically some of the working hypotheses at the basis of earlier work on clusters,[1] and also to illustrate what astrophysical information can be derived from an inextensive survey of one of the globular systems. There is a considerable number of clusters no fainter than Messier 68 concerning whose structure little is now known.

---

[1] For example, that relating to the general applicability of the adopted methods of determining parallax; cf. section 5 on page 8.

1. *Earlier results.*—The position of Messier 68 = N.G.C. 4590 for 1900 is:

Right ascension $= 12^{h}34^{m}.2$ Declination $= -26^{\circ}12'$
Galactic longitude $= 268^{\circ}$ Galactic latitude $= +36^{\circ}.6$

There are no early measures of magnitude for the individual stars, aside from roughly estimated limiting values by Bailey,[1] and no variable stars had been reported prior to this study. Holetschek's[2] integrated visual magnitude of the cluster is 8.2. The diameter estimated from the Franklin-Adams chart, $5'.3$, has led, in *Mount Wilson Contribution* No. 152, to the parallax

$$\pi = 0''.000062, \qquad (1)$$

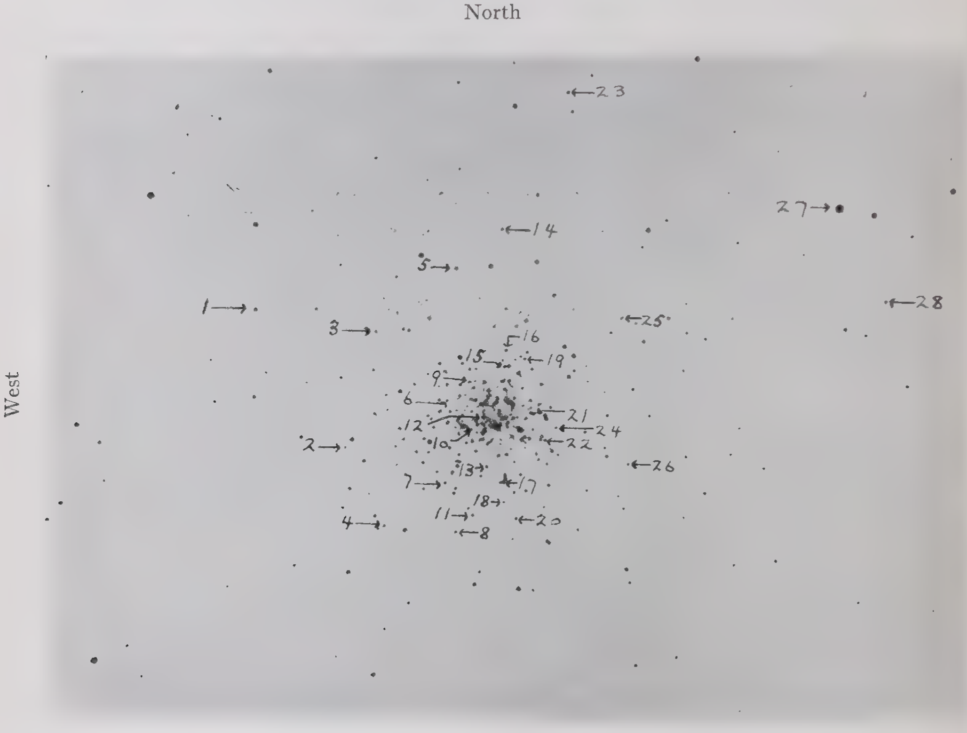

The Variable Stars in Messier 68

---

[1] *Harvard Annals*, **60**, 212, 1908; **76**, 46, 1915.

[2] *Annalen der k.k. Universitäts Sternwarte in Wien*, **20**, 114, 1907.

to which correspond the linear galactic co-ordinates, in units of 100 parsecs,

$$\begin{aligned} R &= 161 \\ R\cos\beta &= 129 \\ R\sin\beta &= +97 \end{aligned}$$

2. *Mount Wilson photographs.*—The observations in Table I have all been made at the primary focus of the 60-inch reflector. The remarks in the last column show to what use the various plates have been put. Although the southern declination of this cluster greatly limits the working season with the 60-inch reflector and is also unfavorable to high accuracy in the comparison with polar standards, the plates are of good quality and the results appear to be trustworthy.

TABLE I

PHOTOGRAPHS OF MESSIER 68 (N.G.C. 4590)

Plate Number	Date G.M.T.	Kind of Plate	Exposure Time	Remarks
4501*.....	1918, July 3.68	S 27	5^m, 5^m, 1^m	Variables
4842......	1919, Feb. 24.91	S 27	15	Variables
4843*.....	1919, Feb. 24.92	S 27	1 1 1	Photographic magnitudes, variables
4844*.....	1919, Feb. 24.93	Iso + C	5 5 5	
4845*.....	1919, Feb. 24.95	S 27	1 1 1 1^m	
4855*.....	1919, Feb. 25.92	Iso + C	5 1 5	Photo-visual magnitudes
4856*.....	1919, Feb. 25.92	S 27	2 2 2	Photographic magnitudes, variables
4857*.....	1919, Feb. 25.93	S 27	10 10 2	Variables
4858*.....	1919, Feb. 25.94	Iso + C	15 15 2	Photo-visual magnitudes, variables
4859*.....	1919, Feb. 25.95	S 27	1 1 1	Photographic magnitudes, variables
4863......	1919, Feb. 27.88	S 27	12	Variables, luminosity-curve
4864......	1919, Feb. 27.90	S 27	35	Variables, chart
4911......	1919, May 24.68	S 30	20	Variables
4924......	1919, May 25.670	S 30	50	Variables, positions, ellipticity, luminosity-curve
4935......	1919, May 26.68	S 30	20	Variables

* Plates with multiple exposures are polar comparisons.

3. *Variable stars.*—By comparing the various plates in a stereocomparator, Miss Ritchie has found that the 28 stars listed in Table II undergo appreciable variation in light. The x and y co-ordinates in the second and third columns give the intervals of right ascension and of declination from the center; x is positive east, and y is positive north of the cluster. The positions are believed to be sufficiently accurate for identification. On the accompanying reproduction of Plate 4864 the variable stars are indicated by arrowheads.

The magnitudes have been determined as usual through the intermediary of polar comparison plates and by the measurement of some twenty comparison stars on all photographs listed in Table II. The last column of the table shows the differences between the photo-visual magnitude on Plate 4858 and the mean of the photographic magnitudes on Plates 4857 and 4859; these values of the variable color-index apply, of course, only to one phase of the light variation of each star. The bluish color for all but No. 27 indicates that the variables are of the usual cluster type. The observed ranges of light-variation and the similarity of the median magnitudes also support this view, although neither range nor median brightness is definitively determined.

A comparison of the magnitudes for any variable in Table II with the corresponding dates of observation in Table I shows that probably all except No. 27 have periods of less than a day. It appears reasonable to assume that these 27 stars belong to one or more of the sub-types[1] of Cepheid variables whose absolute photographic median magnitudes are approximately −0.2 (*Mount Wilson Contribution* No. 151, p. 27).

The apparent photographic median magnitude cannot be derived with certainty for a given variable because of insufficient observations to determine the light-curve completely. The tabulated medians vary from 15.65 to 16.21; the average median is 15.90± 0.10 (average deviation). Considering that all observations refer to a typical star, however, we derive the following fairly reliable mean value for the 27 variables:

$$\text{Median} = 15^{\text{M}}.90 \pm 0.02 \text{ (p.e.)}. \qquad (2)$$

As a further check of this value, the median of the means for the ten brightest and for the fifteen faintest[2] magnitudes in Table II is

$$(16.42 + 15.33)/2 = 15^{\text{M}}.88.$$

---

[1] On the basis of the observed range and the relative number of bright and faint magnitudes, we infer that the variables numbered 4, 6, 8, 13, and 28 may belong to Bailey's sub-class *c*, for which the characteristics are very short period, small amplitude of variation, and light-curves practically symmetrical.

[2] For the average cluster-type star the duration of "brighter than median" is to the duration of "fainter than median" approximately as two to three.

TABLE II

Positions and Observations of 28 New Variable Stars in Messier 68

Variable	Position		Magnitudes on Photographic Plates										Observed Range	Median Magnitude	Provisional Color-Index
	x	*y*	4842	4843	4856	4857	4859	4863	4864	4911	4924	4935			
1.....	−4′40″	+1′49″	15.99	....	16.03	15.88	....	15.43	15.28	15.65	15.66	15.52	0.75	15.66	+0.07:
2.....	−2 48	−0 45	16.39	....	16.24	16.02	16.11:	16.18	16.16	15.69	16.08	16.28	0.70	16.04	+0.34
3.....	−2 20	+1 31	16.34	....	15.96	15.79	16.09:	15.76	15.54	15.93	15.93	15.86	0.80	15.94	+0.46
4.....	−1 57	−2 11	15.93	....	16.02	15.79	15.77	15.84	15.65	15.98	15.56	16.01	0.46	15.79	+0.21
5.....	−0 56	+2 50	16.14	....	15.85	15.76	15.90	15.02	15.51	15.69	15.77	15.91	0.63	15.82	+0.21
6.....	−0 54	+0 17	15.90	15.74	16.00	15.64	15.71	15.73	15.77	15.65	15.93	16.03	0.39	15.84	+0.25
7.....	−0 50	−1 19	15.85	....	15.87	15.56	15.65	15.78	15.48	15.65	16.16	15.94	0.68	15.82	+0.26
8.....	−0 38	−2 14	16.12	....	16.03	15.79	16.00	15.84	15.82	15.69	16.14	15.74	0.45	15.92	+0.43
9.....	−0 31	+0 40	16.12	15.72	16.07	16.10	....	15.88	15.89	15.90	15.43	16.28	0.85	15.86	+0.40
10.....	−0 25	−0 16	16.62:	15.02	15.93	16.20	15.84	16.21	15.28:	16.15	16.20	15.60	0.61	15.90	+0.47
11.....	−0 18	−1 52	15.93	....	16.11	16.06	16.02	15.60	15.31	15.53	15.87	15.97	0.80	15.71	+0.33
12.....	−0 10	−0 1	16.23	15.70	15.75	15.64	15.07	15.56	16.08	16.01	15.85	16.14	1.16	15.65	+0.27
13.....	−0 6	−0 56	15.90	....	16.28	16.20	16.07	15.62	15.77	15.74	15.66	16.22	0.66	15.95	+0.24:
14.....	−0 4	+3 38	15.55	15.56	16.29	16.10	....	15.16	15.92	15.98	15.82	15.50	0.79	15.90	+0.29:
15.....	+0 9	+0 58	16.14	....	15.89	15.69	15.65	15.76	16.08	16.36	16.08	15.78	0.71	16.00	+0.21
16.....	+0 11	+1 20	16.12	15.90	15.89	15.74	15.71	15.73	15.95	16.43	16.16	15.86	0.72	16.07	+0.17
17.....	+0 16	−1 15	16.60:	....	15.76	15.95	15.65	15.78	16.16	16.56	16.04	16.39	0.91	16.10	+0.50
18.....	+0 19	−1 36	16.28	15.90	16.05	15.97	16.02	16.15	16.16	15.72	15.59	16.22	0.69	15.94	+0.29
19.....	+0 33	+1 10	16.21	15.94	15.89	15.74	15.74	15.82	15.98	15.65	16.11	15.84	0.56	15.93	+0.24
20.....	+0 34	−1 54	15.82	15.74	16.02	15.81	15.93	15.80	15.45	15.78	15.59	16.01	0.57	15.74	+0.45
21.....	+0 48	+0 8	16.60	15.92	16.05	16.20	16.00	15.82	16.19	16.26	16.16	16.35	0.78	16.21	+0.57
22.....	+1 1	−0 22	16.52	15.92	16.42	16.32	16.07	15.78	16.14	16.41	16.04	15.30	1.22	15.91	+0.46
23.....	+1 4	+6 20	16.34	....	16.00	15.88	....	15.76	15.85	15.78	15.08	16.16	1.26	15.71	+0.22
24.....	+1 14	−0 8	15.90	15.86	16.09	16.10	16.00	16.11	16.01	16.34	16.00	15.74	0.60	16.04	+0.26
25.....	+2 21	+2 3	15.93	15.77	16.07	16.10	....	16.21	16.19	15.90	16.00	15.99	0.44	15.99	+0.39
26.....	+2 38	−0 44	15.68	15.67	16.11	16.10	....	16.11	15.89	16.09	16.35	15.72	0.68	16.01	+0.39
27.....	+6 20	+4 23	....	11.62	....	....	11.36	10.88	....	14.89	15.04	14.94	4.0±	13.0±	+2.0±
28.....	+7 20	+2 40	15.93	15.74	16.14	16.04	....	15.67	15.62	16.04	15.66	15.97	0.52	15.88	+0.76
Means*..............													0.72	15.90	+0.34

---

* Excluding No. 27.

Arranging the color-indices of Table II in order of the corresponding photographic magnitudes, we make the following tabulation, showing the anticipated increase of color-index with decreasing brightness, which is typical of this kind of variation (cf. Figs. 3, 4, and 5 of *Mount Wilson Contribution* No. 154).

Mean Pg. Magnitude	Number of Variables	Mean Color-Index
15.61	5	$+0^{\mathrm{M}}.23$
15.80	5	0.32
15.91	5	0.29
16.05	6	0.41
16.12	6	+0.41

4. *Relation of absolute magnitude to color-index.*—From the polar comparison plates the magnitudes have been determined both for a series of selected comparison stars, to be used in studying the variables, and for a complete list of all the brighter stars (outside the central nucleus but within $3'.5$ of the center), to be used in determining the parallax of the cluster and the upper limits of luminosity. Table III contains the positions, magnitudes, and colors of these stars. By accepting the value of the parallax adopted in a following section, the apparent photographic and photo-visual magnitudes may be transformed into absolute values by subtracting 16.15 from the magnitudes given in Table III. It is then seen that these stars are all giants, most of them red and yellow, but a few of the fainter ones blue.

The interdependence of color and magnitude among the giant stars is illustrated by Table IV and Fig. 1. The usual color law for giant stars in clusters, already found in several systems,[1] holds also in this case; that is, the fainter the giant, the bluer is the color, and, if the star is a Cepheid variable, the shorter is its period. The last group of Table IV (not plotted in Fig. 1) contains 27 variables; the next to the last group contains 3 stars, and the preceding groups contain 5 stars each. The variables agree perfectly with invariable stars in the relation of median color to absolute luminosity.

---

[1] *Mt. Wilson Communications*, No. 34, 1916.

TABLE III

MAGNITUDES AND COLORS OF 56 STARS IN MESSIER 68

STAR	POSITION		MAGNITUDE		COLOR-INDEX	STAR	POSITION		MAGNITUDE		COLOR-INDEX
	x	y	Photographic	Photovisual			x	y	Photographic	Photovisual	
101†	−7′ 25″	−5′ 9″	12.06	11.06	+1.00	129*†	+0′ 15″	+0′ 58″	15.07	14.16	+0.91
102†	−2 48	−1 53	15.97	15.53	+0.44	130*	+0 16	+0 43	14.85	13.98	+0.87
103	−2 39	−1 32	15.33	14.60	+0.73	131*	+0 18	−1 10	14.92	14.02	+0.90
104*	−2 39	−0 35	14.35	13.12	+1.23	132*	+0 22	+0 19	14.32	12.93	+1.39
105*	−2 26	−0 57	15.06	14.16	+0.90	133*	+0 26	+0 54	14.76	13.80	+0.96
106†	−2 16	−0 4	15.92	15.20	+0.72	134†	+0 28	−1 24	16.01	15.30	+0.71
107	−2 8	−2 2	15.60	14.56	+1.04	135*	+0 32	+2 24	15.02	14.18	+0.84
108†	−2 3	+0 2	16.18	>16.0	<+0.2	136†	+0 36	+4 19	15.80	15.15	+0.65
109†	−2 2	+2 36	15.92	15.34	+0.58	137*	+0 39	+3 2	15.06	14.41	+0.65
110*	−1 49	+0 24	14.75	13.69	+1.06	138†	+0 54	+0 42	15.62	14.58	+1.04
111	−1 46	−0 20	15.84	15.11	+0.73	139*	+0 58	+0 8	14.81	13.98	+0.83
112†	−1 41	+1 37	15.44	14.53	+0.91	140	+1 2	+2 24	15.58	14.99	+0.59
113	−1 34	+3 2	13.98	12.42	+1.56	141*	+1 2	+0 3	14.45	13.29	+1.16
114	−1 34	−2 15	14.00	12.46	+1.54	142	+1 8	−1 13	15.67	15.36	+0.31
115†	−1 9	−0 33	13.86	12.38	+1.48	143*	+1 9	−0 34	15.02	14.34	+0.68
116†	−1 6	+0 57	15.74	14.97	+0.77	144*	+1 14	−2 19	14.99	14.11	+0.88
117*	−1 3	+0 4	15.07	14.26	+0.81	145*	+1 17	+1 26	14.31	12.88	+1.43
118	−0 40	−1 28	15.40	14.39	+1.01	146*	+1 24	+0 52	14.60	13.26	+1.34
119	−0 40	+1 7	13.99	12.40	+1.59	147	+1 27	+1 16	14.08	12.66	+1.42
120*	−0 37	−0 57	15.08	13.98	+1.10	148†	+1 52	−1 18	15.82	15.32	+0.50
121	−0 26	+0 20	15.66	15.32	+0.34	149	+2 9	+0 10	15.80	15.66	+0.14
122*†	−0 14	+2 53	14.63	13.56	+1.07	150†	+2 9	+1 45	15.74	14.97	+0.77
123*	−0 13	+0 40	15.02	14.20	+0.82	151*	+2 13	−0 37	15.02	14.15	+0.87
124*	−0 10	−0 15	14.67	13.70	+0.97	152†	+2 26	−1 21	16.40	15.32	+1.08
125*	−0 10	−3 12	14.64	13.44	+1.20	153†	+2 36	+1 57	15.20	15.56	+0.64
126	−0 8	+0 32	15.41	14.54	+0.87	154†	+2 38	+0 42	15.82	15.61	+0.21
127†	−0 7	+1 44	16.32	15.48	+0.84	155*	+2 47	+1 38	14.67	14.20	+0.47
128*	+0 6	−0 10	14.79	13.67	+1.12	156†	+8 26	+4 50	12.87	11.78	+1.09

* Bright stars used for the determination of distance.

† Comparison stars used for the study of variables.

5. *The distance of Messier 68.*—As described in *Mount Wilson Contribution* No. 151, section V, the mean apparent photographic magnitude of the bright stars can be used as a measure of distance.

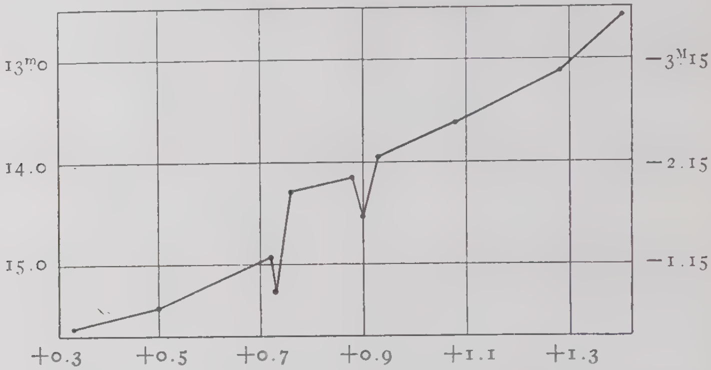

FIG. 1.—The color of giant stars in Messier 68. Abscissae are mean color indices; ordinates are apparent and absolute magnitudes.

Excluding the five brightest stars, we obtain from Table III for the next twenty-five stars in order of brightness the mean value of 14.80±0.21 (average deviation) with extremes of 14^{M}31 and 15^{M}08.[1]

TABLE IV

COLOR OF GIANT STARS

Mean Photo-visual Magnitude		Mean Color-Index
Apparent	Absolute	
12.59	−3.56	+1^{M}40
13.12	−3.03	+1.28
13.61	−2.54	+1.08
13.95	−2.20	+0.93
14.15	−2.00	+0.88
14.28	−1.87	+0.76
14.52	−1.63	+0.90
14.93	−1.27	+0.72
15.26	−0.89	+0.73
15.41	−0.74	+0.50
15.61	−0.54	+0.33
15.57	−0.58	+0.34

If, as previously adopted, this mean value corresponds to absolute magnitude −1.5, we derive as the parallax of the cluster

$$\pi = 0''.000055. \qquad (3)$$

---

[1] Cf. Table II of *Mt. Wilson Contr.*, No. 152, 1917.

A better determination of the distance may be based on the variable stars, whose intrinsic luminosity is known with higher accuracy than that of the brighter stars. Accepting -0.23 as the absolute value of the median photographic magnitude,[1] we compute from the observed value (2)

$$\pi=0.''0000595. \tag{4}$$

These new determinations are of much higher weight than (1), which is based on the measured diameter alone. Assigning weights 1, 2, and 4 to (1), (3), and (4), respectively, we derive the definitive value

$$\pi=0.''000059,$$

which differs from the earlier determination by less than 5 per cent. Corresponding to the adopted parallax, we have, in units of 100 parsecs,

$$\begin{aligned} R &= 170 \\ R\cos\beta &= 137 \\ R\sin\beta &= +102 \end{aligned}$$

and, to reduce from apparent to absolute magnitude, we compute the factor $m-M=16.15$.

The difference, median *minus* "mean of 25 brightest," $+1.10$, is somewhat small; but it differs by less than the adopted probable error from the mean value (derived from several clusters in *Contribution* 151) that was used in *Contribution* 152 for the determination of the distance of a considerable number of clusters in which variable stars are infrequent or unknown.

6. *The general luminosity-curve.*—The relation of the frequency of stars to absolute brightness is tabulated for two photographs in Table V. Numbers in parentheses show the frequencies when the known variable stars are excluded. On the plate of longer exposure, No. 4924, the magnitudes have been determined for more than 800 stars in representative selected areas that cover about one-fourth of the whole cluster; on Plate 4863 all stars in the cluster brighter than magnitude 17.5 were measured, excepting those within half a minute of arc of the center. Because of the

---

[1] *Mt. Wilson Contr.*, No. 151, p. 27, 1917.

small apparent diameter and the fairly high galactic latitude of Messier 68, no correction for background stars has been considered necessary. The reduction of the measures has involved, however, the usual correction for irregularities of the measuring scale and for distance from the center of the plate, and also for the unlike magnitude intervals in Table V.

TABLE V

Luminosity and Frequency of Stars

Plate 4863		Plate 4924	
Absolute Pg. Mag.	Number of Stars	Absolute Pg. Mag.	Number of Stars
−2.2	2.7	−2.4	0.7
−1.76	4.3	−2.06	1.4
−1.38	5.	−1.64	1.4
−1.01	9	−1.25	3
−0.68	24 (23)	−0.86	6 (5)
−0.46	61 (55)	−0.56	11 (10)
−0.28	72 (65)	−0.28	14 (12)
−0.11	60 (53)	0.00	14 (12)
+0.11	31 (29)	+0.27	11 (10)
+0.4	24 (22)	+0.55	9
+0.7	25	+0.83	13
+1.0	41	+1.1	17
+1.3	70	+1.4	19
		+1.7	25
		+1.9	42
		+2.2	74
		+2.5	130
		+2.7	234

The relatively high frequency of stars near the median magnitude, Fig. 2, appears to be much the same in this cluster as in five other globular clusters previously studied.[1] With the variable stars omitted, the phenomenon of a secondary maximum is still distinctly shown. From these results it appears that the general luminosity-curve in a star cluster cannot be accepted as a symmetrical probability-curve. The computation by Schouten[2] and Coeberg[3] of the distance of clusters, on the basis of the relative frequency of stars of the brightest few magnitudes, is therefore open to serious objection because they assume the luminosities to be distributed according to a normal error-curve. The questionable assumption is obviously responsible for the anomalous results obtained by them for the absolute magnitudes of all stars in clusters.

---

[1] *Mt. Wilson Contr.*, No. 155, 1917.

[2] *Verslagen Koninklijke Akademie van Wetenschappen te Amsterdam*, **20**, 1147, 1293, 1918.

[3] *Hemel en Dampkring*, November 1918.

7. *The maximum luminosity in Messier 68.*—The mean absolute magnitude of the five brightest cluster stars is −2.16 photographic and −3.55 photovisual. Variable No. 27 is excluded from this group as possibly not a member of the cluster; if a cluster star, its absolute photographic magnitude at maximum would be of the order of −5.0. The brightest blue star in the cluster appears to be No. 20 with the absolute photo-visual magnitude −0.5.

In Messier 68 there are about 250 stars brighter than absolute magnitude zero; in Messier 13 and Messier 3 there are something like twice as many stars brighter than the same limit of absolute brightness.

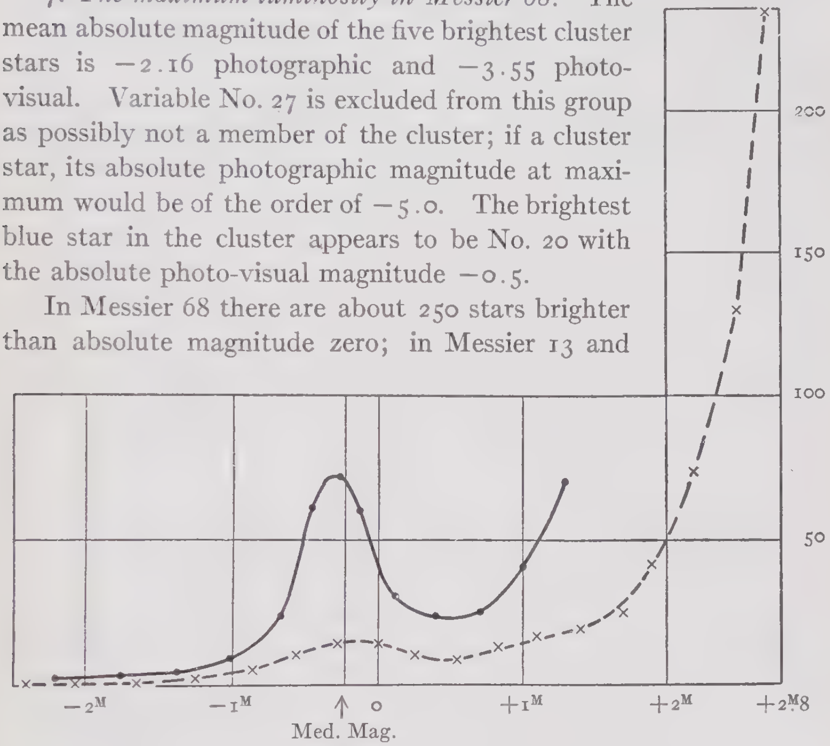

Fig. 2.—General luminosity-curves for Messier 68, from Plates 4863 (full line) and 4924; abscissae are absolute photographic magnitudes; ordinates, numbers of stars.

8. *The form of the cluster.*—Using the system of superposed sectors and rings, described in earlier discussions of the ellipticity of clusters, we have counted 1700 stars brighter than absolute magnitude +2.7 on Plate 4924. There is no appreciable deviation from perfect circularity. The results appear in Table VI, where opposite 30° sectors are combined to eliminate error in centering.

9. *Summary and conclusions.*—A. The results of a characteristic photometric study of Messier 68, a hitherto unexplored southern globular cluster, include the following items: (1) discovery of 28 variable stars, all but one of which appear to be typical cluster variables; (2) verification of the earlier result that cluster-type variables are characteristically bluer at maximum light than at minimum; (3) tabulation of the magnitudes and colors of the brightest giant stars of the cluster; (4) a new determination of the distance (55,000 light-years), based on diameter, variables, and bright stars, which differs very little from an earlier value based on diameter alone; (5) proof of the circularity of the cluster, so far as the two thousand brightest stars are concerned; (6) discovery of a secondary maximum in the general luminosity-curve at about the median magnitude of the short-period variable stars; (7) evidence that this cluster, which is less concentrated to the center than usual, is much poorer in giant stars than some other globular systems.

TABLE VI

DISTRIBUTION OF STARS

POSITION ANGLE	NUMBER OF STARS	
	Distance from Center 0.5 to 5.0 mm	Distance from Center 1.0 to 4.0 mm
15°	293	205
45	279	207
75	284	212
105	277	209
135	280	208
165	288	209
Mean	284	208

B. The following general conclusions, resulting from previous studies of clusters, are directly supported by the evidence from Messier 68: (1) The general luminosity-curve for the stars in a cluster differs so widely from a symmetrical probability-curve that the former is of little value in determining the distance of clusters by the method tentatively suggested by Kapteyn (cf. Fig. 2). (2) The median brightness of the short-period variables in any globular cluster appears to be an astrophysical constant whose value is a little more than one magnitude fainter than the mean of the magnitudes of the 25 brightest stars in the cluster; this result gives weight to the distances of clusters derived from measures of their brightest stars. (3) The diameter of the image of a globular cluster on a photographic chart is a valuable criterion of distance. (4) The brightest giant stars in globular clusters are always very red and have absolute photo-visual magnitudes between −4 and −3. (5) With decreasing brightness, at least as far as absolute magnitude zero, the average color-index of the giant stars decreases (cf. Fig. 1).

Mount Wilson Observatory
October 1919

Contributions from the Mount Wilson Observatory, No. 176
Reprinted from the *Astrophysical Journal*, Vol. LI, pp. 140-178, 1920

STUDIES BASED ON THE COLORS AND MAGNITUDES IN STELLAR CLUSTERS

SIXTEENTH PAPER: PHOTOMETRIC CATALOGUE OF 848 STARS IN MESSIER 3

By HARLOW SHAPLEY and HELEN N. DAVIS

ABSTRACT

Globular cluster Messier 3.—The paper reports in detail measurements of 14 photographic plates taken at the primary focus of the 60-inch reflector during 1915 and 1917. Table II is a *photometric catalogue of 848 stars*, giving the photographic and photo-visual magnitudes and the color-index of each. Of these stars, 750 are suitable for statistical work. The known variables are omitted, but it appears from a comparison of the different plates that at least 17 others are probably *variable stars*. As for the *distribution of stars of various magnitudes and color-type*, a statistical study of the measurements shows that stars of all types and magnitudes are very well mixed, at least for angular distances from the center greater than 2′. The *spectral curve*, omitting variables, shows a maximum frequency near color-class $f5$ and differs from the corresponding curve for Messier 13 in being without a secondary maximum for the blue stars (Fig. 1). The *magnitude curve* shows a maximum frequency for photo-visual magnitude 15.5 which is near absolute magnitude zero, as computed on the basis of the previously determined *parallax* of 0″000072; the curve, as usual, is far from being symmetrical. The *relation of color-index to magnitude* shows the usual decrease of index with decreasing brightness (Fig. 3). In general these results corroborate those yielded by the previous analysis of Messier 13. The *position coordinates of 370 stars* which were not listed by von Zeipel are given in Table III.

An extended investigation of the photographic and photo-visual magnitudes of stars in the globular cluster Messier 13 is described in the second paper of this series, *Mt. Wilson Contr.* No. 116. The study yielded results of sufficient novelty and importance to justify the detailed corroborative analysis of another globular cluster. For this purpose the bright northern system Messier 3 was chosen because of the excellent catalogue of positions by von Zeipel[1] and the published and unpublished studies of variable stars at Harvard[2] and Mount Wilson.[3] The work was begun in

---

[1] *Annales de l'Observatoire de Paris, Mémoires*, **25**, F1-101, 1908.

[2] *Harvard Annals*, **78**, 1-98, 1913.

[3] *Mt. Wilson Contr.*, No. 154, 1917; *Mt. Wilson Communications*, No. 47, 1917; *Publications of the Astronomical Society of the Pacific*, **29**, 110, 140, 1917.

1915 and completed nearly two years ago, some of the results appearing meanwhile in *Mt. Wilson Contr.* Nos. 151 and 152, and particularly in *Mt. Wilson Contr.* No. 155. An illustrated discussion of the dimensions of Messier 3 was printed in *Publications of the Astronomical Society of the Pacific*, **29**, 245, 1917.

Stars in the central part of Messier 3 have not been measured for magnitudes because of the uncertainties introduced by the Eberhard effect into photographic work in crowded regions. Between distances 1ʹ.8 and 11ʹ.3, however, the survey is practically complete to photo-visual magnitude 16.8, and about 140 fainter stars have also been measured. Altogether the catalogue contains 848 stars, less than 100 being within 2ʹ of the center.

The catalogue of Messier 13 (Table IX, *Mt. Wilson Contr.* No. 116) contains 616 stars, all more distant than 2ʹ from the center of the cluster, and complete to photo-visual magnitude 15.6, approximately. Because of the greater distance of Messier 3, the gain of 1.2 in apparent magnitude is partly lost when absolute magnitudes are considered. Thus, using the parallaxes given in *Mt. Wilson Contr.* No. 152, we have

	Messier 3	Messier 13
Parallax	0ʺ.000072	0ʺ.000090
$m-M$	15.72	15.23
Limit of Abs. Mag.	+1.08	+0.37

1. *Observational data.*—The photographs used in the present work are described in Table I. All were made at the primary focus of the 60-inch reflector. In addition to these plates more than eighty others have been made at Mount Wilson, largely for work on variable stars. The ten thousand measures of magnitude for the photometric catalogue are mainly the work of Miss Davis. Miss Ritchie has assisted in preparing the tables and figures for the press.

2. *Description of the catalogue.*—The numbers in the first column are those of von Zeipel's catalogue. Postscript letters are assigned to stars fainter than those listed by him. Miss Ritchie has measured position co-ordinates on photographic enlargements of the cluster for the identification of the 370 postscript stars,

referring each object to two or more stars of von Zeipel's catalogue.[1] The results appear in Table III. The center of the cluster is

$$\left.\begin{array}{l}\text{R. A.} = 13^{\text{h}}37^{\text{m}}35^{\text{s}} \\ \text{Decl.} = +28^\circ 52' 56''\end{array}\right\} 1900.0$$

according to the determination by von Zeipel. Approximate galactic co-ordinates are: Longitude = 8°, Latitude = +77°.

TABLE I

List of Plates

Plate		Date	Length of Exposure	No. Exposures on Pole	Use
Number	Kind				
2371...	Iso	1915, Apr. 16	10^{m}	2	Photo-visual magnitudes
2372...	S 27	Apr. 16	2	2	Comparison stars
2462...	Iso	June 7	10	1	Photo-visual magnitudes
2463...	S 27	June 7	3	2	Photographic magnitudes
2505...	Iso	July 6	20	1	Photo-visual magnitudes
2506...	S 27	July 6	3	2	Photographic magnitudes
3678...	Iso	1917, Mar. 28	5	2	Photo-visual zero point
3679...	S 27	Mar. 28	3	2	Photographic magnitudes
3680...	S 27	Mar. 28	2	2	Photographic magnitudes
3684...	Iso	Apr. 19	120, 20	0	Photo-visual magnitudes
3774...	Iso	May 27	52, 10	0	Photo-visual magnitudes
3775...	Iso	May 27	90, 15	0	Photo-visual magnitudes
3846...	S 27	July 25	4	2	Postscript stars, photographic
3847...	S 27	July 25	5	2	Postscript stars, photographic

An asterisk following the number in the first column indicates that the deduced magnitude is uncertain because of duplicity, bad image, or similar cause. Such stars are excluded from the statistical discussion. A dagger following the number indicates a comparison star used at Harvard and Mount Wilson for the study of variable stars. The magnitudes for these stars, collected in Table VI, depend upon a rather extensive discussion, which will be described in a later contribution dealing with the variables. The three stars marked with a double dagger, Nos. 612, 752, 982, were measured by Miss Ritchie after the completion of the catalogue and are not included in the following discussion; their spectra have been determined by Mr. Sanford and will be reported by him in another place.

---

[1] Corrections to von Zeipel's catalogue: No. 502 is about 10″ south of catalogued declination, which refers to our 502*a;* No. 1227 (on our chart made in 1915) is about 4″ north of the catalogued position; No. 184 is not found on Mount Wilson plates.

The second column contains the distance from the center of the cluster in minutes of arc. The final photographic and photo-visual magnitudes in the third and fifth columns, and the color-index in the last, are followed by colons when special uncertainty has affected the measurements; these doubtful results are also excluded from the statistical treatment. A few stars impossible of accurate measurement (brighter than photo-visual magnitude 17 and outside distance 1ʹ.8) may have been omitted entirely, but it is very unlikely that any of the omissions noted above have prejudiced the general interpretation of the observations.

For all determinations of a star's brightness the residuals from the mean are given in hundredths of a magnitude in the fourth and sixth columns of the catalogue. The photographic residuals refer, in order of the sub-column, to Plates 2463, 2506, 3679, and 3680, respectively, except that when in parentheses in the first two sub-columns the residuals refer to Plates 3846 and 3847. Similarly, the photo-visual residuals refer to Plates 2371, 2462, 2505, and 3684, respectively, with residuals for Plates 3774 and 3775 appearing in parentheses in the first two sub-columns. The letter "m" indicates that the tabulated magnitude depends upon only one plate. An asterisk following the photo-visual magnitude (six instances) means that the star was also measured on Plate 3678, but the residual for that plate is not entered in the following column; its value is the algebraic sum of the residuals there given with sign changed. Occasionally, in forming mean magnitudes, uncertain values were given half-weight; such cases are shown by the residuals; for example, see No. 926*a*.

To eliminate errors as far as possible, all color-indices less than −0.30 or greater than +1.40 have been independently redetermined from special series of measures, and all magnitude determinations showing residuals greater than 0.20 have been re-examined. Some corrections to the catalogue resulted from this supplementary work; its main outcome, however, is the conviction that many of the stars, whose magnitudes are similar to those of the variables, undergo slight variations of light. (Cf. discussion of their residuals in *Mt. Wilson Contr.* No. 155, p. 5.) The following

17 stars have photographic residuals greater than 0.25 and in most cases are probably variable stars:

251
357
603
606
632
665
845
935
962
1146
1170
1214
1241
1244
1374
1437
1439

There are 49 stars, including the comparison star *h*, with photographic residuals between 0.20 and 0.25. All of these stars will be included in future investigations of the variables.

The photographic and photo-visual residuals are summarized for the principal plates in Tables IV and V.[1] The systematic errors are satisfactorily small and no serious divergence of scale has been found. The average probable error of the final magnitudes is ±0.04, which is of the same order of accuracy as that attained in the comparable study of Messier 13.

The contents of the catalogue (which does not include any of the 150 known variable stars) may be summarized as follows:

	Number of Stars
With asterisks	27
With no color-index	21
Color-index with colon (uncertain) . . .	10
Fainter than 16.99 (Pv. mag.)	64
Supplementary	3
Suitable for statistical work (Tables VII, VIII, etc.)	750
Total	875
Subtract for duplicate listing . . .	27
Net total in catalogue	848

3. *Statistical tables and diagrams.*—Tables VII and VIII are in the usual form for the correlation of magnitude, color, number, and distance. Tables IX and X give convenient summaries or rearrangements of the larger tables. From the various tables, and from the figures illustrating these tabular results, it is clear that distance from the center[2] plays no very important part in the

---

[1] Some stars were measured after the tables were formed, so that altogether more than 3600 residuals appear in the catalogue.

[2] This does not apply to distances less than 1′.5.

interrelations of color, magnitude, and number of stars. This conclusion supports the earlier one that the stars of all types and absolute magnitudes are very well mixed in a globular cluster.

The spectral curve of Messier 3 (Fig. 1) has its maximum near color-class *f*5, in that respect agreeing with Messier 13; but the form of the curve as it now stands differs conspicuously in the absence of a preliminary maximum for the blue stars. If colors for the 100 variables, within our present limits of distance from the center, were also included in the diagram, it is probable that this dissimilarity between Messier 3 and Messier 13 would largely disappear. As noted before,[1] the many blue stars of Messier 13 appear to be represented in Messier 3 by cluster-type variables.

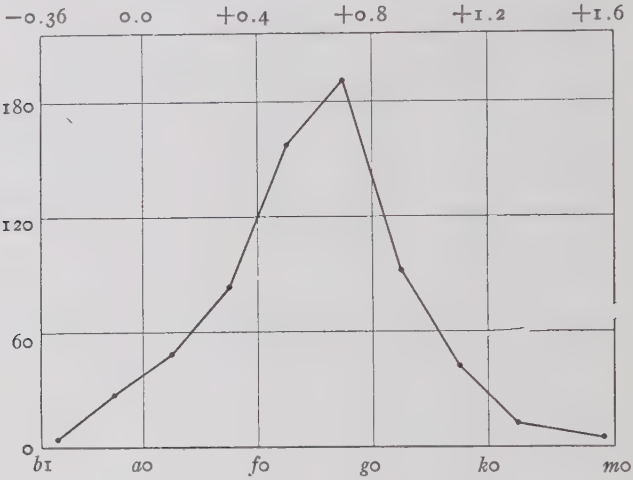

FIG. 1.—Spectral curve of giant stars in Messier 3; ordinates are numbers of stars in each half color-class; abscissae are color-indices and color-classes. Variable stars are not included; there are about 100 within the region studied, and their average median color-index, which varies with the light, is probably +0.25. (Cf. *Contribution*, No. 154, Fig. 4.)

The photographic and photo-visual luminosity-curves for Messier 3 have been fully discussed in *Mt. Wilson Contr.* No. 155. The maximum frequency of stars in the vicinity of absolute magnitude zero is conspicuously shown, for all intervals of distance from the center, by the numbers in the last column of Table VIII. The wide divergence of these observed luminosity-curves from a symmetrical probability-curve again points to the inadvisability of assuming them comparable for the purpose of estimating the distances of clusters.[1]

---

[1] *Mt. Wilson Contr.*, No. 155, p. 12, 1917.

Although the galactic latitude of Messier 3 is so high that superposed foreground stars are few, there may be some evidence in the shape of the curves in Fig. 2 of the influence of non-cluster stars on mean magnitude and color at distances greater than 7′. It is more likely, however, that the brighter average magnitudes at the greatest distances, and also near the center, are due to incompleteness of the catalogue to the seventeenth photo-visual magnitude in those regions.

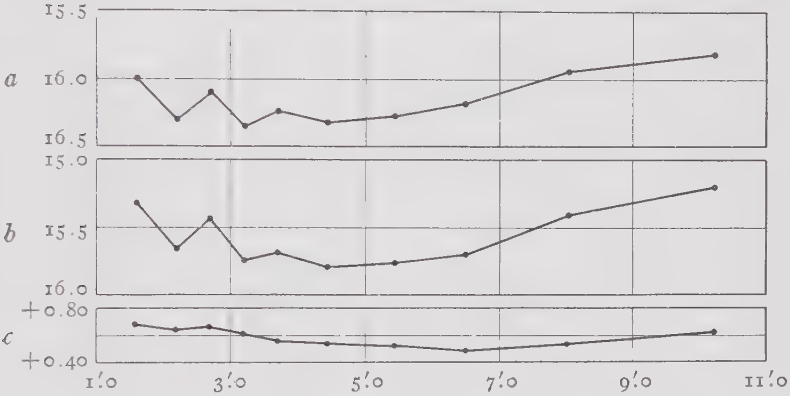

FIG. 2.—Average magnitudes and colors for different distances from the center: *a*) photographic magnitude; *b*) photo-visual magnitude; *c*) color-index. Abscissae are distances in minutes of arc.

Figure 3*a* illustrates for Messier 3 the decrease of color-index with decreasing brightness, which has been found to be a typical characteristic of the giant stars in globular clusters. A similar diagram for Messier 13 based on data given in *Mt. Wilson Contr.* No. 116 is given in Fig. 3*b*. In both cases the mean absolute magnitudes are derived from the parallaxes given earlier in this paper.

---

[1] Cf. *Mt. Wilson Contr.*, No. 175, 1919.

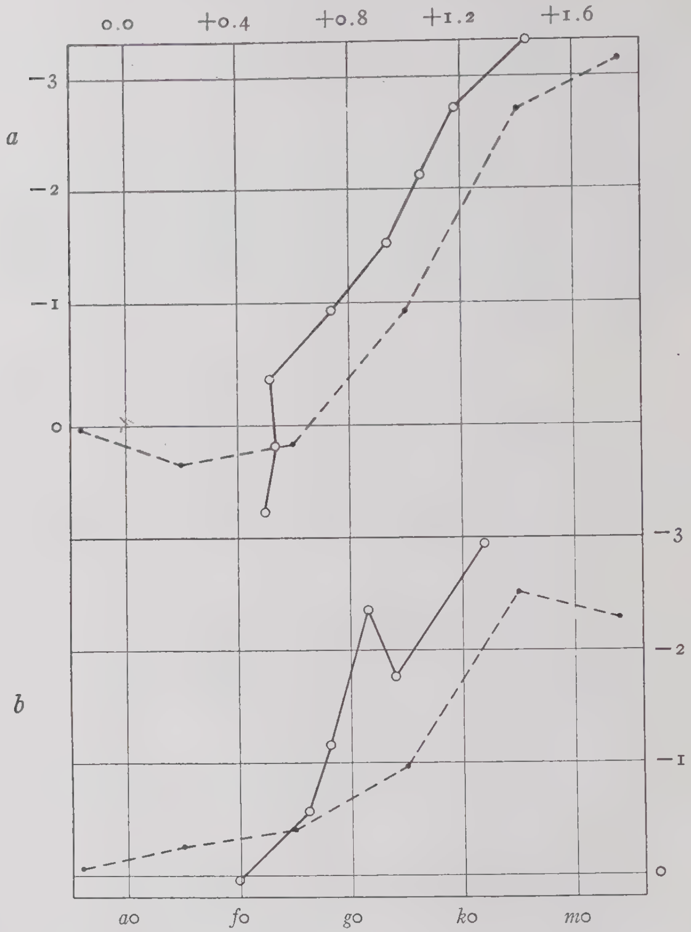

FIG. 3, *a* and *b*

a) The color of giant stars in Messier 3 (distance ⋝ 2′). The circles indicate the mean color-index for equal intervals of magnitude (Table X); the dots indicate mean magnitudes for equal intervals of color-index (Table IX). Abscissae are color-classes and color-indices; ordinates are absolute photo-visual magnitudes. The form of the broken curve is of course affected by the absence from the catalogue of stars fainter than photo-visual magnitude 17. The continuous curve, however, accurately represents the change of average color with brightness down to photo-visual magnitude 16.8; fainter stars are not included.

b) Similar representation of the color of giant stars in Messier 13 (distance ⋝ 2′ except for *m* stars).

TABLE II

PHOTOMETRIC CATALOGUE OF 848 STARS IN MESSIER 3

NUMBER	DISTANCE	PHOTOGRAPHIC		PHOTO-VISUAL		COLOR-INDEX
		Mag.	Residuals	Mag.	Residuals	
145...	11′.4	15.84	+ 8,− 7,....,....	16.02	(−15,+14)....,....	−0.18
155...	9.8	15.12	− 4,+ 5,....,....	14.52	....,...., m,....	+0.60
157...	9.7	15.48	− 9,+ 8,....,....	15.52	(+ 6,− 5)....,....	−0.04
157*a*..	9.8	17.17	(+ 4,− 4)....,....	16.68	(−11,+10)....,....	+0.49
157*b*..	8.9	16.18	(+ 2,− 1)....,....	15.42	(0, 0)....,....	+0.76
157*c*..	8.9	17.42	(...., m)....,....	16.39	(m,....)....,....	+1.03
158...	9.8	15.82	+ 4,− 5,....,....	15.37	(− 5,+ 5)....,....	+0.45
162...	9.2	15.10	+ 5,− 1,− 3,....	14.63	(....,− 2)+ 2,....	+0.47
164...	9.0	14.54	+ 7,+ 7,−13,....	13.62	0,...., 0,....	+0.92
164*a*..	8.8	16.71	(+ 1,− 1)....,....	16.16	(− 4,+ 4)....,....	+0.55
164*b*..	9.2	16.78	(− 6,+ 7)....,....	16.16	(...., m)....,....	+0.62
164*c*..	9.4	16.82	(− 6,+ 7)....,....	16.12	(+ 6,− 6)....,....	+0.70
166...	9.0	16.00	− 2,+ 4,− 2,....	15.30	(− 3,+ 3)....,....	+0.70
167...	8.4	15.68	+ 2,− 3,....,....	14.97	(+ 3,− 3)....,....	+0.71
168...	9.4	16.36	− 4,+ 5,....,....	15.62	(+ 2,− 1)....,....	+0.74
168*a*..	9.1	16.78	(+ 1,− 1)....,....	16.06	(− 6,+ 7)....,....	+0.72
169...	9.6	14.90	+ 1,− 1,....,....	13.86	(+19,−20)....,....	+1.04
174...	13.0	.....	....,....,....,....	11.11:	m,....,....,....	......
175...	8.4	15.85	− 9,+ 5,+ 3,....	15.36	(− 1, 0)....,....	+0.49
175*a*..	8.6	16.04	(+ 6,− 5)....,....	16.64	(−11,+11)....,....	+0.30
177...	7.8	14.45	− 8,+11,− 2,....	13.45	+ 5,....,− 5,....	+1.00
177*a*	7.4	16.19	(− 1,+ 1)....,....	15.58	(+ 3, −2)....,....	+0.61
177*b*..	6.9	17.13	(+12,−12)....,....	16.72	(− 2,+ 3)....,....	+0.41
179...	7.6	14.98	0,− 1,....,....	14.53	....,...., m,....	+0.45
179*a*..	7.3	16.74	(− 2,+ 3)....,....	16.30	(0,− 1)....,....	+0.44
180...	9.3	16.08	+ 4,− 4,....,....	15.03	(0, 0)....,....	+1.05
180*a*..	11.0	16.80	(+ 6,− 7)....,....	16.50	(− 7,+ 8)....,....	+0.30
180*b*..	10.6	16.94	(− 1,+ 2)....,....	15.76	(−12,+11)....,....	+1.18
181*a*..	7.4	17.02	(+ 8,− 9)....,....	.....	....,....,....,....	......
181*b*..	7.9	16.68	(+ 2,− 2)....,....	16.18	(− 6,+ 5)....,....	+0.50
181*c*..	8.2	17.08	(0,+ 1)....,....	16.58	(+ 3,+ 4)....,....	+0.50
182...	10.2	15.39	−17,+17,....,....	15.42	(0, 0)....,....	−0.03
187...	9.1	15.80	+ 3,− 3,....,....	15.00	(− 2,+ 3)....,....	+0.80
188...	7.2	15.12	− 1,+ 1,....,....	14.55	....,...., m,....	+0.57
188*a*	7.0	16.92	(0,+ 1)....,....	16.60	(−10,+ 9)....,....	+0.32
188*b*..	7.8	16.80	(− 1,+ 1)....,....	16.33	(+13,−13)....,....	+0.47
188*c*..	6.7	17.18	(+ 6,− 5)....,....	16.74	(− 4,+ 4)....,....	+0.44
188*d*..	6.3	16.36	(− 6,+ 5)....,....	15.68	(+ 4,− 4)....,....	+0.68
189...	6.5	15.92	+ 3,− 2,...., 0	15.24	(+11,−10)....,....	+0.68
190...	6.6	15.57	− 3,+ 8,....,− 6	15.42	(− 5,+ 5)....,....	+0.15
190*a*..	6.5	17.16	(− 2,+ 1)....,....	16.56	(− 3,+ 4)....,....	+0.60
191...	8.5	15.49	+ 9,+12,−14,− 8	15.40	(− 3,+ 2)....,....	+0.09
192...	6.2	14.65	+10,− 4,− 1,− 4	13.80	....,− 2,+ 1,....	+0.85
193...	9.6	15.36	−14,+15,....,....	14.54	....,+ 3,− 2,....	+0.82
193*a*..	9.3	16.64	(− 2,+ 2)....,....	16.06	(− 3,+ 4)....,....	+0.58
194...	7.0	14.59	− 2,+18,−10,− 5	13.64	− 1,− 5,+ 5,....	+0.95
195...	8.8	16.20	− 5,+ 6,....,....	15.80	(−13,+13)....,....	+0.40
196...	8.0	15.49	− 6,+12,− 5,− 1	15.40	(+ 5,+ 7)....,−11	+0.09
198...	7.6	16.42	+ 5,− 5,....,....	15.73	(− 6,+ 6)....,....	+0.69
199...	6.0	15.50	0,+11,−13,+ 4	14.78	(− 1,+ 1)........,	+0.72

TABLE II—*Continued*

Number	Distance	Photographic		Photo-visual		Color-Index
		Mag.	Residuals	Mag.	Residuals	
200...	7′.1	15.68	− 1,− 3,+15,−10	14.87	(....,+13)−13,....	+0.81
202...	6.0	15.61	+ 6,+12,− 6,−13	15.34	(− 2,+ 2)....,....	+0.27
203...	7.0	15.45	+ 1,+20,−24,+ 3	15.37	(+ 5,+ 8)....,−14	+0.08
204...	7.7	15.71	+21,− 2,− 3,−16	15.74	(− 7,+ 7)....,....	−0.03
205...	6.2	13.81	− 3,−23,+20,+ 6	12.72*	+ 2,− 2,− 9,....	+1.09
205*a*..	6.0	16.78	(− 2,+ 3)....,....	16.10	(−13,+13)....,....	+0.68
206...	7.4	11.27	....,− 2,....,+ 2	10.26*	+ 7,− 3,− 6,....	+1.01
206*a*..	7.5	16.90	(−11,+11)....,....	16.26	(+ 1, 0)....,....	+0.64
208...	8.2	16.76	− 1,+ 1,....,....	16.22	(− 4,+ 4)....,....	+0.54
208*a**.	8.3	17.25	(m,....)....,....	16.65:	(m,....)....,....	+0.60:
210...	5.5	15.40	− 1,+11,−19,+11	15.53	(0, 0)....,....	−0.13
210*a*..	5.7	16.82	(− 3,+ 3)....,....	15.96	(−15,+14)....,....	+0.86
210*b*..	5.7	17.28	(− 3,+ 2)....,....	16.64	(+ 1,− 1)....,....	+0.64
211...	5.5	15.86	+18,+ 4,....,−21	15.33	(− 6,+ 3)....,+ 4	+0.53
211*a*..	5.5	16.06	(− 8,+ 8)....,....	15.26	(− 9,+10)....,....	+0.80
211*b*..	5.2	17.27	(+ 1,− 1)....,....	16.74	(− 9,+10)....,....	+0.53
212...	6.3	16.15	+ 5,+ 3,−10,+ 1	15.40	(+ 5,− 4)....,....	+0.75
212*a*..	5.8	17.28	(− 3,+ 2)....,....	16.88	(0, 0)....,....	+0.40
212*b*..	6.3	17.36	(−18,+18)....,....	16.76	(−15,+15)....,....	+0.60
213...	7.1	15.48	+ 9,+ 8,−18,+ 3	15.44	(+ 3,+ 6)....,−10	+0.04
215...	5.4	16.74	− 2,+ 1,....,....	16.25	(+ 2,− 2)....,....	+0.49
215*a*..	5.4	17.42	(...., m)....,....	16.61	(m,....)....,....	+0.81
216...	9.1	14.77	+14,+ 8,−10,−12	13.83	0,− 2,+ 1,....	+0.94
217...	5.7	16.25	+ 2,+ 5,....,− 7	15.64	(+ 5,− 5)....,....	+0.61
218†..	5.7	15.04	− 2,+ 1,− 2,+ 3	14.51	....,+ 9,− 9,....	+0.53
219...	7.2	16.02	+10,−12,+ 3, 0	15.15	(− 7,+ 7)....,− 1	+0.87
220...	8.2	16.46	+ 6,− 5,....,....	15.71	(− 2,+ 2)....,....	+0.75
225...	5.2	15.62	− 8,+20,− 7,− 4	14.74	....,...., m,....	+0.88
227†..	5.0	15.25	− 1,− 9,− 2,+10	14.60	....,− 8,+ 9,....	+0.65
228...	10.0	15.78	−11,+12,....,....	15.10	(− 5,+ 5)....,....	+0.68
229...	5.8	15.30	−11,+ 8,− 9,+11	14.58	....,...., m,....	+0.72
230...	9.0	15.74	− 4,+ 3,....,....	15.34	(− 7,+ 8)....,....	+0.40
230*a*..	9.3	16.56	(+ 6,− 6)....,....	15.66	(+ 1,− 2)....,....	+0.90
230*b*..	9.6	17.19	(+ 2,− 2)....,....	16.72	(...., m)....,....	+0.47
230*c*..	10.0	16.60	(+ 6,− 7)....,....	16.03	(0, 0)....,....	+0.57
231...	5.5	15.43	0,+18,−18,....	14.78	....,−11,....,+11	+0.65
232...	8.7	15.87	+ 5,− 5,....,....	15.22	(+ 3,− 2)....,....	+0.65
233...	6.4	16.78	+ 2,− 3,....,....	16.11	(− 5,+ 5)....,....	+0.67
235...	7.5	15.53	+21,− 2,−12,− 6	15.50	(+ 3,− 3)....,....	+0.03
236...	5.3	15.87	−10,+ 8,+ 1,+ 1	15.36	(− 4,− 3)....,+ 8	+0.51
237...	6.6	14.33	−15,−10,+10,+16	13.91	+10,− 6,− 3,....	+0.42
238†..	4.5	14.27	−16,+ 3,....,+12	12.48*	+14,....,+ 6,....	+1.79
238*a*..	4.3	16.82	(−12,+11)....,....	16.16	(− 4,+ 4)....,....	+0.66
238*b*..	4.5	16.72	(0,+ 1)....,....	16.22	(− 1,+ 2)....,....	+0.50
240...	4.7	15.34	+ 9,+ 9,−19,+ 1	14.68	....,+14,−13,....	+0.66
241...	5.6	15.55	−20,+18,....,+ 3	15.18	(−10,+10)....,....	+0.37
245...	4.6	15.65	+ 2,+ 8,− 7,− 4	15.63	(+15,+10)....,−24	+0.02
247...	4.2	15.74	+ 2,+12,....,−13	15.43	(− 8,+ 7)...., 0	+0.31
247*a*..	4.0	16.76	(−29,+29)....,....	16.50	(+ 3,− 4)....,....	+0.26
248...	5.4	15.86	+ 6,+ 4,−11,....	15.54	(+ 1,− 1)....,....	+0.32
249*a*..	5.0	17.36	(− 5,+ 6)....,....	16.99	(−11,+11)....,....	+0.37
249*b*..	5.1	16.99	(− 2,+ 2)....,....	16.41	(+ 9,− 9)....,....	+0.58

TABLE II—*Continued*

Number	Distance	Photographic		Photo-visual		Color-Index
		Mag.	Residuals	Mag.	Residuals	
250†..	5′.2	14.81	+ 4,+ 7,− 5,− 6	13.91	− 1, 0,+ 2,....	+0.90
250*a*..	5.4	16.78	(+ 1,− 1)....,....	16.22	(+ 5,− 6)....,....	+0.56
251...	4.4	15.78	+32,− 5,−10,−17	14.89	....,− 9,−10,.... (+19,....)	+0.89
251*a*.	4.3	17.09	(−12,+12)....,....	16.60	(+15,−14)....,....	+0.49
253*a*..	5.2	16.76	(0,+ 1)....,....	16.17	(+ 1,− 1)....,....	+0.59
255...	5.6	15.11	− 7,− 6,....,+13	14.11	− 6,+10,− 4,....	+1.00
255*a*..	5.5	17.16	(+ 2,− 3)....,....	16.63	(− 6,+ 6)....,....	+0.53
256...	9.7	16.07	+ 3,− 3,....,....	14.98	(0,− 1)....,....	+1.09
257...	4.7	16.21	− 4,+ 5,...., 0	15.60	(+ 1,− 1)....,....	+0.61
258†..	4.3	15.52	+15,+ 6,....,−21	15.54	(− 4,+ 5)....,....	−0.02
258*a*..	4.1	17.27	(−19,+19)....,....	16.84	(+ 4,− 3)....,....	+0.43
259...	3.9	15.82	+ 4,+13,....,−17	15.46	(+ 4,− 4)....,....	+0.36
260...	3.9	16.59	− 7,+ 7,....,....	15.75	(− 6,+ 6)....,....	+0.84
260*a*..	3.7	17.32	(+ 3,− 2)....,....	16.97	(−13,+13)....,....	+0.35
261...	5.7	15.90	+ 8,− 8,....,....	15.30	(− 3,+ 3)....,....	+0.60
261*a*..	6.1	17.17	(− 9,+ 9)....,....	10.74	(− 4,+ 4)....,....	+0.43
262...	4.5	15.84	− 1,+ 2,....,....	15.33	(+12,+ 6)....,−17	+0.51
262*a*..	4.8	16.76	(− 6,+ 5)....,....	16.19	(− 1,+ 1)....,....	+0.57
263†..	4.1	14.53	+ 7,−10,− 7,+11	13.41	−10,+ 7,+ 2,....	+1.12
265...	5.0	14.29	−22,+18,+ 4,....	13.15	− 5,+ 3,+ 3,....	+1.14
266...	5.1	16.22	+ 3,− 4,....,....	15.61	(+ 8,− 8)....,....	+0.61
268...	5.7	16.34	− 2,− 4,....,+ 7	15.60	(+ 4,− 4)....,....	+0.74
270...	3.9	16.16	+ 9,− 8,....,....	15.29	(− 4,+ 4)....,....	+0.87
272...	5.1	16.56	− 2,+ 1,....,....	15.84	(− 3,+ 3)....,....	+0.72
273...	3.7	16.00	− 8,+ 4,....,+ 5	15.22	(− 7,+11)....,− 5	+0.78
276...	3.5	16.24	+ 8,− 6,....,+ 1	16.42	(− 6,+ 7)....,....	−0.18
277...	3.6	15.17	− 2,− 4,....,+ 7	14.55	....,...., m,....	+0.62
280*..	4.2	.....	....,....,....,....	17.41	(...., m)....,....	.....
281...	4.8	14.61	− 4,+ 4,...., 0	13.42	− 6,+ 6,+ 1,....	+1.19
281*a*..	4.5	17.01	(...., m)....,....	16.98	(+18,−17)....,....	+0.03
282...	4.1	15.90	+ 5,− 4,....,....	14.99	(+11,− 5)....,− 6	+0.91
283...	3.3	16.55	− 8,+ 5,....,+ 2	15.92	(− 2,+ 1)....,....	+0.63
285...	3.3	16.59	+ 8,+ 4,....,−13	16.05	(− 5,+ 5)....,....	+0.54
286...	3.2	15.77	− 1,+ 9,....,− 9	15.11	(− 1,+ 1)....,....	+0.66
289...	3.3	15.24	+ 5,−11,....,+ 7	14.40	....,.... m,....	+0.84
290...	8.0	15.74	−11,+ 8,− 2,+ 4	15.41	(− 4,+ 4)....,....	+0.33
290*a*..	8.0	17.12	(− 4,+ 5)....,....	16.84	(−19,+19)....,....	+0.28
290*b*..	8.0	16.98	(+10,−10)....,....	16.46	(−10,+10)....,....	+0.52
291...	3.1	14.85	+16,− 8,....,− 9	14.06	+ 4,− 3,− 1,....	+0.79
291*a*..	3.0	17.02	(− 2,+ 3)....,....	16.32	(− 2,+ 3)....,....	+0.70
291*b*..	3.4	17.30	(− 5,+ 4)....,....	16.76	(+12,−11)....,....	+0.54
291*c*..	3.7	17.26	(− 5,+ 4)....,....	16.90	(− 6,+ 5)....,....	+0.36
292...	3.5	15.60	0,+13,−12,....	15.58	(0,+ 1)....,....	+0.02
293...	3.1	15.50	+ 4,− 3,....,....	14.61	....,....,+ 5,− 5	+0.89
296*a*..	3.2	17.42	(− 4,+ 4)....,....	17.11	(−23,+23)....,....	+0.31
296*b*..	3.4	17.38	(− 3,+ 4)....,....	17.17	(...., m)....,....	+0.21
297...	7.4	14.14	−13,+17,− 3,....	12.82	0,−12,+11,....	+1.32
298...	4.2	16.50	0,+ 1,....,....	15.78	(− 6,+ 6)....,....	+0.72
299...	7.0	16.14	+ 3,− 3,....,− 1	15.38	(− 6,+ 7)....,....	+0.76
300...	3.0	16.64	+ 2,− 1,....,....	15.90	(− 6,+ 6)....,....	+0.74
301...	4.5	15.85	+10,+10,....,−20	15.42	(−10,+11)....,− 2	+0.43
301*a*..	4.5	17.16	(+12,−11)....,....	16.62	(+ 3,− 4)....,....	+0.54

TABLE II—*Continued*

Number	Distance	Photographic		Photo-visual		Color-Index
		Mag.	Residuals	Mag.	Residuals	
301*b*..	4′.8	16.68	(− 6,+ 5)....,....	15.94	(−13,+12)....,....	+0.74
301*c*..	5.2	17.13	(−13,+13)....,....	16.78	(+ 6,− 6)....,....	+0.35
301*d*..	5.3	17.24	(− 6,+ 6)....,....	17.14	(...., m)....,....	+0.10
302*..	3.4	14.95	m,....,....,....	.....	....,....,....,....	......
303...	2.8	16.51	+ 3,+ 3,....,− 7	15.82	(+ 8,− 9)....,....	+0.69
303*a*..	2.9	17.02	(− 2,+ 3)....,....	16.42	(− 3,+ 4)....,....	+0.60
304...	2.8	15.49	+14,+ 2,−17,....	15.53	(− 3,+ 3)....,....	−0.04
305*a*..	4.6	17.16	(− 2,+ 1)....,....	16.46	(m,....)....,....	+0.70
306...	2.7	16.12	− 5,− 1,+ 5,....	15.22	(0, 0)....,....	+0.90
307 ..	3.8	15.96	− 4,+12,− 8,....	15.16	(− 1,+ 1)....,....	+0.80
307*a*..	3.9	16.70	(+ 9,− 8)....,....	16.06	(−13,+14)....,....	+0.64
307*b*..	4.1	16.96	(+ 4,− 3). ..,....	16.58	(−12,+11)....,....	+0.38
308...	3.0	15.80	+15,−15,....,....	15.66	(+ 6,− 5)....,....	+0.14
308*a*..	2.7	16.60	(−17,+17)....,....	15.88	(+ 5,− 4)....,....	+0.72
308*b*..	3.4	17.22	(+16,−17)....,....	17.02	(−14,+15)....,....	+0.20
309...	2.7	14.37	−24,+ 6,....,+17	13.18*	−12,+ 7,−11,....	+1.19
310...	2.8	16.92	+ 3,− 4,....,....	15.78	(− 6,+ 6)....,....	+1.14
310*a*..	2.8	17.22	(−12,+12)....,....	16.74	(+ 5,− 5)....,....	+0.48
311...	3.6	15.45	+ 1,+20,−20,....	15.52	(+ 3,− 2)....,....	−0.07
311*a*..	3.5	16.82	(0,− 1)....,....	16.02	(− 9,+ 8)....,....	+0.80
311*b*..	3.4	17.08	(− 4,+ 5)....,....	16.51	(+ 2,− 2)....,....	+0.57
312...	2.7	15.98	+ 3,+ 6,−10,....	14.97	(+ 6,− 6)....,....	+1.01
313...	2.7	16.59	− 7,+ 7,....,....	15.84	(+ 6,− 5)....,....	+0.75
314...	4.8	15.34	+ 1,+22,−22,....	14.40	....,...., m,....	+0.94
315...	3.3	15.49	+11,+12,−24,....	14.77	....,...., m,....	+0.72
317...	3.0	15.92	+15,−15,....,....	15.90	(0, 0)....,....	+0.02
319...	3.6	16.48	− 6,+ 6,....,....	15.73	(+14,−14)....,....	+0.75
320...	6.3	16.66	−10,+ 9,....,....	15.95	(+ 8,− 8)....,....	+0.71
320*a*..	6.3	17.24	(− 3,+ 2)....,....	16.72	(−15,+16)....,....	+0.52
320*b*..	6.2	16.98	(+ 6,− 5)....,....	16.68	(− 3,+ 4)....,....	+0.30
322...	2.9	17.04	− 9,+10,....,....	16.65	(− 4,+ 4)....,....	+0.39
322*a*..	2.9	17.38	(− 7,+ 8)....,....	16.76	(− 1,+ 2)....,....	+0.62
323...	2.7	15.35	+ 8,−14,....,+ 6	14.39	...., 0, 0,....	+0.96
325...	3.8	15.98	+ 3,+13,−15,....	15.40	(+ 7,− 7)....,....	+0.58
326...	2.8	15.64	− 1,+ 5,....,− 3	14.68	....,−11,+11,....	+0.96
326*a*..	3.0	17.30	(− 5,+ 4)....,....	16.77	(− 7,+ 7)....,....	+0.53
326*b*..	3.0	17.26	(...., m)....,....	16.57	(m,....)....,....	+0.69
326*c*..	3.2	17.08	(+13,−12)....,....	16.20	(− 2,+ 3)....,....	+0.88
327...	3.2	15.82	+ 1,+ 8,....,−10	15.44	(−12,− 2)....,+15	+0.38
329...	4.4	15.93	−10,+11,− 2,....	15.12	(− 2,+ 2)....,....	+0.81
330...	2.5	16.39	− 7,+ 2,....,+ 5	15.62	(+ 2,− 1)....,....	+0.77
331...	6.2	15.45	− 6,+16,....,−10	15.40	(− 5,+ 5)....,....	+0.05
332...	3.9	15.85	− 6,+ 5,+ 1,....	15.26	(− 9,+ 7)....,+ 3	+0.59
332*a*..	4.1	17.26	(− 5,+ 4)....,....	16.82	(−17,+17)....,....	+0.44
332*b*..	3.9	17.34	(− 3,+ 3)....,....	16.86	(− 2,+ 2)....,....	+0.48
334...	2.6	14.27	−14,+12,+ 1,....	13.14	− 2,+15,−13,....	+1.13
335...	3.6	16.10	+ 7,+ 5,− 2,− 8	15.44	(− 9,+10)....,....	+0.66
336...	2.9	15.07	+ 4,+ 2,− 6,....	14.05	+13,− 7,− 6,....	+1.02
336*a*..	3.0	17.17	(+ 4,− 4)....,....	.....	....,....,....,....	......
337...	2.4	15.54	+19,− 3,−22,+ 7	15.60	(+ 1,− 1)....,....	−0.06
339...	2.9	15.49	−17,+24,....,− 8	14.76	....,....,+ 5,− 6	+0.73
340...	2.7	16.65	−15,+15,....,....	15.88	(− 1,+ 2)....,....	+0.77

TABLE II—*Continued*

Number	Distance	Photographic		Photo-visual		Color-Index
		Mag.	Residuals	Mag.	Residuals	
341...	3′5	15.55	−12,+22,....,−10	14.69	....,...., m,....	+0.86
342...	5.5	15.75	+ 4,+ 7,....,−10	15.40	(− 3.+ 2)....,....	+0.35
343...	2.6	15.40	+ 6,− 6,....,+ 1	15.26	(−11,+ 7)....,+ 3	+0.14
345...	3.0	14.61	− 4,+ 8,− 5,....	13.35	+ 2,+ 2,− 4,....	+1.26
345*a*..	3.1	17.30	(−12,+12)....,....	16.78	(+10,−11)....,....	+0.52
347...	2.8	16.13	− 1,+ 2, 0,....	15.42	(− 7,+ 8)....,....	+0.71
348...	2.3	14.76	− 4,+ 1,....,+ 4	13.88	+10,− 2,− 8,....	+0.88
348*a*..	2.2	16.76	(+ 3,− 3)....,....	16.14	(− 5,+ 6)....,....	+0.62
349...	3.6	15.89	+21,− 7,−14,....	14.96	(+12,−11)....,....	+0.93
350...	3.0	16.46	−16,+17,....,....	15.60	(+ 1,+ 1)....,− 3	+0.86
350*a*..	2.9	17.36	(− 1,+ 1)....,....	16.76	(− 6,+ 5)....,....	+0.60
352...	2.3	15.24	+ 1,−11,....,+11	14.28	− 6,+ 2,+ 5,....	+0.96
354...	6.5	15.76	+ 3,− 3,....,....	15.47	(m,....)....,....	+0.29
355*a*..	2.4	16.87	(+10,−10)....,....	16.24	(− 3,+ 2)....,....	+0.63
357...	2.4	15.20	+26,+14,−40,....	14.45	(− 3,+ 3)....,....	+0.75
360...	2.1	15.82	− 3.+17,....,−14	15.02	(+ 6,− 5)....,....	+0.80
360*a*..	2.1	16.03	(+ 2,− 2)....,....	15.50	(− 3,+ 3)....,....	+0.53
360*b*..	2.1	16.93	(0, 0)....,....	16.19	(− 7,+ 7)....,....	+0.74
360*c*..	2.1	17.10	(0,− 1)....,....	16.52	(+ 9,− 8)....,....	+0.58
360*d*..	2.2	17.46	(− 8,+ 8)....,....	16.89	(−10,+10)....,....	+0.57
364...	2.1	15.75	−21,+24,....,− 3	15.78	(+ 9,− 8)....,....	−0.03
364*a*..	2.1	16.84	(+ 2,− 3)....,....	15.90	(+ 3,− 3)....,....	+0.94
365...	2.1	15.62	+ 8,+ 3,−11,....	15.54	(+ 4,− 4)....,....	+0.08
367...	2.3	15.10	+ 5,+ 3,− 9,....	13.96	− 6,+ 2,+ 3,....	+1.14
369...	2.0	15.08	+ 3,+ 5,− 9,....	14.40	....,...., m,....	+0.68
370...	1.9	16.85	−13,+13,....,....	16.24	(0,− 1)....,....	+0.61
371...	6.6	15.11	+ 4,−10,− 7,+13	14.81	(− 1,+ 1)....,....	+0.30
372...	2.5	15.63	+ 4,+ 6,....,− 9	14.71	....,...., m,....	+0.92
373...	2.3	16.22	−15,+15,....,....	15.46	(+12,−13)....,....	+0.76
375...	1.9	15.49	+11,+ 7,−19,....	14.77	....,...., m,....	+0.72
376...	1.9	16.06	− 2,+ 2,....,....	15.41	(− 1,+ 1)....,....	+0.65
376*a*.	1.9	16.80	(− 4,+ 5)....,....	16.32	(...., m)....,....	+0.48
377...	2.1	15.92	+12,+ 7,−20,....	15.26	(+ 1,− 1)....,....	+0.66
378*a*..	4.0	17.40	(− 2,+ 2)....,....	16.99	(−15,+15)....,....	+0.41
379*a*..	2.4	17.45	(− 7,+ 7)....,....	16.96	(+ 8,− 8)....,....	+0.49
379*c*..	2.4	17.34	(...., m)....,....	16.58	(+ 8,− 8)....,....	+0.76
380...	1.9	16.05	− 1,+10,....,−10	15.24	(− 7,+ 6)....,....	+0.81
380*a*..	2.1	16.88	(+ 2,− 3)....,....	16.08	(−11,+12)....,....	+0.80
380*b*..	2.2	17.34	(+ 1, 0)....,....	16.98	(− 5,+ 5)....,....	+0.36
381...	2.1	15.22	+ 7,− 9,....,+ 2	14.22	− 7,+10,− 2,....	+1.00
381*a*..	2.0	17.02	(+ 2,− 1)....,....	16.45	(+ 1,− 1)....,....	+0.57
381*b*..	2.0	17.38	(+ 4,− 4)....,....	17.12	(− 8,+ 8)....,....	+0.26
382*..	2.0	15.48	− 2,+21,−18,....	15.10	(+22,−22)....,....	+0.38
383...	2.3	16.40	+ 2,− 3,....,....	15.58	(−13,+12)....,....	+0.82
385...	2.0	15.36	+24,−23,....,....	14.06	(− 4,+ 5)....,....	+1.30
385*a*..	2.1	17.46	(− 8,+ 9)....,....	16.94	(− 1,+ 1)....,....	+0.52
385*b*..	2.0	17.36	(−11,+10)....,....	16.92	(− 8,+ 7)....,....	+0.44
386...	3.4	15.94	+13,+ 5,−19,....	15.40	(−10,+10)....,....	+0.54
386*a*	3.5	17.44	(− 2,+ 2)....,....	16.96	(+ 2,− 1)....,....	+0.48
387...	2.1	14.75	+ 4,− 2,....,− 3	13.85	− 3,+ 1,+ 3,....	+0.90
387*a*..	2.1	16.86	(+14,−13)....,....	16.06	(− 9,+10)....,....	+0.80
389...	1.8	15.46	0,− 3,....,+ 2	14.62	(....,+ 2)− 1,....	+0.84

TABLE II—*Continued*

Number	Distance	Photographic		Photo-visual		Color-Index
		Mag.	Residuals	Mag.	Residuals	
392...	2′9	16.30	− 3,+ 7,....,− 4	15.60	(− 5,+ 4)....,....	+0.70
393...	8.1	15.55	−12,+ 6,+ 7,....	14.63	(....,+ 1)− 1,....	+0.92
394...	1.7	15.94	+ 7,+14,....,−22	15.38	(− 8,+ 7)....,....	+0.56
394*a*..	1.8	16.40	(− 1,+ 1)....,....	15.70	(− 1, 0)....,....	+0.70
396*a*..	2.7	16.83	(−13,+13)....,....	15.97	(−19,+19)....,....	+0.86
397*a*..	1.6	15.49	(+ 1,− 1)....,....	15.61	(...., m)....,....	−0.12
398...	3.0	14.32	−19,− 5,+11,+12	13.19*	− 7,− 4,....,....	+1.13
399...	3.3	16.45	−20,−11,+23,+ 7	15.84	(+ 3,− 3)....,....	+0.61
400...	1.6	15.90	+ 5,+ 9,....,−15	15.34	(−12,+11)....,....	+0.56
401...	2.1	16.16	+ 1,− 1,....,....	15.18	(− 1,+ 2)....,....	+0.98
403...	1.6	15.42	+ 8,− 8,....,....	15.32	(+ 8,− 7)....,....	+0.10
403*a*..	1.7	16.47	(− 8,+ 8)....,....	15.78	(+ 9,− 8)....,....	+0.69
403*b*..	1.7	16.28	(− 6,+ 7)....,....	15.60	(− 5,+ 4)....,....	+0.62
403*c*..	1.5	15.96	(− 8,+ 8)....,....	15.38	(+ 2,− 2)....,....	+0.58
403*d*..	1.7	17.34	(−20,+21)....,....	16.99	(...., m)....,....	+0.35
403*e*..	1.7	17.44	(+ 1,− 2)....,....	17.45	(...., m)....,....	−0.01
403*f*...	1.6	17.41	(+ 4,− 4)....,....	17.24	(...., m)....,....	+0.17
403*g*..	1.6	17.44	(− 9,+ 8)....,....	16.78	(...., m)....,....	+0.66
406...	2.6	16.53	− 6,− 5,+ 5,+ 4	15.71	(+ 7,− 7)....,....	+0.82
411*a*..	4.8	16.96	(+ 1, 0)....,....	16.53	(+12,−12)....,....	+0.43
412...	3.1	15.59	− 5,+14,....,− 8	15.56	(...., m)....,....	+0.03
414...	2.5	16.38	− 4,+ 3,....,....	15.70	(− 1, 0)....,....	+0.68
417...	1.6	14.09	− 2,+ 2,....,....	12.94	+ 8,− 5,− 3,....	+1.15
417*a*..	1.7	15.04	(− 6,+ 7)....,....	15.21	(− 1,+ 1)....,....	−0.17
417*b*..	1.7	16.42	(− 3,+ 2)....,....	16.05	(− 8,+ 8)....,....	+0.37
417*c*..	1.8	17.04	(− 4,+ 5)....,....	16.25	(− 1,+ 1)....,....	+0.79
417*d*..	1.9	17.42	(− 4,+ 4)....,....	16.48	(− 2,+ 3)....,....	−0.06
418...	2.1	15.60	+16,+13,−28,....	15.44	(− 2, +3)....,....	+0.16
418*a**.	2.1	......	....,....,....,....	16.64	(+20,−20)....,....	......
419...	2.6	15.63	−13,+14,....,− 2	15.46	(− 4,+ 4)....,....	+0.17
419*a**.	2.6	17.04	(+ 4,− 3)....,....	16.14	(−14,+15)....,....	+0.90
420*..	1.4	13.59	m,....,....,....	13.40	+ 7,− 6,− 1,....	+0.19
422...	2.4	15.55	+12,+10,−23,....	15.48	(− 8,+ 8)....,....	+0.07
422*a*..	2.3	17.24	(+14,−15)....,....	16.54	(−15,+15)....,....	+0.70
423...	10.6	14.92	− 1,− 7,+ 9,....	14.60	(....,+ 7)− 6,....	+0.32
425*a*..	1.8	16.18	(− 6,+ 5)....,....	15.46	(−16,+15)....,....	+0.72
426...	11.2	14.85	+ 2,− 4,+ 1,....	13.75	....,...., m,....	+1.10
433...	2.9	15.92	− 3,+12,....,−10	15.84	(−12,+12)....,....	+0.08
434...	2.4	16.90	− 5,+ 4,....,....	16.10	(− 1, 0)....,....	+0.80
435...	6.7	15.84	+ 8,− 7,....,....	15.00	(− 2,+ 3)....,....	+0.84
436...	2.1	16.66	0, 0,....,....	15.84	(− 3,+ 3)....,....	+0.82
444...	2.5	15.39	+18,− 1,−16,....	15.42	(+ 3,− 3)....,....	−0.03
450...	2.1	16.86	− 4,+ 5,....,....	16.10	(−10,+10)....,....	+0.76
452...	1.9	15.34	+ 1,−13,....,+11	14.44	(−11,+11)....,....	+0.90
452*a*..	2.1	17.38	(0,− 1)....,....	16.64	(+11,−10)....,....	+0.74
452*b*..	2.2	16.94	(− 8,+ 7)....,....	16.25	(+ 2,− 2)....,....	+0.69
452*c*..	1.9	17.38	(− 7,+ 8)....,....	16.78	(+10,−11)....,....	+0.60
454...	2.5	16.92	−22,+22,....,....	16.20	(− 2,+ 3)....,....	+0.72
455*a*..	5.7	17.52	(0, 0)....,....	16.99	(−15,+15)....,....	+0.53
457...	2.7	16.80	−10,+11,....,....	16.52	(+ 1,− 1)....,....	+0.28
463...	2.4	14.25	−21,+ 2,....,+19	13.12*	− 4,− 3,− 8,....	+1.13
464...	1.9	16.22	− 7,+12,....,− 4	15.40	(−18,+19)....,....	+0.82

TABLE II—*Continued*

Number	Distance	Photographic		Photo-visual		Color-Index
		Mag.	Residuals	Mag.	Residuals	
465...	2′.5	15.01	+ 7,− 4,....,− 3	14.01	+ 5,− 2,− 2,....	+1.00
467...	2.7	15.75	− 8,+20,− 9,− 4	15.67	(− 3,+ 3)....,....	+0.08
467*a*..	2.6	17.36	(+ 2,− 2)....,....	16.66	(− 9,+ 9)....,....	+0.70
467*b*..	2.7	17.28	(− 3,+ 2)....,....	16.76	(+ 8,− 9)....,....	+0.52
471...	3.4	16.14	+23,−24,....,....	15.77	(+ 1,− 1)....,....	+0.37
471*a*..	3.5	16.70	(− 4,+ 3)....,....	15.94	(− 7,+ 6)....,....	+0.76
472...	1.9	14.76	+11,−20,+10,....	14.45	...., m,....,....	+0.31
473...	3.0	16.33	− 1,+ 1,....,....	15.60	(+ 1,− 1)....,....	+0.73
474...	1.7	15.73	−10,+17,....,− 8	15.61	(− 3,+ 3)....,....	+0.12
480...	3.3	16.28	− 3,+ 2,....,....	15.49	(− 7,+ 7)....,....	+0.79
480*a*..	3.7	17.05	(− 8,+ 8)....,....	16.50	(+ 3,− 4)....,....	+0.55
480*b*..	4.0	17.52	(...., m)....,....	17.16	(0,+ 1)....,....	+0.36
482...	2.2	15.92	+ 6,− 6,....,....	15.57	(− 2,+ 2)....,....	+0.35
482*a*..	2.1	16.50	(−13,+12)....,....	15.70	(− 9,+ 9)....,....	+0.80
482*b*..	2.1	16.39	(− 2,+ 2)....,....	15.66	(+ 3,− 2)....,....	+0.73
484...	9.2	16.13	+ 9,− 9,....,....	15.43	(+ 4,− 4)....,....	+0.70
490...	2.0	14.13	+ 5,−14,+10,....	12.33	0,+ 3,− 2,....	+1.80
499...	3.4	16.26	− 1, 0,....,....	15.62	(+ 2,− 3)....,....	+0.64
499*a*..	3.5	17.24	(+11,−11)....,....	16.87	(− 8,+ 8)....,....	+0.37
499*b*..	4.0	17.01	(− 8,+ 8)....,....	16.56	(− 3,+ 2)....,....	+0.45
499*c*..	4.1	17.34	(− 3,+ 3)....,....	16.83	(− 8,+ 8)....,....	+0.51
499*d*..	3.9	17.46	(...., m)....,....	17.31	(...., m)....,....	+0.15
499*e*..	3.9	.....	....,....,....,....	17.48	(...., m)....,....	......
499*f*...	3.0	17.44	(...., m)....,....	17.31	(...., m)....,....	+0.13
499*g*..	4.0	17.19	(−11,+11)....,....	16.88	(− 4,+ 3)....,....	+0.31
499*h*..	4.0	17.59	(...., m)....,....	17.21	(−17,+17)....,....	+0.38
502...	2.4	16.14	+ 3,− 3,....,....	15.21	(− 1,+ 1)....,....	+0 93
502*a*..	2.3	16.20	(0, 0)....,....	15.64	(+ 3,− 3)....,....	+0.56
512...	5.0	15.79	+ 4,+ 7,−11,....	14.94	(+14,−15)....,....	+0.85
513...	2.2	16.03	+ 9,+ 1,....,−11	15.18	(− 6,+ 7)....,....	+0.85
513*a*..	2.3	17.19	(−11,+11)....,....	16.40	(− 7,+ 6)....,....	+0.79
514...	2.9	15.44	+ 2,− 1,....,....	14.58	....,...., m,....	+0.86
522...	3.1	16.54	− 7,+ 6,....,....	15.76	(− 7,+ 8)....,....	+0.78
522*a*..	3.2	16 72	(− 6,+ 5)....,....	16.14	(− 5,+ 6)....,....	+0.58
522*b*..	3.0	16.94	(− 1,+ 2)....,....	16.34	(+ 2,− 2)....,....	+0.60
522*c**.	3.0	.....	....,....,....,....	16.79	(m,....)....,....	......
530...	2.4	16.98	−16,+16,....,....	16.50	(−14,+15)....,....	+0.48
539*..	1.8	15.16	−18,+22,....,− 3	14.98	(m,....)....,....	+0.18
550...	1.8	15.99	+11,+ 9,....,−20	15.10	(− 2,+ 2)....,....	+0.89
550*a*..	1.8	17.36	(−18,+19)....,....	16.86	(+12,−11)....,....	+0.50
564...	1.9	15.94	+16,+ 5,−22,....	14.97	(+ 3,− 6)....,+ 3	+0.97
566...	2.4	16.13	− 1,− 2,....,+ 3	15.17	(0, 0)....,....	+0.96
568...	3.9	16.16	− 6,+ 2,+ 5,....	15.44	(+ 1,− 2)....,....	+0.72
573...	3.4	15.28	− 3,− 7,....,+10	14.62	....,−17,+ 5,.... (....,+11)	+0.66
573*a*..	3.3	17.19	(−11,+11)....,....	16.67	(+21,−21)....,....	+0.52
578...	2.0	16.18	+ 4,− 3,....,....	15.28	(+ 2,− 6)....,+ 4	+0.90
581...	1.6	16.35	− 1,+ 2,− 2,....	15.34	(+ 3,− 4)....,....	+1.01
589...	1.5	13.71	0, 0,....,....	12.80	− 2,+13,−10,....	+0.91
590...	3.5	16.00	−14,+22,....,− 8	15.17	(− 5,+ 5)....,....	+0.83
590*a*..	3.7	17.11	(− 3,+ 2)....,....	16.61	(−11,+11)....,....	+0.50
594...	10.4	15.39	−17,+17,....,....	14.85	(− 3,+ 3)....,....	+0.54
595...	7.9	15.54	−15,+15,....,....	15.40	(− 8,+ 7)....,....	+0.14

TABLE II—*Continued*

NUMBER	DISTANCE	PHOTOGRAPHIC		PHOTO-VISUAL		COLOR-INDEX
		Mag.	Residuals	Mag.	Residuals	
595b*.	7′.4	17.37:	(...., m)....,....	16.92	−22,+22,....,....	+0.45:
596...	2.0	15.80	+ 6,+10,....,−15	15.12	(0, 0)....,....	+0.68
603...	1.8	15.69	+17,+17,−34,....	15.60	(− 2,+ 1)....,+ 2	+0.09
605...	2.3	15.86	+ 6,+ 9,−14,....	15.31	(+11,−11)....,....	+0.55
605a..	2.3	17.10	(− 6,+ 7)....,....	16.48	(+ 2,− 2)....,....	+0.62
606...	1.9	15.64	+22,+ 9,− 32,...	15.47	(0,− 5)....,+ 6	+0.17
609†..	4.1	15.66	− 4,+ 7,....,− 2	15.70	(− 3,+ 3)....,....	−0.04
609a..	4.0	17.42	(−11,+10)....,....	16.94	(− 1,+ 1)....,....	+0.48
609b..	4.3	17.53	(− 5,+ 2)....,....	17.31	(+ 9,− 4)....,....	+0.21
612‡..	1.3	13.96	....,....,− 2,+ 2	12.58	....,− 9,....,....	+1.38
621...	3.1	15.07	+ 1,+ 2,....,− 2	13.97	+ 3,+ 1,− 4,....	+1.10
621a..	3.2	16.92	(− 2,+ 1)....,....	16.26	(− 2,+ 3)....,....	+0.66
621b..	3.2	17.15	(−11,+11)....,....	16.80	(− 5,+ 4)....,....	+0.35
621d..	3.2	17.79:	(− 4,+ 4)....,....	17.38	(...., m)....,....	+0.41:
628...	1.6	16.37	− 3, 0,+ 4,....	15.52	(+ 6,− 7)....,....	+0.85
628a..	1.6	16.34	(+ 3,− 2)....,....	15.38	(+15,−16)....,....	+0.96
632...	5.1	15.62	+ 5,+20,−25,....	15.38	(+ 9,−10)....,....	+0 24
639...	2.1	16.06	− 2,+ 9,....,− 8	15.18	(− 6,+ 7)....,....	+0.88
640†..	2.7	14.40	− 1,+16,−11,− 3	13.22	−10,+ 1,+ 9,....	+1.18
640a..	3.0	17.15	(+ 6,− 6)....,....	16.85	(− 6,+ 6)....,....	+0.30
640b..	3.2	17.05	(+16,−16)....,....	16.48	(+ 2,− 2)....,....	+0.57
640c..	3.0	17.50	(−15,+15)....,....	16.98	(− 5,+ 5)....,....	+0.52
640d..	3.1	17.32	(− 1,+ 2)....,....	16.98	(−23,+22)....,....	+0.34
640e..	3.2	17.30	(−12,+12)....,....	17.04	(−16,+16)....,....	+0.26
640f...	2.8	17.42	(− 7,+ 7)....,....	17.17	(...., m)....,....	+0.25
649...	4.1	15.98	+14,− 3,− 10,....	15.35	(+ 2,− 2)....,....	+0.63
649a..	4.3	17.02	(+ 2,− 1)....,....	16.71	(− 1,+ 1)....,....	+0.31
649b..	4.3	17.16	(− 2,+ 1)....,....	16.82	(− 3,+ 2)....,....	+0.34
649c..	3.8	17.17	(− 9,+ 9)....,....	16.74	(+10,− 9)....,....	+0.43
659...	4.0	15.52	− 6,+ 4,....,+ 2	15.49	(− 7,+ 7)....,....	+0.03
665...	2.0	15.88	+10,+16,−26,....	15.84	(+ 6,− 5)....,....	+0.04
665a..	2.1	17.28	(− 3,+ 2)....,....	16.90	(+14,−15)....,....	+0.38
667*..	1.5	16.14	− 4,....,+ 3,....	.....	....,....,....,....	......
674...	1.8	16.24	+21,−20,....,....	15.53	(m,....)....,....	+0.71
675...	2.5	15.79	+ 4,+ 7,....,−11	16.03	(−13,+13)....,....	−0.24
680...	1.6	14.75	+ 4,− 2,....,− 3	13.66	− 2,−13,+16,....	+1.09
680a..	1.6	15.80	−11,+12,....,....	15.58	(+ 6,− 5)....,....	+0.22
680b..	1.6	15.78	(0,− 1)....,....	15.58	(− 5,+ 6)....,....	+0.20
680c..	1.7	16.37	(+ 2,− 2)....,....	15.60	(− 5,+ 4)....,....	+0.77
700a..	2.4	16.40	(− 3,+ 4)....,....	15.76	(+ 8,− 9)....,....	+0.64
701...	5.0	16.45	+14,−15,....,+ 1	15.68	(− 7,+ 8)....,....	+0.77
701a..	6.0	16.72	(− 2,+ 1)....,....	16.08	(− 5,+ 5)....,....	+0.64
701b..	5.2	17.33	(− 2,+ 2)....,....	16.88	(− 4,+ 3)....,....	+0.45
701c..	5.0	17.35	(− 7,+ 7)....,....	17.06	(−18,+18)....,....	+0.29
701d..	5.0	17.36	(−11,+10)....,....	16.94	(−15,+16)....,....	+0.42
706...	1.5	14.06	−14,+ 5,....,+10	12.90	+14,− 1,−12,....	+1.16
707...	1.8	16.73	+12,− 1,....,−11	15.84	(− 3,+ 3)....,....	+0.89
708...	1.9	15.30	+16,−17,....,− 1	15.43	(−16,+16)....,....	−0.13
709...	11.4	14.26	−16,+16,....,....	14.13	(+ 7,− 7)....,....	+0.13
713a..	9.0	.....	....,....,....,....	16.64	(−14,+14)....,....	......
724...	2.1	16.74	− 2,+ 3,....,....	16.03	(−10,+10)....,....	+0.71
730...	1.6	16.14	....,+ 1,− 1,....	15.15	(+ 2,−15)....,+13	+0.99

TABLE II—*Continued*

NUMBER	DISTANCE	PHOTOGRAPHIC		PHOTO-VISUAL		COLOR-INDEX
		Mag.	Residuals	Mag.	Residuals	
730*a*..	1′6	17.70	(−14,+13)....,....	16.94	(−10,+ 9)....,....	+0.76
738...	1.6	16.70	−11,+10,....,....	16.76	(+12,−13)....,....	−0.06
739...	4.9	15.55	−12,+14,....,− 1	15.50	(− 5,+ 6)....,....	+0.05
739*a*..	4.7	16.64	(− 2,+ 2)....,....	16.12	(+ 6,− 6)....,....	+0.52
739*b*..	5.2	16.81	(0, 0)....,....	16.32	(+11,−12)....,....	+0.49
740†..	3.5	14.10	− 8,+ 4,+ 2,+ 1	13.40	−13,+ 6,+ 6,....	+0.70
740*a*..	3.3	17.24	(−14,+14)....,....	17.25	(−27,+13)....,....	-0.01
740*b*..	3.3	17.40	(− 2,+ 2)....,....	17.14	(−16,+17)....,....	+0.26
752...	1.2	13.06	....,....,− 6,+ 7	12.54	....,− 7,....,....	+1.42
753...	1.5	15.09	−11,+ 4,....,+ 8	13.95	− 2,+ 1,+ 2,....	+1.14
758...	1.6	16.07	+ 3,+ 8,−12,....	15.04	(+ 8,−16)....,+ 9	+1.03
758*a*..	1.7	17.58	(−10,+11)....,....	17.10	(−22,+21)....,....	+0.48
759*a**.	2.2	.....	...., ...,....,....	16.51	(− 5,+ 5)....,....	......
767...	2.0	15.89	−10,+19,....,−10	15.42	(−12,+11)....,....	+0.47
777...	2.4	16.94	− 1, 0,....,....	16.42	(+ 4,− 4)....,....	+0.52
801...	1.3	15.59	+ 1,+23,−24,....	15.47	(+11,−11)....,....	+0.12
801*a* .	1.4	17.06	(− 2,+ 3)....,....	10.25	(− 1,+ 1)....,....	+0.81
801*b*..	1.4	17.47	(+ 1,− 1)....,....	17.14	(−10,+10)....,....	+0.33
801*c*..	1.5	......	....,....,....,....	17.24	(...., m)....,....	......
805...	1.6	15.57	− 3,− 1,....,+ 4	15.57	(− 4,+ 4)....,....	0
810...	2.2	16.06	+ 1,− 2,....,....	15.98	(− 8,+ 8)....,....	+0.08
811...	1.6	15.88	+19,−15,....,− 3	15.14	(+ 8,− 8)....,....	+0.74
832...	2.8	15.23	− 8,+ 2,....,+ 5	14.47	....,− 5,....,.... (....,+ 5)	+0.76
837...	3.9	13.83	− 8,−17,+20,+ 4	12.47	+ 4,+ 9,−12,....	+1.36
837*b*..	4.0	17.13	(−13,+13)....,....	16.75	(0, 0)....,....	+0.38
841...	5.6	15.59	−16,+ 6,+13,− 1	15.36	(+ 6,− 6)....,....	+0.23
845...	1.8	15.62	+14,+28,−41,....	15.58	(+ 6,+ 3)....,− 8	+0.04
845*a*..	1.8	17.26	(−16,+16)....,....	16.52	(+13,−14)....,....	+0.74
853...	4.0	14.56	−19,+21,− 2,....	13.63	− 8, 0,+ 7,....	+0.93
872...	3.4	15.18	− 7,− 5,− 3,+13	14.40	−17,− 8, 0,.... (....,+27)	+0.78
879...	1.5	15.58	− 8,+ 7,...., 0	15.10	(+20,....)−19,....	+0.48
882...	1.7	15.99	+16, 0,−16,....	15.14	(+ 3,....)....,− 3	+0.85
883...	3.7	16.00	− 2,− 1,+17,−15	15.40	(+ 7,− 7)....,....	+0.60
885...	..1.9	14.47	− 6,+ 9,− 4,....	13.27	− 6,+ 2,+ 4,....	+1.20
885*a*..	2.0	17.22	(− 8,+ 8)....,....	16.54	(+ 3,− 3)....,....	+0.68
900...	2.1	16.24	+ 1,− 2,....,....	15.28	(− 3,+ 2)....,....	+0.96
900*a*..	2.4	16.98	(+ 6,− 5)....,....	16.44	(+ 9,− 9)....,....	+0.54
900*b*..	2.5	17.41	(+ 4,− 4)....,....	17.20	(...., m)....,....	+0.21
902...	2.4	15.85	+ 4,+10,....,−13	15.26	(− 1,+ 2)....,....	+0.59
902*a*..	2.4	17.34	(− 3,+ 3)....,....	16.68	(+ 7,− 8)....,....	+0.66
902*b*..	2.3	17.50	(−12,+13)....,....	17.02	(− 4,+ 5)....,....	+0.48
925...	2.8	14.29	−11,− 2,+14,....	12.95	−11,− 2,+12,....	+1.34
925*a*..	2.8	16.28	(+ 2,− 2)....,....	15.54	(− 4,+ 5)....,....	+0.74
925*b*..	2.9	17.66	(−18,+17)....,....	17.24	(− 2,+ 3)....,....	+0.42
925*c*..	3.0	17.46	(− 8,+ 9)....,....	16.92	(−15,+15)....,....	+0.54
925*d**.	2.9	17.31	(− 3,+ 3)....,....	16.96	(−21,+21)....,....	+0.35
925*e*..	2.9	17.38	(− 7,+ 8)....,....	17.11	(−18,+ 9)....,....	+0.27
926*..	4.2	14.65	m,....,....,....	14.43	....,− 5,+ 5,....	+0.22
926*a*..	4.2	17.10	(− 6,+ 7)....,....	16.74	(+14,−28)....,....	+0.36
935...	10.0	15.77	+27,−12,−15,....	14.70	(....,+12)−11,....	+1.07

TABLE II—*Continued*

Number	Distance	Photographic		Photo-visual		Color-Index
		Mag.	Residuals	Mag.	Residuals	
945..	1′.6	16.36	− 2,+ 1,....,....	15.50	(+ 8,− 8)...., 0	+0.86
945*a*.	1.6	16.12	(0,− 1)....,....	15.21	(+ 1,− 1)....,....	+0.91
945*b*.	1.7	16.60	(+ 2,− 2)....,....	15.58	(0,+ 1)....,....	+1.02
952..	1.7	16.16	− 4,+ 6,....,− 3	16.19	(− 7,+ 7)....,....	−0.03
953..	1.5	15.84	−11,+11,....,....	15.22:	(....,+ 8)−17,....	+0.62:
955..	10.1	14.92	+12,− 7,− 4,....	14.55	(...., 0) 0,....	+0.37
962..	10.0	15.79	+31,−14,−17,....	14.86	(....,+ 8)− 8,....	+0.93
969..	8.5	16.15	0, 0,....,....	15.76	(− 7,+ 8)....,....	+0.39
974..	7.7	16.10	0,+ 1,....,....	14.97	(+ 6,− 6)....,....	+1.13
974*a*.	7.0	16.78	(+ 1,− 1)....,....	16.26	(−11,+ 6)....,....	+0.52
982‡.	1.3	15.98	....,....,− 9,+ 9	15.32	....,....,....,....	+0.66
1000..	3.0	14.08	−20,− 9,+15,+12	12.83	+13,− 7,− 5,....	+1.25
1000*a*.	2.8	17.45	(−14,+14)....,....	16.88	(0, 0)....,....	+0.55
1009..	4.0	15.67	− 4,+19,−16,....	15.76	(+ 2,− 3)....,....	−0.09
1012..	1.7	15.72	− 2,+ 1,...., 0	15.64	(0, 0)....,....	+0.08
1014..	1.9	15.69	+ 4,+13,−18,....	14.96	(+12,−11)....,....	+0.73
1017..	6.6	16.39	+ 9,+ 2,....,−12	15.96	(−15,+14)....,....	+0.43
1022..	2.0	16.66	−16,+16,....,....	16.44	(+ 2,− 3)....,....	+0.22
1022*a*.	2.1	16.82	(− 3,+ 3)....,....	16.97	(−13,+13)....,....	−0.15
1028..	2.3	15.66	−12,+11,....,....	14.73	....,− 6,+ 8,.... (....,− 3)	+0.93
1028*a*.	2.3	17.27	(+18,−18)....,....	16.92	(+12,−11)....,....	+0.35
1028*b*.	2.2	16.54	(−17,+16)....,....	15.96	(− 6,+ 7)....,....	+0.58
1028*c*.	2.2	17.46	(...., m)....,....	17.07	(...., m)....,....	+0.39
1039..	2.0	15.02	+ 2,− 9,....,+ 7	13.96	−11,+ 5,+ 5,....	+1.06
1047..	1.8	15.95	0,+ 4,....,− 3	14.99	(− 1,+ 1)....,....	+0.96
1050..	1.6	15.38	+16,−17,....,....	14.17	....,...., m,....	+1.21
1055†.	4.6	15.95	− 7,+ 7,....,+ 1	15.26	(+14,−14)....,....	+0.69
1061..	2.1	16.64	−14,+13,....,....	15.88	(− 1,+ 2)....,....	+0.76
1062..	1.8	15.35	+19,− 6,−14,....	14.60	(....,− 5)+ 5,....	+0.75
1063..	2.2	16.08	− 7,+ 3,....,+ 5	15.14	(+ 3,− 2)....,....	+0.94
1064..	1.8	16.23	−13,+14,....,− 2	15.25	(− 5,+ 5)....,....	+0.98
1070..	2.1	16.19	− 7,+ 3,....,+ 4	16.20	(− 5,+ 6)....,....	−0.01
1076..	1.8	16.12	− 2,+ 3,....,....	15.56	(− 9,+ 8)....,....	+0.56
1076*a*.	1.9	17.08	(− 8,+ 9)....,....	16.16	(−10,+10)....,....	+0.92
1086..	2.0	16.42	− 8,+ 9,....,....	15.66	(− 2,+ 1)....,....	+0.76
1089..	2.2	15.18	+ 7,+ 3,−11,....	14.09	....,...., m,....	+1.09
1090*a*.	2.1	17.08	(− 8,+ 9)....,....	16.48	(+13,−13)....,....	+0.60
1090*b*.	2.3	17.08	(0,+ 1)....,....	16.47	(+ 6,− 6)....,....	+0.61
1090*c*.	2.3	16.34	(− 4,+ 4)....,....	15.60	(− 5,+ 4)....,....	+0.74
1098..	1.8	16.48	+ 4,− 3,....,....,	15.64	(...., m)....,....	+0.84
1101..	4.4	15.90	− 1, 0,....,....	14.88	(+15,−15)....,....	+1.02
1120..	2.2	16.12	+ 5,− 4,....,....	15.96	(− 6,+ 7)....,....	+0.16
1120*a*.	2.3	17.02	(− 2,+ 3)....,....	16.58	(−12,+11)....,....	+0.44
1123..	2.5	15.52	− 2,+21,−20,....	15.52	(+ 9,−10)....,....	0
1123*a*.	2.5	17.32	(− 1,+ 2)....,....	17.03	(...., m)....,....	+0.29
1123*b*.	2.5	17.24	(+11,−11)....,....	16.76	(+ 8,− 7)....,....	+0.48
1123*c*.	2.4	17.56	(m,....)....,....	17.02	(− 4,+ 5)....,....	+0.54
1127..	1.6	13.92	− 9,+ 7,....,+ 3	12.62	....,− 1, 0,....	+1.30
1127*a*.	1.7	16.52	(−13,+14)....,....	15.80	(− 5,+ 4)....,....	+0.72
1128..	3.6	14.08	−20,− 5,+15,+12	14.68	....,−17,+ 1,− 1 (....,+17)	−0.60

TABLE II—*Continued*

NUMBER	DISTANCE	PHOTOGRAPHIC		PHOTO-VISUAL		COLOR-INDEX
		Mag.	Residuals	Mag.	Residuals	
1128*a*.	3′.5	17.08	(− 4,+ 5)....,....	16.51	(+ 2,− 2)....,....	+0.57
1128*b*.	3.4	17.32	(+ 3,− 2)....,....	16.82	(+ 6,− 7)....,....	+0.50
1128*c*.	3.8	.....	....,....,....,....	17.12	(+10,− 5)....,....	......
1130..	3.2	15.53	− 3,+12,....,− 8	15.44	(−12,+12)....,....	+0.09
1131†.	4.0	15.81	− 3,+ 7,− 9,+ 5	15.48	(− 6,+ 5)....,....	+0.33
1131*a*.	4.0	17.30	(+ 1, 0)....,....	16.80	(−15,+15)....,....	+0.50
1131*b*.	3.9	17.31	(− 6,+ 6)....,....	16.72	(+ 3,− 3)....,....	+0.59
1137..	2.2	17.05	m,....,....,....	16.62	(−23,+22)....,....	+0.43
1140..	4.4	15.89	+12,− 7,....,− 4	15.06	(+ 2,− 3)....,....	+0.83
1140*a*.	4.5	16.96	(−20,+21)....,....	16.54	(+11,−10)....,....	+0.42
1140*b*.	4.3	17.34	(+ 4,− 4)....,....	17.02	(−14,+15)....,....	+0.32
1140*c*.	4.5	17.38	(− 3,+ 4)....,....	17.10	(...., m)....,....	+0.28
1140*d*.	4.5	17.29	(− 8,+ 8)....,....	16.84	(...., m)....,....	+0.45
1141..	3.0	16.21	− 4,− 3,+ 8,....	15.31	(+19,− 3)....,−15	+0.90
1143..	2.2	15.71	−11,+15,....,− 3	15.02	(+ 6,− 5)....,....	+0.69
1146..	2.9	15.64	+25,+ 9,−34,....	15.58	(0,+ 3)....,− 2	+0.06
1147..	4.6	16.10	+ 5,+ 1,....,− 5	15.53	(− 3,+ 3)....,....	+0.57
1148..	2.6	15.86	+ 3,+ 9,....,−11	15.28	(− 1, 0)....,....	+0.58
1149..	2.0	16.50	−16,+13,....,+ 4	15.70	(+ 5,− 6)....,....	+0.80
1149*a*.	2.0	17.58	(−16,+16)....,....	17.14	(...., m)....,....	+0.44
1149*b*.	1.9	17.54	(−11,+ 5)....,....	16.56	(+ 1,− 2)....,....	+0.98
1149*c*.	2.1	17.37	(−12,+12)....,....	16.87	(+ 6,− 6)....,....	+0.50
1149*d*.	2.1	17.38	(+ 4,− 4)....,....	16.84	(+ 9,− 9)....,....	+0.54
1149*e*.	2.2	17.46	(− 1, 0)....,....	16.96	(− 8,+ 7)....,....	+0.50
1149*f**	2.3	.....	....,....,....,....	17.24	(...., m)....,....	......
1140*g**	2.3	.....	....,....,....,....	17.20	(...., m)....,....	......
1154..	2.5	15.89	+15,+ 6,....,−21	15.38	(−11,+12)....,....	+0.51
1154*a*.	2.5	17.21	+ 4,− 4,....,....	16.44	(+ 9,− 9)....,....	+0.77
1158..	6.2	16.80	...., m,....,....	16.56	(− 3,+ 2)....,....	+0.24
1162..	7.7	16.08	− 4,+ 3,....,+ 2	15.30	(+ 2,− 2)....,....	+0.78
1168*.	2.0	16.12	+ 3,+18,−21,....	14.87	....,− 9,+ 6,.... (....,+ 4)	+1.25
1170*.	2.0	15.57	+19,+12,−32,....	14.54	....,+ 5,− 6,....	+1.03
1172..	2.8	15.49	− 6,+ 2,....,+ 5	14.62	(....,− 1)+ 2,....	+0.87
1172*a*.	2.9	16.31	(− 1,+ 1)....,....	15.56	(− 3,+ 3)....,....	+0.75
1172*b*.	3.0	17.28	(− 7,+ 6)....,....	16.68	(+ 2,− 1)....,....	+0.60
1172*c*.	2.8	17.08	(0,+ 1)....,....	16.41	(− 5,+ 5)....,....	+0.67
1173..	2.4	15.35	0,+16,−17,....	14.69	....,...., m,....	+0.66
1174..	1.8	16.56	− 6,+ 7,....,....	15.66	(− 2,+ 1)....,....	+0.90
1175..	2.7	15.37	+ 9,+ 1,−10,....	14.34	(....,− 8)+ 9,....	+1.03
1175*a*.	2.7	17.00	(0,+ 1)....,....	.....	....,....,....,....	......
1178..	5.3	16.22	+ 3,− 4,....,....	15.60	(+ 7,− 7)....,....	+0.62
1178*a*.	5.0	17.09	(−12,+12)....,....	16.87	(− 8,+ 8)....,....	+0.22
1178*b*.	4.8	17.01	(− 4,+ 4)....,....	16.62	(+ 3,− 2)....,....	+0.39
1178*c*.	5.4	16.96	(+ 4,− 3)....,....	16.62	(−19,+19)....,....	+0.34
1178*d*.	5.4	17.21	(+ 4,− 4)....,....	17.20	(...., m)....,....	+0.01
1181*a*.	3.0	17.32	(−11,+10)....,....	16.66	(−16,+15)....,....	+0.66
1181*b*.	3.1	17.10	(− 2,+ 3)....,....	16.48	(+ 2,− 2)....,....	+0.62
1182..	2.2	16.18	+ 2,− 3,....,....	15.14	(+ 3,− 2)....,....	+1.04
1186..	2.4	16.01	− 3,+10,....,− 6	15.32	(+ 8,− 7)....,....	+0.69
1192..	2.0	16.22	− 5,+ 4,....,+ 1	15.39	(...., m)....,....	+0.83
1199..	2.8	15.55	− 1,− 4,....,+ 6	14.76	(....,+ 6)− 6,....	+0.79

TABLE II—*Continued*

Number	Distance	Photographic		Photo-visual		Color-Index
		Mag.	Residuals	Mag.	Residuals	
1201*a*.	3′6	17.49:	(...., m)....,....	16.98	(0,+ 1)....,....	+0.51:
1201*b*.	3.6	17.48	(− 3,+ 1)....,....	17.05	(−26,+26)....,....	+0.43
1201*c**	3.5	17.04:	(m,....)....,....	17.31:	(...., m)....,....	−0.27:
1201*d**	3.5	17.35:	(m,....)....,....	17.10	(−22,+21)....,....	+0.25:
1203..	2.7	14.40	−14,− 1,....,+14	13.08	+ 4,− 3,− 2,....	+1.32
1204..	2.6	16.02	....,...., m,....	15.22	(− 2,+ 3)....,....	+0.80
1205..	2.2	16.86	− 9,+ 8,....,....	16.68	(+ 7,− 8)....,....	+0.18
1205*a*.	2.3	.....	....,....,....,....	17.00	(− 2,+ 3)....,....	......
1206..	1.8	16.15	−11,+11,....,....	15.20	(− 3,+ 2)....,....	+0.95
1206*a*.	1.8	17.00	(0,+ 1)....,....	16.08	(−11,+12)....,....	+0.92
1206*b*.	1.7	16.32	(− 2,+ 3)....,....	15.40	(+ 5,− 4)....,....	+0.92
1206*c*.	1.8	16.04	(− 6,+ 7)....,....	15.36	(+ 1, 0)....,....	+0.68
1208..	2.0	14.40	−14,+ 3,....,+11	13.17	0,+ 2,− 2,....	+1.23
1210..	6.4	16.00	+ 4,− 5,....,....	15.57	(+ 4,− 4)....,....	+0.43
1211..	1.9	15.82	+13,−14,+ 9,−10	15.12	(+10,− 9)....,....	+0.70
1212..	2.0	15.34	+16,− 5,−11,....	14.57	....,+ 2,+13,.... (....,−15)	+0.77
1213..	2.0	15.36	+10,+ 2,−13,....	15.12	(+13,−12)....,....	+0.24
1214..	1.8	14.40	−27,+12,+14,....	13.18	+ 9,−13,+ 4,....	+1.22
1215..	1.9	16.02	+ 2,− 3,....,....	15.75	(m,....)....,....	+0.27
1216..	1.9	16.61	−14,+14,....,....	15.86	(− 2,+ 1)....,....	+0.75
1217..	1.8	14.86	+12,−17,+ 1,+ 5	13.69	...., m,....,....	+1.17
1218..	2.5	16.70	−11,+10,....,....	15.98	(− 5,+ 5)....,....	+0.72
1218*a*.	2.5	17.30	(− 5,+ 4)....,....	16.65	(− 4,+ 4)....,....	+0.65
1218*b*.	2.4	17.31	(− 6,+ 6)....,....	16.84	(+ 9,− 9)....,....	+0.47
1219..	1.9	14.04	− 3,−12,+16,....	12.64	+11,−13,+ 2,....	+1.40
1222*a*.	2.0	17.40	(− 9,+ 9)....,....	16.65	(+14,−14)....,....	+0.75
1222*b*.	2.1	17.22	(−12,+12)....,....	16.44	(+ 2,− 3)....,....	+0.78
1222*c*.	2.2	17.36	(+ 9,−10)....,....	17.03	(...., m)....,....	+0.33
1223..	5.3	16.61	+ 9,− 1,....,− 7	15.82	(− 4,+ 5)....,....	+0.79
1223*a*.	5.1	17.10	(−10,+11)....,....	16.90	(− 2,+ 1)....,....	+0.20
1223*b*.	5.4	17.28	(+ 7,− 7)....,....	16.92	(−27,+28)....,....	+0.36
1224..	2.9	14.78	+ 5,− 9,....,+ 5	13.57	+ 4,− 5,+ 1,....	+1.21
1225..	1.9	15.33	+ 6,− 4,− 3,....	14.46	....,− 8,+11,.... (....,− 4)	+0.87
1225*a*.	2.0	17.04	(− 4,+ 3)....,....	16.44	(+ 6,− 6)....,....	+0.60
1225*b*.	2.0	17.01	(− 8,+ 8)....,....	16.36	(+10,−10)....,....	+0.65
1225*c*.	1.9	17.18	(− 8,+ 7)....,....	16.50	(m,....)....,....	+0.68
1226..	2.1	16.02	− 1,+ 2,....,....	15.47	(+11,−11)....,....	+0.55
1227*.	4.0	16.36	+ 6,− 6,....,....	15.57	(− 2,+ 2)....,....	+0.79
1227*a*.	4.1	16.98	(+ 6,− 5)....,....	16.31	(−10,+10)....,....	+0.67
1227*b*.	4.1	17.28	(− 3,+ 2)....,....	17.00	(+ 4,− 5)....,....	+0.28
1227*c*.	4.0	17.40	(− 5,+ 6)....,....	16.94	(− 1,+ 1)....,....	+0.46
1227*d*.	3.8	17.34	(− 9,+ 8)....,....	17.12	(− 2,+ 2)....,....	+0.22
1229..	2.1	15.63	− 9,+ 9,....,....	14.64	(....,+ 3)− 3,....	+0.99
1230..	2.3	16.71	+ 6,−11,....,+ 6	16.03	(−13,+13)....,....	+0.68
1235..	2.2	16.31	− 4,+ 4,....,....	15.24	(− 4,+ 4)....,....	+1.07
1236..	2.0	15.35	+15,− 6,− 8,....	14.32	(....,+ 1) 0,....	+1.03
1236*a*.	1.9	16.52	(+10,−11)....,....	15.71	(+ 1,− 1)....,....	+0.81
1238..	2.1	15.78	− 8,+ 8,....,....	15.64	(0, 0)....,....	+0.14
1239..	2.2	15.24	+ 1,+ 5,− 6,....	14.56	....,....,− 6,+ 7	+0.68
1240..	3.0	15.84	−11,+11,....,....	15.22	(− 5,+ 6)....,....	+0.62

TABLE II—*Continued*

Number	Distance	Photographic		Photo-visual		Color-Index
		Mag.	Residuals	Mag.	Residuals	
1241*.	2′.1	15.00	+ 8,+21,−29,....	13.70	....,− 4,+ 5,....	+1.30
1242..	2.1	15.98	+ 3,+ 5,− 7,....	15.77	(+ 7,− 7)....,....	+0.21
1242*a*.	2.3	16.55	(+11,−11)....,....	15.68	(+ 4,− 4)....,....	+0.87
1243..	2.8	16.37	−10,− 7,+15,+ 1	15.60	(− 5,+ 4)....,....	+0.77
1243*a*.	2.8	16.67	(+ 5,− 5)....,....	16.24	(0,− 1)....,....	+0.43
1244*.	2.1	15.79	− 3,+25,−21,....	14.59	....,−32,+ 2,.... (....,+14)	+1.20
1244*a*.	2.1	17.16	(− 2,+ 1)....,....	16.42	(− 3,+ 4)....,....	+0.74
1246..	2.5	15.01	0, 0,....,....	14.01	+ 4,− 3,− 2,....	+1.00
1247..	2.2	15.81	−14,+14,....,....	15.70	(− 1, 0)....,....	+0.11
1247*a*.	2.4	16.94	(+ 6,− 5)....,....	16.34	(− 7,+ 7)....,....	+0.60
1247*b*.	2.3	17.04	(0,+ 1)....,....	16.40	(− 7,+ 6)....,....	+0.64
1249..	2.4	16.18	+ 4,− 3,....,....	16.13	(−10,+10)....,....	+0.05
1250*a*.	5.6	16.94	(− 8,+ 7)....,....	16.28	(−10,+10)....,....	+0.66
1251..	7.1	16.50	0,+ 1,....,....	15.74	(− 2,+ 2)....,....	+0.76
1254..	7.4	15.82	+ 1, 0,....,....	15.57	(+ 4,− 4)....,....	+0.25
1254*a*.	7.5	16.01	(− 7,+ 7)....,....	15.62	(− 1,+ 2)....,....	+0.39
1255..	2.4	15.01	+ 6,−14,....,+ 7	15.48	(− 3,+ 2)....,....	+0.13
1258..	2.1	15.21	+ 4,+ 8,−12,....	14.26	(....,− 1)+ 1,....	+0.95
1260..	2.2	15.80	+ 6,− 7, 0,....	15.24	(− 2,+ 1)....,....	+0.56
1261..	3.2	15.30	+13,−13,− 7,+ 8	14.58	(....,+ 2)− 3,....	+0.72
1261*a*.	3.4	15.98	(− 7,+ 6)....,....	15.52	(+ 1,− 2)....,....	+0.46
1262..	2.2	15.43	− 8,+22,−13,....	15.30	(+ 2,− 2)....,....	+0.13
1263..	7.3	15.35	+ 4,−10,+ 6,....	15.38	(− 8,+ 9)....,....	−0.03
1264..	8.2	15.98	+ 8,− 8,....,....	15.36	(− 4,+ 3)....,....	+0.62
1265*a*.	3.4	16.84	(−12,+12)....,....	16.37	(− 1,+ 1)....,....	+0.47
1265*b*.	3.4	16.45	(− 8,+ 8)....,....	15.82	(+ 2,− 3)....,....	+0.63
1265*c*.	3.4	17.28	(− 7,+ 6)....,....	16.88	(− 4,+ 3)....,....	+0.40
1265*d*.	3.5	17.42	(− 7,+ 7)....,....	16.94	(− 6,+ 5)....,....	+0.48
1265*e*.	3.7	16.76	(− 6,+ 5)....,....	16.24	(+ 3,− 4)....,....	+0.52
1265*f*.	3.6	17.30	(+ 5,− 4)....,....	17.12	(−19,+19)....,....	+0.18
1265*g*.	3.5	15.96	(− 2,+ 1)....,....	15.08	(−10,+ 9)....,....	+0.88
1269..	6.0	14.73	+ 8,+ 8,−14,− 1	13.86	− 9,.... + 9,....	+0.87
1270..	6.5	14.85	−24,+20,....,+ 5	13.86	+ 1,− 5,+ 5,....	+0.99
1270*a*.	6.4	17.21	(−13,+13)....,....	16.84	(− 5,+ 4)....,....	+0.37
1270*b*.	6.4	17.02	(+ 6,− 6)....,....	16.84	(− 5,+ 4)....,....	+0.18
1271..	2.7	15.69	+20, 0,−18,− 1	14.68	....,+10,....,.... (....,− 9)	+1.01
1271*a*.	2.8	16.64	(+ 2,− 2)....,....	15.96	(− 6,+ 7)....,....	+0.68
1273..	2.8	14.53	−20,+ 3,+ 1,+15	13.29	+ 3, 0,− 4,....	+1.24
1274..	2.6	15.24	+ 1,− 7,− 6,+14	14.57	....,− 2,− 3,.... (....,+ 4)	+0.67
1275..	5.1	16.22	− 2,− 7,+ 7,+ 1	15.37	(−10,+10)....,....	+0.85
1278..	2.4	16.24	− 7,+ 6,....,....	15.29	(−14,+ 4)....,+11	+0.95
1278*a*.	2.3	17.61	(+17,− 9)....,....	17.24	(...., m)....,....	+0.37
1279..	2.4	15.94	− 5,....,+ 4,....	15.09	(−11,+11)....,....	+0.85
1280..	3.1	16.75	+ 5,+ 2,....,− 7	16.34	(+ 2,− 2)....,....	+0.41
1280*a*.	3.0	17.36	(− 5,+ 6)....,....	16.84	(−14,+15)....,....	+0.52
1280*b*.	2.9	17.36	(− 1,+ 1)....,....	17.21	(+ 1,− 1)....,....	+0.15
1283..	2.6	16.04	− 6,+ 7,− 2,....	15.03	(+12,−12)....,....	+1.01
1283*a*.	2.7	16.67	(+ 5,− 5)....,....	16.08	(−15,+15)....,....	+0.59
1285..	2.8	15.97	− 8,+ 7,+ 1,+ 1	15.96	(+ 1, 0)....,....	+0.01

TABLE II—*Continued*

NUMBER	DISTANCE	PHOTOGRAPHIC		PHOTO-VISUAL		COLOR-INDEX
		Mag.	Residuals	Mag.	Residuals	
1285*a*.	3′.1	17.35	(− 7,+ 7)....,....	17.23	(+ 6,− 6)....,....	+0.12
1285*b*.	3.2	17.34	(− 3,+ 3)....,....	17.08	(−10,+ 9)....,....	+0.26
1286..	2.5	16.30	− 3,+ 4,....,....	15.57	(− 7,+ 4)....,+ 2	+0.73
1287..	4.4	15.89	+ 6,+ 1,− 6,....	15.50	(+ 3,+ 6)....,−10	+0.39
1287*a*.	4.4	17.13	(+ 8,− 8)....,....	16.82	(− 3,+ 2)....,....	+0.31
1289..	3.2	16.24	−14,+ 6,....,+ 8	15.38	(−11,+12)....,....	+0.86
1289*a*.	3.1	16.34	(0,+ 1)....,....	15.94	(− 7,+ 6)....,....	+0.40
1290..	2.8	15.46	+17,+ 1,−19,....	14.62	(0,− 1)....,....	+0.84
1290*a*.	3.0	17.34	(− 9,+ 8)....,....	16.90	(− 2,+ 1)....,....	+0.44
1290*b*.	3.0	17.48	(0,+ 1)....,....	16.84	(− 5,+ 4)....,....	+0.64
1292*a*.	2.5	17.36	(+ 2,− 2)....,....	16.86	(+18,−17)....,....	+0.50
1292*b*.	2.5	17.49	(+ 3,− 3)....,....	17.22	(− 6,+ 5)....,....	+0.27
1293..	3.8	16.24	+10,− 9,....,....	15.54	(− 1,+ 2)....,....	+0.70
1293*b*.	3.9	17.34	(− 3,+ 3)....,....	16.94	(−10,+ 9)....,....	+0.40
1293*c*.	3.9	16.27	(+10,−10)....,....	15.58	(0,+ 1)....,....	+0.69
1294..	4.4	15.76	− 9,+10,....,− 1	15.25	(− 3,+ 3)....,....	+0.51
1294*a*.	4.3	17.24	(− 6,+ 6)....,....	16.81	(+ 7,− 7)....,....	+0.43
1294*b*.	4.1	17.38	(− 3,+ 4)....,....	17.05	(−12,+12)....,....	+0.33
1294*c*.	4.1	17.64:	(+ 1,− 1)....,....	17.12	(−14,+15)....,....	+0.52:
1296..	2.5	15.34	+16,− 9,− 7,....	15.18	(+ 7,− 6)....,....	+0.16
1296*a*.	2.5	15.81	(0, 0)....,....	15.84	(0, 0)....,....	−0.03
1296*b*.	2.7	17.45	(− 7,+ 7)....,....	17.20	(...., m)....,....	+0.25
1296*c*.	2.7	17.42	(− 4,+ 4)....,....	17.10	(...., m)....,....	+0.32
1299..	4.0	15.78	− 8,− 9,+17,+ 1	15.37	(− 5,+ 5)....,....	+0.41
1299*a*.	4.1	16.92	(− 2,+ 1)....,....	16.36	(− 9,+ 8)....,....	+0.56
1300..	2.7	15.98	+ 9,+ 6,−15,....	15.32	(− 5,− 4)....,+ 8	+0.66
1301..	3.4	15.35	−10,−10,....,+19	14.57	(− 4,+ 4)....,....	+0.78
1302..	2.9	16.84	− 2,+ 1,....,....	16.03	(−13,+13)....,....	+0.81
1303..	4.7	15.98	0,− 8,+ 7,....	15.00	(+10,− 6)....,− 3	+0.98
1303*a*.	4.4	16.22	(− 2,+ 1)....,....	15.52	(− 2,+ 1)....,....	+0.70
1304..	2.8	16.33	− 1,+ 1,....,....	15.61	(...., m)....,....	+0.72
1304*a*.	2.9	16.59	(−37,+37)....,....	16.08	(−15,+15)....,....	+0.51
1304*b*.	2.9	17.31	(−10,+21)....,....	16.96	(−12,+11)....,....	+0.42
1304*c*.	2.8	17.15	(−15,+15)....,....	16.64	(−14,+14)....,....	+0.51
1304*d**	2.9	17.38:	(−28,+27)....,....	17.17	(...., m)....,....	+0.21:
1305..	4.6	15.22	− 4,−13,+ 2,+15	14.50	(....,+ 4)− 5,....	+0.72
1306..	6.6	15.92	0,− 2,+ 3,....	15.50	(0, 0)....,....	+0.42
1307*a*.	3.3	17.38	(−13,+14)....,....	17.20	(+ 4,− 3)....,....	+0.18
1309..	3.4	16.07	+ 5,−12,+ 6,....	16.00	(−13,+13)....,....	+0.07
1309*a*	3.6	17.16	(+12,−11)....,....	17.00	(−21,+20)....,....	+0.16
1310..	3.0	15.48	−13,+13,....,....	14.64	(+ 4,− 6)+ 3,....	+0.84
1312..	4.1	16.11	− 4,− 7,....,+12	15.32	(+ 3,− 4)....,....	+0.79
1313..	3.0	14.90	− 3,− 1,+ 3,....	13.86	− 6,+ 7,− 1,....	+1.04
1313*a*.	2.9	16.98	(+ 6,− 5)....,....	16.68	(+16,−17)....,....	+0.30
1314..	10.5	15.86	− 3,+ 4,....,....	15.22	(−10,+11)....,....	+0.64
1315..	3.2	15.25	+ 4, 0,− 4,....	14.43	(+12,−12)....,....	+0.82
1315*a*.	3.4	17.34	(− 3,+ 3)....,....	16.90	(− 2,+ 1)....,....	+0.44
1316..	3.5	15.90	+ 2, 0,− 2,....	15.46	(+ 1, −1)....,....	+0.44
1318..	8.0	15.68	−22,− 3,+20,+ 4	15.72	(−11,+12)....,....	−0.04
1318*a*.	7.8	16.38	(−18,+17)....,....	15.82	(− 7,+ 8)....,....	+0.56
1319..	3.1	15.94	+ 4,+ 1,− 6,....	15.48	(−11,+ 2)....,+ 8	+0.46
1319*a*.	3.0	17.32	(−14,+14)....,....	17.02	(− 4,+ 5)....,....	+0.30

TABLE II—*Continued*

Number	Distance	Photographic		Photo-visual		Color-Index
		Mag.	Residuals	Mag.	Residuals	
1319b.	3′.0	17.24	(− 3,+ 2)....,....	16.82	(−12,+13)....,....	+0.42
1322..	6.7	15.62	+ 1,+11,−11,....	15.81	(− 6,+ 6)....,....	−0.19
1323..	3.4	16.08	+ 4,− 4,....,....	15.24	(+ 1,− 2)....,....	+0.84
1324..	5.5	15.64	− 1,+ 1,....,+ 1	15.74	(− 7,+ 7)....,....	−0.10
1324a.	5.6	17.12	(− 2,+ 1)....,....	16.86	(− 2,+ 2)....,....	+0.26
1324b.	5.5	16.99	(− 2,+ 2)....,....	16.63	(− 6,+ 6)....,....	+0.36
1324c.	5.8	16.96	(+ 4,− 3)....,....	16.78	(− 3,+ 3)....,....	+0.18
1324d.	6.2	17.31	(− 3,+ 3)....,....	16.98	(−19,+19)....,....	+0.33
1325..	5.0	15.23	+ 9,− 6,− 2,....	14.45	....,...., m,....	+0.78
1327†.	5.9	16.17	− 7,− 5,....,+11	15.49	(− 4,+ 4)....,....	+0.68
1329..	3.4	15.93	+11,−11,....,....	15.50	(− 8,+ 9)....,....	+0.43
1329a.	3.2	17.04	(+ 4,− 3)....,....	16.46	(0, 0)....,....	+0.58
1329b.	3.2	17.32	(− 4,+ 5)....,....	17.15	(− 5,+ 5)....,....	+0.17
1331..	9.3	15.89	+ 3,− 3,....,....	15.15	(− 7,+ 7)....,....	+0.74
1331a.	9.5	16.06	(+ 6,− 5)....,....	15.46	(− 1,+ 1)....,....	+0.60
1332..	5.1	15.60	−10,+13,....,− 2	14.82	(− 5,+ 6)....,....	+0.78
1333..	3.9	16.48	−14,+15,....,....	15.74	(−10,+10)....,....	+0.74
1334..	3.8	16.12	+ 3,− 4,....,....	15.40	(− 3,+ 2)....,....	+0.72
1335..	3.5	15.60	− 6,+ 5,....,....	15.53	(− 8,+ 8)....,....	+0.07
1336..	4.3	16.26	+ 1, 0,....,....	15.56	(− 1, 0)....,....	+0.70
1338..	3.5	15.48	+15,−14,....,....	14.70	(− 8,− 9)....,+17	+0.78
1338a.	3.6	17.40	(− 5,+ 6)....,....	17.14	(− 4,+ 3)....,....	+0.26
1339..	5.9	15.90	+11,− 8,− 2,....	15.08	(0,+ 1)....,....	+0.82
1339a.	5.6	17.30	(+18,− 9)....,....	16.96	(−17,+18)....,....	+0.34
1340..	5.9	15.68	− 9,+ 9, 0,....	15.58	(− 3,+ 3)....,....	+0.10
1340a.	6.5	17.07	(−10,+10)....,....	16.81	(+ 7,− 3)....,....	+0.26
1340b.	6.4	17.08	(0,+ 1) ....,....	16.91	(−16,+16)....,....	+0.17
1342..	5.2	15.03	+ 8,+ 2,−10,....	14.08	− 5,+13,− 7,.... (0,....)	+0.95
1343a*	10.1	16.17	(...., m)....,....	16.69	(...., m)....,....	−0.52
1343b.	9.6	17.08	(0,+ 1)....,....	16.74	(− 4,+ 4)....,....	+0.34
1344*.	4.2	16.48	−16,+15,....,....	16.98	(− 5,+ 5)....,....	−0.50
1344a*	4.2	.....	....,....,....,....	17.27	(...., m)....,....	......
1345..	4.1	14.76	+ 7,− 7,....,....	13.62	− 9,....,+10,....	+1.14
1345a.	4.4	17.16	(−19,+18)....,....	16.78	(+ 1, 0)....,....	+0.38
1346..	10.0	11.80	+ 3,− 4,....,....	10.57	+36,− 5,−30,....	+1.23
1346a.	9.6	16.92	(−16,+17)....,....	16.51	(−12,+12)....,....	+0.41
1346b.	10.4	16.93	(− 3,+ 3)....,....	16.48	(−12,+12)....,....	+0.45
1347..	5.5	15.48	− 9,− 1’....,+10	15.50	(+ 5,− 5)....,....	−0.02
1347a†	5.7	16.79	− 2,+ 2,....,....	16.38	(− 2,+ 3)....,....	+0.41
1350..	4.1	15.89	+ 6,+ 1,+16,−24	15.29	(+ 1,− 1)....,....	+0.60
1352..	4.4	15.97	+ 4,− 2,− 1,....	16.02	(−15,+14)....,....	−0.05
1352a.	4.0	17.20	(− 2,+ 1)....,....	16.66	(−13,+12)....,....	+0.54
1354..	9.0	16.02	+ 8,− 7,....,....	15.42	(− 2,+ 3)....,....	+0.60
1354a.	9.0	17.20	(− 6,+ 6)....,....	16.76	(−23 +23)....,....	+0.44
1356*.	6.8	16.22	0, 0,....,....	16.10	(+51,−51)....,....	+0.12
1360..	4.4	14.73	+ 6,− 4,+ 2,− 5	13.69	−12,....,+12,....	+1.06
1360a.	4.1	17.40	(− 2,+ 2)....,....	17.26	(− 4,+ 5)....,....	+0.14
1360b.	4.0	17.22	(−14,+15)....,....	16.85	(−10,+10)....,....	+0.37
1361..	9.8	16.86	−11,+12,....,....	16.91	(...., m)....,....	−0.05
1362..	6.3	14.72	+ 3,−11,−10,+18	13.75	−10,+ 4,+ 6,....	+0.97

TABLE II—*Continued*

Number	Distance	Photographic		Photo-visual		Color-Index
		Mag.	Residuals	Mag.	Residuals	
1363..	4′.5	15.21	+ 1,− 4,+ 2,....	14.45	....,...., m,....	+0.76
1363*a*.	5.0	16.74	(− 4,+ 3)....,....	16.37	(− 1,+ 1)....,....	+0.37
1363*b*.	4.9	17.17	(+ 4,− 4)....,....	16.56	(− 6,+ 7)....,....	+0.61
1364..	4.7	15.96	− 7,−19,+18,+ 6	15.31	(−16,+16)....,....	+0.65
1364*a*.	4.6	17.05	(+ 9,− 9)....,....	16.54	(+11,−10)....,....	+0.51
1365..	4.7	15.64	+ 3,− 3,....,....	15.63	(+ 4,− 4)....,....	+0.01
1365*a*.	5.2	16.98	(+ 2,− 2)....,....	16.62	(− 1,+ 1)....,....	+0.36
1365*b*.	4.5	17.27	(+ 1,− 1)....,....	17.17	(...., m)....,....	+0.10
1366..	9.6	15.85	− 2,−12,+ 3,+10	15.09	(+ 3,− 3)....,....	+0.76
1367..	4.7	16.54	−12,+12,....,....	15.70	(− 1, 0)....,....	+0.84
1368..	6.1	16.20	+ 2,− 2,....,....	15.54	(+ 1,− 1)....,....	+0.66
1369..	5.0	15.94	+ 4,− 4,....,....	16.16	(− 4,+ 4)....,....	−0.22
1371..	5.8	15.36	+ 7,− 7,....,....	15.32	(+ 5,− 4)....,....	+0.04
1371*a*.	5.6	17.38	(− 7,+ 8)....,....	16.94	(−15,+16)....,....	+0.44
1372..	5.6	15.27	+12,−22,− 5,+15	14.45	(+ 1,− 1)....,....	+0.82
1372*a*.	5.7	16.42	(+13,−13)....,....	15.99	(−15,+14)....,....	+0.43
1372*b*†	6.6	16.43	+ 9,−12,....,+ 2	15.78	(−14,+15)....,....	+0.65
1373*a*.	6.7	17.02	(+12,−13)....,....	17.04:	(m,....)....,....	−0.02:
1374..	6.3	15.30	+ 5,−25,+11,+ 8	14.68	(− 2,+ 2)....,....	+0.62
1375..	12.1	.....	....,....,....,....	12.68	....,...., m,....	......
1376..	5.9	14.63	+ 2,− 2,+ 1,....	13.52	− 5,− 4,+ 9,....	+1.11
1376*a*.	5.1	15.66	(− 1,+ 1)....,....	15.72	(− 3,+ 4)....,....	−0.06
1376*b*.	4.6	17.07	(−10,+10)....,....	16.63	(− 2,+ 2)....,....	+0.44
1377..	5.5	16.55	−11,+11,....,....	15.76	(− 7,+ 8)....,....	+0.79
1378..	6.2	16.02	− 1,+ 2,....,....	15.52	(− 2,+ 1)....,....	+0.50
1379..	5.6	16.68	+ 4,− 5,....,....	16.00	(−13,+13)....,....	+0.68
1380*a*.	7.7	16.08	(+ 1, 0)....,....	15.46	(+ 7,− 7)....,....	+0.62
1381..	5.6	16.54	− 4,+ 3,....,....	15.84	(− 3,+ 3)....,....	+0.70
1382..	5.7	16.01	+ 6,−11,+ 4,....	15.53	(0, 0)....,....	+0.48
1383..	8.3	15.04	+15,−15,....,....	13.91	....,...., m,....	+1.13
1383*a*.	8.2	16.99	(+ 1,− 1)....,....	16.13	(−13,+13)....,....	+0.86
1385..	7.4	16.24	+ 6,− 6,....,....	15.50	(0, 0)....,....	+0.74
1386*a*.	5.6	17.00	(0,+ 1),....,....	16.56	(−13,+13)....,....	+0.44
1387..	9.6	15.56	−10,+ 9,....,....	14.96	(−11,+10)....,....	+0.60
1388*a*.	6.8	17.00	(0, 0)....,....	16.36	(0,− 1)....,....	+0.64
1389..	9.6	15.58	− 8,+ 7,....,....	.....	....,....,....,....	......
1390..	6.0	15.85	+13,− 8,+15,−20	15.46	(− 6,+ 7)....,....	+0.39
1391..	6.1	15.12	− 1,− 7, 0,+ 9	14.13	(....,+ 9)− 9,....	+0.99
1391*a*.	6.4	16.90	(0,− 1)....,....	16.32	(− 2,+ 3)....,....	+0.58
1391*b*.	6.1	17.02	(+ 6,− 6)....,....	16.72	(− 2,+ 3)....,....	+0.30
1392..	8.1	14.14	−16,−11,+11,+18	12.92	−12,+ 7,+ 4,....	+1.22
1392*a*.	7.5	17.01	(− 8,+ 8)....,....	16.82	(− 7,+ 6)....,....	+0.19
1393..	6.5	15.57	+ 3,− 1,− 2,....	15.53	(− 8,+ 8)....,....	+0.04
1393*a*.	6.6	16.80	(+ 6,− 7)....,....	16.48	(− 9,+10)....,....	+0.32
1393*b*.	6.5	17.24	(−10,+10)....,....	16.80	(−10,+11)....,....	+0.44
1393*c*.	6.4	16.68	(− 6,+ 5)....,....	16.38	(+ 1, 0)....,....	+0.30
1393*d*.	6.0	17.45	(m,....)....,....	.....	....,....,....,....	......
1396..	9.9	16.07	+ 3,− 3,....,....	15.36	(− 4,+ 3)....,....	+0.71
1396*a*.	9.2	16.86	(0, 0)....,....	16.61	(−11,+11)....,....	+0.25
1396*b*.	9.1	16.96	(+ 1, 0)....,....	16.69	(...., m)....,....	+0.27
1397..	7.4	14.29	− 7,+ 2,+ 4,....	12.60	− 6,−11,+17,....	+1.69
1397*a*.	7.1	16.90	(− 4,+ 3)....,....	16.58	(− 1, 0)....,....	+0.32

TABLE II—*Continued*

NUMBER	DISTANCE	PHOTOGRAPHIC		PHOTO-VISUAL		COLOR INDEX
		Mag.	Residuals	Mag.	Residuals	
1401..	8′.8	15.32	− 7,+ 6,....,....	15.44	(− 2,+ 1)....,....	−0.12
1402..	9.6	13.44	−29,+30,....,....	12.78	....,...., m,....	+0.66
1403..	10.6	16.00	− 6,+ 6,....,....	16.14	(− 5,+ 6)....,....	+0.46
1403*a*.	10.5	16.96	(+ 1, 0)....,....	16.60	(−21,+20)....,....	+0.36
1405..	7.1	16.26	−11,+11,....,....	15.47	(0, 0)....,....	+0.79
1405*a*.	6.8	17.10	(−10,+11)....,....	16.61	(− 8,+ 8)....,....	+0.49
1408..	9.6	15.91	+ 1,− 1,....,....	15.12	(− 4,+ 5)....,....	+0.79
1408*a*.	9.2	17.01	(...., m)....,....	16.35	(...., m)....,....	+0.66
1412..	7.6	15.72	+ 4,− 3,....,....	14.87	(+ 5,− 5)....,....	+0.85
1412*a*.	8.6	16.82	(− 3,+ 3)....,....	16.48	(− 2,+ 3)....,....	+0.34
1412*b*.	8.1	16.08	(+ 2,− 2)....,....	16.78	(−17,+17)....,....	+0.20
1413..	7.7	15.68	+ 5,−11,+21,−13	15.50	(+ 3,− 3)....,....	+0.18
1417..	9.6	16.24	−17,+17,....,....	15.82	(−13,+14)....,....	+0.42
1417*a*.	9.4	16.66	(− 4,+ 4)....,....	16.20	(− 8,+ 9)....,....	+0.46
1418..	8.3	15.44	− 5,−10,+14,....	14.55	(+ 1,− 1)....,....	−0.11
1420..	9.4	14.92	+ 6,− 7,+ 1,....	14.14	(+12,−11)....,....	+0.78
1422*b*	8.3	17.10	(−10,+11)....,....	16.81	(...., m)....,....	+0.29
1422*c*.	8.5	16.70	(+ 9,− 8)....,....	16.34	(−10,+10)....,....	+0.36
1423..	10.0	15.01	0, 0,....,....	14.35	(+ 7,− 7)....,....	+0.66
1426..	9.7	15.28	+15,−23,+ 9,....	14.55	(+ 9,− 9)....,....	+0.73
1426*a*.	8.8	16.72	(0,+ 1)....,....	16.25	(− 1,+ 1)....,....	+0.47
1429..	10.4	15.73	−13,+13,....,....	15.38	(− 1,+ 1)....,....	+0.35
1433..	9.5	16.30	+ 4,− 4,....,....	15.72	(− 3,+ 4)....,....	+0.58
1435..	9.6	15.92	+ 9,−10,....,....	15.36	(+ 4,− 3)....,....	+0.56
1437..	10.7	12.10	+12,−28,+13,+ 2	11.75	(− 7,+ 7)....,....	+0.35
1439..	10.7	13.61	−26,+10,+16,....	12.86	(−11,+10)....,....	+0.75
1441..	10.5	16.75	−19,+19,....,....	15.93	(0, 0)....,....	+0.82
1441*a*.	10.6	16.98	(+ 6,− 5)....,....	16.64	(−11,+11)....,....	+0.34
1448..	11.3	16.70	+ 2,− 1,....,....	16.32	(−26,+26)....,....	+0.38
1449..	11.3	14.18	−14,+13,....,....	12.78	− 9,....,....,.... (+ 9,....)	+1.40

TABLE III

Co-ordinates of Postscript Stars (1900.0)

No.	R.A.	Decl.	No.	R.A.	Decl.
	13^{h}	28°		13^{h}	28°
157*a*	$36^{m}50^{s}.9$	54′ 58″	290*b*	$37^{m}26^{s}.4$	60′ 36″
157*b*	36 55.1	54 30	291*a*	37 21.1	52 47
157*c*	36 55.1	54 40	291*b*	37 19.4	52 55
164*a*	36 55.2	52 58	291*c*	37 20.8	52 54
164*b*	36 52.8	52 37	296*a*	37 20.8	52 15
164*c*	36 52.0	52 37	296*b*	37 20.0	52 19
168*a*	37 0	57 56	301*a*	37 23.3	56 29
175*a*	36 57.7	50 20	301*b*	37 22.4	56 39
177*a*	37 1.8	51 23	301*c*	37 21.7	57 4
177*b*	37 4.2	51 9	301*d*	37 20.8	57 5
179*a*	37 1.6	52 38	303*a*	37 22.0	52 41
180*a*	37 56.2	45 52	305*a*	37 23.0	49 9
180*b*	36 58.8	45 53	307*a*	37 22.6	50 4
181*a*	37 2.3	54 26	307*b*	37 22.1	50 0
181*b*	37 0.7	55 26	308*a*	37 24.2	51 38
181*c*	36 59.2	55 17	308*b*	37 20.8	51 33
188*a*	37 7.6	49 18	310*a*	37 22.7	51 58
188*b*	37 2.1	49 38	311*a*	37 23.8	50 27
188*c*	37 6.4	50 35	311*b*	37 23.9	50 32
188*d*	37 8.0	50 29	320*a*	37 21.1	47 31
190*a*	37 7.2	54 49	320*b*	37 21.0	47 24
193*a*	37 7.4	59 52	322*a*	37 22.7	51 51
205*a*	37 10.0	55 10	326*a*	37 22.8	54 12
206*a*	37 9.6	57 53	326*b*	37 22.8	54 19
208*a*	37 6.7	47 25	326*c*	37 22.6	54 28
210*a*	37 10.0	53 58	332*a*	37 23.7	56 4
210*b*	37 10.0	54 8	332*b*	37 23.2	55 44
211*a*	37 10.3	52 23	336*a*	37 23.6	51 16
211*b*	37 11.9	52 12	345*a*	37 24.1	50 55
212*a*	37 12.4	55 56	348*a*	37 25.2	53 25
212*b*	37 11.7	56 21	350*a*	37 25.2	54 44
215*a*	37 10.6	52 49	355*a*	37 25.1	52 0
230*a*	37 12.3	60 52	360*a*	37 25.3	52 54
230*b*	37 11.6	61 1	360*b*	37 25.3	52 51
230*c*	37 11.3	61 15	360*c*	37 25.3	52 44
238*a*	37 15.5	52 55	360*d*	37 24.8	52 56
238*b*	37 14.7	52 55	364*a*	37 25.7	53 14
247*a*	37 17.1	53 37	376*a*	37 26.4	53 20
249*a*	37 15.4	55 17	378*a*	37 27.6	49 19
249*b*	37 14.7	55 14	379*a*	37 27.0	51 18
250*a*	37 16.0	49 30	379*c*	37 27.3	51 10
251*a*	37 16.8	51 10	380*a*	37 26.1	53 33
253*a*	37 15.3	55 52	380*b*	37 25.7	53 41
255*a*	37 18.1	56 55	381*a*	37 27.2	53 58
258*a*	37 18.4	54 48	381*b*	37 27.4	53 59
260*a*	37 18.5	52 15	385*a*	37 26.9	51 44
261*a*	37 18.4	48 12	385*b*	37 27.2	51 54
262*a*	37 17.2	50 12	386*a*	37 26.7	49 56
281*a*	37 20.7	56 8	387*a*	37 27.3	54 9
290*a*	37 21.5	60 21	394*a*	37 26.9	53 7

TABLE III—*Continued*

No.	R.A.	Decl.	No.	R.A.	Decl.
	13^{h}	28°		13^{h}	28°
396*a*....	37^{m}27^{s}.6	55′ 4″	640*a*...	37^{m}32^{s}.8	49′ 56″
397*a*....	37 27.8	52 53	640*b*...	37 32.4	49 49
403*a*....	37 27.4	52 38	640*c*...	37 33.2	49 52
403*b*....	37 27.2	52 37	640*d*...	37 33.3	49 47
403*c*....	37 27.9	52 43	640*e*...	37 33.6	49 41
403*d*....	37 27.2	52 29	640*f*...	37 32.4	50 6
403*e*....	37 27.5	52 31	649*a*...	37 32.8	48 34
403*f*....	37 27.7	52 33	649*b*...	37 32.5	48 34
403*g*....	37 27.9	52 34	649*c*...	37 33.7	49 4
411*a*....	37 28.3	48 19	665*a*...	37 33.3	50 48
417*a*....	37 28.0	52 15	680*a*...	37 33.0	54 24
417*b*....	37 27.7	52 20	680*b*...	37 32.5	54 27
417*c*....	37 27.5	52 12	680*c*...	37 33.0	54 30
417*d*....	37 26.8	52 10	700*a*...	37 33.5	50 29
418*a*....	37 28.4	51 25	701*a*...	37 33.7	58 52
419*a*....	37 28.5	55 3	701*b*...	37 31.3	57 59
422*a*....	37 28.8	51 0	701*c*...	37 31.0	57 50
425*a*....	37 27.9	53 54	701*d*...	37 30.7	57 49
452*a*....	37 27.8	54 15	713*a*...	37 37.1	43 46
452*b*....	37 27.8	54 26	730*a*...	37 34.1	51 16
452*c*....	37 29.2	51 14	739*a*...	37 31.4	57 30
455*a*....	37 28.8	58 27	739*b*...	37 35.1	57 63
467*a*....	37 30.6	55 18	740*a*...	37 35.4	49 34
467*b*....	37 30.5	55 22	740*b*...	37 35.0	49 35
471*a*....	37 29.4	49 34	758*a*...	37 34.3	51 10
480*a*....	37 30.1	56 22	759*a*...	37 34.1	55 7
480*b*....	37 30.0	56 46	801*a*...	37 35.0	51 24
482*a*....	37 30.2	51 2	801*b*...	37 35.8	51 24
482*b*....	37 30.9	51 1	801*c*...	37 36.3	51 20
499*a*....	37 27.5	55 59	837*b*...	37 36.5	56 49
499*b*....	37 25.1	56 10	845*a*...	37 36.2	51 4
499*c*....	37 24.9	56 19	885*a*...	37 35.5	51 4
499*d*....	37 24.8	56 4	900*a*...	37 36.8	50 32
499*e*....	37 24.9	56 2	900*b*...	37 36.3	50 26
499*f*....	37 25.1	56 4	902*a*...	37 36.0	55 16
499*g*....	37 24.4	56 8	902*b*...	37 35.7	55 12
499*h*....	37 24.3	56 8	925*a*...	37 36.4	50 6
502*a*....	37 30.5	50 46	925*b*...	37 37.1	49 59
513*a*....	37 31.1	55 3	925*c*...	37 36.8	49 54
522*a*....	37 30.5	55 53	925*d*...	37 36.6	50 1
522*b*....	37 30.2	55 40	925*e*...	37 38.2	50 3
522*c*....	37 30.0	55 44	926*a*...	37 36.8	57 5
550*a*....	37 32.1	54 39	945*a*...	37 37.6	51 20
573*a*....	37 32.3	56 8	945*b*...	37 38.1	51 15
590*a*....	37 32.0	56 29	974*a*...	37 35.1	45 48
595*b*....	37 30.3	60 10	1000*a*..	37 37.5	55 36
605*a*....	37 32.6	50 36	1022*a*..	37 38.3	50 55
609*a*....	37 32.0	56 51	1028*a*..	37 38.4	55 4
609*b*....	37 32.5	57 9	1028*b*..	37 37.8	55 4
621*a*....	37 34.2	56 4	1028*c*..	37 37.4	55 5
621*b*....	37 33.9	56 5	1076*a*..	37 39.2	51 14
621*d*....	37 32.4	55 58	1090*a*..	37 39.5	54 45
628*a*....	37 32.3	51 22	1090*b*..	37 40.0	54 54

TABLE III—*Continued*

No.	R.A.	Decl:	No.	R.A.	Decl.
	13^{h}	28°		13^{h}	28°
1090*c*...	$37^{\mathrm{m}}39^{\mathrm{s}}.5$	54′ 58″	1227*c*..	$37^{\mathrm{m}}42^{\mathrm{s}}.2$	49′ 9″
1120*a*...	37 40.8	51 0	1227*d*..	37 41.7	49 25
1123*a*...	37 39.7	50 38	1236*a*..	37 43.6	52 34
1123*b*...	37 39.1	50 32	1242*a*..	37 44.4	52 11
1123*c*...	37 38.7	50 36	1243*a*..	37 46.3	54 53
1127*a*...	37 40.9	54 7	1244*a*..	37 44.6	53 29
1128*a*...	37 39.8	56 10	1247*a*..	37 45.5	53 42
1128*b*...	37 41.2	55 58	1247*b*..	37 45.2	53 42
1128*c*...	37 42.6	56 21	1250*a*..	37 44.0	58 15
1131*a*...	37 39.5	56 50	1254*a*..	37 44.3	45 47
1131*b*...	37 38.7	56 44	1261*a*..	37 45.9	50 29
1140*a*...	37 39.9	57 15	1265*a*..	37 43.8	55 44
1140*b*...	37 39.8	57 2	1265*b*..	37 43.1	55 49
1140*c*...	37 43.4	57 0	1265*c*..	37 42.6	55 54
1140*d*...	37 44.9	56 48	1265*d*..	37 43.0	55 59
1149*a*...	37 41.0	54 20	1265*e*..	37 45.8	55 46
1149*b*...	37 40.6	54 19	1265*f*...	37 45.3	55 45
1149*c*...	37 41.8	54 24	1265*g*..	37 45.8	55 34
1149*d*...	37 41.2	54 28	1270*a*..	37 45.8	58 49
1149*e*...	37 42.1	54 29	1270*b*..	37 46.7	58 46
1149*f*...	37 43.7	54 16	1271*a*..	37 46.3	54 13
1149*g*...	37 43.5	54 19	1278*a*..	37 45.8	53 1
1154*a*...	37 41.4	54 59	1280*a*..	37 45.5	50 51
1172*a*...	37 41.0	55 33	1280*b*..	37 45.1	50 55
1172*b*...	37 41.1	55 29	1283*a*..	37 46.7	51 54
1172*c*...	37 41.0	55 34	1285*a*..	37 47.8	54 22
1175*a*...	37 41.4	50 37	1285*b*..	37 47.8	54 28
1178*a*...	37 40.7	48 4	1287*a*..	37 46.6	49 19
1178*b*...	37 42.8	48 20	1289*a*..	37 46.2	54 54
1178*c*...	37 42.7	47 48	1290*a*..	37 47.4	51 30
1178*d*...	37 41.8	47 40	1290*b*..	37 47.0	51 28
1181*a*...	37 42.6	55 28	1292*a*..	37 46.6	52 51
1181*b*...	37 42.7	55 31	1292*b*..	37 46.7	52 53
1201*a*...	37 41.4	49 35	1293*b*..	37 48.0	50 11
1201*b*...	37 41.0	49 34	1293*c*..	37 48.4	50 20
1201*c*...	37 41.4	49 38	1294*a*..	37 47.4	56 16
1201*d*...	37 41.1	49 39	1294*b*..	37 46.9	56 6
1205*a*...	37 43.3	51 24	1294*c*..	37 47.1	56 1
1206*a*...	37 42.8	53 36	1296*a*..	37 46.2	52 17
1206*b*...	37 42.3	53 43	1296*b*..	37 47.2	52 20
1206*c*...	37 42.5	53 46	1296*c*..	37 47.4	52 23
1218*a*...	37 43.5	51 11	1299*a*..	37 48.1	55 50
1218*b*...	37 43.2	51 18	1303*a*..	37 48.1	49 26
1222*a*...	37 43.5	53 50	1304*a*..	37 48.2	53 26
1222*b*...	37 43.9	53 51	1304*b*..	37 47.5	53 24
1222*c*...	37 44.0	53 59	1304*c*..	37 48.0	53 12
1223*a*...	37 43.0	57 40	1304*d*..	37 48.4	53 16
1223*b*...	37 44.0	57 52	1307*a*..	37 47.6	54 42
1225*a*...	37 44.3	53 18	1309*a*..	37 48.8	50 51
1225*b*...	37 43.9	53 22	1313*a*..	37 48.4	52 36
1225*c*...	37 43.7	53 9	1315*a*..	37 48.9	51 26
1227*a*...	37 43.8	49 16	1318*a*..	37 48.9	60 5
1227*b*...	37 44.1	49 20	1319*a*..	37 49.0	52 26

TABLE III—*Continued*

No.	R.A.	Decl.	No.	R.A.	Decl.
	13^{h}	28°		13^{h}	28°
1319*b*...	$37^{m}48^{s}.8$	52′ 31″	1372*a*..	$37^{m}59^{s}.3$	54′ 55″
1324*a*...	37 40.0	57 33	1372*b*..	38 1.2	56 11
1324*b*...	37 47.3	57 37	1373*a*..	37 58.4	57 7
1324*c*...	37 48.0	58 0	1376*a*..	37 55.7	50 36
1324*d*...	37 40.0	58 15	1376*b*..	37 54.0	50 51
1329*a*...	37 40.4	53 23	1380*a*..	38 1.3	48 1
1329*b*...	37 40.5	53 31	1383*a*..	37 56.8	46 13
1331*a*...	37 48.4	43 42	1386*a*..	38 0.8	53 8
1338*a*...	37 51.3	52 16	1388*a*..	38 0.3	49 1
1339*a*...	37 50.5	48 19	1391*a*..	38 4.1	53 45
1340*a*...	37 53.9	47 49	1391*b*..	38 2.0	54 39
1340*b*...	37 54.8	48 13	1392*a*..	38 1.1	57 44
1343*a*...	37 44.4	42 57	1393*a*..	38 3.7	50 51
1343*b*...	37 44.0	43 29	1393*b*..	38 3.1	50 46
1344*a*...	37 52.4	54 52	1393*c*..	38 3.4	51 16
1345*a*...	37 53.9	54 34	1393*d*..	38 1.9	51 31
1346*a*...	37 53.9	61 45	1396*a*..	38 4.2	59 53
1346*b*...	37 55.6	62 20	1396*b*..	38 2.8	60 1
1347*a*...	37 54.7	56 35	1397*a*..	38 4.9	50 5
1352*a*...	37 53.2	53 32	1403*a*..	38 5.2	61 7
1354*a*...	37 52.7	44 36	1405*a*..	38 6.4	53 16
1360*a*...	37 54.1	53 2	1408*a*..	38 8.2	59 3
1360*b*...	37 53.2	52 57	1412*a*..	38 13.1	55 20
1363*a*...	37 57.6	53 21	1412*b*..	38 9.2	56 16
1363*b*...	37 57.2	53 29	1417*a*..	38 12.1	58 1
1364*a*...	37 55.2	54 1	1422*b*..	38 12.6	51 3
1365*a*...	37 58.4	51 56	1422*c*..	38 13.6	51 34
1365*b*...	37 55.2	51 59	1426*a*..	38 13.0	49 36
1371*a*...	37 54.0	56 12	1441*a*..	38 21.8	56 10

TABLE IV

PHOTOGRAPHIC RESIDUALS

	PLATE NUMBER						
	2463	2506	3679	3680	3846	3847	All
Number of Magnitudes.....	466	465	186	188	332	332	1969
Systematic Deviation.......	0.00	+0.02	−0.05	0.00	−0.03	+0.03	0.00
Average Deviation.......	±0.08	±0.08	±0.11	±0.07	±0.06	±0.06	±0.075

TABLE V

PHOTO-VISUAL RESIDUALS

	PLATE NUMBER						
	2371	2462	2505	3684	3774	3775	All
Number of Magnitudes.....	64	80	85	39	661	661	1569
Systematic Deviation.......	−0.01	−0.01	+0.01	0.00	−0.02	+0.02	0.00
Average Deviation.......	±0.07	±0.05	±0.06	±0.07	±0.067	±0.067	±0.066

TABLE VI

COMPARISON STARS

DESIGNATION		PHOTOGRAPHIC MAGNITUDE		COLOR-INDEX
Bailey	Von Zeipel	Harvard	Mt. Wilson	
a...........	740	13.50	14.04	+0.70
b...........	238	13.58	14.05	+1.79
c...........	640	13.98	14.57	+1.18
d...........	263	14.22	14.53	+1.12
e...........	250	14.50	14.81	+0.90
f...........	218	14.98	15.06	+0.53
g...........	227	15.28	15.22	+0.65
*h**..........	258	15.70	15.53	−0.02
k...........	609	16.00	15.63	−0.04
l...........	1131	16.23	15.83	+0.33
m...........	1055	16.49	15.94	+0.69
n...........	1327	16.82	16.16	+0.68
o...........	1372*b*	17.15	16.37	+0.65
p...........	1347*a*	17.63	16.84	+0.41

TABLE VII

Color-Class and Distance

Distance	Tabulated Quantity	Color-Class						All Colors
		b	*a*	*f*	*g*	*k*	*m*	
1'.3 to 1'.5	No. Stars....	0	1	2	4	0	0	7
	Av. C. I.	....	+0.12	+0.53	+1.00	....	....	+0.74
	Av. Pv. mag.	....	15.47	15.24	13.98	....	....	14.55
1'.6......	No. stars....	2	4	4	9	2	0	21
	Av. C. I.....	−0.09	+0.13	+0.68	+0.98	+1.26	....	+0.69
	Av. Pv. mag.	16.18	15.51	16.05	14.86	13.40	....	15.20
1'.7......	No. stars....	2	4	5	3	0	0	14
	Av. C. I.....	−0.10	+0.23	+0.67	+0.93	....	....	+0.49
	Av. Pv. mag.	15.70	16.07	15.63	15.37	....	....	15.71
1'.8......	No. stars....	0	2	9	10	1	0	22
	Av. C. I.....	....	+0.06	+0.68	+0.93	+1.22	....	+0.77
	Av. Pv. mag.	....	15.59	15.76	15.21	13.18	....	15.38
1'.9	No. stars	2	3	9	8	2	0	24
	Av. C. I.....	−0.10	+0.25	+0.66	+0.88	+1.30	....	+0.67
	Av. Pv. mag.	15.96	15.22	15.77	15.37	12.96	....	15.35
2'.0......	No. stars....	0	3	11	5	2	1	22
	Av. C. I.....	....	+0.17	+0.64	+0.92	+1.26	+1.80	+0.75
	Av. Pv. mag.	....	15.80	15.87	14.93	13.62	12.33	15.28
2'.1......	No. stars	3	5	16	13	0	0	37
	Av. C. I.....	−0.06	+0.19	+0.65	+0.89	....	....	+0.62
	Av. Pv. mag.	16.32	15.86	16.20	15.17	....	....	15.80
2'.2......	No. stars....	0	7	9	5	0	0	21
	Av. C. I.....	....	+0.20	+0.59	+1.00	....	....	+0.56
	Av. Pv. mag.	....	16.02	15.96	14.96	....	....	15.74
2'.3......	No. stars....	0	1	11	6	0	0	18
	Av. C. I.....	....	+0.35	+0.64	+0.93	....	....	+0.72
	Av. Pv. mag.	....	16.92	16.08	14.68	....	....	15.66
2'.4......	No. stars	1	3	14	6	0	0	24
	Av. C. I.....	−0.06	+0.08	+0.61	+0.94	....	....	+0.60
	Av. Pv. mag.	15.60	15.70	16.03	15.00	....	....	15.71
2'.5......	No. stars....	3	2	10	3	0	0	18
	Av. C. I.....	−0.10	+0.08	+0.65	+0.97	....	....	+0.52
	Av. Pv. mag.	15.76	15.35	16.12	14.24	....	....	15.66
2'.6......	No. stars....	0	2	3	4	0	0	9
	Av. C. I.....	....	+0.16	+0.65	+0.94	....	....	+0.67
	Av. Pv. mag.	....	15.36	15.50	14.78	....	....	15.15
2'.7......	No. stars....	0	2	6	8	1	0	17
	Av. C. I.....	....	+0.18	+0.67	+1.02	+1.32	....	+0.81
	Av. Pv. mag.	....	16.10	15.96	14.50	13.08	....	15.12

TABLE VII—*Continued*

DISTANCE	TABULATED QUANTITY	COLOR-CLASS						ALL COLORS
		b	*a*	*f*	*g*	*k*	*m*	
2′.8......	No. stars....	1	1	13	4	2	0	21
	Av. C. I.....	−0.04	+0.01	+0.65	+0.95	+1.29	....	+0.71
	Av. Pv. mag.	15.53	15.96	15.85	14.92	13.12	....	15.41
2′.9......	No. stars....	0	4	8	3	1	10	16
	Av. C. I.....	....	+0.21	+0.62	+0.90	+1.21	....	+0.60
	Av. Pv. mag.	....	16.19	16.11	14.89	13.57	....	15.74
3′.0......	No. stars....	0	3	15	5	2	....	25
	Av. C. I.....	....	+0.15	+0.60	+0.95	+1.26	....	+0.67
	Av. Pv. mag.	....	16.14	16.49	14.52	13.09	....	15.78
3′.1......	No. stars....	0	2	7	2	0	0	11
	Av. C. I.....	....	+0.18	+0.57	+1.00	....	....	+0.58
	Av. Pv. mag.	....	16.27	15.83	14.29	....	....	15.63
3′.2......	No. stars....	0	3	6	3	0	0	12
	Av. C. I.....	....	+0.27	+0.63	+0.85	....	....	+0.60
	Av. Pv. mag.	....	15.89	15.84	15.34	....	....	15.73
3′.3......	No. stars....	0	0	6	1	0	0	7
	Av. C. I.....	....	....	+0.64	+0.84	....	....	+0.66
	Av. Pv. mag.	....	....	15.79	14.40	....	....	15.59
3′.4......	No. stars....	0	2	14	1	0	0	17
	Av. C. I.....	....	+0.22	+0.56	+0.84	....	....	+0.54
	Av. Pv. mag.	....	15.88	15.84	15.24	....	....	15.81
3′.5......	No. stars....	1	3	7	4	0	0	15
	Av. C. I.....	−0.18	+0.15	+0.60	+0.84	....	....	+0.52
	Av. Pv. mag.	16.42	15.99	15.70	15.24	....	....	15.68
3′.6 and 3′.7......	No. stars....	2	2	8	1	0	0	13
	Av. C. I.....	−0.34	+0.36	+0.62	+0.93	....	....	+0.46
	Av. Pv. mag.	15.10	16.94	15.71	14.96	....	....	15.75
3′.8 and 3′.9......	No. stars....	0	1	12	3	1	0	17
	Av. C. I.....	....	+0.36	+0.61	+0.84	+1.36	....	+0.68
	Av. Pv. mag.	....	15.46	15.97	15.40	12.47	....	15.64
4′.0 and 4′.1......	No. stars....	2	7	16	4	0	0	29
	Av. C. I.....	−0.06	+0.29	+0.54	+1.02	....	....	+0.51
	Av. Pv. mag.	15.73	16.36	16.31	13.91	....	....	15.95
4′.2 and 4′.3......	No. stars....	1	4	5	0	0	0	10
	Av. C. I.....	−0.02	+0.33	+0.60	....	....	....	+0.43
	Av. Pv. mag.	15.54	16.42	16.18	....	....	....	16.21
4′.4 and 4′.5......	No. stars....	1	4	9	5	0	1	20
	Av. C. I.....	−0.05	+0.28	+0.54	+0.92	....	+1.79	+0.61
	Av. Pv. mag.	16.02	16.52	15.80	14.73	....	12.48	15.52

TABLE VII—*Continued*

DISTANCE	TABULATED QUANTITY	COLOR-CLASS						ALL COLORS
		b	*a*	*f*	*g*	*k*	*m*	
4′.6 and 4′.7	No. stars	0	2	10	2	0	0	14
	Av. C. I.	....	+0.02	+0.61	+0.91	....	....	+0.57
	Av. Pv. mag.	....	15.63	15.66	15.35	....	....	15.61
4′.8 and 4′.9	No. stars	0	2	4	2	0	0	8
	Av. C. I.	....	+0.22	+0.59	+1.06	....	....	+0.62
	Av. Pv. mag.	....	16.06	16.30	13.91	....	....	15.64
5′.0 and 5′.1	No. stars	2	5	8	3	0	0	18
	Av. C. I.	−0.14	+0.28	+0.66	+0.95	....	....	+0.52
	Av. Pv. mag.	15.94	16.50	15.54	14.49	....	....	15.68
5′.2 and 5′.3	No. stars	0	2	7	3	0	0	12
	Av. C. I.	....	+0.36	+0.58	+0.91	....	....	+0.62
	Av. Pv. mag.	....	16.70	16.13	14.24	....	....	15.75
5′.4 and 5′.5	No. stars	3	5	6	2	0	0	16
	Av. C. I.	−0.08	+0.35	+0.59	+0.80	....	....	+0.42
	Av. Pv. mag.	15.59	16.22	15.83	15.94	....	....	15.92
5′.6 and 5′.7	No. stars	0	4	14	3	0	0	21
	Av. C. I.	....	+0.30	+0.56	+0.89	....	....	+0.56
	Av. Pv. mag.	....	16.09	16.01	14.84	....	....	15.86
5′.8 and 5′.9	No. stars	0	3	3	2	0	0	8
	Av. C. I.	....	+0.32	+0.60	+0.96	....	....	+0.51
	Av. Pv. mag.	....	15.89	15.65	14.30	....	....	15.40
6′.0 and 6′.1	No. stars	0	3	5	2	0	0	10
	Av. C. I.	....	+0.32	+0.63	+0.93	....	....	+0.60
	Av. Pv. mag.	....	15.84	15.85	14.00	....	....	15.48
6′.2 and 6′.3	No. stars	0	4	7	3	0	0	14
	Av. C. I.	....	+0.23	+0.63	+0.97	....	....	+0.59
	Av. Pv. mag.	....	16.40	15.82	13.42	....	....	15.47
6′.4 and 6′.5	No. stars	1	7	5	1	0	0	14
	Av. C. I.	−0.58	+0.23	+0.56	+0.99	....	....	+0.35
	Av. Pv. mag.	16.32	16.40	16.06	13.86	....	....	16.09
6′.6 to 7′.0	No. stars	1	5	10	2	0	0	18
	Av. C. I.	−0.19	+0.23	+0.52	+0.90	....	....	+0.44
	Av. Pv. mag.	15.81	15.74	15.92	14.32	....	....	15.69
7′.1 to 7′.5	No. stars	1	6	7	3	1	1	19
	Av. C. I.	−0.03	+0.20	+0.65	+0.90	+1.32	+1.69	+0.60
	Av. Pv. mag.	15.38	15.92	15.63	13.43	12.82	12.60	15.05
7′.6 to 8′.0	No. stars	2	5	8	3	0	0	18
	Av. C. I.	−0.04	+0.20	+0.57	+0.99	....	....	+0.47
	Av. Pv. mag.	15.73	15.71	15.73	14.43	....	....	15.51

TABLE VII—*Continued*

DISTANCE	TABULATED QUANTITY	COLOR-CLASS						ALL COLORS
		b	*a*	*f*	*g*	*k*	*m*	
8′.1 to 8′.5.....	No. stars....	1	5	6	3	1	0	16
	Av. C. I.....	−0.11	+0.27	+0.60	+0.97	+1.22	....	+0.56
	Av. Pv. mag.	14.55	16.22	15.70	14.89	12.92	....	15.46
8′.6 to 9′.0.....	No. stars	1	2	9	2	0	0	14
	Av. C. I.....	−0.12	+0.32	+0.55	+0.98	....	....	+0.53
	Av. Pv. mag.	15.44	16.56	15.74	15.00	....	....	15.73
9′.1 to 9′.5.....	No. stars....	0	1	12	4	0	0	17
	Av. C. I.....	....	+0.25	+0.65	+0.92	....	....	+0.69
	Av. Pv. mag.	....	16.61	15.64	14.88	....	....	15.52
9′.6 to 10′.0.....	No. stars....	2	1	16	5	1	0	25
	Av. C. I.....	−0.04	+0.34	+0.59	+0.99	+1.23	....	+0.64
	Av. Pv. mag.	16.22	16.74	15.34	14.59	10.57	....	15.12
10′.1 to 11′.4.....	No. stars	2	9	6	3	1	0	21
	Av. C. I.....	−0.10	+0.32	+0.58	+1.03	+1.40	....	+0.51
	Av. Pv. mag.	15.72	15.16	14.98	15.15	12.78	....	15.05

TABLE VIII

FREQUENCY OF PHOTO-VISUAL MAGNITUDES FOR EACH COLOR-CLASS

DISTANCE FROM CENTER 1′.3 TO 1′.9

Limits of Photo-visual Magnitude	$<b5$	$b5$ to $a0$	$a0$ to $a5$	$a5$ to $f0$	$f0$ to $f5$	$f5$ to $g0$	$g0$ to $g5$	$g5$ to $k0$	$k0$ to $k5$	$>k5$	All Colors
12.60–.79	.....	.....	.....	.....	.....	.....	.....	.....	1	1	2
.80–.99	.....	.....	.....	.....	.....	.....	1	2	.....	.....	3
13.00–.19	.....	.....	.....	.....	.....	.....	.....	.....	1	.....	1
.20–.39	.....	.....	.....	.....	.....	.....	.....	.....	1	.....	1
.40–.59	.....	.....	.....	.....	.....	.....	.....	.....	.....	.....	.....
.60–.79	.....	.....	.....	.....	.....	.....	.....	2	.....	.....	2
.80–.99	.....	.....	.....	.....	.....	.....	.....	1	.....	.....	1
14.00–.19	.....	.....	.....	.....	.....	.....	.....	.....	1	.....	1
.20–.39	.....	.....	.....	.....	.....	.....	.....	.....	.....	.....	.....
.40–.59	.....	.....	.....	1	.....	.....	2	.....	.....	.....	3
.60–.79	.....	.....	.....	.....	.....	2	1	.....	.....	.....	3
.80–.99	.....	.....	.....	.....	.....	1	2	.....	.....	.....	3
15.00–.19	.....	.....	.....	.....	1	2	3	1	.....	.....	7
.20–.39	.....	1	1	.....	3	1	5	1	.....	.....	12
.40–.59	.....	1	4	2	1	3	4	1	.....	.....	16
.60–.79	.....	1	3	1	.....	4	3	.....	.....	.....	12
.80–.99	.....	.....	.....	.....	.....	2	1	.....	.....	.....	3
16.00–.19	.....	1	.....	1	.....	.....	2	.....	.....	.....	4
.20–.39	.....	.....	.....	.....	1	2	1	.....	.....	.....	4
.40–.59	.....	1	.....	.....	.....	2	1	.....	.....	.....	4
.60–.79	.....	1	.....	.....	.....	2	.....	.....	.....	.....	3
.80–.99	.....	.....	.....	1	1	1	.....	.....	.....	.....	3
Total	0	6	8	6	7	22	26	8	4	1	88

DISTANCE FROM CENTER 2′.0 TO 2′.9

Limits of Photo-visual Magnitude	$<b5$	$b5$ to $a0$	$a0$ to $a5$	$a5$ to $f0$	$f0$ to $f5$	$f5$ to $g0$	$g0$ to $g5$	$g5$ to $k0$	$k0$ to $k5$	$>k5$	All Colors
12.20–.39	.....	.....	.....	.....	.....	.....	.....	.....	.....	1	1
.40–.59	.....	.....	.....	.....	.....	.....	.....	.....	.....	.....	.....
.60–.79	.....	.....	.....	.....	.....	.....	.....	.....	.....	.....	.....
.80–.99	.....	.....	.....	.....	.....	.....	.....	.....	1	.....	1
13.00–.19	.....	.....	.....	.....	.....	.....	.....	3	2	.....	5
.20–.39	.....	.....	.....	.....	.....	.....	.....	1	1	.....	2
.40–.59	.....	.....	.....	.....	.....	.....	.....	.....	1	.....	1
.60–.79	.....	.....	.....	.....	.....	.....	.....	.....	.....	.....	.....
.80–.99	.....	.....	.....	.....	.....	.....	2	2	.....	.....	4
14.00–.19	.....	.....	.....	.....	.....	.....	.....	4	1	.....	5
.20–.39	.....	.....	.....	.....	.....	.....	3	3	.....	.....	6
.40–.59	.....	.....	.....	.....	.....	6	1	.....	.....	.....	7
.60–.79	.....	.....	.....	.....	.....	3	6	1	.....	.....	10
.80–.99	.....	.....	.....	.....	.....	.....	.....	1	.....	.....	1
15.00–.19	.....	.....	1	1	.....	2	7	2	.....	.....	13
.20–.39	.....	.....	2	.....	5	3	7	1	.....	.....	18
.40–.59	.....	2	7	1	3	5	1	.....	.....	.....	19
.60–.79	.....	2	3	1	1	9	4	1	.....	.....	21
.80–.99	.....	1	5	.....	1	7	3	.....	.....	.....	17
16.00–.19	1	.....	1	.....	2	5	4	.....	.....	.....	13
.20–.39	.....	1	.....	.....	1	5	.....	.....	.....	.....	7
.40–.59	.....	.....	.....	2	6	14	.....	.....	.....	.....	22
.60–.79	.....	.....	1	2	5	7	.....	.....	.....	.....	15
.80–.99	.....	1	.....	3	11	.....	.....	.....	.....	.....	15
Total	1	7	20	10	35	66	38	19	6	1	203

TABLE VIII—*Continued*

DISTANCE FROM CENTER 3′.0 TO 3′.9

Limits of Photo-visual Magnitude	<*b*5	*b*5 to *a*0	*a*0 to *a*5	*a*5 to *f*0	*f*0 to *f*5	*f*5 to *g*0	*g*0 to *g*5	*g*5 to *k*0	*k*0 to *k*5	>*k*5	All Colors
12.40–.59									1		1
.60–.79											
.80–.99									1		1
13.00–.19								1			1
.20–.39									1		1
.40–.59						1					1
.60–.79											
.80–.99								2			2
14.00–.19						1					1
.20–.39											
.40–.59						4	2				6
.60–.79	1					3	3				7
.80–.99							1				1
15.00–.19						1	3				4
.20–.39					1	2	4				7
.40–.59		1	4	2	6	7					20
.60–.79			1	1		5	2				9
.80–.99			1		1	5					7
16.00–.19			1		2	1	1				5
.20–.39					3	3	1				7
.40–.59		1			5	2					8
.60–.79					7	2					9
.80–.99				6	12	1					19
Total	1	2	7	9	37	38	17	3	3	0	117

DISTANCE FROM CENTER 4′.0 TO 5′.9

Limits of Photo-visual Magnitude	<*b*5	*b*5 to *a*0	*a*0 to *a*5	*a*5 to *f*0	*f*0 to *f*5	*f*5 to *g*0	*g*0 to *g*5	*g*5 to *k*0	*k*0 to *k*5	>*k*5	All Colors
12.40–.59										1	1
.60–.79											
.80–.99											
13.00–.19								1			1
.20–.39											
.40–.59								3			3
.60–.79							1	2			3
.80–.99							1				1
14.00–.19							1	1			2
.20–.39											
.40–.59					1	4	2				7
.60–.79						3	1				4
.80–.99						1	3	1			5
15.00–.19				1			4				5
.20–.39			1	2	5	6	2				16
.40–.59		3	3	5	3	4					18
.60–.79		4	2			8	1				15
.80–.99					1	4	1				6
16.00–.19	1	1			3	2					7
.20–.39				1	6	2					9
.40–.59				2	6	2					10
.60–.79			1	9	6	1	1				18
.80–.99			1	10	14						25
Total	1	8	8	30	45	37	18	8	0	1	156

TABLE VIII—*Continued*

DISTANCE FROM CENTER ≧ 6′0

Limits of Photo-visual Magnitude	< *b*5	*b*5 to *a*0	*a*0 to *a*5	*a*5 to *f*0	*f*0 to *f*5	*f*5 to *g*0	*g*0 to *g*5	*g*5 to *k*0	*k*0 to *k*5	> *k*5	All Colors
< 12.00	.....	.....	.....	1	.....	.....	.....	1	1	.....	3
12.00–.19	.....	.....	.....	.....	.....	.....	.....	.....	.....	.....	.....
.20–.39	.....	.....	.....	.....	.....	.....	.....	.....	.....	.....	.....
.40–.59	.....	.....	.....	.....	.....	.....	.....	.....	.....	.....	.....
.60–.79	.....	.....	.....	.....	.....	1	.....	1	.....	2	4
.80–.99	.....	.....	.....	.....	.....	1	.....	.....	2	.....	3
13.00–.19	.....	.....	.....	.....	.....	.....	.....	.....	.....	.....	.....
.20–.39	.....	.....	.....	.....	.....	.....	.....	.....	.....	.....	.....
.40–.59	.....	.....	.....	.....	.....	.....	.....	1	.....	.....	1
.60–.79	.....	.....	.....	.....	.....	.....	3	1	.....	.....	4
.80–.99	.....	.....	.....	.....	1	.....	4	2	.....	.....	7
14.00–.19	.....	.....	1	.....	.....	1	1	.....	.....	.....	3
.20–.39	.....	.....	.....	.....	.....	1	.....	.....	.....	.....	1
.40–.59	.....	1	.....	1	2	2	1	.....	.....	.....	7
.60–.79	.....	.....	.....	1	1	2	1	1	.....	.....	6
.80–.99	.....	.....	.....	1	1	2	3	2	.....	.....	9
15.00–.19	.....	.....	.....	.....	.....	4	3	1	.....	.....	8
.20–.39	.....	1	1	2	4	8	.....	.....	.....	.....	16
.40–.59	.....	3	9	4	3	10	.....	.....	.....	.....	29
.60–.79	.....	2	.....	2	1	6	1	1	.....	.....	13
.80–.99	.....	1	.....	.....	4	1	1	.....	.....	.....	7
16.00–.19	.....	1	.....	.....	5	6	1	.....	.....	.....	13
.20–.39	1	.....	.....	3	6	3	.....	1	.....	.....	14
.40–.59	.....	.....	.....	5	4	1	.....	.....	.....	.....	10
.60–.79	.....	.....	.....	9	8	1	.....	.....	.....	.....	18
.80–.99	.....	1	3	5	1	.....	.....	.....	.....	.....	10
Total	1	10	14	34	41	50	19	12	3	2	186

DISTANCE FROM CENTER 2′0 TO 11′3

< 12.00	.....	.....	.....	1	.....	.....	.....	1	1	.....	3
12.00–.19	.....	.....	.....	.....	.....	.....	.....	.....	.....	.....	.....
.20–.39	.....	.....	.....	.....	.....	.....	.....	.....	.....	1	1
.40–.59	.....	.....	.....	.....	.....	.....	.....	.....	1	1	2
.60–.79	.....	.....	.....	.....	.....	1	.....	1	.....	2	4
.80–.99	.....	.....	.....	.....	...	1	.....	.....	4	.....	5
13.00–.19	.....	.....	.....	.....	.....	.....	.....	5	2	.....	7
.20–.39	.....	.....	.....	.....	.....	.....	.....	1	2	.....	3
.40–.59	.....	.....	.....	.....	.....	1	.....	4	1	.....	6
.60–.79	.....	.....	.....	.....	.....	.....	4	3	.....	.....	7
.80–.99	.....	.....	.....	.....	1	.....	7	6	.....	.....	14
14.00–.19	.....	.....	1	.....	.....	2	2	5	1	.....	11
.20–.39	.....	.....	.....	.....	.....	1	3	3	.....	.....	7
.40–.59	.....	1	.....	1	3	16	6	.....	.....	.....	27
.60–.79	1	.....	.....	1	1	11	11	2	.....	.....	27
.80–.99	.....	.....	.....	1	1	3	7	4	.....	.....	16
15.00–.19	.....	.....	1	2	.....	7	17	3	.....	.....	30
.20–.39	.....	1	4	4	15	19	13	1	.....	.....	57
.40–.59	.....	9	23	12	15	26	1	.....	.....	.....	86
.60–.79	.....	8	6	4	2	28	8	2	.....	.....	58
.80–.99	.....	2	6	.....	7	17	5	.....	.....	.....	37
16.00–.19	2	2	2	.....	12	14	6	.....	.....	.....	38
.20–.39	1	1	.....	4	16	13	1	1	.....	.....	37
.40–.59	.....	1	.....	9	21	19	.....	.....	.....	.....	50
.60–.79	.....	.....	2	20	26	11	1	.....	.....	.....	60
.80–.99	.....	2	4	24	38	1	.....	.....	.....	.....	69
Total	4	27	49	83	158	191	92	42	12	4	662

TABLE IX

COLOR-CLASS, DISTANCE, AND PHOTO-VISUAL MAGNITUDE

(Summary of Table VII)

INTERVAL OF DISTANCE	COLOR-CLASS						ALL COLORS	AVERAGE COLOR-INDEX
	b	*a*	*f*	*g*	*k*	*m*		
1′.3–1′.9	15.95(6)	15.62(14)	15.75(29)	15.02(34)	13.18(5)	....	15.32(88)	+0.68
2.0–2.4	16.14(4)	15.94(19)	16.05(61)	14.99(35)	13.62(2)	12.33(1)	15.66(122)	+0.64
2.5–2.9	15.70(4)	15.85(11)	15.96(40)	14.64(22)	13.22(4)	....	15.44(81)	+0.66
3.0–3.4	....	16.04(10)	16.03(48)	14.74(12)	13.09(2)	....	15.74(72)	+0.61
3.5–3.9	15.54(3)	16.22(6)	15.83(27)	15.26(8)	12.47(1)	....	15.68(45)	+0.56
4.0–4.9	15.76(4)	16.30(19)	16.04(44)	14.45(13)	....	12.48(1)	15.79(81)	+0.54
5.0–5.9	15.73(5)	16.27(19)	15.88(38)	14.71(13)	....	....	15.76(75)	+0.52
6.0–7.0	16.06(2)	16.14(19)	15.91(27)	13.84(8)	....	....	15.70(56)	+0.48
7.1–9.0	15.37(5)	16.02(18)	15.70(30)	14.39(11)	12.87(2)	12.60(1)	15.41(67)	+0.54
9.1–11.3	15.97(4)	15.44(11)	15.38(34)	14.82(12)	11.68(2)	....	15.20(63)	+0.61
1′.3–11′.3	15.79(37)	16.01(146)	15.86(378)	14.78(168)	12.99(18)	12.47(3)	15.57(750)	+0.59
Outside Distance 2′......	15.76(31)	16.06(132)	15.89(349)	14.71(134)	12.91(13)	12.47(3)	15.61(662)	+0.58

TABLE X

THE COLOR OF GIANT STARS

Interval of Photo-visual Magnitude	Number of Stars	Average Color-Index
12.0−12.6..........	3	+1.43
12.6−13.2..........	16	+1.18
13.2−13.8..........	16	+1.06
13.8−14.4..........	32	+0.94
14.4−15.0..........	70	+0.74
15.0−15.6..........	173	+0.52
15.6−16.2..........	133	+0.54
16.2−16.8..........	147	+0.50

MOUNT WILSON OBSERVATORY
October 1919

Contributions from the Mount Wilson Observatory, No. 177
Reprinted from the *Astrophysical Journal*, Vol. LI, No. 1, pp. 4–12, 1920

BRIGHT NEBULAE AND STAR CLUSTERS IN SAGITTARIUS AND SCUTUM

PHOTOGRAPHED WITH THE 60-INCH REFLECTOR[1]

By JOHN C. DUNCAN

ABSTRACT

Photographs obtained with the 60-inch reflector are reproduced in five plates. They include the following interesting objects:

In Sagittarius: *Nebula N.G.C. 6523 (Messier 8);*
Star Cluster N.G.C. 6530 (Messier 8);
Globular Star Cluster N.G.C. 6656 (Messier 22).
In Scutum: *Star Cluster and Nebula N.G.C. 6611 (Messier 16);*
Swan Nebula N.G.C. 6618 (Messier 17).

The author refers to previous observations regarding these objects, calls attention to interesting details and identifies some of the brighter stars.

On Plate VII, showing the globular cluster Messier 22, there are about 75,000 stars, of which Shapley estimates that one-third are cluster stars.

Dark markings are clearly evident in the photographs of the nebulae N.G.C. 6523, 6611, and 6618.

Spectrum of nebula N.G.C. 6611 (Messier 16).—A spectrogram obtained by Slipher shows the nebulium lines weaker than the hydrogen series, and indicates that the nebula has a small radial velocity.

Star Córdoba No. 12431. The *right ascension* of this star seems to be incorrectly given in the Córdoba Observatory Catalogue.

Long-exposure photographs of nebulae and clusters made with the 60-inch reflector have been confined chiefly to objects north of the equator because of the better seeing at the high altitudes which they attain. It was the writer's privilege, during the summers of 1918 and 1919, to use this instrument on a number of nights, and the opportunity was utilized for photographing some of the more interesting of the objects that lie farther south. The four objects that form the subject of this article lie within a few degrees of each other in the rich region south of the bright star-cloud of Scutum Sobieskii, a region that includes also the Trifid nebula.

The photographs were made at the 25-foot focus of the 60-inch mirror, which was used at its full aperture. The plates were backed with a burnt-sienna mixture to prevent halation.

---

[1] *Astrophysical Journal*, 51, 4.

Plate III.—The chaotic nebula N.G.C. 6523 and the star cluster N.G.C. 6530 (Messier 8), in Sagittarius. Center of plate (1900.0), $\alpha = 17^h 57^m\!.9$, $\delta = -24°21'$. 1919, June 27. Exposure three hours. Seed 23 plate. Seeing very good. In preparing the positive for reproduction, the brightest part of the nebula was given a longer exposure than the remainder of the plate in order to bring out the detail.

The object known as Messier 8 is a bright open cluster (N.G.C. 6530) combined with a bright nebula (N.G.C. 6523), the combination being visible to the unaided eye as a hazy condensation in the Milky Way, not far from μ Sagittarii. It is a little more than one degree south of the Trifid nebula, which the nebula of Messier 8 much resembles. Messier's description[1] is concerned chiefly with the cluster, his only reference to the nebula being the remark that near the cluster is a bright star (9 Sagittarii) that is "surrounded by a very feeble light"; but modern instruments show that the nebula is one of the brightest and most extraordinary in the sky. Barnard[2] says of it that, "though seldom mentioned, it is far more remarkable than the celebrated Trifid." Sir John Herschel[3] gives a description and an elaborate drawing, and eloquent descriptions are also given in the catalogues of celestial objects of Smyth and Webb. Barnard has described the nebula in considerable detail,[4] and published photographs[5] of it made with the Willard lens. The only large-scale photograph that, to my knowledge, has appeared in any astronomical publication is the fine Crossley photograph[6] made by Keeler in 1899, although excellent plates have been obtained by Ritchey and Pease at Williams Bay, by Lampland at Flagstaff, and doubtless by others. Keeler[7] describes the spectrum as consisting of three bright lines. Lampland[8] has detected in the nebula eighteen variable stars.

The position given by Dreyer for N.G.C. 6523 is that of the brightest part of the nebula, at the left of the center of Plate III.

---

[1] Quoted by Flammarion, *L'Astronomie*, **32**, 26, 1918.

[2] *Astronomy and Astrophysics*, **13**, 792, 1894.

[3] *Cape Observations*, 1847, p. 116 and Plate I.

[4] *Loc. cit.* and *Astronomische Nachrichten*, **130**, 234, 1892.

[5] *Publications of the Lick Observatory*, **11**, 1913, Plates 51 and 52.

[6] *Ibid.*, **8**, 1908, Plate 56. [7] *Ibid.*, **3**, 205, 1904. [8] *Popular Astronomy*, **26**, 32, 1919.

PLATE III

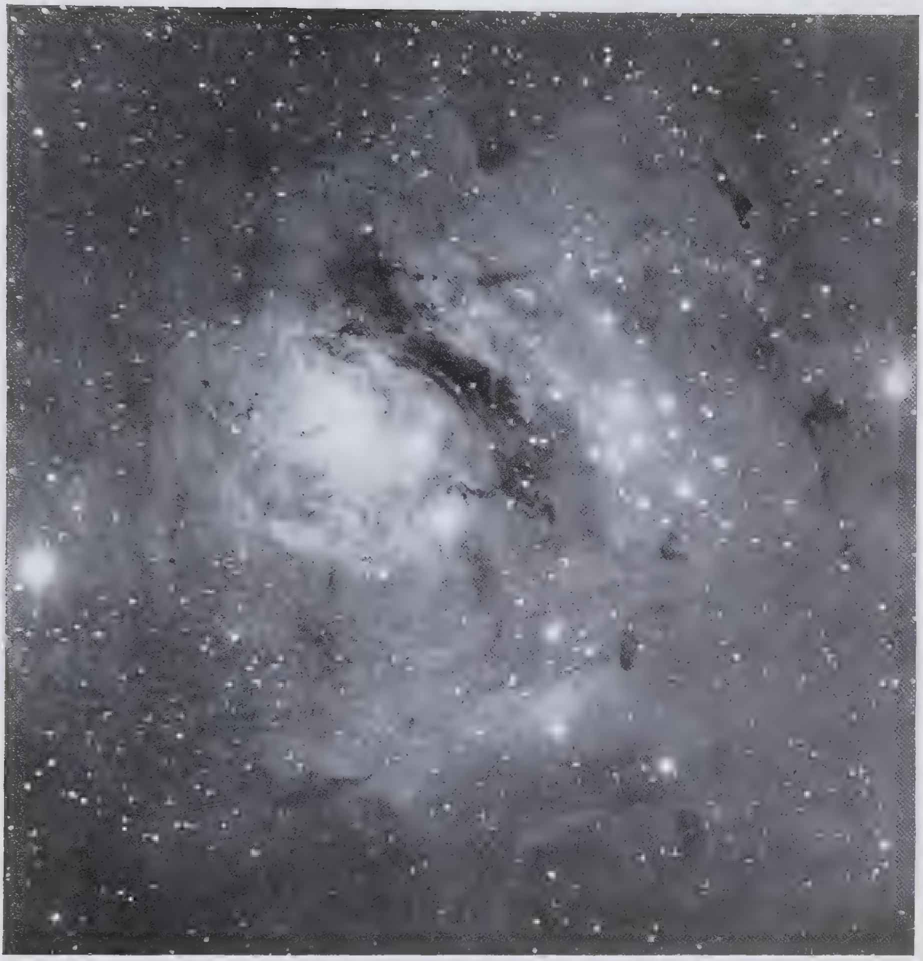

Messier 8, Consisting of the Nebula N.G.C. 6523 and the Star Cluster N.G.C. 6530

Scale: 1 mm = 16″.8 Enlargement 1.64

The center of the bright cluster appears on the right side of the plate, about 10^s farther west than Dreyer's position for N.G.C. 6530. Perhaps the most striking feature of the photograph is the dark rift that cleaves the nebula from northwest to southeast, passing between the cluster and the brightest part of the nebula. This rift is not perfectly dark, but contains certain bright filaments that recall the nebula about Merope in the Pleiades. This filamentous structure occurs also on the left side of the plate, east of the bright star 7 Sagittarii. Besides the great rift, there are many smaller, irregular, sharply defined dark markings in all parts of the nebula, resembling the dark regions of the neighboring Milky Way which are interpreted by Barnard as due to obscuring matter. Some of these small dark markings occur in the very brightest part of the nebula; these, however, are not so dark as those in the fainter portions and would not be easily seen in the reproduction had not this part of the plate been given a longer exposure than the remainder in making the positive. Possibly the absorbing material is not perfectly opaque, but allows some light from the brightest nebulosity to pass through. The abrupt edge of the faint nebulosity on the north and south sides of the nebula may perhaps also be due to obscuring masses. The dark spots in Messier 8 suggested to Miss Clerke the name of "Lagoon";[1] but she seems to have found the name unsatisfactory, as it does not appear in the second edition of her book. Professor Ritchey applies the term "chaotic" to nebulae of this class.

Two of the dark spots shown in Plate III are listed in Professor Barnard's "Catalogue of 182 Dark Markings in the Sky."[2] No. 88 of that catalogue is 38 mm from the right edge and 39 mm from the bottom, and No. 89 is 13 mm from the right and 53 mm from the top, near the bright star Córdoba 12446—not very well brought out in the engraving, though easily seen on the original plate. South of the stars Córdoba 12431 and 12437 and extending eastward almost to 12446 is a remarkable irregular bright line of nebulosity which suggests a thin fold turned edgewise to the observer. About 3′ west and 1′ south of Córdoba 12431 is a shorter, brighter line of the same nature. In the upper right corner of the plate, about 7′ south of Córdoba 12446, is a fainter line of the same general appearance. The appearance of slightly brighter nebulosity just below Córdoba 12466 is due to halation.

---

[1] *The System of the Stars*, first edition (1890), p. 284.

[2] *Astrophysical Journal*, **49**, 16, 1919.

The positions and magnitudes of bright stars given in the following table were taken from the *Catálogo de 15,975 Estrellas* of the Córdoba Observatory.[1] The right ascension of No. 12431 as given in that catalogue seems to be in error, as the only star near its place and comparable with it in brightness appears on the photograph with about 2^{s} less right ascension. It is stated in the notes at the end of the Córdoba publication that the position of this star rests on a single observation.

Córdoba No.	Name	Visual Mag.	Place, 1900.0		Distance in mm from Edge of Plate III
			α	δ	
12383	7 Sagittarii	5.9	$17^{h}56^{m}43^{s}.33$	$-24°16′53″.1$	L 4, B 50
12403		9.4	57 37.20	22 12.8	L 47, T 56
12407	9 Sagittarii	6.0	44.55	21 45.6	L 53, T 57
12411		8.1	49.02	18 52.7	L 57, B 57
12417		9.0	58 7.09	14 46.0	R 48, B 43
12418		9.6	7.42	5 41.3	R 48, B 11
12420		8.2	7.73	11 9.6	R 48, B 30
12430		8.0	17.84	23 22.2	R 40, T 52
12431		9.0	18.17(?)	26 27.3	R 42, T 41
12435		8.4	25.65	9 50.1	R 33, B 25
12437		8.8	27.89	27 2.4	R 31, T 39
12446	Piazzi 342	8.0	59 2.52	24 12.3	R 3, T 49

The following defects in Plate III might prove deceptive:

Description	Distance in mm from Edge of Plate
Round, like faint star	R 31, B 58
Round, like faint star	R 22, B 64
Irregular, nebulous, 1 mm diameter	R 13, B 56

Plate IV.—The nebula and star cluster N.G.C. 6611 (Messier 16), in Scutum Sobieskii. Center of plate (1900.0), $\alpha = 18^{h}13^{m}.1$, $\delta = -13°51′$. 1919, August 25–26. Exposure 205 minutes. Seed 30 plate. Thick sky and poor seeing.

This object was discovered by Messier in 1764.[2] In the catalogues of Herschel, Webb, Smyth, and Dreyer it is described simply

---

[1] *Resultados del Observatorio Nacional Argentino en Córdoba*, **22**, 1913.

[2] Captain W. H. Smyth, *A Cycle of Celestial Objects*, **2**, 415, 1844.

PLATE IV

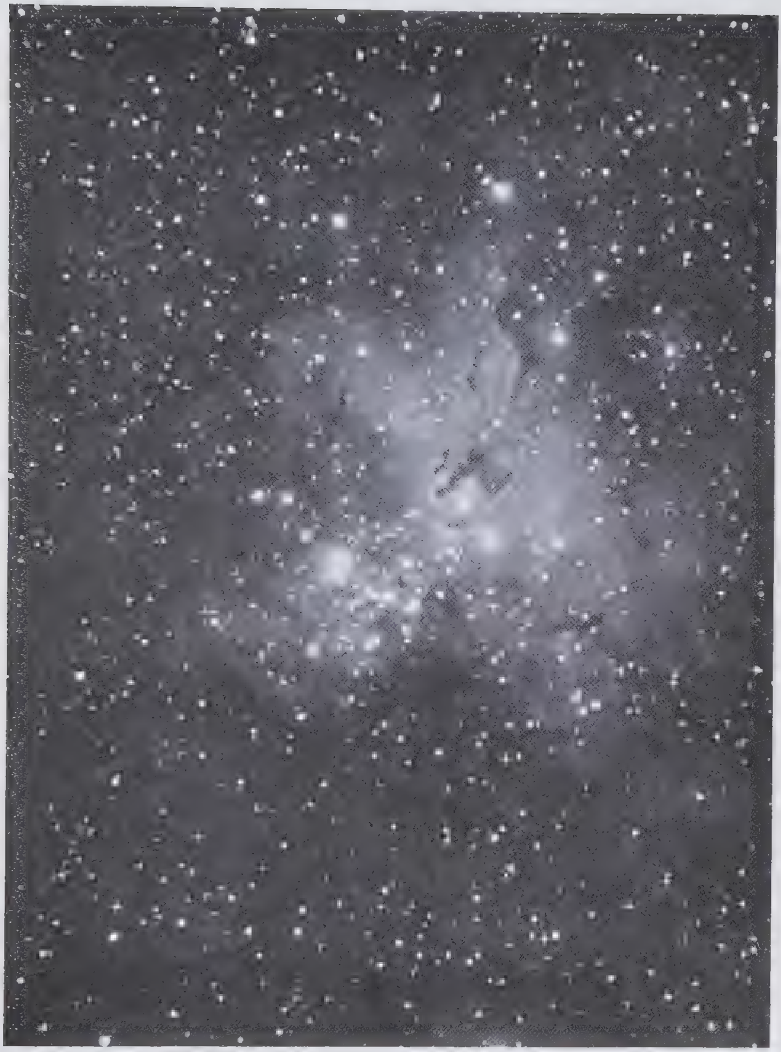

The Nebula and Star Cluster N.G.C. 6611=M 16

Scale: 1 mm=14″.4 Enlargement 1.85

as a star cluster, no mention being made of the nebula, though Messier says[1] the stars are "mixed with a feeble light." The nebula was detected photographically by Barnard[2] in 1895 and Roberts[3] in 1897. Though Messier seems to have been the only early observer to perceive the nebula visually, it is no more difficult than the nebula in the Pleiades, and I have seen it easily with the 12-inch refractor of the Whitin Observatory.

S. DM.	Visual Mag.	Place, 1855.0		Distance in mm from Edge of Plate IV
		α	δ	
−13°4914.....	9.5	$18^{h}9^{m}49^{s}.1$	−13°47′.9	L 10, B 49
15.....	9.2	52.6	35.8	L 13, B 1
17.....	9.5	55.2	39.7	L 14, B 15
−14 4985.....	8.9	10 13.0	−14 7.7	L 31, T 4
86.....	9.1	13.8	2.7	L 33, T 26
−13 4920.....	9.2	14.3	53.3	L 33, T 64
21.....	9.2	17.0	53.2	L 37, T 65
23.....	9.3	19.4	48.2	L 40, B 52
24.....	9.5	20.6	57.5	L 41, T 46
25.....	8.3	22.7	50.7	L 43, B 63
26.....	8.3	23.2	50.8	L 43, B 65
−14 4988.....	8.5	23.4	−14 1.7	L 43, T 28
−13 4927.....	9.2	27.1	−13 48.4	L 48, B 53
30.....	9.1	39.6	52.6	R 41, T 65
31.....	8.2	42.3	35.6	R 36, B 0
32.....	9.0	43.1	51.7	R 37, B 67
−14 4991.....	8.2	45.0	−14 2.6	R 36, T 24
−13 4933.....	9.8	51.8	−13 52.0	R 28, B 67
34.....	9.3	52.2	58.2	R 29, T 43
36.....	9.4	56.7	59.8	R 23, T 35
37.....	9.8	11 6.1	57.9	R 14, T 45

The large gap in the north side of the nebula led Barnard[4] to compare it to the nebula in Orion. The most interesting feature, however, as disclosed by the present photograph, is the system of sharply defined dark markings of which the most conspicuous is on the southeast side, extending inward beyond the center. This marking so resembles the result of irregular flow of developer that, when it appeared on an earlier negative, its reality was questioned until it was fully verified by the present plate. The nebulosity in a thin line lying along the northern rim of the great dark marking is brighter than elsewhere.

---

[1] C. Flammarion, *L'Astronomie*, **32**, 239, 1918.

[2] *Publications of the Lick Observatory*, **11**, 1913, Plate 57.

[3] *Celestial Photographs*, **2**, 151, 1899.

[4] *Astronomische Nachrichten*, **177**, 233, 1908.

Dr. V. M. Slipher, of the Lowell Observatory, has written me that he obtained a spectrogram of this nebula in September, 1919, showing a spectrum "similar to that of the Trifid nebula and the outer parts of the Orion nebula, in that the nebulium lines N_1 and N_2 are weaker than the hydrogen series" and that, like the Trifid, the nebula has a small radial velocity.

The magnitudes and positions of bright stars given in the table on page 5 were taken from Schönfeld's Southern *Durchmusterung.*

Plates V and VI.—The Swan Nebula, N.G.C. 6618 (Messier 17), in Scutum Sobieskii. Center of Plate V (1900.0), $\alpha = 18^{\mathrm{h}}15^{\mathrm{m}}.1$, $\delta = -16^\circ 14'$. 1919, July 29. Exposure three hours. Seed 23 plate. Seeing fair.

This nebula was discovered by Messier in 1764[1] and attracted considerable attention from observers throughout the last century. Drawings of it were made by Sir John Herschel in 1833[2] and 1837,[3] Lord Rosse in 1854,[4] Lassell in 1862,[5] Trouvelot and Holden in 1875,[6] and a number of others. It was photographed in 1893 by Roberts,[7] using his 20-inch reflector and giving an exposure of two hours, and in 1899 by Keeler[8] with the 36-inch Crossley reflector and an exposure of four hours. Huggins[9] described the spectrum as consisting of a single bright line ($H\beta$ or λ 5007 ?), together with a faint continuous spectrum when the image of the brightest part of the nebula was thrown upon the slit.

Messier perceived only a "train of light without stars, 5′ or 6′ in extent"[10]—evidently the brightest part shown in the photographs, lying northwest and southeast. Herschel, in his drawing of 1833, shows the bright, curved part extending southward

---

[1] Smyth, *A Cycle of Celestial Objects*, **2**, 416, 1844.

[2] *Phil. Trans.*, **123**, 461 and Plate XII, 1833.

[3] *Cape Observations*, 1847, p. 7 and Plate II.

[4] *Observations of Nebulae and Clusters*, p. 151 and Plate VI.

[5] *Memoirs, R.A.S.*, **36**, 49 and Plates VII and VIII, 1867.

[6] *Americal Journal of Science* (3), **11**, 341, 1876.

[7] *Celestial Photographs*, **1**, 101, 1893.

[8] *Publications of the Lick Observatory*, **8**, Plate 58, 1908.

[9] *Phil. Trans.*, **156**, 385, 1866.

[10] Flammarion, *L'Astronomie*, **32**, 241, 1918.

PLATE V

W

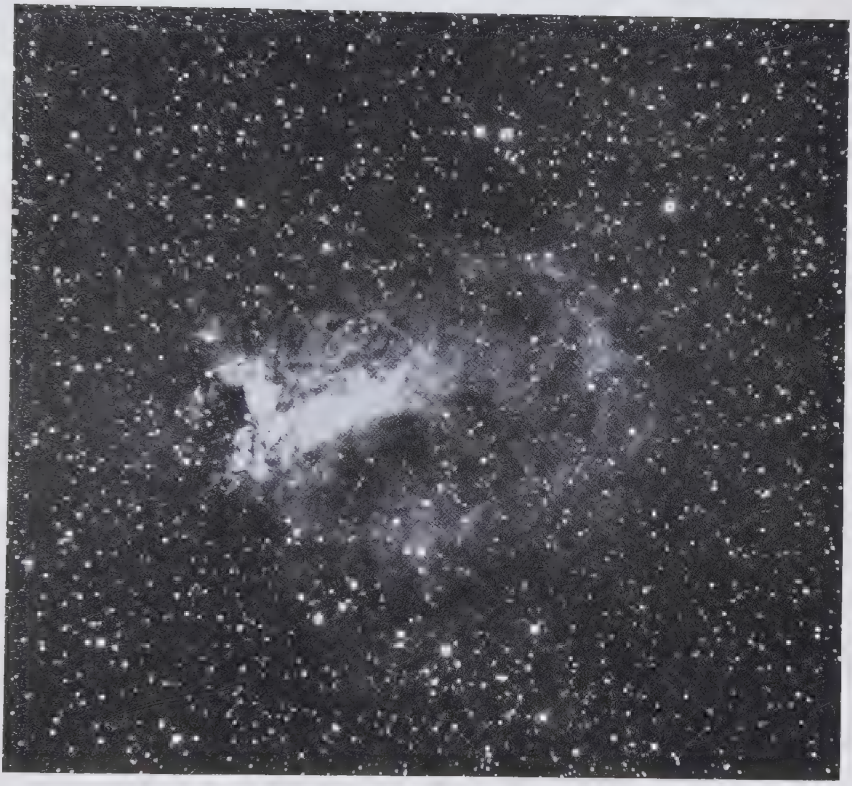

E

THE SWAN NEBULA N.G.C. 6618=M 17

Scale: 1 mm=19″.5 Enlargement 1.4

PLATE VI

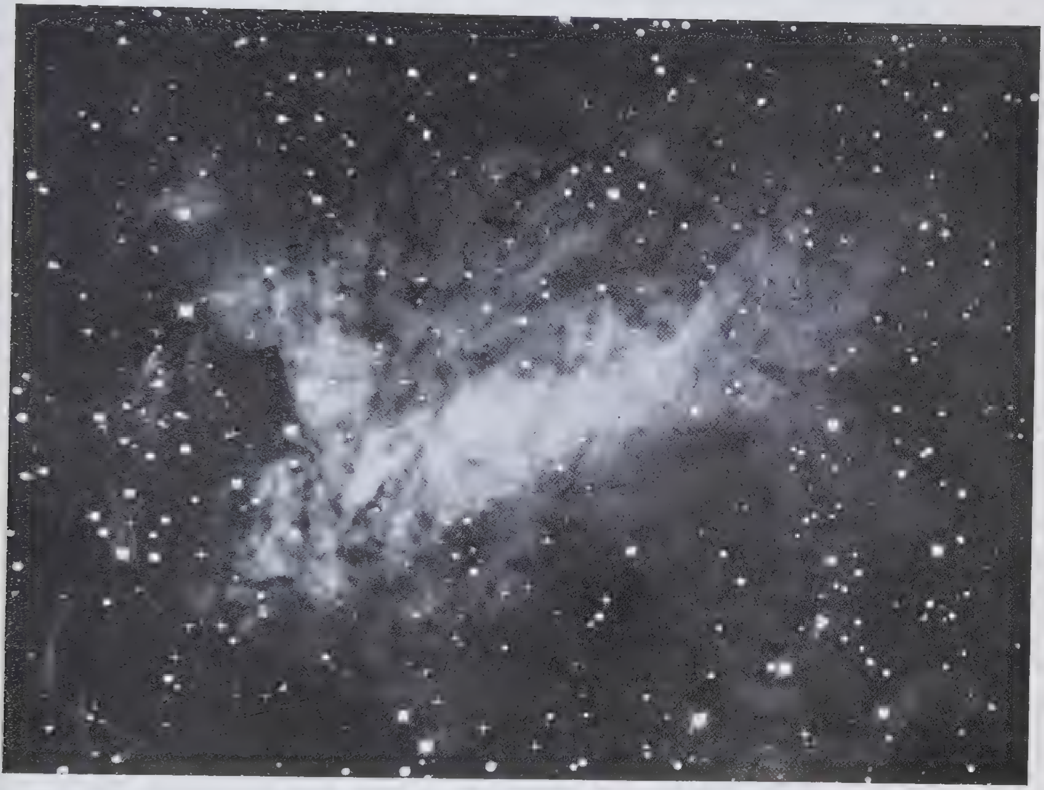

Central Part of the Swan Nebula

Scale: 1 mm = 7″.2 Enlargement 3.8

from the west end of Messier's streak and giving the nebula, in Herschel's mind, the appearance of a capital Ω with the right hook exaggerated. This appearance has led to the various names of Omega, Horseshoe, and Swan—the last applying more appropriately than the others, perhaps, to the view obtained with a moderate-sized telescope. Herschel's drawing of 1837 shows a second curve at the other end of Messier's streak, which explains the description "2-hooked" in the N.G.C. This is evidently the brightest part of the diffuse nebulosity shown near the center and eastern edge of Plate V. Holden, in comparing his own observations with those of other observers, comes to the conclusion that conspicuous motion took place within the nebula between 1833 and 1875; but a comparison of the photographs shows that no changes on such a large scale occurred between 1893 and 1919, and it seems certain that the apparent changes noted by Holden were due to inaccuracies in drawing.

S. DM.	Visual Mag.	Place, 1855.0		Distance in mm from Edge of Plate V
		α	δ	
-16°4813.....	9.4	$18^h 11^m 47^s.6$	$-16^\circ\ 4'.3$	L 13, B 17
15.....	9.5	12 2.0	0.3	L 22, B 5
16.....	9.6	5.7	15.7	L 26, B 53
17.....	10	9.4	22.6	L 30, T 26
18.....	9.4	13.4	14.2	L 31, B 47
19.....	9.7	22.5	8.6	L 38, B 32
21.....	9.2	25.8	21.0	L 41, T 31
22.....	9.2	26.3	5.6	L 41, B 21
23.....	10	29.4	0.9	L 44, B 6
26.....	9.6	41.8	4.9	L 52, B 19
27.....	9.5	44.5	8.3	L 54, B 29
28.....	9.1	49.5	4.0	R 52, B 17
29.....	8.7	52.2	26.2	R 49, T 16
30.....	8.9	57.7	26.4	R 45, T 16
32.....	9.3	13 5.0	5.0	R 41, B 19
34.....	9.3	8.4	0.6	R 39, B 8
35.....	9.5	12.8	16.3	R 34, B 52
36.....	7.8	26.5	23.0	R 24, T 25

The photograph brings out much faint nebulosity that cannot be perceived visually, especially to the east and north of the region of Messier. This nebulosity is of a filamentous structure, somewhat remotely resembling that of the Network Nebula in Cygnus, N.G.C. 6992. Like M 8 and M 16, this nebula shows a set of dark markings, but they seem of a different kind from those of the former nebulae. The most conspicuous is the square-cornered, sharply outlined space under the neck of the "swan," which is so devoid of light that its contrast with the bright part of the nebula at first gives the impression that it is blacker than the surrounding sky. This dark space is closed on the west by nebulosity which, though faint even on the photograph, was seen and drawn by Lassell. At the north edge of the faint northern extension of the nebula is a dark tree-like structure (almost lost in the engraving). Most interesting of all are the dark streaks that cross the region of Messier and especially the head and neck of the swan. They are well shown in Plate VI. Some of these seem to radiate from a point near the base of the swan's neck.

The magnitudes and positions of bright stars in the table on page 7 were taken from Schönfeld's Southern *Durchmusterung*. The nebula is S. DM. $-16°4820$.

Plate VII.—The globular star cluster N.G.C. 6656 (Messier 22), in Sagittarius. Center of plate (1900.0), $\alpha = 18^{h}30^{m}.3$, $\delta = -23°59'$. 1918, August 6. Exposure three hours. Seed 23 plate. Seeing good. Part of the guiding for this photograph was by Mr. Hoge.

This cluster has been known since the early days of the telescope, and is one of the six "nebulae" in the list drawn up by Halley[1] (the others were the great nebulae of Andromeda and Orion and the star clusters ω Centauri, M 11 and M 13). Smyth says,[2] "Halley ascribes the discovery of this in 1665 to Abraham Ihle, a German; but it has been thought this name should have been Abraham Hill, who was one of the first council of the Royal Society, and was wont to dabble with astronomy. Hevelius, however, appears to have noticed it previous to 1665 so that neither Ihle nor Hill can be supported."

A photograph made in 1897 has been published by Bailey,[3] who discovered sixteen variable stars in the cluster.

Mr. Shapley[4] places the cluster at a distance of 8300 parsecs (or 27,000 light-years) from the sun and 1200 parsecs from the

---

[1] *Phil. Trans.*, **29**, 390; abridged edition, **4**, 224, 1749.

[2] *Cycle of Celestial Objects*, 1844, p. 422.

[3] *Annals of Harvard College Observatory*, **38**, Plate IX, Fig 2, 1902.

[4] *Mt. Wilson Contr.*, No. 160; *Astrophysical Journal*, **50**, 42, 1919.

PLATE VII

W

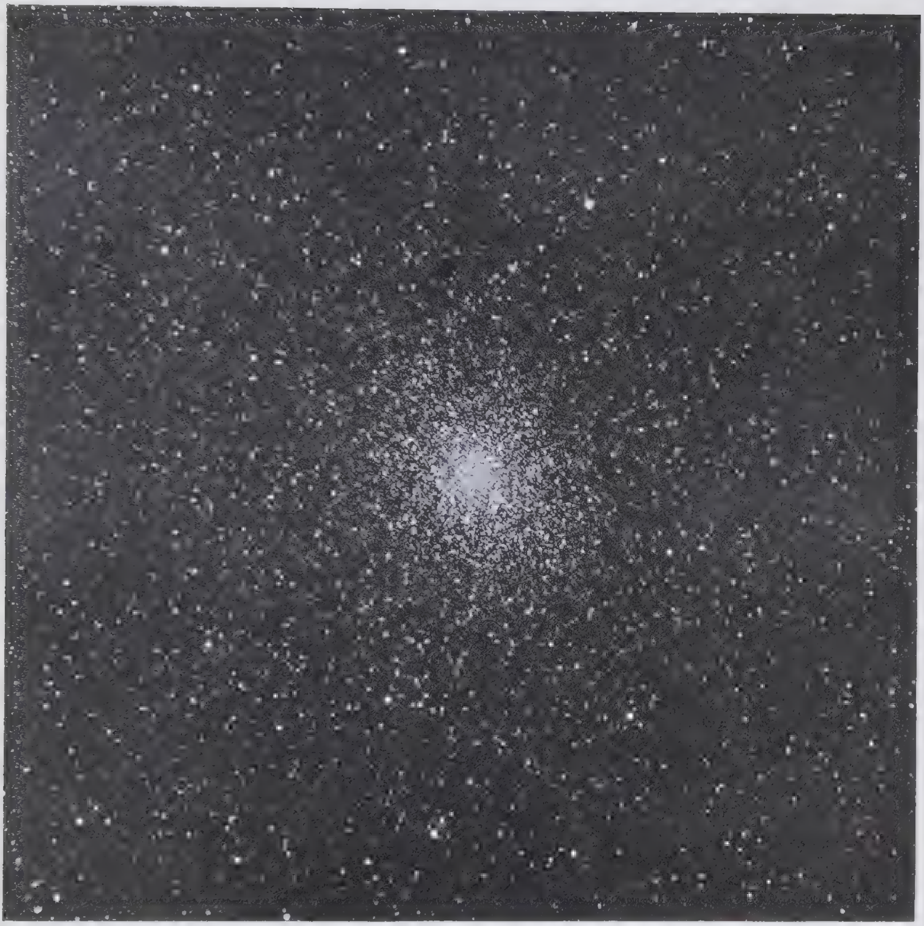

E

The Globular Star Cluster N.G.C. 6656=M 22

Scale: 1 mm=16″.0 Enlargement 1.7

plane of the galaxy—nearer the galactic plane than any other known cluster. Its diameter is at least 30′, so that the light of a star at one end of a diameter must require more than two hundred and forty years to travel to the other end. On the plate reproduced here, Miss Davis has counted about 75,000 stars, of which Shapley estimates that one-third are cluster stars, while the others belong to the Milky Way background. The faintest stars on the original plate are of about the twentieth magnitude, or, on the basis of Shapley's distance, between absolute magnitudes +5 and +6, about like the sun. From counts made on this plate and on others of shorter exposure, Shapley finds that the projection of the major axis of the cluster lies in position angle 25°, and is parallel to the galactic plane.

Two dark spots appear in the reproduction, one 13 mm from the left edge and 32 mm from the top, and the other 57 mm from the left and 34 mm from the top. These are defects due to insensitive spots in the original plate.

The following stars were identified in the Córdoba catalogue referred to in the discussion of Plate III.

Córdoba No.	Visual Mag.	Place, 1900.0		Distance in mm from Edge of Plate VII
		α	δ	
12919.........	9.0	$18^{h}30^{m}35^{s}.26$	$-24^{\circ}\ 8'38''.7$	R 44, T 26
12922.........	8.5	18 30 41.49	−23 50 42.0	R 38, B 27

I desire to record here my keen appreciation of the kindness of Mr. Hale and Mr. Adams in giving me a place among the Mount Wilson observers during two summers, and to Mr. Ritchey and Mr. Pease for practical suggestions and for allowing me the use of the 60-inch reflector on certain nights when that privilege would regularly have been theirs.

Whitin Observatory
Wellesley, Mass.
October 1919

Contributions from the Mount Wilson Observatory, No. 178
Reprinted from the *Astrophysical Journal*, Vol. LI, pp. 37–48, 1920

THE SPECTRUM OF ELECTRICALLY EXPLODED WIRES[1]

By J. A. ANDERSON

ABSTRACT

High-temperature absorption spectra, such as those given by the sun and some stars have not been reproduced fully in the laboratory. The absorption spectra obtained with the arc and the electric furnace have been limited to wave-lengths below 0.56 μ for iron and have not included the high-temperature lines. The author has developed *a method of obtaining high-temperature absorption spectra,* which consists in electrically exploding a fine wire in a confined space. When the explosion occurs in air confined in a tube or slot, the flash gives a brilliant continuous spectrum crossed by the absorption lines of the elements composing the wire. The spectrograms reproduced show that for *iron* an absorption spectrum was obtained which extends to 0.66 μ and includes all classes of lines except the pronounced enhanced lines. *Copper, nickel,* and *manganin* were also investigated. When the method has been more fully developed it may be possible to imitate stellar absorption spectra of the solar type.

New laboratory source of light.—By discharging a large condenser, charged to 26,000 volts, through a fine wire 5 cm long, about 30 calories of energy were dissipated in about 10^{-5} sec. If all of this energy had gone into the two milligrams of wire it would have raised its temperature to about 300,000°. Actually, the brilliant flash which resulted had an intrinsic intensity corresponding to a temperature of about 20,000°, or about one hundred times the intrinsic brilliancy of the sun. The character of the spectrum and also the pressure developed depend, of course, upon the energy per unit mass and also upon the initial pressure and volume of the surrounding gas. When the wire was exploded within a tube or slot under a bell jar exhausted to 2 cm pressure, a line *emission spectrum* was obtained. As the air pressure was raised the continuous background increased in intensity and the spectrum became more and more an *absorption spectrum.* Because of the high temperature the *continuous spectrum* extends far into the ultra-violet. This source should be useful in studying the *pressure-shift* of lines, as pressures of 50 atmospheres can readily be obtained. The spectrograms already secured show the effect clearly. The *appearance* of the flash is shown by direct photographs. Its size corresponds to a speed of propagation in open air of about 3.3 km per second. Some striking *mechanical effects of the explosion* are briefly described.

Meteorites falling into the sun.—In a *theoretical discussion* the author points out that meteorites falling into the sun would be given a relatively enormous amount of energy in a short time and hence would be exploded by mechanical means much as his wires were exploded by electrical means.

Fine wires.—A simple method of producing on a lathe wires weighing down to 0.1 mg per cm was developed.

Laboratory investigations deal almost exclusively with emission spectra, that is, spectra consisting of bright lines on a more or less completely dark background. Absorption spectra such as are given by the sun and stars, not being readily produced in the laboratory, must be interpreted in terms of the knowledge derived from a study of emission spectra, which would not be a serious drawback if the mechanism of emission and of absorption were known; since, however, neither is at all well understood, one never feels absolutely sure of his ground in discussing solar or stellar spectra.

---

[1] *Astrophysical Journal*, 51, 37, 1920.

Absorption spectra are encountered in the laboratory: (1) in self-reversals of arc or spark lines; (2) by passing white light through cooler vapors or gases. In the arc or spark at atmospheric pressure only a small percentage of the lines are found to be reversed; in the spark at high pressures or in liquids more lines may be reversed, and in the experiments of Hale and Kent[1] at the highest pressure a fair absorption spectrum was produced, though the background was not quite uniform. Possibly at still higher pressures this method would yield a pure absorption spectrum. The high pressure required is, however, a disadvantage in more ways than one.

By passing white light through vapors or gases a pure absorption spectrum is obtained, but, since the hottest source of white light at our disposal is the crater of the arc, it has been found possible to reverse only those lines which are usually found self-reversed in the arc, and naturally very little can be done in the region beyond λ 2500. As an illustration consider the spectrum of iron, perhaps the most important element from the standpoint of the astrophysicist. The low-temperature lines (Groups *a* and *b* of Gale and Adams) are found self-reversed in the arc from the extreme ultraviolet up to about λ 5500, although reversals above λ 4500 are not common. The same lines are also obtained as absorption lines in the electric furnace, either by passing white light from the crater of the arc through the furnace tube or by inserting a graphite plug near the middle of the tube;[2] but no lines beyond λ 5500 have been reversed by this means. Liveing and Dewar mention λ 5615 as having been reversed in one of their experiments, but this is the only case of reversal for iron in the region less refrangible than λ 5500 that I have come across. The high-temperature lines, and in fact the great majority of iron lines, are nearly unknown as absorption lines except in the sun and stars.

---

[1] *Publications of the Yerkes Observatory*, **3**, Part II.

[2] A. S. King, *Mt. Wilson Contr.*, No. 174; *Astrophysical Journal*, **51**, 13, 1920.

In the course of the experiments described below the absorption spectrum of iron from λ 2250 to λ 6600 has been photographed; all classes of lines except the pronounced enhanced lines are present, as may be seen from the reproductions. Of course only a beginning has been made so far; but the results obtained are quite promising, and it seems reasonable to expect that when the method is fully developed we may be able to imitate successfully the spectra given by the sun and stars. The object of the present communication is to call attention to the method in the hope that other workers may be induced to aid in developing it as rapidly as possible.

It may be of interest to state briefly the idea which led to these experiments: Consider a meteoric particle falling into the sun or a similar center of attraction. Let its mass be m and its velocity v; its kinetic energy is therefore $\frac{1}{2} mv^2$. With the sun as the center of attraction we have $v = 6 \times 10^7$ cm/sec., and hence, for $m = 1$ gram, the energy is 1.8×10^{15} ergs or about 4×10^7 calories. How far such a particle would travel before being consumed will of course depend upon the density of the atmosphere through which it moves. In general the path would not be long; hence the time would be short, perhaps a second or, more probably, only a very small fraction thereof. The conditions thus indicate that *a very large quantity of energy is thrown into a small amount of matter in a short space of time.* The effects, spectroscopic and otherwise, of such conditions cannot of course be predicted; hence if any of the circumstances could be produced experimentally they might lead to interesting results.

The conditions to be satisfied are as just stated: to throw a large amount of energy into a small amount of matter in as short a time as possible. By purely mechanical means this does not appear to be easy, but by electrical methods it seemed worth trying.

In the first attempts a small iron wire was inserted in a circuit containing two fair-sized 110-volt direct-current generators in series. On closing the circuit the wire blew up like an ordinary fuse with a blinding flash of light, the spectrum of which was easily photographed. On account of the large inductance of the circuit containing the armatures of the two generators, the duration of the flash was rather long and the amount of energy developed per gram per second not, therefore, very large. An estimate placed this at about 10^5 calories. A large storage battery would undoubtedly discharge at a much greater rate, but for obvious reasons this was not tried. Instead, a large glass plate condenser was built, which, when charged to about 25,000 volts, contains an amount of energy equal to 30 calories. When discharged through an iron wire 5 cm long and weighing 2 milligrams, this gives very good results. The circuit was so arranged that the frequency of the electrical oscillations as determined by a rotating mirror was 150,000 cycles per second, and the damping large enough to confine most of the energy to the first cycle. (See Plate VIII *a*, which is a photograph of the flash as seen in the rotating mirror.) If we assume that the effective time of a discharge is of the order of 10^{-5} seconds and that the larger part of the energy of the condenser charge is expended in the exploding wire, we arrive at a rate of energy development per gram which is of the right order of magnitude. The discharge of this condenser was used throughout the present work.

DETAILS OF APPARATUS AND EXPERIMENTS

The condenser consists of 98 plates of single-strength window glass 40×50 cm (16×20) inches having tin-foil coatings 35×43 cm laid on with shellac. It is charged from a 500-watt, 26,000-volt transformer through a mechanical rectifier, the arrangement of the circuit being as shown in Figure 1. The difference of potential of the condenser plates can be regulated to some extent by varying the length of the series spark-gap *S*. When this is short, 2 mm approximately, and the gap *W* closed by a heavy conductor, sparks pass through *S* at the rate of 2 or 3 per second. When the gap *S* is lengthened to 2 cm, the sparks pass at the rate of one in about 2 seconds. The entire circuit *CSW* is made as short and compact as possible in order to keep the inductance low and the

PLATE VIII

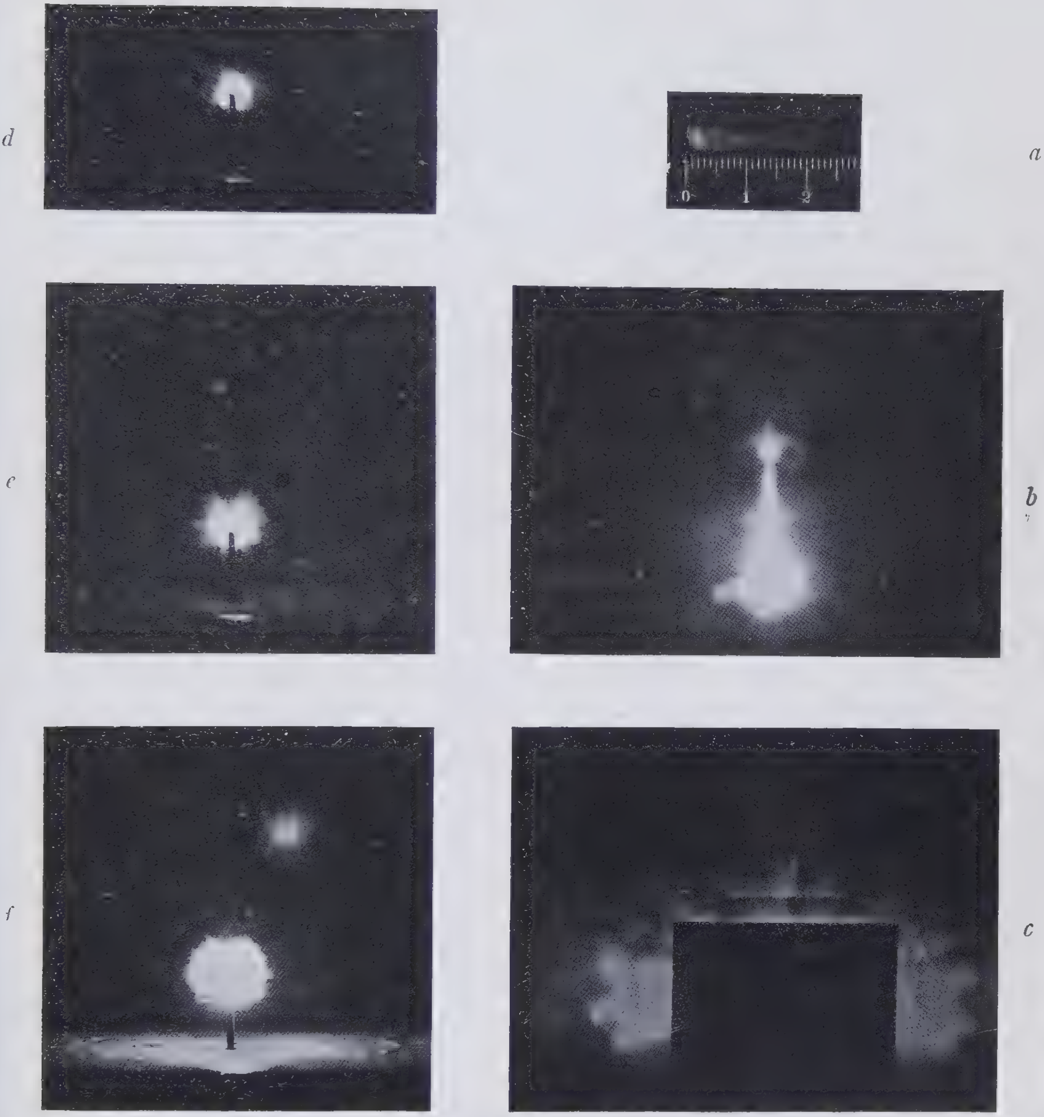

Photographs of Electrically Exploded Wires

- *a* Explosion photographed by rotating mirror. Numbered divisions of scale correspond to one one-hundred-thousandth of a second
- *b* Explosion in block of wood; end view
- *c* Explosion in block of wood; side view
- *d* Explosion in open air; aperture F/44
- *e* Explosion in open air; aperture F/22
- Explosion in open air; aperture F/5.6. The faint image above is a ghost from the camera objective

frequency high. Since the capacity of the condenser is about 0.4 microfarad, and the frequency 150,000 cycles per second, it follows that the total inductance is only about $\frac{1}{400}$ millihenry. The sparks are very noisy and the observer must not go too close without protecting his ears. This is especially true when a wire is exploded in the circuit. The sound-wave then sent out can be felt as a distinct sharp blow on the face or hands at a distance of 50 cm or more.

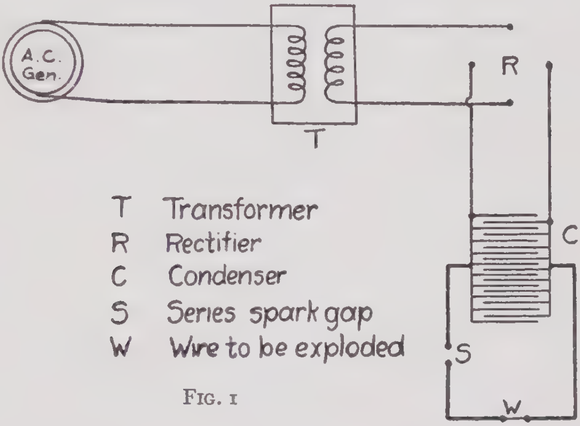

FIG. 1

The mechanical effects of exploding wires are interesting. Some of these have been described by Singer[1] and by F. E. Nipher.[2] If a glass tube with open ends be slipped over the wire the explosion breaks the tube into fragments, which are scattered all over the room; if the ends of the tube are closed by cork stoppers and the tube filled with water, the water disappears completely and the tube is broken into powder so fine that it is sometimes difficult to recognize it as glass. With the wire a few millimeters below the free surface of water in a large glass jar, the sound-wave transmitted through the water by the explosion thoroughly wrecks the containing vessel. The apparent absence of any heat effect is also quite striking. A No. 40 B. and S. gauge (0.080 mm) copper wire with double cotton insulation may be exploded, and in most cases the insulation remains nearly unchanged. Tissue paper wrapped tightly around the wire is torn into small bits, but not burned or even charred.

---

[1] *Philosophical Magazine*, 46, 161, 1815.

[2] *Experimental Studies in Electricity and Magnetism.* Blakiston, 1914.

With the present condenser and voltage, it is not possible to obtain good effects with wires larger than No. 36 B. and S. gauge (0.127 mm), or longer than 8 cm; in fact smaller and shorter wires give better results. At first this was a great inconvenience, as it was found impossible to procure such small wires on the Pacific Coast. The difficulty was overcome by one of the mechanicians, who found a neat way of making practically straight lathe turnings of any length, in sizes from less than 0.1 milligram per centimeter up.

In photographing the spectrum of the explosions a plane grating spectrograph was used. The collimator is a 12.5 cm (5 in.) Brashear telescope lens of 150 cm (60 in.) focus. The grating is a 10 cm (4 in.) Rowland, known as the "Kenwood grating," having bright second and third orders. The camera lens is a Bausch and Lomb Tessar Ic, F/4.5 of 39 cm (15 $\frac{3}{4}$ in.) focus. The second-order spectrum was used and the grating so inclined to the axis of the camera lens that the dispersion at the middle of the plate is 6 A per millimeter. The ultra-violet region was photographed with a large Fuess quartz spectrograph, giving a scale at λ 2300 of about 4.5 A per millimeter.

RESULTS

The following are the general conclusions from the work up to the present time:

1. *Wire exploded in the open air.*—When viewed side on, the spectrum consists of bright lines, with faint self-reversals in the green region and more prominent reversals in the violet. There is a continuous background of increasing intensity toward shorter wave-lengths, but not very strong. Viewed end on, the reversals are more prominent throughout and the continuous background very much strengthened. At λ 3700 the strength of the background is so great that this portion of the spectrum looks very much like a normal absorption spectrum. Open-air explosions were not studied in the region beyond λ 3600.

PLATE IX

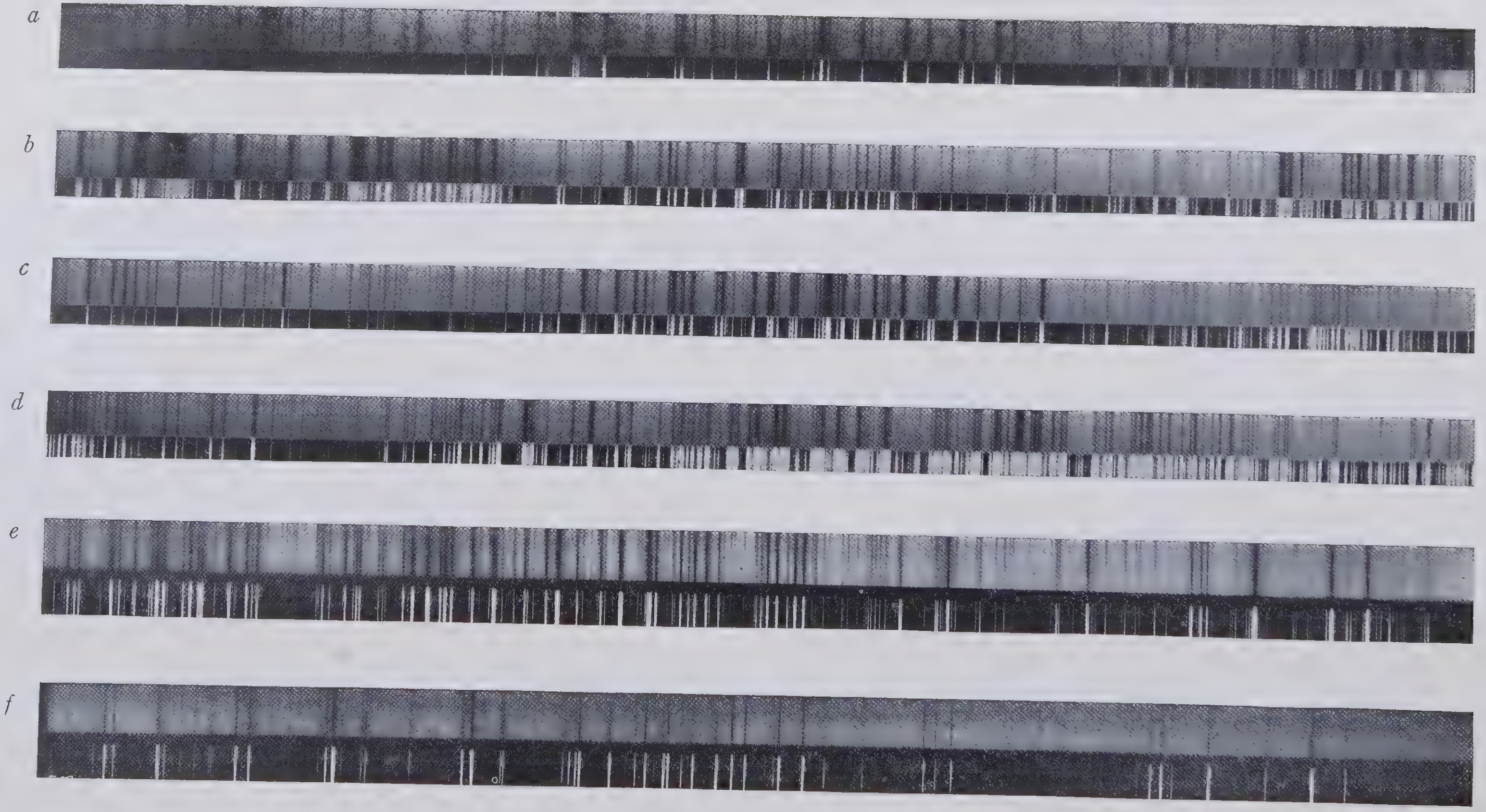

Spectra of Electrically Exploded Iron Wires with Iron Arc Comparison

Quartz Spectrograph: *a*, λ 2270 to λ 2490; *b*, λ 2472 to λ 2764; *c*, λ 2780 to λ 3280; *d*, λ 3216 to λ 4075
Grating Spectrograph: *e*, λ 3700 to λ 4090; *f*, λ 5143 to λ 5645

2. *Wire surrounded by a wooden tube 1 cm in diameter and viewed end on.*—At atmospheric pressure the spectrum is perfectly continuous with absorption lines only, from λ 2250 to above λ 5700. To the violet of λ 4500 the lines are in general quite narrow and sharp; to the red of λ 4500 the flame lines are sharp, while lines of groups *d* and *e* are rather wide and diffuse. A spectrogram of the region λ 6100–λ 6600 shows also a continuous spectrum with absorption lines, but there are faint traces of emission lines (enhanced iron lines). Using this arrangement under a bell jar, the region λ 3600–λ 4200 was studied in air at pressures ranging from 2 cm to 20 cm. At 2 cm all lines were bright and very few showed self-reversals, except H and K (these came no doubt from the wood). From 5 cm to 13 cm pressure the continuous background increased rapidly in intensity; reversals became gradually more prominent, and the bright lines broadened and in general shifted toward longer wave-lengths, so that at 10 cm numerous lines showed as a fine absorption line in the normal position with a broad emission line lying wholly on its red side. At 15 cm and 20 cm there was no trace of bright lines, the spectrum being perfectly continuous with the absorption lines in general very fine.

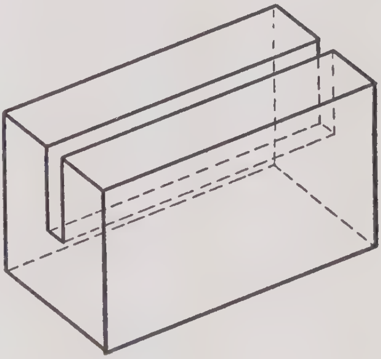

Fig. 2

3. *Wire placed in a cut in a block of wood as indicated in Figure 2.*—The cut mostly used was 4 cm long, 2.5 cm deep, and 3 mm wide. This gives the same spectrum as that produced by the tube just described; it is, however, much easier to load, and is better adapted for projection on the slit of the spectroscope. The spectra reproduced in Plate IX were taken with this arrangement, viewed end on.

4. *Brightness of the explosion as a source of light.*—Since the spectrum is continuous it becomes possible to compare the brightness of the source with that of the sun, for example, by merely

comparing the exposure-times which give the same density on the photographic plate, using the same spectroscope and projecting apparatus in both cases. The method is simply one of direct substitution. Such a comparison was made in the region λ 3900–λ 4000, using both the quartz and grating spectrographs, and in the region of λ 5500 using the grating instrument. The results are as shown in the accompanying table:

No. of Successive Explosions	Exposure to Sun for Equal Density	Region	Spectrograph
	Sec.		
3	1/200	λ 3900–λ 4000	Quartz
10	1/40	λ 3900–λ 4000	Grating
48	1/10	λ 5200–λ 5600	Grating

It remains to estimate the equivalent duration of an explosion. Plate VIII*a* shows that the total duration of light of sufficient intensity to affect the photographic plate exposed with the rotating mirror is not over 1/20,000 sec. It also shows that the greater part of this light is concentrated in the first half-cycle, the duration of which is 1/300,000 sec. Hence if we call the equivalent time 1/100,000 sec. we are overestimating rather than underestimating it. Using this value we find for the ratio of exposure to sun to that of the explosions for the three comparisons given above 167:1, 250:1, 200:1, respectively, or in the mean that it requires 200 times the exposure to the sun to produce the same density as that given by the explosions. The sunlight is of course considerably reduced in intensity in passing through the atmosphere, and there is an additional loss at the speculum mirror which reflects it into the projection system. If we say that only one-half of the light from the sun reached the projection system we still find this new source to be 100 times as bright as the solar surface.

5. *Direct photographs of the explosion.*—Plate VIII*b* shows an end view of the explosion in the block of wood, and Plate VIII*c* is a side view of the same. The contraction of the luminous column above the slot in the end view is evidently connected with the sharply defined "shadow" above the block in the side view. This apparent shadow is a little surprising and an explanation does not readily suggest itself.

Plate VIII*d*, *e*, *f* shows end views of the explosion of a wire in the open air. They were taken with the camera lens stopped to F/44, F/22, and F/5.6, respectively, so as to get the effect of exposures of different "lengths." The F/44 exposure, together with a similar one taken side on (not reproduced), show plainly a central core of luminous vapor, having the form of a solid cylinder 22 mm in diameter and of a length somewhat greater than that of the wire used, the ends of the cylinder being roughly hemispherical caps. The remarkably sharp outer boundary of this cylinder indicates that it marks the limit reached by the expanding gases at the end of the first half-cycle, that is, at the end of 1/300,000 sec. The F/22 exposure shows clearly a fainter second cylinder outside the first, whose diameter is roughly 45 mm. Its outer boundary is, however, rather ragged in this exposure, and even in the F/5.6 exposure it is far from being as sharp as that of the inner cylinder. The outer cylinder probably marks the limit reached by the gases at the end of the first cycle, and its light is chiefly derived from the current during the second half-cycle, the greater part of which must have passed through the inner core.

The vapors undoubtedly go on expanding through the succeeding cycles, but partly on account of their rapid cooling due to expansion, and partly because of the great diminution of the current intensity, the corresponding cylinders fail to be registered on the photographs.

If the explanation just given is correct, we find for the velocity of the expanding gases 3.3 km per second, or about 10 times the velocity of sound in air at normal temperatures.

When the wire is exploded in the slot in the block of wood, the two regions corresponding to the two cylinders can still be seen quite well on the photographs, but they lack the sharp outline shown in the open air, perhaps owing to the resistance to motion offered by the confining walls of wood. It is clear, however, that the velocity in this case is considerably greater, measurements on one of the best plates giving 30 mm and 54 mm respectively, instead of 22 mm and 45 mm for the open air.

6. *Pressure in the gases of the explosion.*—The experiments of Hale and Kent, showing that a spark discharge in gases at a pressure

of 50 atmospheres or more gives a spectrum at least partially continuous, suggested that the cause of the continuous spectrum observed in these experiments may be a very high pressure in the gases formed by the explosion. An effort to estimate the order of magnitude of this pressure was made as follows: A hole 7 mm in diameter was bored through a block of wood weighing 130 grams. The block was then split into two parts by a cut passing through the axis of the hole. One-half was rigidly mounted, and the other suspended as a pendulum so as to hang in contact with the immovable half. The wire was mounted centrally in the hole and the velocity of the movable half produced by the explosion was measured and found to be 135 cm/sec. The mass of the movable block being 65 grams, its momentum was 65×135 = 8775 gr. cm/sec. The wire in this case was a No. 36 B. and S. gauge (0.127 mm) nickel wire, 6 cm long, 48 mm being inside the opening in the split block. The mass of 48 mm of this wire is 4.8 mg. The momentum is of course equal to the product of the pressure, area, and the time. The pressure varies and is a function of the time. Not knowing the law of variation or the exact value of the time, only very rough estimates of the pressures could be made. The time in this case is of course not the same as the duration of the light, because the emission of light, being largely due to the flow of current through the gases, will cease after a few cycles; the gases, however, go on expanding until atmospheric pressure has been reached. If we assume the equivalent time to be that during which the maximum pressure would produce the momentum observed, we may reasonably suppose that its value would be somewhere between 1/50,000 and 1/10,000 sec., and probably nearer the latter figure. This gives, for the pressure, a value lying between 135 and 27 atmospheres, with the probability in favor of a value of 40 or 50 atmospheres. An independent method of estimating the pressure is as follows: Assume that the nickel wire is transformed into monatomic nickel vapor at a temperature of 20,000° C., which is the order of temperature to be expected from the intensity of the light. The volume at atmospheric pressure would be 136 cu. cm, and if we neglect leakage through the open ends of the tube and merely divide by the volume of the tube, viz., 1.82 cu. cm, we find 75 atmospheres as an upper limit for the pressure, which is in fair agreement with the estimate from the momentum of the block. We cannot be far from the truth if we say that in this experiment the pressure was of the order of 50 atmospheres.

The iron wires exploded in making the spectrograms accompanying this paper weighed only 0.4 as much as the nickel wire used in the experiment just described, and the volume of the slot in which the wires were placed was 2.5 cu. cm, or 1.4 times as great, so that in this case the pressure could hardly have been more than one-third of that just estimated, or of the order of 20 atmospheres. It seems reasonable to conclude, therefore, that the pressures developed in these explosions are not nearly as high as those which have often been used in spectroscopic investigations, and hence that *very high pressure in a gas is not at all necessary for the production of a continuous spectrum.*

7. *Experiments with other elements.*—A few spectrograms were made using copper, nickel, and manganin wires. With manganin the continuous spectrum has about the same brightness as with iron; with nickel it is brighter; while with copper it is very much fainter.

DISCUSSION

It may not be out of place to return for a moment to the idea which prompted these experiments. As stated above, this was to determine if possible the spectroscopic result of the fall of a meteoric particle of very high velocity into a resisting medium, such as the solar atmosphere. The general effect would be an extremely rapid vaporization of the materials forming the particle. In these experiments we have a rapid vaporization of a metal in the form of a thin wire. The analogy ends here, for in one case the vaporization is produced by mechanical, in the other by electrical, means. That the two methods would yield identical results is not to be expected; but on the other hand it is hard to advance any valid reason why they should be radically different. There is another difference, and an important one, in the amounts of energy available in the two cases. In our experiments the total energy of the condenser charge was 30 calories, and not all of this small amount went into the wire. The same wire falling into the sun would develop 80,000 calories—in a longer time it is true, yet one cannot help feeling that an adequate imitation of what must happen in the sun requires much more energy than was available in the present work. The following general conclusions seem to be reasonable: A very small particle would be consumed in the extreme outer regions of the sun's atmosphere where the pressure is exceedingly low. The path of the particle would therefore be long and the rate of development of heat energy low. Under such conditions the spectrum would most likely consist of bright lines, with little if any continuous background. Particles large enough to reach a level where the pressure is appreciable would encounter an enormous resistance, and the development of heat energy would be extremely rapid, perhaps hundreds of times as rapid as in the present experiments. Here it seems likely that a continuous spectrum with absorption lines would be produced.

The experiments will be continued with a larger condenser and higher voltage. Attempts will also be made to observe the explosions in gases other than air; hydrogen, for example, should be interesting.

The author desires to express his thanks to Mr. Ellerman for help in some of the photographic work, and for his kindness in preparing the plates for reproduction. The author is also indebted to Mr. Sinclair Smith, who assisted throughout the experimental work.

SUMMARY

1. Fine wires exploded by a condenser discharge give a brilliant continuous spectrum crossed by the absorption lines of the element composing the wire.

2. The continuous spectrum extends into the extreme ultraviolet.

3. The intrinsic brightness of the explosion as a source of light is very high, being apparently much greater than that of the solar surface.

4. The pressure in the gases giving the continuous spectrum is not excessive, being at most of the order of 20 atmospheres.

Mount Wilson Observatory
December 1, 1919

Contributions from the Mount Wilson Observatory, No. 179
Reprinted from the *Astrophysical Journal*, Vol. LI, pp. 121–26, 1920

THE SPECTRUM OF NOVA OPHIUCHI 1919

By WALTER S. ADAMS and CORA G. BURWELL

ABSTRACT

Spectrum of Nova Ophiuchi.—The paper reports in detail *measurements* of a spectrogram obtained with the 100-inch reflector on November 2. Although the star had reached its maximum brightness over six weeks before, the general features of the spectrum are characteristic of novae at a comparatively early stage of development. The strong continuous background is crossed by bright bands, with absorption lines forming their violet edges, which correspond mainly to hydrogen and calcium lines and to the enhanced lines of iron and titanium. The middle of each band is displaced about 1 A to the red, while the absorption lines are displaced from 4.5 to 5.5 A to the violet. The shifts for the various lines are proportional to the wave-length and are about half the width of the associated bands. The *radial velocity* indicated by the calcium absorption lines is about +6 km.

Spectra of novae; a simple interpretation of the observed displacements.—The fact that for Nova Persei, Nova Geminorum No. 2, Nova Aurigae, and Nova Ophiuchi the displacement of the absorption lines is in each case about twice the width of the corresponding bands, suggests that both phenomena are mainly Doppler effects, and lends some support to the *hypothesis* of a shell of gas moving rapidly out from each star.

The spectrum of the nova in Ophiuchus discovered by Miss Mackie on photographs made at the Harvard College Observatory[1] was observed at Mount Wilson on the nights of November 1 and 2. The magnitude of the star was estimated at about 8.0, and for this reason and because of its low altitude it was necessary to use a spectrograph of small dispersion. For the first photograph the 60-inch reflector and the Cassegrain spectrograph with one prism and a camera of 18 cm focal length were employed; the second spectrogram was made with the 100-inch reflector and a spectrograph containing one prism and a camera with a focal length of 46 cm. The latter negative obtained with an exposure time of 110 minutes was most satisfactory, and the results given in this communication are based upon its measurement.

---

[1] *Harvard College Observatory Bulletin*, No. 696.

The general features of the spectrum are those characteristic of novae at a comparatively early stage of development. This is in itself remarkable, since the maximum of light of the star apparently occurred about September 13, over six weeks previous to these observations. The continuous spectrum is strong and a large number of fairly well-defined absorption lines are present. In many cases these are associated with bright bands upon the side of longer wave-length. These bands, as has been found in other novae, are due to hydrogen, calcium, and the more prominent enhanced lines of iron, titanium, and other elements. It is probable that all the absorption lines are accompanied by bright bands, but unless the latter are rather strong it is not possible to distinguish them with certainty against the continuous background. There is little difficulty in identifying essentially all of the absorption lines with the enhanced or the stronger arc lines of various elements. The lines present are nearly identical with those found in the spectrum of Nova Aquilae No. 3 a few days after maximum of light, but their displacement is only about -4.7 angstroms at λ 4500, against a displacement of -23 angstroms in Nova Aquilae.

RADIAL VELOCITY

A bright band is present in the position of the calcium line K and another band is made up of calcium H and the hydrogen line $H\epsilon$. Across these bands are dark lines due to calcium, the measurement of which affords a means of determining the radial velocity of the star. The lines are somewhat stronger than in most novae, but the measurements are subject to considerable uncertainty because of the inferior focus in this part of the spectrum. The mean of the determinations by two observers, after correction for the earth's motion, is $+6$ km.

ABSORPTION LINES

The principal dark lines measured in the spectrum are given in Table I. Successive columns show the wave-length, as taken from Rowland's table, of the line with which the stellar line is identified, the element to which it is due, the wave-length in Nova Ophiuchi, the displacement, and the corresponding displacement

TABLE I

Sun	Element	Nova Ophiuchi	Displacement	
			Nova Oph.	Nova Aquilae
			A	A
3900.68	Enh. Ti	3895.79	−4.9	....
3913.61	Enh. Ti	3909.08	4.5	....
3933.82	Ca	3928.94	4.9	−19.5
3970.25	Hε	3965.17	5.1	20.9
4012.54	Enh. Ti	4007.94	4.60	20.45
4028.50	Enh. Ti	4024.24	4.26	19.28
4101.90	Hδ	4097.57	4.33	20.54
4163.82	Enh. Ti	4159.33	4.49	20.68
4172.84	Enh. Ti, Fe	4168.29	4.55	20.41
4179.02	Enh. Fe	4174.01	5.01	20.86
4184.47	Enh. Ti	4180.03	4.44	20.59
4226.90	Ca	4222.38	4.52	20.96
4233.33	Enh. Fe	4228.78	4.55	21.44
4247.00	Enh. Sc	4242.52	4.48	21.10
4290.38	Enh. Ti	4285.74	4.64	21.60
4294.20	Enh. Ti	4289.61	4.59	21.58
4296.74	Enh. Fe	4292.31	4.43	22.09
4300.21	Enh. Ti	4295.59	4.62	21.61
4308.08	Fe, Enh. Ti	4303.30	4.78	21.48
4314.09	Enh. Ti	4309.68	4.41	21.31
4321.12	Enh. Ti	4315.92	5.20	21.62
4325.94	Fe	4321.37	4.57	21.98
4340.63	Hγ	4336.03	4.60	21.68
4352.01	Cr, Mg.	4347.21	4.80	21.69
		4363.83		
4375.10	....	4370.28	4.82	21.84
4385.55	Enh. Fe.	4380.57	4.98	20.14
4395.20	Enh. Ti	4390.49	4.71	21.98
4399.94	Enh. Ti	4395.66	4.28	21.50
		4401.51		
4417.43	Enh. Fe, Ti	4412.33	5.10	21.20
4443.98	Enh. Ti	4439.22	4.76	22.12
4468.66	Enh. Ti	4463.89	4.77	22.27
4489.06	Enh. Ti, Fe	4484.09	4.97	22.47
4501.44	Enh. Ti	4496.56	4.88	22.36
4508.46	Enh. Fe	4503.36	5.10	22.45
4515.51	Enh. Fe	4510.13	5.38	22.39
4520.40	Enh. Fe	4515.48	4.92	22.82
4522.80	Enh. Fe	4517.94	4.86	22.35
4528.80	Fe	4523.70	5.10	....
4534.14	Enh. Ti	4529.44	4.70	22.50
4549.77	Enh. Fe, Ti	4544.57	5.20	22.79
4563.94	Enh. Ti	4558.92	5.02	22.65
4572.16	Enh. Ti	4567.16	5.00	22.39
4576.51	Enh. Fe	4571.98	4.53	....
4584.02	Enh. Fe	4579.06	4.96	23.15
4805.29	Enh. Ti	4800.58	4.71	23.86
4861.53	Hβ	4855.88	5.65	....
4924.11	Enh. Fe	4918.44	5.67	24.86
5018.63	Enh. Fe	5011.6	7.0	24.97

in the spectrum of Nova Aquilae on June 11, 1918, the date on which the spectrum was most nearly comparable with that of Nova Ophiuchi. The wave-lengths at the beginning and end of the table are less accurate than the others. Corrections have been applied for radial velocity.

The well-known proportionality between displacement and wave-length characteristic of the spectra of novae is marked in these results. Thus if we form means for each 200 angstrom units beginning at λ 4000 we find the following displacements:

λ 4120 -4.52 λ 4320 -4.65 λ 4520 -4.95 λ 4900 -5.76

These values are satisfied by the equation $\Delta\lambda = 0.00110\,\lambda$ with the following residuals, weights being assigned according to the number of lines:

λ 4120 0.00 λ 4320 -0.09 λ 4520 -0.01 λ 4900 $+0.38$

The ratio of the displacement of the absorption lines in Nova Ophiuchi to that in Nova Aquilae as obtained from Table I is 1 to 4.53. A similar comparison of the displacements in Nova Aurigae, Nova Persei, Nova Geminorum No. 2, and Nova Aquilae was made by Adams,[1] and attention was called to the remarkably close agreement of the ratios with the integer numbers 1, 2, and 3, the largest value belonging to the more refrangible component of the hydrogen lines. The corresponding value in the case of Nova Ophiuchi should apparently be 4, and the departure from the whole number is too large to come within the limits of error of the determination. Although the relationship found for the four earlier novae may well be regarded as a coincidence, attention should be called to the fact that in the case of at least one, Nova Aquilae, the displacement varied with the interval after maximum of light. Accordingly, results obtained at the same relative light-phase should be used, and no strict comparison can be made between the displacements found in the case of Nova Ophiuchi six weeks after apparent maximum and those in Nova Aquilae only three days after maximum.

One other possible effect may be referred to. As will appear later, the bright bands in Nova Ophiuchi are displaced about one angstrom toward the red, and those in Nova Aquilae the same amount toward the violet. If these displacements are in any way related to those of the absorption lines, allowance should be made for the difference.

---

[1] *Proceedings of the National Academy of Sciences*, **4**, 355, 1918.

BRIGHT BANDS

A list of the bright bands measured in the spectrum is given in Table II. The values for the first few bands are necessarily uncertain.

TABLE II

Sun	Element	Center of Band	Width in A	Displacement in A
3889.2	Hζ	3890	....	+1
3933.8	Ca	3935	7	+1
3970.2	Hε	3971	8	+1
4028.5	Enh. Ti	4029.7	7.3	+1.2
4101.9	Hδ	4102.9	7.6	+1.0
4233.3	Enh. Fe	4233.8	8.0	+0.5
4340.6	Hγ	4341.7	8.8	+1.1
4417.4	Enh. Fe, Ti	4418.5	8.6	+1.1
4444.0	Enh. Ti	4444.9	9.1	+0.9
4468.7	Enh. Ti	4469.6	8.7	+0.9
4481.4	Enh. Mg.	4482.1	....	+0.7
		4513		
4522.8	Enh. Fe	4523.8	8.9	+1.0
4584.0	Enh. Fe	4585.7	10.7	+1.7
		4633		
4861.5	Hβ	4863.2	9.2	+1.7
4924.1	Enh. Fe	4925.7	10.1	+1.6
5018.6	Enh. Fe	5020	11	+1

It is clear from these results that there is a displacement of the center of these bands of the order of one angstrom unit to the red. It also seems probable that both the displacement and the width of the bands increase in proportion to the wave-length. This result is well known in the case of previous novae. The following summary shows the values of the width and displacement at λ 4500 for the four principal stars of this character:

	Width of Bands in A	Displacement in A
Nova Persei	48	+1.0
Nova Geminorum	25	+1.2
Nova Aquilae	49	−1.0
Nova Ophiuchi	9	+1.1

The displacement to the violet in the case of Nova Aquilae is of especial interest. It is well established from the observations of Harper at Ottawa[1] and from the Mount Wilson measurements.

A comparison of the widths of the bands in these stars shows that their ratio is closely the same as that between the displacements of the absorption lines, and that in each case the width is very nearly twice that of the corresponding displacement. The absorption lines, therefore, may be regarded as marking definitely the violet edges of the bright bands, and the conclusion is obvious that the cause which produces the displacements of the dark lines must be mainly responsible for the widening of the bright bands. This would favor the view that the Doppler effect is the principal agent involved, since in such laboratory investigations as that of the spectrum of the spark in liquids and under high pressures, in which a slight degree of resemblance to the spectra of novae has been attained, the dark lines and the bright bands have been very differently affected. The hypothesis of a shell of gas moving rapidly outward from the star may, accordingly, be regarded as receiving some slight degree of support from these results.

In conclusion the suggestion may be made that the displacements of the absorption lines and the widths of the bright bands are to some extent an indication of the disturbances present in the star, and so perhaps form a rough measure of its absolute magnitude. From this point of view Nova Ophiuchi would be of especial interest as being intrinsically the faintest of the last five prominent novae.

Mount Wilson Observatory
December 15, 1919

---

[1] *Journal of the Royal Astronomical Society of Canada*, **12**, 494, 1918.

Contributions from the Mount Wilson Observatory, No. 180
Reprinted from the *Astrophysical Journal*, Vol. LI, pp. 107–120, 1920

PRELIMINARY OBSERVATIONS OF THE ZEEMAN EFFECT FOR ELECTRIC FURNACE SPECTRA

By ARTHUR S. KING

ABSTRACT

Zeeman effect for furnace spectra of iron and vanadium.—Hitherto Zeeman effect observations have been almost exclusively confined to spark spectra. Because the electric furnace emits or absorbs strongly many lines which are weak or absent in spark spectra, and because it is desirable to compare the effects of a magnetic field on spectra from different sources, the present investigation was undertaken. The furnace tube was placed parallel to the lines of force, in a field varying from 6500 gauss in the center to 9000 gauss near the ends, and it was heated to a maximum temperature of 2200°. To obtain the inverse effect, a carbon plug was placed so as to supply a continuous high-temperature spectrum as a background. Spectrograms were taken with a concave grating giving a scale of about 1.83 A per mm. Table I contains the observed separations for both *the direct and the inverse effects, viewed along the lines of force*, for 100 iron furnace lines together with the corresponding separations obtained with the spark as source. Table II contains similar data for the direct effect for 90 vanadium lines. Twenty of the iron lines and eleven of the vanadium lines had not previously been investigated. It was found that the character and magnitude of the separations for the *n*-components of furnace lines both in emission and in absorption agree closely with those of the corresponding spark lines, reduced to the same field intensity; that is, the effect is independent of the source used. Since these three methods give identical results for each line, they may be used to supplement each other in studying the effect. Among other advantages of the furnace, the non-uniformity of the magnetic field enables the location and temperature of the active centers of absorption or emission for various lines to be determined. Spectrograms are reproduced in Plates X and XI.

Zeeman effect for the D-lines of the sodium spectrum.—The author suggests a possible *explanation of a variation* of the effect with the source of light, which was *observed by Woltjer.*

On account of the difficulty of maintaining an arc in the magnetic field, investigations of the Zeeman effect have thus far been carried out almost exclusively with the electric spark as the source of light. While the spark is satisfactory for much work of this kind, certain disadvantages make it desirable to supplement the spark experiments with those from a source quite different in character. Two features of the spark spectrum are especially troublesome. First, many lines characteristic of the low-temperature sources, and important in sun-spot spectra, are faint or absent in the spark, though, on the other hand, the spark emits strongly the enhanced lines and others requiring high excitation. Second, the condensed spark in air, made more disruptive by the magnetic field, is an unfavorable source for obtaining the sharp Zeeman components required for measurements of high precision. A sharpening of the lines by the use of self-induction, which also removes the disturbing air lines, is accompanied by a reduction in the luminosity of the spark.

The electric furnace is especially effective in emitting the lines which are weak in the spark. When inclosed in a vacuum chamber, the furnace lines can be made extremely sharp, and, unlike the sources involving an electric discharge, neither the action of the furnace nor the character of its spectrum undergoes material modification when operated *in vacuo*. A third useful feature of the furnace is the unique facilities afforded for the study of the inverse Zeeman effect by the production of absorption spectra when a diaphragm of graphite is placed at the center of the tube. The absorption spectra produced in the regular furnace by this means were described in a recent paper.[1]

The obvious disadvantage of the furnace when used with the usual type of electromagnet is its relatively large size, which prevents the use of high magnetic fields. While an equipment designed to overcome this difficulty is being prepared, it seemed desirable, by operating a small furnace between the poles of a Weiss electromagnet, to examine the character of the magnetic separations given by the moderate field available. The possibilities of the furnace for this work could thus be determined and it could be seen whether any decided peculiarities appeared for a source very different from the spark.

This investigation has been limited to the spectra of iron and vanadium, with the addition of a few impurity lines, but the material is sufficient to show clearly the nature of the magnetic separations for the furnace spectrum.

---

[1] *Mt. Wilson Contr.*, No. 174; *Astrophysical Journal*, 51, 13, 1920.

EXPERIMENTAL METHOD

A graphite tube 10 cm long, of 6 mm internal and 12.5 mm external diameter, was placed axially between the poles of a large Weiss electromagnet. The latter was provided with pole-pieces 5.1 cm in diameter, one of which was perforated to enable the light from the furnace tube to pass through the hollow core to the spectrograph. The tube was clamped at each end in a graphite bushing 12.5 mm wide held in a brass ring of the same width, the two halves of which were bolted tightly together. This ring was of rectangular cross-section and made hollow to permit of water-cooling. The alternating current, at potentials of 5 to 20 volts, was led to the clamping rings by flexible copper tubes, also water-cooled, from the massive transformer terminals some 2 meters distant. The portion of the furnace tube between the clamps was turned down to a slightly smaller diameter, varying in different experiments, and, since no vacuum chamber was used, it was surrounded by a protecting jacket. Various jacketing methods were tried, but the most satisfactory was to inclose the furnace tube in a thick-walled graphite tube, with an air space of 2 to 3 mm between, and to cool this outer tube with a tubular water-jacket of brass.

A magnetic gap of about 10.5 cm was required to allow space for the furnace. The field in this gap, when the magnet was fully excited, was measured with a bismuth spiral as 6500 gausses at the center, and increased to 9000 gausses 1 cm from the pole, which, however, was considerably beyond the heated portion of the tube. The bearing of this field variation on the observed phenomena of the furnace will be noted later.

The material to be vaporized, either iron filings or powdered vanadium, was placed in the central part of the tube when the emission spectrum was desired, or in front of a graphite plug placed at the center when the absorption spectrum was to be observed. The metal was fused at a moderate temperature before the field was turned on. This, in the case of the iron, which sticks to the graphite when melted, prevented the metal from being drawn out of the tube. The largest current usable with the rather fragile tube was 800–900 amperes, the temperature attained, judging from the spectrum, being in the neighborhood of 2200° C. The fact that the current passed through the contact blocks for a short distance at right angles to the field caused a vibration which, in spite of fairly rigid clamping in a wooden frame, eventually broke the tube. The limited exposures possible on this account were sufficient to allow photographing with the first order of the 30-foot plane-grating spectrograph and the second order of the 15-foot concave grating, the scales being about 1 mm = 1.83 A and 1 mm = 1.86 A, respectively.

OBSERVATIONS OF THE ZEEMAN EFFECT

1. *Character of the separations.*—As the spark has hitherto been the only source extensively used in studies of the Zeeman effect, it cannot be assumed without proof that a source so different in its action as the furnace would show no differences in the magnetic behavior of spectrum lines as compared with the spark. The present investigation has therefore had as one of its chief objects a comparison of the furnace and spark material extensive enough to show whether for a given field-strength the number of components and the amount of their separation is the same for the two sources. Since the observations were made entirely along the lines of force, the data collected are for the n-components only. Measurements of the spark separations for iron have been published by the writer,[1] and those for vanadium by Mr. Babcock,[2] for fields of 16,000 and 20,000 gausses, respectively. These have furnished comparisons of furnace and spark separations for nearly all of the lines except those which are strong in the furnace as compared with the arc or spark. These are chiefly IA lines of the furnace classification and in most cases the measurements given here are the first that have been made for such lines.

A large variety is found in the appearance of the lines emitted by the furnace in the magnetic field, but this is readily explained in every case by the data at hand on the temperature class and the character of the magnetic separations shown for the spark in high fields. For lines of triplet separation, the furnace shows a pair of sharp *n*-components, their sharpness when viewed along the varying field in which the furnace is placed indicating that the particles emitting them are rather definitely localized in the tube. Many cases of blurred components occur, the line sometimes appearing as a diffuse patch. These are found to be either complex lines in which the four or more *n*-components are not resolved by the low field, or low-temperature lines whose components are self-reversed, or sometimes a combination of both effects. Interesting cases are observed in which a line has the same appearance as a triplet when viewed at right angles to the lines of force, there being a sharp middle component twice as strong as either side component. This is caused by reversals of the two *n*-components for which the amount of separation and the width of reversal happen to be such that the red side of one reversed component falls exactly upon the violet side of the other. The furnace results, including the absorption spectra to be discussed later, supply ample evidence that reversed magnetic components, when observed along the lines of force, show no peculiarities as compared with unreversed components of the same lines. A certain amount of evidence on this point has appeared in work with the spark, the difficulty of obtaining some of the ultra-violet iron lines with unreversed components having been noted by the writer.[1]

---

[1] *Papers of the Mt. Wilson Observatory*, **2**, Part I, 1912.

[2] *Mt. Wilson Contr.*, No. 55; *Astrophysical Journal*, **34**, 209, 1911.

Lines such as λλ 5124 and 5435 of iron, which show no separation for high fields with the spark, are sharp also in the furnace spectrum. Several lines which give a quartet of *n*-components in the spark show the same resolution in the furnace, and the iron line λ 5497 is resolved into five *n*-components in both sources. The field used with the furnace was too low to separate the more complex types, but in every case of lines common to both, the appearance of the furnace line is explained by the character of its separation in the spark.

2. *The inverse effect.*—Experiments on the magnetic separation of absorption lines were carried out for the iron spectrum to a sufficient extent to show what may be expected of the furnace when operated in this way. The absorption lines obtained with

---

[1] *Papers of the Mt. Wilson Observatory,* **2,** Part I, p. 19, 1912.

a plug in the center of the tube and their dependence on temperature class were discussed in a former paper.[1] It was shown there that successive classes of lines appeared as the temperature was raised, so that the production of narrow absorption lines for a given class is a matter of temperature adjustment. With the absorption furnace in the magnetic field, the components follow closely the character of the no-field absorption line, so that a proper temperature must be chosen for the desired set of lines. Proceeding according to this principle, a large part of the iron lines for which the direct Zeeman effect had been observed were obtained with their components in absorption. Complete similarity as to character and number of components was found for the direct and inverse effects. The absorption method is useful for obtaining low-temperature lines with short exposures, this requiring, as for the no-field spectrum, a higher temperature than that needed for the same lines in emission. For the regular work of obtaining measurable lines under the special conditions supplied by the furnace, the direct effect—adjusting the temperature and vapor-density to the character of various groups of lines—will probably be more used than the inverse effect. The absorption method, however, will have its place in many problems, especially in those connected with solar spectra. For the n-components observed along the lines of force, the present results show that the character of the magnetic resolution is the same for the two effects, so that the components in absorption may be studied by this means when it is of advantage to do so.

3. *Magnitude of furnace separations.*—The separations measured for iron and vanadium are recorded in Tables I and II. A field measurement was first made by selecting a number of lines, each of which has a pair of sharp n-components in both furnace and spark. A comparison of the separations gave for the direct effect a strength of 6400 gausses for the field generally used with the furnace, while a value of slightly less than 6500 gausses was given by a bismuth spiral placed midway between the poles. There is thus excellent agreement of furnace and spark separations, provided the furnace components are emitted by vapor near the center

---

[1] *Mt. Wilson Contr.*, No. 174; *Astrophysical Journal*, 51, 13, 1920.

of the tube. This is probably the case, as the lines compared were as a rule furnace lines of moderate strength which the central vapor should emit most strongly, the strongest low-temperature lines being usually either overexposed or complex. In Tables I and II, therefore, the spark values, so far as they are available for the given lines, are reduced to a field of 6400 for comparison with the furnace separations.

A comparison of the inverse and direct effects for the same lines showed the separation of the absorption components to be consistently larger than in emission, the separations of the best lines being in the ratio of 1 to 0.87, a result repeated on a number of plates for which the same field was used. This indicated a larger field-strength in the part of the tube where the absorbing vapor was effective. Measurements along the pole-gap with the bismuth spiral brought out the interesting fact that at about 25 mm from the center the field increased to the value indicated by the absorption lines. It follows that the absorbing particles were centered about a position at this distance from the plug. The distance probably varies for different sets of lines; the field and dispersion now used are not sufficient to test this point.

Besides explaining the larger separations of the absorption components in the present experiments, this result suggests a method of locating the section of the furnace tube in which any line is emitted or where the vapor absorbs the line most strongly, and from this the corresponding temperature. A knowledge of the variation of field-strength along the axis of the magnet would be required, and also the temperature-gradient along the tube, which can be measured by moving a plug from end to center and recording its temperature at different points. A high precision in the measurement of the magnetic separations should then give valuable information as to the origin of different groups of lines.

4. *Comparison with spark separations.*—The list of iron lines in Table I gives in the second column the temperature class, in the third the emission separations as measured, in the fourth the absorption separations reduced by the factor required on account of the larger field apparently operating in this case, and in the fifth the

TABLE I

SEPARATION OF IRON LINES IN MAGNETIC FIELD

λ	CLASS	Δλ		
		Emission	Absorption	Spark
3940.885	IA	....	.186	.184
4100.745	IA	.176	.185	....
4147.675	I	.231	.220	.270
4152.176	IA	.114	....	....
4172.748	IA	....	.116	....
4174.917	IA	....	.116	.150
4177.598	IA	....	.142	....
4206.696	IA	....	.191	.135
4216.185	I	....	.188	.183
*4222.225	III	.174	....	.190
4232.724	IA	.317	....	....
*4235.953	II	.174	.180	.181
4250.134	III	.163	.157	.153
4258.386	IA	.264	.285	....
*4260.489	III	.173	.185	.169
*4271.171	III	.161	.161	.158
4282.406	II	.150	.150	.124
4291.472	IA	.233	.250	....
*4299.254	II	.172	.161	.162
4315.092	III	.216	.216	.207
4337.052	II	.097	....	.106
4347.239	IA	.182	....	....
4352.740	II	.178	....	.166
*4375.934	I	....	.180	.170
4389.251	IA	....	.166	....
*4427.313	I	....	.193	.172
4430.622	II	.304	....	.288
4435.154	IA	.174	.176	....
4442.349	III	.193	....	.194
4447.727	II	.244	....	.234†
4459.128	II	.200	....	.180
*4461.658	I	....	.182	.174
4466.557	I	.180	.172	.137
4482.176	I	....	.186	.160
4489.744	IA	.178	.190	....
4494.571	II	.134	.128	.121
4528.624	II	.147	....	.143
4531.155	I	.147	....	.159
4592.658	I	.152	....	.166
4602.946	I	.224	....	.226
*4878.226	III	.455	....	.437
4939.689	I	.221	....	.232
4957.612	III	.181	....	.200
4994.133	I	.234	.211	.232
*5012.073	I	.212	.222	.215
5041.079	I	.232	.228	.199
5041.763	III	.223	.221	.200
*5051.643	I	.209	.206	.208
5079.742	I	.337	.321	.295
5083.344	I	.196	.200	.190
5110.414	I	.238	.260	.216

TABLE I—*Continued*

λ	Class	Δλ		
		Emission	Absorption	Spark
5127.364	I†	.257	.254	.270
5142.934	I	.238	.231	.231
5150.845	I	.246	.256	.252
5166.288	IA	.293	.301	....
5167.492	II	.173	.181	.185
5168.904	IA	.260	.266	....
*5171.601	II	.209	.214	.208
*5194.950	I	.177	.175	.183
5204.585	IA	.293	.284	....
5216.277	II	.094	.104	.122
5225.533	IA	.506 .260	....	....
5227.187	II	.169	.171	.163
5232.954	III	....	.204	.223
5247.052	IA	.349	.341	....
5250.212	IA	.513	.506	....
5254.956	IA	.400	.381	....
*5270.357	II	.120	.117	.120
5328.539	II	.217	.217	.195
5397.135	I	....	.260	.252
5429.701	I	....	.240	.243
5497.521	I	.568†† .288	....	.556†† .277
5501.471	I	.368	....	.400
5506.785	I	.404	....	.410
5615.663	IV	.239	....	.234
5658.836	IV	.280	....	.290
5701.555	III	.224	....	.243
*6137.704	III	.254	....	.262
6173.346	III	.605	....	.636
*6191.568	II	.191	....	.216
6213.440	III	.456	....	.480§
6219.290	III	.396	....	.396
*6230.732	III	.299	....	.307
*6252.567	III	.213	....	.233
*6254.266	III	.355	....	.381
6265.145	III	.392	....	.388
6280.622	IA	.359	....	....
6301.524	IV	.404	....	.425
6322.696	III	.389	....	.386
6335.341	III	.288	....	.266
6358.684	IA	.447	....	.298
6393.609	III	.213	....	.237
*6421.361	III	.389	....	.397
6430.859	III	.310	....	....
*6494.993	II	.258	....	.273
6546.251	III	.209	....	.234
*6592.928	III	.262	....	.280
6663.452	IV	.411	....	.435
*6678.001	III	.292	....	.315

† Mean of two pairs.

†† Five *n*-components. Measurements for outer and inner pairs.

§ Mean of two pairs.

spark values reduced to the furnace field. Table II, for vanadium, is similar, except that the absorption method was not used for this element.

These lists include the lines for which more or less sharply defined doublets could be measured. When the furnace components were not sharp, those of the spark showed a pronounced widening or a resolution into an inner and an outer pair. Many strong furnace lines, whose complex character allowed no resolution in this field, are omitted.

A general close agreement of the furnace and spark separations in the tables indicates that the action of the field is the same for the two sources. In Table I the iron lines which in the spark show two sharp *n*-components and yield measurements of high weight are marked with an asterisk. The agreement for these lines is good. For the other lines, the furnace and spark values often agree closely, and when different show no systematic variation. The mean separations of 67 iron doublets measured for both furnace and spark are 0.2516 and 0.2537 respectively for the two sources. A similar comparison of 79 vanadium doublets gives means of 0.3083 and 0.3100. In the few cases where the discrepancy is considerable, the line is invariably found to be especially difficult to measure in one or both sources, usually owing to a shading of the complex *n*-components toward one side or the other. The vanadium lines of Table II are usually less difficult to measure than those of iron, the only notable discrepancies being for lines of complex structure.

This observational material is presented in some detail on account of the difficulty in handling magnetic-field data if the character or magnitude of the separations depends upon the nature of the source. No indication of such a dependence in the iron or vanadium spectrum has appeared. The field possible with the present form of furnace has not enabled me to check the observations of Woltjer[1] on the components of the D lines of sodium. He examined these lines as emitted by a vacuum tube and as given in absorption by the oxy-acetylene flame, and found that while the spacing remained the same, the relative intensities of the five

---

[1] *Amsterdam Dissertation*, 1914; (Abstract) *Physikalische Zeitschrift*, **15**, 918, 1914.

TABLE II

Separations of Vanadium Lines in Magnetic Field

λ (Exner and Haschek)	Class	Δλ	
		Furnace	Spark
5176.95	III	.178	.177
5193.20	III	.230	.245
5193.84	III	.197	.165
5195.65	III	.245	.204
5213.82	III	.208	....
5216.76	IV	.279	.260
5225.90	III	.256	.260
5234.26	III	.156	.153
5241.03	III	.188	.184
5353.56	III	.198	....
5402.17	III	.174	.175
5415.47	III	.197	.193
5487.42	III	.219	.237
5488.10	III	.182	.217
5517.40	IIA	.342	....
5542.91	IIA	.182	....
5546.13	IIIA	.357	.361
5547.26	II	.342	.344
5574.20	IIA	.208	....
5584.77	I	.290	.299
5586.21	III	.200	.214
5592.63	I	.290	.300
5601.60	III	.208	.216
5604.41	IV	.204	....
5605.18	II	.327	.362
5627.85	I	.271	.288
5646.29	II	.342	.360
5657.70	II	.290	.309
5668.55	II	.297	.305
5683.37	III	.226	.232
5725.80	III	.215	.219
5733.29	IV	.193	.191
5734.21	III	.189	.199
5737.25	II	.234	.256
5743.66	II	.260	.273
5747.92	III	.200	.228
5749.05	III	.222	.185
5786.43	III	.230	.210
5807.38	III	.197	.180
5826.83	III	.200	....
5850.57	IIIA	.301	.325
5979.11	IIIA	.241	.229
5981.02	IIIA	.238	.227
6002.89	IIA	.416	.457
6008.90	IIIA	.331	.280
6018.16	IIIA	.301	....
6025.64	IIIA	.222	.209
6039.95	I	.332	.331
6087.70	IIIA	.312	....
6090.45	I	.272	.286
6111.90	II	.294	.293

TABLE II—*Continued*

λ (Exner and Haschek)	Class	Δλ Furnace	Δλ Spark
6119.70	I	.239	.240
6150.32	I	.280	.282
6170.55	IA	.286	.269
6189.55	IIA	.244	.240
6199.40	I	.355	.351
6214.04	I	.355	.359
6216.52	I	.337	.352
6224.70	I	.356	.357
6230.92	I	.336	.339
6233.31	IA	.356	.349
6240.30	IIA	.357	.364
6245.35	IIA	.359	.359
6252.02	I	.376	.378
6257.03	IIA	.394	.396
6258.73	IIA	.797	.785
6261.39	IIA	.743 .181	.770 .190
6266.49	IIA	.508	.563
6268.98	IIA	.458	.469
6274.80	I	.587 .303	.607 .308
6285.32	I	.379	.385
6293.02	I	.380	.371
6296.69	I	.368	.377
6327.00	III	.268	.278
6339.23	III	.257	.260
6349.61	III	.238	.234
6357.47	III	.186	.196
6358.99	III	.297	.278
6430.68	III	.370	.330
6433.37	IIIA	.279	.269
6452.55	IIA	.394	.384
6488.22	IV	.249	.292
6504.38	IIA	.348	.582 .464
6531.65	II	.433	.421
6543.71	IIIA	.456	....
6566.10	IIIA	.732	.708
6606.22	IIIA	.388	.368
6608.06	IIIA	.264	....
6625.10	IIIA	.407	.375

n-components of D_2 were quite different in the two cases. This difference Woltjer provisionally ascribes to temperature. The results of the writer's recent study of absorption spectra[1] with the furnace may, however, have some bearing on this case. Instances were there noted of the weakening of spectral lines through a

---

[1] *Loc. cit.*

PLATE X

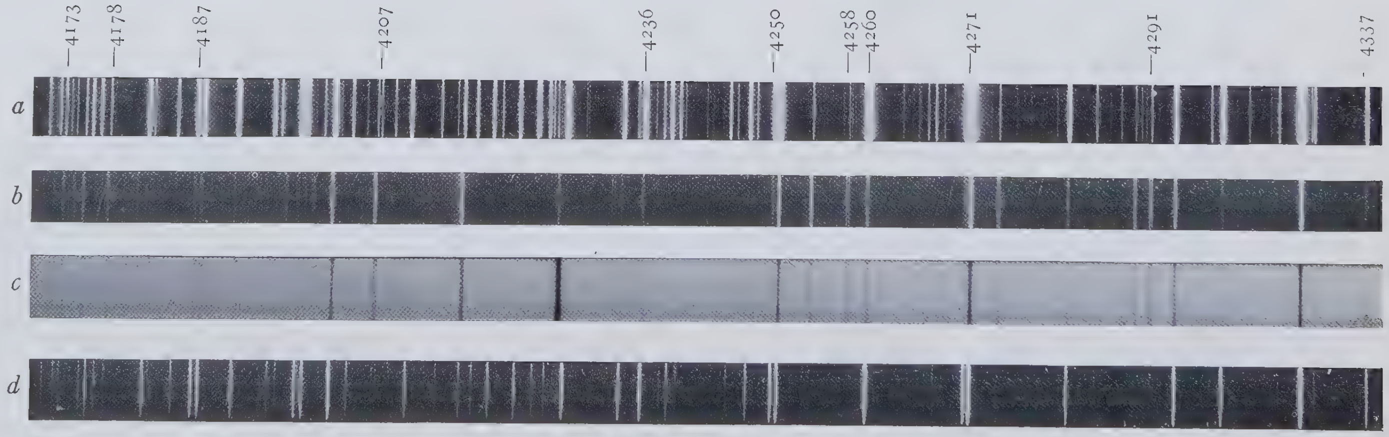

Effect of a Magnetic Field on the Electric Furnace Spectrum of Iron

a, *d*. Comparison arc spectra of iron without field
b. Emission spectrum of furnace in magnetic field
c. Absorption spectrum of furnace in magnetic field

PLATE XI

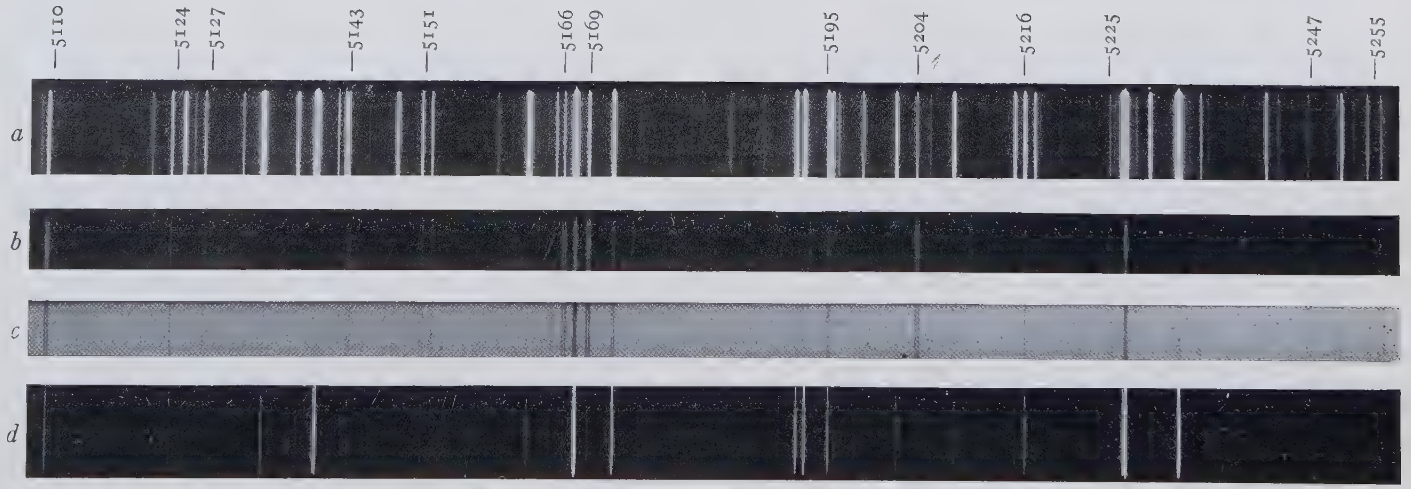

Effect of a Magnetic Field on the Electric Furnace Spectrum of Iron

a, *d*. Comparison arc spectra of iron without field
b. Emission spectrum of furnace in magnetic field
c. Absorption spectrum of furnace in magnetic field

partial balancing of emission and absorption. The effect of large differences in furnace temperatures on the magnetic separations has not been fully tested, owing to the long exposures required at low temperature, but a temperature difference of at least 400° produced no perceptible changes other than those clearly due to reversals at the higher stage.

5. *Magnetic characteristics of Class IA lines.*—This class, especially in the iron spectrum, presents interesting features. It is an important group of lines for which the magnetic data must depend largely on furnace observations, since these lines are very difficult in the spark when they can be measured at all. In number they include 23 per cent of the lines given in Table I. The sharpness of the components in a large majority of cases indicates a greater prevalence of the triplet type than is found among the lines of other classes. In the blue the average separation of IA lines is about the same as for others, but in the green it is nearly twice as great. Simple and often large separations appear to be characteristic of these lines, which are strong in the low-temperature furnace, and very faint in the arc and spark.

Other large groups of lines, for which the furnace is not so necessary as for those of Class IA, are yet relatively strong in the furnace and their Zeeman components appear with less difficulty than with the spark. For a large proportion of the lines in a spectrum the usefulness of the furnace in observations supplementary to those of the spark seems thus to be assured.

DESCRIPTION OF THE PLATES

Plates X and XI illustrate the results obtained for both emission and absorption spectra. Arc spectra with long and short exposures, respectively, are given above and below for each section, with the furnace spectra between. The plates selected for reproduction favor the weaker furnace lines so that many of the strong lines are overexposed, some of these showing in the negative the apparent triplet structure resulting from the reversal of both n-components. It will be noted that numerous lines, well defined in the furnace, are scarcely visible in the lower arc exposure, which is a normal one for the stronger arc lines. The very strong arc spectrum above is necessary to show these IA lines for which the furnace is especially effective.

SUMMARY

1. The action of a magnetic field on the furnace spectrum has been examined both for the direct and inverse effects.

2. The character and magnitude of the separations for the *n*-components of furnace lines in emission agree closely with those of the spark in a corresponding field. Self-reversed components are frequent and follow the character of the no-field line.

3. The use of a plug in the furnace tube gives the Zeeman components in absorption. The effects agree with those obtained for emission, except that uniformly larger separations for absorption components indicate that the absorption particles are localized in a part of the tube having a higher field-strength.

4. The large class of lines which are relatively strong in the furnace spectrum makes this source especially useful in supplementing the results for the spark in the magnetic field. For the more pronounced type of these lines, not usually obtainable with the spark, the furnace provides an effective method of increasing the data on magnetic separations.

The writer is indebted to Miss Brayton, of the Computing Division, for assistance in measuring a part of the spectrograms.

Mount Wilson Observatory
December 1919

Contributions from the Mount Wilson Observatory, No. 181
Reprinted from the *Astrophysical Journal*, Vol. LI, pp. 179–186, 1920

OBSERVATIONS OF THE ELECTRIC FURNACE SPECTRA OF COBALT, NICKEL, BARIUM, STRONTIUM, AND CALCIUM IN THE REGION OF GREATER WAVE-LENGTH

By ARTHUR S. KING

ABSTRACT

Infra-red electric furnace spectra to λ 9200.—By using plates stained with dicyanin, the author has extended his study of the furnace spectra of *cobalt, nickel, barium, strontium, and calcium* beyond λ 7000; the longest wave-lengths photographed were λλ 8094, 7798, 8560, 7673, and 7326 respectively. By comparing the spectra obtained with low, medium, and high furnace temperatures, the *lines were grouped into temperature classes*, as in previous work of the author's, according to the temperature at which each appeared and to the rate of increase of intensity with rising temperature. While all the furnace lines obtained appear in the arc, the relative intensities often vary widely; some lines strong in the furnace are faint in the arc and some lines strong in the arc were not found in the furnace.

The material presented in this paper was collected during a series of experiments designed to extend as far as possible into the infra-red several furnace spectra which had previously been studied through the range λ 3000 to λ 7000.[1]

Since photographic emulsions stained with dicyanin are sensitive far beyond the red limit of the visible spectrum, it is possible to observe the characteristics of infra-red lines without extraordinary difficulties. For the weaker light-sources, however, faster plates than those now available are highly desirable, and this lack of speed has been much felt in the photography of furnace spectra. It has been noted repeatedly in former furnace investigations that the region of greater wave-length is relatively weak in the furnace. The present study of the infra-red bears out this observation, and long exposures were often required to bring out the spectra that have been obtained. It has been possible, however, to photograph the spectrum to about λ 9200 and to classify the lines which the furnace was able to emit within this range.

---

[1] *Mt. Wilson Contr.*, Nos. 108, 150; *Astrophysical Journal*, **42**, 344, 1915; **48**, 13, 1918.

Seed "23" plates or Eastman Portrait Films were treated with a dicyanin bath according to the method recommended by Merrill.[1] The plates were used for the first-order spectrum of the 15-ft. concave grating to about λ 8250, while the films exposed with a 1-meter concave grating gave the extension farther into the infra-red.

The tube-resistance furnace was operated as usual *in vacuo*, and photographs were made for three temperature stages selected according to the element under examination. This treatment brought out the groups of lines appearing at the successive temperatures and showed the relative changes in line intensity as the temperature rises.

The resulting classification is given in the last column of Tables I–IV and follows the method of previous work. Lines of Classes I and II appear at low temperatures; those of Class II strengthen more rapidly at higher temperatures and are usually strong arc lines. Class III lines appear at medium temperature, while those of Classes IV and V are high-temperature lines. Those lines which are especially characteristic of the furnace spectrum and are relatively faint in the arc are denoted by "A" after the class number. The predominating lines of this type are those of Classes I A and III A.

COBALT

The cobalt lines obtained in this investigation are listed in Table I, the wave-lengths (and also those of Table II) being the measures of Meggers and Kiess,[2] which are on the international system. The metal used in the furnace was a purified powder prepared by Kahlbaum.

The results are presented in the usual form, with intensities for the arc and three furnace temperatures. The latter were approximately 2400°, 2100°, and 1900° C. Some of the low-temperature lines as far as λ 7085 were also listed in the former tables.[3] The classification of these lines remains the same, but the relative intensities are changed owing to the use of dicyanin plates. The low-temperature spectrograms required long exposure, and, in order to make sure that all possible lines for this temperature were recorded, the results with the 15-ft. spectrograph were checked by a strongly exposed film taken with the 1-meter concave grating.

---

[1] *Bulletin of the Bureau of Standards*, **14**, 487, 1919.

[2] *Ibid.*, **14**, 637, 1919.

[3] *Mt. Wilson Contr.*, No. 108; *Astrophysical Journal*, **42**, 344, 1915.

TABLE I

TEMPERATURE CLASSIFICATION OF COBALT LINES

λ (MEGGERS AND KIESS)	ARC INTENSITY	FURNACE INTENSITIES			CLASS
		High Temperature	Medium Temperature	Low Temperature	
6678.84	5	5	4	2	II
6771.05	50	50	40	40	I
6814.99	40	40	30	25	I
6872.42	40	40	30	20	I
6937.85	4	2	1	....	III
6997.30*	4	....	....	....	V
7004.82	3	3	2	....	III
7016.65	35	35	25	25	I
7027.86	6	tr	....	....	V
7052.84	60	60	40	50	I
7054.08	10	8	5	....	III
7084.99	100	80	80	80	I
7094.64	1	1	....	....	IV
7113.74	5	....	....	....	V
7124.45	1	1	1	....	III
7134.37	5	....	....	....	V
7154.71	8	8	6	2	II
7159.23	6	....	....	....	V
7193.63	4	....	....	....	V
7250.09	1	3	2	....	III A
7285.29	4	1	....	....	IV
7354.61	3	4	2	....	III
7388.66	5	2	1	....	III
7417.40	10	10	5	2	II
7437.15	1	2	1	....	III A
7457.43	6	....	....	....	V
7533.52	1	1	....	....	IV
7554.04	4	1	....	....	IV
7590.60	2	2	1	....	III
7606.30	2	....	....	....	V
7610.29	2	1	....	....	IV
7712.68	6	5	2	....	III
7838.18	3	....	....	....	V
7869.92	2	....	....	....	V
7871.43	2	....	....	....	V
7908.75†	6	3?	3?	....	III ?
7926.59	3	....	....	....	V
7987.38	5	5	3	....	III
8007.34	5	....	....	....	V
8043.33	2	....	....	....	V
8056.03	2	....	....	....	V
8094.03	8	4	2	....	III

* Probably double.

† Furnace line may be due to carbon.

The variety of types observed for the visible spectrum continues in the region of longer waves. A number of moderately strong arc lines did not appear in the furnace and are placed in Class V. Two very faint arc lines λλ 7250 and 7437 are relatively strong in the furnace. The low-temperature spectrum ceases at λ 7417, but that for medium temperature holds up to the end of the list at λ 8094.

NICKEL

The nickel lines listed in Table II were obtained for about the same temperature stages as the cobalt lines in Table I. The

TABLE II

TEMPERATURE CLASSIFICATION OF NICKEL LINES

λ (Meggers and Kiess)	Arc Intensity	Furnace Intensities			Class
		High Temperature	Medium Temperature	Low Temperature	
6842.10	8	....	....	....	V
6876.77	2	2	....	....	IV
6914.60	50	50	20	15	II
6955.10	3	....	....	....	V
7001.55	1	1	....	....	IV
7024.76	3	....	....	....	V
7030.10	3	....	....	....	V
7034.42	1	....	....	....	V
7110.98	3	15	8	....	III A
7122.31*	100	4?	2?	....	IV?
7182.06	8	....	....	....	V
7197.07	5	15	5	....	III A
7261.94	3	8	3	....	III A
7291.30	1	3	1	....	III A
7385.23†	1	1?	....	....	IV?
7386.24†	1	3?	2?	....	III A?
7393.67	10	2	1	....	III
7409.35	8	1	....	....	IV
7414.51	2	6	4	....	III A
7422.34	15	4	3	....	III
7522.87	3	2	1	....	III
7525.18	2	1	tr	....	III
7555.67	5	2	2	....	III
7574.10	1	....	....	....	V
7617.02	5	2	1	....	III
7619.24	1	1	tr	....	III
7714.27	3	8	8	6	I A
7727.68	3	1	....	....	IV
7748.94	3	tr	....	....	IV
7788.95	2	6	6	....	III A
7797.66	3	....	....	....	V

* Difficult on account of strong carbon spectrum. Line, if present, is faint in furnace.
† Furnace lines may be due to carbon.

metallic nickel was a purified preparation from Kahlbaum. In some cases cobalt and nickel were used together in the furnace.

The low-temperature stage, at which many lines appear in the visible spectrum, shows in the region now studied only λλ 6915 and 7714. About one-fourth of the lines in Table II, however, are relatively strong in the furnace as compared with the arc. The most notable of this type is the I A line λ 7714, the others belonging to Class III A. This feature causes the occurrence of various contrasting pairs of neighboring lines, one of which is a decided arc line and the other a furnace line. Such pairs are λλ 7111 and 7122, 7414 and 7422, 7714 and 7728, 7789 and 7798. The relative intensities of the members of any of these pairs in a given source will decide its resemblance to the furnace or the arc.

BARIUM

The barium lines in Table III were obtained at temperatures of 2400°, 2000°, and 1650° C. for the three stages. Desiccated barium chloride was used in the furnace. First-order plates taken with the 15-ft. concave grating supplied the data except for the last two lines, which were photographed on films with the 1-meter concave grating.

The wave-lengths are those measured by Hermann,[1] by Saunders,[2] and by Meggers,[3] as indicated by the initials in the second column. The values of Meggers are on the international system.

The low-temperature spectrum yields a considerable number of lines in this region. Besides the strong arc lines of Class II, which are present at low temperature, there is an important set of five Class I lines, of which the I A line λ 7911 is the most interesting. This line widens at high temperature and its low density may be due to incipient reversal, but the high intensity of this weak arc line at low temperature is very striking. Several lines just visible in the arc with moderate exposure attain considerable strength at the high and medium furnace temperatures and are placed in Class III A. Lines which in the arc show a diffuse structure are indicated by "n" after the arc intensity. Some of these are shaded toward red or violet. In all such cases the vacuum furnace gives a sharply defined line. Three lines, λλ 7060, 7281, 7672, are reversible both in the arc and in the high-temperature furnace. The reversals are narrow, however, compared with those of the potassium pair, λλ 7665, 7699, which, though given merely by an impurity, often appear widely reversed.

---

[1] *Tübingen Dissertation*, 1904; *Annalen der Physik* (4), **16**, 684, 1905.

[2] *Astrophysical Journal*, **32**, 153, 1910.

[3] *Bulletin of the Bureau of Standards*, **14**, 371, 1918.

TABLE III

TEMPERATURE CLASSIFICATION OF BARIUM LINES

λ	Measured by	Arc Intensity	Furnace Intensities			Class
			High Temperature	Medium Temperature	Low Temperature	
6772.07.....	H	2n	1	1	....	III
6865.93.....	H	30	10	6	3	II
6868.04*....	H	8n	2	?	....	IV?
7060.26†....	H	400r	200R	100	40	II
7090.51.....	H	5n	5	3	....	III
7120.73.....	H	200	100	40	20	II
7153.72.....	S	5	5	2	....	III
7195.71.....	H	80	40	30	4	III
7208.50.....	H	1n	1	1	....	III
7213.83.....	H	1	6	4	....	III A
7229.40.....	H	25	10	5	....	III
7280.58.....	H	150r	100R	40	15	II
7359.67.....	H	1	4	2	....	III A
7376.10.....	H	2n	2	1	....	III
7392.83.....	H	30	15	12	4	II
7410.6......	S	1	1	....	....	IV
7417.80.....	H	5	6	5	2	II
7460.27.....	H	5n	5	2	....	III
7488.38.....	H	10	10	10	8	I
7610.50.....	M	2	4	4	....	III A
7636.88.....	M	2n	3	2	....	III
7642.92.....	M	4n	4	2	....	III
7672.12.....	M	25r	20r	15	12	I
7706.58.....	M	1n	1	1	....	III
7780.49.....	M	10	10	8	7	I
7905.80.....	M	6	6	6	1	III
7911.36.....	M	3	3	6	10	I A
8210.28‡....	M	4	3	2	?	III?
8559.90.....	M	4	3	2	2	I

* Difficult at medium temperature on account of band.

† Intensities much affected by vapor density.

‡ May be concealed by band at low temperature.

STRONTIUM

The strontium lines in Table IV were obtained with the dried chloride in the tube at the same temperatures as were used with barium. No lines showed a higher relative intensity in the furnace than in the arc. λ 6892.62 is the most conspicuous low-temperature line, the only one falling in Class I. The other strong lines fade rapidly at low temperature. λ 7153.08 seems usually to have been ascribed to barium, which has a line at λ 7153.72, but the two lines are clearly shown by these photographs to be distinct.

TABLE IV

Temperature Classification of Strontium Lines

λ (Meggers)	Arc Intensity	Furnace Intensities			Class
		High Temperature	Medium Temperature	Low Temperature	
6791.08	100	20	20	5	II
6878.36	300	40	30	10	II
6892.62	50	50r	50	50	I
7070.15	400	100	100	30	II
7153.08*	5	1 ?	....	....	IV ?
7167.24†	50	10	4	....	III
7232.24‡	20	6	2	....	III
7287.44	1	1	....	....	IV
7309.47	70	15	10	1	III
7621.54	10	4	2	....	III
7673.11§	15	4	1	....	III

* Furnace line may be due to carbon.

† Widens to red in arc.

‡ Widens to red in arc.

§ Widens to violet in arc.

CALCIUM

Spectrograms were made with metallic calcium in the furnace for the same temperatures as were used with barium and strontium. The lines measured by Meggers at λλ 7148.15, 7202.21, 7326.12 were obtained with the furnace. These come within the range covered in the former investigation.[1] Numerous attempts were made to photograph the lines λλ 8497.98, 8542.06, 8662.10, but these, while strong in the arc, did not appear with certainty in the furnace, though a trace of the strongest may have been present. These lines are of special interest as in the solar spectrum they are the strongest in that part of the infra-red at present reached by photography. This high solar intensity and the fact that they are stronger in the spark than in the arc are features which they have in common with the H and K lines. They are, however, enhanced lines of a more pronounced type than H and K, the latter appearing even at low temperatures in the furnace, while those of the infra-red triplet belong clearly in Class V.

---

[1] *Mt. Wilson Contr.*, No. 150; *Astrophysical Journal*, **48**, 13, 1918.

SUMMARY

1. By means of plates bathed with dicyanin, a study of the cobalt, nickel, barium, strontium, and calcium spectra extending into the infra-red has been made for three temperatures of the electric furnace.

2. The lines of the arc spectrum, above a certain minimum intensity, appear for the most part in the furnace. Some strong arc lines, however, were not obtained in the furnace, and, on the other hand, a number of examples appear of lines strong in the furnace which are faint in the arc.

3. Besides these features, the same variety as to rate of increase of line intensity with temperature was observed as for the visible spectrum, and the resulting classification is based on the differing response to varying temperature.

Mount Wilson Observatory
January 1920

Contributions from the Mount Wilson Observatory, No. 182

THE PHOTOGRAPHIC DETERMINATION OF STELLAR PARALLAXES WITH THE 60-INCH REFLECTOR

FOURTH SERIES

By ADRIAAN VAN MAANEN

The present publication is a continuation of the three previous series[1] of parallaxes. As the work has been carried out in practically the same way as for the former series, only a few details need to be mentioned in regard to the taking, measuring, and discussion of the plates.

The exposures for N.G.C. 6804, 7008, and 7662 were 25, 20, and 25 minutes, respectively, while for all other fields they were as a rule 15 minutes.

For some fields it has been necessary to use a few comparison stars whose distance from the center of the plates is greater than 8′; in no case, however, does the distance exceed 10′.

The detailed results for each field are collected in the tables, which are arranged in the same way as in the previous papers.

SUMMARY OF RESULTS

The results are in Table I; at the end are values for nine objects not contained in Boss's *Preliminary General Catalogue*.

The mean number of exposures is a little over 16; the mean probable error of a final parallax is 0″.0058.

It has previously been noted that in the case of some of the double stars the probable errors are considerably larger than for the other fields. An investigation shows that in general the accidental error is large when the distance between the components is large. For the 100 fields discussed in the four series the mean probable error is 0″.0056; for the six double stars for which the distance is less than 10″ it is 0″.0060; while for Boss 5682–5683, 5433–5434, 3983–3986, and 592–593, whose separations are 14″,

---

[1] *Mt. Wilson Contr.*, Nos. 111, 1916; 136, 1917; 158, 1918.

16″, 30″, and 39″, respectively, the probable errors are 0.″0075, 0.″0095, 0.″0160, and 0.″0145. The increase is probably due to the diffraction images caused by the small rotating sector. In the case of single stars and of close doubles the diffraction pattern can be kept nearly symmetrical with respect to the hour circle, and thus with the measuring thread; but this is not possible for double stars of large separation. The difficulty could be avoided by using a considerably larger sector, which on the other hand would have the great disadvantage of cutting out the nearest comparison stars, or by treating the components of such stars as separate objects.

TABLE I

Number in Boss *P.G.C.*	Mag. Harvard	Spectrum	P.M. Boss	Relative Parallax	P.E.	No. of Exp.	μ_a Boss	μ_a vM	Boss−vM
217..........	6.31	Mb(G6)	0.″023	−0.″003	0.″007	18	+0.″021	+0.″022	−0.″001
340..........	5.77	B9	0.025	+0.015	0.007	18	+0.019	+0.009	+0.010
373..........	6.26	F2p	0.135	+0.034	0.004	16	+0.128	+0.120	+0.008
889..........	5.92	G9	0.058	+0.018	0.002	16	+0.055	+0.043	+0.012
1182..........	6.00	F0	0.013	0.000	0.003	18	−0.013	−0.017	+0.004
1256..........	5.88	Mb*	0.049	+0.005	0.004	16	+0.045	+0.023	+0.022
1267..........	6.22	K0	0.048	+0.019	0.005	18	−0.038	−0.038	0.000
1629..........	var.	F8p	0.024	+0.006	0.004	14	−0.006	+0.018	−0.024
1846..........	5.69	Mb(G9)	0.019	+0.008	0.003	16	+0.019	0.000	+0.019
2663..........	5.93	K1	0.090	+0.008	0.007	16	−0.090	−0.052	−0.038
2800..........	5.74	Ma*	0.041	+0.003	0.003	14	−0.039	0.000	−0.039
2915..........	6.05	Mc	0.023	−0.006	0.005	16	−0.021	+0.039	−0.060
3141..........	5.62	K0	0.136	+0.034	0.006	14	−0.095	−0.056	−0.039
3581..........	6.00	Ma*	0.072	+0.010	0.004	16	−0.006	−0.008	+0.002
3983..........	6.93	G3	0.246	+0.010	0.016	16	−0.217	−0.207	−0.010
3986..........	7.61	....	0.230	+0.031	0.016	16	−0.205	−0.226	+0.021
4195..........	5.47	K5	0.076	+0.014	0.007	16	−0.001	−0.006	+0.005
4817..........	5.37	F8	0.009	−0.001	0.004	16	−0.003	+0.015	−0.018
*Anon. 1......	12.34	F0	3.01	+0.244	0.008	16	....	+1.267	....
†Anon. 2......	12.1	....	....	−0.003	0.009	16	....	+0.011	....
‡Anon. 3......	10.4	....	....	+0.011	0.009	16	....	−0.016	....
W.B. 4^h1189...	6.50	K4	1.25	+0.107	0.006	20	....	+0.555	....
§Anon. 4......	9.67	Mb	10.30	+0.519	0.006	18	....	−0.728	....
‖N.G.C. 6804 .	13.4	Pl. Neb.	....	+0.020	0.003	18	....	−0.004	....
‖N.G.C. 6905 .	14.5	Pl. Neb.	....	+0.013	0.002	18	....	−0.021	....
‖N.G.C. 7008 .	12.8	Pl. Neb.	....	+0.014	0.004	20	....	−0.022	....
‖N.G.C. 7662 .	12.9	Pl. Neb.	....	+0.021	0.004	16	....	−0.003	....

* Anonymous 1: $\alpha = 0^h\ 43^m\ 52^s$, $\delta = +4°\ 55'$; $\mu = 3.''01$, van Maanen; mag. by Seares.

† Anonymous 2: $\alpha = 2^h\ 45^m\ 44^s$, $\delta = +22°\ 38'$; mag. as given in the *Carte du Ciel*, Paris.

‡ Anonymous 3: $\alpha = 2^h\ 45^m\ 54^s$, $\delta = +22°\ 37'$; mag. as given by Burnham, *Measures of Proper Motion Stars*.

§ Anonymous 4: $\alpha = 17^h\ 52^m\ 54^s$, $\delta = +4°\ 28'$; $\mu = 10.''30$, Barnard; mag. by Seares.

‖ The magnitudes for the central stars of the four planetary nebulae are photographic, derived from counts of the number of stars of equal and brighter magnitudes and based on Table IV of *Groningen Publications*, No. 27.

Special notes may be made concerning the following fields:

a) **Anonymous 1,** $\alpha=0^h43^m52^s$, $\delta=+4°55'$. In *Publications of the Astronomical Society of the Pacific*, December 1917, I announced that this star has a proper motion of 3″.01 annually; Seares found the photo-visual and photographic magnitudes to be 12.34 and 12.91, respectively. The spectrum is F0. The absolute parallax of +0″.246 gives for the absolute magnitudes, +14.3 photo-visual and +14.8 photographic. It is, therefore, by far the faintest F-type star known at the present time.

b) **Anonymous 2 and 3,** $\alpha=2^h45^m44^s$, $\delta=+22°38'$ and
$\alpha=2^h45^m54^s$, $\delta=+22°37'$

In 1909 Puiseux[1] announced that the second of the two stars has a proper motion of 0″.708 annually. Burnham, measuring this field in 1910 and comparing the positions of some neighboring stars with those of the *Carte du Ciel* print of 1908 for this region, found that the first star, which he estimated to be of mag. 12.1, also has a considerable motion of 0″.87 annually. Both are entered in my list of stars with proper motions exceeding 0″.50 annually,[2] as Nos. 73 and 72, respectively. The field was added to the parallax program of both the Dearborn and the Mount Wilson observatories. Comparing a Mount Wilson plate of 1918 with the *Carte du Ciel* position of 1892, I found that Puiseux' star showed no appreciable motion whatever, but that a third star, No. 26 of plate 382, showed a considerable displacement as compared with the catalogue position. I then requested Professor Frost to send me plates of the region taken with the 40-inch refractor. He kindly forwarded two taken in 1911 and one taken in 1913, mentioning at the same time that Professor Slocum had measured the plates and that according to his records "they do not show that there is an appreciable motion." Professor Barnard about the same time wrote that he had measured both stars, and that neither showed any appreciable motion. The position of the third star on the Mount Wilson plate of 1918 also agrees very well with those of the Yerkes plates of 1911 and 1913, and we must therefore conclude that none of the three stars has any large motion. The best explanation is that the position of star 26 of plate 382 of the Paris *Carte du Ciel* is in error by $0'.3$ in declination. In measuring the parallaxes of the stars of Puiseux and Burnham, I incidentally measured that of star 26, and found as the mean value for its relative parallax $-0''.023 \pm 0''.008$.

---

[1] *Bulletin Astronomique,* **26,** 416, 1909.

[2] *Mt. Wilson Contr.,* No. 96; *Astrophysical Journal,* **41,** 187, 1915.

c) **Boss 1182.** In measuring the parallax of this object one of the comparison stars was found to have a considerable proper motion; it was accordingly dropped for comparison purposes, but its proper motion and parallax were determined. The star is now placed on the regular parallax program. Its preliminary data are:

$\alpha\ 1900 = 4^h 53^m 11^s$, $\delta\ 1900 = +39^\circ 13'$
$\mu = 0''.377$ in p. $114^\circ.6$ $\pi = -0''.010 \pm 0''.006$
Photographic mag. = 13.2

d) **W.B. 4^h1189.** This star was put on the parallax program at the request of Mr. Adams, as the value derived by him for its spectroscopic parallax, viz., $+0''.095$, was irreconcilable with that published by Flint, viz., $+0''.290$. Several other values of its parallax have now been published: Yale $+0''.104$, Miller $+0''.111$, and Mitchell $+0''.124$, all in good agreement with the Mount Wilson values.

TABLE II

N.G.C.	π abs.	m	M	Diameter	
				Angular	Light-Years
2392	$+0''.022$	10.0	+ 6.7	46″	0.03
6720	+0.008	14.7	+ 9.2	80	0.16
6804	+0.022	13.4	+10.1	32	0.02
6905	+0.015	14.5	+10.4	47	0.05
7008	+0.016	12.8	+ 8.8	95	0.09
7662	+0.023	12.9	+ 9.7	31	0.02

e) **Boss 1629.** This star is a Cepheid variable, its magnitude ranging from 5.0 to 5.9; through the use of the period-luminosity curve the absolute magnitude and thus the parallax was determined by Shapley to be $+0''.004$.[1]

f) In the third series of parallaxes results for the three planetary nebulae N.G.C. 2392, 6720, and 7662 were discussed. Material is now available for six of these remarkable objects. This has been fully discussed in *Proceedings of the National Academy of Sciences*, 4, 394–396, 1918;[1] a condensed summary of the results is given in Table II.

---

[1] *Mt. Wilson Contr.*, No. 153; *Astrophysical Journal*, **48**, 279, 1918.

DISCUSSION OF SYSTEMATIC ERRORS

The four series of Mount Wilson parallaxes now published can be tested for systematic errors by comparing the results with those from other sources. Several methods of procedure are open:

a) A direct comparison with other observers. Fairly good parallaxes are available for sixteen objects. The earlier values for the nebulae N.G.C. 224 and 2392 have been omitted as too unreliable. The parallaxes for the three Wolf-Rayet stars B.D. +35° 4001, +35° 4013, and +36° 3956, published by Kapteyn,[2] have been corrected for a magnitude error.[3] The results are collected in Table III, whose successive columns give the name of the object, the parallax by other observers, that by van Maanen, the difference, others − van Maanen, and the weight of the difference. The weights are of course functions of the probable errors of both values

TABLE III

Object	π_{others}	$\pi_{\text{van Maanen}}$	$\pi_o - \pi_{vM}$	Weight
Boss 592	+0″.039	+0″.010	+0″.029	0.6
593	+0.035	+0.030	+0.005	0.6
Nova Persei	+0.015	+0.009	+0.006	1.8
W.B. 4^h1189	+0.116	+0.109	+0.007	1.7
Boss 1629	+0.042	+0.008	+0.034	0.9
2378	0.000	+0.001	−0.001	0.9
Barnard's star	+0.506	+0.521	−0.015	2.0
N.G.C. 6720	+0.015	+0.004	+0.011	0.9
Boss 4817	+0.010	+0.001	+0.009	0.9
4892	+0.048	+0.046	+0.002	1.3
4893	+0.032	+0.044	−0.012	1.3
B.D. +35°4001	−0.006	+0.013	−0.019	0.2
+35°4013	+0.011	+0.004	+0.007	0.2
+36°3956	+0.066	−0.003	+0.069	0.2
Boss 5433	+0.302	+0.327	−0.025	0.9
5434	+0.302	+0.322	−0.020	0.9

---

[1] *Mt. Wilson Communications*, No. 56.

[2] *Groningen Publications*, No. 1, p. 81, 1900.

[3] *Publications of the Astronomical Society of the Pacific*, **28**, 280, 1916.

of the parallaxes. For the Mount Wilson values the probable error 0″.0056 was used, except in the case of the wide double stars Boss 592, 593, and Boss 5433, 5434, where, on account of the greater uncertainty for wide doubles mentioned above, the value 0″.010 was used. The weighted mean difference $\pi_{\text{others}}-\pi_{\text{van Maanen}}$ is +0″.0013.

b) It has been noted before[1] that an error in the parallaxes will be reflected in the proper motions and vice versa. A second solution was therefore made for each star appearing in Boss's *Preliminary General Catalogue*, using Boss's value for μ_a in the equations of condition; the resulting mean correction to the parallaxes of the ninety-two stars available is +0″.0006.

c) From Kapteyn's tables in *Groningen Publications*, No. 8, we may interpolate the parallax of each individual star as a function of its magnitude and proper motion. The mean deviation of the parallaxes so determined, without regard to sign, is 0″.011. The five stars showing deviations exceeding 0″.050 are collected in Table IV. The spectroscopically determined parallaxes, kindly supplied by Mr. Adams, are also included. The last two columns give the differences $\pi_{\text{Kapteyn}}-\pi_{\text{van Maanen}}$ and $\pi_{\text{Adams}}-\pi_{\text{van Maanen}}$. For Boss 2921 and 3650 the differences are all so large that we must admit the possibility of a considerable error in the directly measured parallaxes; both stars have therefore been placed on the program for redetermination. For the following discussion they have been rejected. For Boss 5433 and 5434 the large difference $\pi_{\text{Kapteyn}}-\pi_{\text{van Maanen}}$ is likely due to the uncertainty in the parallax derived from *Groningen Publications*, No. 8. When the proper motion is exceptionally large, as is the case with the stars in question

TABLE IV

Boss *P.G.C.*	π Kapteyn	π Adams	π van Maanen	$\pi_K-\pi_{vM}$	$\pi_A-\pi_{vM}$
2921........	+0″.019	+0″.013	+0″.080	−0″.061	−0″.067
3650........	+0.040	+0.060	+0.098	−0.058	−0.038
5433........	+0.275	+0.331	+0.327	−0.052	+0.004
5434........	+0.255	+0.331	+0.322	−0.067	+0.009
6129........	+0.042	+0.138	+0.099	−0.057	+0.039

---

[1] *Mt. Wilson Contr.*, No. 136, p. 37, 1917.

which form the well-known double 61 Cygni, the tables of Kapteyn, which refer to mean values, cannot be expected to give close approximations for individual stars. These stars are accordingly omitted from the comparison with Kapteyn, but are retained for the rest of the discussion. For Boss 6129 no obvious explanation of the large differences is available and the star is retained throughout.

In order to investigate a possible dependence of the Mount Wilson parallaxes upon the right ascension, the remaining eighty-nine stars were divided into groups covering three hours each;

TABLE V

α	$\pi_K - \pi_{vM}$	n	Wt.
$0^h - 2^h$	+0.″001	15	33
3 − 5	−0.002	9	20
6 − 8	−0.001	13	30
9 −10	+0.003	12	18
12 −14	−0.012	7	12
15 −17	−0.002	12	22
18 −20	−0.003	11	21
21 −23	0.000	10	13

Table V gives the mean differences and the numbers of stars n. These results show no systematic error which is a function of the right ascension. Taking into account, in the case of stars of large proper motion, the larger deviations of the individual parallaxes from Kapteyn's formula, the weighted mean difference $\pi_K - \pi_{vM}$ is −0.″0013.

To compare the results with the formula

$$\bar{\pi} = (0.905)^{m-5.5} \sqrt[1\ 54]{0.0262}$$

used by Kapteyn for stars of type II,[1] the stars of this type were all reduced to the same magnitude. Since most of them have magnitudes between 5.0 and 7.0, they were reduced to magnitude 6.0 with the help of Tables 45–48, *Groningen Publications*, No. 29; for the few stars fainter than 7.0 it was not thought wise to apply a correction for magnitude; it seemed better to omit them altogether.

---

[1] *Groningen Publications*, No. 8, p. 24, 1901.

The results are given in Table VI and illustrated by Figure 1, from which the last two values of the table based on two stars and on one star, respectively, are omitted. The curve represents the mean parallaxes according to Kapteyn's formula for magnitude 6.0. The agreement with the Mount Wilson parallaxes is extremely close, especially for the smaller values of the proper motion.

TABLE VI

$\bar{\mu}$	π_{Kapteyn}	$\pi_{\text{van Maanen}}$	$\pi_{\text{K}}-\pi_{\text{vM}}$	n	Wt.
0″.012	+0″.0051	+0″.0042	+0″.0009	10	30
0.020	+0.0070	+0.0077	−0.0007	10	29
0.037	+0.0105	+0.0093	+0.0012	10	22
0.055	+0.0136	+0.0130	+0.0006	10	20
0.070	+0.0159	+0.0202	−0.0043	10	17
0.090	+0.0187	+0.0237	−0.0050	10	15
0.136	+0.0244	+0.0233	+0.0011	10	10
0.274	+0.0385	+0.0451	−0.0066	7	3.5
0.692	+0.0670	+0.0445	+0.0215	2	0.4
1.250	+0.1035	+0.1110	−0.0075	1	0.1

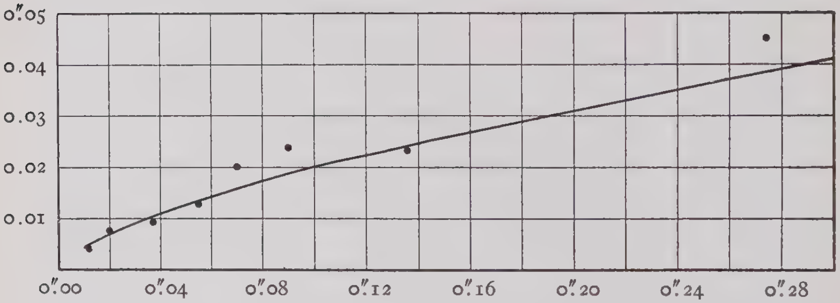

FIG. 1.—Comparison of Mount Wilson parallaxes with Kapteyn's formula for mean parallax. Abscissae, proper motion; ordinates, mean parallax. The curve represents the formula for stars of magnitude 6.0.

The table shows that the difference $\pi_{\text{K}}-\pi_{\text{vM}}$ is independent of the amount of proper motion. For the 80 second-type stars with magnitudes 5.0 to 7.0 the mean difference is −0″.0008.

d) We can derive $\overline{M}$, the mean absolute magnitude, and $\overline{V}$, the mean τ-component of the proper motion expressed in kilometers per second, for different groups of stars and see how these values agree with our present knowledge of intrinsic brightness and stellar velocity. For this purpose the stars were subdivided into two groups, including types F and G, and K and M. Each group was further subdivided according to proper motion, with limits 0″.000 to 0″.049, 0″.050 to 0″.099, 0″.100 to 0″.199, and 0″.200 to 0″.499; $\overline{M}$ and $\overline{V}$ were then computed by:

$$\overline{M} = 5 \log \overline{\pi} + 5 - 5 \log 10^{-0.2\overline{m}}$$

$$\overline{V} = 4.74 \frac{\overline{\tau}}{\overline{\pi}}$$

The first formula, based on the supposition of constant absolute magnitude, is due to Mr. Strömberg. $\overline{M}$ and $\overline{V}$ were derived for three values of the parallax, viz., $\pi = \pi_{\text{abs.}}$, $\pi_1 = \pi_{\text{abs.}} - 0''.003$, and $\pi_2 = \pi_{\text{abs.}} - 0''.006$. The results are shown in Table VII.

TABLE VII

Parallax	0″.000–0″.049		0″.050–0″.099		0″.100–0″.199		0″.200–0″.499	
	$\overline{M}$	$\overline{V}$	$\overline{M}$	$\overline{V}$	$\overline{M}$	$\overline{V}$	$\overline{M}$	$\overline{V}$
	Stars of Types F and G							
$\pi = \pi_{\text{abs.}}$	−0.11	10	+1.43	18	+3.20	14	+4.53	11
$\pi_1 = \pi_{\text{abs.}} - 0''.003$	−1.50	20	+0.79	23	+2.90	16	+4.39	12
$\pi_2 = \pi_{\text{abs.}} - 0''.006$	−6.71	216	+0.03	34	+2.56	19	+4.24	13
No. stars	10		7		14		6	
	Stars of Types K and M							
$\pi = \pi_{\text{abs.}}$	+0.68	9	+2.91	10	+2.58	31	+6.53	4
$\pi_1 = \pi_{\text{abs.}} - 0''.003$	−0.23	14	+2.63	12	+2.23	36	+6.46	4
$\pi_2 = \pi_{\text{abs.}} - 0''.006$	−1.83	29	+2.31	13	+1.80	44	+6.23	4
No. stars	23		20		3		1	

For the larger proper motions the changes in $\overline{M}$ and $\overline{V}$ produced by modifying the parallaxes are slight. For these groups, therefore, the comparison gives no indication as to the systematic errors in the parallaxes. But for the first group, including the smallest proper motions, which must consist almost exclusively of giants, the case is different. When the parallaxes for these stars are corrected by $-0''.006$, the resulting values of $\overline{M}$ and $\overline{V}$ are quite incompatible with our knowledge of these quantities. For the F and G stars $\pi=\pi_{\text{abs.}}$ yields decidedly better results than $\pi_1=\pi_{\text{abs.}}-0\overset{''}{.}003$; for the K and M stars π_1 seems to give results a trifle better than π. From this we might conclude that the systematic correction to the Mount Wilson parallaxes is $-0\overset{''}{.}001$ or $-0\overset{''}{.}002$.

e) Since the spectroscopically determined parallaxes are in process of revision, a comparison with these will be postponed to a later paper.

f) An investigation of the systematic errors of different parallax observers has recently been made. The discussion is based on all the directly determined parallaxes of stars whose magnitudes, spectral types, and proper motions are known; in all, 1538 observations of 901 stars were available for this purpose. The result for the Mount Wilson parallaxes is, that they seem to require a correction of $-0\overset{''}{.}002$ to reduce them to the mean system defined by the measures of all the observers.

Summarizing the points discussed under *a* to *f* we may conclude that the systematic error of the Mount Wilson trigonometric parallaxes does not appear to exceed $0\overset{''}{.}001$ or $0\overset{''}{.}002$; it seems to be independent of both right ascension and proper motion.

I wish to express my acknowledgment to Mr. Hoge and Mr. Humason for their valuable aid in securing the plates, and to Miss Coral Wolfe, of the Computing Division, who has performed a large share of the necessary computations.

Anonymous 1 $\alpha=0^h43^m52^s$ $\delta=+4°55'$ ($\mu=3''$, van Maanen)

Pl. No.	Date			t	Obs.	Qy	p	m	Remarks
1568...	1917	Oct.	8	$-3°.0$	vM	g	-0.053	$+2.77$	Trail of Boss 171
1638_1..		Dec.	8	$+1.5$	vM	fg	-0.816	$+2.94$	
1638_2..			8	$+5.5$	H	fg	-0.816	$+2.94$	
1670...	1918	Jan.	6	$+13.5$	vM	g	-0.901	$+3.02$	Clouds, 25^m exp.
1865_1..		Aug.	12	-6.7	Hum	g	$+0.739$	$+3.62$	
1865_2..			12	-2.5	vM	g	$+0.739$	$+3.62$	
1866...			12	$+1.7$	Hum	g	$+0.739$	$+3.62$	
1879_1..			13	-14.5	vM	g	$+0.731$	$+3.62$	
1879_2..			13	-10.2	H	fg	$+0.731$	$+3.62$	
1893_1..		Sept.	2	$+1.5$	Hum	fg	$+0.493$	$+3.67$	
1893_2..			2	$+6.2$	vM	fg	$+0.493$	$+3.67$	
1919...			4	$+10.5$	vM	g	$+0.459$	$+3.68$	
2026_1..		Nov.	10	$+8.0$	H	g	-0.534	$+3.86$	
2026_2..			10	$+12.0$	vM	g	-0.534	$+3.86$	
2052...			26	-6.5	vM	f	-0.714	$+3.91$	20^m exp.
2055...			27	-12.5	H	f	-0.724	$+3.91$	20^m exp.

Mor.-Ev.	Δp	Δm	M	v	Δt
1865_1-1568....	$+0.79$	$+0.85$	$+727$	-51	$-3°.7$
1865_2-1638_1...	$+1.56$	$+0.68$	$+764$	$+2$	-4.0
$1866-1638_2$...	$+1.56$	$+0.68$	$+775$	$+13$	-3.8
1879_1-2055....	$+1.46$	-0.29	-24	-18	-2.0
1879_2-2052....	$+1.45$	-0.29	$+2$	$+10$	-3.7
1893_1-2026_1...	$+1.03$	-0.19	$+2$	-4	-6.5
1893_2-1670....	$+1.39$	$+0.65$	$+735$	$+22$	-7.3
$1919-2026_2$...	$+0.99$	-0.18	-3	-11	-1.5

$$+2.31\,\mu_\alpha+2.48\,\pi=+2150 \qquad \pi=+149.8=+0''.244\pm0''.008$$
$$+2.48\,\mu_\alpha+13.70\,\pi=+3964 \qquad \mu_\alpha=+777.1=+1''.267\pm0''.020$$

Comp. Star	Br.	x	y	π	P.E.
1.........	b	$+1'.8$	$+3'.6$	$+0''.004$	$\pm0''.010$
2.........	bf	$+7.1$	-3.0	-0.002	0.008
3.........	f	$+0.4$	-5.5	$+0.006$	0.008
4.........	f	-1.6	-2.1	-0.007	0.005
5.........	f	-5.2	-1.1	$+0.004$	0.010
6.........	f	-4.1	$+1.2$	-0.009	0.008
7.........	bf	-3.6	$+5.1$	$+0.003$	±0.006

Boss 217 $\alpha = 0^h54^m39^s$ $\delta = +5°57'$

Pl. No.	Date			t	Obs.	Qy	p	m	Remarks
1145	1916	Nov.	16	$+4°.5$	H	g	-0.579	$+1.88$	Clouds, 20^m exp.
1146			16	$+9.5$	vM	g	-0.579	$+1.88$	Clouds, 20^m exp.
1168_1			17	$+7.0$	vM	fg	-0.592	$+1.88$	Thick, 25^m exp.
1168_2			17	$+13.2$	H	fg	-0.594	$+1.88$	Thick, 25^m exp.
1521_1	1917	Aug.	12	$+2.5$	vM	fg	$+0.767$	$+2.62$	
1521_2			12	$+7.0$	H	g	$+0.767$	$+2.62$	
1652	1918	Jan.	5	$+15.5$	vM	fg	-0.907	$+3.02$	
1880_1		Aug.	13	-6.0	vM	g	$+0.761$	$+3.62$	
1880_2			13	-1.7	H	g	$+0.761$	$+3.62$	Trail
1905_1		Sept.	3	$+8.0$	Hum	f	$+0.522$	$+3.68$	Clouds, 25^m exp.
1905_2			3	$+15.0$	vM	f	$+0.521$	$+3.68$	Clouds, 23^m exp.
1918			4	$+2.0$	H	g	$+0.507$	$+3.68$	
1932_1			5	$+1.0$	vM	g	$+0.495$	$+3.68$	
1932_2			5	$+5.5$	H	g	$+0.495$	$+3.68$	
2025_1		Nov.	10	-5.0	H	g	-0.497	$+3.86$	
2025_2			10	-1.0	vM	g	-0.497	$+3.86$	
2041_1			11	-7.5	vM	g	-0.509	$+3.87$	
2041_2			11	-3.0	H	g	-0.509	$+3.87$	

Mor.-Ev.	Δp	Δm	M	v	Δt	Remarks
1880_1-2041_1	$+1.27$	-0.25	$+3$	$+8$	$+1°.5$	
1880_2-2025_1	$+1.26$	-0.24	-4	$+1$	$+3.3$	
1932_1-2041_2	$+1.00$	-0.19	-10	-5	$+4.0$	
$1918-1145$	$+1.09$	$+1.80$	$+22$	0	-2.5	
1521_1-2025_2	$+1.26$	-1.24	-31	-12	$+3.5$	
1932_2-1168_1	$+1.09$	$+1.80$	$+12$	-10	-1.5	
1521_2-1146	$+1.35$	$+0.74$	-20	-28	-2.5	Star 5 not measured
1905_1-1168_2	$+1.12$	$+1.80$	$+21$	-1	-5.2	
1905_2-1652	$+1.43$	$+0.66$	$+48$	$+41$	-0.5	

$$+12.41\,\mu_a + 5.51\,\pi = +157 \qquad \pi = -1.6 = -0''.003 \pm 0''.007$$

$$+5.51\,\mu_a + 13.28\,\pi = +53 \qquad \mu_a = +13.4 = +0''.022 \pm 0''.007$$

Comp. Star	Br.	x	y	π	P.E.
1	f	$+1'.2$	$0'.0$	$+0''.009$	$\pm 0''.010$
2	bf	$+3.3$	$+2.9$	$+0.010$	0.012
3	bf	$+6.5$	-6.3	-0.014	0.008
4	b	-4.1	-6.0	0.000	0.006
5	f	-0.4	$+0.4$	$+0.009$	0.014
6	ff	-4.3	$+8.9$	-0.013	± 0.007

Boss 340 $\alpha = 1^h28^m30^s$ $\delta = +36°43'$

Pl. No.	Date	t	Obs.	Qy	p	m	Remarks
1176_1..	1916 Nov. 18	+3.°5	vM	f	−0.492	+1.89	20^m exp.
1176_2..	18	+9.0	vM	f	−0.492	+1.89	20^m exp.
1189_1..	Dec. 16	+0.5	vM	fg	−0.797	+1.96	
1189_2..	16	+5.0	H	g	−0.797	+1.96	Trail
1867_1..	1918 Aug. 12	−3.2	vM	g	+0.851	+3.62	
1867_2..	12	+0.7	Hum	g	+0.851	+3.62	
1881_1..	13	−3.0	vM	fg	+0.843	+3.62	
1881_2..	13	+0.5	H	f	+0.843	+3.62	
1894_1..	Sept. 2	+2.5	Hum	fg	+0.652	+3.67	
1894_2..	2	+7.0	vM	fg	+0.652	+3.67	
1904_1..	3	−14.0	Hum	fg	+0.642	+3.68	Clouds, 20^m exp.
1904_2..	3	−9.0	vM	fg	+0.642	+3.68	Clouds, 20^m exp.
1920...	4	+6.0	H	fas	+0.629	+3.68	
2053_1..	Nov. 26	−9.2	H	f	−0.587	+3.91	20^m exp.
2053_2..	26	−3.5	vM	f	−0.587	+3.91	20^m exp.
2056...	27	−9.5	vM	fg	−0.599	+3.91	9^m exp.
2060_1..	Dec. 9	0.0	vM	fg	−0.731	+3.94	
2060_2..	9	+4.2	H	fg	−0.731	+3.94	

Mor.-Ev.	Δp	Δm	M	v	Δt
1904_1–2056....	+1.24	−0.23	−1	−11	−4.°5
1904_2–2053_1...	+1.23	−0.23	−11	−21	+0.2
1867_1–2053_2...	+1.44	−0.29	+46	+35	+0.3
1881_1–2060_1...	+1.57	−0.32	+2	−10	−3.0
1867_2–1176_1...	+1.34	+1.73	+14	−7	−2.8
1894_1–2060_2...	+1.38	−0.27	+15	+4	−1.7
1920 –1189_2...	+1.43	+1.72	−5	−27	+1.0
1894_2–1176_2...	+1.14	+1.78	+41	+21	−2.0
1881_2–1189_1...	+1.64	+1.66	+37	+13	0.0

$$+12.23\,\mu_a + 7.66\,\pi = +134 \qquad \pi = +8.9 = +0''.015 \pm 0''.007$$
$$+7.66\,\mu_a + 17.31\,\pi = +195 \qquad \mu_a = +5.4 = +0''.009 \pm 0''.008$$

Comp. Star	Br.	x	y	π	P.E.
1.........	bf	+4'.0	+1'.2	+0''.009	±0''.011
2.........	bf	+6.7	−1.0	−0.007	0.011
3.........	bf	+1.8	−7.7	+0.002	0.010
4.........	bf	−4.5	−5.6	−0.003	0.012
5.........	f	−1.5	−0.3	+0.011	0.010
6.........	f	−4.4	+3.3	+0.012	0.008
7.........	bf	0.0	+6.3	−0.005	0.009
8.........	f	−2.2	+0.7	−0.020	±0.007

Boss 373 = Bu 870 $\alpha = 1^h35^m44^s$ $\delta = +25^\circ14'$

Pl. No.	Date	t	Obs.	Qy	p	m	Remarks
1207$_1$..	1916 Dec. 17	−3°5	H	g	−0.792	+1.96	
1207$_2$..	17	+0.7	vM	g	−0.792	+1.96	
1228$_1$..	18	−6.5	H	g	−0.800	+1.97	
1228$_2$..	18	−2.0	vM	g	−0.800	+1.97	Trail
1546$_1$..	1917 Sept. 13	−10.0	vM	fg	+0.539	+2.70	
1546$_2$..	13	−6.0	H	fg	+0.538	+2.70	
1547$_1$..	13	−1.0	vM	g	+0.538	+2.70	
1547$_2$..	13	+3.7	H	gas	+0.538	+2.70	
1557$_1$..	14	−1.5	H	fg	+0.525	+2.71	
1557$_2$..	14	+2.7	vM	g	+0.525	+2.71	
1639$_1$..	Dec. 8	−0.5	vM	g	−0.705	+2.94	
1639$_2$..	8	+3.7	H	fg	−0.707	+2.94	
1854$_1$..	1918 Aug. 11	−8.0	Hum	g	+0.871	+3.61	
1854$_2$..	11	−3.7	vM	g	+0.871	+3.61	
2059$_1$..	Dec. 9	−12.0	vM	fg	−0.714	+3.94	
2059$_2$..	9	−7.5	H	fg	−0.714	+3.94	

Mor.-Ev.	Δp	Δm	M	v	Δt
1546$_1$–2059$_1$...	+1.25	−1.24	−84	−19	+2°0
1854$_1$–2059$_2$...	+1.59	−0.33	+9	0	−0.5
1546$_2$–1228$_1$...	+1.34	+0.73	+80	−2	+0.5
1854$_2$–1207$_1$...	+1.66	+1.65	+145	−11	−0.2
1557$_1$–1228$_2$...	+1.33	+0.74	+83	+1	+0.5
1547$_1$–1639$_1$...	+1.24	−0.24	+22	+14	−0.5
1557$_2$–1207$_2$...	+1.32	+0.75	+88	+5	+2.0
1547$_2$–1639$_2$...	+1.25	−0.24	+24	+16	0.0

$$+6.13\,\mu_\alpha + 3.02\,\pi = +514 \qquad \pi = +20.9 = +0''034 \pm 0''004$$
$$+3.02\,\mu_\alpha + 15.26\,\pi = +540 \qquad \mu_\alpha = +73.6 = +0''120 \pm 0''006$$

The 10$^{\mathrm{M}}$6 companion, being covered by the sector, does not show images on the plates.

Comp. Star	Br.	x	y	π	P.E.
1.........	f	+0′4	+3′3	+0″011	±0″007
2.........	b	+2.3	+5.6	+0.002	0.009
3.........	f	+3.7	+2.5	−0.003	0.006
4.........	ff	+5.9	−4.3	−0.002	0.007
5.........	bf	−3.6	−5.9	+0.004	0.011
6.........	f	−5.6	−1.4	+0.007	0.006
7.........	f	−3.7	+1.1	−0.018	0.012
8.........	bf	−0.4	+1.2	−0.002	±0.006

Anonymous 2 $\alpha=2^h45^m44^s$ $\delta=+22^{\circ}38'$
3 $\alpha=2^h45^m54^s$ $\delta=+22^{\circ}37'$

Pl. No.	Date			t	Obs.	Qy	p	m	Remarks
1640_1..	1917	Dec.	8	$-5^{\circ}.0$	vM	g	-0.504	$+2.94$	
1640_2..			8	-0.7	H	fg	-0.504	$+2.94$	
1701...	1918	Feb.	3	$+13.5$	vM	fg	-0.941	$+3.10$	Thick, 20^m exp. Trail of Boss 674
1720...			4	$+13.0$	vM	fg	-0.940	$+3.10$	
1921...		Sept.	4	-6.5	vM	fg	$+0.850$	$+3.68$	
1922...			4	$+3.0$	vM	fg	$+0.848$	$+3.68$	
1935_1..			5	$+3.7$	vM	fg	$+0.841$	$+3.68$	
1935_2..			5	$+7.7$	H	fg	$+0.841$	$+3.68$	
1946_1..			28	-13.7	H	fg	$+0.599$	$+3.75$	
1946_2..			28	-10.0	vM	fg	$+0.598$	$+3.75$	
1953_1..			29	$+2.2$	H	fg	$+0.585$	$+3.75$	Hazy, 20^m exp.
1953_2..			29	$+7.5$	vM	g	$+0.585$	$+3.75$	Hazy, 19^m exp.
2062_1..		Dec.	9	$+3.0$	vM	fg	-0.515	$+3.94$	
2062_2..			9	$+7.0$	H	fg	-0.515	$+3.94$	
2097_1..			28	-9.0	H	fg	-0.745	$+3.99$	
2097_2..			28	-5.0	vM	fg	-0.745	$+3.99$	

Mor.-Ev.	Δp	Δm	M (72)	M (73)	v (72)	v (73)	Δt
$1921-1640_1$......	$+1.35$	$+0.74$	-11	-5	-14	-7	$-1^{\circ}.5$
$1922-1640_2$......	$+1.35$	$+0.74$	$+16$	$+41$	$+13$	$+39$	$+3.7$
1935_1-2062_2......	$+1.36$	-0.26	$+12$	$+38$	$+16$	$+26$	-3.3
1935_2-1720......	$+1.78$	$+0.58$	$+11$	-13	$+10$	-19	-5.3
1946_1-2097_1......	$+1.34$	-0.24	-46	-24	-42	-35	-4.7
1946_2-2097_2......	$+1.34$	-0.24	-21	$+16$	-17	$+5$	-5.0
1953_1-2062_1......	$+1.10$	-0.19	$+46$	$+26$	$+49$	$+17$	-0.8
1953_2-1701......	$+1.53$	$+0.65$	-8	-10	-10	-14	-6.0

$$\left.\begin{array}{l} +2.09\,\mu_a+2.82\,\pi=+9 \\ +2.82\,\mu_a+15.80\,\pi=-8 \end{array}\right\}(2) \qquad \left.\begin{array}{r} -1 \\ +80 \end{array}\right\}(3)$$

$$(2)\begin{cases}\pi=-1.6=-0''.003\pm0''.009\\ \mu_a=+6.5=+0''.011\pm0''.026\end{cases} \qquad (3)\begin{cases}\pi=+6.8=+0''.011\pm0''.009\\ \mu_a=-9.7=-0''.016\pm0''.023\end{cases}$$

Comp. Star	Br.	x	y	π	P.E.
1........	f	$+0'.8$	$+4'.5$	$-0''.017$	$\pm0''.011$
2........	bf	$+1.2$	$+4.1$	$+0.029$	0.012
3........	bf	$+0.8$	$+7.6$	-0.036	0.007
4........	bb	$+4.8$	$+6.0$	$+0.021$	0.005
5........	ff	$+3.8$	$+1.5$	-0.027	0.007
6........	bf	$+5.2$	-5.5	$+0.033$	0.014
7........	f	$+2.5$	-8.2	-0.020	0.006
8........	bf	$+1.1$	-8.0	$+0.003$	0.012
9........	f	$+1.2$	-3.7	-0.025	0.009
10........	f	-1.0	-4.8	$+0.013$	0.011
11........	ff	-4.4	-0.8	$+0.006$	0.005
12........	f	-6.0	0.0	-0.026	0.014
13........	bf	-2.7	$+1.2$	$+0.028$	0.009
14........	b	-6.9	$+6.2$	$+0.018$	±0.012

Boss 889 $\alpha=3^h46^m24^s$ $\delta=+48°21'$

Pl. No.	Date			t	Obs.	Qy	p	m	Remarks
710...	1915	Sept.	29	$-10°7$	C	fg	+0.781	+0.75	
711...			29	-6.2	vM	g	+0.780	+0.75	
712...			29	-0.5	C	fg	+0.779	+0.75	
727...			30	-11.0	vM	g	+0.768	+0.75	
788...	1916	Jan.	3	-0.5	H	f	−0.659	+1.01	Hazy, 20^m exp.
1654$_1$..	1918	Jan.	5	-7.2	H	fg	−0.689	+3.02	
1654$_2$..			5	-3.2	vM	fg	−0.689	+3.02	
1655...			5	$+1.7$	H	fg	−0.690	+3.02	Trail
1672$_1$..			6	-5.0	H	fg	−0.702	+3.02	Hazy, 25^m exp.
1672$_2$..			6	$+1.5$	vM	fg	−0.702	+3.02	Hazy, 25^m exp.
1683$_1$..		Feb.	2	-4.7	vM	fg	−0.926	+3.09	
1683$_2$..			2	-0.7	H	g	−0.926	+3.09	
1948$_1$..		Sept.	28	-3.0	H	fg	+0.787	+3.75	Clouds, 20^m exp.
1948$_2$..			28	$+2.0$	vM	g	+0.787	+3.75	Clouds, 16^m exp.
1979$_1$..		Oct.	14	-6.0	H	fg	+0.598	+3.79	
1979$_2$..			14	-2.0	vM	fg	+0.598	+3.79	

Mor.-Ev.	Δp	Δm	M	v	Δt
727 −1654$_1$...	+1.46	−2.27	−55	−12	$-3°8$
710 −1672$_1$...	+1.48	−2.27	−47	− 4	−5.7
711 −1683$_1$...	+1.71	−2.34	−37	+ 5	−1.5
1948$_1$−1654$_2$...	+1.48	+0.73	+39	+ 4	+0.2
1979$_1$−1683$_2$...	+1.52	+0.70	+29	− 6	−5.3
1979$_2$− 788....	+1.26	+2.78	+85	− 4	−1.5
1948$_2$−1672$_2$...	+1.49	+0.73	+40	+ 5	+0.5
712 −1655....	+1.47	−2.27	−35	+ 8	−2.2

$$+30.21\,\mu_a-7.28\,\pi=+711 \qquad \pi=+11.0=+0\overset{''}{.}018\pm0\overset{''}{.}002$$
$$-7.28\,\mu_a+17.71\,\pi=+5 \qquad \mu_a=+26.2=+0\overset{''}{.}043\pm0\overset{''}{.}002$$

Comp. Star	Br.	x	y	π	P.E.
1........	f	$+1\overset{'}{.}0$	$+1\overset{'}{.}6$	$+0\overset{''}{.}015$	$\pm0\overset{''}{.}008$
2........	f	+1.4	+1.8	−0.010	0.008
3........	f	+3.3	+2.7	−0.002	0.007
4........	bf	+4.5	+1.0	0.000	0.011
5........	bf	+4.1	−2.7	−0.003	0.009
6........	bf	+0.1	−4.7	+0.004	0.003
7........	bf	−2.3	−5.1	−0.001	0.006
8........	f	−3.4	−1.6	+0.006	0.006
9........	b	−3.3	+1.8	−0.018	0.008
10........	bf	−3.2	+1.8	−0.009	0.005
11........	ff	−2.6	+3.8	+0.017	±0.009

Boss 1182 = Bu 2445 $\alpha=4^h53^m26^s$ $\delta=39^\circ15'$

Pl. No.	Date			t	Obs.	Qy	p	m	Remarks
362_1..	1914	Oct.	15	−13°0	vM	g	+0.787	−0.21	
362_2..			15	− 8.5	C	fg	+0.787	−0.21	
363_1..			15	− 2.0	vM	g	+0.787	−0.21	
363_2..			15	+ 2.5	C	fg	+0.787	−0.21	Trail
794...	1916	Jan.	11	− 2.0	vM	f	−0.573	+1.03	
1682_1..	1918	Jan.	7	+ 4.5	vM	f	−0.524	+3.02	25^m exp.
1682_2..			7	+11.0	H	f	−0.524	+3.02	25^m exp.
1684_1..		Feb.	2	−11.5	vM	fg	−0.836	+3.09	
1684_2..			2	− 7.5	H	g	−0.836	+3.09	
1685_1..			2	− 2.2	vM	g	−0.838	+3.09	
1685_2..			2	+ 1.7	H	g	−0.838	+3.09	
1702_1..			3	−10.2	H	fg	−0.847	+3.10	Thick, 20^m exp.
1702_2..			3	− 4.7	vM	fg	−0.847	+3.10	Thick, 20^m exp.
1980_1..		Oct.	14	−11.5	H	fg	+0.797	+3.79	
1980_2..			14	− 7.2	vM	fas	+0.797	+3.79	
2004_1..			28	+ 0.5	vM	f	+0.630	+3.83	20^m exp.
2004_2..			28	+ 5.5	H	fg	+0.628	+3.83	20^m exp.
2017...			29	+12.0	vM	fg	+0.614	+3.83	

Mor.-Ev.	Δp	Δm	M	v	Δt
362_1–1684_1...	+1.62	−3.30	+30	− 6	−1°5
1980_1–1702_1...	+1.64	+0.69	+ 6	+12	−1.3
362_2–1684_2...	+1.62	−3.30	+45	+ 9	−1.0
1980_2–1702_2...	+1.64	+0.69	− 7	− 1	−2.5
2004_1–1685_1...	+1.47	+0.74	−20	−12	+2.7
363_1– 794....	+1.36	−1.24	+18	+ 5	0.0
363_2–1685_2...	+1.63	−3.30	+30	− 6	+0.8
2004_2–1682_1...	+1.15	+0.81	−25	−16	+1.0
2017 –1682_2...	+1.14	+0.81	+ 4	+13	+1.0

$$+37.04\,\mu_\alpha-12.57\,\pi=-402 \qquad \pi=+\ 0.3=0\overset{''}{.}000\pm0\overset{''}{.}003$$
$$-12.57\,\mu_\alpha+19.91\,\pi=+141 \qquad \mu_\alpha=-10.7=-0\overset{''}{.}017\pm0\overset{''}{.}002$$

The 9^M7 companion, being covered by the sector, shows no measurable images on the plates.

Comp. Star	Br.	x	y	π	P.E.
1.........	bf	+5′9	+4′5	−0″015	±0″006
2.........	f	+6.0	−0.1	+0.009	0.004
3.........	f	+4.9	−1.2	+0.003	0.012
4.........	bf	+0.3	−5.4	+0.002	0.007
5.........	bf	−2.9	−4.9	−0.004	0.006
6.........	f	−1.4	+0.7	−0.016	0.006
7.........	f	−1.2	+3.4	+0.022	0.006
8.........	bf	−7.1	+5.5	−0.001	±0.006

W.B. 4^h1189 $\alpha=4^h55^m51^s$ $\delta=-5^\circ52'$

Pl. No.	Date	t	Obs.	Qy	p	m	Remarks
347_1..	1914 Oct. 14	$-13^\circ.0$	vM	g	$+0.803$	-0.21	
347_2..	14	-8.2	H	g	$+0.803$	-0.21	
348...	14	$+2.5$	vM	g	$+0.803$	-0.21	Trail
714...	1915 Sept. 29	-2.5	vM	fg	$+0.931$	$+0.75$	
715...	29	$+1.7$	vM	g	$+0.931$	$+0.75$	
805...	1916 Jan. 12	$+4.0$	vM	fg	-0.579	$+1.04$	
806...	12	$+8.2$	vM	fg	-0.579	$+1.04$	Clouds
812...	Feb. 24	$+12.5$	vM	g	-0.970	$+1.15$	Hazy, 20^m exp.
1656_1..	1918 Jan. 5	-8.0	H	fg	-0.484	$+3.02$	
1656_2..	5	-3.5	vM	g	-0.485	$+3.02$	
1657_1..	5	$+2.2$	H	fg	-0.485	$+3.02$	
1657_2..	5	$+7.0$	vM	g	-0.485	$+3.02$	Trail
1673_1..	6	-7.0	H	fg	-0.499	$+3.02$	Hazy, 25^m exp.
1673_2..	6	0.0	vM	gas	-0.499	$+3.02$	Hazy, 25^m exp.
1674...	6	$+8.0$	H	g	-0.499	$+3.02$	Hazy, 25^m exp.
1982_1..	Oct. 14	$+8.7$	H	g	$+0.802$	$+3.79$	
1982_2..	14	$+13.0$	vM	fg	$+0.802$	$+3.79$	
2016_1..	29	$+1.0$	vM	g	$+0.623$	$+3.83$	
2016_2..	29	$+5.7$	H	g	$+0.623$	$+3.83$	
2032...	Nov. 10	$+10.2$	vM	g	$+0.450$	$+3.86$	

Mor.-Ev.	Δp	Δm	M	v	Δt
347_1–1656_1...	$+1.29$	-3.23	-1006	$+6$	$-5^\circ.0$
347_2–1673_1...	$+1.30$	-3.23	-1002	$+13$	-1.2
714–1656_2...	$+1.42$	-2.27	-718	-38	$+1.0$
715–1673_2...	$+1.43$	-2.27	-651	$+26$	$+1.7$
348–1657_1...	$+1.29$	-3.23	-1028	-12	$+0.3$
2016_1– 805....	$+1.20$	$+2.79$	$+1027$	-2	-3.0
2016_2–1657_2...	$+1.11$	$+0.81$	$+379$	$+30$	-1.3
2032–1674....	$+0.95$	$+0.84$	$+318$	-30	$+2.2$
1982_1– 806....	$+1.38$	$+2.75$	$+1044$	$+17$	$+0.5$
1982_2– 812....	$+1.77$	$+2.64$	$+999$	-16	$+0.5$

$$+65.27\,\mu_a-5.49\,\pi=+21860 \qquad \pi=+65.4=+0''.107\pm0''.006$$

$$-5.49\,\mu_a+17.67\,\pi=-714 \qquad \mu_a=+340.4=+0''.555\pm0''.003$$

Comp. Star	Br.	x	y	π	P.E.
1.........	f	$+0'.7$	$+3'.6$	$-0''.018$	$\pm0''.005$
2.........	ff	$+5.2$	$+3.2$	$+0.006$	0.010
3.........	bf	$+4.4$	$+0.8$	0.000	0.008
4.........	ff	$+2.6$	-4.9	$+0.001$	0.006
5.........	b	-4.3	-4.3	-0.003	0.007
6.........	f	-2.3	-0.7	0.000	0.008
7.........	bf	-3.8	$+0.5$	$+0.001$	0.006
8.........	f	-2.3	$+2.2$	$+0.014$	±0.008

Boss 1256 $\alpha=5^h11^m7^s$ $\delta=+42^\circ41'$

Pl. No.	Date	t	Obs.	Qy	p	m	Remarks
1134_1..	1916 Oct. 21	$+3^\circ.5$	vM	fg	+0.766	+1.81	Trail of asteroid (31), 20^m exp.
1134_2..	21	+11.2	H	fg	+0.764	+1.81	20^m exp.
1275_1..	1917 Feb. 13	+ 6.2	H	fg	−0.898	+2.12	20^m exp.
1275_2..	13	+13.0	vM	f	−0.898	+2.12	20^m exp.
1576_1..	Oct. 8	+ 4.2	vM	fg	+0.890	+2.77	
1576_2..	8	+ 8.5	vM	fg	+0.890	+2.77	
1703_1..	1918 Feb. 3	− 2.2	H	fg	−0.810	+3.10	Thick, 20^m exp.
1703_2..	3	+ 3.5	vM	g	−0.810	+3.10	Thick, 20^m exp.
1721_1..	4	−16.5	H	fg	−0.818	+3.10	
1721_2..	4	−12.0	vM	g	−0.818	+3.10	Trail
1725...	Mar. 3	+ 7.7	vM	g	−0.981	+3.17	20^m exp.
1726...	3	+14.7	Hum	fg	−0.981	+3.17	20^m exp.
1981_1..	Oct. 14	− 5.5	H	fg	+0.842	+3.79	
1981_2..	14	− 1.5	vM	fg	+0.842	+3.79	
2003...	28	−11.2	H	f	+0.686	+3.83	20^m exp.
2018...	29	+13.2	H	g	+0.674	+3.83	

Mor.-Ev.	Δp	Δm	M	v	Δt
2003 −1721_1...	+1.50	+0.73	+50	+35	$+5^\circ.3$
1981_1−1721_2...	+1.66	+0.69	+15	0	+6.5
1981_2−1703_1...	+1.65	+0.69	− 7	−22	+0.7
1134_1−1275_1...	+1.66	−0.31	− 4	− 5	−2.7
1576_1−1703_2...	+1.70	−0.33	+ 9	+ 8	+0.7
1576_2−1725....	+1.87	−0.40	+ 4	+ 4	+0.8
1134_2−1726....	+1.75	−1.36	−19	− 6	−3.5
2018 −1275_2...	+1.57	+1.71	+20	− 9	+0.2

$$+6.63\,\mu_\alpha+\ 1.87\,\pi=+\ 98 \qquad \pi\ =+\ 3.3=+0''.005\pm0''.004$$

$$+1.87\,\mu_\alpha+22.40\,\pi=+101 \qquad \mu_\alpha=+13.9=+0''.023\pm0''.008$$

Comp. Star	Br.	x	y	π	P.E.
1.........	bf	$+1'.2$	$+4'.7$	$+0''.013$	$\pm0''.003$
2.........	f	+2.5	+2.5	−0.014	0.004
3.........	bf	+2.6	−0.4	+0.004	0.005
4.........	f	+3.3	−7.4	+0.011	0.002
5.........	bf	+0.4	−3.4	−0.022	0.003
6.........	f	−1.4	−2.6	+0.010	0.006
7.........	bf	−4.0	+1.4	+0.007	0.008
8.........	bf	−3.0	+2.1	−0.012	0.008
9.........	f	−1.9	+4.3	+0.004	±0.008

Boss 1267=Bu 2644 $\alpha=5^h13^m20^s$ $\delta=20°2'$

Pl. No.	Date	t	Obs.	Qy	p	m	Remarks
298...	1914 Oct. 11	$-3°0$	H	g	$+0.873$	-0.22	Trail
315...	12	-5.7	vM	fg	$+0.863$	-0.22	
747_1..	1915 Oct. 1	-3.5	vM	fg	$+0.945$	$+0.75$	
747_2..	1	$+0.7$	H	fg	$+0.945$	$+0.75$	
1243...	1917 Jan. 29	-4.5	vM	fg	-0.760	$+2.08$	
1244...	29	-0.2	vM	f	-0.760	$+2.08$	
1245...	29	$+6.5$	vM	fg	-0.760	$+2.08$	
1246...	29	$+10.7$	vM	fg	-0.760	$+2.08$	
1592_1..	Oct. 24	$+6.5$	vM	fg	$+0.737$	$+2.82$	
1592_2..	24	$+11.2$	H	fg	$+0.735$	$+2.82$	20^m exp.
1597_1..	Nov. 7	-8.5	H	g	$+0.554$	$+2.85$	
1597_2..	7	-4.0	vM	g	$+0.553$	$+2.85$	
1704...	1918 Feb. 3	$+10.5$	H	g	-0.807	$+3.10$	Thick, 20^m exp.
1722_1..	4	-6.0	Hum	g	-0.816	$+3.10$	
1722_2..	4	-2.0	vM	g	-0.816	$+3.10$	
2005...	Oct. 28	$+7.5$	vM	fg	$+0.691$	$+3.83$	20^m exp.
2113...	1919 Jan. 23	-3.0	vM	fg	-0.678	$+4.07$	20^m exp.
2126...	24	-3.2	H	g	-0.689	$+4.07$	

Mor.-Ev.	Δp	Δm	M	v	Δt
1597_1–1243....	$+1.31$	$+0.77$	-2	$+1$	$-4°0$
315 –2126....	$+1.55$	-4.29	$+148$	$+30$	-2.5
1597_2–1722_1...	$+1.37$	-0.25	$+28$	$+6$	$+2.0$
747_1–1722_2...	$+1.76$	-2.35	$+50$	-25	-1.5
298 –2113....	$+1.55$	-4.29	$+96$	-22	0.0
747_2–1244....	$+1.71$	-1.33	$+60$	$+10$	$+0.9$
1592_1–1245....	$+1.50$	$+0.74$	-17	-17	0.0
2005 –1704....	$+1.50$	$+0.73$	$+10$	$+10$	-3.0
1592_2–1246....	$+1.50$	$+0.74$	$+8$	$+8$	$+0.5$

$$+46.37\,\mu_\alpha-15.72\,\pi=-1254 \qquad \pi=+11.4=+0''.019\pm0''.005$$
$$-15.72\,\mu_\alpha+21.17\,\pi=+605 \qquad \mu_\alpha=-23.2=-0''.038\pm0''.004$$

The $10^M.2$ companion, being covered by the sector, does not show any images on the plates.

Comp. Star	Br.	x	y	π	P.E.
1........	f	$+1'.5$	$+7'.1$	$-0''.004$	$\pm0''.010$
2........	bb	$+2.6$	$+5.1$	-0.011	0.009
3........	f	$+4.0$	$+0.8$	$+0.008$	0.013
4........	f	$+7.4$	-3.3	$+0.008$	0.007
5........	bf	-0.1	-8.5	-0.013	0.010
6........	f	-1.6	-5.9	-0.022	0.011
7........	bf	-6.5	-5.1	$+0.024$	0.006
8........	f	-1.4	-1.9	$+0.011$	0.006
9........	bf	-5.5	$+7.0$	-0.012	0.007
10........	b	-0.1	$+7.8$	$+0.012$	±0.008

Boss 1629 $\alpha=6^h22^m8^s$ $\delta=+30°33'$

Pl. No.	Date			t	Obs.	Qy	p	m	Remarks
1687_1..	1918	Feb.	2	$+5°.2$	vM	g	-0.610	$+3.09$	
1687_2..			2	$+9.5$	H	fg	-0.610	$+3.09$	Trail
1737...		Mar.	4	$+1.0$	vM	fg	-0.911	$+3.17$	Hazy, 25^m exp.
2007_1..		Oct.	28	$+4.2$	vM	fg	$+0.860$	$+3.83$	
2007_2..			28	$+9.2$	H	fg	$+0.860$	$+3.83$	
2008...			28	$+13.2$	vM	fg	$+0.860$	$+3.83$	
2019_1..			29	$+1.5$	vM	fg	$+0.852$	$+3.83$	
2019_2..			29	$+5.7$	H	gas	$+0.852$	$+3.83$	
2033_1..		Nov.	10	-4.2	H	fg	$+0.724$	$+3.86$	
2033_2..			10	0.0	vM	fg	$+0.724$	$+3.86$	
2156_1..	1919	Feb.	21	$+6.5$	vM	g	-0.830	$+4.15$	
2156_2..			21	$+11.7$	H	g	-0.830	$+4.15$	
2167...		Mar.	24	$+12.0$	vM	fg	-0.997	$+4.23$	
2181...			25	$+13.5$	vM	fg	-0.997	$+4.23$	

Mor.-Ev.	Δp	Δm	M	v	Δt	Remarks
2033_1–1737.......	$+1.64$	$+0.69$	$+5$	-9	$-5°.2$	
2033_2–1687_1......	$+1.33$	$+0.77$	$+18$	$+5$	-5.2	
2019_1–2156_1......	$+1.68$	-0.32	-10	-12	-5.0	
2007_1–1687_2......	$+1.47$	$+0.74$	$+16$	$+3$	-5.3	
2019_2–2156_2......	$+1.68$	-0.32	$+29$	$+27$	-6.0	
2007_2–2167.......	$+1.86$	-0.40	-14	-17	-2.8	
2008 –2181.......	$+1.86$	-0.40	$+8$	$+5$	-0.3	Star 4 not measured

$$+2.14\,\mu_\alpha+0.68\,\pi=+26 \qquad \pi=+3.6=+0''.006\pm0''.004$$
$$+0.68\,\mu_\alpha+19.18\,\pi=+77 \qquad \mu_\alpha=+11.0=+0''.018\pm0''.012$$

Comp. Star	Br.	x	y	π	P.E.
1.........	f	$+2'.7$	$+2'.7$	$-0''.011$	$\pm0''.005$
2.........	f	$+6.3$	$+1.2$	-0.009	0.004
3.........	bf	$+6.2$	-2.3	-0.004	0.008
4.........	f	$+3.4$	-3.4	$+0.044$	0.014
5.........	bf	-3.2	-4.9	-0.027	0.006
6.........	f	-5.9	0.0	$+0.001$	0.006
7.........	bf	-4.1	$+1.0$	$+0.012$	0.006
8.........	bf	-3.4	$+1.6$	$+0.011$	0.007
9.........	f	-1.1	$+2.7$	-0.006	±0.008

Boss 1846 $\alpha = 7^h5^m36^s$ $\delta = +51°36'$

Pl. No.	Date	t	Obs.	Qy	p	m	Remarks
1135_1..	1916 Oct. 21	−10°5	vM	f	+0.961	+1.81	20^m exp.
1135_2..	21	− 3.5	H	fg	+0.961	+1.81	20^m exp.
1155...	Nov. 16	− 4.5	vM	g	+0.760	+1.88	
1156...	16	0.0	H	fg	+0.760	+1.88	
1290_1..	1917 Mar. 15	− 1.5	H	fg	−0.927	+2.21	
1290_2..	15	+ 2.5	vM	fg	−0.927	+2.21	
1291_1..	15	+ 7.7	H	g	−0.927	+2.21	
1291_2..	15	+12.0	vM	g	−0.927	+2.21	
1304_1..	16	− 5.2	vM	fg	−0.933	+2.21	
1304_2..	16	− 1.0	H	fg	−0.933	+2.21	
1646_1..	Dec. 8	− 5.2	vM	g	+0.469	+2.94	
1646_2..	8	− 0.5	H	g	+0.469	+2.94	
2035...	1918 Nov. 10	+13.7	H	fg	+0.825	+3.86	Trail
2049...	11	+11.7	H	fg	+0.816	+3.87	
2157...	1919 Feb. 21	+ 6.7	vM	g	−0.719	+4.15	
2190...	Mar. 26	+ 5.5	vM	fg	−0.975	+4.24	Hazy, 20^m exp.

Mor.-Ev.	Δp	Δm	M	v	Δt
1135_1-1304_1...	+1.89	−0.40	+ 7	− 2	−5°3
1646_1-1290_1...	+1.40	+0.73	+24	+17	−3.7
$1155-1304_2$...	+1.69	−0.33	− 7	−15	−3.5
1135_2-2190....	+1.94	−2.43	+16	+ 7	−9.0
1646_2-1290_2...	+1.40	+0.73	+13	+ 6	−3.0
$1156-2157$....	+1.48	−2.27	+ 5	− 1	−6.7
$2049-1291_1$...	+1.74	+1.66	− 3	−12	+4.0
$2035-1291_2$...	+1.75	+1.65	+15	+ 6	+1.7

$$+17.86\,\mu_\alpha - 1.57\,\pi = -4 \qquad \pi = +5.0 = +0\overset{''}{.}008 \pm 0\overset{''}{.}003$$
$$-1.57\,\mu_\alpha + 22.39\,\pi = +112 \qquad \mu_\alpha = +0.2 = 0\overset{''}{.}000 \pm 0\overset{''}{.}003$$

Comp. Star	Br.	x	y	π	P.E.
1.........	ff	+2′3	+1′5	+0″018	±0″010
2.........	f	+7.4	+3.7	+0.005	0.005
3.........	f	+4.5	−2.1	+0.002	0.005
4.........	bf	+2.3	−1.6	−0.026	0.010
5.........	ff	−3.7	−2.5	+0.010	0.007
6.........	f	−3.2	−0.1	+0.007	0.006
7.........	b	−6.0	−0.5	+0.005	0.006
8.........	bf	−2.7	+2.7	−0.022	±0.005

Boss 2663 $\alpha=9^h51^m8^s$ $\delta=+9°24'$

Pl. No.	Date			*t*	Obs.	Qy	*p*	*m*	Remarks
811_1..	1916	Jan.	12	− 5°2	vM	fg	+0.514	+1.04	
811_2..			12	− 0.5	vM	fg	+0.514	+1.04	Clouds
870_1..		Mar.	26	+ 8.7	vM	g	−0.611	+1.24	
870_2..			26	+13.0	H	g	−0.611	+1.24	Trail
1203...		Dec.	16	+13.0	H	fg	+0.806	+1.96	
1222...			17	+ 4.7	H	fg	+0.798	+1.96	
1223...			17	+ 9.0	vM	fg	+0.798	+1.96	
1319_1..	1917	Apr.	12	− 9.5	H	g	−0.791	+2.28	
1219_2..			12	− 5.0	vM	fg	−0.791	+2.28	
1651_1..		Dec.	8	+ 2.5	H	gas	+0.863	+2.94	
1651_2..			8	+ 6.7	vM	fg	+0.863	+2.94	
1747...	1918	Apr.	4	− 2.7	vM	g	−0.710	+3.26	Clouds, 22^m exp.
2076...		Dec.	26	− 6.0	H	f	+0.718	+3.99	25^m exp.
2172_1..	1919	Mar.	24	+ 7.2	vM	fg	−0.577	+4.23	
2172_2..			24	+12.7	Hum	g	−0.577	+4.23	
2185...			25	− 2.0	vM	g	−0.589	+4.23	

Mor.-Ev.	Δ*p*	Δ*m*	M	*v*	Δ*t*
2076 −1747....	+1.43	+0.73	− 2	+14	−3°3
811_1−1319_1...	+1.31	−1.24	+ 58	+11	+4.3
811_2−2185....	+1.10	−3.19	+102	− 6	+1.5
1651_1−1319_2...	+1.65	+0.66	− 44	−31	+7.5
1222 −2172_1...	+1.38	−2.27	+ 54	−26	−2.5
1651_2−2172_2...	+1.44	−1.29	+ 88	+40	−6.0
1223 − 870_1...	+1.41	+0 72	− 8	+ 8	+0.3
1203 − 870_2...	+1.42	+0.72	− 23	− 7	0.0

$$+20.54\,\mu_\alpha - 5.95\,\pi = -687 \qquad \pi = +5.1 = +0''.008 \pm 0''.007$$
$$-5.95\,\mu_\alpha + 15.67\,\pi = +270 \qquad \mu_\alpha = -32.0 = -0''.052 \pm 0''.006$$

Comp. Star	Br.	*x*	*y*	π	P.E.
1.........	bf	+0′3	+5′5	−0″037	±0″009
2.........	ff	+2.5	+4.8	+0.006	0.007
3.........	b	+5.2	−1.1	+0.002	0.008
4.........	f	+2.6	−3.2	+0.016	0.006
5.........	bf	+4.4	−5.5	−0.009	0.006
6.........	f	−1.4	−6.7	+0.008	0.008
7.........	ff	−4.5	−4.8	−0.019	0.011
8.........	bf	−3.0	+4.3	+0.020	0.006
9.........	f	−3.2	+5.4	+0.012	±0.004

Boss 2800 $\alpha = 10^h 26^m 52^s$ $\delta = +14^\circ 39'$

Pl. No.	Date			t	Obs.	Qy	p	m	Remarks
1765_1..	1918	May	3	+ 8°.0	vM	fg	−0.868	+3.34	
1765_2..			3	+12.0	H	fg	−0.868	+3.34	
1780...			4	+ 9.7	H	fg	−0.876	+3.34	Hazy, 25^m exp.
2070_1..		Dec.	10	−11.0	vM	g	+0.889	+3.95	
2070_2..			10	− 7.0	H	fg	+0.889	+3.95	
2077...			26	+ 0.2	H	f	+0.793	+3.99	25^m exp.
2091_1..			27	−16.0	vM	fg	+0.785	+3.99	
2091_2..			27	−11.5	H	g	+0.785	+3.99	
2120_1..	1919	Jan.	23	+ 3.5	vM	g	+0.482	+4.07	
2120_2..			23	+ 7.5	H	fg	+0.482	+4.07	
2206...		Apr.	22	−10.0	vM	g	−0.782	+4.31	Clouds, 25^m exp.
2211...			23	−11.0	vM	f	−0.792	+4.31	
2212_1..			23	− 5.7	H	fg	−0.792	+4.31	
2212_2..			23	0.0	vM	f	−0.792	+4.31	Trail, clouds, 23^m exp.

Mor.-Ev.	Δp	Δm	M	v	Δt
2091_1–2211....	+1,58	−0.32	+ 7	+ 4	−5°.0
2091_2–2206....	+1.57	−0.32	− 7	−10	−1.5
2070_1–2212_1...	+1.68	−0.36	+13	+10	−5.3
2070_2–2212_2...	+1.68	−0.36	+ 4	+ 1	−7.0
2077 –1765_1...	+1.66	+0.65	−16	−19	−7.8
2120_1–1780....	+1.36	+0.73	+18	+15	−6.2
2120_2–1765_2...	+1.35	+0.73	+ 5	+ 2	−4.5

$$+1.95\,\mu_\alpha + 0.84\,\pi = +1 \qquad \pi = +2.0 = +0''.003 \pm 0''.003$$
$$+0.84\,\mu_\alpha + 17.03\,\pi = +33 \qquad \mu_\alpha = -0.3 = 0''.000 \pm 0''.010$$

Comp. Star	Br.	x	y	π	P.E.
1.........	f	+4′.8	+1′.1	−0″.015	±0″.012
2.........	ff	+6.3	+1.4	+0.014	0.014
3.........	bf	+1.9	−6.5	−0.008	0.005
4.........	bf	−6.7	−6.0	+0.003	0.005
5.........	ff	−5.6	+3.6	−0.011	0.009
6.........	f	−1.9	+2.5	+0.028	0.015
7.........	f	−1.2	+5.4	−0.012	±0.005

Boss 2915 $\alpha = 10^h 50^m 50^s$ $\delta = +6°43'$

Pl. No.	Date	t	Obs.	Qy	p	m	Remarks
1252_1..	1917 Jan. 29	−10°.5	vM	fg	+0.466	+2.08	
1252_2..	29	− 6.5	vM	fg	+0.465	+2.08	
1321_1..	Apr. 12	− 2.5	vM	g	−0.611	+2.28	
1321_2..	12	+ 1.7	H	fg	−0.611	+2.28	
1335_1..	13	− 0.2	H	fg	−0.624	+2.28	
1335_2..	13	+ 4.0	vM	g	−0.624	+2.28	
1349...	May 12	+ 7.0	vM	gas	−0.882	+2.36	
1668_1..	1918 Jan. 5	+ 4.5	vM	g	+0.754	+3.02	
1668_2..	5	+ 9.2	H	g	+0.754	+3.02	
1680...	6	+ 2.0	H	fg	+0.745	+3.02	Clouds, 25^m exp.
1692_1..	Feb. 2	− 8.7	H	g	+0.424	+3.09	
1692_2..	2	− 4.5	vM	g	+0.423	+3.09	
1693...	2	+ 1.0	H	fg	+0.423	+3.09	
1742...	Apr. 3	− 5.2	vM	pf	−0.493	+3.26	
1748...	4	− 3.0	H	g	−0.506	+3.26	Clouds, 23^m exp. Trail of β Leonis
1764...	May 3	− 3.7	H	fg	−0.820	+3.34	

Mor.-Ev.	Δp	Δm	M	v	Δt
1252_1–1742....	+0.96	−1.18	−23	+ 8	−5°.3
1692_1–1764....	+1.24	−0.25	−37	−27	−5.0
1252_2–1321_1...	+1.08	−0.20	− 1	+ 8	−4.0
1692_2–1748....	+0.93	−0.17	−10	− 3	−1.5
1693 −1335_1...	+1.05	+0.81	+ 1	−15	+1.2
1680 −1321_2...	+1.36	+0.74	+17	+ 4	+0.3
1668_1–1335_2...	+1.38	+0.74	+29	+16	+0.5
1668_2–1349....	+1.64	+0.66	+14	− 4	+2.2

$+3.72\,\mu_a + 2.14\,\pi = +82$ $\pi = -3.5 = -0''.006 \pm 0''.005$

$+2.14\,\mu_a + 12.03\,\pi = +9$ $\mu_a = +24.1 = +0''.039 \pm 0''.009$

Comp. Star	Br.	x	y	π	P.E.
1.........	f	+1'.4	+4'.9	−0''.012	±0''.018
2.........	bf	+7.6	+2.6	+0.017	0.010
3.........	f	+8.0	−2.1	−0.019	0.009
4.........	f	+2.2	−2.9	+0.014	0.012
5.........	bf	−6.9	−5.9	+0.003	0.011
6.........	f	−4.8	+0.1	−0.022	0.014
7.........	ff	−5.6	+0.1	+0.007	0.013
9.........	ff	−2.7	+2.6	+0.014	±0.022

Boss 3141 $\alpha = 11^h 56^m 32^s$ $\delta = +36°36'$

Pl. No.	Date	t	Obs.	Qy	p	m	Remarks
1204...	1916 Dec. 16	−11°0	vM	fg	+0.900	+1.96	
1277...	1917 Feb. 13	− 9.0	H	fg	+0.508	+2.12	20^m exp.
1336_1..	Apr. 13	− 6.0	H	g	−0.381	+2.28	
1336_2..	13	− 1.0	vM	g	−0.381	+2.28	
1350_1..	May 12	− 2.5	H	g	−0.737	+2.36	
1350_2..	12	+ 1.5	vM	fg	−0.738	+2.36	
1363_1..	13	− 7.0	vM	fg	−0.747	+2.37	
1363_2..	13	− 3.0	vM	fg	−0.747	+2.37	
1669_1..	1918 Jan. 5	− 1.0	vM	fg	+0.866	+3.02	
1669_2..	5	+ 3.2	H	gas	+0.866	+3.02	
1694_1..	Feb. 2	− 9.0	vM	g	+0.646	+3.09	
1694_2..	2	− 4.7	H	fg	+0.644	+3.09	
1715...	3	+ 0.5	H	fg	+0.634	+3.10	Hazy, 20^m exp.
1766..	May 3	− 5.0	vM	fg	−0.629	+3.34	Trail

Mor.-Ev.	Δp	Δm	M	v	Δt
1204 −1363_1...	+1.65	−0.41	+60	+11	−4°0
1277 −1336_1...	+0.89	−0.16	+33	+ 8	−3.0
1694_1−1766....	+1.28	−0.25	+ 5	−31	−4.0
1694_2−1363_2...	+1.39	+0.72	− 6	−10	−1.7
1669_1−1350_1...	+1.60	+0.66	+28	+17	+1.5
1715 −1336_2...	+1.02	+0.82	−19	−12	+1.5
1669_2−1350_2...	+1.60	+0.66	+18	+ 7	+1.7

$+2.33\,\mu_\alpha + 2.82\,\pi = -21$ $\pi = +21.0 = +0''.034 \pm 0''.006$

$+2.82\,\mu_\alpha + 13.24\,\pi = +181$ $\mu_\alpha = -34.4 = -0''.056 \pm 0''.016$

Comp. Star	Br.	x	y	π	P.E.
1.........	bf	+4′7	+4′7	+0″005	±0″005
2.........	f	+5.1	−3.2	−0.002	0.006
3.........	f	+1.8	−5.2	−0.010	0.008
4.........	ff	−3.6	−1.8	+0.016	0.009
5.........	bf	−0.8	+2.2	+0.009	0.010
6.........	ff	−4.3	+3.8	−0.019	±0.009

Boss 3581 $\alpha = 13^h 46^m 44^s$ $\delta = +35°10'$

Pl. No.	Date			t	Obs.	Qy	p	m	Remarks
1280...	1917	Feb.	13	$-9°.5$	vM	f	$+0.828$	$+2.12$	Clouds, 25^m exp.
1718...	1918	Feb.	3	-5.5	vM	fg	$+0.885$	$+3.10$	Hazy, 20^m exp.
1734...		Mar.	3	-0.5	vM	fg	$+0.664$	$+3.17$	Hazy, 25^m exp.
1735...			3	$+7.5$	Hum	fg	$+0.664$	$+3.17$	Hazy, 25^m exp.
1786_1..		May	31	$+2.5$	H	gas	-0.623	$+3.42$	
1786_2..			31	$+6.5$	vM	gas	-0.623	$+3.42$	Trail
1799_1..		June	1	-8.2	H	fg	-0.634	$+3.42$	
1799_2..			1	-4.0	vM	fg	-0.634	$+3.42$	
1800_1..			1	$+1.2$	H	fg	-0.634	$+3.42$	
1800_2..			1	$+5.5$	vM	g	-0.634	$+3.42$	
1812_1..			2	-13.0	vM	g	-0.644	$+3.42$	
1812_2..			2	-8.7	H	g	-0.644	$+3.42$	
2123...	1919	Jan.	23	-15.0	vM	fg	$+0.915$	$+4.07$	
2143_1..			25	-8.0	Hum	fg	$+0.912$	$+4.07$	
2143_2..			25	-3.7	vM	fg	$+0.912$	$+4.07$	
2144...			25	$+0.7$	Hum	fg	$+0.912$	$+4.07$	

Mor.-Ev.	Δp	Δm	M	v	Δt
$2123-1812_1$...	$+1.56$	$+0.65$	$+3$	-4	$-2°.0$
$1280-1812_2$...	$+1.47$	-1.30	$+5$	-10	-0.8
2143_1-1799_1...	$+1.55$	$+0.65$	0	-6	$+0.2$
$1718-1799_2$...	$+1.52$	-0.32	$+27$	$+16$	-1.5
2143_2-1800_1...	$+1.55$	$+0.65$	-10	-16	-4.9
$1734-1786_1$...	$+1.29$	-0.25	$+27$	$+18$	-3.0
$2144-1800_2$...	$+1.55$	$+0.65$	$+22$	$+16$	-4.8
$1735-1786_2$...	$+1.29$	-0.25	-4	-13	$+1.0$

$$+3.59\,\mu_a + 1.00\,\pi = -12 \qquad \pi = +6.1 = +0''.010 \pm 0''.004$$

$$+1.00\,\mu_a + 17.42\,\pi = +101 \qquad \mu_a = -5.0 = -0''.008 \pm 0''.009$$

Comp. Star	Br.	x	y	π	P.E.
1.........	bb	$+2'.5$	$+1'.2$	$+0''.031$	$\pm 0''.011$
2.........	b	$+3.3$	$+1.4$	$+0.022$	0.008
3.........	f	$+6.7$	$+2.5$	-0.027	0.010
4.........	f	-0.1	-3.0	-0.016	0.006
5.........	f	-8.0	-1.5	-0.013	0.007
6.........	f	-4.7	-0.4	$+0.019$	0.005
7.........	f	-1.1	$+3.2$	-0.017	± 0.007

Boss 3983, 3986 = Bu 7362 $\alpha = 15^h34^m59^s$ and $15^h35^m12^s$ $\delta = +80^\circ 47'$

Pl. No.	Date	t	Obs.	Qy	p	m	Remarks
844_1	1916 Mar. 24	$-7^{\circ}.0$	vM	f	$+0.757$	$+1.23$	
844_2	24	-2.2	H	f	$+0.757$	$+1.23$	
981_1	June 23	$+5.0$	vM	g	-0.589	$+1.48$	
981_2	23	$+9.5$	H	g	-0.589	$+1.48$	Trail
994_1	24	$+1.5$	H	g	-0.601	$+1.48$	
994_2	24	$+6.0$	vM	g	-0.603	$+1.48$	
1326_1	1917 Apr. 12	-11.0	vM	fg	$+0.529$	$+2.28$	
1326_2	12	-7.0	H	fg	$+0.527$	$+2.28$	
1343_1	13	$+6.0$	H	fg	$+0.512$	$+2.28$	
1343_2	13	$+10.5$	vM	fg	$+0.512$	$+2.28$	
1391	June 11	$+4.7$	H	fg	-0.416	$+2.45$	
1417_1	13	-12.5	vM	g	-0.445	$+2.45$	
1417_2	13	-8.2	H	fg	-0.445	$+2.45$	
1418	13	-3.0	vM	g	-0.445	$+2.45$	
2179	1919 Mar. 24	$+8.5$	Hum	f	$+0.763$	$+4.23$	20^m exp.
2202	Apr. 21	$+11.5$	H	fg	$+0.405$	$+4.31$	

Mor.-Ev.	Δp	Δm	M (3983)	M (3986)	v (3983)	v (3986)	Δt
1326_1-1417_1	$+0.97$	-0.17	$+66$	$+36$	$+38$	-7	$+1^{\circ}.5$
844_1-1417_2	$+1.20$	-1.22	$+144$	$+184$	-19	-8	$+1.2$
1326_2-1418	$+0.97$	-0.17	$+24$	$+34$	-4	-9	-4.0
844_2-994_1	$+1.36$	-0.25	$+38$	$+51$	-3	-10	-3.7
1343_1-981_1	$+1.10$	$+0.80$	-90	-106	$+5$	-26	$+1.0$
$2179-1391$	$+1.18$	$+1.78$	-150	-144	$+68$	$+79$	$+3.8$
1343_2-994_2	$+1.12$	$+0.80$	-147	-75	-52	$+14$	$+4.5$
$2202-981_2$	$+0.99$	$+2.83$	-389	-429	-35	-56	$+2.0$

$$\left.\begin{array}{l} +14.07\,\mu_a + 4.55\,\pi = -1759 \\ +\ 4.55\,\mu_a + 10.00\,\pi = -\ 514 \end{array}\right\} (3983) \qquad \left.\begin{array}{r} -1864 \\ -\ 438 \end{array}\right\} (3986)$$

$$(3983)\begin{cases} \pi = +\ 6.4 = +0''.010 \pm 0''.016 \\ \mu_a = -127.1 = -0''.207 \pm 0''.013 \end{cases} \qquad (3986)\begin{cases} \pi = +\ 19.3 = +0''.031 \pm 0''.016 \\ \mu_a = -138.4 = -0''.226 \pm 0''.013 \end{cases}$$

Comp. Star	Br.	x	y	π	P.E.
1	f	$+7'.6$	$+0'.1$	$-0''.053$	$\pm 0''.013$
2	f	$+6.6$	-3.2	$+0.052$	0.014
3	bf	$+2.6$	-0.4	-0.008	0.015
4	f	-5.1	-2.2	-0.029	0.005
5	f	-5.6	$+1.6$	$+0.009$	0.009
6	ff	-2.3	$+0.8$	-0.001	0.011
7	f	-0.4	$+3.3$	$+0.029$	± 0.017

Boss 4195 $\alpha = 16^h 23^m 28^s$ $\delta = +0°53'$

Pl. No.	Date			t	Obs.	Qy	p	m	Remarks
905_1..	1916	Apr.	23	−12.°5	vM	fg	+0.555	+1.31	
905_2..			23	− 8.2	H	fg	+0.554	+1.31	
920_1..			24	−15.5	vM	g	+0.541	+1.32	
920_2..			24	−11.5	H	fg	+0.541	+1.32	
1429_1..	1917	June	26	−13.7	vM	g	−0.457	+2.49	
1429_2..			26	− 9.2	H	fg	−0.457	+2.49	
1443_1..			27	− 3.0	H	g	−0.473	+2.49	
1443_2..			27	+ 2.0	vM	fg	−0.473	+2.49	
1453...		July	11	−12.5	vM	fg	−0.663	+2.53	
1486...		Aug.	10	+13.2	vM	g	−0.942	+2.61	
1495...			11	+13.0	vM	g	−0.946	+2.61	
1512...			12	+13.5	vM	g	−0.952	+2.62	
1758...	1918	May	2	+ 4.0	vM	gas	+0.432	+3.34	Hazy, 20^m exp.
1759...			2	+10.0	H	gas	+0.432	+3.34	Hazy, 20^m exp. Trail
1775_1..			3	+ 6.2	H	fg	+0.417	+3.34	
1775_2..			3	+10.5	vM	g	+0.417	+3.34	

Mor.-Ev.	Δp	Δm	M	v	Δt
920_1–1429_1...	+1.00	−1.17	− 3	−16	−1.°8
905_1–1453....	+1.22	−1.22	+20	+ 5	0.0
920_2–1429_2...	+1.00	−1.17	− 1	−14	−2.3
905_2–1443_1...	+1.03	−1.18	+45	+32	−5.2
1758 –1443_2...	+0.91	+0.85	+35	+30	+2.0
1775_1–1495....	+1.36	+0.73	−14	−23	−6.8
1759 –1486....	+1.37	+0.73	+ 5	+ 4	−3.2
1775_2–1512....	+1.37	+0.72	+10	− 1	−3.0

$+7.92\,\mu_\alpha - 1.30\,\pi = -41$ $\pi = +8.6 = +0''.014 \pm 0''.007$

$-1.30\,\mu_\alpha + 10.99\,\pi = +100$ $\mu_\alpha = -3.8 = -0''.006 \pm 0''.009$

Comp. Star	Br.	x	y	π	P.E.
1........	f	+0′.8	+0′.1	−0″.014	±0″.013
2........	f	+1.1	+1.0	+0.007	0.010
3........	bf	+2.9	+1.2	+0.009	0.009
4........	ff	+1.5	−0.4	−0.016	0.014
5........	f	+1.9	−1.0	+0.013	0.007
6........	ff	+0.3	−3.7	−0.012	0.015
7........	bf	−1.4	−1.8	+0.009	0.014
8........	f	−1.6	−1.4	+0.012	0.009
9........	f	−2.6	−1.0	−0.008	0.007
10........	f	−3.6	+2.1	+0.005	0.008
11........	f	+0.1	+4.8	−0.006	±0.006

Anonymous 4 $\alpha=17^h52^m54^s$ $\delta=+4°28'$ ($\mu=10''$, Barnard)

Pl. No.	Date			t	Obs.	Qy	p	m	Remarks
1118...	1916	Sept.	21	+26°5	H	gas	−1.002	+1.73	
1359_1..	1917	May	12	− 8.7	H	g	+0.602	+2.36	
1359_2..			12	− 4.0	vM	fg	+0.602	+2.36	
1373_1..			13	−11.5	vM	fg	+0.588	+2.37	
1373_2..			13	− 7.2	vM	fg	+0.588	+2.37	
1387...			14	+20.0	Pt	fg	+0.572	+2.37	20^m exp.
1469...		July	28	− 9.7	vM	fg	−0.610	+2.58	
1470...			28	− 4.7	H	fg	−0.610	+2.58	
1471...			28	+ 1.2	vM	fg	−0.610	+2.58	
1476...			29	−13.2	H	g	−0.622	+2.58	
1477...			29	− 9.0	vM	g	−0.623	+2.58	
1478...			29	− 2.7	H	fg	−0.623	+2.58	Trail of Boss 4545
1487_1..		Aug.	10	− 3.0	H	g	−0.769	+2.61	
1487_2..			10	+ 1.0	vM	g	−0.769	+2.61	
1760_1..	1918	May	2	− 4.7	vM	fg	+0.731	+3.34	
1760_2..			2	− 0.5	H	fg	+0.731	+3.34	
1776_1..			3	− 5.5	H	fg	+0.720	+3.34	
1776_2..			3	− 1.5	vM	fg	+0.720	+3.34	

Mor.-Ev.	Δp	Δm	M	v	Δt
1387−1118....	+1.57	+0.64	+215	+ 1	−6°5
1373_1−1476....	+1.21	−0.21	+484	+ 5	+1.7
1359_1−1469....	+1.21	−0.22	+494	+11	+1.0
1373_2−1470....	+1.20	−0.21	+458	−18	−2.5
1359_2−1478....	+1.23	−0.22	+492	+ 2	−1.3
1776_1−1477....	+1.34	+0.76	+113	+25	+3.5
1760_1−1487_1...	+1.50	+0.73	+146	− 6	−1.7
1776_2−1487_2...	+1.49	+0.73	+152	+ 4	−2.5
1760_2−1471....	+1.34	+0.76	+ 62	−26	−1.7

$$+2.82\,\mu_\alpha+4.18\,\pi=+73 \qquad \pi=+318.4=+0''.519\pm0''.006$$
$$+4.18\,\mu_\alpha+16.41\,\pi=+3356 \qquad \mu_\alpha=-446.7=-0''.728\pm0''.014$$

Comp. Star	Br.	x	y	π	P.E.
1.........	bf	+0′.7	+4′.0	+0″.021	±0″.018
2.........	f	+2.2	+2.5	−0.017	0.016
3.........	bf	+1.2	+0.1	+0.016	0.015
4.........	f	+1.1	−0.1	−0.007	0.010
5.........	f	+3.0	−1.9	+0.006	0.010
6.........	bf	0.0	−3.2	−0.010	0.012
7.........	f	−5.2	−4.1	+0.007	0.007
8.........	bf	−2.6	+2.9	−0.015	±0.012

Boss 4817=Bu 8936 $\alpha=18^h53^m48^s$ $\delta=+17°14'$

Pl. No.	Date			t	Obs.	Qy	p	m	Remarks
683...	1915	Sept.	2	$-10°5$	vM	f	-0.843	$+0.67$	Clouds, 20^m exp.
684_1..			2	-5.0	H	fg	-0.843	$+0.67$	
684_2..			2	-1.0	vM	fg	-0.843	$+0.67$	
685...			2	$+4.2$	H	fg	-0.843	$+0.67$	
1761_1..	1918	May	2	-9.0	vM	fg	$+0.871$	$+3.34$	
1761_2..			2	-5.0	H	fg	$+0.871$	$+3.34$	
1762...			2	0.0	vM	f	$+0.871$	$+3.34$	
1777_1..			3	-10.5	H	fg	$+0.863$	$+3.34$	
1777_2..			3	-6.2	vM	fg	$+0.863$	$+3.34$	
1778...			3	-1.5	H	fg	$+0.863$	$+3.34$	Trail
1793_1..			31	-8.2	H	g	$+0.541$	$+3.42$	
1793_2..			31	-4.0	vM	g	$+0.541$	$+3.42$	
1844_1..		Aug.	11	-6.5	Hum	fg	-0.596	$+3.61$	
1844_2..			11	-2.0	vM	fg	-0.596	$+3.61$	
1857_1..			12	-3.2	vM	g	-0.609	$+3.62$	
1857_2..			12	$+1.0$	Hum	g	-0.610	$+3.62$	

Mor.-Ev.	Δp	Δm	M	v	Δt
1777_1-683....	$+1.71$	$+2.67$	$+26$	$+4$	$0°0$
1761_1-1844_1...	$+1.47$	-0.27	$+8$	$+11$	-2.5
1793_1-684_1...	$+1.38$	$+2.75$	$+11$	-13	-3.2
1777_2-1857_1...	$+1.47$	-0.28	$+5$	$+9$	-3.0
1761_2-1844_2...	$+1.47$	-0.27	-7	-4	-3.0
1793_2-684_2...	$+1.38$	$+2.75$	$+38$	$+14$	-3.0
$1778-1857_2$...	$+1.47$	-0.28	-20	-16	-2.5
$1762-685$....	$+1.71$	$+2.67$	$+17$	-5	-4.2

$$+29.68\,\mu_a+15.11\,\pi=+254 \qquad \pi=-0.9=-0''.001\pm0''.004$$
$$+15.11\,\mu_a+18.28\,\pi=+120 \qquad \mu_a=+9.0=+0''.015\pm0''.003$$

The 11^M7 companion, being covered by the sector, does not show any images on the plates.

Comp. Star	Br.	x	y	π	P.E.
1.........	b	$+3'.0$	$+2'.7$	$-0''.007$	$\pm0''.006$
2.........	f	$+3.3$	$+1.5$	$+0.005$	0.004
3.........	bf	$+4.8$	-2.3	$+0.004$	0.009
4.........	f	$+1.1$	-3.8	$+0.002$	0.014
5.........	f	-1.6	-4.9	$+0.002$	0.005
6.........	f	-4.8	-2.3	-0.010	0.008
7.........	b	-4.8	$+2.7$	$+0.013$	0.004
8.........	bf	-1.1	$+3.3$	-0.009	±0.009

N.G.C. 6804 $\alpha=19^h26^m48^s$ $\delta=+9°1'$

Pl. No.	Date	t	Obs.	Qy	p	m	Remarks
1423...	1917 June 13	−12.°0	vM	g	+0.465	+2.45	20^m exp.
1538...	Sept. 13	− 6.2	vM	fg	−0.864	+2.70	Hazy, 30^m exp.
1539...	13	+ 2.7	H	fg	−0.864	+2.70	Hazy, 30^m exp.
1551...	14	− 7.0	vM	g	−0.873	+2.71	
1552...	14	+ 1.0	H	g	−0.873	+2.71	
1807...	1918 June 1	−15.7	H	fg	+0.633	+3.42	
1808...	1	− 9.0	vM	g	+0.633	+3.42	
1816...	2	−12.2	H	fg	+0.621	+3.42	
1817...	2	− 5.5	vM	fg	+0.621	+3.42	
1818...	2	+ 3.2	H	g	+0.621	+3.42	
1824...	3	−12.5	Hum	fg	+0.608	+3.42	Hazy, 40^m exp.
1825...	3	− 2.0	vM	g	+0.608	+3.42	Hazy, 40^m exp.
1826...	3	+10.7	Hum	fg	+0.608	+3.42	Hazy, 35^m exp.
1845...	Aug. 11	− 3.0	Hum	g	−0.477	+3.61	Trail of Boss 4995
1846...	11	+ 6.2	vM	vg	−0.477	+3.61	
1883...	Sept. 2	− 7.5	Hum	g	−0.761	+3.67	
1896...	3	−13.5	vM	g	−0.771	+3.68	
1906...	4	−12.5	vM	g	−0.781	+3.68	

Mor.-Ev.	Δp	Δm	M	v	Δt
1423–1906....	+1.25	−1.23	+19	0	+0.°5
1807–1896....	+1.40	−0.26	+16	− 3	−2.2
1824–1883....	+1.37	−0.25	+20	+ 2	−5.0
1816–1551....	+1.49	+0.71	+ 9	− 8	−5.2
1808–1538....	+1.50	+0.72	+10	− 7	−2.8
1817–1845....	+1.10	−0.19	+29	+14	−2.5
1825–1552....	+1.48	+0.71	+18	+ 1	−3.0
1818–1539....	+1.49	+0.72	+30	+13	+0.5
1826–1846....	+1.09	−0.19	− 1	−16	+4.5

$+3.76\,\mu_\alpha+1.60\,\pi=+10$ $\qquad\pi=+12.5=+0.''020\pm0.''003$

$+1.60\,\mu_\alpha+16.68\,\pi=+204$ $\qquad\mu_\alpha=-2.7=-0.''004\pm0.''006$

Comp. Star	Br.	x	y	π	P.E.
1.........	bf	+2.′6	+2.′7	+0.″003	±0.″008
2.........	f	+2.6	+0.7	−0.008	0.006
3.........	bf	+1.6	−4.8	0.000	0.002
4.........	ff	+0.8	−1.6	0.000	0.007
5.........	f	−0.7	−1.0	+0.005	0.007
6.........	f	−3.8	−2.2	+0.002	0.007
7.........	f	−2.6	+1.5	−0.007	0.008
8.........	f	−0.8	+4.8	+0.003	±0.004

N.G.C. 6905 $\alpha = 20^h 17^m 56^s$ $\delta = +19°47'$

Pl. No.	Date	t	Obs.	Qy	p	m	Remarks
1448	1917 June 27	−14°0	vM	g	+0.439	+2.49	
1553_1	Sept. 14	− 4.0	vM	g	−0.743	+2.71	
1553_2	14	+ 1.2	H	fg	−0.743	+2.71	
1562	Oct. 8	− 2.2	vM	g	−0.930	+2.77	
1578	9	− 4.5	vM	g	−0.933	+2.78	
1794	1918 May 31	−18.2	H	g	+0.781	+3.42	
1795	31	−12.5	vM	fg	+0.781	+3.42	
1809	June 1	−13.5	H	g	+0.772	+3.42	
1810	1	− 8.0	vM	fg	+0.772	+3.42	
1811	1	− 1.7	H	fg	+0.772	+3.42	Trail of Boss 5224
1832_1	July 1	−10.0	vM	g	+0.383	+3.50	
1832_2	1	− 3.5	Hum	g	+0.383	+3.50	
1839	2	− 1.0	vM	fg	+0.367	+3.50	
1884_1	Sept. 2	−12.0	vM	fg	−0.598	+3.67	
1884_2	2	− 6.7	Hum	g	−0.598	+3.67	
1897_1	3	−18.0	Hum	fg	−0.611	+3.68	
1897_2	3	−12.5	vM	fg	−0.611	+3.68	
1907	4	−18.0	Hum	g	−0.622	+3.68	

Mor.-Ev.	Δp	Δm	M	v	Δt
1448 − 1897_1	+1.05	−1.19	+26	+ 3	+4°0
1794 − 1907	+1.40	−0.26	+17	+ 3	−0.2
1809 − 1897_2	+1.38	−0.26	+19	+ 5	−1.0
1795 − 1884_1	+1.38	−0.25	+ 7	− 7	−0.5
1832_1 − 1884_2	+0.98	−0.17	+ 1	− 9	−3.3
1810 − 1578	+1.71	+0.64	+ 7	+ 1	−3.5
1832_2 − 1553_1	+1.13	+0.79	+13	+14	+0.5
1811 − 1562	+1.70	+0.65	+ 4	− 1	+0.5
1839 − 1553_2	+1.11	+0.79	−13	−12	−2.2

$$+3.72\,\mu_a + 1.48\,\pi = -35 \qquad \pi = +7.9 = +0''013 \pm 0''002$$

$$+1.48\,\mu_a + 16.12\,\pi = +108 \qquad \mu_a = -12.6 = -0''021 \pm 0''005$$

Comp. Star	Br.	x	y	π	P.E.
1	f	+0′7	+0′8	−0″007	±0″005
2	f	+1.1	+1.9	+0.004	0.010
3	b	+1.0	−0.1	+0.007	0.009
4	f	+2.5	−0.8	−0.007	0.007
5	f	+0.1	−0.5	+0.014	0.006
6	f	−1.2	−2.2	+0.006	0.006
7	f	−1.2	−1.6	−0.012	0.007
8	f	−1.4	+1.1	−0.006	0.007
9	bf	−1.8	+2.1	+0.001	±0.007

N.G.C. 7008 $\alpha=20^h57^m38^s$ $\delta=+54°10'$

Pl. No.	Date	t	Obs.	Qy	p	m	Remarks
1449	1917 June 27	$-16°0$	H	fg	$+0.574$	$+2.49$	
1554_1	Sept. 14	-0.5	vM	g	-0.616	$+2.71$	
1554_2	14	$+4.7$	H	g	-0.616	$+2.71$	
1563_1	Oct. 8	-4.0	vM	g	-0.856	$+2.77$	
1563_2	8	$+1.5$	Pt	g	-0.856	$+2.77$	
1583	10	-7.0	vM	gas	-0.870	$+2.78$	Hazy, 25^m exp.
1796	1918 May 31	-14.7	H	g	$+0.859$	$+3.42$	
1797	31	-9.2	vM	g	$+0.859$	$+3.42$	18^m exp.
1819	June 2	-12.0	vM	g	$+0.845$	$+3.42$	Trail of Boss 5405
1833_1	July 1	-6.7	vM	g	$+0.523$	$+3.50$	
1833_2	1	-0.2	Hum	g	$+0.523$	$+3.50$	
1834_1	1	$+6.0$	vM	fg	$+0.521$	$+3.50$	
1834_2	1	$+11.2$	Hum	fg	$+0.521$	$+3.50$	
1840_1	2	-2.0	Hum	g	$+0.508$	$+3.50$	
1840_2	2	$+3.5$	vM	g	$+0.508$	$+3.50$	
1885	Sept. 2	-8.7	vM	fg	-0.439	$+3.67$	
1898_1	3	-15.2	Hum	fg	-0.453	$+3.68$	
1898_2	3	-9.7	vM	fg	-0.453	$+3.68$	
1908	4	-20.5	H	g	-0.467	$+3.68$	
1938	28	$+4.0$	vM	g	-0.768	$+3.75$	Hazy, 25^m exp.

Mor.-Ev.	Δp	Δm	M	v	Δt
1449 – 1908	$+1.04$	-1.19	$+1$	-24	$+4°5$
1796 – 1898_1	$+1.31$	-0.26	$+28$	$+14$	$+0.5$
1819 – 1898_2	$+1.30$	-0.26	$+30$	$+16$	-2.3
1797 – 1885	$+1.30$	-0.25	$+20$	$+6$	-0.5
1833_1 – 1583	$+1.39$	$+0.72$	-1	-3	$+0.3$
1840_1 – 1563_1	$+1.36$	$+0.73$	$+5$	$+4$	$+2.0$
1833_2 – 1554_1	$+1.14$	$+0.79$	-6	-5	$+0.3$
1840_2 – 1563_2	$+1.36$	$+0.73$	-18	-19	$+2.0$
1834_1 – 1554_2	$+1.14$	$+0.79$	0	$+1$	$+1.3$
1834_2 – 1938	$+1.29$	-0.25	$+21$	$+7$	$+7.2$

$$+4.50\,\mu_a+2.21\,\pi=-41 \qquad \pi=+8.3=+0''014\pm0''004$$

$$+2.21\,\mu_a+16.07\,\pi=+105 \qquad \mu_a=-13.2=-0''022\pm0''007$$

Comp. Star	Br.	x	y	π	P.E.
1	f	$+1'1$	$+2'1$	$+0''002$	$\pm0''006$
2	f	$+0.5$	$+5.8$	-0.013	0.003
3	f	$+2.7$	$+0.1$	$+0.021$	0.011
4	bf	$+2.2$	-0.8	$+0.004$	0.007
5	b	$+0.3$	-1.1	-0.023	0.010
6	f	-1.5	-3.7	-0.012	0.005
7	f	-2.7	-2.9	$+0.007$	0.007
8	f	-0.7	0.0	-0.001	0.011
9	ff	-3.6	$+1.5$	$+0.014$	±0.006

N.G.C. 7662 $\alpha = 23^h 21^m 6^s$ $\delta = +41°59'$

Pl. No.	Date	t	Obs.	Qy	p	m	Remarks
749...	1915 Nov. 2	−7°7	vM	f	−0.699	+0.84	Hazy, 30^m exp.
750...	2	+3.9	H	fg	−0.699	+0.84	Hazy, 30^m exp.
758...	4	−13.2	H	fg	−0.719	+0.85	30^m exp. Trail of Boss 6002
759...	4	−2.7	vM	fg	−0.719	+0.85	30^m exp.
1050...	1916 July 23	−5.7	H	g	+0.701	+1.56	30^m exp.
1061...	Aug. 3	−14.2	H	g	+0.574	+1.59	
1062...	3	−7.0	vM	g	+0.574	+1.59	
1063...	3	+1.2	H	g	+0.574	+1.59	
1079...	5	−6.5	H	fg	+0.549	+1.60	
1080...	5	0.0	vM	fg	+0.549	+1.60	
1081...	5	+8.2	H	g	+0.549	+1.60	
1082...	5	+15.0	vM	g	+0.549	+1.60	
1126...	Oct. 21	0.0	vM	f	−0.575	+1.81	
1127...	21	+8.7	H	fg	−0.575	+1.81	30^m exp.
1143...	Nov. 16	+4.5	vM	g	−0.822	+1.88	Clouds, 28^m exp.
1163...	17	−5.5	H	fg	−0.827	+1.88	Hazy, 35^m exp.

Mor.-Ev.	Δp	Δm	M	v	Δt
1061– 758....	+1.29	+0.74	+29	+15	−1°0
1062– 749....	+1.27	+0.75	+3	−11	+0.7
1079–1163....	+1.38	−0.28	+13	−6	−1.0
1050– 759....	+1.42	+0.71	+20	+3	−3.0
1080–1126....	+1.12	−0.21	+8	−6	0.0
1063– 750....	+1.27	+0.75	+10	−4	−1.8
1081–1143....	+1.37	−0.28	+31	+13	+3.7
1082–1127....	+1.12	−0.21	+10	−4	+6.3

$$+2.41\,\mu_a + 2.61\,\pi = +28 \qquad \pi = +12.7 = +0.''021 \pm 0.''004$$
$$+2.61\,\mu_a + 13.18\,\pi = +161 \qquad \mu_a = -2.1 = -0.''003 \pm 0.''008$$

Comp. Star	Br.	x	y	π	P.E.
1.........	bf	+0.′7	+0.′4	+0.″019	±0.″010
2.........	bf	+4.1	+2.1	−0.003	0.006
3.........	f	+2.9	−2.3	−0.002	0.009
4.........	f	+1.5	−2.2	−0.011	0.008
5.........	f	−0.5	−3.3	+0.011	0.007
6.........	f	−2.3	−1.8	−0.001	0.014
7.........	f	−3.0	+2.5	−0.024	0.009
8.........	bf	−2.9	+5.1	+0.014	±0.005

MOUNT WILSON OBSERVATORY
November 1919

Contributions from the Mount Wilson Observatory, No. 183
Reprinted from the *Astrophysical Journal*, Vol. LI, pp. 236–243, 1920

NOTE ON THE AIR LINES IN SPARK SPECTRA FROM λ 5927 TO λ 8719[1]

By PAUL W. MERRILL

ABSTRACT

Air lines in condensed spark spectra, λ 5927 to λ 8719.—As an essential preliminary to the investigation of spark spectra in this region, a study of the air lines has been begun by comparing spectra obtained with different elements as electrodes, both in air and in oxygen. (1) The *wave-lengths* of 58 air lines, so determined, are given in Table I with an accuracy which is limited by the fact that the lines are usually ill-defined and sometimes broad and hazy. Twenty of them correspond to known H, N, O, or A lines, including six lines of the *red spectrum of argon* and four *oxygen lines* which had not previously been observed in spark spectra. Except for two more, which are probably due to oxygen, the rest have not, as yet, been identified. (2) All of the identified lines are found to be *shifted with reference to vacuum tube spectra;* the increase of wave-length is about 0.1 A for the *oxygen lines* and two *nitrogen lines,* 0.3 A for three other N lines, 0.6 A for the *argon lines,* and 0.7 A for *hydrogen alpha* and for three other N lines. (3) The *effect of adding self-inductance* is to weaken the two *nitrogen lines* λλ 6482 and 6610.

Spectrum of condensed spark in oxygen.—Several identifications of oxygen and nitrogen lines by previous observers using vacuum tubes are confirmed, and the doubtful identification of λ 7157 as due to oxygen is strengthened.

In the spectrum of the condensed spark in air there appear numerous lines which are to be ascribed to the gases of the surrounding atmosphere rather than to the material of the electrodes. These lines may be stronger and more numerous than the electrode lines. They are usually ill-defined and often broad and nebulous. Lines of nitrogen, oxygen, hydrogen, and argon are present in the spectrum of the disruptive discharge in ordinary air.

Very little information in regard to spark spectra beyond λ 6600 is available at present, although the need for it is becoming pressing. The recognition of the air lines is an essential preliminary to the investigation of spark spectra in a new region; and since it is always of interest to study spectral lines as produced under different modes of excitation, the observation of the air lines in spark spectra is desirable for the additional reason that many of these lines occur both in vacuum tube discharges and in the tube-arc.[1] Moreover, certain of these lines are present in astronomical spectra. The best-known examples are the hydrogen lines, but the presence of the spark lines of oxygen and nitrogen in stellar spectra has been recognized for some time.

---

[1] *Contributions from the Mount Wilson Observatory,* No. 183.

In the present investigation fifty-eight lines which are thought to be due to air have been observed in spark spectra from λ 5927 to λ 8719. These lines have all been photographed in the spectrum of the spark between electrodes of at least two elements, carbon and aluminum. Most of them have been photographed with several other elements also. For the region of wave-length greater than λ 7000 the air lines are the most striking features of the spectra of all the elements observed, including Al, C, Ca, Co, Cu, Fe, Ni, Ti, so that the photographed infra-red spark spectra of these elements appear much alike.

Wave-length measurements.—The lines which have been measured in the present investigation appear in the first column of Table I. Their relative intensities are in the second column. All the lines are more or less hazy and diffuse; those which are especially so are marked "h." The voltage employed was 8000, the capacity about 0.1 microfarad. No auxiliary spark-gap was used. No special temperature control was provided for the electrodes but care was taken that they did not become excessively hot, for in that case the characteristic spark features are weakened and the spectrum tends to become like that of the arc.

At λλ 6456 and 6950 are broad hazy patches which cannot be accurately measured. λ 7479 is a curious feature extending from λ 7476.7 to λ 7482.1. It is markedly unsymmetrical, being stronger toward the violet. Presumably it is composed of several ill-defined lines completely blended. Most of the other lines are fairly symmetrical, though lack of symmetry was especially noted for λλ 7424, 7442, and 7468. With high dispersion the lines of the oxygen triplet λλ 7772, 7774, 7775 appear slightly unsymmetrical.

All the lines have been measured with a dispersion of 16.8 A per mm; the stronger ones with 3.7 A per mm, and λλ 6482 and

---

[1] Arthur S. King and Paul W. Merrill, "Recent Observations of Tube-Arc Spectra Especially in the Infra-Red," *Physical Review*, 14, 271, 1919.

TABLE I

Air Lines in Spark Spectra

I. A.	Int.	Probable Error	Previous Observers	Probable Error	Vacuum Tubes
5927.83	5	.02	5927.88	.03	5927.57 N
5931.78	7	.02	5931.85	.04	5931.50 N
5941.54	11	.02	5941.65	.05	5941.49 N
5952.33	4	.02	5952.48	.03	5952.20 N
6160.72	1h	(.04)			
6171.0	3h	(.4)	6170.4	.1	
6284.22	1	(.03)	6284.4	(.2)	6283.29 N
6358.13	0h	(.08)			6356.78 N
6370.92	0h	(.06)			
6379.52	3h	.03	6379.7	(.2)	6378.79 N
6456	vh				O
6482.054	7	.004	6482.045	.01	6481.34 N
6563.5	12vh	.06	6563.3	.1	6562.79 H
6610.39	8	.007	6610.41	.04	6610.06 N
6640.7	0	(.3)			
6654.78	2	.05			
6721.25	1	.02			
6811.9	0	(.3)			
6864	00				
6887.61	1	(.06)			
6950	vh				
6965.95	1	.04			6965.43 A
7067.6	0	(.08)			7067.22 A
7157.36	9	.01			7157. O
7384.53	1	(.04)			7383.98 A
7424.04	8	.02			
7432.9	0	(.1)			
7442.70	10	.01			
7458.7	0	(.1)			
7468.72	14	.02			(7474. O)?
7479					
7504.84	0	(.04)			7503.87 A
7515.16	0	(.07)			7514.65 A
7635.70	1	(.07)			7635.11 A
7772.07	10	.01			7771.97 O
7774.33	7	.01			(7774.00)O
7775.60	6	.01			(7775.67)O
7947.83	4	.01			
7951.10	3	(.06)			
7952.3	2	(.2)			
8185.26	4	(.02)			
8188.42	4	(.02)			
8200.72	1	(.03)			
8211.12	2	(.02)			
8216.72	7	(.02)			
8223.48	4	(.02)			
8230.20	0	(.05)			
8242.80	4	(.03)			
8446.84	5	(.03)			8446.42 O
8594	00				
8630.02	0	(.04)			

TABLE I—*Continued*

I. A.	Int.	Probable Error	Previous Observers	Probable Error	Vacuum Tubes
8680.63	2	(.04)			
8683.70	1	(.04)			
8686.41	0	(.04)			
8692	00				
8703.8	00	(.2)			
8712.00	0	(.1)			
8719.2	00	(.2)			

6610 with 1.8 A per mm in addition, first-order grating spectra being used in every observation. The spectra having 16.8 A per mm and some of those having 3.7 A per mm were obtained on films, the remainder on glass plates. The wave-lengths were determined in most cases by reference to iron-arc comparison spectra, usually in the second order, but on some plates in the first order. Wherever possible, however, lines in the spark spectra themselves were used as standards. For this purpose the exposures to the calcium and copper sparks were especially suitable. The wave-lengths of the metallic lines were taken from *Scientific Papers of the Bureau of Standards*, Nos. 312 and 324.

In the fourth column appear the mean wave-lengths found by previous observers.[1] In the third and fifth columns are the probable errors; those in parentheses, depending on a small number of determinations, have been estimated; the others have been computed from the residuals in the usual way.

Hydrogen.—The hydrogen line Hα which appears on all of the photographs is exceedingly diffuse and difficult to measure. Measurements on a considerable number of exposures, however, have given the wave-length λ6563.5, with a probable error of 0.06 A. The effective wave-length thus found is 0.7 A greater than that obtained from vacuum tubes.[1] The values of previous observers give a slightly smaller displacement, 0.5 A. The interpretation of this apparent displacement should be considered in connection with the similar displacements shown by the lines of nitrogen and argon.

---

[1] The principal sources from which these wave-lengths have been taken are Otto Schulemann, "Das Funkenspektrum des Indiums," *Zeitschrift für wissenschaftliche Photographie*, **10**, 263, 1911–1912; Franz Joseph Kasper, "Messungen am Silberspektrum," *ibid.*, p. 53; A. Kretzer, "Untersuchungen über das Antimonspektrum," *ibid.*, **8**, 45, 1909–1910; Wilhelm Schwetz, "Die Spektren des Wismuts," *ibid.*, p. 301; Matthias Aretz, "Über den langwelligen Teil des Kupferfunken- und Kupferbogenspektrum," *ibid.*, **9**, 256, 1910–1911; J. M. Eder and E. Valenta, "Wellenlängenmessungen im roten Bezirke der Funkenspektra," *Sitzungsberichte Akad. der Wiss. Wien, Math-naturw. Kl.*, **118**, IIa, 511, 1909.

Nitrogen and oxygen.—Most of the air lines are due to nitrogen and oxygen. The vacuum tube wave-lengths of nitrogen are by Porlezza,[2] those of oxygen are by Runge and Paschen,[3] reduced to the international system.[4]

Confirmation of several of the identifications was obtained by operating the spark in an atmosphere of oxygen. The oxygen used was a commercial product and probably was not free from nitrogen, as the nitrogen lines were not eliminated from the spectrum and in fact were not greatly reduced in intensity. When the exposures in oxygen were so timed as to give the same general intensity as exposures in air, only two lines were found to be certainly weakened, namely λλ 6482.054 and 6610.39. The following lines were strengthened in an atmosphere of oxygen: λλ 6158, 6456, 7003, 7157.36, 7772.07, 7774.33, 7775.60, 8446.84. The lines at λλ 6158, 6456, and 7003 are very wide and diffuse. The first and third are absent or very weak in air and do not appear in Table I. λλ 6158 and 6456 probably correspond to triplets, and λ 7003 to a single line, all observed by Runge and Paschen in the series spectrum of oxygen. The last four lines are well-known oxygen lines, and λ 7157.36 is probably due to oxygen. A line at approximately this wave-length was observed in an oxygen tube by Runge and Paschen, though not included by them in their table of oxygen lines.

The exposures with the spark in oxygen did not give sufficiently great changes in the relative intensities of the remaining lines in

---

[1] W. E. Curtis, "Wave-Lengths of Hydrogen Lines and Determination of the Series Constant," *Proceedings of the Royal Society*, A **90**, 605, 1914.

[2] C. Porlezza, "Lo Spettro a righe dell'azoto in tubo di Geissler," *Atti R. Accademia dei Lincei*, Serie 5, **20**, 584, 1911.

[3] Runge and Paschen, *Annalen der Physik*, **61**, 641, 1897; Paschen, *Annalen der Physik*, **27**, 562, 1908.

[4] K. W. Meissner, "Untersuchungen und Wellenlängenbestimmungen im roten und infraroten Spektralbezirk," *Annalen der Physik*, **50**, 713, 1916.

Table I to make it possible to assign their origins. They may be due to nitrogen, but this is not certain except for those of shorter wave-length corresponding to lines found by previous observers in nitrogen tubes. The identification of the remaining lines must await further work with the spark in atmospheres of pure gases or with vacuum tubes containing pure gases.

Comparison of the spark wave-lengths of nitrogen lines with those by Porlezza in the vacuum tube shows a large positive displacement. For eight lines the mean displacement is 0.43±0.08 A, the probable error being computed as though the shift were actually of the same amount for all lines. This is not necessarily the case, but even so the displacement is more than five times the probable error. Including one more line (λ 6358), poorly determined, gives 0.53±0.1 A. Using values of previous observers for eight lines we get a displacement of 0.52±0.08 A. The chance that these displacements are due to accidental errors is negligible, and it would be surprising if systematic errors to the amount of 0.4 or 0.5 A should exist in either series.

TABLE II

WAVE-LENGTHS OF OXYGEN LINES

SPARK	TUBE RUNGE AND PASCHEN*	ARC		SUN MEISSNER*
		Meissner*	Meggers and Kiess†	
7772.07........	7771.97	7771.98	7771.93	7771.97
7774.33........	7774.00	7774.19	7774.14	7774.20
7775.60........	7775.67	7775.42	7775.43	7775.42
8446.84........	8446.42	8446.36 8446.76	8446.42	8446.38 8446.78

* K. W. Meissner, *Annalen der Physik*, 50, 713, 1916.

† *Bulletin of the Bureau of Standards*, 14, 637, 1918.

The wave-lengths of four oxygen lines as found in various sources are collected in Table II. The spark lines seem to be displaced toward longer wave-lengths as compared with other sources, though by smaller amounts than occur in the similar displacements shown by the lines of hydrogen, nitrogen, and argon. The vacuum-tube values of Runge and Paschen for the second and third lines are admittedly inaccurate.

These four infra-red oxygen lines are essentially spark lines. They are faintly present in the arc[1] and are fairly strong in the solar spectrum.[2] A preliminary photograph by Mr. Ellerman and the writer indicated that the triplet at λλ 7772–7775 is much weakened in the spot spectrum as compared with the disk. This is conclusively shown by an excellent photograph secured by Mr. Brackett. It would not be surprising if this triplet were found to be strong in the spectra of certain stars of types B and A.

Argon.—The photographs show six faint lines near the positions of six of the strongest lines of the so-called "red" spectrum of argon. Lines of wave-length 4000–5000 in the "blue" argon spectrum have been previously observed in spark spectra,[3] but the writer is not familiar with any record of observation of lines of the "red" spectrum in the spark. As these lines are produced in the vacuum tube without capacity, it seems somewhat peculiar that they should appear in the condensed spark. Their effective wave-lengths in the spark appear to be greater than the vacuum-tube values.[4] The six lines give a mean displacement of 0.59±0.06 A.

Self-induction.—A few exposures were made with about 0.1 millihenrys self-induction in the electric circuit. The only striking change in the appearance of the spectrum is the pronounced weakening of the nitrogen lines λλ 6482 and 6610, though many of the lines probably become narrower.

SUMMARY

1. Fifty-eight air lines have been photographed in spark spectra from λ 5927 to λ 8719 and their wave-lengths determined with varying degrees of accuracy.

2. The lines which can be identified at present are due to argon, hydrogen, nitrogen, and oxygen.

---

[1] An unpublished observation by Mr. Babcock to which he kindly permits reference in this connection shows that the three lines at λλ 7772, 7774, and 7775 are quite strong at the *poles* of the iron arc, especially at the *positive* pole, as would be expected of spark lines.

[2] That λλ 7772, 7774, and 7775 are not caused by the earth's atmosphere, but are true solar lines, was shown by St. John (*Annual Report of the Director of Mount Wilson Observatory for 1911*).

[3] See discussion by A. S. King, *Astrophysical Journal*, **21**, 344, 1905.

[4] K. W. Meissner, *Annalen der Physik*, **51**, 115, 1916.

3. An attempt to distinguish between the nitrogen and oxygen lines by operating the spark in an atmosphere of oxygen confirmed several previous identifications, but was inconclusive in regard to most of the new lines.

4. The effective wave-lengths of the lines of argon, hydrogen, and nitrogen appear to be greater in the spark than in vacuum tubes by several tenths of an angstrom unit. The oxygen lines show the same effect to a smaller degree.

5. Self-induction in the spark circuit causes a relative weakening of the nitrogen lines λλ 6482.054 and 6610.39.

In conclusion it may be noted that this investigation is preliminary and incomplete. Further work on the apparent displacement of the lines is required in order that its true character and interpretation may be found. Chemical identifications should be established for the unknown lines by operating the spark in very pure atmospheres of oxygen, nitrogen, and argon.

Mount Wilson Observatory
February 1920

Contributions from the Mount Wilson Observatory, No. 184
Reprinted from the *Astrophysical Journal*, Vol. LI, pp. 257–262, 1920

ON THE APPLICATION OF INTERFERENCE METHODS TO ASTRONOMICAL MEASUREMENTS

By A. A. MICHELSON[1]

ABSTRACT

An interference method of measuring extremely small angles and changes of angle.—Thirty years ago the author called attention to the possibility of measuring such minute angles as the *diameters of planetoids and satellites* and the *distance between the components of double stars* by observing the interference fringes produced at the focus of a telescope when only two portions of the objective, located on the same diameter, are used; for it was shown that as the distance apart of the apertures is increased the visibility of the fringes reaches a minimum for a distance equal to $1.22\ \lambda/\alpha$, or $0.5\ \lambda/\alpha$, for a disk or double star respectively, when λ is the effective wave-length and α is the desired angle. This beautiful and simple method was applied successfully by the author in 1891 to the accurate measurement of the size of Jupiter's satellites but was not tested on stellar objects, probably because it was supposed to require ideal seeing conditions. Last year, however, the author discovered by tests at Yerkes Observatory and at Mount Wilson that even when the "seeing" was bad, clear and relatively steady fringes could be obtained; and Anderson, using the 100-inch reflector, has recently measured the separation of the components of Capella, $0''.0545$, within less than 1 per cent by the application of this method. In fact the 100-inch could measure with accuracy separations as small as $0''.025$. But to determine the *diameter of a fixed star*, a distance between apertures of at least 10 meters would be required; so that an interferometer arrangement would have to be substituted for the telescope. The author also suggests that by the use of prisms to superpose the fringe systems of two stars, small *relative motions* and *parallaxes* could be measured.

Relative brightness of components of double stars may also be determined from the relative visibility of the focal fringes at minimum and maximum visibility.

In the number of the *Philosophical Magazine* for July, 1890 (**30**, 1), a method was described for the measurement of the angular magnitude of astronomical objects such as the diameter of planetoids and satellites and the distance between double stars, when these are beyond the powers of the largest telescopes, and the hope was there expressed that it might not be impossible thus to measure the diameter of the fixed stars.

Briefly, the process consists in utilizing only the two portions of a large objective at opposite ends of a diameter. The interference fringes at the focus under these conditions will be a series of equidistant interference bands which are most distinct with a source subtending an infinitesimal angle. For an object presenting an appreciable angle the visibility is less and may become zero—the exact relation being readily expressed for any given distribution of light in the source. Thus if $\phi(a)da$ represent the intensity of a strip of the source of angular width da, and s the distance between the apertures (supposed small compared with s), and

---

[1] Research Associate of the Carnegie Institution of Washington, Mount Wilson Observatory.

if $P=\int\phi(a)da$, $C=\int\phi(a)da\ \cos 2\pi\frac{s}{\lambda}a$, and $S=\int\phi(a)da\ \sin 2\pi\frac{s}{\lambda}a$,

then the visibility of the interference bands is

$$V=\frac{\sqrt{C^2+S^2}}{P}\ .$$

Thus for a double star, the brightness of whose components is in the ratio $1:r$ and whose angular distance $=a$,

$$V=\frac{\sqrt{1+r^2+2r\cos 2\pi\frac{s}{\lambda}a}}{1+r}\ .$$

For equal components this reduces to $\cos\frac{\pi sa}{\lambda}$, which vanishes for $a=\frac{1}{2}\frac{\lambda}{s}$. Accordingly this angle can be accurately measured when it is only half of the limit of resolution of the full-apertured telescope.

Again, by comparing the visibility at maximum and at minimum, the ratio of the brightness of the component stars may be found by

$$r=\frac{V_1-V_2}{V_1+V_2}.$$

For a uniformly illuminated disk

$$V=\int_0^1\sqrt{1+\omega^2}\cos\omega n d\omega$$

where $n=\pi\frac{sa}{\lambda}$, a being the angular diameter. For such an object the fringes vanish for an angular diameter $a=1.22\frac{\lambda}{s}$.

A series of observations was taken on the satellites of Jupiter at the Lick Observatory the following year with results which amply confirmed the practicability and accuracy of the method.

It is clear, however, that as in all probability the stars present an angular diameter less than one-hundredth of a second, it would be almost hopeless to make such measurements, utilizing the largest telescope in existence; for it would require a distance between the apertures of at least 10 meters to observe the vanishing of the fringes.[1] While such a large telescope would be entirely out of question, the interferometer arrangements figured in the article referred to may serve the purpose, as there is theoretically no limit to the effective base line and practically only that which depends on the atmospheric disturbances.

With a view to testing the effect of these, a trial was made (August 25, 1919) with the 40-inch refractor at Yerkes Observatory, using two apertures 4 inches by 5 inches at opposite ends of a diameter. The result was very encouraging, the interference bands being remarkably steady, notwithstanding the relatively poor "seeing"—2 to 3 on a scale of 5.

On invitation from Dr. George E. Hale the test was applied (September 18, 1919) to the 60-inch reflector of the Mount Wilson Observatory and then to the 100-inch reflector, and in both cases the experience at the Yerkes Observatory was confirmed.

In the case of the 60-inch telescope the apertures were applied, as in the case of the 40-inch, to the objective; while for the 100-inch, it was found quite as effective and far more convenient to use a small screen with two apertures near the eyepiece, the distance and orientation being thus much more readily controlled while the effective size and separation of the two interfering pencils remain the same.

The interference fringes in both observations remained remarkably clear and steady, notwithstanding the excessive "boiling" of the highly magnified images corresponding to "seeing" 2 on a scale of 10.

---

[1] A diminution in visibility, however, might be observed with a diameter of 2 meters.

Subsequent observations showed that the interference bands remain visible even when the seeing is so poor that the usual type of observation is impracticable.

A statement of results obtained by this method by Dr. J. A. Anderson of the staff of the Mount Wilson Observatory from observations of the spectroscopic binary Capella is herewith appended.

STATEMENT OF RESULTS FROM OBSERVATIONS OF CAPELLA WITH THE MICHELSON INTERFEROMETER

Date of Observation	Distance	Position Angle	Remarks
December 30.6 1919	0″.0418	(153°.9)	P.A. calculated. Only the distance observed accurately*
February 13.6 1920	0.0458	5.0	
February 14.6 1920	0.0451	1.0	
February 15.6 1920	0.0443	356.4	
March 15.6 1920	0.0505	242.0	
April 23.6 1920	(0.0439)	107.0	Distance calculated. Only the position angle observed accurately†

* The rough observation of position angle was 148°±10°.

† Observation made in strong daylight. The blue background shifted the effective wave-length to the red, causing the observed distance of 0″.0402 to be much too low. The background could not affect the position angle.

Using the following elements[1] for the orbit, these observations are satisfied as indicated:

$$a_1+a_2 = 0''.05249 \qquad (a_1+a_2)\sin i = 83{,}277{,}900 \text{ km}$$

$$e = 0.016$$

$$\omega = 117^\circ.3$$

$$i = 140^\circ 30'$$

Position angle of $\Omega = 45^\circ 55'$

$$T = \text{J.D. } 2{,}422{,}387.9 \qquad \text{or} \qquad P = 104.006 \text{ days}$$

---

[1] See orbit by H. M. Reese, *Astrophysical Journal*, **14**, 263, 1901, for values of $(a_1+a_2)\sin i$, of e, and of ω. a_1 and a_2 are the semi-major axes; e, the eccentricity (same for each orbit); omega is the distance of periastron from the ascending node in the plane of the orbit; i is the inclination of the orbit to the line of sight; Ω is the symbol for the ascending node and is here equivalent to the position angle on the tangential plane.

Date	$t-T$	a	i	r	Position Angle
1. December 30.6 1919	$39^{d}.7$	1 and 5 $0''.05249$	$180°-39°31'$	$0''.04180$	$153°.9$
2. February 13.6 1920	84.7	2 and 5 0.05250	$-39\ 36$	0.04583	4.6
3. February 14.6 1920	85.7	3 and 5 0.05248	$-39\ 22$	0.04506	1.0
4. February 15.6 1920	86.7	4 and 5 0.05249	$-39\ 31$	0.04430	357.3
5. March 15.6 1920	11.7	....	$-39\ 30$	0.05050	242.4
6. April 23.6 1920	50.7			0.04391	107.2
		Means 0.05249	$180°-39\ 30$		

Parallax of Capella $0''.0600$.

It appears from a comparison of these results with the orbit that an order of accuracy of one ten-thousandth of a second of arc is attainable in the case of Capella with a base line of 100 inches.

In these observations the distance between the apertures was fixed, and the vanishing of the fringes was observed at the appropriate position angle.

The complete disappearance of the interference bands showed that the component stars are of equal brightness; otherwise the visibility would have a minimum from which the ratio of the brightness may be obtained as indicated above.

For this, however, it would be necessary to measure the visibility, or at least to calibrate the eye estimates.

This may be effected by adjusting the relative width of two auxiliary apertures so that the resulting visibility of a single comparison star (or of the double star in a direction perpendicular to the plane of the components) is the same as that which is actually observed.

If the ratio of the width of the apertures is ρ, then when the visibilities are equal in the two systems of fringes

$$V=\frac{2}{\rho+\frac{1}{\rho}}.$$

Other problems which involve the comparison of two stars, such as the measurement of stellar parallax, proper motion, variation of latitude, etc., may also be undertaken by a modification of the interference method. For this two prisms or prism couples are similarly placed in front of the apertures, with the plane of refraction parallel with that passing through the two apertures and the axis. This plane is rotated until the direction coincides with that of the stars to be compared. The refraction by the prisms is then altered (by rotating the single prisms in the same plane, or by equal and opposite rotations of the elements of the prism couples) until the two systems of fringes are superposed. Any change in the relative position of the stars is accompanied by a corresponding alteration in the appearance of the fringes, which is then compensated by rotation of the prisms, from which the change in position may be determined.

Preparations are now under way at Mount Wilson for testing the possibilities of the interferometer method with a base line of 18 to 20 feet.

Ryerson Physical Laboratory
June 1920

Contributions from the Mount Wilson Observatory, No. 185
Reprinted from the *Astrophysical Journal*, Vol. LI, pp. 263–275, 1920

APPLICATION OF MICHELSON'S INTERFEROMETER METHOD TO THE MEASUREMENT OF CLOSE DOUBLE STARS

By J. A. ANDERSON

ABSTRACT

Michelson interference method of measuring close double stars.—It is surprising that this method of accurately measuring angles as minute even as half the limit of resolution of the telescope used has heretofore been applied only to Jupiter's satellites. But after Michelson found by tests last year at the Yerkes Observatory and at Mount Wilson that clear and relatively steady fringes can be obtained even when the "seeing" is bad, steps were taken to apply the method to the measurement of the separation of the components of Capella. The *arrangement of apparatus* adopted is described in full. The apertures were placed near the focus instead of at the objective and set at a fixed distance apart, somewhat greater than the distance for minimum visibility, and were then rotated and the four position angles which gave minimum visibility were determined. After the *effective wave-length* for a G-type star had been found by laboratory experiments with sunlight to be about 0.550 μ, the position readings gave both the angular separation of the components and the direction of the line joining them. The *effect of atmospheric dispersion* is in general to shift the center of the system. Two methods of compensating for this effect are suggested. A method of determining the *relative brightness of components* when the ratio is not more than 1.5 is described and illustrated.

Accuracy.—In the case of Capella, the separation, about $0\overset{''}{.}05$, was determined within considerably less than 1 per cent. As to the *limits of applicability of the 100-inch reflector* in such measurements, the theoretical resolution limit with the interferometer is $0\overset{''}{.}025$, and double stars down to about the eleventh magnitude should be measurable under ordinary observing conditions.

Elements for Capella as determined by the Michelson interference method.—Observations made on six dates, December 1919 to April 1920, give the following results: $a=0\overset{''}{.}05249$; $T=\text{J.D. } 2{,}422{,}387.9$; $i=140°30'$. These combined with spectroscopic elements give: $P=104.006$ days; $a_1+a_2=130{,}924{,}000$ km; $m_1=4.62\odot$; $m_2=3.65\odot$.

Interference method of measuring atmospheric dispersion, by its effect on the fringe systems of stars at various zenith distances, is suggested by the author as likely to prove very sensitive.

The astronomical applications of the interferometer have been discussed by Professor Michelson in a number of papers.[1] He explains how the diameters of stars can be measured, considered as uniformly luminous disks; and, in case there is darkening toward the limb, how the amount of darkening can be determined. Further, if a celestial object is not circular in apparent shape, he explains how its exact shape may be found. Special cases, such as double stars, are fully treated.

---

[1] *Philosophical Magazine* (5), **30**, 1, 1890; (5), **31**, 338, 1891; (5), **34**, 280, 1892; *American Journal of Science* (3), **39**, 115, 1890.

In view of the great beauty and simplicity of the method, it is rather surprising to find that the only application it has had up to the present time is to the determination of the diameters of Jupiter's satellites, and this was done by Professor Michelson himself. It is possible that astronomers who in general are so much troubled by the phenomena of "bad seeing" have had a feeling that an instrument so extraordinarily sensitive as the interferometer is known to be could hardly, if ever, be used, especially with the larger telescopes.

On September 18, 1919, Professor Michelson made a final test of this point by applying the interferometer to the 60-inch and 100-inch telescopes of the Mount Wilson Observatory, and found that the interference fringes were easily observed, although the seeing at the time was rated about 2 on a scale of 10. He had on August 25 found similar results with the 40-inch refractor of the Yerkes Observatory. Accordingly, it was decided to give the method a trial with the 100-inch reflector, and Mr. Hale requested the writer to undertake the experiments described below.

As it appeared probable that an aperture much larger than 100 inches would be required for effective work in measuring stellar diameters, it was decided to apply the method to the measurement of some double star, if possible, to one too close to be measured with the usual method. Capella was selected, because an estimate of the separation of its components, based on knowledge of its spectroscopic orbit and parallax, places this around $\frac{1}{20}$ second of arc, which should be easy to measure with the interferometer applied to the 100-inch telescope.

A preliminary observation (by Mr. Pease and the writer) was made on December 30, 1919, the chief object of which was to learn just how the interferometer should be constructed in order that it might be suited to the measurement of double stars. This observation gave the distance between the components of Capella with a probable error of about 1 per cent; a reading of the position angle was also made, but it was so very rough that it might easily be in error by 10° either way. Regular observations with the improved form of apparatus were made on February 13, 14, and 15, March 15, and April 23, 1920.

As shown in the diagram (Fig. 1) the interferometer consists simply of a plate (*A*) having two apertures in it, placed in the converging beam of light coming from the telescope objective or mirror. The interference fringes formed in the focal plane are viewed with a high-power eyepiece *E*. The entire interferometer can be rotated about the telescope axis so as to vary the position of the line joining the centers of the two apertures; and the apertures themselves are so arranged that their distance apart can be varied, the actual separation being read on a scale at the eye end of the instrument, where the circle is also located from which the position angle of the apertures is read. The plate carrying the apertures can also be moved entirely out of the beam of light to facilitate the accurate centering of the star to be observed.

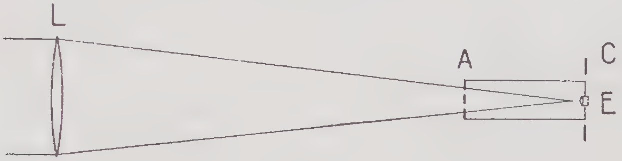

FIG. 1

The method of making the measurements differs slightly from that described by Professor Michelson,[1] and will therefore be described in sufficient detail to be clear even without reference to any previous work.

Let the light from a star fall upon two apertures placed (for simplicity) in front of the telescope objective or mirror. Let the width of each aperture measured along the line joining their centers be *d;* let the distance between their centers be *D*. The shape of the diffraction pattern seen in the focal plane of the telescope will depend upon that of the apertures; but we are here concerned only with its dimension in the direction of the line joining the two apertures, and this, in angular measure, as seen from a distance equal to the equivalent focal length of the telescope, is $\alpha = 2C\lambda/d$. The intensity, being, say, unity at the center of the pattern, falls to the first zero value at an angle $\alpha/2$ from this point. C is a factor depending on the shape of the apertures. For rectangular slits, $C=1$; for circular apertures, $C=1.22$ nearly. Upon the diffraction pattern will appear the interference fringes, these being at right angles to the line joining the two apertures. The angular distance between two bright fringes is λ/D. Hence the number of fringes which can be seen on the central diffraction disk depends on the ratio D/d, and is equal to $2CD/d$. If this number is greater than 10, the fringes farthest from the center will, in general, be invisible in white light, because of the overlapping of the different colors.

---

[1] *Philosophical Magazine* (5), **30**, 1, 1890.

Now assume that this arrangement is pointed at a double star, the angular separation of its components being β. If β is larger than $2C\lambda/d$, two separate diffraction patterns will be seen, each with its own system of interference fringes. When β is less than $2C\lambda/d$ the patterns will overlap more or less; and if β is just equal to $\lambda/2D$ and the position angle of the double star is the same as that of the line joining the two apertures, the conditions are such that a bright fringe due to one component falls on a dark fringe due to the other component, or we may say that the two fringe systems are out of step by just one-half a fringe; and hence, if the two component stars are of the same intensity the visibility of the fringes near the center of the pattern will be zero. (It is, of course, clear that minima of visibility will occur for $\beta = N\lambda/2D$, where N is any odd integer.) Hence we may say that the interferometer "resolves" two stars whose angular separation is $\lambda/2D$, just as a circular telescope objective of diameter D will resolve two stars whose separation is $1.22\lambda/D$; that is, the resolving power of the interferometer is somewhat more than twice that of a telescope of the same aperture. It should also be borne in mind that useful measurements may be made with the interferometer even when the angular separation is much less than $\lambda/2D$, as will be discussed more fully below.

Let D_0 denote the smallest value of D which will cause the fringes to disappear for a double star having equal components. If we choose D a little larger than D_0, so that $D_0 = D\cos\theta$, it is evident that the fringes will be visible when the position angle of the apertures is the same as that of the double star. If now the interferometer be rotated through an angle $\pm\theta$, the fringes will just disappear; and the same thing will happen when the instrument is rotated through an angle $180° \pm \theta$. For any value of D greater than D_0 there are, therefore, four values of the position angle, for each of which the fringes disappear, or have minimum visibility, according as the two components of the double star are of equal or of unequal intensity. From these four position angles and the known value D one can obviously find the value of D_0 and the position angle of the double star. There will, of course, be two possible position angles differing by 180°, but, as will be explained presently, unless the two components have exactly the same intensity and the same color, even this uncertainty may be removed.

The method just described was employed in the present work on Capella. As a rule, a complete observation included three complete rotations of the interferometer for each of three values of D, making a total of thirty-six readings of position angle. The values of D were so chosen that θ, as defined above, should lie between 30° and 50°. Under these conditions and with reasonably good seeing the probable error of a single reading should not exceed 3°. It is the author's opinion that with a little practice a good observer will be able to reduce the probable error of a single setting to about 1°. The corresponding error in the distance is about 1.8 per cent. The time required for a complete observation was about one hour, but it is reasonable to expect that when one becomes accustomed to observations of this kind no more than fifteen minutes will be required.

Given a suitable arrangement for measuring the "visibility" of the fringes, the following method of observation may be used. Choose a value of D smaller than D_0. Determine the visibility at position angles differing from each other by, say, 15° all the way around the circle. If the object is a double star, the visibility will show two maxima and two minima in a revolution. (This will also be true if the object has the form of a luminous surface longer in one dimension than at right angles thereto. Further measures will, however, readily distinguish between this case and that of a double star.) Repeat twice, using two other values of D. The data thus obtained should be sufficient to determine both position angle and distance of the double star, with a high degree of accuracy, and without requiring a value of D as large as D_0.

Having found D_0 as explained above, we need to know only λ in order to compute β, since $\beta=\lambda/2\,D_0$. The value of λ for the sun was found from laboratory measures, using as an artificial double star two small round holes illuminated by sunlight reflected from freshly silvered mirrors. The constants of the apparatus were determined by direct measurements, and also by observations on the artificial double star illuminated by very nearly monochromatic light of known wave-length. The results from two series of observations with sunlight were 5498 A and 5500 A. It seems safe, therefore, to use for a G-type star $\lambda=0.0000550$ cm, and this value was employed in reducing the observations of Capella.

In this connection it is important to bear in mind the rôle played by the background on which the interference pattern is observed. On April 23 an observation of Capella was made in full daylight. The observation was very easy to make, but on being reduced, using the value of λ given above, the distance between the components came out approximately 10 per cent too small. A little consideration shows that this might have been predicted, for the skylight, being relatively very rich in blue light, would reduce the visibility of the blue fringes much more than that of the yellow or red fringes, thus resulting in a considerable increase in the value of the effective wave-length.

EFFECTS OF ATMOSPHERIC DISPERSION

When observations are made at some distance from the zenith it is found that for certain position angles of the interferometer the center of the fringe system does not fall on the center of the diffraction pattern and may even be displaced to such an extent that the fringes cannot be seen at all. This happens when the line joining the apertures is perpendicular to the horizon. The cause of the phenomenon is atmospheric dispersion, as became evident from a series of observations on a star at zenith distances between 50° and 20°. The phenomenon is well known to physicists who have used interferometers. For completeness, however, the explanation will be reproduced here.

To fix ideas, let us consider a star at zenith distance 45°. As seen on the sky it is really a short spectrum, the violet end above and the red end pointing down toward the horizon. Set the interferometer at right angles to this spectrum, that is, with the line joining the apertures parallel to the horizon. The fringe system will be seen central on the diffraction pattern, but the fringes will be closer together at the upper edge than at the lower, for the former are in violet light, the latter in red light. Hence the fringe system is fan-shaped, very much as indicated in the diagram (Fig. 2). Now, if we rotate the interferometer through an angle of 90°, the central fringe will no longer be white, but colored—a spectrum whose width is equal to the length of the little stellar spectrum seen on the sky. The order of colors in this fringe is violet above, red below. The angular width of this fringe for the case we are considering ($z=45°$) is about 0″.8, and is therefore equal to about ten times the distance between two bright fringes when $D=113$ cm. Consequently, in this part of the system the fringes overlap to such an extent that the result is perfectly uniform illumination. Let us for a moment imagine the atmospheric dispersion removed, all other conditions being the same. The diffraction pattern will then show a perfectly normal fringe system, the central fringe being white, the others being spectra whose dispersion increases linearly with the distance from the central fringe. For convenience let us number the fringes, calling the central fringe 0; then +1, +2, +3, etc., upward, and −1, −2, −3, etc., downward. The order of colors in the + fringes is red above, violet below, this order being just the reverse for the − fringes. Since the dispersion

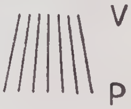

FIG. 2

increases with the order, it is evident that we can find some fringe which will have a given width, say $0''.8$, and hence will be an inverted duplicate of the central fringe as seen with atmospheric dispersion. This will evidently be one of the $+$ fringes, say the $+p$th. If we now introduce atmospheric dispersion, the $+p$th fringe will be white or very approximately so, and will accordingly be regarded as the center of the system. Indeed, the fringes $p-1$, $p-2$, etc., will be violet above, red below, while the fringes $p+1$, $p+2$, etc., will be violet below, red above, as they should be. Now if p is greater than CD/d, the new central fringe will be off the diffraction pattern, in the direction away from the horizon.

We may calculate p as a function of D and the zenith distance as follows: Let the limits of the spectrum be taken as λ 4500 and λ 6500. Let the width of the $+1$st fringe be w, and its distance from the 0 fringe be W. The width of the pth fringe will be pw, or since $w/W=4/11$, the width of the pth fringe is $4pW/11$. In angular measure $W=\lambda/D$ or, in seconds of arc, $W=11''.3/D$. Hence the width of the pth fringe in seconds of arc is $45''.2\,p/11\,D$ where D is, of course, in centimeters.

The mean atmospheric refraction in seconds of arc for zenith distances less than about 70° is given to a sufficient approximation by $r''=60 \tan z$. The atmospheric dispersion between the wave-length limits chosen is 0.0138 times this, according to the values given in *Bulletin of the Bureau of Standards*, **14**, No. 4, 697–740, 1919. Hence the dispersion will be given by $\delta''=0.83 \tan z$ $=45''.2\,p/11\,D$, whence $p=0.22\,D \tan z$. Taking $D=150$ cm, $z=45°$, we have $p=33$, which indicates that with good conditions of seeing this should be a very sensitive method for the actual determination of atmospheric dispersion.

In order to make observations at all zenith distances, it is necessary to be able to compensate for this effect of atmospheric dispersion. The method thus far used is not entirely satisfactory. Two plates of plane parallel glass of exactly the same thickness are mounted, one in front of each of the apertures of the interferometer. The normals to the plane faces of these plates make an angle of about 5° with the axis of the telescope, and hence, by tilting one of the plates slightly so as to vary the angle, one of the two beams can be retarded or accelerated with respect to the other sufficiently to bring the fringe system back to the center of the diffraction disk. Unfortunately, as the interferometer is rotated, one must constantly vary the tilt of the movable plate, and this is annoying, especially with bad seeing, when the fringes are none too easy to observe anyway. A much better way, which, however, has not been tried yet, would be to place a prism with a variable angle in front of the interferometer, but mounted so as not to rotate with the latter. By maintaining its refracting edge always downward it would then only be necessary to vary the refracting angle with the zenith distance. It should be easy to arrange the mounting so that the adjustments would be made automatically by the action of gravity.

SIZE OF APERTURES AND BRIGHTNESS

The apertures which were used with the 100-inch reflector measure 18.3×27.5 cm as seen in projection on the telescope mirror. Their distance apart was varied from about 120 to 200 cm. On the average, then, $D = 160$ cm, and $d = 0.12\,D$. With d as small as this, the diffraction disk is, of course, quite large compared to the size of the fringe system. A relatively small amount of light is admitted by the small apertures, and this is spread over a rather large area in the focal plane; hence the intensity is low. A little consideration will show that doubling the size of the apertures will result in a 16-fold increase in the intensity of the image; consequently, if we are interested in faint stars, we must use apertures as large as possible. In the present work on Capella this question was of no importance, for with such a bright star there is plenty of light for observations with small apertures even in daytime. Sufficient data were gathered, however, both with the large telescope and from laboratory experiments, to enable us to see pretty clearly just what can be done.

With $d = 0.12\,D$ it was found possible with the 100-inch reflector to observe stars down to the seventh magnitude, the seeing being usually 1 on a scale of 10. With good seeing perhaps one might reach a magnitude fainter. Laboratory experiments showed that there is practically no loss in the distinctness of the fringes when d

is as large as 0.5 D, which would increase the intensity two hundred and fifty-six times, or about six magnitudes. Hence with an instrument as large as the 100-inch, one might be able to observe stars down to the thirteenth magnitude, and there should be no difficulty in reaching the eleventh magnitude under ordinary conditions of observing. It is, of course, important to bear in mind that, as d is increased, the size of the diffraction disk decreases according to theory only if the seeing is very good. A small instrument will, therefore, be much more likely to reach the theoretical limiting magnitude than one as large as the 100-inch.

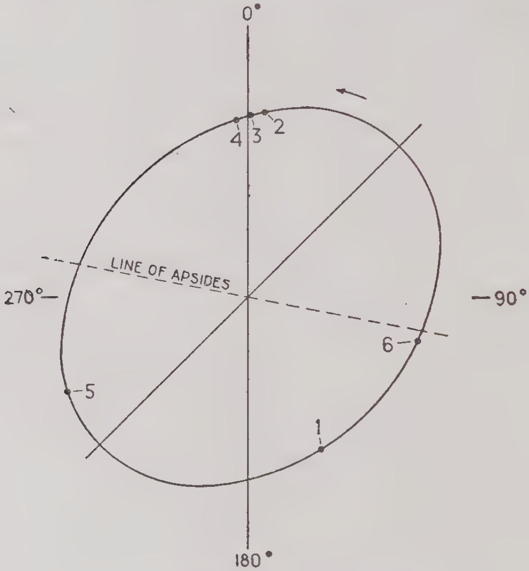

FIG. 3.—Apparent orbit of Capella

When d is greater than 0.3 D, so that the fringe system covers all of the diffraction disk, the normal phase-changes over the latter begin to produce an appreciable effect. If, for example, two stars of equal intensity are observed, d being greater than 0.3 D, and D being so chosen that the fringes should just disappear, one finds that although they do disappear at the center of the disk, they may still be seen at the ends of a diameter parallel to the line

PLATE XII

a

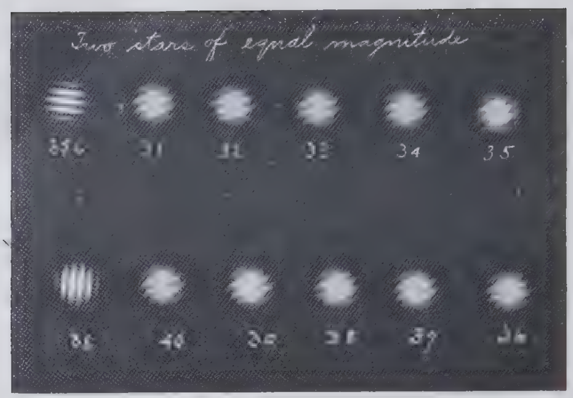

Position Angle of Stars 266°

b

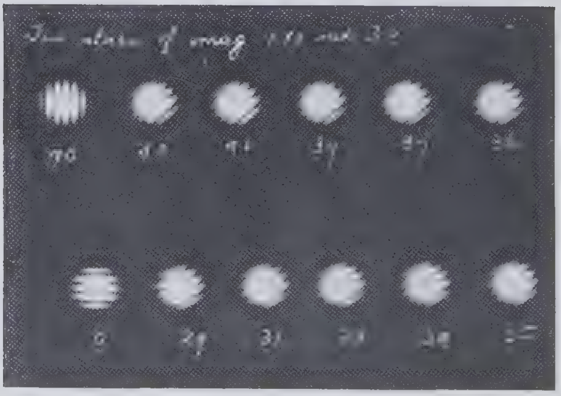

Position Angle of Stars 270°

APPEARANCE OF INTERFERENCE SYSTEM FROM ARTIFICIAL STARS IN THE LABORATORY joining the two stars. If, say, the star on the right side is brighter than that on the left, the fringes will be visible at the center, but will disappear at some point between the center and the left side. These phenomena are beautifully shown if D is so chosen that θ is around 45°, the fringes being inclined at 45° to the line joining the two stars. Plate XII is reproduced from two series of photographs made to illustrate this point. The position angle of the artificial double star used in Plate XII *a* was 266°, and the two stars had the same magnitude. The number under each image shows the position angle of the interferometer when the photograph was made. Plate XII *b* shows a similar set for two stars in position angle 270°, their magnitudes differing by 1.17. It will be observed that in each set the image made at 35° shows the fringes on the right side out of step by half a fringe with the fringes on the left side. In *a*, however, the two systems meet in a vertical line across the center of the image, while in *b* this line is near the left edge. From this it is clear that if one uses a relatively large value of d, and the seeing is good enough to enable one to see the phenomena just described, there should be no difficulty in estimating the difference in brightness of the components, provided this does not exceed say 1.5 mag., or in removing completely the uncertainty of 180° in the value of the position angle. Experience also shows that with a pattern such as shown in Plate XII the probable error of a single setting for θ is not greater than 1°; in fact, the probable error of the mean of 10 settings seldom exceeded 0°15. The observed co-ordinates of Capella are as follows:

RESULTS FOR CAPELLA

Observation	Date G.M.T.	Distance	Position Angle	Remarks
1.......	1919 Dec. 30.6	0″0418	148° ±10°	Position angle only roughly estimated
2.......	1920 Feb. 13.6	0.0458	5.0	
3.......	Feb. 14.6	0.0451	1.0	
4.......	Feb. 15.6	0.0443	356.4	
5.......	Mar. 15.6	0.0505	242.0	
6.......	Apr. 23.6	....	107.0	Observed distance (0″0402) greatly in error on account of daylight

The following spectroscopic elements for Capella are taken from Campbell's *Second Catalogue of Spectroscopic Binaries:*[1]

P	T	ω	e	$a \sin i$	$m \sin^3 i$
104.022	J.D. 2,414,899.5	117.3	0.016	36,847,900 km	0.19
....	....	(297.3)	....	46,430,000 km	0.94

Adding 72 P to T, we have $T' =$ J.D. 2,422,389.1 as a convenient time of periastron for our calculations. The data are not well distributed and indeed are insufficient for a complete revision of the elements; but a slight change in P is, of course, allowable, and for purposes of fitting the observed and calculated positions we may regard T' as variable with limits of ±2 days.

Let ρ and v be the radius vector and true anomaly in the orbit plane. Let r and ϕ be the radius and angle from the node in the apparent orbit. Then

$$\begin{aligned} \rho \cos (v+\omega) &= r \cos \phi \\ \rho \sin (v+\omega) \cos i &= r \sin \phi \end{aligned}$$

Since the eccentricity is small, we may set $\rho = a(1-e \cos v)$ so that

$$\begin{aligned} r^2 &= a^2(1-e \cos v)^2[\cos^2(v+\omega)+\sin^2(v+\omega) \cos^2 i] \\ &= a^2(1-e \cos v)^2[1-\sin^2 (v+\omega) \sin^2 i] \end{aligned}$$

Combining the fifth observation with each of the first four we can derive four values of a. With the mean value of a we can then find five values of i. The values of a and i thus obtained should agree except for errors in the observations or in the given elements. We have assumed that the given elements are all accurate except P, as indicated above. Using $T' = 2,422,389.1$ we derive:

Observation	$t-T'$	M	v	a	i
1...........	38ᵈ5	133°25	134°59	0″05334	137° 51′
2...........	85.5	289.00	287.27	.05394	132 49
3...........	84.5	292.45	290.75	.05377	134 2
4...........	85.5	295.92	294.27	.05368	134 42
5...........	10.5	36.34	37.43	....	134 42
6...........	49.5	171.32	171.60	....	....
			Mean	0.05368	

---

[1] *Lick Observatory Bulletin*, No. 181.

Reducing T' by 0.9 and then by 1.2 days we have:

Observation	$t-T'$	a	i	$t-T'$	a	i
1	$39^{\mathrm{d}}.4$	$0''.05270$	139°56′	$39^{\mathrm{d}}.7$	$0''.05249$	140°29′
2	84.4	.05280	138 46	84.7	.05250	140 24
3	85.4	.05276	139 11	85.7	.05248	140 38
4	86.4	.05276	139 6	86.7	.05249	140 29
5	11.4	....	139 14	11.7	....	140 30
	Mean	0.05275	....	Mean	0.05249	140 30

By subtracting 1.2 days from T, we arrive at a remarkable constancy in the values of a and i, and conclude that the observations to date are best represented by

$$T'=\text{J.D. }2{,}422{,}387.9,\qquad a=0''.05249,\qquad i=140^\circ 30'$$

Computing the distance and position angle with these values we have:

Observation	r (Observed)	Pos. Ang. (Observed)	r (Calc.)	Pos. Ang. (Calc.)	O−C	
					r	Pos. Ang.
1	$0''.0418$	148° ±10°	$0''.04180$	153°54′	$0''.00000$	....
2	.0458	5.0	.04583	4 34	−0.00003	+0°.4
3	.0451	1.0	.04506	1 0	+0.00004	0.0
4	.0443	356.4	.04430	357 18	0.00000	−0.9
5	.0505	242.0	.05050	242 26	0.00000	−0.4
6	....	107.0	0.04391	107 12	....	−0.2

The agreement is, perhaps, better than we have any reason to expect, due possibly to the fact that the number of observations is small. However, taking the results as they stand, we can substitute in the elements as given by Campbell and derive:

$$P=104.006\text{ days.}\quad a_1+a_2=130{,}924{,}000\text{ km.}$$
$$\pi=0''.0600;\quad m_1=4.62\odot;\quad m_2=3.65\odot.$$

It remains to be seen whether recent spectroscopic observations are in agreement with this new value of the period.

Mount Wilson Observatory
June 1920

Contributions from the Mount Wilson Observatory, No. 186
Reprinted from the *Astrophysical Journal*, Vol. LI, pp. 276–308, 1920

PHOTOGRAPHS OF NEBULAE WITH THE 60-INCH REFLECTOR, 1917–1919

By FRANCIS G. PEASE

ABSTRACT

Photographs of nebulae with the 60-inch reflector.—About 330 of the nebulae found on the 66 plates taken by the author during the years 1917–1919 are listed or described in this article, and 27 of these are illustrated on the 18 plates reproduced. The most remarkable are: N.G.C. 2146, Camelopardus, with its handlike dark marking, a spiral with an abnormal center; N.G.C. 3379, resembling an unresolved star cluster; N.G.C. 3384, with a dual, Saturn-like nucleus and symmetrical wings; N.G.C. 4395–4399–4400–4401, which together form a remarkable spiral; N.G.C. 4656–4657, which constitute a single right-handed spiral without a well-defined nucleus; and I.C.II 5146 Cygnus, a unique array of light and dark markings. In addition the following are described: (1) Spirals: N.G.C. 48, 1186, 1699, 2290, 2291, 2964, 2968, 3310, 3367, 3389, 3395–3396, 3786, 3788, 5257, 5258, 5278–5279, 5544, 5545, 6014 (?), 6906, 6928, 6930, 7722; I.C.II 1441, 2233. (2) Round or elongated: N.G.C. 49, 51, 1700, 2274, 2275, 2288, 2289, 2970, 3377, 3391, 5557, 5868, 5869, 6017, 6927, 7240, 7242, 7435, 7436, 7611, 7615, 7617, 7619, 7621, 7623, 7627, 7631; I.C.I 922, 928; I.C.II 5192, 5194, 5195. (3) Misc.: N.G.C. 955, 2294 (spindles); 1491, 1555, 2024, 2245, 2247, 2359, 2403, 2537, 6820, 6888, 7023 (irregular); 3357 (stellar); 6703(?), 7048 (planetary); I.C.I 931 (stellar); 1470 (irregular); I.C.II 5191 (spindle). (4) Uncatalogued nebulae numbering 255. *Variations from N.G.C.*—The positions for N.G.C. 48, 49, 51, 2247, 5544, 5545, 6927, 6928, and 6930 were given incorrectly. N.G.C. 5865, 5871, and 7433 were not found. N.G.C. 6823 is a cluster and N.G.C. 6846 is a group of stars. In four cases, indicated above by dashes, two or more nebulae seem to form parts of a single system. *Variable nebulae.*—The changes in N.G.C. 1555 are described and also possible differences in the nuclear region of N.G.C. 2245, which will be investigated further. Other nebulae, N.G.C. 955, 1186, 2024, and 7023, showed no change.

Spectra of two nebulae.—N.G.C. 1700 is of type G0 or later and has a large radial velocity. The spectrum of the nucleus of N.G.C. 3379 is G0 or later and the radial velocity is +850 km per sec.

This series of observations of nebulae covers the writer's work in direct photography with the 60-inch reflector during the years 1917–1919. The program included (*a*) peculiar nebulae, e.g., N.G.C. 3395–3396; (*b*) groups of nebulae with a view to future measurement, e.g., N.G.C. 48, 49, 51; I.C.I 922, etc.; (*c*) variable nebulae such as N.G.C. 1555; (*d*) previously observed nebulae requiring additional photographic data, these being indicated with an asterisk thus: N.G.C 955*; (*e*) a few objects for special purposes, and several affording data for classification photographed during intervals in the regular program. In addition a search for spirals was made along the Milky Way among the smaller nebulae with no success thus far.

Trails for orientation were made on practically all the plates. Many of the measures have been made with a polar co-ordinate machine; and while this serves admirably for the determination of orientation and distances, the magnification (12) is too high for use in determining the size of the objects. For these data recourse was had to the polar co-ordinate réseau and a low-power magnifier. Many objects appearing near the edges of the plates have been listed; but it is to be remembered that at 10′ from the center of the field a star image is oval, and at 15′ it is comate or arrow-shaped, although poor seeing rounds out these forms, with some increase in size. The smaller nebulae not listed in the N.G.C., or the *Index Catalogue*, are listed as *a*, *b*, *c*, etc., in order of their right ascension.

The descriptions apply to a particular plate or to the general results from a number of plates of the same object, and are not co-ordinated into a homogeneous series of intensities corresponding to the N.G.C. The nebulae have been separated into four orders of brightness: faint, F; medium faint, MF; medium bright, MB; bright, B. The following abbreviations have also been used in the descriptions: R, round; Irr., irregularly; gbM, gradually brighter in the middle; lbM, little brighter in the middle; Nu., nucleus; sbM, suddenly brighter in the middle. All illustrations are placed with N at the top, *p* on the right.

As before, the positions are those of the N.G.C. brought forward to the year 1920. A number of these have been found incorrect, and recourse has been had to Bigourdan's *Observations des Nebuleuses et d'Amas Stellaires* to obtain the correct data.

Photographs of several objects taken with the 100-inch reflector have been used in this paper and are designated with the prefix 100−. Several of Mr. Shapley's photographs showing nebulae have been used in compiling the descriptions. These are designated as *Shapley* 2968, etc.

TABLE I

NEGATIVES WITH THE 60-INCH REFLECTOR

N.G.C.	α 1920	δ 1920	Constellation	G.C.	H and Others	*h*	Type	Plate No.	Illustration	Remarks
48......	$0^h\ 9^m 52^s$	+47°47′.8	Lacerta	....	Barnard	......	Spl.	309		8 additional Nebulae on plate
49......	0 10 13	48.0	Lacerta	....	A.N.	......	Elong.	309		
50......	0 10 26	48.9	Lacerta	....	4136	......	Elong.	309		
955*.....	2 26 29	− 1 27.8	Cetus	551	II 278	229	Spe.	319		15 additional
1186*.....	3 0 16	+42 30.9	Perseus	639	IV 43	281	Spl.	310	XIII*d*	20 additional
1491......	3 57 21	+51 5.6	Perseus	791	I 258	......	Irr.	308	XIII*c*	
1555*.....	4 17 17	+19 20.1	Taurus	839	Hind	......	Var.	312, 322		
1699......	4 53 3	− 4 52.8	Eridanus	....	....	......	Spl.	314, Hoge 3		
1700......	4 53 0	− 4 59.3	Eridanus	932	IV 32	336	R	314, Hoge 3		
2024......	5 37 49	− 1 53.6	Orion	1227	V 28	......	Irr.	316		
2146......	6 5 53	+78 23.	Camelopardus	5357	Winnecke	TI	Spl.	358	XIII*f*	
2245......	6 28 17	+10 13.2	Monoceros	1425	IV 3	393	Fan.	323, 329	XIV*a*	
2247......	6 28 45	+10 23.7	Monoceros	....	Ld. R, SwI	......	Irr.	323, 329		
2274......	6 42 2	+33 39.0	Gemini	1448	II 615	406	R	313		
2275......	6 42 3	41.0	Gemini	1449	II 614	407	R	313		
2288......	6 45 28	29.1	Gemini	1455	Ld. R	......	R	311, 315	XIV*a*	12 additional
2289......	6 45 29	30.9	Gemini	1456–7	II 898	410	Elong.	311, 315		
2290......	6 45 33	27.7	Gemini	5369	III 897?	......	Spl.	311, 315		
2291......	6 45 35	33.0	Gemini	1458	III 897?	409	Spl.	311, 315		
2294......	6 45 47	33.2	Gemini	1460	Ld. R	......	Spe.	311, 315		
2359......	7 13 50	−13 4.1	Canis Major	1511	V 21	3075	....	320	XIV*b*	
2403*.....	7 29 7	+65 46.5	Camelopardus	1541	V 44	......	....	307		
2537......	8 7 35	+46 14	Lynx	....	....	......	Irr.	359, Sh.2968		
2903......	9 27 39	+21 51.2	Leo Major	1861	I 56	6041	Single	282		No text given
2905......	9 27 41	+21 52.3	Leo Major	1863	I 57	6042	Spl.			
2964......	9 38 11	+32 12.8	Leo Minor	1896	I 114	622	Spl.	321, 324		15 additional
2968......	9 38 28	+32 17.7	Leo Minor	1899	II 491	624	El. Spl.	321, 324		
2970......	9 38 48	+32 20.7	Leo Minor	1901	....	627	Elong.	321, 324		
3310......	10 33 48	+53 55.1	Ursa Major	2158	IV 60	731	Spl.	356		
3357......	10 40 6	+14 30.3	Leo Major	5533	....	......	Neb. Star	291		No text given
3367......	10 42 21	+14 10.2	Leo Major	2193	II 78	748	Spl.	289, 327	XIII*e*	9 additional
3377......	10 43 28	+13 24.4	Leo Major	2201	II 99	754	Elong.	289, 327		4 additional
3379......	10 43 37	+13 0.2	Leo Major	2203	I 17	757	R	290, 334	XV*a*	See text 3377
3384......	10 44 4	+12 3.1	Leo Major	2207	I 18	758	Elong.	290. 334		
3389......	10 44 14	+12 57.0	Leo Major	2211	II 41	761	Spl.	290, 334		
3391......	10 44 45	+14 38.6	Leo Major	5535	....	......	Elong.	289, 327		
3395......	10 45 23	+33 24.4	Leo Minor	2216	I 116	765	Double	286, 332	XVI*a*	
3396......	10 45 28	+33 24.9	Leo Minor	2217	I 117	766	Spiral			
3786......	11 35 29	+32 21.3	Ursa Major	2479	....	931	Spiral	337, 338	XIII*b*	26 additional
3788......	11 35 32	+32 22.8	Ursa Major	2480	....	932	Spiral			
4395......	12 21 51	+33 59.4	Canes Venatici	2958	V 29.1	1252	Single	330,331,333	XV*b*	
4399......	12 22 ±	+34 ±	Canes Venatici	2959	V 29.2	......	.....			
4400......	12 22 ±	+34 ±	Canes Venatici	2960	Ld. R	......	Spiral			
4401......	12 22 1	+33 57.5	Canes Venatici	2962	Ld. R	......	.....			

4656	12 40 5	+32 36.2	Canes Venatici	3189	I 176	1414	Single }	336, 339	XVI*b*	11 additional
4657	12 40 14	+32 39.4	Canes Venatici	3190	I 177	1415	Spl. }			
5257	13 35 49	+ 1 14.7	Virgo	3624	II 895	1654	Spl.	345 }	XVII*b*	
5258	13 35 53	+ 1 14.3	Virgo	3625	II 896	1655	Spl.	345 }		
5278	13 38 40	+56 4.3	Ursa Major	3639	II 798	1665	Single }	341, 342	XVII*a*	
5279	13 38 45	+56 4.5	Ursa Major	....	Ld. R	1665a	Spl. }			
5544*	14 13 40	+36 56.5	Boötes	3833	II 419	1771	Spl.	127, 260, 261 }	XVIII*b*	13 additional
5545*	14 13 41	+36 56.8	Boötes	3834	Ld. R	......	Spl.	127, 260, 261 }		
5557	14 15 5	+36 51.6	Boötes	3843	I 99	1776	Elong.	127, 260, 261		
5865	15 5 43	+ 0 48.	Serpens	4057	II 684	......	....	328, 335		Not on plate
5868	15 5 44	+ 0 50.2	Serpens	4060	dA	......	R	328, 335		
5869	15 5 45	+ 0 46.6	Serpens	4061	II 545	1908	Elong.	328, 335		
5871	15 5 57	+ 0 49.1	Serpens	....	....	T V	....	328, 335		Not on plate
6014	15 52 1	+ 6 9.7	Serpens	4148	....	1940	Spl?	325		
6017	15 53 19	+ 6 13.6	Serpens	4150	....	1941	Elong.	325		
6703*	18 45 0	+45 27.7	Lyra	5931	....	......	Plan?	344		10 additional
6820	19 39 3	+22 53.3	Vulpecula	5945	....	......	Irr.	298		
6823	19 39 48	+23 6.5	Vulpecula	4512	VII 18	2049	Cluster	298		
6846	19 53 22	+32 8.4	Cygnus	5948	....	......	Group of stars	295		
6888	20 9 33	+38 9.1	Cygnus	4561	IV 72	......	Irr.	299, 301, 348	XVIII*c*	
6906	20 19 36	+ 6 12.3	Sagitta	5956	m 40	......	Sp.	352		
6927	20 28 46	+ 9 38.6	Delphinius	5962	....	......	Elong.	347, 350		4 additional
6928	20 28 58	+ 9 39.2	Delphinius	5963	....	......	Spl.	347, 350		
6930	20 29 7	+ 9 34.6	Delphinius	5964	....	......	Spl.	347, 350		
7023*	21 0 37	+67 51.	Draco	4634	IV 74	......	Irr.	343		
7048	21 11 23	+45 57.4	Cygnus	....	St. IV	......	Plan.	296		
7240	22 11 53	+36 52.7	Lacerta	6033	St. V	......	Elong.	292, 354, 357		19 additional
7242	22 12 10	+36 53.7	Lacerta	6035	St. V	......	Elong.	292, 354, 357		
7431	22 53 47	+25 44.2	Pegasus	....	Bigourdan	......	....	293		Star on plate
7433	22 54 2	+25 43.2	Pegasus	4872	Ld. R	......	....	293		Not on plate
7435	22 54 6	+25 42.2	Pegasus	4873	Ld. R	......	R	293		
7436	22 54 6	+25 43.3	Pegasus	4871	III 243	2195	R	293		14 additional
7611	23 15 33	+ 7 22.5	Pegasus	4934	dA	......	Elong.	351		
7615	23 15 53	+ 7 58.5	Pegasus	4935	....	2229	Elong.	351		
7617	23 16 2	+ 7 43.7	Pegasus	6186	m 572	......	Elong.	351		
7619	23 16 12	+ 7 46.	Pegasus	4936	II 439	2230	R	351		
7621	23 16 20	+ 7 55.7	Pegasus	6188	m 574	......	Elong.	351		
7623	23 16 27	+ 7 57.5	Pegasus	4938	III 435	2231	R	351		
7626	23 16 39	+ 7 46.7	Pegasus	4940	II 440	2233	R	351		
7631	23 17 24	+ 7 46.7	Pegasus	4942–3	Ld. R	......	Elong.	351		
7722	23 34 41	+15 31.0	Pegasus	6216	....	......	Spl.	353		
I 922	13 40 17	+56 0.4 }		Barnard						
I 928	13 40 43	+56 1.2 }	Ursa Major	AN	....	......	....	341, 342		72 additional
I 931	13 40 49	+56 1.3 }		4136						
I 1441	22 11 47	+36 53.8	Lacerta	....	Bigourdan	......	....	292		See text N.G.C. 7240
I 1470	23 1 51	+59 48.9	Cassiopeia	Spitalier 62	Barnard 3110	......	Irr.	297	XVIII*a*	3 additional
II 2233	8 8 19	+45 59.5	Lynx	....	....	......	Spl.	Sh.2968, 359		
II 5146	21 50 25	+46 53.2	Cygnus	Espin	Wolf	......	Irr.	276, 349	XVII*c*	
II 5191 }										
II 5192 }	22 12 7±	+36 52.8±	Lacerta	....	....	......	....	292		See text N.G.C. 7240
II 5194 }										
II 5195	22 12 11	+36 53.8		....	....	......	....	....		

PLATE XIII

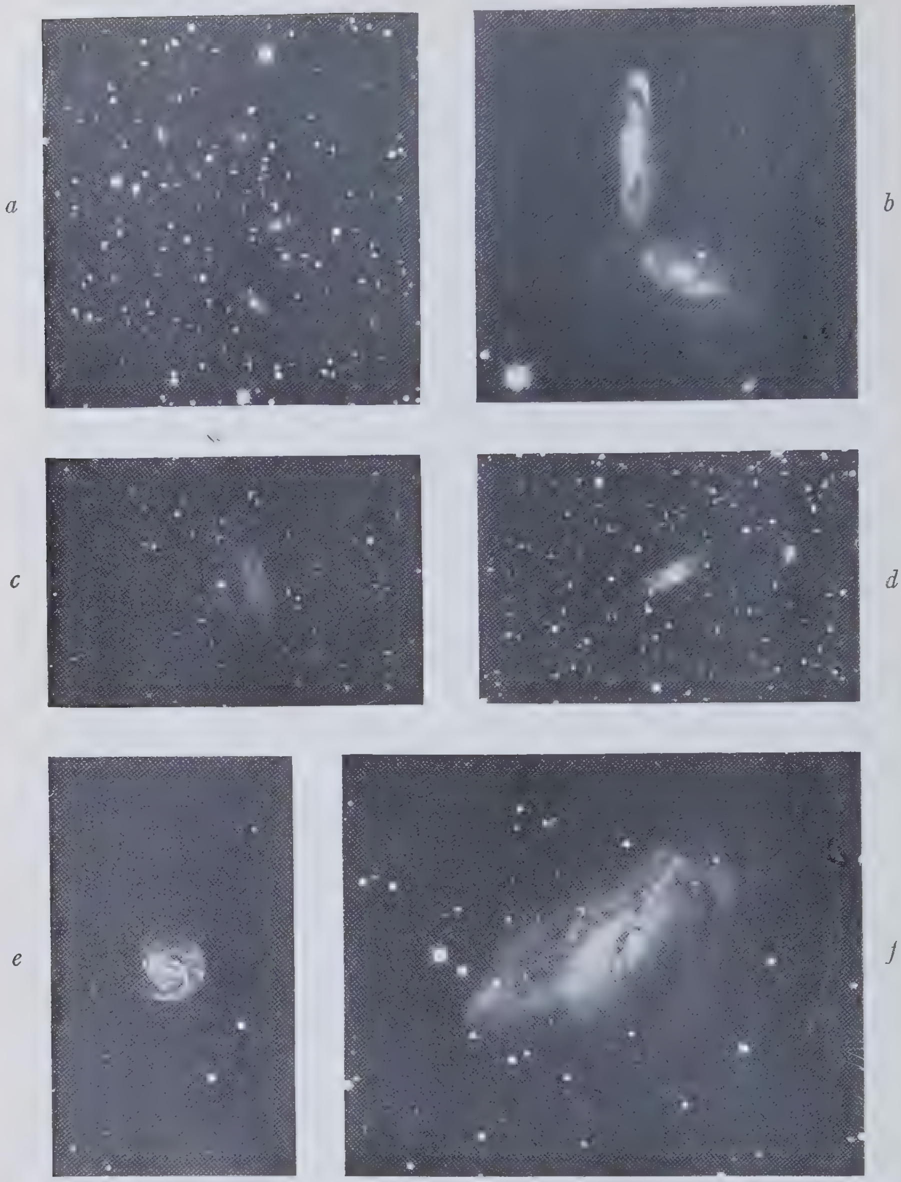

a. N.G.C. 2288, 2289, 2290, 2291, 2294, Exposure, 210^{m} S 27, Enlargement, 1.9, 1 mm = 14.″4
b. N.G.C. 3786, 3788 Exposure, 135 S 27, Enlargement, 5.6, 1 mm = 4.9
c. N.G.C. 1491 Exposure, 160 S 23, Enlargement, 1.9, 1 mm = 14.4
d. N.G.C. 1186 Exposure, 220 S 27, Enlargement, 1.9, 1 mm = 14.4
e. N.G.C. 3367 Exposure, 150 S 30, Enlargement, 2.4, 1 mm = 11.2
f. N.G.C. 2146 Exposure, 258 S 23, Enlargement, 3.5, 1 mm = 7.8

PLATE XIV

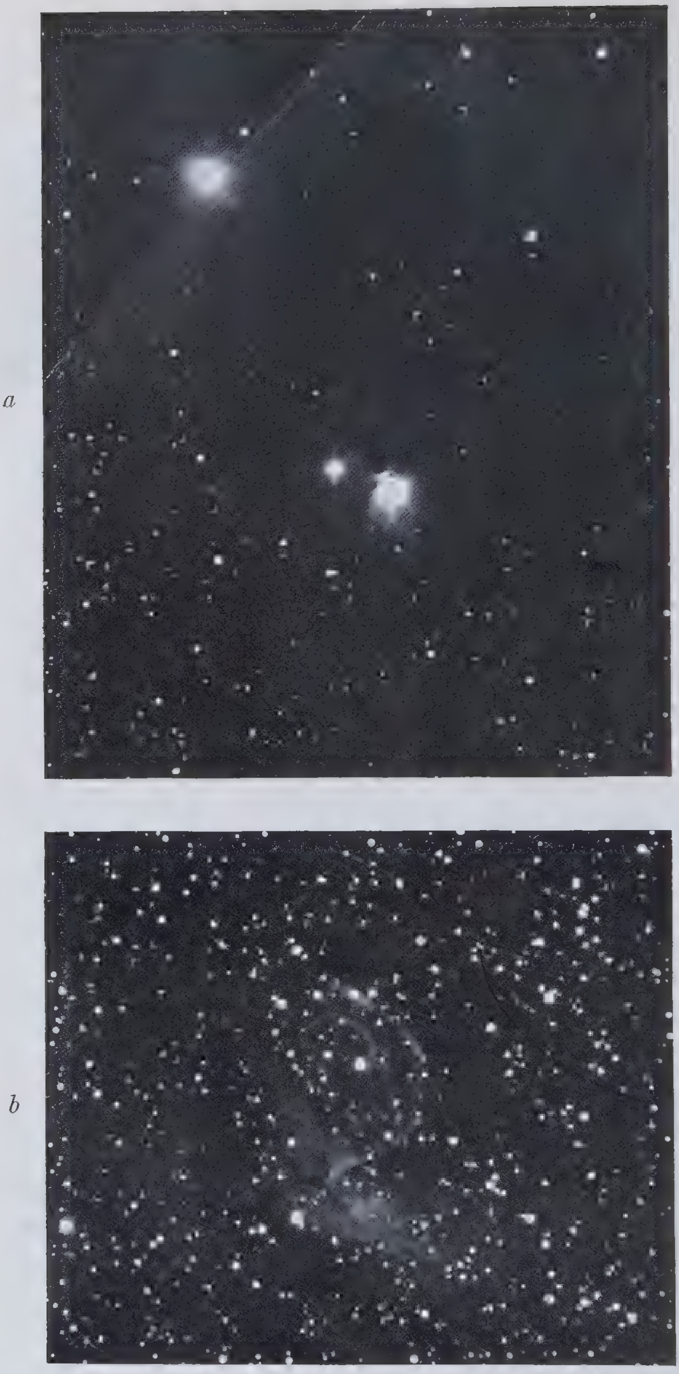

a. N.G.C. 2245, 2247, Exposure, 95^{m} S 30, Enlargement, 1.9, 1 mm = 14″4
b. N.G.C. 2359, Exposure, 210 S 23, Enlargement, 2.5, 1 mm = 11.0

PLATE XV

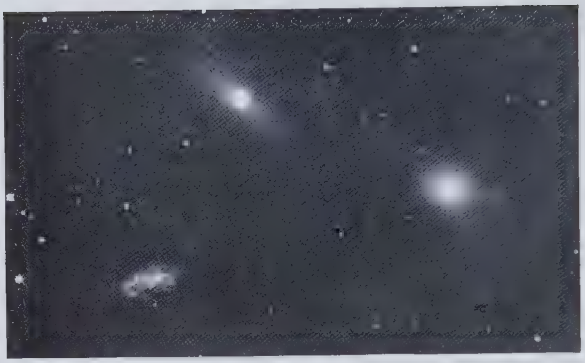

a

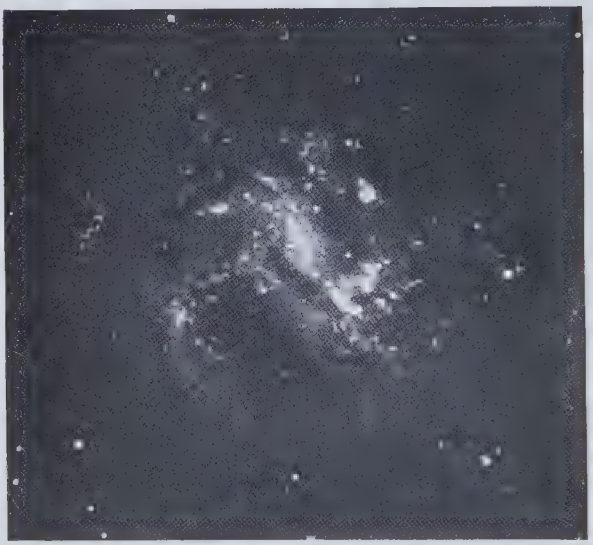

b

a. N.G.C. 3379, 3384, 3389, Exposure, 120^m S 23, Enlargement, 1.9, 1 mm = $14.''4$
b. N.G.C. 4395, 4399, 4400, 4401, Exposure, 450 S 30, Enlargement, 2.0, 1 mm = 13.3

PLATE XVI

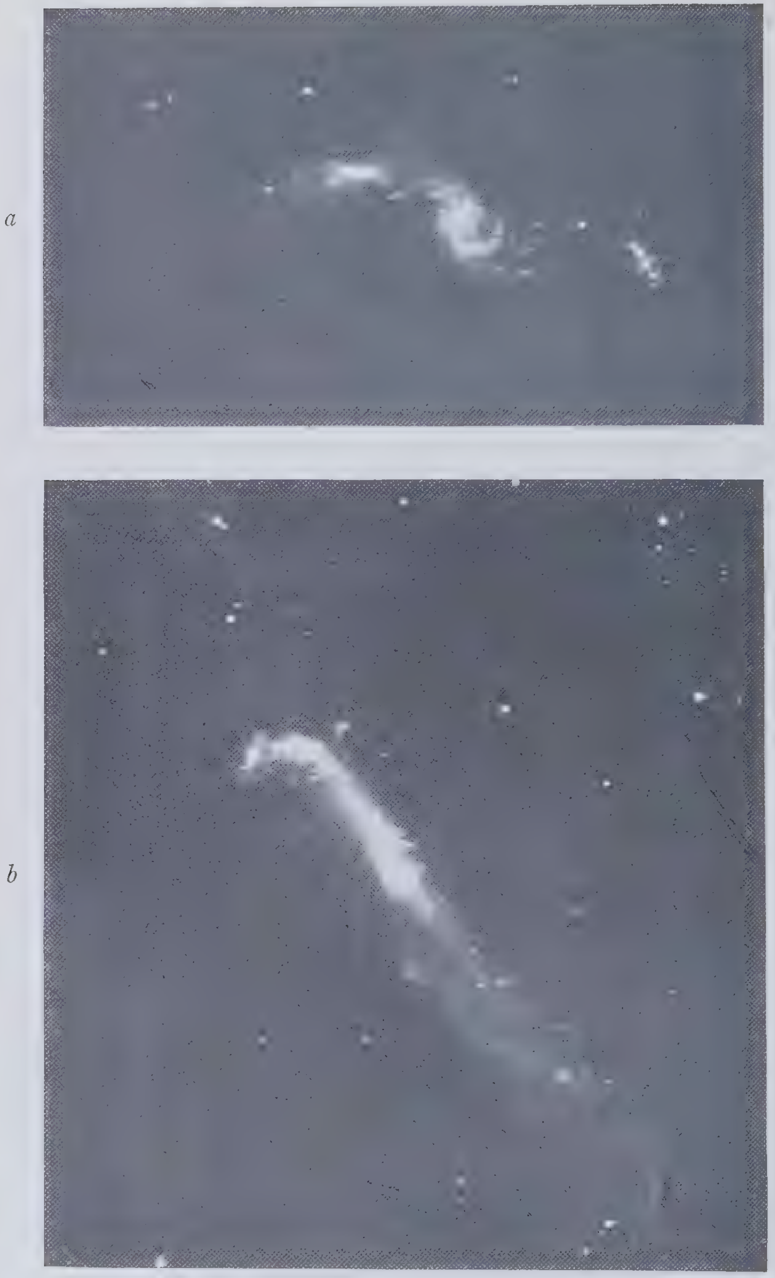

a. N.G.C. 3395–96, Exposure, 120^{m} S 23, Enlargement, 5.6, 1 mm = $4\overset{\prime\prime}{.}9$
b. N.G.C. 4656–57, Exposure, 240 S 30, Enlargement, 1.9, 1 mm = 8.5 (100-inch)

PLATE XVII

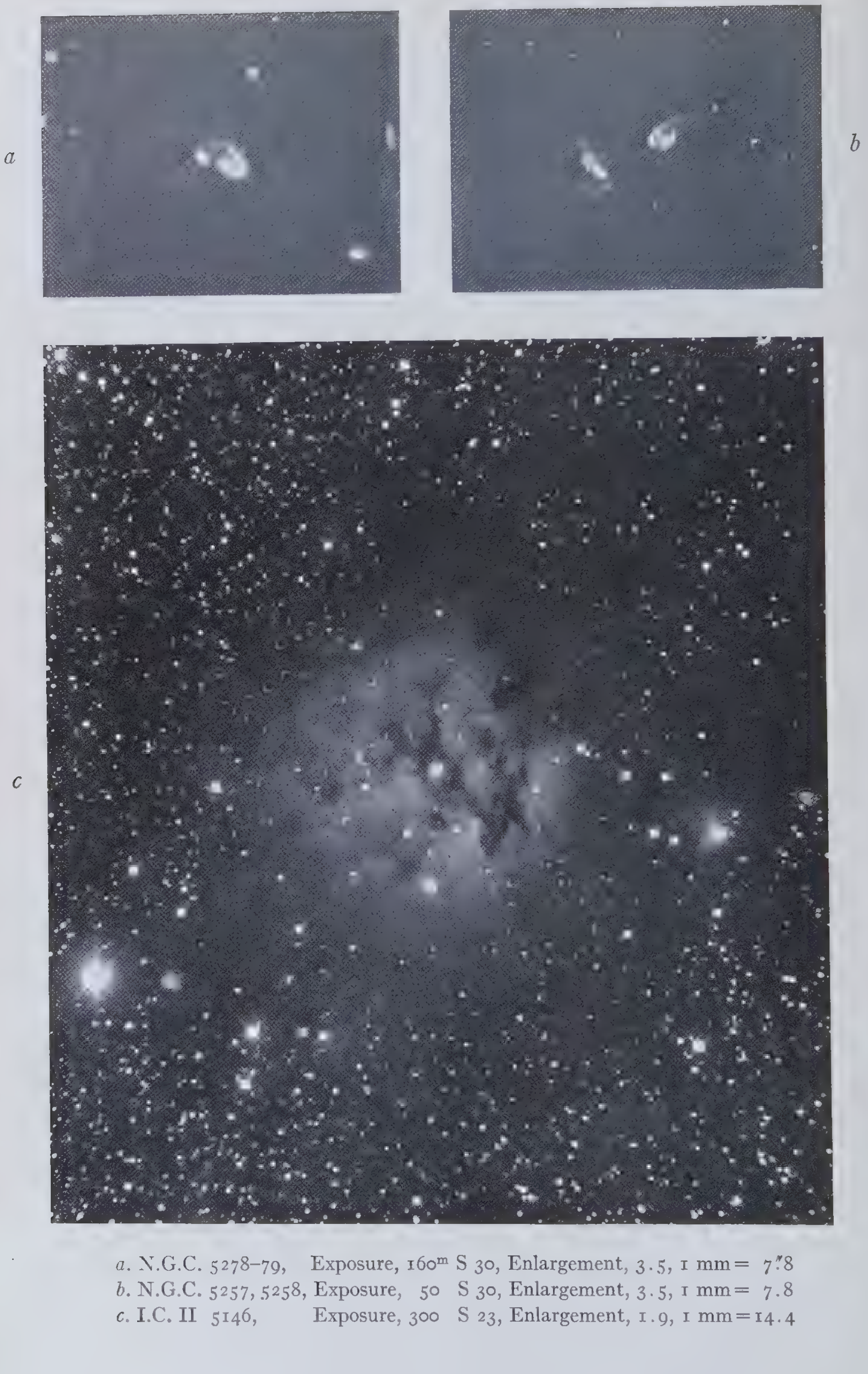

a. N.G.C. 5278–79, Exposure, 160^m S 30, Enlargement, 3.5, 1 mm = 7″.8
b. N.G.C. 5257, 5258, Exposure, 50 S 30, Enlargement, 3.5, 1 mm = 7.8
c. I.C. II 5146, Exposure, 300 S 23, Enlargement, 1.9, 1 mm = 14.4

PLATE XVIII

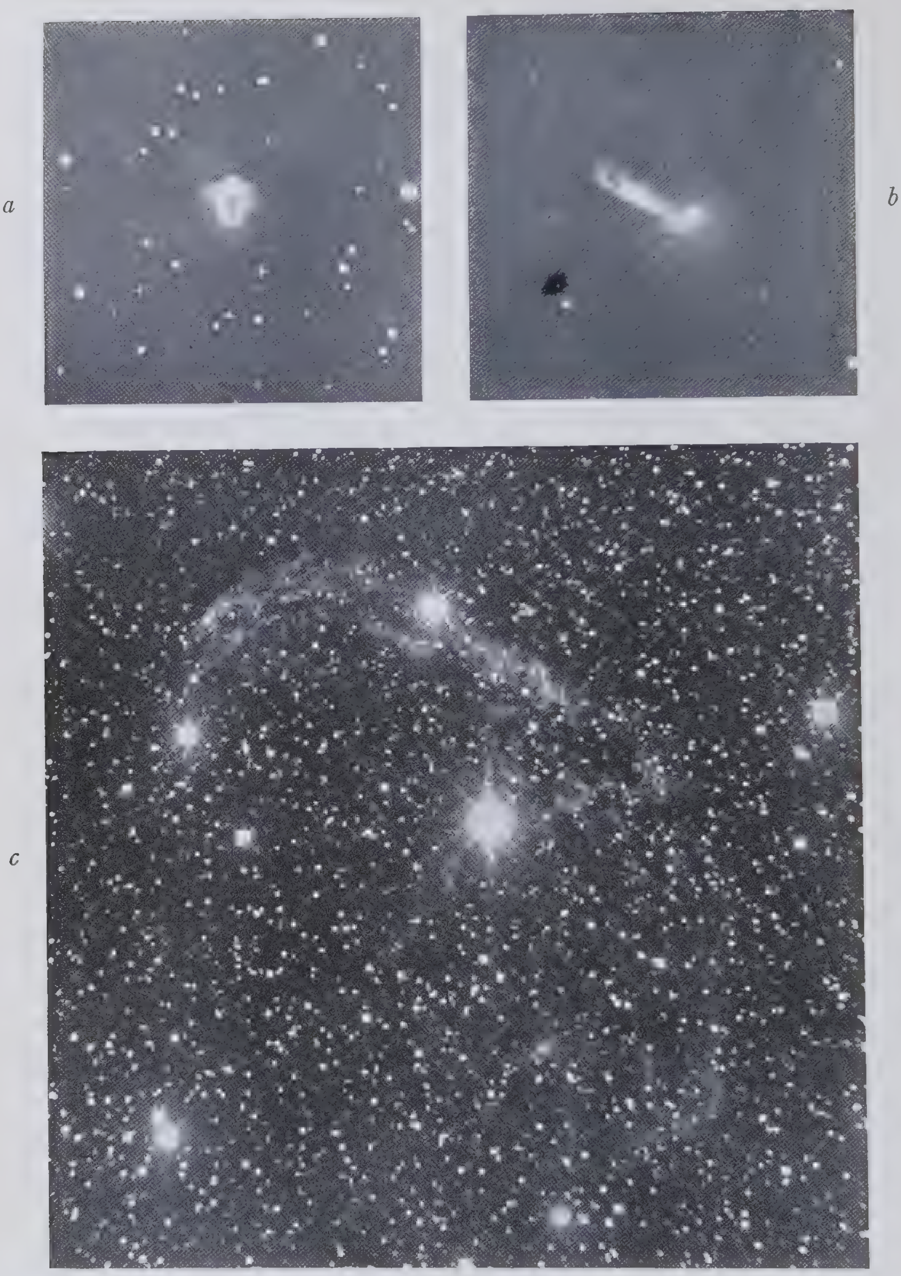

a. I.C. I 1470, Exposure, 190^{m} S 23, Enlargement, 5.5, 1 mm = 5″.0
b. N.G.C. 5544, 5545, Exposure, 360 S 27, Enlargement, 5.5, 1 mm = 5.0
c. N.G.C. 6888, Exposure, 300 S 30, Enlargement, 2.4, 1 mm = 11.2

To increase their sensitiveness, the plates were given a preliminary exposure. Before use at the telescope they were exposed to an 8 c. p. red lamp at a distance of six feet. The amount varied from twenty to forty seconds, depending upon the length of exposure to be given at the telescope.

Mr. W. P. Hoge, Mr. J. C. Duncan, Mr. Hugo Benioff, and Mr. Milton Humason have assisted in making the plates, and to them the writer wishes to express his gratitude for the help rendered. I am indebted to Mr. Ellerman for the preparation of the positives for the half-tones.

N.G.C. 48, 49, and 51, Lacerta

N.G.C. 48 $\alpha=0^h\ 9^m 52^s$, $\delta=+47^\circ 47'.8$
N.G.C. 49 $\alpha=0\ 10\ 13$, $\delta=+47\ 48.0$ (1920); $\lambda=84^\circ$, $\beta=-14^\circ$
N.G.C. 51 $\alpha=0\ 10\ 26$, $\delta=+47\ 48.9$

Plate No. 309, 1917, November 16, 130^m. Images large

A group of eleven nebulae, six of which are described by Barnard in *A.N.* 4136. Eight are elliptical in shape, the other three irregularly round. Two have distinct spiral structure, four have strong bright, almost stellar, nuclei. Two are medium-faint, almost uniform spindles, and the remainder, faint patches with slightly brighter middle.

The positions given in the N.G.C. are not correct, those above being obtained from Barnard's corrected values. The following is a description of the nebulae, measures being referred to the nucleus of N.G.C. 51.

a, *p*	250°	*d*	15′.5	MF	12″×6″, *p* 161°.
b,	234		10.5	MB	20″×10″, *p* 65°, almost stellar Nu.; Barnard No. 1.
c,	227		8.7	MB	Spiral, 45″×15″, *p* 168°, gbM, vs almost stellar Nu.; Barnard No. 2.
d,	257		5.7	MB	Spiral, 45″×30″, *p* 11°, N.G.C. 48, Barnard No. 3.
e,	202		7.3	MF	9″ diameter with almost stellar Nu., Barnard No. 4.
f,	308		2.7	F	10″ diameter gbM.
g,	256		2.1	MF	12″×9″, *p* 161°, gbM, B almost stellar Nu., N.G.C. 49, Barnard No. 5.
h,			0	MB	30″×18″, *p* 59°, B, almost stellar Nu. on sp edge of central B patch 10″ diameter, N.G.C. 51, Barnard No. 6.

i,	0	8.0	F	Patch 10″ diameter.
j,	13	6.4	MF	Patch 10″ gbM.
k,	18	10.7	MF	Spindle 30″×6″, *p* 19°, gbM.

N.G.C. 955,* Cetus

$\alpha=2^h26^m29^s$, $\delta=-1°27'.8$ (1920); $\lambda=138°$, $\beta=-54°$

Plate No. 319, 1917, December 17, 30^m; 18, 65^m. Total 95^m. Images large

A so-called variable nebula, but thought by Dreyer to be unchanging. This plate was made for comparison with No. 229. It is stronger than the 1913 plate; the general dimensions are increased to 113″×10″, but there is no change of relative intensity in the different parts of the nebula. Many small nebulae are shown on both plates; 15 of the more important ones are as follows, the measures referring to the nucleus of N.G.C. 955:

a, *p*	249°, *d*	16′.3		Nebulous spot.
b,	346	15.1	F,	uniform, 8″ diameter.
c,	214	4.9	F,	spindle, 20″×4″, *p* 32°, BM.
d,	31	8.2	F,	sliver, 10″×2″, *p* 15°.
e,	35	6.9	MF,	spindle, 12″×3″, *p* 115°, gbM.
f,	162	13.6	MF,	spindle, 20″×6″, *p* 44″, gbM, Nu.
g,	156	16.0	MF,	spindle, 5″ diameter, gbM, Nu.
h,	59	7.9	F,	sliver, uniform, 15″×3″, *p* 30°.
i,	88	8.5	MF,	uniform 12″ diameter, with Nu. 2″ diameter elongated 143°.
j,	146	14.3	F,	uniform, 6″ diameter.
k,	146	20.0	MF,	8″ diameter, gbM.
l,	84	16.5	MF,	spindle, 10″×4″, *p* 63°, gbM, Nu.
m,	61	20.5	MB,	spindle, 13″×6″, *p* 40°, gbM, Nu. (edge of plate).
n,	94	17.8	F,	8″ diameter gbM (edge of plate).
o,	98	19.2	MF,	10″ diameter gbM (edge of plate).

N.G.C. 1186,* Perseus

$\alpha=3^h0^m16^s$, $\delta=+42°30'.9$ (1920); $\lambda=115°$, $\beta=-13°$

Plate No. 310, 1917, November 16, 220^m. S 27.
Images large. Illustrated Plate XIII*d*

This photograph was made for comparison with No. 245, taken in 1914. This supposedly variable nebula has undergone no relative change since 1914. The longer exposure brings out, however, the spiral structure more clearly and shows the nebulosity extending to 2′.5×0′.8. The arrangement of the arm is not regular.

Many small nebulae are on the plate, among them the following. The measures refer to the nucleus of N.G.C. 1186, and not to the star.

a, *p*	233°, *d*	18″.8	MF,	9″ diameter, nebulous spot, fades at edges.
b,	326	19.9	MF,	8″ diameter, nebulous spot, fades at edges.
c,	229	13.7	MF,	10″ diameter, nebulous spot, gbM.
d,	229	12.2	MF,	6″ diameter, nebulous spot, gbM.
e,	312	11.1	F,	7″×2″, *p* 135°, nebulous patch.
f,	262	8.0	MF,	7″×2″, *p* 50°, nebulous spot.
g,	331	15.8	MF,	5″ diameter, nebulous spot, gbM.
h,	346	12.5	F,	4″ diameter, nebulous spot, gbM.
i,	349	13.3	F,	4″ diameter, nebulous spot, gbM.
j,	190	10.6	MF,	5″ diameter, nebulous spot, gbM.
k,	350	7.3	F,	5″ diameter, nebulous spot, gbM.
l,	353	11.2	MF,	11″ diameter, nebulous spot, gbM.
m,	357	9.5	MF,	3″ diameter, nebulous spot, gbM.
n,	178	5.3	MB,	35″×6″, *p* 65°, spindle, stellar Nu.
o,	87	1.8	F,	10″×2″, *p* 23°, thread.
p,	55	2.5	MF,	10″×8″, *p* 9°, nebulous spot, gbM.
q,	141	7.6	MB,	8″ diameter, almost a nebulous star.
r,	73	7.0	F,	5″ diameter, nebulous spot, gbM.
s,	90	13.6	B,	9″ diameter, nebulous star.
t,	55	17.4	MB,	7″ diameter, nebulous spot.

N.G.C. 1491, Perseus

$\alpha=3^h57^m21^s$, $\delta=+51°5'.6$ (1920); $\lambda=118°$, $\beta=-1°$

Plate No. 308, 1917, October 20, 45^m. Cramer Crown.
Images small and round
Plate No. 355, 1919, December 22, 160^m. S 23. Images
small and round. Illustrated Plate XIII*c*

A tuft of wispy nebulosity, roughly triangular in shape, about 3′ on a side. The effect is produced by three principal V-shaped streamers or filaments, included angle 80°–90°, pointing *p* 225°. They are displaced with respect to one another and thus cross. A star of magnitude 10–11 lies in the fainter nebulosity filling the V.

N.G.C. 1555, Taurus

$\alpha=4^h17^m17^s$, $\delta=+19°20'.1$ (1920); $\lambda=144°$, $\beta=-20°$

Plate No. 312, 1917, November 17, 195^m. S 27. Images small and elongated
Plate No. 322, 1918, February 11, 110^m; 12, 100^m; 13, 110^m. Total 320^m. S 27.
Images medium and round
Plate No. 326, 1919, March 1, 90^m. S 30. Images small and round

For previous descriptions and chart see *Mount Wilson Contribution*, No. 127; *Astrophysical Journal*, **45**, 89, 1917. All three plates show nebulosity *A* remaining about the same, nebulosity *C* extending farther to the W and N. Traces of *G* show as before, while dark regions not sketched show S and E of *K* and *H*.

N.G.C. 1699, 1700, Eridanus

N.G.C. 1699, $\alpha=4^{h}53^{m}3^{s}$, $\delta=-4^{\circ}52'.8$ } (1920); $\lambda=172^{\circ}$, $\beta=-26^{\circ}$
N.G.C. 1700, $\alpha=4\ 53\ 0$, $\delta=-4\ 59.3$

Plate No. 314, 1917, November 18, 120^{m}. S 27. Large images, fairly round
Plate No. 3 (Hoge), 1919, December 24, 110^{m}. S 30. Small round images

N.G.C. 1700 has a very bright center fading away in several gradual steps and forming an ellipse 50″×30″, *p* 92°. The entire mass is soft, having no detail or structure other than the changes in intensity between center and edge. A 23-hour exposure made with the focal-plane spectrograph on the 60-inch reflector gave a spectrum of sufficient strength to show that the type is G0 or later, and that the nebula has large positive radial velocity.

There are two other nebulae on the plate whose positions are given with respect to the nucleus of N.G.C. 1700.

a, N.G.C. 1699, *p* 6°, *d* 6′.6, MB, 30″×17″, *p* 161°. Almost uniform left-handed spiral, vs B Nu. Position given in N.G.C. is incorrect.

b, 129, 13.6 MF, 15″×10″, *p* 9° lbM, vs B Nu.

N.G.C. 2024, Auriga

$\alpha=5^{h}37^{m}49^{s}$, $\delta=+51^{\circ}5'.6$ (1920); $\lambda=174^{\circ}$, $\beta=-15^{\circ}$
Plate No. 316, 1917, November 19, 30^{m}. Cramer Crown.
Images large and round

Comparison of this plate with Keeler's photograph, taken June 28, 1902, shows no apparent change in the nebula (*Lick Observatory Publications*, **8**, Plate 13).

N.G.C. 2146, Camelopard

$\alpha=6^{h}5^{m}53^{s}$, $\delta=+78^{\circ}23'$ (1920); $\lambda=102^{\circ}$, $\beta=+25^{\circ}$
Plate No. 358, 1919, December 23, 258^{m}. S 23. Images medium
and a little elongated. Illustrated Plate XIII*f*

A most remarkable nebula, best described in parts, although actually all blended together. (1) An irregular mass of nebulosity 3′.5×1′, *p* 150° greatly differing in intensity, with dark markings in the direction of its elongation. The nucleus lies a little S of the center of this mass; the nebulosity is brightest around the nucleus. Superimposed on this bright mass is a dark marking in the form of a hand, with four talon-like fingers stretching S*p* and with three stars standing out upon it. (2) A lobe in the form of an elongated ellipse 3'.3×1', *p* 125°, with greatest density along the periphery. This extends about 1'.4 beyond the S end of (1) and its axis produced would intersect (1) at its N end. The interior is filled with soft nebulosity, has a line of bright knots toward its N end, and some tufts projecting over its *f* side. (3) A spiral arm leaving the N*p* point of (1) and sweeping to the S in such a way as to give the effect of a left-handed spiral. It ends *p* 200°, *d* 2', with respect to the nucleus.

One might describe the system as a spiral with abnormal center, attached to a single arm or to double arms in the latter case, the lobe forming one of the arms. In the former case a single arm emerges from the S corner of (1), sweeping around the *f* side and under the N end of (1), and emerging on the *p* side as (3). In either case the major axis of the arm or arms would be 5'.2 long and lie in *p* 120°. At the extremities there is the effect of a turn in the arm, but there is no increase in density where the single arm and element (1) are superimposed.

A medium-bright right-handed spiral, 8'×2', *p* 30° lies *p* 54°, *d* 19' with respect to nucleus of N.G.C. 2146. The plate shows many small nebulae.

N.G.C. 2245, Monoceros

$\alpha = 6^h28^m17^s$, $\delta = +10°13'.2$ (1920); $\lambda = 169°$, $\beta = +2°$

Plate No. 323, 1918, February 14, 60^m. S 27. Poor seeing.
Large round images
Plate No. 329, 1919, March 28, 95^m. S 30. Excellent seeing.
Small round images. Illustrated Plate XIV*a*

A fan-shaped nebula fading away irregularly from an almost stellar point toward the circumference, beyond which extends, torch fashion, nebulosity similar to that of the Orion nebula. A few seconds from its apex and almost at right angles to its axis is a line of nebulosity 30''–40'' long. Alongside this line, away from the nebula, is a fan-shaped dark area, appearing to be a shadow cast by an opaque portion of the line, the light source being the fan itself. Evidently the whole region is nebulous, as detail can be seen in the shadow, particularly a looped thread formation. The two photographs appear to show a striking difference about the head, but this may be due to the differences in the plates. The 1918 plate shows a round stellar nucleus standing out from the nebulosity, while the 1919 plate shows an almost solid mass completely covering the nucleus. Further observations will be made.

N.G.C. 2247, Monoceros

$\alpha=6^h28^m45^s$, $\delta=+10^\circ22'.8$ (1920); $\lambda=169^\circ$, $\beta=+2^\circ$

Plate No. 323, 1918, February 14, 60^m. S 27. Poor seeing. Large round images

Plate No. 329, 1919, March 28, 95^m. S 30. Excellent seeing. Small round images. Illustrated Plate XIV*a*

This nebula lies $9'.9$ N of and $5'.7$ *f* N.G.C. 2245 involving centrally the star B.D.+10° 1172. It surrounds the star irregularly, streamers radiating $2'$ to $3'$ from the center. In addition to the streamers there is a small patch $1'$ N and a line about $1'$ S. Both N.G.C. 2245 and N.G.C. 2247 lie in a dark lane. While Hubble's variable N.G.C. 2261 is related to a variable star, neither of these stars has been mentioned as variable.

The position given in the N.G.C. is not correct. Swift's original description is so exactly like that surrounding B.D.+10° 1172 that there is no question of this being the object. The position given is that of the B.D. star.

N.G.C. 2274, 2275, Gemini

$$\left.\begin{array}{lll} \text{N.G.C. 2274,} & \alpha=6^h42^m2^s, & \delta=+33^\circ39'.0 \\ \text{N.G.C. 2275,} & \alpha=6\ \ 42\ \ 3\ , & \delta=+33\ \ 41\ .0 \end{array}\right\} \text{(1920);} \quad \lambda=149^\circ, \quad \beta=+15^\circ$$

Plate No. 313, 1917, November 17, 20^m. Cramer Crown. Poor seeing. Images medium and elongated

Plate No. 100-137, 1919, December 19, 30^m. S 23. Images small and comate

N.G.C. 2274. Nebulosity $7''$ diameter, gradually brighter toward the middle, with bright almost stellar nucleus. There is trace of a wing N*p*.

N.G.C. 2275. Nebulosity 10″ diameter, gradually brighter toward the middle, with bright stellar nucleus. There are traces of faint surrounding nebulosity 30″ in diameter.

N.G.C. 2288, 2289, 2290, 2291, and 2294, Gemini

N.G.C. 2288,	$\alpha=6^{\rm h}45^{\rm m}28^{\rm s}$,	$\delta=+33^\circ 29'.1$	(1920); $\lambda=149^\circ$, $\beta=+15^\circ$
N.C.C. 2289,	$\alpha=6\ 45\ 29$,	$\delta=+33\ 30.9$	
N.G.C. 2290,	$\alpha=6\ 45\ 33$,	$\delta=+33\ 27.7$	
N.G.C. 2291,	$\alpha=6\ 45\ 35$,	$\delta=+33\ 33.0$	
N.G.C. 2294,	$\alpha=6\ 45\ 47$,	$\delta=+33\ 33.2$	

Plate No. 311, 1917, November 16, 90$^{\rm m}$. Cramer Crown. Good plate. Small images

Plate No. 315, 1917, November 18, 70$^{\rm m}$; 19, 140$^{\rm m}$. Total 210$^{\rm m}$. S 27. Poor seeing. Large images. Illustrated Plate XIII*a*

This group is mentioned by Lord Rosse in his *Observations* and is shown by the photographs to be composed of spirals with a background of ill-defined nebulae of similar character.

The following is a brief description of all the nebulae on the plates. The positions are referred to the nucleus of N.G.C. 2290.

N.G.C. 2288, *p* 325°, *d* 1′.8, MB nebulosity, 7″ diameter. B Nu. almost stellar.

N.G.C. 2289, *p* 343, *d* 2′.6, 15″×10″, *p* 100°. gbM, B almost stellar Nu.

N.G.C. 2290, MF ring 5″ to 15″ wide, broken in places, outside diameter 1′.10×0′.54 and mean diameter 0′.9×0′.45. B stellar Nu. in MB nebulosity 10″ diameter connecting with outer ring. Almost certainly a left-handed spiral.

N.G.C. 2291, *p* 3°, *d* 5′.3, B almost stellar Nu. in F, R, nebulosity 35″ diameter showing traces of rings, almost certainly spiral.

N.G.C. 2294, *p* 28°, *d* 6′.2, B almost uniform spindle 27″×9″, *p* 7′.5. Surrounded by faint nebulosity 40″×10″ and having a vs B diffuse elongated Nu.

a, *p*	263°, *d*	16′.2	F	Patch, 8″ diameter.
b,	285	11.9	F	3″ diameter, gbM, Nu.
c,	220	11.7	MB	10″ diameter, gbM, Nu.
d,	349	11.0		Semicircular, 10″ radius, MB on curve, fades back of Nu. From vertex to central Nu. is a bright line 2″ wide, *p* 137°.
e,	96	5.2	F	Sliver, 10″×5″, *p* 130°.
f,	95	5.4	F	Spot, 3″ diameter.
g,	108	6.0	F	Diffuse spot, 8″ diameter.

h,	130	8.7	F	20″×5″, *p* 116″, MB Nu. near *f* end.
i,	146	12.9	MB	Nebulous star.
j,	96	7.5	F	15″×10″, *p* 85° elongated diffuse spot.
k,	127	9.4		15″×8″, *p* 32° gbM Nu., looks S-shaped.
l,	67	13.5	F	Diffuse patch, 15″ diameter.

N.G.C. 2359, Canis Major

$\alpha=7^h13^m50^s$, $\delta=-13°\ 4'.1$ (1920); $\lambda=197°$, $\beta=0°$

Plate No. 320, 1917, December 17, 60^m; 18, 150^m. Total 210^m. S 23.
Images large and round. Illustrated Plate XIV*b*

The brighter parts of the nebula agree closely with the drawings by the earlier observers. Sir John Herschel pictured it as resembling a bust, while Lassell drew it as like a balloon, with a long neck twisted in the S*p* direction. The balloon or head is approximately 5′ in diameter; the neck is to the S, with nebulosity about 1′ wide extending 8′ *p*, concave on the N and gradually narrowing and fading out. From the top (N) of the head a symmetrical streamer concave to S extends in *p* direction. The radius of curvature of the two streamers is roughly 15′ and their ends are about 8′ apart. A second streamer about 1′ wide extends *f* from the top of the head to a distance of 9′.

N.G.C. 2403,* Camelopard

$\alpha=7^h29^m7^s$, $\delta=+65°46'.5$, (1920); $\lambda=118°$, $\beta=+30°$

Plate No. 307, 1917, October 19, 100^m. Cramer Crown.
Images small and round

The illustration of N.G.C. 2403 (*Mount Wilson Contribution*, No. 132, Plate X*c; Astrophysical Journal*, **46**, 35, 1917, Plate V) was made from Plate No. 307, and not from No. 169 as there stated.

The nebulous spot *p* 50°, *d* 3′.4, with respect to the center of the nebula is probably a flaw, as there is a difference in character between it and the rest of the nebulosity on the plate.

N.G.C. 2537, Lynx

$\alpha=8^h7^m35^s$, $\delta=+46°14'$ (1920); $\lambda=141°$, $\beta=+33°$

Plate No. 2968 (Shapley), 1916, March 27, 30^m. S 27
Plate No. 359, 1919, December 23, 60^m. S 30. Images
small and elongated

Nebulosity of the form of a horseshoe or a semi-elliptical line, major axis N–S, concave to the S, together with a line of nebulosity $30''$ long lying in the center of the ellipse on the major axis. Two faint lines of nebulosity extend from the N end of this line to the outer nebulosity, the included angle being about 150°. The axes of the complete ellipse would measure $75''\times45''$. The nebulosity is of the mixed type, there being a number of well-defined knots in it.

I.C.II 2233 falls near the edge of the plates and appears to be a faint edge-on spiral $4'\times10''$, *p* 170°±, with faint stellar nucleus. A faint patch $20''$ diameter lies $4'.6$ *f* N.G.C. 2357.

N.G.C. 2964, Leo Minor

$\alpha=9^h38^m11^s$, $\delta=+32°12.8$ (1920); $\lambda=162°$, $\beta=+50°$

Plate No. 321, 1917, December 18, 60^m. Cramer Crown. Images small and round

Plate No. 324, 1919, February 28, 210^m. S 30. Images small and round

A right-handed spiral, with bright inner arms extending to $75''\times45''$, *p* 90°, and exterior arms to $2'.5\times1'.2$. The inner arms are dotted with bright condensations, the outer are faint and soft. Several peculiar details suggest a drift of the component parts relative to each other; among these may be noted the winged knots on the *p* side, the disjunction of the nucleus and the *f* arm, and a left-handed wisp crossing the *p* arm N of the nucleus.

N.G.C. 2968, Leo Minor

$\alpha=9^h38^m28^s$, $\delta=+32°17'.7$ (1920); $\lambda=162°$, $\beta=+50°$

Plate No. 321, 1917, December 18, 60^m. Cramer Crown. Images small and round

Plate No. 324, 1919, February 28, 210^m. S 30. Images small and round

Probably an edge-on spiral, since it shows an irregular ellipse of nebulosity $1'.2\times7'$, *p* 31°, gradually increasing in brightness toward the central nucleus $2''$ diameter, and has an absorption streak running irregularly along the major axis.

The plate shows many small nebulae; measures were made of 15 with the nucleus of N.G.C. 2968 as a center.

a,	*p* 305°,	*d* $13'.4$	MB,	uniform ellipse, $7''\times3''$, *p* 142°.
b,	247	11.3	MB,	uniform ellipse, $8''\times4''$, *p* 140°, sbM.
c,	282	10.0	MF,	uniform, $3''$ diameter.

d,	196	9.2	F,	spindle, 20″×6″, *p* 129°, F Nu.
e,	329	2.7	MF,	uniform patch, 9″×4″, *p* 48°.
f,	242	0.8	MB,	10″×2″, *p* 179°, gbM.
g,	4	14.1	MB,	10″ diameter, gbM.
h,	166	6.5	MB,	10″ diameter, *f* side stronger.
i,	168	13.6	MB,	gbM, 11″×8″, *p* 60°.
j,	154	7.7	F,	uniform, 12″×3″, *p* 132°.
k,	61	4.9	MB,	sbM, 12″×6″, *p* 75°.
l,	19	13.0	MF,	spindle, gbM, 10″×4″, *p* 23°.
m,	124	13.7	MF,	nebulous star, 4″ diameter.
n,	56	14.0	F,	uniform, lbM, 10″×3″, *p* 23°.
o,	47	15.9	MF,	gbM, Nu, 10″×3″, *p* 29°.

N.G.C. 2970, Leo Minor

$\alpha=9^h38^m48^s$, $\delta=+32°20'.7$ (1920); $\lambda=162°$, $\beta=+50°$

Plate No. 321, 1917, December 18, 60^m. Cramer Crown. Images small and elongated

Plate No. 324, 1919, February 28, 210^m. S 30. Images small and round

Bright nebulosity gradually fading away, 15″×10″, *p* 80°, with a bright stellar nucleus about 5″ diameter centrally located.

N.G.C. 3310, Ursa Major

$\alpha=10^h33^m48^s$, $\delta=+53°55'.1$ (1920); $\lambda=124°$, $\beta=+55°$

Plate No. 356, 1919, December 22, 12^m and 90^m. Exp. on same plate. S 30. Images small and round

A left-handed spiral, 90″×50″, *p* 170°. The short exposure shows a bright nucleus surrounded by a bright elliptical ring, 22″×15″, *p* 140°, from which springs an arm of much smaller density in *p* 130°, bending to the north and running for a length of about 25″. A faint star with faint surrounding nebulosity lies just adjoining the ring at *p* 230°, *d* 14″, from the center. The long exposure shows a mass 30″×25″, *p* 130°, with the arm emerging as above and ending at *p* 20°, *d* 25″. The nucleus, ring, and two stars show plainly. There are traces of other arms lying around the bright mass, particularly one emerging opposite the strong arm running southward and ending at *p* 165°, *d* 30″. The ring is strongest in its N and S sections.

N.G.C. 3367, Leo Major

$\alpha = 10^h42^m21^s$, $\delta = +14°10'.2$ (1920); $\lambda = 200°$, $\beta = +59°$

Plate No. 289, 1917, April 22, 70^m. S 23. Images small and comate

Plate No. 327, 1919, March 1, 150^m. S 30. Small round images.

Illustrated Plate XIII*e*

A left-handed spiral about 1′.8 diameter, almost circular, with a bright sharp stellar nucleus. The periphery is well defined on the *p* side but lacking on the *f*. It is similar in type to N.G.C. 5921[1] in that an almost straight bar crosses the center *p* 70°, from the ends of which emerge arms almost at right angles to the bar, a single arm at one end, a double one at the other. The bar is slightly concave on the N side and its *f* end continues in a series of condensations across the arm to the periphery. The arm emerges from the bar 14″ from the nucleus and turns to the N. The *p* end of the bar spreads into soft nebulosity and just touches the arm from the *f* end; the arm on the *p* end leaves at about 16″ from the nucleus, turns to the south, and at about 10″ spreads into two parallel arms with nebulosity between them, which run parallel for about 90°; the outer one then fades away into the rim, while the inner one continues and is merged in the *p* rim. There are a number of branching and crossing threads, and a bright knot *p* 267°, *d* 47″, from the nucleus lying in the periphery. The greatest extent of the nebulosity is 60″, *p* 40°. The double arm brightens at a point just *f* the nucleus. The plate shows a number of nebulous spots, the more prominent of which are as follows, the measures referring to the nucleus of 3367.

a,	*p* 269°, *d*	14′.4	5″ diameter, uniform.
b,	193	11.0	3″ diameter, gbM, B, stellar Nu.
c,	151	4.9	3″ diameter, stellar Nu.
d,	149	13.0	11″×5″, *p* 126°, gbM.
e,	150	15.0	10″×4″, *p* 145°, lbM.
f,	25	18.1	5″ diameter, gbM.
g,	34	14.3	5″ diameter, lbM.
h,	45	17.7	4″ diameter, lbM.
i,	57	15.3	5″ diameter, gbM.
N.G.C. 3377	49	21.8	

[1] *Publications of the Astronomical Society of the Pacific*, **24**, 227, 1912.

N.G.C. 3371	Should lie about one-third the distance from 3367 to 3377, but there is nothing on the plate.
N.G.C. 3373	Should lie in the region *f* 3367 and a little S, but there is nothing on the plate.

N.G.C. 3377, Leo Major

$\alpha=10^h43^m28^s$, $\delta=14^\circ24'.4$ (1920); $\lambda=201^\circ$, $\beta=+60^\circ$

Plate No. 289, 1917, April 22, 70^m. S 23. Small astigmatic images
Plate 327, 1919, March 1, 150^m. S 30. Small comate images

A diffuse ellipse $90''\times30''$, *p* 40°, gradually increasing in brightness toward the center, where there is a great increase in brightness in an elongated nucleus $20''\times13''$. A number of faint nebulae not listed under N.G.C. 3367 appear in the field. The measures refer to the nucleus of N.G.C. 3377.

a,	*p* 315°,	*d* 9′.1	Very faint, 1′ diameter.
b,	60	8.2	MF, uniform, 10″ diameter.
c,	110	12.9	MF, uniform, $12''\times4''$, *p* 129°.
d,	64	19.4	MF, lbM, 8″ diameter.
N.G.C. 3391	52	22.9	($10^h\ 44^m\ 45^s$, $+14^\circ\ 38'.6$) (1920); appears on the corner of plate 289. The image is bright, $20''\times11''$, *p* 26°, and suggestive of spiral formation, but the image is too comate to say for certain.

N.G.C. 3379, Leo Major

$\alpha=10^h43^m37^s$, $\delta=+13^\circ0'.2$ (1920); $\lambda=203^\circ$, $\beta=+59^\circ$

Plate No. 290, 1917, April 23, 75^m. S 23. Small, slightly elongated image
Plate No. 334, 1919, March 30, 120^m. S 23. Small, slightly elongated image
Illustrated Plate XV*a*

A nebula which long since attracted attention, owing to its resemblance to an unresolved star cluster. It has a very bright nucleus 10″–12″ diameter, surrounded by a bright atmosphere, 30″ diameter, which gradually fades away at 90″ diameter. The nebula differs from many others, such as N.G.C. 4374 (M 84) and N.G.C. 4402, in having a planet-like nucleus, whereas usually the nebulosity gradually increases toward the center, with a possible sudden increase in brightness to form a semi-diffuse nucleus. A spectrogram[1] made with the focal-plane spectrograph at the

---

[1] *Publications of the Astronomical Society of the Pacific*, **30**, 255, 1918.

Newtonian focus of the 60-inch reflector shows the nucleus to be G5 or later, and to have a radial velocity of about +850 km/sec. Slipher obtained a value of 780 km/sec. Faint traces of the outer nebulosity show a maximum of continuous spectrum corresponding to the nucleus.

N.G.C. 3384, Leo Major

$\alpha = 10^h 44^m 4^s$, $\delta = +13^\circ 3'.1$ (1920); $\lambda = 203^\circ$, $\beta = +59^\circ$

Plate 290, 1917, April 23, 75^m. S 23. Small, slightly comate images
Plate 334, 1919, March 30, 120^m. S 23. Small, slightly comate images
Illustrated plate XV*a*

An astonishing nebula consisting of a bright center $40''$ diameter, on which is superimposed a very bright elongated nucleus $19'' \times 10''$, *p* 45°, crossed by a second bright nucleus $40'' \times 5''$, *p* 130°, presenting a Saturn-like appearance. Finally, from this mass wings or branches extend in *p* 53° on either side, to a distance of $1'.5$ The wings gradually broaden to a width of $1'$ at $1'$ from the center, where they are rounded off.

The three nebulae, N.G.C. 3379, 3384, 3389, appearing on the same plate present very different features. N.G.C. 3389 is a well-defined spiral, N.G.C. 3384 presents spiral and planetary characteristics, while N.G.C. 3379 leads one to believe it a very distant, unresolved cluster or group of spirals.

N.G.C. 3389, Leo Major

$\alpha = 10^h 44^m 14^s$, $\delta = +12^\circ 57'.0$ (1920); $\lambda = 204$, $\beta = +60^\circ$

Plate No. 290, 1917, April 23, 75^m. S 23. Small slightly comate images
Plate No. 334, 1919, March 30, 120^m. S 23. Small slightly elongated images. Illustrated Plate XV*a*

A medium-bright right-handed spiral $110'' \times 52''$, *p* 107°, having a very small stellar nucleus. The arms are fairly dense, with condensations along them, but are not strictly regular in form.

N.G.C. 3395–3396, Leo Minor

$$\left.\begin{array}{lll} \text{N.G.C. 3395,} & \alpha = 10^h 45^m 23^s, & \delta = +33^\circ 24'.4 \\ \text{N.G.C. 3396,} & \alpha = 10\ 45\ 28\ , & \delta = +33\ 24.9 \end{array}\right\} (1920);\quad \lambda = 160^\circ,\quad \beta = +64^\circ$$

Plate No. 286, 1917, March 26, 120^m. S 23. Small round images
Illustrated Plate XVI*a*
Plate No. 332, 1919, March 29, 110^m. S 30. Small round images

N.G.C. 3395 is a right-handed spiral with its major axis in *p* 32°. Its S*p* portion is well defined and extends about 52″ along the major axis from the nucleus. The N*f* portion is markedly deficient in size and in density of material. N.G.C. 3396 lies *p* 66°, *d* 73″ N*f* with respect to the nucleus of 3395. It is composed of a bright elongated nucleus 10″×5″, *p* 97°, with which is blended a knot about 3″ diameter 9″ *f* and a short line diagonally opposite. Surrounding this is a mass whose general axis is in *p* 94° and which extends 42″ *f* the nucleus. Between the two nebulae is evidence of a great disturbance, since material which would ordinarily belong to the N*f* arm of 3395 is absent, while stream lines indicate its presence about 3396. It remains to be ascertained whether the formation is the result of two separate centers or whether 3395 has separated from 3396, or, finally, whether 3396 has wrenched material away from 3395. The stream line of 3395 suggests a right-hand twist. There is more than enough material in 3396 to make up for that lost in the arm of 3395; in fact, it is just about equal to the complete arm of 3395.

There are many small nebulae on the plates, the more prominent of which are the following, the measures referring to the nucleus of N.G.C. 3395:

I.C.II 2603			Not on plates.
a,	*p* 278°, *d*	15′.9	10″×4″, *p* 56°, bM.
Big. 270			Not on plates.
b,	280	11.1	MF, 5″ diameter, bM.
c,	210	15.2	MF, 10″×5″, *p* 99°, lbM.
I.C.II 2604	203	13.8	MB, Irr. R, 50″ diameter, RH spiral.
d,	339	11.9	MF, 6″ diameter, lbM.
e,	330	4.3	MF, 6″ diameter, lbM.
f,	342	5.4	MB, 2″ diameter, stellar.
I.C.II 2605			Part of arm of N.G.C. 3395.
Big. 402			
I.C.II 2608	157	14.1	MB, 45″×6″, *p* 118°, B Nu., spindle.
g,	40	13.0	MB, 10″ diameter, lbM.
h,	98	9.2	MF, 3″ diameter, lbM.
i,	46	17.4	MF, 4″ diameter, lbM.
j,	80	12.7	F, 9″×5″, *p* 116°, lbM.
k,	124	23.2	MB, 60″×10″, *p* 170°, B Nu., spindle.

N.G.C. 3786, 3788, Ursa Major

$$\left.\begin{array}{lll}\text{N.G.C. 3786,} & \alpha=11^{h}35^{m}29^{s}, & \delta=+32^{\circ}21'.3\\ \text{N.G.C. 3788,} & \alpha=11\ 35\ 32\ , & \delta=+32\ 22.8\end{array}\right\}(1920);\ \lambda=159^{\circ},\ \beta=+75^{\circ}$$

Plate No. 337, 1919, April 29, 30^{m}. S 23. Images small and slightly elongated

Plate No. 338, 1919, April 29, 135^{m}. S 27. Images large and fairly round. Illustrated Plate XIII*b*

N.G.C. 3786 is a right-handed spiral with a bright nucleus, a fairly bright central part 60″×30″, *p* 67°, and a faint interrupted ring, not strictly elliptical, 2′×1′, *p* 75°, which is probably an extended arm. The central part is weaker on the N side, which shows an irregular dark marking. The outer ring just touches a faint prolongation from the S end of N.G.C. 3788.

N.G.C. 3788 is a right-handed elliptical spiral 92″×20″, *p* 179°, very similar to N.G.C. 5545 lying *p* 18°, *d* 1′.4 N*f* N.G.C. 3788. The nebulosity on and between the arms is soft, with traces of condensation near the center. The brightest spot is a knot *p* 40°, *d* 10″. The center and the N end of the major axis in the curve of the arm are bright.

N.G.C. 3791 and 3793 do not appear on the plates. Plate No. 338 is literally covered with small nebulae, some of them spindles, and many of them merely rounded masses with relatively bright, ill-defined centers. Presumably these are related to the spiral family. The measures of some of them, referred to the nucleus of N.G.C. 3786, are as follows:

a, *p*	314°, *d*	22′.4	MF, R, 7″, lbM.
b,	311	16.6	F, 9″×4″, *p* 135°.
c,	285	12.4	F, Irr. R, 6″.
d,	273	11.0	MF, R, 7″, lbM.
e,	330	17.4	MF, R, 4″, lbM.
f,	325	14.4	MB, R, 5″, BM.
g,	331	16.7	F, Irr. R, 8″.
h,	336	18.5	MB, R, 7″, BM.
i,	331	14.9	F, Irr. R, 6″, lbM.
j,	322	11.4	MF, R, 5″, bM.
k,	238	6.1	MF, Irr. R, 9″, lb near end.
l,	226	4.8	MF, 20″×4″, *p* 132°, knots at middle and ends.
l^{1},	225	4.7	MB, 8″×3″, *p* 87°, other F nebulosity *f*.

m,	285	2.9	F, Irr. R, 6″, uniform.
n,	351	16.0	MF, R, 5″, bM.
o,	210	1.4	MB, 10″×3″, *p* 139°, BM.
p,	181	10.5	MF, R, 6″, lbM.
q,	6	8.4	MB, R, 6″, bM.
r,	167	8.5	MF, R, 5″, lbM.
s,	10	11.4	MF, R, 4″, bM.
t,	70	4.6	MF, 14″×4″, *p* 3°, bM, spindle.
u,	44	10.7	MF, R, 4″, lbM.
v,	115	8.6	F, Irr. R, 4″, lbM.
w,	34	15.0	MF, 10″×2″, *p* 135°, lbM.
x,	115	11.4	F, In R, 6″, lbM.
y,	60	12.4	F, R, 2″.
z,	112	15.3	MF, Irr. R, 10″, uniform.

N.G.C. 4395, 4399, 4400, 4401, Canes Venatici

$$\left.\begin{array}{lll} \text{N.G.C. 4395,} & \alpha=12^{h}21^{m}51^{s}, & \delta=+33^{\circ}59'.4 \\ \text{N.G.C. 4399,} & \alpha=12\ 22\ \pm & \delta=+34\ \ 0\pm \\ \text{N.G.C. 4400,} & \alpha=12\ 22\ \pm & \delta=+34\ \ 0\pm \\ \text{N.G.C. 4401,} & \alpha=12\ 22\ \ 1 & \delta=+33\ 57.5 \end{array}\right\}\ (1920);\ \lambda=121^{\circ},\ \beta=+82^{\circ}$$

Plate No. 330, 1919, March 28, 270^{m}. S 23. Images small and elongated
Plate No. 331, 1919, March 28, 20^{m}. S 30. Images small and round
Plate No. 333, 1919, March 29, 30, 450^{m}. S 30. Images small and slightly elongated. Illustrated Plate XV*b*

These four nebulae, together with a large amount of fainter nebulosity, form a remarkable spiral. The configuration is approximately circular in outline, with indications of a three-armed spiral or pinwheel and a two-armed spiral with one detached arm (similar to N.G.C. 3395–3396), all of which are blended and not simply superimposed. The brightest nebulosity is not at the center of either, but lies in the S*f* portion of the whole. Aside from these predominating features, large faint whorls are also seen which indicate that the nebula is roughly spherical in form. N.G.C. 4395 is the two-armed portion, N.G.C. 4399 the S*f* arm of the pinwheel, and N.G.C. 4401 the brightest knot of the whole. The nebula as a whole is roughly 12′×10′, elongated in *p* 128°, with N.G.C. 4395 as center; beyond this, and, in fact, scattered over the plate, are many small nebulous stars or spots similar to those within the nebula. The plates are not strong enough to show definitely the relation of the component parts, and further descriptions will be reserved for a longer exposure.

N.G.C. 4656–4657, Canes Venatici

$$\left.\begin{array}{ll}\text{N.G.C. 4656}, & \alpha=12^{h}40^{m}\ 5^{s},\ \delta=+32^{\circ}36'.2\\ \text{N.G.C. 4657}, & \alpha=12\ 40\ 14\ ,\ \delta=+32\ 39.4\end{array}\right\}(1920);\ \lambda=90^{\circ},\ \beta=+86^{\circ}$$

Plate No. 336, 1919, April 28, 20^{m}. S 27. Images comate
Plate No. 339, 1919, April 29, 140^{m}. S 27. Images medium and elongated
Plate No. 100–145, 1920, February 16, 240^{m}. S 30. Images small and round.
Illustrated Plate XVI*b*

The objects listed as N.G.C. 4656 and 4657 constitute a most interesting single right-handed spiral. It appears as though a section were scaling off from a streamer of nebulosity which extends across the plate for a distance of 20′. The nebulosity strongly resembles that of N.G.C. 4449. There is no well-defined center or nucleus, but the inner end of the stronger arm is relatively bright, and this is taken as the center in the discussion. The strong N*f* arm consists of well-defined soft nebulosity dotted with about 50 condensations and having much fainter material lying on its concave side. The position angle at the center is about 26°, but the direction changes rapidly, the arm becomes concave on the *f* side and turns south at *p* 50°, *d* 3′.6 from the center, and after a return of 25″ stops. The width is from 20″ to 30″. The S*p* arm is not so well defined and the material is distributed in several bands. It consists of a *p* member emerging from the center in *p* 220° to a distance of 3′.4, which then branches, one branch continuing straight on, the other curving slightly concave N for a distance of 5′. The second member starts in *p* 185°, runs straight for 2′, then gradually curves for about 5′, ending in *p* 223°. There are traces of other lines of material extending to a distance of 8′.

In addition to a number of very small nebulae on the plate there is a well-defined two-armed right-handed spiral *p* 260°, *d* 3′.4 with respect to the center of 4656–7; it is 30″×20″, *p* 10°.

N.G.C. 5257, 5258, Virgo

$$\left.\begin{array}{l}\text{N.G.C. 5257, } \alpha=13^h35^m49^s,\ \delta=+1^\circ14'.7\\ \text{N.G.C. 5258, } \alpha=13\ 35\ 53\ ,\ \delta=+1\ 14.3\end{array}\right\}(1920);\ \lambda=298^\circ,\ \beta=+61^\circ$$

Plate No. 345, 1919, June 27, 50^m. S 30. Images small and elongated. Illustrated Plate XVII*b*

N.G.C. 5257 is a left-handed spiral with two principal arms, each making a complete revolution before fading out. It forms an irregular ellipse 80″×40″, *p* 120° (no trail). For a length of 20″, beginning a half-turn from the center, there are several bright knots in line in each arm. Beyond this the nebulosity is soft and spreads into brushes at the ends. The curvature at the ends is very small, and there is indication that the *f* one extends to N.G.C. 5258.

N.G.C. 5258 is a left-handed spiral whose brighter parts lie within an ellipse 60″×18″, *p* 30° (no trail), from the extremities of which spring the two main opposite arms forming a letter **S**, the arms themselves being opposite arcs of a circle of 30″ radius. The central nucleus is brighter than that of N.G.C. 5257, and two knots as bright as the nucleus lie one to the N end and one to the S. The arms are soft and brushy, as in N.G.C. 5257.

N.G.C. 5278–5279, Ursa Major

$$\left.\begin{array}{l}\text{N.G.C. 5278, } \alpha=13^h38^m40^s,\ \delta=+56^\circ4'.3\\ \text{N.G.C. 5279, } \alpha=13\ 38\ 45\ ,\ \delta=+56\ 4.5\end{array}\right\}(1920);\ \lambda=74^\circ,\ \beta=+60^\circ$$

Plate No. 341, 1919, May 28, 30^m. S 30. Fair images

Plate No. 342, 1919, June 25, 160^m. S 30. Fair images. Illustrated Plate XVII*a*

These separately listed objects are parts of the same nebula, consisting of a stellar center and a ribbon of nebulosity which encircles the nucleus for a little more than one turn, then abruptly decreases in intensity and widens out, and continuing in a curve, concave to the S, ends abruptly in a bright twist or hook, at about *p* 70°, *d* 40″. The first coil is roughly 30″×20″, *p* 60°, and the whole lies within an ellipse 65″×30″, *p* 60°. The curl on the end forms a semicircle of about 7″ radius and points *p* 320°.

This nebula appears on the same plates as the group of objects listed by Barnard under I.C. 917 to 928; the illustration is from Plate No. 342 where it appears near the edge.

N.G.C. 5544,* 5545,* 5557, Boötes

$$\left.\begin{array}{llll} \text{N.G.C. } 5544, & \alpha=14^{h}13^{m}40^{s}, & \delta=+36^{\circ}56'.5 \\ \text{N.G.C. } 5545, & \alpha=14\ 13\ 41\ , & \delta=+36\ 56.8 \\ \text{N.G.C. } 5557, & \alpha=14\ 15\ \ \ 5\ , & \delta=+36\ 51.6 \end{array}\right\}(1920);\ \lambda=32^{\circ},\ \beta=+68^{\circ}$$

Plate No. 127, 1912, June 13, 180^{m}. S 23

Plate No. 260, 1916, April 30, 50^{m}. S 23. Images small and round

Plate No. 261, 1916, May 1, 2, 3, 4, 5, 360^{m}. S 27. Images small. Illustrated Plate XVIII*b*

In *Mount Wilson Contribution*, No. 132, the orientation of these plates is in error 180°, consequently the descriptions of N.G.C. 5544 and 5545 are interchanged and Plate XIII*c* is shown S at top and *f* at right. The positions in N.G.C. are incorrect, as that of 5545 is given S of 5544, while actually it is to the N. Bigourdan's value (*Annales Observatoire de Paris, Observations*, 1899) for N.G.C. 5544 is $\alpha=14^{h}12^{m}50^{s}.62$, $\delta=+37^{\circ}2'7''.2$ (1900), the relative position of the nebulae *p* 244°±, *d* 37″, but he states that the measures are uncertain and difficult. The corrected description is as follows:

N.G.C. 5544 and 5545 are two overlapping spirals, the former in plan, the latter very much inclined to the line of sight.

N.G.C. 5544 consists of a bright stellar nucleus, a nebular ring about 5″ wide and 28″ outside diameter, a fainter diametral streak crossing the nucleus in *p* 130° and an outer ring of about the same intensity as the inner one, irregularly round, 8″ wide and 45″ outside diameter; both rings are slightly elongated in *p* 115°. The nebulosity is entirely soft.

N.G.C. 5545 is a left-handed spiral 70″×15″, *p* 60°, its *p* end just tangent to the *f* point of the nucleus of N.G.C. 5544. The nucleus is faint and stellar. The arms are about equal in intensity where they start from the nucleus, but that on the *p* side continues bright for a much greater distance, being interrupted, however, at several points. Several knots and condensations appear. Its extremely small, bright nucleus lies in *p* 68°, *d* 36″, with respect to nucleus of N.G.C. 5544.

N.G.C. 5557 appears at the *f* side of the plates; it is so distorted that one cannot more than suspect it to be a spiral. Its position with respect to N.G.C. 5544 is *p* 105°, *d* 17.4 and, allowing for distortion, seems to be a bright mass 18″×14″ surrounded with fainter nebulosity 40″ diameter.

The plates are covered with a multitude of faint nebulae, a number of which are as follows, their positions being given with respect to the nucleus of N.G.C. 5544:

a,	*p* 235°,	*d* 20′.7	MB, Irr. R, 12″ diameter BM (edge of plate).
b,	216	21.3	F, nebulous spot, 5″ diameter (edge of plate).
c,	329	9.8	F, uniform sliver, 20″×2″, *p* 24°.
d,	205	7.5	MB, elongated Nu., 4″×2″, *p* 4°, in MF nebulosity, 11″ diameter.
e,	228	3.8	F, 5″ diameter, gbM.
f,	356	6.6	Faint, MF at center, 10″×3″, *p* 42°.
g,	179	4.8	Bright Nu., 2″ to 3″ diameter, surrounded by F nebulosity, 13″ diameter, *p* 79.
h,	173	16.1	MF center, 10″×2″, *p* 145°, in F nebulosity 15″×5″.
i,	23	7.8	Two F slivers each 11″ long lying *p* 37° and 52° intersecting to form a V on S*p* end.
j,	139	18.5	F, 8″ diameter, gbM.
k,	97	13.0	F, 10″×2″, *p* 130°.
l,	124	16.0	F, Wisp, 13″×3″, *p* 76°.
m,	130	23.1	Nebulous spot, 10″×5″, *p* 51° (edge of plate).

N.G.C. 5868, 5869, Serpens

$$\left.\begin{array}{l}\text{N.G.C. 5868},\ \alpha=15^{h}5^{m}44^{s},\ \delta=+0^{\circ}50'.2\\ \text{N.G.C. 5869},\ \alpha=15\ \ 5\ \ 45\ ,\ \delta=+0\ \ 46.6\end{array}\right\}(1920);\ \lambda=328^{\circ},\ \beta=+47^{\circ}$$

Plate No. 328, 1919, March 1, 50^m, S 23. Images small and almost round

Plate No. 335, 1919, March 30, 30^m, S 30. Images small and elongated

N.G.C. 5868 is a medium bright, semi-diffuse stellar nucleus 2″–3″ diameter with a faint halo 5″ diameter.

N.G.C. 5869 is a medium bright, diffuse stellar nucleus 5″×4″, *p* 133°, surrounded with nebulosity gradually fading away at 10″×7″.

N.G.C. 5865 and N.G.C. 5871, for which positions are given in this vicinity, do not appear on the plates.

There is a very faint diffuse spot roughly 7″ diameter, p 116°, d $1'.9$, with respect to the nucleus of 5868.

N.G.C. 6014, 6017, Serpens

$$\left.\begin{array}{l}\text{N.G.C. 6014,}\ \ \alpha=15^{h}52^{m}\ 1^{s},\ \ \delta=+6^{\circ}\ 9'.7\\ \text{N.G.C. 6017,}\ \ \alpha=15\ 53\ 19\ ,\ \ \delta=+6\ 13.6\end{array}\right\}(1920);\ \ \lambda=341^{\circ},\ \ \beta=+39^{\circ}$$

Plate No. 325, 1919, February, 28, 30^{m}. S 30. Images small and slightly elongated

N.G.C. 6014. Medium bright stellar nucleus lying centrally in faint nebulosity 30″ diameter, showing traces of rings. It is probably a spiral. There is a faint nebula of the same character, 15″ diameter, at p 51°, d $11'.0$, with respect to N.G.C. 6014.

N.G.C. 6017. A faint elliptical nebula 18″×6″, p 133°, with bright nucleus 7″×5″.

N.G.C. 6703,* Lyra

$\alpha=18^{h}45^{m}0^{s}$, $\delta=+45^{\circ}27'.7$ (1920); $\lambda=42^{\circ}$, $\beta=+18^{\circ}$

Plate No. 344 (Duncan and Hoge), 1919, June 26, 315^{m}. S 30. Images medium and elongated

This plate was taken for classification, but the results are not conclusive and the type must be settled spectroscopically. The nucleus is lost in the very strong central part, 30″ in diameter. The ring, 80″ diameter, shows more plainly, and there is nebulosity between the ring and the central mass; but it is not clear whether the nebula is a planetary or a spiral in plan. Ten small faint nebulae, in addition to the six mentioned previously, are shown on the plate.

N.G.C. 6820, Vulpes

$\alpha=19^{h}39^{m}3^{s}$, $\delta=+22^{\circ}53'.3$ (1920); $\lambda=27^{\circ}$, $\beta=-1^{\circ}$

Plate No. 298, 1917, July 23, 90^{m}. S 23. Images small and nearly round

The nebula lies in a rich region of the Milky Way. It has a stellar nucleus lying eccentrically to the south in a mass of soft, irregular, patchy nebulosity, roughly 30″ in diameter.

N.G.C. 6823, an open cluster, appears on the N*f* corner of the plate.

N.G.C. 6846, Cygnus

$\alpha=19^h53^m22^s$, $\delta=+32^\circ 8'.4$ (1920); $\lambda=37^\circ$, $\beta=+1^\circ$

Plate No. 295, 1917, July 20, 150^m. S 23. Images small and elongated

A small group of twelve stars, approximate magnitude 17, in a very rich region of the Milky Way, clustered about three stars of magnitude 15.

N.G.C. 6888, Cygnus

$\alpha=20^h9^m33^s$, $\delta=+38^\circ 9'.1$ (1920); $\lambda=43^\circ$, $\beta=+1^\circ$

Plate No. 299, 1917, August 21, 60^m. S 23. Images small and slightly elongated

Plate No. 301, 1917, August 22, 60^m. S 27. Images small and slightly elongated

Plate No. 348, 1919, July 25, 300^m. S 30. Images medium. Illustrated Plate XVIII*c*

A network nebula in the heart of the Milky Way, about 13° N*p* N.G.C. 6960 and 6992, which it resembles in shape and character of nebulosity. It is roughly elliptical, $18'\times 9'$, *p* 42°. The N, N*p*, and S*p* edges include the bulk of the nebulosity, which gives it a crescent form, the bowl of which is filled with faint and scattered nebulosity.

N.G.C. 6906, Sagitta

$\alpha=20^h19^m36^s$, $\delta=+6^\circ 12'.3$ (1920); $\lambda=18^\circ$, $\beta=-18^\circ$

Plate No. 352 (Benioff), 1919, August 27, 120^m. Images small and nearly round

A right-handed spiral lying at the edge of the Milky Way where the star density, for this plate, is five to six stars per square minute of arc. The nebula measures $90''\times 35''$, *p* 35°, the arms are soft and delicate, though increased exposure may show parts to be granular. A short line 12″ long projects equally beyond the nucleus in *p* 165° and 345°.

N.G.C. 6927, 6928, 6930, Delphin

$$\left.\begin{array}{lll} \text{N.G.C. 6927,} & \alpha=20^h28^m46^s, & \delta=+9^\circ 38'.6 \\ \text{N.G.C. 6928,} & \alpha=20\ 28\ 58\ , & \delta=+9\ 39.2 \\ \text{N.G.C. 6930,} & \alpha=20\ 29\ \ 7\ , & \delta=+9\ 34.6 \end{array}\right\}\text{(1920);}\quad \lambda=22^\circ,\quad \beta=-18^\circ$$

Plate No. 347 (Duncan and Hoge), 1919, June 27, 60^m. Images small and elongated

Plate No. 350, 1919, August 21, 140^m. S 23. Images small and elongated

These plates show three N.G.C. nebulae in addition to the several small nebulae given below. The foregoing positions have been corrected from Bigourdan's observations.

The following measures refer to the brightest spot of N.G.C. 6928.

a,	*p* 231°, *d*	4′.2	10″×5″, *p* 20°, gbM, BM.
N.G.C. 6927	257	3.0	18″×8″, *p* 10°, gbM, BM.
N.G.C. 6928			100″×28″, *p* 110°, left-handed spiral, two arms making about three-fourths of a turn each. Brightest in the middle where the two arms join with a slight offset, forming a bent line 35″ long.
b,	161	1.6	MF, nebulous spot, 4″ diameter.
N.G.C. 6930	146	3.9	30″×12″, *p* 9°, left-handed spiral nebula with slight traces of outside arms at end of major axis.
c,	139	5.6	Nebulous spot, 3″ diameter.
d,	126	13.2	20″×6″, *p* 70°, lbM.

N.G.C. 7023, Draco

$\alpha=21^h0^m37^s$, $\delta=+67°51'$ (1920); $\lambda=72°$, $\beta=+14°$

Plate No. 343, 1919, June 25, 160^m. S 23. Images small and slightly elongated

Comparison of this plate with No. 12 (1911, July 23, 149^m, S 23) in the stereocomparator gave no indication of change.

N.G.C. 7048, Cygnus

$\alpha=21^h11^m23^s$, $\delta=+45°57'.4$ (1920); $\lambda=57°$, $\beta=-2°$

Plate No. 296, 1917, July 20, 60^m. S 23. Images round and large

A planetary resembling the Dumb-bell nebula, about 1′ diameter, weak axis in *p* 170°. The central star is very faint. A longer exposure is necessary to bring out the detail.

N.G.C. 7240, 7242, Lacerta

$$\left.\begin{array}{lll}\text{N.G.C. 7240,} & \alpha=22^h11^m53^s, & \delta=+36°52'.7\\ \text{N.G.C. 7242,} & \alpha=22\ \ 12\ \ 10, & \delta=+36\ \ 53.7\end{array}\right\}(1920);\quad \lambda=59°,\quad \beta=-17°$$

Plate No. 292, 1917, June 21, 22, 195^m. S 23. Images round and medium
Plate No. 354, 1919, December 22, 50^m. S 23. Images round and small
Plate No. 357, 1919, December 23, 145^m. S 23. Images small and elongated

A group including twenty in addition to the six nebulae described by Barnard in *A.N.*, 137, 717, 1906. The measures refer to the nucleus of N.G.C. 7242.

N.G.C. 7240	*p* 0°,	*d* 0′.	18″×5″, *p* 108°, gbM, B stellar Nu., Barnard *c*.
N.G.C. 7242	73	3.6	12″×6″, *p* 33°, gbM, B stellar Nu., Barnard *a*.
a,	217	8.7	MB, 9″×1″.5, *p* 178°, gbM.
b, I.C.II 5191?	287	4.1	Spindle, 45″×6″, *p* 66°, BNu., Barnard *f*.
c,	214	6.0	F, 3″ diameter.
d,	203	8.2	F, 8″×2″, *p* 170°.
e,	217	3.6	B, 3″ diameter, almost stellar, F wings *p* 58°.
f, I.C.II 5192?	251	1.8	12″×6″, *p* 160°, gbM, Barnard *d*.
g,	193	6.5	F, 2″ diameter, bM.
h, I.C.I 1441	332	1.4	Spiral, 30″×15″, *p* 40°, Barnard *e*, Bigourdan 233.
i,	171	4.6	F, 4″×2″, *p* 140°.
j,	4	9.7	F, 10″×2″, *p* 143°.
k,	15	4.1	MB, 4″ diameter, stellar.
l,	175	14.0	MB, 3″ diameter.
m,	95	2.3	F, 2″ diameter.
n,	157	6.2	Spindle, 20″×6″, *p* 120°, B stellar Nu.
o,	141	4.1	F, 6″×3″, *p* 100°.
p, I.C.II 5195	71	4.0	B, 4″ diameter, gbM, almost stellar.
q,	140	5.7	F, 3″ diameter, Nu.
r, I.C.II 5194?	119	4.8	10″ diameter, gbM, B stellar Nu., Barnard *b*.
s,	41	6.3	F, 3″ diameter.
t,	68	7.3	B, 3″ diameter, almost stellar.
u,	40	15.4	F, 20″×6″, *p* 124°, B stellar Nu.
v,	51	12.5	F, 2″ diameter.
w,	83	10.0	F, 2″ diameter.
x,	117	13.6	18″×5″, *p* 118°, stellar Nu.

N.G.C. 7435, 7436, Pegasus

$$\left.\begin{array}{lll}\text{N.G.C. 7435,} & \alpha=22^h54^m6^s, & \delta=+25^\circ42'.2 \\ \text{N.G.C. 7436,} & \alpha=22\ 54\ 6\ , & \delta=+25\ 43.3\end{array}\right\}(1920); \quad \lambda=62^\circ, \quad \beta=-31^\circ$$

Plate No. 293, 1917, June 23, 120^m. S 23. Images small and round

The plate shows a rich field of small nebulae consisting of elongated masses with bright almost stellar nuclei. They are probably spiral.

N.G.C. 7431, $a=22^h53^m47^s$, $\delta=+25^\circ44'.2$ (1920), is a star with faint companion *f*.

N.G.C. 7433, $a=22^h\ 54^m\ 2^s$, $\delta=+25^\circ43'.2$ (1920), does not appear on the plate.

N.G.C. 7436 has a bright stellar nucleus surrounded by faint nebulosity, 7″ diameter.

The positions of the following nebulae are referred to N.G.C. 7436.

a, *p*	239°, *d*	14′.9	MB, 20″×8″, *p* 40°, lbM.
b,	273	7.9	F, 15″×5″, *p* 150, lbM.
c,	249	7.2	MB, 30″×8″, *p* 140, spindle, bM.
d,	332	12.6	F, 15″×10″, *p* 30, lbM.
e,	238	5.7	F, 20″×10″, *p* 150, lbM.
f,	334	5.8	MF, 10″×5″, *p* 150, spindle, stellar Nu.
g,	313	3.5	MF, 5″ diameter, stellar Nu.
h,	300	1.6	MB, 30″×10″, *p* 45, ellipse, stellar Nu.
i,	232	1.0	MB, 30″×10″, *p* 160, spiral, stellar Nu.
j,	187	2.4	MB, 5″ diameter.
k,	270	0.4	B, 20″×6″, *p* 95, spindle, stellar Nu.
l,	168	1.1	MF, 4″ diameter stellar nucleus, N.G.C. 7435.
m,	136	7.3	MB, 20″×10″, *p* 130.
n,	141	9.4	F, 30″×8″, *p* 40, uniform.
o,	47	8.9	MF, 6″ diameter, bM.

N.G.C. 7611, 7615, 7617, 7619, 7621, 7623, 7626, 7631, Pegasus

N.G.C. 7611,	$\alpha=23^h15^m33^s$,	$\delta=+7°22'.5$	(1920); $\lambda=56°$, $\beta=-51°$
N.G.C. 7615,	$\alpha=23\ 15\ 53$,	$\delta=+7\ 58.5$	
N.G.C. 7617,	$\alpha=23\ 16\ \ 2$,	$\delta=+7\ 43.7$	
N.G.C. 7619,	$\alpha=23\ 16\ 12$,	$\delta=+7\ 46.0$	
N.G.C. 7621,	$\alpha=23\ 16\ 20$,	$\delta=+7\ 55.7$	
N.G.C. 7623,	$\alpha=23\ 16\ 27$,	$\delta=+7\ 57.5$	
N.G.C. 7626,	$\alpha=23\ 16\ 39$,	$\delta=+7\ 46.7$	
N.G.C. 7631,	$\alpha=23\ 17\ 24$,	$\delta=+7\ 46.7$	

Plate No. 351, 1919, August 21, 130^m. S 23. Images small and round

N.G.C. 7611, B, stellar Nu., 10″ diameter in F nebulosity. 60″×15″, *p* 140°, edge of plate.
N.G.C. 7615, MF, uniform, 40″×20″, *p* 140°.
N.G.C. 7617, B, stellar Nu., 8″×5″, *p* 32°.
N.G.C. 7619, B, Nu., 12″×10″, *p* 32°, in F nebulosity.
N.G.C. 7621, Stellar Nu., 3″ diameter in nebulosity 20″×5″, *p* 170°.
N.G.C. 7623, B, stellar Nu., 8″×6″, *p* 170°, in F nebulosity 15″ diameter.
N.G.C. 7626, B, stellar Nu., 8″ diameter, in F nebulosity 40″ diameter.
N.G.C. 7631, MF, stellar Nu., 3″ diameter, in F nebulosity 90″×30″, *p* 80°.

There are many other small nebulae on the plate, which will be listed when a duplicate plate has been made.

N.G.C. 7722, Pegasus

$\alpha=23^h34^m41^s$, $\delta=+15^\circ31'.0$ (1920); $\lambda=68^\circ$, $\beta=-44^\circ$

Plate No. 353, 1919, August 27, 27^m. S 23. Images small, almost round

The exposure is sufficient to show a spiral with bright nucleus and strong absorption streak *f* the nucleus. The portion shown on the plate covers $45''\times30''$, *p* 150° (no trail).

I.C.I 922, 928, 931, Ursa Major, and a Group of 72 Others

$$\left.\begin{array}{ll}\text{I.C.I 922,} & \alpha=13^h40^m17^s,\ \delta=+56^\circ0'.4\\ \text{I.C.I 928,} & \alpha=13\ 40\ 43\ ,\ \delta=+56\ 1.2\\ \text{I.C.I 931,} & \alpha=13\ 40\ 49\ ,\ \delta=+56\ 1.3\end{array}\right\}\text{(1920);}\quad \lambda=73^\circ,\quad \beta=+59^\circ$$

Plate No. 341, 1919, May 28, 30^m. S 30. Fair images
Plate No. 342, 1919, June 25, 160^m. S 30. Fair images

Barnard originally called attention to this group in *A.N.*, **125**, 379, 1890, and numbers from 917 to 938 (with a few exceptions) were assigned to it in the *Index Catalogue*. Of the seventy-five nebulae shown on the plates only three (not including N.G.C. 5278–5279, which appear among them) have been identified, namely, I.C.I 922, 928, 913. Many of the objects are almost stellar, but they have been listed because of some peculiarity of appearance which distinguishes them from the neighboring star images. Measurements were made on the plate relative to B.D.+56° 1677, for which the reduced co-ordinates are $\alpha=13^h37^m19^s.6$, $\delta=+56^\circ25'.2$ (1860). Positions are given for right ascension and declination 1860. Hubble's paper[1] on this field which has just been published identifies twenty-five of the objects given here; they are indicated as H22, etc.

---

[1] E. P. Hubble, "Photographic Investigations of Faint Nebulae," *Publications of the Yerkes Observatory*, 4, Part II, 1919.

Description		α 1860	δ 1860
MB, Spindle, 30″×9″, *p* 10°, lbM		$13^h36^m\ 7^s.0$	$+56°22'.4$
MF, 7″, gbM	H22	9.1	15.9
B, 14″×8″, *p* 70°		11.6	20.4
MB, 7″, gbM		19.6	25.5
B, Nucleus, N.G.C. 5278		27.2	22.0
B, Tail, N.G.C. 5279		31.5	22.2
MF, 10″, patch	H31	47.3	28.8
MB, 5″		52.5	36.3
MF, 5″, lbM		56.7	36.0
F, 10″, patch		37 4.6	8.9
MF, 5″, lbM		5.6	19.9
MF, 12″ diameter, patch		13.0	40.6
MB, 12″×8″, *p* 135°, spindle, gbM		13.7	31.1
F, 6″, lbM		14.1	14.7
MB, 10″, gbM	H34	14.1	8.9
MF, 20″×5″, *p* 170°, uniform		16.7	31.2
B, B.D.+56° 1677		19.6	25.2
MF, 12″×8″, *p* 100°, lbM	H35	21.9	14.0
MF, 12″×8″, *p* 70°, lbM		23.2	10.2
MB, 4″		23.5	15.9
B, 20″×8″, *p* 100°, gbM	H36	26.1	13.8
MB, 12″×8″, *p* 135°, gbM	H37	34.3	12.6
MF, 4″		38.7	24.8
B, 6″, stellar	H40	45.1	17.8
F, 8″, patch		46.9	10.2
MF, 10″, lbM		47.1	40.1
MB, 10″, patch		48.2	35.1
MB, 12″×4″, *p* 60°, uniform		48.5	33.0
MB, 8″×4″, *p* 135°, lbM	H41	52.0	22.0
MF, 5″, lbM		53.7	26.8
MB, 5″, lbM		54.6	17.4
MB, 8″, I.C.I 922, gbM	H42	38 02.7	18.6
B, 5″, gbM	H43	3.4	17.7
MB, 20″×5″, *p* 100°, spindle, gbM	H44	5.4	18.5
F, 5″, patch		7.5	13.7
MF, 5″, lbM		8.9	17.4
B.D.+56° 1679		14.8	19.7
B, 5″, stellar		16.0	28.1
F, Patch 8″		16.0	14.7
MF, Patch 8″		19.0	14.6
MB, 10″×4″, *p* 90°, patch		26.1	16.7
MB, 3″		28.0	20.4
B, 8″×4″, *p* 120°, gbM, I.C.I 928		29.2	19.4
MF, 6″, gbM		32.0	24.8
MF, 8″, patch		32.7	16.7
MB, 10″×8″, *p* 90, lbM		33.0	25.3
B, 5″, I.C.I 931, stellar	H48	34.8	19.5
MB, 7″×3″, *p* 30°, lbM		35.2	30.4
B, 4″, almost stellar	H49	35.5	20.3
B, Star?		36.6	15.8
B, Star? 4″	H51	37.3	15.6
MF, 10″×4″, *p* 140°, lbM		38.9	24.3
B, 5″, almost stellar		39.4	18.9
B, 6″, almost stellar	H53	41.4	20.3
MB, 4″, almost stellar		42.7	20.9
F, 7″, lbM		43.1	15.0

Description		α 1860	δ 1860
F, 8″×4″, *p* 95°		$13^h38^m47^s.2$	+56°19′.4
F, 10″×5″, *p* 135°	H56	51.0	15.5
B.D.+56° 1682		56.4	19.6
B, 8″×5″, *p* 40°, gbM		58.9	25.4
B, 15″×6″, *p* 90°, gbM	H59	59.2	23.8
MF, 7″, patch, lbM		39 0.0	28.3
B, 30″×6″, *p* 80°, BNu., spindle	H60	12.7	32.8
F, 6″, patch		13.6	11.4
B, 30″×6″, *p* 30°, gbM	H61	13.7	38.9
F, 5″, patch		14.0	12.1
B, 8″×5″, *p* 135°		19.6	19.3
B, 10″×6″, *p* 150°	H62	25.5	19.1
MB, 25″, patch, gbM	H63	31.6	41.2
B, 15″×10″, *p* 40°, patch	H64	33.5	34.8
F, 30″×4″, *p* 10°, sliver		33.5	34.1
MB, 4″, almost stellar		36.1	22.4
MB, 4″, almost stellar		37.3	23.1
F, 5″		40.8	28.7
MF, 3″		41.5	19.7
F, 11″×6″, *p* 135°		47.5	11.1
MF, 8″, patch, lbM		51.6	24.5
MF, 8″×4″, *p* 40°, patch		53.6	24.3
MB, 10″×4″, *p* 130°, spindle, bM	H66	55.0	16.1

I.C.I 1470, Cassiopeia

$\alpha=23^h1^m51^s$, $\delta=+59°48'.9$ (1920); $\lambda=78°$, $\beta=-1°$

Plate No. 297, 1917, July 21, 190^m. S 23. Images intermediate and fairly round. Illustrated Plate XVIII*a*

A gaseous nebula lying in a rich region of the Milky Way. Its prominent feature is a bright thread of nebulosity irregularly triangular in shape, superimposed on the fainter nebulosity. The sides of the triangle are roughly 30″ long; the north side lies in *p* 88° and is straight, except for an abrupt bend to the N around a star directly in its middle; the *f* side in *p* 60° is shaped like an integral sign, while the *p* side, *p* 140°, is V-shaped, points inward, and has a faint star at its apex. The N and *p* sides do not quite join. The faint nebulosity is roughly 70″×45″ and is quite full of markings, which a longer exposure will show to advantage. A dark marking cuts across the nebula north of the triangle.

Three nebulous stars appear in the plate:

a,	314°	14′.8	Three stars involved in F nebulosity.
b,	197	10.7	Bright star in group of 5, involved in nebulosity.
c,	84	6.2	Two stars involved in nebulosity.

I.C.II 2233, Lynx

$\alpha=8^h8^m19^s$, $\delta=+45°59'.5$ (1920); $\lambda=141°$, $\beta=+35°$
Plate No. 2968 (Shapley), 1916, March 27, 30^m. S 27
Plate No. 359, 1919, December 23, 60^m. S 30. Images elliptical

The nebula falls near the edge of the plates of N.G.C. 2537 and appears to be a faint edge-on spiral 240″×10″, *p* 170° (no trail), with a faint stellar nucleus.

I.C.II 5146, Cygnus

$\alpha=21^h50^m25^s$, $\delta=+46°53'.2$ (1920); $\lambda=62°$, $\beta=-7°$
Plate No. 276, 1916, August 4, 60^m. S 23. Images small and round.
Plate No. 349, 1919, July 26, 300^m. S 23. Images small and elongated.
Illustrated Plate XVII*c*

This well-known nebula lies at the end of a dark lane which is well shown on Plate No. 349 and on the various published photographs of Barnard, Curtis, Franks, and Wolf. It surrounds the star B.D.+46° 3474 $9^M.5$, and its strong parts are 12′ in diameter, while extensions run to the boundaries of the dark region in which it lies. Two of these extensions end at stars involved in nebulosity, *a*, *p* 257, *d* 9′.7, which is preceded by a bright patch, and *b*, *p* 156°, *d* 9′.8, where the nebulosity brightens on the preceding side of the star. The nebula is a wonderful array of dark and light markings and cannot be likened to any other object, although counterparts of certain configurations may be found in some of the other large gaseous nebulae. For example, the dark birdlike or torchlike dark markings in the S*p* section, of which there are two, are similar to a marking in the *p* section of M 16; two dark indentations on the N*p* side resemble some of the indentations about the rim of M 8; and some of the canopied structure resembles the outlying parts of the Orion nebula.

MOUNT WILSON OBSERVATORY
April 1920

ERRATA in *Mount Wilson Contr.*, No. 132,

Astrophysical Journal, 46, 24, 1917

Page 12: N.G.C. 2403, Plate V*c* was made from negative No. 307 (of the present series) instead of No. 169.

Page 18: N.G.C. 4594, the equation should read $V = -2.78x + 1180$.

Plate XIII*c*: N.G.C. 5544–5545, orientation of the plate is S at top, *f* at right; identification of nebulae in text is not correct; true description is found in the present series.

Page 19: N.G.C. 4900, $\alpha = 12^h 56^m 28^s$.

Contributions from the Mount Wilson Observatory, No. 187
Reprinted from the *Astrophysical Journal*, Vol. LII, pp. 8–22, 1920

THE COLOR OF THE NEBULOUS STARS

BY FREDERICK H. SEARES AND EDWIN P. HUBBLE

ABSTRACT

Color of forty-seven nebulous stars.—The ratio of the times of exposure with and without a yellow filter, producing images of the same size on an isochromatic plate, varies regularly with the spectral type for normal stars of a given absolute magnitude. Most nebulous stars, however, as the results in this paper show, are abnormally red for their spectral type. The color-indices of thirty-six out of the forty-two nebulous stars for which complete data are available are from 0.4 to about 3 color-classes in advance of their respective spectral types. The average *color excess* is about one color-class, which is five times the probable error. Two methods were used. The color-indices obtained from the *blue-yellow exposure ratios* determined with the 60-inch reflector were checked in part by those obtained from *polar comparisons of photographic and photo-visual magnitudes* made with the 10-inch Cooke refractor. The stars investigated are in R.A. 6^h to 7^h and 16^h to 18^h and include among others ρ Ophiuchi, σ Scorpii, 22 Scorpii, N.G.C. 1514, 2170, 2175, 2182, 2245, 2247, 2282, 2283, I.C. 444, 446. Several possible *explanations* of these results are discussed.

Suspected variable star.—The behavior of B.D.+10°1771, $8^{M}.0$, spectrum K0, suggests that it may be a variable.

Spectrum of nebulosity around nebulous stars N.G.C. 2245, 2247, 2282, I.C. 446, and ρ Ophiuchi is continuous, whereas the nebulosity around N.G.C. 1514 is gaseous.

In a paper presented to the Royal Society in 1791,[1] Sir William Herschel described a class of objects that he called "nebulous stars, properly so-called." These objects are found in or near the Galaxy, and are characterized by the fact that visually they present nothing to differentiate them from ordinary stars, except a surrounding mass of nebulosity; they are perfectly sharp and show none of the diffuseness found in those extra-galactic objects to which the name "nebulous star" is often applied. The nebulosity itself is frequently inconspicuous, and in some cases can be detected only on photographs of long exposure.

Historically, the nebulous stars of Herschel are of great interest, for it was through them that he first became convinced of the existence of luminous matter widely scattered throughout space, in a form quite different from that which constitutes the stars, and was led to generalizations that have long dominated the field of stellar evolution. Their important contribution dates back a hundred and thirty years, but the interest which attaches to nebulous stars is not wholly historical, as will appear from the following.

---

[1] *Phil. Trans.*, 81, 71, 1791; *Collected Scientific Papers*, Vol. I, 415 (London, 1912).

The observations described below have grown out of a remark by Hubble that visually the central star of N.G.C. 1514 and of one or two similar objects are appreciably redder than their spectral types would indicate them to be.[1] Measures of the color of N.G.C. 1514 and 2245 by the method of exposure-ratios confirmed this suspicion. An examination of the color-indices available for certain other nebulous stars, although inconclusive, was suggestive that a real excess of color might be associated with these objects as a class. Systematic observations were then undertaken and sufficient data have been accumulated to put the matter largely beyond doubt. For the great majority of the objects observed there seems to be no doubt whatever; two or three stars appear to be exceptional, and two or three others included in the program are open to question, because their intimate association with nebulosity is not yet fully established.

Herschel's original list[2] of nebulous stars included eighteen. The number at present known is approximately one hundred; many of the later discoveries are due to Professor Barnard, to whom we are much indebted for unpublished data. The stars thus far observed, about fifty in all, occur in two groups, in R.A. 6^h–7^h and 16^h–18^h, and are mainly in southern declinations ranging from the equator to $-24°$. Their spectra are mostly of type B; a very few seem to be early A's; one is Oe5 and one G5.

The observations have been made with the 60-inch reflector by the method of exposure-ratios,[3] controlled in part by photographic polar comparisons with the 10-inch Cooke refractor. To reduce the measurement to a differential procedure, all the nebulous stars in the same part of the sky were photographed on the same plate, along with a half-dozen other stars of known spectrum, not associated with nebulosity, whose colors are assumed to be normal. As a further aid in the elimination of systematic errors, the check stars were observed at approximately the same mean zenith distance as the nebulous stars.

---

[1] Russell (*Proceedings of the National Academy of Sciences*, **5**, 398, 1919) has called attention to the abnormal color-indices of ζ, o, and ξ Persei, all situated in a region full of diffuse nebulosity.

[2] *Loc. cit.*

[3] Seares, *Proceedings of the National Academy of Sciences*, **2**, 521, 1916; **3**, 29, 1917; **5**, 232, 1919.

Three stars of the group in 6^h–7^h were already out of reach toward the west when the observations were begun. Of this group we have observed thirteen nebulous stars and six check stars. For the second group the numbers are thirty-one and seven, respectively, although several of the nebulous stars occur on a single plate. The polar comparison plates supply results for two additional nebulous stars in the second group.

TABLE I

OBSERVATIONS OF NEBULOUS STARS

Exposure Ratio, 60-inch Reflector		Polar Comparisons, 10-inch Refractor	
1920, Feb. 16, Plate	5209, 5210	1920, Apr. 12, Plate	5, Iso, 10^m
Apr. 21	5241		6 S30, 1
22	5244, 5250		7 S30, 1
23	5254		8 Iso, 10
24	5266	Iso plates used with filter D	

To determine the ratio of exposures necessary to produce blue and yellow images of equal intensity, exposures, usually of 2, 4, and 8 seconds, are made on a Cramer Instantaneous Iso plate, thus giving a series of "blue" images. The yellow images are produced by exposing the same plate behind a yellow filter—32 and 64 seconds for B and A stars, 16 and 32 seconds for F and early G stars, and 8 and 16 seconds for later G's and for K and M stars. To identify the images additional 2-second exposures are made, and the order of one or both of the series is inverted. The blue images serve as a scale with which the exposure required to produce a blue image equal to a given yellow image may be read directly from the plate. The logarithm of the exposure-ratio (log E) is used as the measure of color.

Since the relative size of the blue and yellow images depends upon their actual size, it is important that the images be kept within certain narrow limits. To this end each star photographed is reduced to a standard apparent magnitude—usually the tenth, with a possible range of half a magnitude in either direction—by means of diaphragms and screens. In refined work the remaining small deviations may be compensated by slight corrections, although it is doubtful if anything is thereby gained, since the corrections are of the order of the unavoidable uncertainties. The exposure-ratio also depends upon the emulsion and, indeed, to some extent upon the individual plate.

The relation of $\log E$ to spectral type and Mount Wilson color-indices (color system of the 60-inch reflector) for a provisional mean curve is shown in Table II. The values refer to stars of zero absolute magnitude. For dwarf stars quite another series must be used,[1] but this is not needed for the present discussion. In the region of the B stars the curve is possibly a little too steep; but this cannot appreciably affect the present results.

TABLE II

SPECTRUM, EXPOSURE-RATIO, AND COLOR-INDEX

(Blue-Yellow, Provisional Values for $M=0$)

Sp.	log E	C.I.	Sp.	log E	C.I.
B0	8.80	−0.40	G0	9.26	+0.80
B5	8.86	−0.20	G5	9.35	+1.00
A0	8.94	0.00	K0	9.45	+1.20
A5	9.02	+0.20	K5	9.55	+1.40
F0	9.10	+0.40	Ma	9.55	+1.40
F5	9.18	+0.60	Mb	9.55	+1.40

The effect of atmospheric extinction and fluctuations from plate to plate in the relative blue-yellow sensitiveness is to displace vertically the curve of $\log E$ and the spectrum. These and other similar factors, such as abnormal values of the coefficients of reflection from the mirror, all combine to form a plate constant whose value is determined by comparing the observed values of $\log E$ for the check stars with the normal curve. The application of the plate constant to the observed values of $\log E$ for the stars of unknown color reduces them to the curve from which the color-class[2] or color-index can be determined.

---

[1] Seares, *Proceedings of the National Academy of Sciences*, **5**, 232, 1919.

[2] Seares, *op. cit.*, **1**, 481, 1915.

Table III gives the values of the plate constants derived from the individual check stars and the adopted means. The check stars are all giants, but several of them deviate appreciably from zero absolute magnitude, to which the values of Table II refer. Allowance for this fact has been made with the aid of the curves in the *Proceedings of the National Academy of Sciences* (**5**, 232, 1919, Figs. 2 and 3). The results in Table III are affected both by the errors of measurement and the uncertainties in the spectral classification. Their combined influence upon a single value of the plate constant averages ±0.041, or ±0.10 mag. The average uncertainty for a plate is therefore ±0.017, or ±0.04 mag.

TABLE III

CHECK STARS AND PLATE CONSTANTS

(Unit=0.01 in log E)

Star	Sp.	5241	5244	5254	Star	Sp.	5250	5266
Boss 1751.....	B8	− 4	−13	+ 1	Boss 3758....	F3	− 5	+ 5
1788.....	B8	− 3	−10	− 3	3810....	K0	−16	− 5
1944.....	B8	− 4	−13	−19	4137....	F9	− 9	−11
2008.....	F3	......	− 6	− 5	4193....	Ma	− 6	−11
2020.....	Mb	− 6	− 5	−11	4731....	F3	− 4	+ 4
2330.....	B3	−10	−14	− 6	5003....	B0	− 6	−12
....	......	......	......	......	5062....	A4	− 1	......
Means.......	......	− 5	−10	− 7	Means.....	......	− 7	− 5

Freed from plate error, the results for all the stars observed are in Tables IV and V. It should be noted that the application of the plate constants has really been effective in reducing the results to a homogeneous system. If the mean log E be formed for each star, and then the deviations of the individual values from these means, we obtain data for the calculation of any residual systematic differences between the plates. Excluding B.D.+10°1771, which is peculiar, the results are

Plate	5210	5241	5244	5254	5250	5266	
Systematic	−0.013	+0.004	−0.002	+0.007	−0.005	+0.005	log E
Deviation	−0.032	+0.010	−0.005	+0.017	−0.012	+0.012	mag.

The average value of the probable error of a single determination of color from these measures, including residual errors in the plate constants, is $\pm 0\overset{\mathrm{M}}{.}066$.

TABLE IV

COLORS FROM EXPOSURE-RATIOS, REGION 6^h–7^h

Object	Vis. Mag.	Sp.	Log *E* (Blue-Yellow)						Color Excess (Unit, 1 Spectral Subdivision)					
			5209	5210	5241	5244	5254	Mean	5209	5210	5241	5244	5254	Mean
Nebulous stars														
N.G.C. 1514	9.0	B8	9.09	......	......	......	......	9.09	+1.2	......	......	......	......	+1.2
2175	7.40	Oe5	......	......	8.87	......	8.87	8.87	......	......	+1.0	......	+1.0	+1.0
2245	11.	A0	......	9.14	9.15	9.16	9.18	9.16	......	+1.3	+1.3	+1.4	+1.5	+1.4
2247	8.5	......	......	9.14	9.07	9.08	9.07	9.09	......	......	......	......	......	......
2282	9.7	B5	......	......	......	8.97	8.95	8.96	......	......	......	+0.7	+0.6	+0.6
I.C. 444	7.03	B9	......	......	9.15	9.09	9.11	9.12	......	......	+1.4	+1.1	+1.2	+1.2
446	10.5	B5	......	......	9.19	9.09	9.11	9.13	......	......	+2.1	+1.5	+1.6	+1.7
B.D.+10°1771	8.0	K0	......	9.46	9.29	9.27	9.31	......	......	+0.1	−0.9	−1.0	−0.7	......
− 6 1415*	10.2	B1	......	......	......	9.21	9.24	9.22	......	......	......	+2.6	+2.8	+2.7
− 6 1417	9.1	B9	......	......	9.09	9.09	9.05	9.08	......	......	+1.1	+1.1	+0.8	+1.0
− 6 1418	9.1	B5	......	......	9.08	9.14	9.15	9.12	......	......	+1.4	+1.4	+1.8	+1.5
− 6 1431†	9.1	B5	......	......	8.99‡	9.15	9.06	9.07	......	......	+0.08	+1.8	+1.3	+1.3
−10 1848	7.01	B0	......	......	......	9.09	9.06	9.08	......	......	......	+2.0	+1.8	+1.9
−12 1771	8.5	B9	......	......	8.91	8.87	......	8.89	......	......	−0.1	−0.4	......	−0.2
													Mean	+1.28
Check stars														
Boss 1751	6.0	B8	6 B	8.91	8.90	8.94	8.83	8.90	......	0.0	−0.1	+0.2	−0.5	−0.1
1788	6.0	B8	and	and	8.89	8.91	8.87	8.89	......	......	−0.1	0.0	−0.2	−0.1
1944	2.9	B8	11 A	9	8.90	8.94	9.03	8.96	......	......	−0.1	+0.2	+0.8	+0.3
2008	0.2	F3	stars	other	......	9.15	9.17	9.16	......	......	......	0.0	+0.1	+0.1
2020	6.0	Mb	......	B stars	9.56	9.50	9.59	9.55	......	......	+0.1	−0.3	+0.2	0.0
2330	4.4	B3	......	......	8.89	8.88	8.83	8.87	......	......	+0.3	+0.2	−0.1	+0.1
													Mean	+0.05

* N.G.C. 2170. † N.G.C. 2182. ‡ Images bad.

Spectra of N.G.C. 1514 and 2245 by Sanford with focal plane slit spectrograph and 100-inch reflector; N.G.C. 2282 and I.C. 446, 6° objective prism and 10-inch refractor (uncertain); B.D. −6°1415 and −6°1418, 15° objective prism and 10-inch refractor; spectra of other nebulous stars are from the *Revised Draper Catalogue;* those of check stars are by Adams and from the *Revised Draper Catalogue.* In all cases the spectrum refers to the star—not to the surrounding nebulosity.

Magnitudes of N.G.C. 2245 and I.C. 446 are estimates; those of N.G.C. 2175, I.C. 444, and B.D. −10° 1848 are from *Harvard Annals*, **54**; those for the other nebulous stars are B.D. values corrected by *Harvard Annals*, **72.**

The very large color excess for B.D. −6°1415 seems to be real; but the result requires confirmation, for the images are very faint on both plates.

TABLE V

Colors from Exposure-Ratios, Region 16h–18h

Object	Vis. and Pv. Magnitude	Sp.	Log *E*			Color Excess		
			5250	5266	Mean	5250	5266	Mean
Nebulous stars								
ρ Ophiuchi Bt.	5.22	B5	9.05	9.00	9.03	+1.2	+0.9	+1.1
ρ Ophiuchi Ft.	5.92		9.06			+1.3		
σ Scorpii	3.08	B1	9.05	8.94	9.00	+1.6	+0.9*	+1.2
22 Scorpii	4.87	B5	9.88	8.89	9.88	+0.1	+0.2	+0.2
B.D. −10°4713	5.80	B5	9.03	9.11	9.07	+1.1	+1.6	+1.4
−19 4357	6.2	G5	9.33	9.31	9.32	−0.1	−0.2	−0.2
−19 4359 Bt.	7.1	B9	8.99	9.01	9.00	+0.4	+0.5	+0.4
−19 4359 Ft.	8.0	A0	9.05	8.99	9.02	+0.7	+0.3	+0.5
−19 4361 Bt.	7.0	B9	9.07	9.07	9.07	+0.9	+0.9	+0.9
−19 4361 Ft.	8.4	A0	9.06	9.07	9.06	+0.8	+0.8	+0.8
−19 4940	9.6	B3	......	8.99	8.99	......	+1.0	+1.0
−19 4943	9.0	B9	......	9.05	9.05	......	+0.8	+0.8
−19 4946 Bt.	10.9	B3	......	9.01	9.01	......	+1.1	+1.1
−19 4946 Ft.	10.9	B3	......	8.97	8.97	......	+0.9	+0.9
−19 4948	9.0	B1	......	8.95	8.95	......	+1.0	+1.0
−19 4953	7.5	B5	......	9.02	9.02	......	+1.0	+1.0
−19 4954	9.9	......	......	9.37	9.37	......	......	......
C.D. −23 12860	6.56	B8	9.09	9.07	9.08	+1.1	+1.3	+1.2
−23 12862	......	......	9.09	9.09	9.09	......	......	......
−23 13908	10.1	B3	9.09	8.97	9.03	+1.6*	+0.9*	+1.2
−23 13983	9.6	B5	......	9.14	9.14	......	+1.8†	+1.8
−23 13997	9.1	B5	8.95	8.96	8.96	+0.6	+0.6	+0.6
−23 13998	8.6	B3	8.93	8.97	8.95	+0.6	+0.9	+0.8
−23 13999	9.9	A2	9.00	8.96	8.98	+0.2	−0.1	0.0
−23 14002	9.9	A2	8.95	8.99	8.97	−0.1	+0.1	0.0
−23 14004	9.7	......	8.99	8.95	8.97	......	......	......
−23 14005	7.4	B3	8.97	8.98	8.98	+0.7	+0.7	+0.7
−23 14017	8.5	B5	8.97	9.04	9.00	+0.7	+1.1	+0.9
−24 12684	8.0	B5	9.18	9.13	9.16	+2.0	+1.7	+1.8
−24 13962	7.2	B1	8.97	8.97	8.97	+0.9	+1.1	+1.0
−24 13984	9.8	B1	......	9.08	9.08	......	+1.7	+1.7
							Mean	+0.88
Check stars								
Boss 3758	3.9	F3	9.17	9.09	9.13	−0.1	−0.6	−0.4
3810	5.8	K0	9.54	9.45	9.50	+0.8	+0.2	+0.5
4137	5.6	F9	9.24	9.28	9.26	−0.1	+0.1	0.0
4193	0.8	Ma	9.54	9.61	9.58	−0.1	+0.4	+0.2
4731	4.8	F3	9.09	9.03	9.06	−0.2	−0.6	−0.4
5003	5.1	B0	8.82	8.91	8.86	+0.1	+0.7	+0.4
5062	0.6	A4	9.03	......	9.03	−0.2	......	−0.2
							Mean	+0.01

* Images bad.

† Images at edge of plate.

NOTES TO TABLE V

For those stars included in the polar comparisons given in Tables VI and VII the magnitudes are photo-visual. Magnitudes for the remaining nebulous stars are visual, from *Harvard Annals*, **50** or **54**, and the C.D. corrected by *Harvard Annals*, **72**.

ρ Ophiuchi: Sp. from *Harvard Annals*, Frost and others, is probably of brighter component only.

σ Scorpii: Sp. from *Harvard Annals*, Campbell and others. A spectroscopic binary with stationary H and K lines. *Harvard Annals*, **76**, gives a color excess of $+0^{M}33$ mag.

22 Scorpii, and B.D. $-10°4713$: Sp. from *Harvard Annals*, checked by MW slit spectrogram.

B.D. $-19°4357$: Slit spectrogram, 60-inch. Abs. mag. by Adams, one plate, -0.3.

B.D. $-19°4359$, $-19°4361$: Sp. from *OP* 10-inch refractor, and *FP* slit, 60-inch reflector.

B.D. $-19°4940$: Sp. from *OP* 10-inch refractor. Lines very diffuse.

B.D. $-19°4943$: Sp. from *OP* 10-inch refractor. Lines very wide, especially Hδ.

B.D. $-19°4946$: Sp. from *FP* slit, 60-inch reflector.

B.D. $-19°4948$: Sp. from *OP* 10-inch refractor.

B.D. $-19°4953$: Sp. from *FP* slit, 60-inch reflector.

C.D. $-23°12860$: 3′ *p* ρ Ophiuchi. Sp. from *OP* 10-inch refractor.

C.D. $-23°12862$: 2′ N ρ Ophiuchi.

Spectra of remaining nebulous stars from *OP* 10-inch refractor.

C.D. $-23°13908$: Sp. very faint.

C.D. $-23°13983$: Lines widely double.

C.D. $-23°14005$ and $-24°13962$: Sp. checked by *FP* slit, 60-inch reflector.

Spectra of check stars are by Adams or from *Harvard Annals*.

The significant quantities are those in the two columns headed "Color Excess." These are expressed in spectral subdivisions and were obtained by subtracting the spectral type from the color-class corresponding to log E. Their values in magnitudes on the color system of the reflector may be found by multiplying by 0.4. Thus for N.G.C. 1514, Plate 5209, log $E=9.09$; the color-class is *f*0 and the spectrum B8, whence the color excess is $+1.2$, or in magnitudes, $+0.48$.

The values of the color excess for the check stars are merely residuals, inasmuch as the color of these stars is assumed to be normal. In contrast with these, the large and persistently positive values of the color excess for the nebulous stars show that their colors are well in advance of their spectral types. The phenomenon seems to be somewhat more pronounced for the group in 6^{h}–7^{h} than for that in the later hours of right ascension, the respective means being $+1.28$ and 0.88. The corresponding values in magnitudes are $+0.51$ and $+0.35$.

The star B.D. +10°1771, $8^{M}_{.}0$, is not nebulous, but follows the nebulous star N.G.C. 2245 closely and lies in the dark lane connecting this object with N.G.C. 2247. The spectrum, K0, is from the *Revised Draper Catalogue*. The values of log E are subject to a systematic correction because of the size of the images, the exposures and aperture having been adjusted to N.G.C. 2245 and I.C. 446, which are both in the same field and much fainter; but their relative values should be reliable. The accordant results from Plates 5241, 5244, 5254 can be reconciled with the spectrum only by supposing the star to be of low luminosity, $M = +6$ or fainter. The value from Plate 5210, on the other hand, indicates high luminosity. The images on this plate are excellent. The possibility of an error in the record which would explain the discordance seems to be excluded by the results for N.G.C 2245 and 2247 (observed simultaneously with B.D. +10°1771), which are in agreement with those from the other plates. The behavior of the star suggests variability.

These results have been tested by a direct determination of the color-indices of two groups of nebulous stars in $18^{h}\,5^{m}_{.}5, -24°$ and $18^{h}12^{m}, -19°$, respectively, with the aid of polar comparisons made with the 10-inch Cooke triplet. One pair of plates for the determination of photographic and photo-visual magnitudes was made for each region; and, as a check on the zero-points of the magnitude scales, several stars near the nebulous objects, but not involved in nebulosity, were also included in the comparison. The results are given in Tables VI and VII.

The photographic and photo-visual magnitudes are on the Mount Wilson system,[1] reduced to the color system of the 10-inch refractor by the formula

$$Pg_{10} = Pg_{60} - 0.19\, C_{60},$$

in which Pg_{60} represents the photographic magnitude of a polar standard on the color system of the reflector and C_{60} its corresponding color-index. The photo-visual magnitudes require no reduction.

---

[1] *Mt. Wilson Contr.*, No. 97; *Astrophysical Journal*, **41**, 206, 1915.

The spectra are from an objective prism plate with the same instrument. The relation between color-index and spectrum for the check stars is shown in Figure 1, from which it appears that the zero-points of the magnitude scales are well determined. For Region II there is a slight systematic effect, but for Region I spectrum A0 corresponds to zero color-index very accurately. For K0, $C_{10}=0.96$. For the reflector the corresponding value is $C_{60}=1.20$, whence the coefficient of the color equation is 0.20, in agreement with the value given above.

TABLE VI

COLORS BY POLAR COMPARISONS. REGION I, R.A. $18^h5^m.5$ DEC. −24°

OBJECT	MAGNITUDE		COLOR-INDEX	COLOR-CLASS	SP.	COLOR EXCESS	
	Pg.	Pv.				CC−Sp.	Table V
Nebulous stars							
B.D. −22°4510*.....	8.04	7.25	+0.79	*g5*	A3	+2.2	....
C.D. −23 13836.....	8.34	8.74	−0.40	*o8*	B0	−0.2	....
−23 13908.....	10.23	10.10	+0.13	*a4*	B3	+1.1	+1.2
−23 13954.....	9.64	9.55	+0.09	*a3*	B3	+1.0	....
−23 13983.....	9.78	9.64	+0.14	*a4*	B5	+0.9	+1.8†
−23 13997.....	9.08	9.10	−0.02	*b9*	B5	+0.4	+0.6
−23 13998.....	8.45	8.56	−0.11	*b7*	B3	+0.4	+0.8
−23 13999.....	10.02	9.87	+0.15	*a5*	A2	+0.3	0.0
−23 14002.....	9.95	9.82	+0.13	*a4*	A2	+0.2	0.0
−23 14004.....	9.82	9.73	+0.09	*a3*‡	....	....	....
−23 14005.....	7.64	7.38	+0.26	*a8*	B5	+1.3	+0.7
−23 14017.....	8.47	8.46	+0.01	*a0*	B5	+0.5	+0.9
−24 13962.....	7.38	7.20	+0.18	*a6*	B1	+1.5	+1.0
−24 13984.....	9.93	9.78	+0.15	*a5*	B1	+1.4	+1.7
Check stars							
C.D. −23°13909.....	9.45	8.37	+1.08	*k4*	K2	+0.2	
−23 13991.....	7.62	7.60	+0.02	*a1*	A2	−0.1	
−23 13881.....	7.67	8.01	−0.34	*o9*	B2	−0.3	
−24 13893.....	9.03	8.96	+0.07	*a2*	A2	0.0	
−24 13880.....	7.54	7.65	−0.11	*b7*	B5	+0.2	
−23 14016.....	8.80	8.42	+0.38	*f1*	F2	−0.1	
−23 14012.....	9.43	9.37	+0.06	*a2*	B9	+0.3	
−23 14001.....	9.08	8.19	+0.89	*g8*	K0	−0.2	
Systematic difference for check stars						0.00	

* The bright central star in the northern mass of the Trifid nebula.

† Images at edge of plate.

‡ Color-class from exposure-ratio *a2*.

Assuming the increase in color to be linear, we find from the color-indices by the formula, color-class$=C_{10}/0.32$, the values given in the fifth column of Tables VI and VII. The differences, color-class *minus* spectrum, expressed in spectral subdivisions, are the values of the color excess. The mean differences for the check stars are small, as was to have been expected. Their values are 0.00 and +0.14, respectively, or in magnitudes, 0.00 and +0.03. The nebulous stars, on the other hand, with the exception of C.D. −23°13836, 13999, and 14002 (Table VI), show large values of the color excess, in agreement with the results obtained from the exposure-ratios, which are inserted in the last column of Tables VI and VII. Correcting the values of the color excess derived in Table VII for the small outstanding systematic difference shown by the check stars, which is probably to be attributed to zero-point errors in the magnitudes, we find means for the stars observed by both methods as follows:

TABLE VII

COLORS BY POLAR COMPARISONS, REGION II, R.A. 18^h12^m DEC. −19°

OBJECT	MAGNITUDE		COLOR-INDEX	COLOR-CLASS	SP.	COLOR EXCESS	
	Pg.	Pv.				CC−Sp.	Table V
Nebulous stars.							
B.D. −19°4940......	9.55	9.50	+0.05	*a*2	B3	+0.9	+1.0
−19 4943......	9.09	9.00	+0.09	*a*3	B9	+0.4	+0.8
−19 4946 Bt....	10.88	10.76	+0.12	*a*4	B5	+0.9	+1.1
−19 4946 Ft....	10.91	10.90	+0.01	*a*0	B3	+0.7	+0.9
−19 4948......	8.75	8.80	−0.05	*b*9	B1	+0.8	+1.0
−19 4953......	7.56	7.49	+0.07	*a*2	B5	+0.7	+1.0
−19 4954......	10.78	9.80	+0.98	*k*1*	....	....	....
Check stars							
B.D. −19°4970......	7.91	7.75	+0.16	*a*5	A3	+0.2	
−19 4965......	9.07	8.44	+0.63	*g*0	F8	+0.2	
−19 4969......	9.21	9.00	+0.21	*a*7	A2	+0.5	
−19 4952......	7.98	7.62	+0.36	*f*1	F2	−0.1	
−20 5065......	9.24	9.30	−0.06	*b*8	B5	+0.3	
−19 4935......	9.45	9.22	+0.23	*a*7	A5	+0.2	
−19 4929......	8.56	8.09	+0.47	*f*5	F8	−0.3	
	Systematic difference for check stars					+0.14	

* Color-class from exposure-ratio *g*6.

	From C.-I.	From log *E*	No. of Stars
Table VI..........	0.80	0.87	10
Table VII.........	0.59	0.97	6

Summarizing the results we find:

	Nebulous Objects Observed	Spectra Lacking	Positive Effect	Exceptions	Doubtful
Table IV............	13	1	11	B.D. −12° 1771	....
Table V............	31	4	23	B.D. −19 4357	22 Scorpii
				C.D. −23 13999	....
				C.D. −23 14002	....
Additional, Table VI..	3	....	2	C.D. −23 13836	....
Totals............	47	5	36	5	1

Of the forty-two objects for which complete data are available, thirty-six show a positive effect whose reality can scarcely be doubted. A revision of the spectral classification may modify the number slightly; but the close accordance of the spectra for the check stars in Tables VI and VII and the corresponding color-indices (see Fig. 1) lead us to hope that no serious uncertainty arises from this source. As for the exceptional cases, it has already

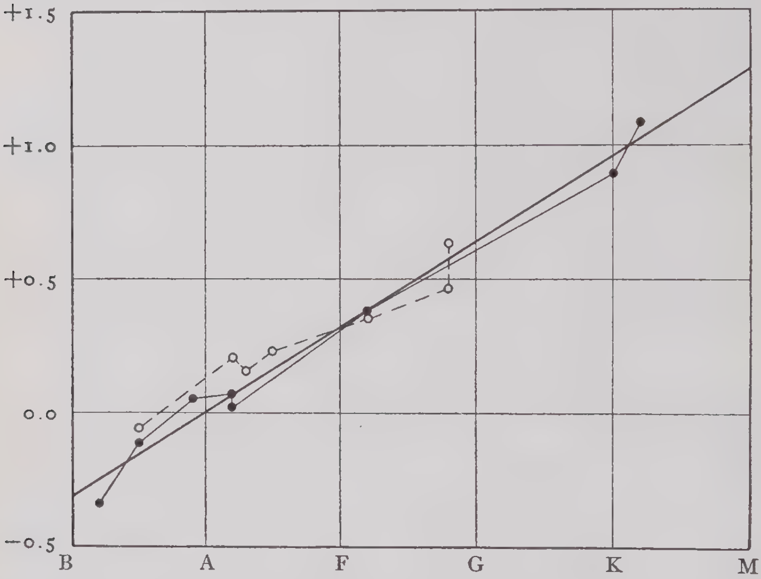

FIG. 1.—Spectral type and color-index for the 10-inch Cooke refractor. Full line, Table VI; broken line, Table VII.

been remarked that, in some cases at least, a close association with nebulosity has not certainly been established. In any event it seems clear that a large majority of these objects are approximately one color-class in advance of their spectral types.

It would be premature at this stage of the investigation to express an opinion as to the cause of the phenomenon. An explanation that will occur to everyone, perhaps the most plausible at hand, is that of molecular scattering produced by the nebulosity surrounding the star. But there is also the chance of some form of fluorescent excitation in the nebulous material closely adjacent to the stars; and one should likewise bear in mind the possibility that peculiar internal conditions may occur in stars intimately involved in nebulosity, producing something similar to the luminosity effect that is now well established for the G and K stars at large. Narrowly considered, this last suggestion does not seem immediately applicable. Almost without exception the nebulous stars have B or early A spectra; and the luminosity effect for these types, if present at all, is certainly much less than the color excess observed in the nebulous stars. But if we think of the luminosity effect upon color as being primarily atmospheric in origin, and if at the same time we look upon the luminous material surrounding the nebulous stars as an integral part of its atmosphere, chaotic and unorganized through a neutralization of gravitational attraction by repulsive forces, the connection may not be so remote. This, however, leads us back to the suggestion of molecular scattering as the primary phenomenon.

Finally, a scattering by particles of more than molecular size should not be forgotten. In this connection it is at least suggestive that the nebulosity surrounding N.G.C. 2245, 2247, 2282, and I.C. 446,[1] as well as that covering the region of ρ Ophiuchi, shows a continuous spectrum. Moreover, all through that part of the sky including the group of nebulous stars in 16^h–18^h of right ascension we find extended areas of low star density, dark lanes, and vacant patches that seem to indicate an obstruction of starlight by masses of non-luminous obscuring material. These regions are too well known through the observations of Barnard and others to

[1] The nebulosity about N.G.C. 1514, on the other hand, is gaseous.

need comment. It may be pertinent to remark, however, that ρ Ophiuchi and the two seventh-magnitude stars near it, C.D. $-23°12860$ and 12862, are the only objects brighter than the tenth magnitude in an area of more than three square degrees.[1] The average number to this limit per square degree in the regions immediately adjoining is from 10 to 15.

These circumstances may have some bearing upon the exceptional cases of nebulous objects which show no appreciable excess of color. If the particles of the nebulous mass be above a certain size, the characteristic phenomenon of scattering does not occur, and we have a reduction in the intensity of the transmitted light which affects all wave-lengths equally. It is instructive in this connection to attempt to correlate the excess of color with the density of the surrounding nebulosity. Subdividing the stars into three groups, we find the following mean values of the color excess:

Nebulosity	Color Excess	No. of Stars	No. of Exceptions
Moderate........	+1.0	27	4
Dense...........	+1.5	6	0
Very Dense......	+0.9	9	2
All..............	+1.04	42	6

There is no certain evidence of correlation; but it is perhaps significant that of the nine stars involved in very dense nebulosity, two are exceptional or doubtful, and four others have values of the color excess below the average for the entire group of forty-two stars.

MOUNT WILSON OBSERVATORY
May 14, 1920

NOTE.—Photographs taken with the 60-inch and 100-inch reflectors after the foregoing paper was written show C.D. $-23°13999$, 14002, and 14004 (Table VI) apparently superimposed upon a background of smooth nebulosity, which does not condense about the stars. This is also the case with B.D. $-19°4954$ (Tables V and VII). The nebulous nature of these objects is therefore doubtful.

[1] See the C.D. charts.

The condensation about B.D. $-19°4357$ (Table V) is very feeble, especially as compared with that of its neighbors B.D. $-19°4359$ and 4361.

22 Scorpii (Table V) itself is apparently free from nebulosity, although two intricate streamers bend around it to form what Professor Barnard calls "the eye nebula," of which 22 Scorpii is the pupil. The symmetrical arrangement of the streamers suggests a repulsive force emanating from the star. Professor Barnard has published an excellent photograph of the region, taken with the Bruce 10-inch camera, in *Astrophysical Journal*, **31**, 10, 1910.

A recent photograph of C.D. $-23°13836$ shows that the star is not nebulous.

B.D. $-12°1771$ alone therefore remains as an exception of a real and very striking nature.

Recent exposure-ratio photographs confirm the very large color excess found by polar comparisons for B.D. $-22°4510$ (Table VI), and place it in color-class g4. Additional spectrograms leave no doubt that the spectrum is really A3. The lines are normal in distribution and number, and there is no trace of bright-line radiation in the red. The very pronounced color, which visually is in striking contrast to that of the companion star B.D. $-23°338$ in the principal mass of the Trifid nebula, must therefore be attributed to peculiarities in the continuous spectrum.

June 28, 1920

Contributions from the Mount Wilson Observatory, No. 188
Reprinted from the *Astrophysical Journal*, Vol. LII, pp. 23–38, 1920

ON THE DISTRIBUTION OF THE STARS IN SPACE ESPECIALLY IN THE HIGH GALACTIC LATITUDES

By J. C. KAPTEYN[1] AND P. J. VAN RHIJN

ABSTRACT

Distribution of stars in space.—While the results reported in this paper are provisional, in that some recently available parallaxes are not included and the investigation of the lower galactic latitudes has not been completed, it is unlikely that more complete data will materially modify them. (1) *In galactic latitudes* $\pm 40°$ *to* $\pm 90°$. The *average parallax for all stars of a given magnitude* (m) *and proper motion* (μ) is found to be represented satisfactorily by the formula $\log \pi = -0.691 - 0.0682\, m + 0.645 \log \mu$. By combining this result with the law of dispersion of parallax for stars of given m and μ, which had already been determined, the two fundamental laws which determine the arrangement of stars in space were found. The first of these is the *luminosity-curve* or frequency of the several absolute magnitudes per unit volume, which, at least near the sun, is found to correspond accurately, from $-10\overset{\mathrm{M}}{.}6$ to $+7\overset{\mathrm{M}}{.}4$, to a symmetrical probability-curve with the equation: $\log \phi(M) = -2.394 + 0.1858M - 0.03450M^2$ (see Table IV and Fig. 1). Assuming that the luminosity-curve is the same for all distances from the sun, the median absolute magnitude of all stars is 2.7 (which is about 2.9 magnitudes fainter than the sun), with a probable error of $\pm 1\overset{\mathrm{M}}{.}69$. The second law is the *law of stellar densities* as a function of parallax. For distances below 1000 parsecs the densities can be determined directly (see Table V). For greater distances the following formula was derived from the luminosity-curve and the distribution-curve of apparent magnitudes, assuming no extinction of light in space: $\log \Delta(\rho) = -3.425 + 3.526 \log \rho - 0.943 (\log \rho)^2$ (see Table VI). (2) *In galactic latitudes* 0°, 30°, 60°, *and* 90°. A less refined investigation of all stars in these latitudes has led to formulae for the densities as a function of parallax which are similar to that given above (see Tables VI and VII). These results enable us to draw a *section of the galactic system* at right angles to the galactic plane, with the sun at the center (Fig. 2), which shows that in the direction of the galactic poles about 1500 parsecs may be taken as practically the limit of the system, while in a direction in the plane of the Milky Way the same small density is eight times more distant. The authors point out that, since symmetry around the galactic poles is assumed, this work is merely a second approximation to the complete solution of the problem.

1. The investigations contained in *G.P.*[2] 27, 29, and 30 were carried out for the purpose of making possible an elaborate treatment of the arrangement of the stars in space. At least two more

---

[1] Research Associate of the Mount Wilson Observatory.

[2] By *G.P.* we will denote the *Publications of the Astronomical Laboratory at Groningen.*

publications will be necessary to complete this investigation. Now that, after so many years of preparation, our data seem at last to be sufficient for the purpose, we have been unable to restrain our curiosity and have resolved to carry through completely a small part of the work, even though, by so doing, the rules for strict economy of labor cannot be altogether adhered to.

The present paper is the outcome of this more or less provisional work. In the main it relates to the stars as a whole between galactic latitudes ±40° and ±90°. It is provisional in that the extremely valuable parallaxes now placed at our disposal by Mitchell have not yet been used, and moreover because the thorough discussion which will have to be made of the measured parallaxes in all galactic latitudes is not yet completed. We expect little to be changed, however, in the definitive treatment of the subject, which will form a part of the more comprehensive work.

A somewhat less refined investigation of all the stars (irrespective of spectrum) in galactic latitudes 0°, 30°, 60°, and 90° has also been added.

2. In *G.P.* 30 were found the numbers of stars for each magnitude down to $m = 12.0$ and for every value of the proper motion μ. These numbers, corrected for observational errors, are contained in Table 19, which also gives for magnitudes 13 and 14 the numbers for proper motions exceeding $0''.200$.

We begin by deriving the average parallax for each of these classes of stars, i.e., for stars having given values of m and μ. Following the method indicated in *G.P.* 8, we tentatively start from the formula arrived at in that publication,

$$\log \pi_{m,\mu} = A + Bm + C \log \mu. \tag{1}$$

It turns out that this formula represents all our data satisfactorily. It is true that some of the divergences are larger than seems desirable, but there is reason to believe that the defect is not in the formula. At all events, the question whether a still more satisfactory formula can be assigned can be settled only by the later definitive treatment of the data for the whole of the sky.

The measured parallaxes available for our investigation embrace all the published results that seem to deserve confidence, excluding those whose probable errors exceed 0″.025. In addition we are indebted to Professor Schlesinger for a magnificent list of unpublished determinations. We cordially thank him for this generous act of courtesy. Professor Mitchell, too, as already mentioned, has communicated his invaluable results. These will, of course, play a prominent part in our more elaborate work, but they arrived too late for the present note.

For those cases in which several determinations are available for the same star, weights were adopted, not exactly in accordance with the probable errors as given by the authors, but modified somewhat by the supposition that small systematic errors still attach to all the results.

For proper motions exceeding 1″.00, the stars in all galactic latitudes were used. For smaller motions we confined ourselves for the present to galactic latitudes higher than 40°.

In order to find the change of π with μ (the constant C in (1)) we divided the stars with measured parallaxes into two groups according to brightness—magnitudes 3.5 to 6.5, and those that are fainter. Both these groups were subdivided according to proper motion. We thus obtained the normal values in Tables I and II, which, by means of small corrections derived from *G.P.* 8, were all reduced to magnitudes 5.0 and 8.0.

The data obtained from direct parallax determinations given in these tables were supplemented by results derived from the parallactic motions in Table 25 of *G.P.* 29. The latter parallaxes were obtained by adopting 19.5 km for the sun's velocity, and are entered in the last lines of Tables I and II.

The constants in formula (1) were then determined in such a way that the values from the parallactic motions are almost exactly represented, while at the same time the measured parallaxes are represented as well as possible. The results thus found are

$$\log \pi_{5.0} = -1.040 + 0.630 \log \mu \tag{2}$$

$$\log \pi_{8.0} = -1.163 + 0.659 \log \mu. \tag{3}$$

The parallaxes computed with these formulae have been designated by π_1 in Tables I and II. Although the residuals $O-\pi_1$

may not seem to be all that can be desired, we believe our tables prove that, at least as far as the change with proper motion is concerned, formula (1) cannot be materially in error. As we have already remarked, however, it seems best to reserve a closer discussion of this point until later. As the combined result of (2) and (3) we adopt

$$C = +0.645. \tag{4}$$

TABLE I

MAGNITUDE 3.5 TO 6.5

m	True μ	$\bar{\pi}$	No.	π_1	π_2	$O-\pi_1$	$O-\pi_2$
5.0.....	0″.048	+0″.018	31	0″.0135	0″.013	+0″.0045	+0″.005
5.0.....	.123	+ .034	23	.0245	.024	+ .0095	+ .010
5.0.....	.251	+ .043	27	.038	.038	+ .005	+ .005
5.0.....	.436	+ .047	15	.054	.054	− .007	− .007
5.0.....	.670	+ .072	18	.071	.072	+ .001	.000
5.0.....	1.260	+ .134	23	.105	.108	+ .029	+ .026
5.0.....	3.77	+ .174	9	.211	.218	− .037	− .044
5.0 (mean) *G.P.* 29..		+0.0204	....	0.0200	0.0192	+0.0004	+0.0012

TABLE II

MAGNITUDE 6.5 AND FAINTER

m	True μ	π	No.	π_1	π_2	$O-\pi_1$	$O-\pi_2$
8.0.....	0″.202	+0″.021	29	+0″.024	0″.021	−0″.003	0″.000
8.0.....	.486	+ .032	22	+ .043	.036	− .011	− .004
8.0.....	.714	+ .040	31	+ .055	.047	− .015	− .007
8.0.....	1.30	+ .085	28	+ .082	.069	+ .003	+ .016
8.0.....	4.05	+ .214	13	+ .173	.143	+ .041	+ .071
8.0 (mean) *G.P.* 29..		+0.0079	....	0.0079	0.0072	0.0000	+0.0007

3. We derive the constants A and B exclusively from the mean parallaxes found from parallactic motions. Writing (1), in which C has the value (4), in the form

$$\pi = 10^{A+Bm} \times 10^{0.645 \log \mu}, \tag{5}$$

we find for the mean parallax of all the stars of magnitude m,

$$\pi = 10^{A+Bm} \times 10^{\overline{0.645 \log \mu}}, \tag{6}$$

where the dashes indicate average values.

Since the total number of stars for every value of m and μ is given in Table 19 of *G.P.* 30, we can at once find the average value occurring in the second member. The values of $\bar{\pi}$ are obtained from Table 25 (in which the sun's velocity = 19.5 km). Introducing logarithms, we find the equations of condition in Table III.

TABLE III

EQUATIONS OF CONDITION

Magnitude	Equation	$\log \pi_{\text{comp.}}$	$O-C$ $\log \pi_{29} - \log \pi_{\text{comp.}}$
4	$A+4B=-1.033$	-0.975	-0.058
5	$A+5B=-1.019$	-1.046	$+.027$
6	$A+6B=-1.121$	-1.118	$-.003$
7	$A+7B=-1.156$	-1.189	$+.033$
8	$A+8B=-1.215$	-1.260	$+.045$
9	$A+9B=-1.326$	-1.332	$+.006$
10	$A+10B=-1.429$	-1.403	$-.026$
11	$A+11B=-1.499$	-1.474	-0.025

Solved by least squares, these equations yield

$$A = -0.690 \qquad B = -0.0713, \tag{7}$$

so that finally

$$\log \pi_{m,\mu} = -0.690 - 0.0713\, m + 0.645 \log \mu, \tag{8}$$

with which the third column in Table III was computed. Instead of this formula, however, the one actually used in what follows is

$$\log \pi_{m,\mu} = -0.691 - 0.0682\, m + 0.645 \log \mu. \tag{9}$$

Since the two equations represent the observations almost equally well, we have not repeated the computations.

The coefficient of m corresponds to log ϵ in *G.P.* 8, formula (3). Hence from (9), $\epsilon=0.855$, whereas in *G.P.* 8 the value $\epsilon=0.905$ was adopted. In the meantime this value of ϵ has already been corrected in *G.P.* 11 (p. 20) to $\epsilon=0.87$, in good agreement with the present value.

The parallaxes obtained by means of (9) are given in Tables I and II under the heading π_2. The residuals for this definitive solution are given under the heading $O-\pi_2$. Only in the case of the largest proper motions are they somewhat excessive. That this is not due to a defect in our formula is proved by the fact that the sign in the case of magnitude 8.0 is the opposite of that for magnitude 5.0. For the present purpose we do not consider these residuals for the largest proper motions to be of prime importance, since they are extremely rare.[1] Had this not been the case we might have lessened these extreme values somewhat by adopting a slightly larger value of C.

4. Formula (9) contains the solution of the problem presented in section 2, viz., to find the average parallax for each of the classes of stars of given m and μ contained in Table 19 of *G.P.* 30. The stars of apparent magnitudes 13 and 14 in this table, all having large proper motions, must be of extremely low absolute magnitude; they are accordingly very valuable for extending the luminosity-curve at its fainter extremity. That the frequency of the smaller proper motions is not known for these stars is of small importance. Their influence on the computations actually used for what follows is so small that we can quite safely introduce extrapolated values.

Although by (9) we can find the *average* parallax of the stars of any m and μ, it is of course evident that the parallax of any single star of the given m and μ will in general differ from the mean parallax. But for the problem of the general arrangement of the stars in space it is not necessary to know the distance of each individual star. It suffices to know how many stars have such and such a distance. This knowledge may be obtained if, in addition to the average parallaxes already found, we can find the dispersion law of the parallaxes, that is, the law which, for the stars of given

---

[1] In further computations the best plan will probably be to use for these stars the individual parallaxes as found by direct determination.

m and μ, specifies, for any value of a, the frequency of a parallax a times the average parallax.

Having found the number of stars of given magnitude m and a given parallax, we shall know of course for these same stars the absolute magnitude M.

It has been shown in *G.P.* 11 (pp. 17–20) that widely differing assumptions as to the dispersion law lead to results that differ but little. In this preliminary solution, therefore, we have not deemed it necessary to derive this law anew, but have adopted the one found and tabulated in *G.P.* 8 (solution D).

Since it thus becomes possible to find, for any given distance, the number of stars of each absolute magnitude, we can evidently derive the two fundamental laws which determine the arrangement of the stars in space, viz., the luminosity-curve and the law of stellar densities. A convenient manner of conducting the computations is explained at length in *G.P.* 11 and need not be repeated here. It should be remembered, however, that it introduces the two assumptions: (1) there is no appreciable extinction of light in space; (2) the frequency of the several absolute magnitudes (luminosity-curve) does not change with the distance from the sun. These assumptions can be avoided, at least to a considerable extent. They will be discussed in the definitive solution.

Different units of distance have been used by different astronomers. That most widely used at present is the parsec. For the sake of uniformity we have resolved henceforth not only to use this unit but also to use the name, which is very convenient (though very ugly). To conform with this new unit, the value of the absolute magnitude, which must still be defined to be the magnitude of a star as it would appear at the unit of distance, must also be changed. Its numerical value will now be five less than it was according to former publications, and may be found by the formula

$$M=m+5\log\pi=m-5\log\rho. \qquad \text{(A)}$$

The results obtained in the present case are in Tables IV and V. The table giving the densities will presently be extended to greater distances through the consideration of other data.

The result for the luminosity-curve may be considered to be the final result of this paper. Its general high accuracy appears in the agreement of the large overlapping portions of the independent curves found for different distances from the sun. For brevity's sake we omit the numbers which show this, but even without

TABLE IV

LOG NUMBER OF STARS PER CUBIC PARSEC NEAR THE SUN

(Determining Luminosity-Curve)

M	log $\phi(M)$	Computed	O−C
−11.64	1.2 −10	0.8 −10	+0.4
−10.64	1.6	1.7	− .1
− 9.64	2.55	2.61	− .06
− 8.64	3.373	3.425	− .052
− 7.64	4.148	4.173	− .025
− 6.64	4.843	4.851	− .008
− 5.64	5.474	5.461	+ .013
− 4.64	6.020	6.001	+ .019
− 3.64	6.493	6.473	+ .020
− 2.64	6.894	6.875	+ .019
− 1.64	7.215	7.209	+ .006
− 0.64	7.472	7.473	− .001
+ 0.36	7.662	7.669	− .007
+ 1.36	7.776	7.795	− .019
+ 2.36	7.836	7.853	− .017
+ 3.36	7.819	7.841	− .022
+ 4.36	7.737	7.761	− .024
+ 5.36	7.627	7.611	+ .016
+ 6.36	7.364	7.393	− .029
+ 7.36	7.200	7.105	+ .095
+ 8.36	7.00	6.75	+ .25
+ 9.36	6.4	6.3	+0.1

TABLE V

DENSITY (=1 NEAR SUN)

π	Density	π	Density
0″.00118	0.089	0″.0296	0.918
.00187	.179	.0469	1.000
.00296	.298	.0743	1.000
.00469	.451	.118	1.000
.00743	.600	.187	1.000
.0118	.760	0.296	1.000
0.0187	0.864		

them we gain an insight into the accuracy through the astonishingly close approach of the values in Table IV to the simple analytical curve

$$\log \phi(M) = -2.394 + 0.1858\, M - 0.03450\, M^2 . \qquad (10)$$

The last column of the table shows the residuals.

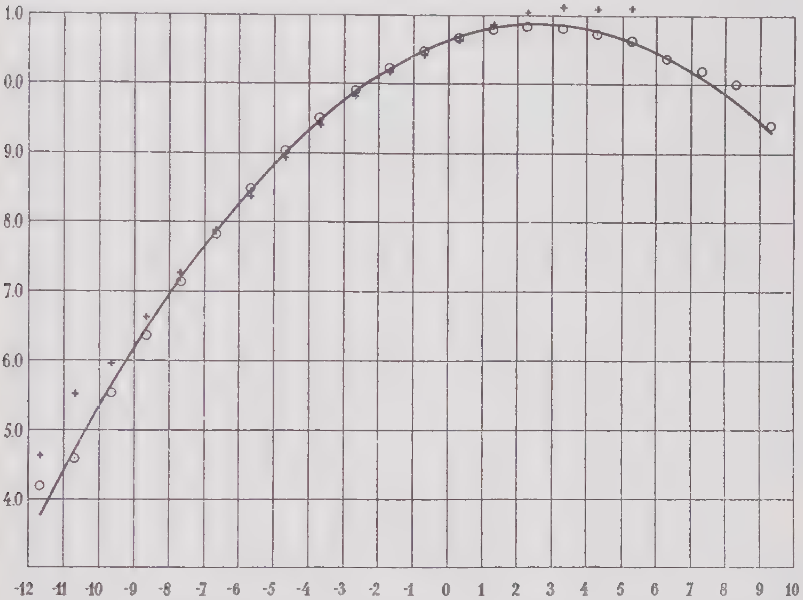

FIG. 1.—Luminosity-curve, all spectral types together. Abscissae are absolute magnitudes (unit of distance, 1 parsec). Ordinates are logarithms of numbers of stars per 1000 cubic parsecs near the sun.

A still better appreciation of the close approach of theory and observation may be obtained by inspecting Figure 1, which shows the curve (10) and the observed values, represented by small circles. With absolute magnitudes as abscissae, this curve gives the logarithm of the number of stars per 1000 cubic parsecs, instead of per cubic parsec, as does formula (10).

We may write (10) in the form

$$\phi(M) = A \frac{h}{\sqrt{\pi}} e^{-h^2 (M - M_0)^2} \qquad (11)$$

where

$$\left.\begin{aligned} A=0.0451,\ M_0=2.693,\ h=0.2818 \\ r=\frac{0.4769}{h}=1.692 \end{aligned}\right\} \qquad (12)$$

It thus appears that the luminosity-curve (or rather the absolute-magnitude curve) is represented very closely by an error-curve spread round the median value $M=2.7$, with a probable error of ± 1.69. If we assume that the agreement of the two curves holds for absolute magnitudes beyond those afforded by our data, the total number of stars per cubic parsec in the vicinity of the sun from the very brightest, absolutely, to the faintest is 0.0451.

The crosses in Figure 1 represent the results found in *G.P.* 11 from wholly different and very scanty material.[1] In *G.P.* 11 only the data for stars brighter than 6.0 or 6.5 may be considered as fairly reliable, whereas in the present paper most of the data are certainly trustworthy down to magnitude 11 (inclusive), and even down to magnitude 12 (inclusive) for the all-important proper motions of considerable amount, and begin to fail altogether only beyond magnitude 14.

Although the present curve is therefore infinitely preferable to the old one, it is still eminently satisfactory to see how closely the old curve agrees with the present result. The extremities were of necessity unreliable; the data on which it was based were defective not only in the proper motions and magnitudes but even more so in the measured parallaxes.

The most gratifying advance is the determination of the maximum of the curve. Owing to the inclusion of material for stars as faint as twelfth, thirteenth, and fourteenth magnitudes, we are at last well beyond the maximum, which can now be located with considerable precision. In many respects this will prove a very important gain, indeed, since it allows us for the first time to express with some certainty the relation between the average absolute magnitude of the stars and that of the sun. The absolute magnitude of the sun[1] appears to be near -0.2, which is 2.9 magnitudes *brighter* than the average magnitude of all the stars.

---

[1] Reduced from the Potsdam scale to the Harvard scale by subtracting 0.16 from the magnitudes.

If in Table IV we disregard the first two and the last two values, which are of necessity very uncertain, there still remain values ranging over no less than eighteen magnitudes, that is, over luminosities varying from one to sixteen millions, all of which lie with extreme precision on the same Gaussian curve. We doubt whether any other case is known in the whole domain of science of so close an agreement over so large a range—a range of more than ten times the probable error. It is difficult to avoid the conclusion that we have here to do with a law of nature, a law which plays a dominant part in the most diverse natural phenomena. This in itself would lead us to assume that the curve (11) will still hold for the remainder of the descending branch of the luminosity-curve. There is at least one other fact which tends to confirm our belief that this will be the case. For the B0, B1, B2, and B3 stars practically the whole curve is covered by the observations,[2] and no assured deviation from an error curve has been found. It is true that in this case the number of observations is very small. Be this as it may, it would be more satisfactory if the curve could still be prolonged somewhat by observation. We hope to consider elsewhere the possibility of doing so.

5. The densities in Table V do not extend to distances greater than a thousand parsecs and cannot claim any very great accuracy even for distances somewhat below this limit. It is evident that much would be gained by introducing a consideration of the known total number of stars of any given magnitude m.[3]

As before let $\phi(M)dM$ represent the luminosity-curve, i.e., the number of stars per cubic parsec near the sun having absolute magnitudes between M and $M+dM$. Further let $N_m dM$ represent the number of stars per 10,000 square degrees having apparent magnitudes m to $m+dm$. Finally let $\Delta(\rho)$ represent the total number of stars of any absolute magnitude per cubic parsec, taking as unit the number in the neighborhood of the sun. It is easy to show, ρ being the distance, that

---

[1] *Astrophysical Journal*, **43**, 105, 1916.

[2] *Mt. Wilson Contr.*, No. 147, p. 72; for the B3 stars in particular see Table XXXIII.

[3] See *Proceedings Roy. Acad. Amsterdam*, March 1908.

$$N_m = 0.9696\pi \int_0^\infty \rho^2 \Delta(\rho)\phi(m-5\log\rho)d\rho\ . \tag{13}$$

Schwarzschild[1] has shown that if

$$\phi(M) = e^{p+qM+rM^2} \tag{14}$$

and

$$N_m = e^{a+bm+cm^2} \tag{15}$$

we shall have

$$\Delta(\rho) = e^{h+k\log\rho+l(\log\rho)^2}\ . \tag{16}$$

Since (10) or (11) shows that $\phi(M)$ has indeed the form (14), and since it was long ago shown (see for example *G.P.* 27, p. 24) that with astonishing approximation N_m has also the form (15), we can find the density $\Delta(\rho)$ at once from (16). The relation between the constants is found to be

$$l = \frac{25cr}{r-c}, \tag{17}$$

and further, if we write

$$G = -l - 25r \tag{18}$$

$$k = 5q - 6.9078 - \frac{G(b-q)}{5r} \tag{19}$$

$$h = a - p - 2.5203 + \frac{\log G}{0.8686} - \frac{(k-5q+6.9078)^2}{4G}\ . \tag{20}$$

6. By means of these formulae we have computed the densities from the values of N_m in Table V of *G.P.* 27. Since the labor involved is small, we were not able to resist the temptation to treat in the same way the data for galactic latitudes 0°, 30°, 60°, and 90°, for this must give a first insight into the arrangement of the

---

[1] *Astronomische Nachrichten*, 185, 81, 1910.

stars of the whole stellar system in space. In executing this plan we had of course to assume that the luminosity-curve is the same for all galactic latitudes, which seems little doubtful, although naturally we intend to investigate the matter in our definitive solution.

A little preliminary computation gave the following values of the constants in formula (15) by which the values of N_m in *G.P.* 27 are excellently represented:

Galactic Latitude	0°	30°	60°	90°	40° to 90°	Luminosity-Curve
a	−1.249	−1.296	−1.748	−2.079	−1.605	$p=-5.512$
b	+1.668	+1.593	+1.692	+1.783	+1.659	$q=+0.4279$
c	−0.0325	−0.0343	−0.0438	−0.0509	−0.0415	$r=-0.07944$

The constants of the luminosity-curve in accordance with (10) have also been added. Using these data we find by means of formulae (17) to (20):

Galactic Latitude	0°	30°	60°	90°	40° to 90°
h	−5.830	−5.193	−9.221	−14.319	−7.885
k	+5.705	+5.481	+9.320	+14.092	+8.120
l	−1.366	−1.508	−2.441	− 3.542	−2.171

which lead to the very convenient formulae

$$\left.\begin{array}{llll}
\text{Gal. Lat. } 0°, & \log\Delta(\rho) = -2.532+2.478 & \log\rho - 0.593 & (\log\rho)^2 \\
30, & = -2.256+2.381 & -0.655 & \\
60, & = -4.005+4.048 & -1.060 & \\
90, & = -6.219+6.120 & -1.538 & \\
40 \text{ to } 90, & = -3.425+3.526 & -0.943 &
\end{array}\right\} \quad (21)$$

The evident and well-recognized defect of these solutions is that the formula gives $\Delta(0)=0$, which is inadmissible. The values of $\Delta(\rho)$ furnished by (16) or (21) for the smaller distances cannot therefore be accepted. Fortunately our former solution gives good values for these very distances. The comparison of the results obtained by the two methods, which can be made for galactic latitudes 40° to 90° and which is given below, proves that the

TABLE VI

LOG $\Delta(\rho)$

LOG ρ	ρ IN PARSECS	LATITUDE				LATITUDE 40° TO 90°		
		0°	30°	60°	90°	Formula (16)	Table V	Adopted
1.0......	10.0	0.00	0.00	0.00	0.00	9.16	0.00	0.00
1.2......	15.8	.00	.00	.00	.00	.45	.00	.00
1.4......	25.1	.00	.00	.00	.00	.66	9.99	9.99
1.6......	39.8	.00	.00	.00	.00	.80	.96	.96
1.8......	63.1	.00	.00	.00	.00	.87	.92	.92
2.0......	100	.00	9.89	9.85	9.87	.85	.84	.84
2.2......	158	.00	.81	.77	.80	.77	.73	.75
2.4......	251	.00	.68	.60	.61	.61	.59	.60
2.6......	398	9.90	.51	.35	.30	.37	.39	.38
2.8......	631	.76	.28	.02	8.86	.06	.14	.08
3.0......	1000	.56	8.99	8.60	.30	8.67	....	8.67
3.2......	1580	.32	.66	8.10	7.62	8.20	....	8.20
3.4......	2510	.04	.27	7.50	6.81	7.66	....	7.66
3.6......	3980	8.70	7.83	6.83	5.88	7.05	....	7.05
3.8......	6310	.32	.33	6.07	4.83	6.36	....	6.36
4.0......	10000	7.89	6.79	5.23	3.65	5.59	....	5.59
4.2......	15800	7.42	6.19	4.30	2.35	4.75	....	4.75
4.4......	25100	6.89	5.54	3.28	0.93	3.83	....	3.83
4.6......	39800	6.32	4.84	2.19	9.39	2.84	....	2.84
4.8......	63100	5.70	4.08	1.00	7.72	1.77	....	1.77
5.0......	100000	5.03	3.27	9.74	5.93	0.63	....	0.63

TABLE VII

ρ

$\Delta(\rho)$	0°	30°	60°	90°
1.00.............	0	0	0	0
0.40.............	910	320	250	250
.16.............	1920	710	490	450
.063............	3550	1320	800	660
.025............	5750	2140	1200	910
.010............	8910	3310	1700	1230
.0040...........	13200	4900	2340	1580
.0016...........	19100	7080	3090	2000
.00063..........	26900	10000	4070	2510
.00025..........	37200	13500	5130	3090
0.00010..........	50100	18200	6460	3720

present method yields good results as soon as the maximum is well passed.

For distances less than 100 parsecs[1] we have accordingly adopted the first solution for galactic latitudes 40° to 90.° For distances beyond this limit the two solutions give results which agree surprisingly well, and we have adopted the mean of the two. Beyond 630 parsecs the second solution is the only one available. For galactic latitudes 0°, 30°, 60°, and 90° the first solution has not been carried out. In close agreement with the result just found for the high galactic latitudes, we have assumed the density to be constant up to the maximum of the second solution, while, from that value on, the second solution was adopted. Table VI shows the values thus obtained, from which by interpolation we derive Table VII.

Figure 2 was constructed with the aid of Table VII. If we imagine this figure completed by the addition of its reflected image on the other side of the line *AB*, it will represent a complete section through the galactic system at right angles to the galactic plane. The lines shown are lines of constant density. The sun lies at the center *S*. The numbers along the bottom line show the distances expressed in parsecs. The density is

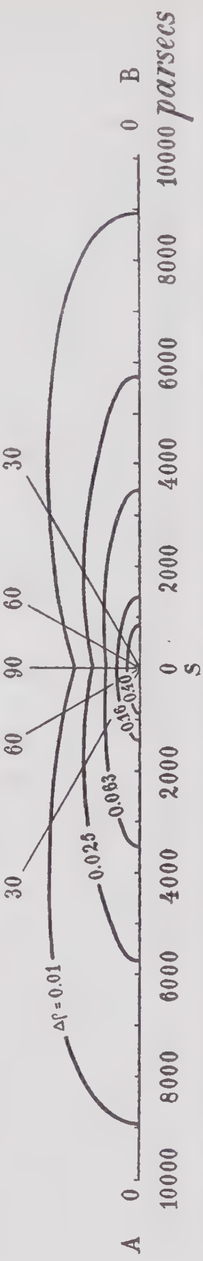

FIG. 2.—Distribution of density in a plane perpendicular to the galactic circle passing through the center of the stellar system. AB is the plane of the galaxy; the marginal numbers 0, 30, 60, and 90 are galactic latitudes. The curves are lines of equal density, the density at the sun (assumed to be at the center of the system) being taken as unity.

---

[1] By the substitution, below the maximum, of the first solution for the second, the total number of stars N_m which the theory yields exceeds somewhat the total found from observation. But since the volume of space below the maximum of formula (16) is very small, we have assumed that no serious error is introduced.

unity at *S*, and 0.40, 0.16, 0.063, 0.025, and 0.01, respectively, along the lines shown in the figure.

Whether the inflection near the pole in the lines of small density is real we are not at the moment prepared to say. If it is not, the layers of small density become singularly flat for an enormous range in distance.

We have not yet studied the question of the limits to which our results for the density are fairly reliable; but there is hardly a doubt that we can safely adopt them as a good approximation up to at least 1500 parsecs. In the direction of the pole of the Galaxy this brings us to what many will be inclined to take as practically the limit of the system. At least the density at that distance cannot be 1/200 of that near the sun. In any direction along the plane of the Milky Way, on the contrary, this same limit must be eight times more distant.

Leaving further considerations for the definitive solution, we conclude by expressing the hope that our present attempt to derive the arrangement of the stars will not be misunderstood. We have always considered this problem to be one that must be solved by successive approximations. The first was that attempted in *G.P.* 11, in which the system was considered as a whole, without regard to the differences shown in different galactic latitudes. The present solution constitutes a second approximation. It assumes that the center lies near or in the sun; that the system is symmetrical with respect to the galactic plane, which is supposed to pass through the sun; and that the normal to the plane through the center is an axis of symmetry. In subsequent approximations these assumptions will be dropped. Although perhaps something in the right direction has already been accomplished, much still remains to be done, especially in the study of the galactic clouds, before the solution will be complete.

ASTRONOMICAL LABORATORY, GRONINGEN
January 1920

Contributions from the Mount Wilson Observatory, No. 189

ON THE SYSTEMATIC DIFFERENCES IN TRIGONOMETRICALLY DETERMINED PARALLAXES

By ADRIAAN VAN MAANEN and CORAL WOLFE

The determination of the systematic errors of directly measured parallaxes would be an easy problem if we knew the real parallaxes of any considerable number of objects, for a comparison of the values found by the different parallax observers with the real parallaxes would at once yield the required data. The method fails, however, because we do not know with certainty the distance of a single star.

Several ways, however, may be followed in order to derive a useful approximation for the systematic error of any observer. An obvious method is to compare the results of the observer with the mean parallaxes of the same stars as derived by all observers. The systematic errors of the different observers enter into the mean as accidental errors, and, if the number of observers is considerable, compensate each other to such an extent that the systematic error of the mean will be very small. The systematic deviation of the observer from mean parallaxes based on the measures of a number of observers should, therefore, agree closely with his systematic error. The drawback is that relatively few objects have been measured by several observers. For only 19 objects are there six or more determinations of the parallax available; for 26 objects there are five; while for the majority only one or two observations are at hand. This method would therefore necessarily exclude most of the observational material.

Another method was used for a preliminary investigation by one of the authors in *Mt. Wilson Contr.* Nos. 136 and 158, where the trigonometrically determined parallax of every star of known spectral type, magnitude, and proper motion was compared with the corresponding value derived from van Rhijn's tables of mean parallaxes.[1] The differences thus found were combined according to spectral type, magnitude, and proper motion, and were used to derive corrections to the tables. The corrected tables represent the system determined by the mean of the results of all the observers contributing data to the comparison and should be comparatively free from systematic observational error. The average systematic deviation of any observer from the corrected tables is then approximately his systematic error. The results are practically the same as before; they represent the systematic deviation of the observer from the mean of the directly determined parallaxes of all observers combined, but with the advantage that it is not necessary for them to have observed the same stars. This is the method followed in the present discussion.

---

[1] *Derivation of the Change of Colour with Distance and Apparent Magnitude.* Dissertation, Groningen, 1915.

Several points require comment. For simplicity, consider stars of a single spectral type. The corrections to the table depend upon differences of the form $\pi_O-\pi_T$, where π_O is an observed parallax measured by any observer, and $\bar{\pi}_T$ the tabular mean parallax of stars having the same magnitude and proper motion as the given star. The correction itself is the mean of a number of such differences for different observers and different stars whose magnitudes and proper motions lie within narrow limits. Thus

$$C_{m,\mu}=\frac{1}{n}\Sigma(\pi_O-\bar{\pi}_T)_{m,\mu} \qquad (1)$$

where the subscripts represent the mean magnitude and proper motion of the stars in question.

The first point to be noted is that the results of the discussion in nowise depend upon the tabular values $\bar{\pi}_T$. These are eliminated. For example, when the correction (1) is applied to the tabular value $(\bar{\pi}_T)_{m,\mu}$, the "corrected" mean parallax becomes

$$\bar{\pi}_{m,\mu}=(\bar{\pi}_T)_{m,\mu}+C_{m,\mu}=(\bar{\pi}_T)_{m,\mu}+\frac{1}{n}\Sigma(\pi_O)_{m,\mu}-\frac{1}{n}\Sigma(\bar{\pi}_T)_{m,\mu} \qquad (2)$$

The last term of (2) is the mean of n tabular values of $\bar{\pi}_T$ corresponding to magnitudes and proper motions lying within narrow limits. The means of these magnitudes and proper motions are m and μ, respectively. The first term in the right member of (2) is the tabular parallax corresponding to these means. Since for moderate intervals of m and μ the variation of $\bar{\pi}_T$ is nearly linear, this first term is sensibly equal to the last, and the "corrected" tabular value is simply

$$\bar{\pi}_{m,\,\mu}=\frac{1}{n}\Sigma(\pi_O)_{m,\,\mu}=(\bar{\pi}_O)_{m,\,\mu} \tag{3}$$

that is, the mean of the observed parallaxes whose corresponding magnitudes and proper motions lie within certain narrow limits. These means might have been formed directly, without using tables of mean parallaxes at all, except for the fact that the method outlined affords a simpler numerical treatment. In practice the corrections of the form of (1) are not added directly to the tabular values of the mean parallaxes, but, as will be seen presently, are used to compute differential corrections to the constants of the exponential functions whose numerical values are the tabular mean parallaxes. The process is therefore merely a device for obtaining a corrected exponential relation between $\bar{\pi}$, m, and μ which will represent the available data.

Second, it must not be supposed that, when the stars as a whole are considered, the modified relation is necessarily an improvement over that upon which the tables are based; it is only an interpolation formula representing the measured parallaxes of stars of known spectrum, magnitude, and proper motion.

Third, the systematic deviations of the different observers are obtained by comparing their *individual* results with the *mean* parallaxes calculated from the "corrected" formula. Any single difference of this sort $\bar{\pi}_F-\pi_O$ is composed of the following parts: (1) the accidental error in π_O; (2) the systematic error in π_O; (3) the difference between the true parallax of the given star and the value π_F from the formula. The problem is to separate (2) from (1) and (3). For a given observer (2) enters with the same sign, while (1) and (3) have a random distribution. The algebraic mean of a sufficient number of differences of the form $\pi_F-\pi_O$ should therefore isolate the systematic deviation (2).

The influence of (1) or (3) for any group of stars of a given spectral type, magnitude, and proper motion will be the smaller the more stars there are included in a group. It will be shown later that several groups may be combined to form the systematic deviations, because the deviations as a whole seem to be independent

TABLE I

SPECTRUM	MAG.	<0″.050		0″.050–0″.099		0″.100–0″.199		0″.200–0″.499	
		n	n'	n	n'	n	n'	n	n'
O	<3	......	......	......	......	......	......	......	......
	3–5	2	3	......	......	......	......	......	......
	5–7	4	4	......	......	......	......	......	......
	7–9	4	7	......	......	......	......	......	......
	>9	......	......	......	......	......	......	......	......
B	<3	17	27	5	6	3	4	2	2
	3–5	15	16	2	2	......	......	......	......
	5–7	10	12	......	......	......	......	......	......
	7–9	......	......	1	1	......	......	......	......
	>9	......	......	......	......	......	......	......	......
A	<3	3	8	6	7	8	13	7	17
	3–5	13	14	12	16	18	25	7	15
	5–7	6	6	8	14	7	8	5	8
	7–9	......	......	1	1	2	2	......	......
	>9	......	......	......	......	1	1	......	......
F	<3	6	11	......	......	1	1	......	......
	3–5	9	19	3	4	14	23	25	46
	5–7	6	8	5	6	24	23	42	58
	7–9	......	......	2	2	1	1	11	14
	>9	......	......	......	......	1	1	1	1
G	<3	2	3	3	5	1	1	3	10
	3–5	16	23	12	18	9	17	7	16
	5–7	7	7	6	7	5	8	21	31
	7–9	......	......	1	1	6	6	35	37
	>9	......	......	......	......	1	1	3	4
K	<3	6	14	1	4	4	7	4	14
	3–5	19	22	15	18	30	38	14	23
	5–7	13	13	19	19	10	10	7	9
	7–9	......	......	1	1	2	2	13	16
	>9	......	......	1	1	1	1	2	2
M	<3	2	3	1	2	......	......	2	6
	3–5	3	4	3	4	2	4	1	1
	5–7	15	17	7	7	1	1	1	1
	7–9	......	......	......	......	......	......	......	......
	>9	......	......	......	......	......	......	1	3

of spectral type and proper motion, although for several observers they are found to be a function of the magnitude. We shall, however, be able to combine for each observer all groups of the same magnitude, which gives enough material to reduce the influence of (1) and (3) considerably. Moreover, even if the

TABLE I.—*Continued*

Spectrum	Mag.	0″.500–0″.999		1″–2″		2″–5″		>5″	
		n	n′	n	n′	n	n′	n	n′
O......	<3	......	......	......	......	......	......	......	......
	3–5	......	......	......	......	......	......	......	......
	5–7	......	......	......	......	......	......	......	......
	7–9	......	......	......	......	......	......	......	......
	>9	......	......	......	......	......	......	......	......
B......	<3	......	......	......	......	......	......	......	......
	3–5	......	......	......	......	......	......	......	......
	5–7	......	......	......	......	......	......	......	......
	7–9	......	......	......	......	......	......	......	......
	>9	......	......	......	......	......	......	......	......
A............	<4	2	8	1	2	......	......	......	......
	3–5	1	3	......	......	......	......	......	......
	5–7	3	6	2	6	......	......	......	......
	7–9	......	......	......	......	......	......	......	......
	>9	......	......	......	......	......	......	......	......
F........	<3	1	6	1	5	......	......	......	......
	3–5	7	21	3	17	1	1	......	......
	5–7	17	35	3	7	......	......	......	......
	7–9	12	22	3	9	......	......	......	......
	>8	......	......	......	......	1	1	......	......
G............	3<	1	1	......	......	2	2	......	......
	3–5	10	39	5	20	1	1	......	......
	5–7	24	57	9	30	1	5	1	6
	7–9	27	38	2	11	......	......	......	......
	>9	1	1	......	......	......	......	......	......
K	<3	2	2	......	......	1	2	......	......
	3–5	1	3	1	7	2	5	......	......
	5–7	12	26	7	19	3	11	1	14
	7–9	39	72	8	22	2	11	1	1
	>9	5	7	4	8	......	......	......	......
M............	<3	......	......	......	......	......	......	......	......
	3–5	......	......	......	......	......	......	......	......
	5–7	......	......	......	......	......	......	......	......
	7–9	......	......	2	7	5	25	1	1
	>9	1	3	2	5	1	1	1	4

systematic deviation proves to be a function of magnitude, the adopted values will be those given by the smooth curves defined by the results for the successive magnitudes, which will again reduce the uncertainty. As (1) has less influence when the probable error of the observer is small, its influence is less for the better observations; the uncertainty in the final mean deviations will therefore be less for the observer who has attained the higher accuracy and the greater number of observations.

The circumstances affecting the elimination of the quantity (3) are as follows. Kapteyn has shown that it is an even chance that the true parallax of a star of given magnitude and proper motion lies within the limits $0.52\ \bar{\pi}$ and $1.25\ \bar{\pi}$, where $\bar{\pi}$ is the mean parallax of stars of the given magnitude and proper motion.[1] This is for all spectral types together. If we separate the types, we should expect the dispersion to be somewhat less, and, in fact, van Rhijn finds this to be the case.[2] Roughly speaking, the probable value of the difference (3) is of the order of $\frac{1}{3}\ \pi$; and to obtain reliable results, the number of observations must be sufficient to render the effect of (3) negligible as compared with the systematic differences which are to be determined. For small proper motions the probable values of (3) are small, and a comparatively small number of stars is sufficient to reduce to a negligible quantity the resulting uncertainty in the systematic error. With proper attention to weighting, the data for the large proper motions can be used, but they will contribute little to the result.

Although the ideal condition of a uniform distribution of the observed parallaxes is not satisfied, sufficient material is available to afford valuable indications as to the probable systematic deviations of the various observers from the system defined by means of all the measured parallaxes that can be used for this investigation.

This material is indicated in Table I, which gives for each spectral type the number of stars (n) and of observations (n') for the different limits of magnitude and proper motion used. It includes 901 stars with 1538 parallax observations. The companions of double stars have been excluded. Part of the material is unpublished, and we are under great obligation to Professor Miller, Professor Mitchell, and Professor Schlesinger for kindly allowing us to use their data. The various observers (or observatories) have contributed as shown in Table II, the last column of which gives the weights assigned to the individual parallaxes on the basis of their probable errors.

---

[1] *Groningen Publications*, No. 8, 23, 1901.

[2] *Loc. cit.*

TABLE II

Observer	n	w	Observer	n	w
Abetti	41	0.4	Russell	40	0.3
Allegheny	259	1.2	Yale	241	0.5
Flint I	95	0.2	Yerkes	131	1.0
Flint II	120	0.3	Cape	20	0.5
Greenwich	38	1.2	Fox	15	1.0
Jewdokimow	57	0.2	Groningen	21	0.3
Jost	47	0.4	Kapteyn	15	0.5
van Maanen	89	1.5	Kostinsky	8	0.7
Sproul	84	1.0	Peter	13	0.4
McCormick	201	1.0	Voûte	3	1.0

It is hardly necessary to mention that throughout the work absolute parallaxes were used. The reductions from relative to absolute parallaxes were derived from the tables published by Kapteyn in *Groningen Publications*, No. 8.

For each spectral type we combine the weighted observations of each group of stars between adopted limits of magnitude and proper motion. The limits chosen for the magnitudes are: <3 3–5, 5–7, 7–9, and >9; for the proper motions: $<0''.050$, $0''.050$–$0''.099$, $0''.100$–$0''.199$, $0''.200$–$0''.499$, $0''.500$–$0''.999$, $1''$–$2''$, $2''$–$5''$, and $>5''$. For each spectral type we can derive from the corresponding means the constants of the formula giving the mean parallax as a function of m and μ.

In practice several difficulties present themselves:

A) The true formula giving the mean parallax of a star as a function of magnitude and proper motion is unknown. But we require only an interpolation formula which will represent the observed results. We may use either the equation of Kapteyn, $\bar{\pi}=ab^m\mu^c$, or that of Strömberg, $\bar{\pi}=ab^m(\mu+C)^c$. The former, involving only three constants, is adopted. It may more conveniently be expressed in the form: $\log\bar{\pi}=a'+b'm+c'\log\mu$. It holds with sufficient precision for all but the smallest proper motions and is simpler for our present purposes. As already indicated, we do not deal with the parallaxes themselves, but, in order to use smaller quantities, derive differential corrections to the constants used by Kapteyn for the calculation of his tables of mean parallaxes. We therefore compare the weighted mean of the observed parallaxes for each magnitude-proper-motion group with the corresponding value of Kapteyn's mean parallax; the difference $\bar{\pi}_O - \bar{\pi}_K$ then serves as the absolute term in an equation of condition

$$(da' + mdb' + \log \mu \cdot dc')\bar{\pi} = \bar{\pi}_O - \bar{\pi}_K = d\bar{\pi} \tag{4}$$

involving the corrections to the constants. (For the B and A stars the differences of the observed parallaxes and those which can be derived from Kapteyn's tables were found to be so considerable that the use of the differential formula is questionable. In both cases the constants were accordingly derived from the equation $\bar{\pi} = ab^m\mu^c$ itself.)

B) The material of the different observers is distributed very unevenly over the groups of different magnitude and proper motion. This involves an error in the constants to be determined as soon as any observer whose systematic error is considerable predominates in a specific group. To illustrate this, we give in Table III the number of observations for the K-type stars as functions of m and μ. The successive columns under each magnitude interval refer to the different groups of proper motions which are the same as in Table I. For the different magnitudes the numbers of parallaxes by the individual observers are distributed very unevenly. Using the weights given in Table II, we find, for instance, that for stars of magnitudes 3–5 Allegheny supplies 66 per cent of the weight and for stars of magnitudes 5–7 van Maanen 47 per cent. In order to meet this difficulty, two systems of weighting were introduced; as the matter of treatment is one of opinion, two radically different methods have been followed:

a) For each spectral type the weight of any observer who would predominate in the derivation of the constants was reduced to such a figure that the total weight of his material for that type would not exceed 20 per cent of the total available; an exception was made for the M-type stars, where practically all the parallaxes

TABLE III

	Mag. <3								Mag. 3–5								Mag. 5–7								Mag. 7–9								Mag. >9								Total
Abetti	...	...	...	...	...	...	...	...	...	...	2	1	...	...	...	...	2	3	1	...	...	...	...	1	...	...	...	...	...	1	...	...	...	...	...	...	...	...	...	...	11
Allegheny	2	1	2	1	...	...	...	...	19	10	22	10	...	1	...	...	...	1	1	...	3	...	...	1	...	...	...	1	3	...	...	...	...	...	...	...	...	...	...	...	78
Flint I	...	...	...	2	...	...	1	...	...	1	...	2	...	1	1	...	...	...	1	...	...	6	3	1	...	...	...	1	1	7	2	...	...	...	...	...	...	...	...	...	30
Flint II	6	1	3	3	2	...	...	...	...	...	...	1	1	...	...	...	...	...	...	1	...	3	...	...	...	...	...	...	4	1	...	...	...	...	...	...	...	...	...	...	26
Greenwich	...	...	...	...	...	...	...	...	...	...	...	...	...	...	...	...	...	...	...	1	...	...	...	...	...	...	...	...	...	1	...	...	...	...	...	2	...	...	...	...	4
Jewdokimow	1	...	...	2	...	...	...	...	...	...	...	...	...	1	1	...	...	...	...	...	1	...	2	1	...	...	...	...	4	1	2	...	...	...	...	...	...	...	...	...	16
Jost	...	...	...	...	...	...	...	...	...	...	...	3	...	...	...	...	...	...	1	...	3	...	...	1	...	...	...	1	1	...	...	...	...	...	...	...	...	...	...	...	10
van Maanen	...	...	...	...	...	...	...	...	...	...	...	...	...	...	...	...	10	13	5	1	...	1	...	1	...	...	...	...	...	...	...	...	...	...	...	...	...	...	...	...	31
Sproul	...	1	...	...	...	...	...	...	...	...	2	1	...	1	...	...	...	...	...	...	3	1	1	1	...	...	...	...	4	...	1	...	...	...	...	...	...	...	...	...	16
McCormick	3	...	2	2	...	...	...	...	2	5	8	4	1	1	1	...	1	1	1	...	3	1	2	1	...	...	...	3	5	1	...	...	...	...	...	...	...	...	...	...	48
Russell	...	...	...	...	...	...	...	...	...	1	...	...	...	...	...	...	...	...	...	...	1	...	...	1	...	1	...	1	1	1	2	...	...	...	...	...	...	3	...	...	12
Yale	1	1	...	2	...	...	...	...	1	1	1	1	1	...	...	...	...	1	...	4	12	3	1	1	...	...	...	6	31	4	2	...	...	...	...	...	3	...	...	...	77
Yerkes	...	...	...	1	...	...	...	...	...	...	3	...	...	1	...	...	...	...	...	2	...	1	...	1	...	...	...	...	11	3	2	...	...	1	...	...	3	4	...	...	33
Cape	...	...	...	...	...	...	...	...	...	...	...	...	...	...	2	...	...	...	...	...	...	...	1	...	...	...	...	...	...	...	...	1	...	...	...	...	...	...	...	...	4
Fox	...	...	...	...	...	...	...	...	...	...	...	...	...	...	...	...	...	...	...	...	...	...	...	...	...	...	...	2	5	...	...	...	...	...	...	...	...	1	...	...	8
Groningen	...	...	...	1	...	...	...	...	...	...	...	...	...	...	...	...	...	...	...	...	...	...	...	1	...	...	2	1	1	...	...	...	...	...	1	...	1	...	...	...	8
Kapteyn	...	...	...	...	...	...	...	...	...	...	...	...	...	...	...	...	...	...	...	...	...	1	...	...	...	...	...	...	1	1	...	...	...	...	...	...	...	...	...	...	3
Kostinsky	1	...	...	...	...	...	...	...	...	...	...	...	...	...	...	...	...	...	...	...	...	...	...	1	...	...	...	...	...	...	...	...	...	...	...	...	...	...	...	...	2
Peter	...	...	...	...	...	...	...	...	...	...	...	...	...	...	...	...	...	...	...	...	...	1	1	1	...	...	...	...	...	1	...	...	...	...	...	...	...	...	...	...	4
Voûte	...	...	...	...	...	...	...	...	...	...	...	...	...	...	...	...	...	...	...	...	...	1	...	...	...	...	...	...	...	...	...	...	...	...	...	...	...	...	...	...	1

are due to Allegheny, van Maanen, and McCormick. The percentage weight for each observer for the different types is given in Table IV under the heading *a*.

TABLE IV

PERCENTAGES OF WEIGHTS OF DIFFERENT OBSERVERS

OBSERVER	B		A		F		G		K		M	
	a	*b*	*a*	*b*	*a*	*b*	*a*	*b*	*a*	*b*	*a*	*b*
Abetti	1	0	6	10	2	0	2	8	2	11	2	0
Allegheny	10	0	16	10	13	9	12	8	17	11	23	33
Flint I	0	0	3	10	2	9	2	0	1	0	0	0
Flint II	15	20	11	10	3	9	4	8	4	11	2	0
Greenwich	0	0	0	0	6	9	13	8	1	0	0	0
Jewdokimow	1	0	2	10	2	9	1	8	1	0	1	0
Jost	1	0	5	10	4	9	2	8	2	11	1	0
van Maanen	12	0	0	0	14	9	8	8	16	11	31	33
Sproul	8	0	13	10	16	9	9	8	6	11	0	0
McCormick	11	20	15	10	14	9	12	8	16	11	32	33
Russell	2	0	1	0	1	0	2	8	1	0	2	0
Yale	12	20	13	10	13	9	15	8	18	11	4	0
Yerkes	15	20	12	10	8	9	13	8	10	11	0	0
Cape	9	20	1	0	0	0	1	0	0	0	2	0
Fox	0	0	0	0	1	0	1	0	4	0	0	0
Groningen	0	0	1	0	0	0	1	0	1	0	0	0
Kapteyn	0	0	0	0	1	0	1	0	0	0	0	0
Kostinsky	0	0	0	0	0	0	1	0	1	0	0	0
Peter	0	0	1	0	0	0	1	0	0	0	0	0
Voûte	3	0	0	0	1	0	0	0	0	0	0	0

b) The second method of weighting was suggested by Mr. Seares; it is based on the principle that all observers should have the same weight when the number of observations is large enough to make the influence of accidental errors and dispersion negligible as compared with the systematic error, while observers whose material is insufficient to satisfy this condition should have little or no weight. In deriving the constants of the formula for each type, an arbitrary limit of nine observations was adopted for each observer. The results of all observers having nine or more observations were used and given the same total weight in forming the mean system, while the results of those observers who have less than nine observations for the spectral type in question were excluded altogether. For types B, A, and M, where the material is scanty, the limit was reduced to four. The contrast between the two methods is clearly seen from Table IV, which gives the percentage weight assigned to each observer for the different types according to both methods.

C) Since the dispersion (3) mentioned on page 3 is practically proportional to the mean parallaxes, it follows that the equations of condition should receive weights inversely proportional to the squares of the mean parallaxes. In the least-squares solution weights are fully taken into account by multiplying each equation by the square root of the weight, which merely transfers the factor $\bar{\pi}$ from the left member of the equation of condition to the denominator of the right member.

Among the stars of large proper motion exceptional deviations from the mean-parallax formula are frequently encountered; thus for ϵ Eridani and α Canis Minoris we find π_O to be $0''.317$ and $0''.314$, as determined by three and six observers, respectively, while Kapteyn's tables give $0''.109$ and $0''.176$ as the mean parallaxes of stars of corresponding magnitude and proper motion. In order to avoid the influence of individual cases such as these, all groups of stars between the adopted limits of magnitude and motion with $\mu > 0''.200$ were rejected unless the number of observations was more than two; in method *b*, moreover, all stars having $\mu > 1''.000$ were omitted in deriving the constants, as it is chiefly among the stars of large proper motion that considerable differences appear.

Summarizing, we proceeded thus: The stars of each spectral type were arranged according to magnitude and proper motion. For each star $\bar{\pi}_T$ was derived from the tables in *Groningen Publications*, No. 8, and the difference $\pi_O - \pi_T$ (Observer *minus* Kapteyn, corrected from relative to absolute parallax) formed for each observation. The weighted mean of these differences for each group of magnitude and proper motion was used as the numerator of the second member of an equation of the form

$$da' + m db' + (\log \mu) dc' = \frac{\pi_O - \bar{\pi}_T}{\bar{\pi}_T}. \qquad (5)$$

Two complete solutions were made, using the different systems of weighting mentioned under (*a*) and (*b*) on pages 8 and 10. For each type, da', db', and dc' were derived from a set of equations like (5) by a least-squares solution and used with the aid of formula (5) to correct Kapteyn's tabular parallaxes. The mean parallaxes of the individual observers for each magnitude-proper-motion group were then compared with results obtained by this formula. The differences $\pi_F - \bar{\pi}_O$ thus found represent the systematic deviation of each observer as compared with the mean of the parallax material available.

These deviations for the different observers may be a function of the various characteristics of the star: spectral type, magnitude, motion, right ascension, declination, galactic latitude, or some other peculiarity. In order not to subdivide the material too much, we have confined ourselves to the spectral type, magnitude, and motion. Tables V, VI, and VII give for each observer the dependence of the deviation on each of these three characteristics. They indicate the corrections that must be applied to the results of the individual observers in order to reduce them to the mean system. Observers with a total of less than 20 parallaxes have been omitted from these tables. The results derived by the two methods of weighting discussed above are given separately under *a* and *b*, while *n* gives the number of observations used. The fact that *n* is sometimes smaller than the number of observations shown in Table II is due to the rejection of the stars mentioned under (*C*) on page 11.

In forming Tables V to X the weights assigned to each group of stars were proportional to $\frac{n}{r^2+(K\bar{\pi})^2}$, where n is the number of stars in the group, r the probable error of the observer, and $K\bar{\pi}$ the value of the probable dispersion for these stars.

It is remarkable to see how closely in general the systematic deviations, formed by the two methods, agree. Whenever the difference becomes considerable, it can practically always be attributed to the larger number of stars used in method *a*. It is important to note, especially in the case of Table VII, that the systematic deviations for stars of larger proper motion have little weight, even when the number of stars is considerable, owing to the large value of the dispersion $K\bar{\pi}$ which appears in the denominator of the expression for the weight.

TABLE V

UNIT=0″.001

SPECTRAL TYPE	a		b		a		b		a		b	
	Corr.	*n*	Corr.	*n*	Corr.	*n*	Corr.	*n*	Corr.	*n*	Corr.	*n*
	Abetti				Allegheny				Flint I			
B........	−12	1	− 9	1	+10	5	+11	5	.....	.....	.....	....
A........	−27	8	−22	8	+ 7	42	+14	42	−45	8	−63	8
F........	+ 4	9	+ 4	8	+ 7	64	+ 6	60	+10	21	+ 2	15
G........	−28	10	−25	10	0	62	+ 1	59	+29	20	+95	5
K........	+ 2	10	− 5	9	+ 5	77	+ 1	76	−41	29	−49	8
M........	−13	1	−15	1	− 1	8	+ 3	8	−46	6	.....	.....
	Flint II				Greenwich				Jewdokimow			
B........	−18	19	−16	19	.....	.....	.....	.....	−10	1	− 5	1
A........	+16	20	−11	20	.....	.....	.....	.....	+ 3	5	−36	5
F........	− 3	21	− 4	20	+15	9	+19	9	−22	15	−28	14
G........	+ 2	31	+10	28	+ 7	23	+13	20	−20	15	0	9
K........	− 2	26	+ 4	22	+16	4	− 8	1	−16	15	−18	8
M........	+47	2	+42	2	.....	.....	.....	.....	+49	4	+215	1
	Jost				van Maanen				Sproul			
B........	−52	1	−52	1	− 7	3	− 8	3	− 4	3	− 4	3
A........	− 7	7	+ 3	7	.....	.....	.....	.....	+ 8	14	+12	14
F........	−14	16	−15	16	+ 8	17	+11	17	−18	30	−16	28
G........	−25	10	−22	9	− 2	12	− 2	12	−13	19	−12	16
K........	+13	9	+14	9	− 1	30	− 7	29	− 8	15	− 7	11
M........	+27	2	+37	1	− 3	21	− 3	21	−62	2	.....	.....
	McCormick				Russell				Yale			
B........	− 8	4	−10	4	+13	2	+13	2	+16	9	+17	9
A........	+ 1	26	+ 2	26	−27	1	−54	1	+ 1	14	−11	14
F........	+ 4	55	+ 1	51	+ 8	5	−24	3	+ 2	51	0	45
G........	0	51	+ 1	43	+36	10	+35	9	+ 6	80	+13	68
K........	− 8	47	−10	41	+17	11	+23	5	+ 8	77	+12	63
M........	+ 2	12	0	11	−54	7	−44	2	−20	6	+ 9	2
	Yerkes											
B........	+ 2	14	+ 2	14								
A........	+ 4	21	+10	21								
F........	+ 5	17	+15	15								
G........	0	27	0	22								
K........	+ 1	32	+ 1	17								
M........	−46	6	.....	.....								

TABLE VI

UNIT = 0″.001

Mag.	a		b		a		b		a		b	
	Corr.	n	Corr.	n	Corr.	n	Corr.	n	Corr.	n	Corr.	n
	Abetti				Allegheny				Flint I			
<3......	......	....	......	....	+ 9	16	+ 6	16	+48	11	+39	9
3–5......	−31	24	−30	23	+ 4	163	+ 3	161	−38	20	−26	10
5–7......	+15	14	+14	14	+ 4	68	+ 7	64	−26	33	−12	14
7–9......	+42	1	......	....	+ 6	10	+ 7	9	+ 8	23	−95	3
>9......	......	....	......	....	......	....	......	....	......	....	......	....
	Flint II				Greenwich				Jewdokimow			
<3......	+ 1	65	− 3	65	......	....	......	....	+28	12	+ 8	12
3–5......	+ 1	17	+ 6	16	−22	1	−50	1	−28	13	−22	8
5–7......	− 6	23	0	17	+15	8	+18	8	− 2	15	−18	10
7–9......	−17	14	− 6	13	+ 9	22	+14	21	−46	15	−32	8
>9......	......	....	......	....	+ 5	5	......	....	......	....	......	....
	Jost				van Maanen				Sproul			
<3......	+40	1	+31	1	......	....	......	....	−23	4	−20	3
3–5......	+ 3	9	+ 1	9	......	....	......	....	− 1	33	− 1	30
5–7......	−16	31	−13	30	− 1	82	− 3	81	−12	35	− 9	31
7–9......	+14	4	+14	3	+ 9	1	+17	1	−23	11	−22	8
>9......	......	....	......	....	......	....	......	....	......	....	......	....
	McCormick				Russell				Yale			
<3......	+ 5	30	− 1	29	− 3	3	−24	3	+ 3	25	− 5	23
3–5......	− 2	111	− 3	102	+ 2	8	−11	6	−13	34	−16	30
5–7......	− 3	38	− 2	32	+22	8	+28	8	+11	73	+16	61
7–9......	+ 6	16	+ 4	13	+11	14	+24	5	+ 9	98	+15	84
>9......	......	....	......	....	+16	3	......	....	−20	4	......	....
	Yerkes											
<3......	+ 1	7	− 1	6								
3–5......	+ 3	37	+ 4	35								
5–7......	+ 2	27	+ 6	24								
7–9......	0	36	+ 8	22								
>9......	+ 8	8	......	....								

TABLE VII

UNIT=0″.001

μ	a		b		a		b		a		b	
	Corr.	n	Corr.	n	Corr.	n	Corr.	n	Corr.	n	Corr.	n
	Abetti				Allegheny				Flint I			
<0″.050	+15	8	+18	8	+3	54	+2	54	+24	2	+24	2
0″.050–0.099	−8	8	+2	8	+6	32	+5	32	−18	2	−18	2
0.100–0.199	−33	10	−33	10	+3	66	+3	66	−2	6	0	6
0.200–0.499	+2	6	+2	6	+8	73	+9	73	−14	17	−18	17
0.500–0.999	−65	5	−67	5	+5	25	0	25	+51	9	+24	9
1 – 2	+17	2	.....	....	−4	8	.....	....	−12	39	.....	....
>2	.....	....	.....	....	.....	....	.....	....	−28	12	.....	....
	Flint II				Greenwich				Jewdokimow			
<0.050	−8	31	−8	31	.....	....	.....	....	−24	5	−29	5
0.050–0.099	−4	9	−9	9	.....	....	.....	....	.....	....	.....	....
0.100–0.199	+3	17	0	17	.....	....	.....	....	.....	....	.....	....
0.200–0.499	+2	18	+1	18	+9	32	+15	27	+35	9	+32	9
0.500–0.999	+5	34	+5	34	+7	3	−5	3	−27	21	−34	21
1 – 2	−43	8	.....	....	+6	1	.....	....	−50	10	.....	....
>2	.....	....	.....	....	.....	....	.....	....	+7	7	.....	....
	Jost				van Maanen				Sproul			
<0.050	−52	1	−52	1	−1	36	−3	36	−8	9	−6	9
0.050–0.099	−17	2	−7	2	−3	25	−6	25	−6	11	−4	11
0.100–0.199	−19	14	−15	14	+6	15	+4	15	−11	19	−9	19
0.200–0.499	+4	17	+4	17	−3	5	−5	5	−3	19	−3	19
0.500–0.999	−9	9	−8	9	+14	1	+21	1	−15	14	−20	14
1 – 2	−31	1	.....	....	−20	1	.....	....	−38	5	.....	....
>2	−50	1	.....	....	.....	....	.....	....	−28	4	.....	....
	McCormick				Russell				Yale			
<0.050	−2	44	−2	44	+13	2	+13	2	+7	12	+2	12
0.050–0.099	0	27	0	27	+9	3	+5	3	+11	7	+11	7
0.100–0.199	+2	34	−1	34	−59	1	−60	1	+50	4	+46	4
0.200–0.499	−3	42	−7	42	+12	4	+6	4	+9	41	+3	41
0.500–0.999	+4	29	−4	29	+19	12	+18	12	+6	141	+7	137
1 – 2	−13	15	.....	....	+16	8	.....	....	−20	26	.....	....
>2	−30	4	.....	....	−14	6	.....	....	−50	6	.....	....
	Yerkes											
<0.050	+7	17	+8	17								
0.050–0.099	+3	15	+6	14								
0.100–0.199	+1	10	+1	10								
0.200–0.499	−2	26	0	26								
0.500–0.999	+5	25	+7	22								
1 – 2	−15	18	.....	....								
>2	−41	6	.....	....								

Tables V and VII show that the systematic deviations for each observer are practically independent of the spectral type and the proper motion. For magnitude it is different; only for Allegheny, Greenwich, van Maanen, McCormick, and Yerkes do the systematic differences seem to be practically independent of the magnitude. For these we may accordingly assume a constant correction. Assigning equal weights to methods *a* and *b*, we derive the systematic reductions to the mean system which are given in Table VIII.

TABLE VIII

REDUCTION TO MEAN SYSTEM

Observer	Method *a*	Method *b*	Reduction Adopted	Probable Error
Allegheny	+0.″0044	+0.″0040	+0.″004	±0.″0008
Greenwich	+0.0085	+0.0138	+0.012	0.0011
van Maanen	−0.0010	−0.0030	−0.002	0.0009
McCormick	−0.0009	−0.0023	−0.002	0.0009
Yerkes	+0.0022	+0.0050	+0.004	±0.0010

The last column shows the probable errors of the corrections; their smallness is evidence of the reality of the systematic deviations.

For the other observers the reductions to the mean system are clearly functions of the magnitudes of the stars and have been assumed to be linear functions of the magnitude; the results are given in Table IX.

TABLE IX

UNIT=0.″001

Observer	Magnitude									
	0	1	2	3	4	5	6	7	8	9
Abetti	.....	.....	.....	−52	−30	− 8	+14	+36	+59	.....
Flint I	+18	+12	+ 6	+ 1	− 5	−10	−16	−22	−27	−33
Flint II	+ 4	+ 2	+ 1	− 1	− 2	− 4	− 5	− 7	− 8	−10
Jewdokimow	+27	+19	+11	+ 3	− 5	−13	−21	−29	−37	−45
Jost	+10	+ 6	+ 3	0	− 3	− 6	−10	−13	−16	−19
Sproul	.....	.....	.....	0	− 3	− 7	−10	−14	−18	−21
Russell	−18	−13	− 8	− 3	+ 2	+ 7	+12	+16	+21	+26
Yale	−11	− 8	− 5	− 2	+ 1	+ 4	+ 7	+10	+13	+15

For the observers whose number of observations is less than 20 the systematic reductions have of course little value; but for the sake of completeness they have been collected in Table X.

TABLE X

Observer	Reduction	Probable Error
Cape	−0″.010	±0″.0045
Fox	−0.029	0.0067
Groningen	−0.010	0.0050
Kapteyn	+0.005	0.0029
Kostinsky	−0.044	0.0114
Peter	−0.016	0.0081
Voûte	−0.019	±0.0171

As in Table IX the last column gives the probable errors of the corrections.

To some it may appear doubtful whether the application of these corrections is justifiable. The authors themselves are quite convinced that the results are by no means final. The size of the probable errors as compared with the quantities involved shows, however, that there is good reason to ascribe the greater part of the deviations found to real systematic differences, although in many cases we may see no cause for the existence of such differences.

The following tests indicate that the deviations found do represent the effect of real systematic differences.

1. For the 19 stars with six or more observations available the weighted mean parallaxes were computed, first, without, and second, with, the systematic reductions derived above. Comparing the results of the individual observers with the mean parallaxes, we find that of those having parallaxes for more than 10 of these stars, Allegheny, Jewdokimow, Sproul, Russell, and Yerkes show a considerable improvement when the corrections are applied; for McCormick the result is the same as before, while for only Flint I and Yale is the agreement less satisfactory than before. Including all observers of these 19 stars, we find that the application of the reductions to the mean system improves the agreement in 72 per cent of the cases.

2. Further, for all the stars which have more than one observation in common we have formed the differences $\pi_A - \pi_B$, $\pi_A - \pi_C$, etc., where A, B, C, etc., represent the individual observers. This was done, first, without, and second, with, the use of the systematic reductions. In the latter set of reductions case we find the weighted differences to be improved in 65 per cent of the cases.

3. For the Cepheid variables we know the parallaxes with considerable accuracy from Shapley's period-luminosity curve. For eight[1] of these stars we have directly determined parallaxes available. When systematic corrections are applied, the mean is reduced by 0."002, which brings the result into close agreement with Shapley's mean value for these stars. Owing to the small number of stars, this agreement in itself is by no means conclusive, but in combination with the other points mentioned above the result has considerable weight.

We are under great obligation to Mr. Seares for many valuable suggestions during the progress of this investigation.

Mount Wilson Observatory
May 1920

---

[1] The parallax of δ Cephei, which became available after the systematic differences were derived, is also included in the comparison.

Contributions from the Mount Wilson Observatory, No. 190
Reprinted from the *Astrophysical Journal*, Vol. LII, pp. 73–85, 1920

STUDIES BASED ON THE COLORS AND MAGNITUDES IN STELLAR CLUSTERS

SEVENTEENTH PAPER: MISCELLANEOUS RESULTS

By HARLOW SHAPLEY

ABSTRACT

Discovery and position co-ordinates of 88 variable stars in globular clusters N.G.C. 5024, 6293, 6553, 6779, 6864, 6981, 7006, and 7492 are collected in Table II.

Absolute visual magnitudes of forty globular clusters are given in Table III. More than half lie within the interval −8.3 to −9.3, the mean being −8.8±0.5. This remarkable agreement in absolute magnitude enables parallaxes to be estimated from the apparent brightness with a probable error of less than 25 per cent. The *total light-emission of an average cluster* is about 275,000 times that of the sun.

Galactic cluster N.G.C. 7789 is found from the count of 13,500 stellar images to contain about 1100 stars with magnitudes ranging from 13 to 20. The probable linear diameter is 20 parsecs.

Theoretical conclusions regarding Cepheid variables.—Assuming the average heat content per unit mass and therefore the ratio of mass to radius to be the same for all these variables, the author derives a theoretical period-luminosity curve which fits the observations well if the mean atomic weight has the value indicated by other considerations, viz., between 2.5 and 3.0. This agreement lends support to the theory and to the conclusion that only giant stars with a particular ratio of mass to radius become Cepheid variables.

Globular cluster N.G.C. 7006 is so distant that the faintest stars recorded on the plate, magnitude 20, are probably a hundred times as bright as our sun. The star count indicates that the cluster is similar in constitution to nearer ones.

Density of stars in galactic longitude +32° and latitude −20°, to photographic magnitude 20, is about 23,000 per square degree.

Following the plan of the fourteenth paper, the present contribution includes five notes on various aspects of the investigation of clusters. Three of these contain new observational results; the other two deal with material already published. The subjects are:

I. The discovery of 88 variable stars in eight globular clusters.

II. The total light-emission of an average globular cluster and the absolute visual magnitudes of forty systems.

III. The number of stars in N.G.C. 7789, an open cluster of the galactic system.

IV. Evidence that a giant star must have a particular ratio of mass to radius before it can become a Cepheid variable (a theoretical period-luminosity law).

V. A further investigation of the most distant globular cluster now known, N.G.C. 7006.

I. POSITION CO-ORDINATES OF NEW VARIABLE STARS

Upon the request of the late Professor Pickering we have undertaken at Mount Wilson to supplement the systematic discovery and study of variable stars in globular clusters (carried on at Harvard under Professor Bailey's supervision) by examining those faint and highly condensed systems which cannot be satisfactorily studied with the Harvard telescopes. Also, for the brighter clusters, special series of plates have been made and sent to Professor Bailey to supplement the Harvard material in the study of the light-curves of cluster variables; and some progress has been made in examining the fainter stars in bright clusters for evidence of variability.

The typical variable in a globular cluster is the short-period Cepheid. Through the remarkable law that the length of the period is uniquely related to the absolute brightness, these variables are of paramount importance in determining the distances and space distribution of clusters. Particularly for the most remote clusters it is important to check by means of Cepheid variables the distances already derived through measures of angular diameter and the magnitudes of the brightest stars.

Positions of 23 new variables near the center of Messier 3 are given in *Mount Wilson Contr.*, No. 91, 1914. The variable stars found by Miss Davis on my photographs of clusters were reported in *Publications of the Astronomical Society of the Pacific*, **29**, 210, 260, 1917; and the positions and magnitudes of the 28 variables found in Messier 68 by Miss Ritchie are included in the general discussion of that cluster, *Mount Wilson Contr.*, No. 175, 1919.[1] The clusters in which other variables have been found by Miss

---

[1] Positions of 19 of these variables are also published in *Publications of the Astronomical Society of the Pacific*, **31**, 226, 1919. A faint variable in Messier 9 has also been found on Mount Wilson plates, *ibid.*, **28**, 282, 1916.

PLATE XIX

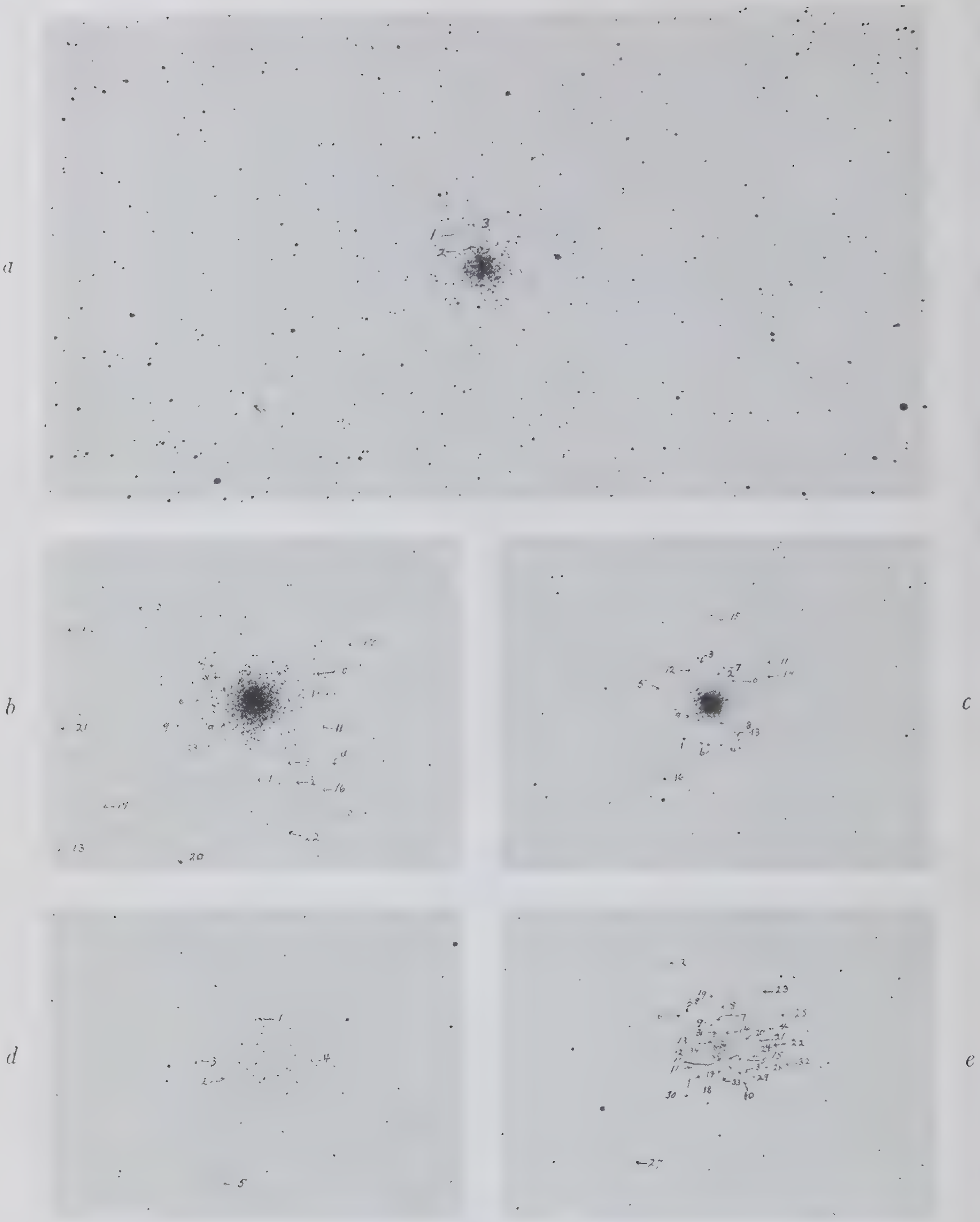

VARIABLE STARS IN CLUSTERS

a. N.G.C. 6779 = Messier 56
b. N.G.C. 5024 = Messier 53
c. N.G.C. 6864 = Messier 75
d. N.G.C. 7492
e. N.G.C. 6981 = Messier 72

Scale: 1 mm = 16″

Ritchie are listed in Table I, taking the co-ordinates and adopted values of the parallax from *Mount Wilson Contr.*, Nos. 152 and 161.

The equatorial co-ordinates of the new variables, in seconds of arc from an adopted center, are given in Table II; the orientation, however, is not exact. An asterisk after the number in the first column indicates that the star is suspected of variation, but the plates now available are insufficient for a definite proof.

On the accompanying reproduction of photographs of five clusters (Plate XIX) the variable stars are indicated by arrows.

TABLE I

N.G.C.	Messier	Right Ascension 1900	Declination 1900	Parallax	Number of Variables	Number Suspected of Variation
5024	53	$13^{\mathrm{h}}\ 8^{\mathrm{m}}.0$	$+18^\circ 42'$	$0''.000053$	23	
6293		17 4.0	−26 26	0.000040	3	
6553		18 3.2	−25 56	0.000031		2
6779	56	19 12.7	+30 0	0.000040	1	2
6864	75	20 0.2	−22 12	0.000022	11	5
6981	72	20 48.0	−12 55	0.000034	31	3
7006		20 56.8	+15 48	0.000015	2	
7492		23 3.1	−16 10	0.000035	1	4

Nearly all of the variables in these clusters appear to have periods of less than a day. This is particularly true for the 23 in Messier 53 and the 31 in Messier 72; for both clusters the median magnitudes of the variables are closely grouped around a mean value, in agreement with the earlier results for Messier 3, 5, 15, 22, 68, and ω Centauri.

A study of the variable stars in Messier 75, at least the determination of their median magnitudes, will be of special interest because the cluster appears to be one of the most distant objects on record, $R=45,000$ parsecs. A photographic study of the variables in the faint cluster Messier 72 will be published as the next contribution of this series.

II. THE ABSOLUTE MAGNITUDES OF FORTY GLOBULAR CLUSTERS

The integrated visual magnitudes of forty globular clusters have been measured at Vienna by Holetschek.[1] Parallaxes have been published for all of them in earlier contributions of this series.

[1] *Annalen der k.k. Universitäts-Sternwarte in Wien*, **20**, 114, 1907.

TABLE II

Variable	x	y
N.G.C. 5024		
1	+0′ 9″.6	−2′51″.0
2	−1 18.0	−3 3.6
3	−1 0.6	−2 18.0
4	−2 49.5	−2 36.6
5	−3 57.0	−4 18.0
6	+2 3.6	+0 13.5
7	+1 19.5	+1 23.5
8	+1 12.0	+1 0
9	+1 7.5	−0 40.5
10	−2 18.6	+0 54.0
11	−2 23.4	−0 58.5
12	+6 49.5	+3 7.5
13	+7 42.0	−4 59.7
14	+5 54.6	−3 27.0
15	+4 8.4	+3 48.0
16	−2 16.5	−3 22.5
17	−3 34.5	+1 54.0
18	−1 36.0	+0 12.6
19	+2 45.6	−0 42.0
20	+3 8.4	−5 51.6
21	+7 17.4	−0 27.0
22	−0 53.4	−4 48.0
23	+1 36.0	−1 29.7
N.G.C. 6293		
1	+1 21.0	+0 49.5
2	−2 15.6	+1 4.5
3	+0 48.6	+0 18.6
N.G.C. 6553		
1*	+0 4.5	+0 0.3
2*	+0 50.4	−0 1.2
N.G.C. 6779		
1	+0 51.0	+1 15.6
2*	+0 21.0	+0 54.4
3*†	+0 33.0	+2 4.5
N.G.C. 6864		
1	+0 15.6	−1 23.4
2	−0 9.0	+0 54.0
3	+0 18.0	+1 25.5
4	−0 18.0	−1 24.6
5	+1′48″.0	−0′36″.0
6	+0 8.4	−1 21.0
7	−0 24.6	+1 18.0
8	−0 13.5	−0 41.4
9	+0 45.6	−0 24.0
10*	−0 43.5	+0 50.4
11	+2 1.2	+1 24.0
12	+0 39.6	+1 15.0
13*	−0 53.4	−1 16.5
14*	−2 4.5	+0 51.0
15*	−0 19.5	+3 3.0
16*	+1 50.4	−2 43.5
N.G.C. 6981		
1	+0 43.5	−0 54.0
2	+1 39.0	+3 14.4
3	−0 52.5	−0 58.5
4	−1 46.5	+0 37.5
5	−0 38.4	−0 21.6
6*	+1 18.0	+1 18.6
7	−0 3.6	+0 55.5
8	−0 6.6	+1 29.4
9	+0 11.4	+0 50.4
10	−0 48.6	−1 13.5
11	+0 57.0	−0 36.6
12	+0 9.0	−0 21.6
13	+0 13.5	+0 17.4
14	−0 13.5	+0 36.0
15	−1 4.5	−0 21.0
16	−0 4.5	−0 19.5
17	+0 3.6	−0 43.5
18	−0 26.4	−0 37.5
19*	+0 3.0	+1 52.5
20	−0 54.6	+0 15.0
21	−1 22.5	+0 12.6
22	−1 53.4	+0 1.5
23	−1 39.0	+1 56.4
24	−0 15.6	−0 24.0
25	−2 13.5	+1 7.5
26	−1 31.5	−0 45.0
27	+3 29.4	−3 54.0
28	−1 5.4	+1 21.0
29	+0 36.0	−0 52.5
30	+1 11.4	−1 37.5
31	+0 5.4	+0 36.6
32	−2 18.0	−0 42.0
33*	+0 2.4	−1 0.6
34	−0 6.0	+0 7.5

---

* Suspected.

† Found independently by Miss Davis, *Publications of the Astronomical Society of the Pacific*, **29**, 210, 1917, where the position is referred to a different origin.

TABLE II—*Continued*

Variable	*x*	*y*	Variable	*x*	*y*
N.G.C. 7006			N.G.C. 7492		
1	−0′22″.5	+0′36″.6	1	+0′ 1″.2	+1′36″.6
2	−0 37.5	−0 39.6	2*	+1 12.0	−0 27.0
			3*	+2 22.5	−0 7.5
			4*	+1 51.0	+0 4.5
			5*	+1 21.0	−4 17.4

These values of distance and apparent brightness permit the computation of the integrated absolute magnitudes presented in Table III.

All but two clusters fall within the magnitude interval from −6.8 to −9.7, and more than half within the interval −8.3 to −9.3. This remarkable similarity in total light-emission again calls attention to the possibility of using apparent brightness as a measure of distance.[1] We have here, in fact, an independent method of determining relative parallaxes of clusters, for although the apparent magnitudes of Cepheids or of bright stars are indirectly involved in computing the absolute magnitudes of Table III, it should be specially noted that the adopted value of the distance of a cluster is not dependent on the apparent brightness of its

TABLE III

ABSOLUTE MAGNITUDE FOR GLOBULAR CLUSTERS

N.G.C.	Abs. Mag.	N.G.C.	Abs. Mag.	N.G.C.	Abs. Mag.	N.G.C.	Abs. Mag.
1904	−9.0	6121	−8.5	6287	−9.0	6712	−8.6
4147	−9.2	6171	−7.0	6293	−8.6	6760	−8.1
4590	−7.8	6205	−9.4	6333	−9.7	6779	−8.7
5024	−8.6	6218	−8.7	6341	−9.2	6864	−10.3
5272	−9.1	6229	−9.6	6356	−9.4	6934	−8.6
5466	−8.0	6235	−8.8	6402	−9.0	6981	−7.8
5634	−7.7	6254	−8.5	6626	−8.4	7006	−9.4
5897	−5.7	6266	−8.9	6637	−7.6	7078	−9.6
5904	−8.8	6273	−9.2	6656	−8.4	7089	−9.2
6093	−8.7	6284	−8.3	6681	−6.8	7099	−7.7

---

[1] The possibility was first noted in *Mt. Wilson Contr.*, No. 115, and discussed further in *Mt. Wilson Contr.*, No. 161, section vi; *Astrophysical Journal*, 50, 107, 1919.

stars as a whole. The 25 brightest stars, for instance, contribute scarcely 2 per cent to the total light of a cluster.

From Table III we may derive the following values of the mean absolute magnitudes and of the average deviation from the mean:

	Number	Absolute Magnitude
All clusters	40	-8.59 ± 0.63
$\pi < 0''.00005$	19	-8.81 ± 0.56
$\pi \geq 0.00005$	21	-8.39 ± 0.70
North of declination $-20°$	23	-8.78 ± 0.54
$\pi < 0''.00005$	12	-8.82 ± 0.57
$\pi \geq 0.00005$	11	-8.74 ± 0.51

There is no indication that distant and nearby clusters differ in total luminosity.

Since the magnitude estimates for clusters south of declination $-20°$ are probably of lower weight than for clusters observable at small distance from the zenith, the average visual absolute magnitude of a globular cluster may be accepted as -8.8 ± 0.5 until further observation justifies revision of the data for distance or apparent magnitude.

By taking -8.8 as the mean value of the absolute visual magnitude, the distance of any globular cluster can be computed, from the apparent magnitude of the system as a whole, with an average probable error of less than 25 per cent. The relation connecting distance in parsecs, r, with apparent visual magnitude, m, is

$$\log r = 0.2\ (m + 13.8).$$

The total light-emission of an average globular cluster is, according to the foregoing result, 275,000 times that of the sun, and its energy of radiation is 10^{39} ergs per second.

III. ON THE DIMENSIONS AND STELLAR CONTENT OF N.G.C. 7789

Although the northern cluster N.G.C. 7789, in galactic latitude $-6°$, is well outside the region of the sky where globular clusters are found, its richness in faint stars suggests that it may be a type intermediate between the loosest of globular clusters and the most populous of bright open systems. The hypothesis that these two main types represent different stages in the evolution of a stellar group makes the richest open systems of particular interest.

An hour's exposure on a fast plate with the 60-inch reflector demonstrates that N.G.C. 7789 is not globular, as it is not closely condensed toward the center, and the number of stars does not increase with decreasing brightness. The angular diameter is approximately 20′. Since the distance of the group has been estimated provisionally as 3300 parsecs,[1] the linear diameter appears to be only 20 parsecs, possibly one-sixth the average value for globular clusters.

On a series of five good photographs, all centered on the cluster, Miss Mayberry has counted the number of stars in a region 22′ by 28′. The exposure times range from one minute to one hour, and the total number of images counted is 13,500. An analysis of the star counts, which were recorded for every fourth of a square minute of arc on all plates, yields the following results for the whole region:

Photographic Magnitude Interval	<16	16–17	17–18	18–19	19–20	Total
Number of cluster stars...	347	210	155	266	126	1104
Number of field stars.....	592	256	666	1178	1475	4167
Ratio..............	0.59	0.82	0.23	0.23	0.09	....

While qualitatively dependable, high weight should not be given to the numerical values in this tabulation, because of difficulty in allowing for the photometric effect of distance from the center in the case of clusters of large angular diameter, and because of uncertainty in the magnitude limits. Apparently the cluster stars lie mainly between magnitudes 15 and 19. The brightest are of photographic magnitude 13, corresponding at the distance given above to the absolute magnitude +0.5.

IV. NOTE ON THE PERIOD-LUMINOSITY CURVE OF CEPHEID VARIATION

The total content of heat in a gaseous mass may be expressed as the sum of the kinetic energy of translation of the molecules (or particles of the gas), and the energy within the molecules. If the mass is a typical giant star, therefore, in a steady state, the total heat, H, is necessarily proportional to the gravitational potential; that is,

---

[1] *Mt. Wilson Communication*, No. 62; *Proceedings of the National Academy of Sciences*, **5**, 344, 1919.

$$H \propto \frac{\mu^2}{R},$$

where μ is the mass and R the radius. The factor of proportionality involves the ratio of the specific heats which conceivably may vary with mass or linear dimensions, but as all the possible values for a gaseous star lie between 4/3 and 5/3, this ratio will be treated below as a constant. The *average* heat-content per unit of mass is

$$C = k_o \frac{\mu}{R} \cdot \tag{1}$$

Let us suppose that C has the same constant value for all Cepheid variables and check this supposition against observation. Then since $\mu = 4\pi R^3 \bar{\rho}/3$, where $\bar{\rho}$ is the mean density, we have, upon substitution for R in (1),

$$\bar{\rho}\mu^2 = \text{a constant;} \tag{1'}$$

and since in a gaseous star the period, P, of a gravitational pulsation is inversely proportional to the square root of the mean density,[1]

$$\frac{\mu}{P} = \text{a constant.} \tag{2}$$

The relation of the masses of two gaseous giant stars to the difference in their absolute (bolometric) magnitude, M, may be written (from Eddington's theory)[2]

$$M_n - M_1 = 2.5 \log_{10} \frac{\mu_1(1-\beta_1)}{\mu_n(1-\beta_n)}, \tag{3}$$

[1] In his mathematical discussion of the Cepheid problem, Eddington deduced $P^2\bar{\rho}f(\gamma) = a$ *constant*, where the function of the ratio of specific heats, γ, changes slightly with the mass because of changes in the elastic constants.

[2] *Astrophysical Journal*, **48**, 205, 1918; cf. also Jeans, *Problems of Cosmogony and Stellar Dynamics*, Cambridge, England (1919), chap. viii.

where β, the ratio of the force of the ordinary gas pressure to gravitation, is given by

$$\frac{1-\beta}{\beta^4}=0.0026\ m^4\mu^2. \tag{4}$$

The unit of μ is the solar mass; and m, the average "molecular" weight, is expressed in terms of the hydrogen atom.

By adopting from data of observation the following values as defining a typical Cepheid variable

$$\left.\begin{aligned} M_1&=-2.2\\ \mu_1&=4.0\\ P_1&=5.4\text{ days}\end{aligned}\right\} \tag{5}$$

we have

$$\log_{10} P=\log_{10}\mu+0.13. \tag{2'}$$

Taking $m=2$, 2.5, 3, and 4, I have used the preceding equations to compute μ, M, and the logarithm of P for selected intervals of β. The results are given in Table IV for $m=2.5$, in which case

$$M=-1.90-2.5\log_{10}\mu(1-\beta). \tag{3'}$$

Figure 1 compares the theoretical period-luminosity curve, computed on this assumption of an average heat-content, with all the available observations. Each plotted point represents the observed period and visual brightness of a Cepheid variable, the data being taken without change from my derivation of the period-luminosity curve in *Mount Wilson Contr.*, No. 151. The visual magnitude of the two brightest stars plotted should be decreased by 0.4 mag., according to a more recent examination of the color-period relation for Cepheids, thus bringing those two points in close agreement with the curve. Open circles indicate determinations of low weight.

For Cepheids with periods of less than three days the theoretical curve no longer fits the observations. This is to be expected, for the central density in such stars is commonly believed to be too great for further comparison with a gas. It has already been found that the cluster-type variables have anomalous physical properties, in that stars of the same absolute magnitude and color differ in length of period by three to one.[1]

The observations are not so well represented by the theoretical period-luminosity curve when the average molecular weight is taken as 2 or 4; but with $m=3$ it is possible to represent the observed values nearly as well as with $m=2.5$, provided small alterations of the adopted quantities (5) are introduced. The value of m adopted by Eddington for theoretical work is 2.8. In an unpublished investigation Russell uses a value very slightly smaller. Jeans, Eddington, Lindemann, and others have noted that m must be of the order of magnitude here used on account of the necessarily high degree of ionization that is believed to prevail at stellar temperatures.

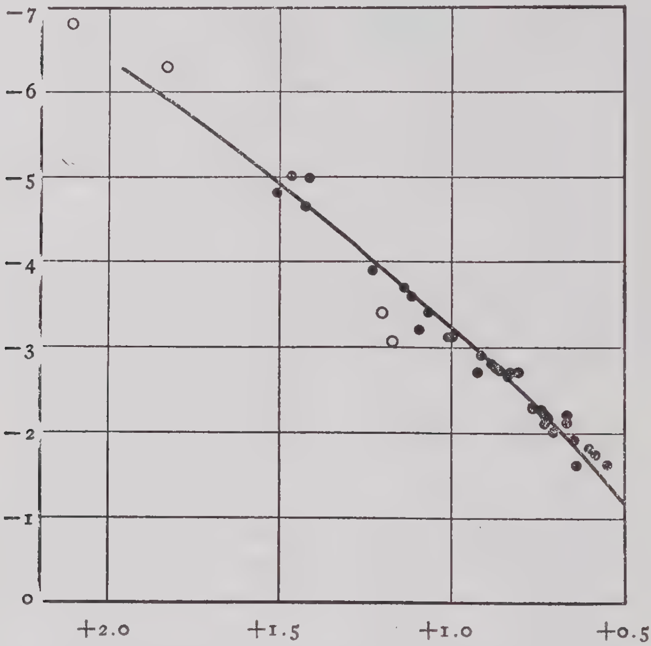

FIG. 1.—Period-luminosity curve. Ordinates are absolute visual magnitudes; abscissae are logarithms of the period.

---

[1] *Mt. Wilson Contr.*, No. 154, 1917; *Astrophysical Journal*, **49**, 24, 1919.

Accepting, therefore, the radiative theory of giant stars and a most probable value of the average molecular weight, we conclude from the foregoing discussion that for all typical Cepheid variables μ/R has practically the same value;[1] and we may reasonably infer that this condition of definite average heat content and corresponding critical central temperature is associated with the origin, and particularly with the persistence, of the pulsations that are believed to underlie the spectral, light, and velocity variations.

TABLE IV

A THEORETICAL PERIOD-LUMINOSITY CURVE

β	μ	M	$\log P$
0.2	70	−6.27	1.97
0.3	29	−5.17	1.59
0.4	15	−4.28	1.31
0.5	9	−3.53	1.08
0.6	5.5	−2.76	0.87
0.67	4.0	−2.20	0.73
0.7	3.5	−1.95	0.67
0.8	2.2	−1.01	0.47

The duration of Cepheid variation is much the same problem as the duration of the giant stages of all gaseous stars. Both problems involve principles of radiation or sources of energy beyond those currently accepted. Russell has made the interesting suggestion that the maintenance of the pulsations may be ascribed to the pulsatory supply of heat from some undescribed internal source at times of greatest contraction.[2] Without some such supplementary means of sustenance it appears improbable that the pulsations could long continue. It seems likely, therefore, that only those pulsatory disturbances, starting with the critical μ/R (and the resulting condition of internal temperature) that is favorable for drawing on the supplementary sources, would sufficiently develop and persist to result in typical stellar variation.

---

[1] Eddington's observation (*Monthly Notices*, **77**, 2, 1918), that for galactic Cepheids the central temperature divided by β is essentially constant, is equivalent to this result, for on his theory of radiative equilibrium the central temperature is proportional to $\mu^{\frac{2}{3}} \bar{\rho}^{\frac{1}{3}} \beta$; cf. equation (1′) above.

[2] *Publications of the Astronomical Society of the Pacific*, **31**, 205, 1919.

V. NOTE ON THE DISTANT CLUSTER N.G.C. 7006

Observations of the extremely distant globular cluster N.G.C. 7006 have been discussed in preceding papers of this series.[1] In addition to the extremely small parallax, the study thus far has given results that bear on the scattering of light in space, on the comparability of near and distant clusters, and on the speed of evolution of giant stars.

A photograph made with the 60-inch reflector in July, 1918, by Professor J. C. Duncan, affords additional data of interest in the comparison with the brighter systems. The exposure of 95 minutes on a Seed 27 plate shows the cluster as a typical system, differing very little in general appearance from Messier 15. A study of the photograph yields the following results:

1. The brightest ten stars of the cluster are photographically somewhat fainter than the seventeenth magnitude. The faintest on the plate are of the twentieth magnitude, corresponding, at the adopted distance of 67,000 parsecs, to the absolute photographic magnitude +1 and to a luminosity one hundred times as great as that of the sun.

2. In the field of the cluster the foreground density averages 6.4 stars per square minute; that is, to the twentieth photographic magnitude there are in this part of the sky about 23,000 stars in a square degree. The galactic longitude and latitude are 32° and −20°. Seven faint nebulae, apparently spirals, are on this plate within ten minutes of arc of the center.

3. Two counts with a superposed réseau give a mean of 505 cluster stars, 200 of which are brighter than magnitude 18.5. The numbers agree very closely with the numbers of stars in Messier 3 and Messier 13 for the corresponding intervals of absolute magnitude, thus emphasizing further the similarity of near and distant globular clusters.

4. The cluster appears to be slightly elliptical. Eight independent estimates give values of the position angle of the major axis ranging from 90° to 135°, with a mean of 115°. The star counts, grouped in quadrants, afford a rough verification. On the

---

[1] *Mt. Wilson Contr.*, No. 152, p. 14, n. 1; *Astrophysical Journal*, **48**, 154, 1918: No. 156, pp. 1–6; *Astrophysical Journal*, **49**, 249, 1919.

Franklin-Adams chart the cluster appears as a diffuse star image and no elongation can be detected. New measures of the diameter on the chart give 46″, in nearly exact agreement with earlier determinations. A distinct (but probably chance) spiral structure can be traced on the plates of shorter exposure; it is absent, however, from this new plate, which brings out the fainter stars.

5. The angular diameter of the cluster on the Mount Wilson photograph is approximately four minutes of arc, corresponding to a linear diameter of 80 parsecs. Extension to still fainter magnitudes would probably give a slightly larger diameter.

MOUNT WILSON OBSERVATORY
May 1920

Contributions from the Mount Wilson Observatory, No. 191
Reprinted from the *Astrophysical Journal*, Vol. LII, pp. 162–182, 1920

THE SURFACE BRIGHTNESS OF THE GALACTIC SYSTEM AS SEEN FROM A DISTANT EXTERNAL POINT AND A COMPARISON WITH SPIRAL NEBULAE

By FREDERICK H. SEARES

ABSTRACT

Comparison of the galactic system with spiral nebulae as to surface brightness.—The results recently obtained by Kapteyn and van Rhijn for the distribution of stars of various magnitudes in our Galaxy have enabled the author to determine the surface-brightness of the galactic system, as viewed from a distant point in the direction of the galactic pole, for various distances from the center. The brightness of the central part is found to correspond to visual magnitude 23 per square second of arc, whereas probably all known spiral nebulae are brighter than this; in fact, many nebulae, including such well-known ones as that in Andromeda, are more than one hundred times as bright. This result indicates that spirals differ from the galactic system by being nebulous, or that they must be much larger or composed of more stars or of brighter stars. Our Galaxy is therefore far from being a typical spiral. Viewed edge on, the brightness of the Galaxy would be magnitude 21.2 per square second. These results are checked by comparison with the total amount of starlight in the direction of the pole and the Galaxy as computed from star counts.

Brightness of nebulous areas may be *determined photographically* by comparing the times of exposure necessary for barely perceptible images, with the exposure necessary to secure a trace of a large extra-focal image of a star of known magnitude. The constants for use with the 60-inch were determined in this way. Since in the case of extended nebulae, atmospheric disturbances and intermittency losses do not interfere with the continuity of exposure, images were obtained for a given magnitude per square second in the time required for images of stars about three magnitudes brighter.

In view of current discussion of the relation of spiral nebulae to the galactic system, it is of interest to compare the surface brightness of the spirals with that of our system as it would appear from a distant external point. This can be done with the aid of results recently obtained by Kapteyn and van Rhijn in an investigation of the density and luminosity laws.[1] The brightness at the center of figure of the system as seen in projection from the outside can also be computed from the numbers of stars in the successive intervals of apparent magnitude; but to determine the brightness at other points, the distribution of the stars in space must be known, and this requires a knowledge of the laws of density and luminosity.

---

[1] *Mt. Wilson Contr.*, No. 188; *Astrophysical Journal*, **52**, 23, 1920.

The density law gives the total number of stars per unit volume of space at various distances from the center of the system; the luminosity law specifies the number of stars of each unit of intrinsic brightness (absolute magnitude) in a unit volume of unit density. It is assumed that the *relative* frequencies of the absolute magnitudes are the same at all distances. For a constant volume, the total number of stars of each absolute magnitude therefore decreases, with increasing distance, in accordance with the density law.

In the form used here, these laws are a second approximation, based upon the data now available. Like the first, published by Kapteyn some years ago, they are mean results for all spectral types. Although still provisional, their precision is ample for the question considered.

I. INTEGRATION OF THE DENSITY-FUNCTION

Assuming the system to be a figure of revolution, symmetrical with respect to the galactic plane and with the sun at the center, Kapteyn and van Rhijn find for latitudes 0°, 30°, 60°, and 90° the stellar densities and corresponding distances given in Table I. The last column shows that in the direction of the pole the number of stars falls off rapidly, and at 1230 parsecs is only 0.01 that at the center of the system. In the plane of the Galaxy, on the other hand, a density of 0.01 occurs at a distance of nearly 9000 parsecs. The difference in these distances exhibits the well-known concentration of the stars toward the galactic plane. The authors estimate that the quantities in Table I are a very good approximation to distances of 1500 parsecs. In the direction of the pole this is practically the limit of the system, and it is clear that the light of the stars in the higher latitudes which are beyond this limit cannot be any important fraction of the whole.

Because of this circumstance, the external point from which the system is supposed to be observed is chosen in the direction of the galactic pole. Thus viewed, the system would be at least approximately circular in outline; and, if the point of observation were very distant, the stars would be unresolved and appear as a luminous surface. It is the brightness of this surface that we wish to determine.

The numbers in Table I lead to the total density, D, in a direction perpendicular to the galactic plane at any distance from the center, while the luminosity law gives the total amount of light, l, in a volume of unit density. The combination of these results gives the quantity of light radiated from any point on the projected system in the direction of the distant external point.

As a preliminary, we must derive values of the density at intervals along the line of sight, i.e., along perpendiculars to the galactic plane, at various distances from the center. For the center of figure itself, the last column of Table I gives directly the required data. Selecting other points at the distances indicated in the heading of Table II, we find by graphical interpolation from the data of Table I the quantities in the body of Table II. Numbers in parentheses are densities in the galactic plane at distances from the center indicated in the heading. The other numbers are the distances from the plane, along the respective perpendiculars, at which occur the densities shown in the first column. Thus, at a point 400 parsecs from the center, the density in the plane is 0.78; and 400 parsecs perpendicularly above (and below) this point the density is 0.16.

TABLE I

STELLAR DENSITY AND DISTANCE FROM CENTER OF GALACTIC SYSTEM

Density	Galactic Latitude			
	0°	30°	60°	90°
1.00	0	0	0	0
0.40	910	320	250	250
0.16	1950*	710	490	450
0.063	3550	1320	800	660
0.025	5750	2140	1200	910
0.010	8910	3310	1700	1230
0.0040	13200	4900	2340	1580
0.0016	19100	7080	3090	2000

* The value by Kapteyn and van Rhijn, *loc. cit.*, Table VII, is 1450. Their results, however, are interpolated from Table VI of their article, which seems to require 1950, the distance used in the present discussion.

To determine the total density D in the line of sight, consider a volume of square cross-section, 1 parsec × 1 parsec, extending from the center of the system to the distant point. From a plot of the numbers in the first two columns of Table II[1] it appears that for the first 100 parsecs from the plane the mean density is 0.87; for the second 100 parsecs it is 0.60; for the third, 0.41; etc. Hence the total density (multiplying by 2 to include stars on both sides of the plane) is

$$D=200(0.87+0.60+0.41+0.27+\ldots\ldots)=527.$$

The volume in question is therefore the equivalent of 527 cubic parsecs of unit density. The values of D for the remaining points were found in a similar manner; the results are in the lower part of Table II.

II. TOTAL LIGHT PER CUBIC PARSEC

If now l be the quantity of light, referred to a unit distance of one parsec, received by the observer from all the stars in a cubic parsec of unit density, the total light from one square parsec of the surface of the system seen in projection will be

$$L=Dl. \qquad (1)$$

Since L is referred to unit distance, its equivalent absolute magnitude is

$$M=-2.5 \log L=-2.5 \log Dl. \qquad (2)$$

We may calculate l approximately by reading from the luminosity-curve of Kapteyn and van Rhijn[2] the data in the second column of Table III, namely, the numbers of stars of each unit interval of absolute magnitude, M, in a volume of 1000 cubic parsecs of unit density. These numbers must be multiplied by the corresponding relative luminosities and summed.

Let the light of a star for which $M=0$ be l_0; that for $M=-1$ will then be $2.512\, l_0$; for $M=-2$, $(2.512)^2\, l_0$, etc. The logarithms

---

[1] Supplemented by a few values interpolated from Table VI of the investigation by Kapteyn and van Rhijn, *Mt. Wilson Contr.*, No. 188.

[2] *Loc. cit.*, Fig. 1.

TABLE II

Densities Along Perpendiculars to the Galactic Plane at Various Distances from Center

Density	Distance (ρ) in Parsecs										
	0	200	400	600	800	1000	1500	2000	3000	4000	5000
....	(1.00)	(0.92)	(0.78)	(0.60)	(0.45)	(0.355)	(0.230)	(0.155)	(0.082)	(0.051)	(0.035)
0.40	250	210	170	120	50	....	....	....	....	....	....
0.16	450	430	400	350	320	270	150	....	....	....	....
0.063	660	690	700	700	680	660	585	500	400	....	....
0.025	910	950	1000	1050	1070	1090	1080	1020	1000	820	600
0.010	1230	1260	1320	1380	1450	1500	1590	1650	1800	1780	1750
0.0040	1580	1700	1780	1850	1920	2000	2200	2250	2400	2500	2600
0.0016	....	....	....	....	....	2500	2700	2800	3100	3300	3450
D	527	490	428	360	306	276	216	183	143	114	93
M sq. ps.)	−3.64	−3.57	−3.42	−3.23	−3.05	−2.94	−2.68	−2.50	−2.23	−1.98	−1.76
m (1 sq. sec)	22.93	23.00	23.15	23.34	23.52	23.63	23.89	24.07	24.34	24.59	24.81

of the coefficients of l_0 for the successive values of M are in the third column of Table III. Adding these to the quantities in the second column, we obtain the logarithms of the total light for each M, expressed in l_0 as a unit. The numbers themselves are in the last column. The total for all the stars is $55.5\ l_0$; hence for 1 cubic parsec $l = 0.0555\ l_0$.

TABLE III

LUMINOSITY-CURVE AND TOTAL LIGHT PER 1000 CUBIC PARSECS OF UNIT DENSITY

M*	Logarithm No. Stars 1000 Cubic Parsecs	Logarithm Relative Luminosity	Logarithm Total Light Each M	Total Light Each M
−11	4.4−10	4.4	8.8−10	0.1
10	5.3	4.0	9.3	0.2
9	6.2	3.6	9.8−10	0.6
8	7.0	3.2	0.2	1.6
7	7.7	2.8	0.5	3.2
6	8.3	2.4	0.7	5.0
5	8.8	2.0	0.8	6.3
4	9.3	1.6	0.9	7.9
3	9.7−10	1.2	0.9	7.9
2	0.1	0.8	0.9	7.9
− 1	0.4	0.4	0.8	6.3
0	0.6	0.0	0.6	4.0
+ 1	0.8	9.6−10	0.4	2.5
2	0.9	9.2	0.1	1.3
3	0.9	8.8	9.7−10	0.5
4	0.8	8.4	9.2	0.2
+ 5	0.6	8.0−10	8.6−10	0.0
			Total	55.5

* Unit of distance for M is 1 parsec.

The value of l can be more precisely obtained as follows: The luminosity law is very accurately expressed by

$$\left.\begin{aligned}\phi(M) &= A\frac{h}{\sqrt{\pi}}e^{-h^2(M-M_0)^2}\\ A=0.0451,\quad M_0&=+2.693,\quad h=0.2218\end{aligned}\right\}\qquad(3)$$

where $\phi(M)$ = number of stars of absolute magnitude M per cubic parsec of unit density. If l_M be the light of a star of magnitude M, then

$$\log\frac{l_M}{l_0} = -0.4\,M,\quad l_M = l_0 e^{-0.9211\,M}.$$

The total light of the stars in a cubic parsec of unit density is therefore

$$l=\int_{-\infty}^{+\infty}\phi(M)l_M dM=Al_0\frac{h}{\sqrt{\pi}}\int_{-\infty}^{+\infty}e^{-h^2\{(M-M_0)^2+11.60\,M\}}dM,$$

which reduces to

$$\left.\begin{aligned}&l=A'l_0\frac{h}{\sqrt{\pi}}\int_{-\infty}^{+\infty}e^{-h^2(M-M_0')^2}dM\\&A'=0.0545,\ \ M_0'=-3.11,\ \ h=0.2818.\end{aligned}\right\}\qquad(4)$$

The integral is that of the ordinary error curve. With the coefficient $h/\sqrt{\pi}$ its value is unity; hence

$$l=0.0545\,l_0\qquad(5)$$

in substantial agreement with the previous result. We adopt the value (5).

It will be noted that the number of stars for a given M is a maximum for $M=M_0=2.69$ (equation 3), while the maximum amount of light radiated by the stars of a given M is that corresponding to $M=M_0'=-3.11$ (equation 4). The latter result is checked, roughly at least, by the numbers in the last column of Table II, which indicate a maximum for $M=-3$. The integration of (3) between $-\infty$ and $+\infty$ with respect to M gives the result of Kapteyn and van Rhijn for the total number of stars of all magnitudes in a cubic parsec of unit density, namely, $A=0.0451$.

III. SURFACE BRIGHTNESS OF GALACTIC SYSTEM. CONTROL OF RESULTS

From (5) it follows that

$l=$ light of one star of absolute magnitude $+3.16$.

Equation (2) for the equivalent absolute magnitude of the light from one square parsec of the surface of the galactic system thus becomes

$$M=3.16-2.5\log D\,,\qquad(6)$$

from which we find the values of M at the bottom of Table II.

For comparisons with spiral nebulae we need the apparent brightness of an area of known *angular* dimensions. Since we are dealing with a luminous surface, this is independent of the distance, for if the distance be doubled, the surface, and hence the amount of light, will be quadrupled; but the increase in light will be exactly compensated by the increase in distance, so that the amount received by the observer remains constant.

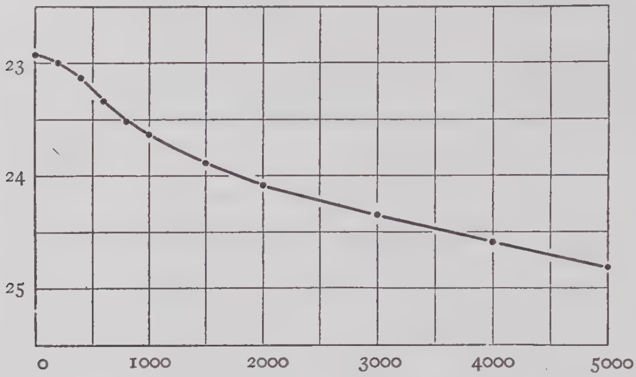

FIG. 1.—Surface brightness of the galactic system as seen from a distant external point in the direction of the galactic pole. Abscissae are distances in parsecs from the center of the system seen in projection; ordinates are the equivalent apparent magnitudes of the light received from an angular area of 1 square second of arc.

As the unit of angular area, we adopt one square second of arc. The required equivalent apparent magnitude is then

$$m = M + 5 \log 206265, \tag{7}$$

where M is the absolute magnitude of the light from one square parsec. The resulting values of m for various distances from the center of the projected system are given in the last line of Table II, and are illustrated in Figure 1.

Assuming the validity of the hypotheses upon which the density and luminosity laws are based—absence of absorption and invariancy of the luminosity law with distance—we may accept these results as reliable to distances of 2000 parsecs or so. Beyond this limit they may require some revision; but in any event it seems clear that the magnitude curve is singularly flat, for in a radial distance of 2000 parsecs the decrease in surface brightness is only slightly in excess of a magnitude. This emphasizes anew the significance of the galactic plane as a structural feature of the system.

As a control upon these results, we may use the alternative method of procedure suggested in the opening paragraph. The surface brightness at the center of the galactic system as seen from an external point bears a simple relation to the quantity of starlight received by an observer on the earth, and this can easily be calculated from the known numbers of stars in successive intervals of apparent magnitude.

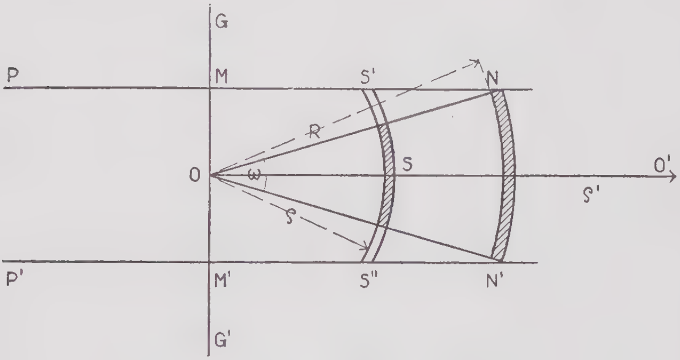

FIG. 2

Let *GG′* (Fig. 2) represent a small portion of the plane of the galaxy, *O* the center of the system, and *OO′* the direction of its pole. The distance, ρ', of the external observer at *O′* is assumed to be large as compared with the dimensions of the system whose limit is at *NN′*.

The light received by *O′* from the circular area *NN′* is that of all the stars in the cylinder *NPP′N′*. If the area of *NN′* be one square parsec, its equivalent magnitudes will be

$$M = 2.5 \log lD; \quad m = M + 5 \log \rho', \tag{8}$$

in which ρ' is the distance of *O′* in parsecs.

An observer at O, on the other hand, receives from an area of the sky defined by the solid angle ω the quantity of light, L', contributed by the stars in the cone NON'. To determine the relation of M and m to M' and m', the equivalent magnitudes of L', consider the thin shell S intercepted by the cone NON'. The volume of S is

$$dV = \omega\rho^2 d\rho,$$

ρ being the radius. If $\Delta(\rho)$ represent the stellar density at the distance ρ, the number of units of standard density in S will be

$$\Delta(\rho)dV = \omega\Delta(\rho)\rho^2 d\rho.$$

Since the light from all the stars in a cubic parsec of unit density, referred to unit distance, is l, the light at O from S is

$$dL' = \frac{l}{\rho^2}\Delta(\rho)dV = \omega l \Delta(\rho)d\rho. \tag{9}$$

This is independent of ρ, differences in distance being compensated by corresponding changes in the volume of the shell.

Thus a shell equal to and occupying the position of NN', and having the same density as S, will contribute the same amount of light as S. But since we are dealing with small values of ω, the shell $S'S''$ intercepted by the cylinder is sensibly equal to the shell NN'. Consequently the observer receives from S, the section intercepted by the cone, the same amount of light as he would receive from $S'S''$ if it occupied the position NN'. The total light at O from all the stars in the cone NON' is therefore the same as would be received from all the stars in the half-cylinder $NMM'N'$ if they were removed to the limit of the system NN' at the distance R.

The equivalent absolute magnitude of L' must therefore equal that of $L/2$, L, as before, being the light received at O' from the entire cylinder $NPP'N'$, reduced to unit distance. For a constant angular area a similar relation holds for the apparent magnitudes m and m'. The percentage error in these relations is of the order of $\sin^2\frac{\alpha}{2}$, where α is the angular aperture of the cone NON', and is altogether negligible.

This result may be verified by integrating (9) to the limit of the system, $\rho = R$, whence

$$L' = \omega l \int_0^R \Delta(\rho) d\rho. \tag{10}$$

The value of the integral, with the approximation indicated above, is $D/2$, where D is the density integral already evaluated; and $\omega = A/R^2$, where $A = 1$ square parsec. Hence

$$m_0' = -2.5 \log L' = -2.5 \log lD + 0.75 + 5 \log R,$$

which is the equivalent apparent magnitude of the light in the cone referred to the distance R. We have, therefore,

$$\left.\begin{aligned} M' &= -2.5 \log lD + 0.75 \\ m' &= M' + 5 \log \rho' \end{aligned}\right\} \tag{11}$$

in which the apparent magnitude has now been referred to the same distance as that occurring in (8). From (8) and (11),

$$M' = M + 0.75, \quad m' = m + 0.75. \tag{12}$$

These relations hold for any direction in space, but it is presupposed that the line of sight passes through the center of the system. For galactic latitude 90°, the first column of Table II gives $m_{90} = 22.93$. This quantity and the value of m' derived from star counts at the galactic pole should satisfy the second relation.

The remaining values of m in Table II cannot be tested directly, but a strong presumption in favor of their reliability would be established should we find relation (12) also to be satisfied for latitude 0°. The density integral gives for the galactic plane $D = 2556$; the corresponding m is 21.22. From the density and luminosity laws we therefore find for a unit area of one square second, $m_0' = 21.97$ and $m_{90}' = 23.68$.

The most reliable star counts at present available are those of Kapteyn, reduced to the normal visual scale by van Rhijn.[1] From these data we derive for latitudes 0° and 90° the numbers of stars for each interval of magnitude, multiply the results by the corresponding relative luminosities, and form the total in the manner followed in the case of the luminosity curve (Table III). The tables of van Rhijn extend only to $m=16$; but, since the fainter stars contribute only a small percentage of the total light received, it is possible to extrapolate the results to $m=19$ without introducing any serious error. The equivalent magnitudes for one square degree are thus found to be

---

[1] *Groningen Publication*, No. 27, Table V, p. 63, 1917.

$$m'_0=4.20 \qquad m'_{90}=5.98. \tag{13}$$

Using a different method of integration, van Rhijn finds 4.15 and 6.00, respectively.[1]

Reducing (13) to unit area and comparing with the results from the density and luminosity laws, we find the *equivalent apparent visual magnitudes of starlight for an area of one square second of arc:*

	Lat. 0°	Lat. 90°	
From density and luminosity laws	21.97	23.68	(14)
From star counts	21.98	23.76	
Difference	−0.01	−0.08	

Considering the uncertainties involved in the various numerical integrations, the agreement is excellent. It not only checks the calculations, in particular the results in Table II, but also shows that the revised density and luminosity laws found by Kapteyn and van Rhijn are in very good agreement with the best data now available.

IV. LIMITING MAGNITUDE OF INSTRUMENT FOR LUMINOUS SURFACES

We must now find values of the surface brightness for representatives of the spiral nebulae. A precise photometric determination is beset with troublesome difficulties; but approximations sufficient for the purpose can easily be obtained by noting the exposure time necessary to produce the first traces of a photographic image. We must know first, however, the limiting magnitude attainable in a given exposure with the instrument used.

---

[1] *Mt. Wilson Contr.*, No. 173, Table XI; *Astrophysical Journal*, **50**, 373, 1919.

For Seed 30 plates and an exposure of one minute with the 60-inch reflector, the limit for stars is from the fifteenth to the sixteenth magnitude, depending on the seeing. Results for point sources, however, cannot be used in the present instance without additional information which is not easily obtained. The limit has therefore been determined with the aid of luminous surfaces of known brightness, using for the purpose extra-focal images, from 2 to 6 mm in diameter, of stars of well-determined magnitude. The influence of seeing is then negligible, and the loss in photographic effect due to intermittent exposure, which always enters in the case of focal images, is avoided altogether, inasmuch as the sensitive film, except at the edge of the image, is constantly illuminated. On the other hand, there is possibly some disturbance arising from the phenomenon noted by Eberhard;[1] but for the very small photographic densities with which we are here concerned, the effect seems to be unimportant.

From several determinations made with plates of the emulsion used in deriving the limiting exposure for most of the nebulae we have:

Equivalent photographic magnitude of one square second of a luminous surface just shown by an exposure of one minute with the 60-inch reflector $= 18.8 \pm 0.3$ (focal ratio 1:5). (15)

Neglecting differences in the absorption losses, this result applies to any telescope whose focal ratio is 1:5. Independent evidence that it is of the right order of magnitude will be given later.

Under good atmospheric conditions the difference in the limits for a point source and for a luminous surface of the area considered is therefore about three magnitudes. The value for surfaces is unexpectedly low and suggests that the intermittency loss is a factor of importance in determining the limiting magnitude for focal images of stars.

In the case of focal exposures to point sources, the optical image is much smaller than the photographic image, the diameter of the first dark ring of the diffraction pattern for the 60-inch reflector being $0''.14$. Owing to atmospheric disturbances, the optical image does not remain fixed in position, but oscillates rapidly, the amplitude of its excursions varying with the degree of the disturbance, so that no point within the boundary of the resulting photographic image is constantly illuminated. Suppose, for example, the area covered by the excursions to be $2''$ in diameter —with good seeing, it is even smaller. If the light of a star of magnitude 15.8 were distributed uniformly over such an area, its equivalent magnitude per square second of arc would be 17.0, which is the *mean* brightness necessary to produce an appreciable photographic effect in one minute under the conditions of intermittent exposure. This is nearly two magnitudes above the limit corresponding to continuous exposure.

---

[1] *Physikalische Zeitschrift*, **13**, 288, 1912.

The difference, for the greater part, is apparently to be ascribed to intermittency loss. A subjective factor may also affect the result, for it is probable that smaller densities can be detected when the deposit covers several millimeters than when it is only 0.1 mm in diameter; this, however, will not affect the comparisons with nebulae whose images are large enough to be comparable with the extra-focal images of stars. In the case of very small nebulae, or of minute details in the larger objects, it may enter to some degree; and here, too, there may be an approach to the conditions that determine the limit for focal images of stars. Very small objects, therefore, may be somewhat brighter than the comparison with the limiting magnitude of luminous surfaces would indicate. Allowance for such an error would only strengthen the conclusion which is to be derived from the comparison of the surface brightness of nebulae with that of the galactic system.

V. SURFACE BRIGHTNESS OF CERTAIN SPIRAL NEBULAE

No great amount of data for the spirals is available at present, but an examination of a few plates of short exposure for such well-known objects as the Andromeda Nebula, N.G.C. 3254, 4254 (M 99), 4565, 4594, 4736, 4826 (M 64), and 5194 (M 51) leads to the conclusion that the surface brightness of the extended nebulosity near the nucleus is between the eighteenth and nineteenth photographic magnitudes. The details are as follows:

The Andromeda nebula.—From a 15^{s} exposure the sharply defined but irregular nucleus is estimated to be of the eleventh magnitude. This exposure shows distinct traces of attendant nebulosity. An exposure of 2^{m} reveals nebulosity covering an area about $2'$ in diameter.

N.G.C. 3254.—The nucleus, which is very diffuse, is discernible on a plate of 30^{s} exposure, and in 1^{m} is well shown, with attendant nebulosity. The inclination of the plane to the line of sight is probably 10° or 15°.

N.G.C. 4254 (M 99).—The diffuse nucleus appears in 30^{s}. The nebulous mass $2'$ *Nf* is well shown in 1^{m}; also one or two nebulous spots closer in. In 2^{m} the whorls are beginning to be outlined.

N.G.C. 4565 (H V 24).—The very diffuse nucleus is clearly shown in 1^{m}. An exposure of 2^{m} extends the nebulosity to a distance of $30''$. The nebula is seen edge-on.

N.G.C. 4594.—Also seen edge-on. The very diffuse nucleus is too bright on a plate of 1^{m} exposure for an estimate of its magnitude. This exposure shows nebulosity on both sides of the "absorption" band, extending, on the brighter side, to a distance of nearly $2'$ from the nucleus.

N.G.C. 4736.—From a 5^{m} exposure it is evident that 1^{m} would show nebulosity near the nucleus.

N.G.C. 4826 (M 64).—An exposure of 16^{s} shows the nucleus as a nebulous star; 32^{s} reveals nebulosity covering an area $10''$ in diameter. The ring $0'.9 \times 1'.5$ is easily traced on a plate of 64^{s} exposure.

N.G.C. 5194 (M 51).—Five minutes is sufficient to outline the arms throughout their length. The central part and the nebulous mass *Sp* are surprisingly strong. An exposure of 1^{m} would certainly show the brighter portions of the nebula.

These nebulae are among the largest and brightest of the spirals; but there are many others whose brighter parts seem to be comparable with those mentioned. Thus the photographs by Curtis, *Publications of the Lick Observatory*, **13**, Plates IV, V, and VI, especially Figures 38–69, suggest a striking similarity in the brightness of the more conspicuous portions of these objects. The reproductions are from exposures ranging from approximately 1^h to 3^h. N.G.C. 4826, mentioned above, is among them (Fig. 54); and, aside from difference in size, is no more conspicuous than many of the others. The very small nebulae found in such numbers in the high galactic latitudes are doubtless fainter than the limit given above, although the difference is probably less than would be inferred from the long exposures necessary to record them; for many of them are so small that they must be compared with stars rather than with surfaces of appreciable extent.

Bearing in mind that the color-index of the central part of a spiral is of the order of 0.8 magnitude, it thus appears that the light of the brightest of these objects corresponds to an equivalent *visual* magnitude of from 17 to 18 per square second of arc; and that many of them are certainly brighter than the nineteenth visual magnitude.

VI. GENERAL REMARKS. CONTROL OF LIMITING MAGNITUDE FOR SURFACES

Certain questions are immediately raised by the values of the surface brightness given above, both for the spirals and for the galactic system. Thus for the Andromeda nebula we find a magnitude of 18, photographic, or possibly 17.5, visual, at a distance of 1′ from the nucleus; and yet the object is easily visible to the unaided eye. The two results are not inconsistent, for it should be remembered that the value of the surface brightness refers to an area of 1 square second of arc.

The resolution limit of the eye may be placed at 2′, which implies that the retinal image of a star has an effective angular diameter of this amount. Further, so far as the visual sensation is concerned, the result seems to be much the same whether the light of the source is concentrated in a point or whether it is distributed uniformly over a disk 2′ in diameter. Referred to this unit of area, the equivalent visual magnitude of the central part of the Andromeda nebula is about 7.0. An adjacent zone 2′ or 3′ in width is not greatly inferior in brightness to the nebulosity near the nucleus, and, remembering the influence of the size of an object upon its visibility, it appears that the observed surface brightness is quite compatible with the fact that the nebula is readily seen with the unaided eye.

Again, we easily see the star clouds of the Milky Way, a circumstance that at first seems irreconcilable with the results given in (14) for the equivalent brightness of star-light in galactic latitude 0°. Referred to an area 2′ in diameter this value becomes $m_0 = 12$. In other words, twelfth-magnitude stars distributed uniformly, at intervals of 2′, would appear as a luminous surface of approximately the same brightness as the average star-light in the Milky Way. The extent of the surface is here the determining factor. An isolated area 2′ in diameter of the brightness of the Milky Way could not be differentiated from the background of the sky, although a larger area of the same brightness would be visible. For stimuli near the threshold of visual sensation, the total energy of the stimulus is more important in fixing the limit of perception than the intensity per unit area of the retina.

Experiments by Russell[1] show that a fully rested eye, shielded from all extraneous light, is capable of perceiving luminous surfaces a degree in diameter when the equivalent brightness per 2′ area is as low as the sixteenth magnitude. In the open, under ordinary conditions of sky illumination, the limit is about 2.5 magnitudes brighter. In other words, the eye should distinguish from the average sky background a luminous area a degree in diameter whose brightness, in excess of the normal sky light, is of magnitude 13.5 per 2′ area. This is 1.5 magnitudes fainter than the calculated mean starlight in the Milky Way. The results above are therefore in no wise inconsistent with the ability of the eye to perceive faint sources of light. Moreover, the value in (14) is of the same order as that derived from the measures of the brightness of the sky by Yntema and by van Rhijn.[2]

Finally, since the estimates of the brightness of the spirals depend directly upon the limiting magnitude of surfaces that can be photographed in one minute, it is important that the value given in (15) be controlled. This has been done by means of photographs of the galactic clouds near Messier 8, placed at my

[1] *Astrophysical Journal*, **45**, 60, 1917.

[2] *Mt. Wilson Contr.*, No. 173, p. 18; *Astrophysical Journal*, **50**, 373, 1919.

disposal by Mr. Hubble. The exposures were made with an Ic Tessar of 6.5 inches focus, ratio 1:4.5, and a Voigtlander doublet of 16 inches focus, ratio 1:4. The limiting exposure that just outlines the clouds is 10^m for the former objective, and 7^m for the latter.

Since a 10-fold increase in the exposure corresponds to a gain of 2 in the limiting magnitude, we find in each case, starting from (15) and allowing for differences in the focal ratios, 21.0 as the photographic magnitude of the brightest parts of the clouds. To reduce to visual magnitude for comparison with the result from star counts, we must subtract the mean color-index. For this we have no exact data; but its value seems to be less than would be inferred from Fath's determination of the spectrum of the Milky Way.[1] Van Rhijn's recent investigation[2] of the brightness of the sky shows that the zodiacal light extends over the entire sky. Its intensity in the regions photographed by Fath seems to have been comparable with the starlight itself, and it is possible that the characteristic solar lines which appeared in his integrated spectrum may have been largely due to this source. Photographs by the method of exposure ratios, and direct determinations of color-indices by Shapley[3] show that there are many faint blue stars in the galactic clouds; and it seems unlikely that the mean color-index for these regions is in excess of 0.4 magnitude. This value is an estimate, but the error involved cannot be serious.

Another correction must also be taken into account, namely, the greater brightness of the sky background in the region photographed by Hubble as compared with that in the vicinity of the stars whose extra-focal images were used to derive the value in (15). This arises partly from difference in the zodiacal light and partly from a source of illumination, probably auroral in origin, whose intensity increases with the zenith distance. The influence of these factors, which has been determined with the aid of van Rhijn's tables,[1] very nearly compensates the effect of the color-index, and we therefore adopt magnitude 21 for the visual brightness of the starlight in the galactic clouds which were photographed. The mean magnitude for latitude 0° found from star counts is 22. Counts for the particular region in question are not available, but from the fluctuations in the numbers of stars in other regions along the Milky Way it is clear that the excess of density in the vicinity of Messier 8 will account for most, if not all, of the remaining difference of one magnitude. This affords an independent check on the limiting brightness for luminous surfaces given in (15). The comparison is rough, but sufficient to confirm the previous result.

---

[1] *Mt. Wilson Contr.*, No. 63; *Astrophysical Journal*, **36**, 362, 1912. Slipher, *Publications of the American Astronomical Society*, 23d meeting, 1919, finds for the Milky Way a composite spectrum—solar type with abnormally strong hydrogen lines, which harmonizes with the suggestion presented here, namely, that the zodiacal light plays an important part in contributing the solar characteristics to the spectrum.

[2] *Mt. Wilson Contr.*, No. 173; *Astrophysical Journal*, **50**, 356, 1919.

[3] *Mt. Wilson Contr.*, No. 133; *Astrophysical Journal*, **46**, 64, 1917.

VII. COMPARISON OF NEBULAE WITH THE GALACTIC SYSTEM

In selecting nebulae for the comparison, preference has been given to those whose planes are nearly perpendicular to the line of sight in order that their magnitudes might be comparable with the brightness of the galactic system as seen from the distant external point on the axis of the system. The surface brightness of the latter at the center of figure we have found to be of the twenty-third magnitude (Table II).

The difference is therefore from 4 to 6 magnitudes. Had the comparison been with the nuclei of spirals, this difference would have been increased by two or more magnitudes; but leaving the nuclei out of consideration, we are led to the result that the surface brightness of many of the spirals is of the order of one hundred times that of the galactic system. The conclusions to be drawn from this result can be stated only as alternatives, and, unfortunately, settle nothing as to the constitution or size of the spirals.

If we suppose the spirals to consist wholly or mainly of extended nebulosity, the supposition in itself admits a structural dissimilarity, as compared with the galactic system, that may cover any sort of observed difference.

On the other hand, suppose the spirals to consist of collections of stars, isolated in space at such distances that they present more or less continuous, luminous surfaces. From a consideration of the quantities of light, l_S and l_G, received from unit angular areas of the surface of a spiral and of the galactic system, we then find

---

[1] *Loc. cit.*

$$\frac{\delta_S}{\delta_G}=I\frac{T_G}{T_S}, \tag{16}$$

in which T_S and T_G are the thicknesses of the two systems measured along their polar axes, δ_S and δ_G, their mean stellar densities along the same axes, and I the ratio of intensities l_S/l_G.

Equation (16) is a relation between mean density, linear dimensions, and the intensity ratio I. If the dimensions of the spirals and the galactic system are of the same order,

$$\delta_S=I\delta_G, \tag{17}$$

in which for the brighter spirals I is of the order of 100.

If these objects are smaller than the galactic system, their stellar densities must be even greater, and exceed the value expressed by (17) in the ratio of T_G/T_S. Finally, if we suppose the densities to be the same,

$$T_S=IT_G, \tag{18}$$

which implies that the brighter spirals are very much larger than our system. The brighter spirals, at least, are therefore not directly comparable with the galactic system in the relation of stellar density to linear dimensions.

It is impossible to specify the percentage of the entire class of spirals to which this conclusion would apply, for we do not know at all accurately the total number within the reach of existing telescopes, and still less the number too faint to be thus revealed. We can say, however, that the value of I appearing in the formulae above is probably greater than unity for every known spiral. The value $I=1$ would imply the existence of spirals with a surface brightness as low as the twenty-third magnitude, visual, or perhaps 23.8, photographic. An object of this brightness, if large enough to escape the photographic intermittency loss, would be just shown with the exposure time which faintly registers stars of the twenty-first photographic magnitude. With fast plates and good conditions this is approximately eight or ten hours, which is near the maximum practicable limit. But the faintest spirals are apparently so small that the loss due to intermittency almost certainly comes into operation, with the result that the surface brightness of all these objects is probably greater than that of the galactic system; whence, for the known spirals, $I > 1$.

The alternative possibilities expressed by (17) and (18), which follow directly enough from the hypothesis of stellar constitution for the spirals, are therefore such that they place our own system at the end, if not actually outside, the series of known spirals when arranged according to one or the other of the two characteristics, density and linear dimensions. At the other end we find the extreme instances indicated by the formulae when we substitute for I a quantity of the order of 100.

Mount Wilson Observatory
July 1920

Contributions from the Mount Wilson Observatory, No. 192
Reprinted from the *Astrophysical Journal*, Vol. LII, pp. 183–186, 1920

MAGNITUDES OF FAINT COMPARISON STARS FOR NOVA PERSEI, NO. 2

By FREDERICK H. SEARES

ABSTRACT

Magnitudes of 36 faint comparison stars for Nova Persei No. 2 were determined by comparison with the Mount Wilson Standards at the North Pole.

Mount Wilson scale of photo-visual magnitudes compared with Barnard's visual scale gives values uniformly 0.8 magnitude larger for the range 12 to 15 magnitudes.

Brightness and color of Nova Persei No. 2 were determined on five dates during 1917–1918.

Photographic and photo-visual magnitudes of the faint comparison stars near Nova Persei, No. 2, which are included in the lists of Hagen,[1] Barnard,[2] and Aitken[3] have been determined by comparison with the Mount Wilson Standards at the North Pole.

TABLE I

OBSERVATIONS

Date	Plate		Exposure	H. A.	Seeing	Extinction
	Number	Brand				
1917 Sept. 22	4020....	Seed 27	2^{m}	50°E	3	$+0^{M}.16$
22	4021....	Iso+C	3	50 E	3	+0.08
1917 Oct. 22	4125....	Iso+C	10	45 E	4	+0.09
22	4126....	Seed 27	8	46 E	4	+0.18
1918 Nov. 7	4778....	Iso+C	10	48 E	3	+0.08
7	4779....	Seed 27	5	38 E	3	+0.20
8	4789....	Seed 27	5	52 E	4	+0.15
8	4790....	Iso+C	10	42 E	4	+0.09
9	4802....	Iso+C	10	56 E	3	+0.06
9	4803....	Seed 30	2	48 E	3	+0.17

Five pairs of photographs were made with the 60-inch reflector as indicated in Table I. The Iso plates (Cramer, Instantaneous) were exposed behind yellow filter C. With the exception of those of the first pair, which received an additional exposure on the Pole, each plate was given three equal exposures in the order: Nova, Pole, Nova.

---

[1] *Astrophysical Journal*, **13**, 233, 1901.

[2] *Astronomische Nachrichten*, **159**, 49, 1902; *Monthly Notices*, **80**, 710, 1920.

[3] *Lick Observatory Bulletin*, No. 8, 1901.

The photographs were measured by Miss Joyner and Miss Richmond in the usual manner. The scale-readings on the Polar Standards were plotted against their adopted magnitudes,[1] and from the resulting curves were read the magnitudes of the comparison stars with the scale-reading as argument. The results were corrected for atmospheric extinction by the quantities in the last column of Table I, which reduce the magnitudes to the zenith.

TABLE II

MAGNITUDES AND RESIDUALS

DESIGNATION			MEAN MAGNITUDES		COLOR-INDEX	RESIDUALS									
Hagen	Barnard	Aitken	Pg.	Pv.		Photographic					Photo-visual				
34	....	......	....	10.63	....	....	....	....	....	....	0	....	....	....	....
42	....	......	....	10.75	....	....	....	....	....	....	0	....	....	....	....
44	....	......	11.96	11.78	+0.18	0	....	....	....	....	+4	−4	....	....	....
48	....	......	13.12	12.47	+0.65	+35	−24	−15	(+67)	+2	+18	−39	+4	+8	+11
49	15	......	13.20	12.32	+0.88	−10	−8	+20	+7	−9	−8	−9	+29	−4	−8
54	....	......	13.24	12.69	+0.55	−10	−4	+12	+7	−5	+9	−13	+26	−9	−12
56	14	*o*	13.37	12.64	+0.73	−2	−24	+16	+24	−16	+1	−7	+12	−8	+2
57	....	......	16.22	15.50	+0.72	+22	+11	−28	+10	−13	....	−9	....	+10	....
58	....	......	13.55	12.72	+0.83	−8	−16	+14	+18	−9	+4	−18	+20	−6	+1
64	....	......	13.96	12.64	+1.32	+33	−28	−4	−20	+17	−4	−12	−4	−8	+30
65	....	......	14.23	12.80	+1.43	+21	−33	−2	+7	+8	+7	−19	−3	+2	+15
66	....	......	13.87	12.86	+1.01	+18	−27	−7	+10	+8	−8	−11	+3	+4	+13
68	....	......	13.61	12.82	+0.79	+24	−34	−2	+17	−3	0	−8	+8	−12	+13
71	....	......	14.62	13.30	+1.32	−19	(−62)	−1	+11	+8	−4	−12	+8	−3	+13
73	....	......	14.19	13.32	+0.87	−14	+5	−3	+9	+4	−7	+20	+4	−11	−8
74	16	......	14.07	13.20	+0.87	+40	−33	−18	+11	−1	−8	+12	−2	−9	+6
75	....	......	14.99	13.21	+1.78	+6	−29	+7	+14	0	−7	−21	+11	+6	+10
76	....	......	14.70	13.36	+1.34	−13	(−54)	−3	+16	−1	−6	−1	−2	+16	−6
77	8	*i*	14.24	13.16	+1.08	+22	−26	−14	+22	−5	−6	−10	0	−17	+31
78	11	*l*	14.44	13.60	+0.84	−7	−6	+2	+22	−10	−11	+5	−3	−15	+24
79	10	*k*	14.57	13.47	+1.10	−9	−31	+12	+28	−2	−16	+7	−3	+8	+5
80	....	......	16.94	15.95	+0.99	....	+22	−24	−1	+3	....	+14	....	+4	−19
81	2	*b*	15.57	14.53	+1.04	−35	−3	+13	+12	+15	....	+19	−9	−6	−4
....	1	......	16.44	15.19	+1.25	−5	+22	−31	+16	−1	....	+22	+3	−4	−21
....	3	*c*	14.42	13.67	+0.75	+2	−21	−6	+13	+13	−9	+10	−5	−10	+16
....	4	*e*	15.62	15.01	+0.61	−18	−1	+5	+6	+7	....	+27	−19	+15	−23
....	5	*f*	14.50	13.68	+0.82	−9	−13	−9	+28	+5	+1	+19	−4	−15	−1
....	6	*g*	15.72	14.74	+0.98	−8	−4	−7	+9	+10	....	+20	−19	+4	−5
....	7	*h*	15.20	14.38	+0.82	−9	−22	+6	+14	+9	....	+7	−3	+1	−6
....	9	*j*	15.61	13.94	+1.67	−14	−4	−2	+16	+6	+18	+4	+4	−23	−1
....	12	*m*	15.35	14.22	+1.13	−31	−4	+17	+6	+14	(+55)	+14	−15	−3	+2
....	13	*n*	15.61	14.20	+1.41	−22	+15	+1	−2	+6	+38	+16	−33	−12	−7
....	17	......	14.71	13.82	+0.89	−16	−13	+1	+20	+9	+6	+14	−8	−11	−2
....	18	......	14.51	13.94	+0.57	−8	−8	+3	+8	+4	....	+23	−18	−2	−1
....	20	*a*	16.86	15.88	+0.98	....	+18	−20	+5	−2	....	+4	....	−3	....
....	....	*d*	16.23	15.62	+0.61	−13	+15	−1	−2	0	....	(+44)	−13	+12	(−44)
Systematic Difference						−2	−10	−2	+11	+2	+1	+2	−1	−3	+2

The collected results are in Table II. The first three columns give the designation in the lists of Hagen, Barnard, and Aitken, respectively. The fourth and fifth columns contain the mean photographic and photo-visual magnitudes, and the sixth the color-indices. The remaining columns give the residuals for the separate plates in hundredths of a magnitude. Six of these exceed the rejection limit of 0.4 magnitude, and the corresponding magnitudes were accordingly omitted in forming the means; their residuals, referred to the adopted means, are inclosed in parentheses. The systematic differences at the bottom of the table are the deviations of the zero-points of the individual plates from the adopted mean zero-point.

---

[1] *Mt. Wilson Contr.*, No. 97; *Astrophysical Journal*, **41**, 206, 1915.

TABLE III

COMPARISON OF BARNARD VISUAL WITH MOUNT WILSON PHOTO-VISUAL MAGNITUDES

Barnard Number	MW Pv. Magnitude	MW Pv. *minus* Barnard Visual	Corrected Difference
1	15.19	+0.69	$-0\overset{\mathrm{M}}{.}11$
2	14.53	.82	+0.02
3	13.67	0.81	+0.01
4	15.01	(1.64)	(+0.84)
5	13.68	0.78	−0.02
6	14.74	1.11	+0.31
7	14.38	.79	−0.01
8	13.16	.95	+0.15
9	13.94	.67	−0.13
10	13.47	.79	−0.01
11	13.60	.80	0.00
12	14.22	.78	−0.02
13	14.20	.70	−0.10
14	12.64	.69	−0.11
15	12.32	.77	−0.03
16	13.20	0.81	+0.01
17	13.82	1.00	+0.20
18	13.94	+0.80	0.00
Mean		+0.80	

The observations—of the photo-visual magnitudes at least—were undertaken at the request of Professor Barnard, as a basis for comparison with his visual measures, which he has kindly placed at my disposal. The large values of MW—Barnard (Table III) arise from the difference of 0.80 magnitude in the zero-points. Allowing for this, we find the differences given in the fourth column. These show no dependence upon magnitude, whence it follows that Professor Barnard's visual scale and the Mount Wilson photo-visual scales are parallel.

The color-indices of most of the stars lie between 0.7 and 1.2 magnitudes. Nevertheless, the range is sufficient to show that the relative color equation of the two series of measures is at least small. The photo-visual magnitudes are therefore directly comparable with the visual measures.

TABLE IV

Brightness and Color of Nova Persei, No. 2

Date	Pg. Mag.	Pv. Mag.	Color-Index
1917 Sept. 22	13.79	13.28	$+0^{\mathrm{M}}.51$
Oct. 22	14.40	13.55	0.85
1918 Nov. 7	13.44	13.16	0.28
8	13.81	13.39	0.42
9	13.45	12.78	+0.67

The differences for Nos. 4 and 6 are the only serious discordances, and suggest that the stars may be variable. In forming the zero-point difference used in Table III, No. 4 has been excluded, and No. 6 has been given reduced weight.

The brightness and color of the Nova derived from the five pairs of plates are as indicated in Table IV.

Only three of the stars in the Harvard list[1] fall within the limits of this investigation. A comparison with Wendell's results gives

Hagen No.	Wendell's Desig.	MW Pv.—Wendell	No. MW Obsns.
34	*c*	+0.06	1
42	*d*	−0.28	1
49	*f*	+0.09	5

---

[1] *Harvard Circular*, No. 66, 1902.

Mount Wilson Observatory
July 1920

Contributions from the Mount Wilson Observatory, No. 193
Reprinted from the *Astrophysical Journal*, Vol. LII, pp. 187–197, 1920

EXPERIMENTS ON THE POSSIBLE INFLUENCE OF POTENTIAL DIFFERENCE ON THE RADIATION OF THE TUBE RESISTANCE FURNACE

By ARTHUR S. KING

ABSTRACT

Radiation from the tube resistance furnace.—(1) *Effect of a small potential gradient.* To determine whether, as Hemsalech asserts, the currents through the ionized vapor, produced by a potential gradient of 1 or 2 volts per centimeter along the heating tube, were responsible for the emission of some of the furnace lines, a series of experiments was performed in which four different methods were used to reduce or eliminate the potential gradient acting on the vapor. In every case the relative intensity of the lines was found the same as with the higher potential gradient, for the same temperature. No evidence of the alleged low-voltage arc spectrum superposed upon the furnace spectrum was found. (2) *Origin of the radiation.* This result confirms the author's contention that whatever reactions between atoms or ions may cause the radiation, these reactions are caused and controlled by the high temperature alone, each temperature giving a definite spectrum. (3) The "*red fringe*" observed by Hemsalech is probably a chemical phenomenon, similar to a flame. It may be obtained when no potential difference is acting on the vapor.

When a substance is vaporized in a graphite tube by the passage of an electric current through the material of the tube or by any other method that will give sufficiently high temperature, it must be conceded that the high thermal condition may be accompanied by chemical actions and by effects resulting from the strongly ionized state known to exist near a hot surface. It has been maintained by the writer that, as the chemical and ionization conditions are caused by the high temperature and their intensities are controlled by it, the observed changes in the spectrum can properly be regarded as resulting from the variations of the temperature.

While, in the studies of metallic spectra thus far carried out, the furnace was usually operated according to a fixed procedure, many experiments have been made as to the effects of other methods of handling. Thus, with air present in the furnace chamber, the pressure has been varied from a few millimeters to over

20 atmospheres. Carbon dioxide, oxygen, nitrogen, and hydrogen have also been used at pressures up to at least one atmosphere. The numerous changes in chemical action which must have resulted have failed to show anything that could be regarded as a real change in relative intensity of metallic lines when a given temperature was employed. The different distributions of vapor in an oxidizing atmosphere cause wider reversals of sensitive lines, and the general intensity of the spectrum, as measured by exposure times, may be greatly altered. Substances such as iron, which form carbides, show a more vigorous combination with the tube material when the furnace contains air at atmospheric pressure than when operated in a partial vacuum, and the intensity of the iron spectrum, as a whole, is increased. In all these cases, however, a certain temperature gives a definite set of lines, and, allowing for reversals, these lines show practically the same relative intensities.

When a potential difference is maintained between the ends of the tube, the presence of ionized vapor within the tube gives opportunity for the conduction of a certain fraction of the current by the metallic and carbon vapors. The potentials employed in my experiments, as measured by an alternating-current voltmeter, have ranged from less than 1 volt to about 2 volts per centimeter of the length of the tube. As the temperature is raised, the increased potential-drop, greater ionization, and higher resistance of the graphite tube will combine to give more current through the vapor. The possibility of such currents through the vapor is thus evident. Whether, under the usual conditions of operating the furnace, these currents have any effect in exciting the emission of lines not produced at the same temperature when there is no current in the tube is another matter, and it is for the purpose of testing this question that the following experiments were undertaken.

In his recent papers[1] Dr. G. A. Hemsalech asserts that a large class of lines requires, before they are emitted, the presence in the furnace tube of a low-tension arc, such as would result from the passage of a considerable current through the vapor. These are

[1] *Philosophical Magazine*, **36**, 209, 281, 1918; **39**, 241, 1920.

lines which I have found to be faint or absent at furnace temperatures which produce another large class, the low-temperature lines; but the lines first named rapidly gain intensity at higher temperatures. The question is whether at these higher temperatures the conductivity of the vapor in the tube has become so great that the radiation of a low-tension arc is superposed on that of the furnace. In a paper[1] published after the appearance of the second article by Dr. Hemsalech, I showed that the lines which he had not observed until his furnace reached a temperature of about 2500° C. were obtainable with temperatures as low as 1800° and were distinct at 2000°, for which Dr. Hemsalech did not suspect a disturbing conductivity of the vapor.

In his last paper, Dr. Hemsalech attempts to account for the discordance between his results and mine on the ground that the potential-drop per cm which I used to produce a temperature of 1800° was about the same as that for which he obtained 2500°. This he attributes to my use of an unprotected tube in a vacuum chamber and of an alternating voltage which has high momentary values, whereas he has used a jacketed tube with direct current. Further, by passing a current through a thin graphite plate, he found that, when this was heated to a high temperature, a red glow appeared on the under side of the plate. This glow was sharply defined and was found to be deflected by a magnetic field in a direction which indicated that a part of the heating current passed through the vapor adjacent to the plate. The "red fringe" thus produced gave a spectrum consisting of carbon flutings and lines of titanium and vanadium, elements regularly found in the Acheson graphite. These flutings and metallic lines showed a sharp falling off in intensity at the limit of the "red fringe," and this fact, together with the deflection of the fringe by a magnetic field, led Dr. Hemsalech to consider that when they occur in a tube furnace (which can be regarded as a rolled-up plate), they are due to a passage of the current through the vapor within the tube.

These two points, the relatively large potential-drop which I used in producing the test lines of iron at low temperature, and the apparent electrical nature of the "red fringe," are the outstanding features of Dr. Hemsalech's argument that the tube furnace is to some extent a low-tension arc.

---

[1] *Mt. Wilson Contr.*, No. 162; *Astrophysical Journal*, **49**, 48, 1919.

The "red fringe," the color of which is due to a band spectrum, is, I believe, mainly a chemical phenomenon which I shall show later occurs near heated carbon when no current is being carried by it. The sharp boundary of the fringe is difficult to account for on electrical grounds, but would seem to be readily explained by the sudden cessation of a chemical reaction, corresponding to the production of the sharply defined envelopes of flames. The well-known deflection of ionized vapors in flames would lead one to expect the effect of the magnetic field which Dr. Hemsalech observed. The evidence from the direction of the deflection that the ions were carrying part of the heating current would have been more complete if the current had been reversed, while the direction of the field remained the same. The temperature of the fringe vapor must have been much below the measured temperature of the graphite plate, on account of the strong gradient inevitable at the exposed surface. The "red fringe" is, I believe, the same as the red glow which appears regularly in the tube furnace at temperatures well below 2000° C. when a fresh tube is first heated. It fades after a short time, with the temperature unchanged. I have always ascribed it to a transient condition while some impurities of the graphite are being burned out.

That certain lines appear in a mass of ionized vapor through which a fraction of the heating current may be passing, clearly does not justify the conclusion that these lines require the current for their production. Experiments are needed in which, with the vapor heated to about the same temperature, the possibility of a current is reduced or eliminated. Such experiments, which I have carried out by four different methods, will now be described. Three of these methods involved different arrangements of the tube furnace, while in the fourth the tube was heated by an external arc.

1. *The use of direct current with protected tube, and comparison of direct and alternating currents with unprotected tube.*—A large direct-current generator, just installed, made it possible to use with the furnace heavy currents which have been available hitherto only with transformer voltage. In order to retain the heat and thus

permit the use of lower potentials, the tube was jacketed with a protecting tube of graphite and outside of this with cakes of partially fused carborundum. In the earlier experiments with this furnace,[1] a protecting jacket of this kind was used. It has the disadvantage that the temperature gradually rises during a considerable interval while the jacket is being heated, and with the alternating current, no method is available for changing the voltage by small steps to counteract this increase. For the regular examination of spectra at different temperatures, where constancy during the exposure is a prime requisite, the tube was left unprotected inside the vacuum chamber. This arrangement, as Dr. Hemsalech has noted, requires relatively high potentials to give the desired temperatures, and the peak voltage during each alternation produces momentary values of the electric field higher than those given by direct current for the same tube temperature. The possible effect of this was easily tested by using a protected tube, with current from the new generator, the adjustment of whose field permits a fine variation of the voltage to allow for heating of the jacket. Temperature measurements were made at the center of the inner wall of the tube by means of a Leeds and Northrup pyrometer of the Morse type, whose readings yield the same temperatures as the less convenient Wanner pyrometer previously used. The potential-drop was measured across the electrode pipes outside the furnace chamber and included not only that over the tube but also across six contacts within the chamber, whose resistance was not negligible.

Photographs of the iron spectrum were made with the furnace at 1950° and 1800° C. For the latter temperature, the voltage, after the jacket was fully heated, remained steady at 12 volts, or 0.6 volt per cm of the tube, neglecting the contact resistances. Allowing for the probable drop over these, it is likely that not more than 10 volts, or 0.5 volt per cm, were involved in the production of the spectrum observed. In this spectrum, all of the strong iron lines of the λ 4900 group were distinctly though faintly registered. These are the test lines which Dr. Hemsalech maintains do not appear in the tube furnace with direct current below 2500°, at which temperature the potential-drop per cm in his experiments was about twice that used here. The rest of the spectrum at 1800° was the regular low-temperature spectrum, with the lines of Classes I and II strong and those of Class III, to which the group near λ 4900 belongs, beginning to develop. For instance, the strong arc line λ 4260 of Class III was less than one-fifth as strong as the adjacent λ 4258 of Class IA, a relation which can be reversed at higher temperatures. The prominent impurity lines of titanium and vanadium were strong, and the "cyanogen" band at λ 3883 was well developed. It has been shown in previous experiments that this band and those of the carbon spectrum are much stronger in air at atmospheric pressure than in the partial vacuum used in these experiments. The spectrum at 1950° differed from that at 1800° chiefly in the rapid strengthening of the lines of Class III, λ 4260 now being only slightly weaker than λ 4258.

---

[1] *Mt. Wilson Contr.*, Nos. 28, 32; *Astrophysical Journal*, **28**, 300, 389, 1908.

Experiments were next made with the usual unprotected tube, charged with iron filings, a photograph being taken at a certain temperature with alternating current, followed by one with direct current adjusted to give the same pyrometer reading. Pairs of spectrograms were thus made for temperatures of 1750°, 1800°, and 2200°. Slightly higher voltages were of course required than in the case of the protected tube. The spectra at a given temperature were practically identical, the same lines being present, with the same relative intensities, whether alternating or direct current was used.

These experiments serve to establish the emission of lines of Class III, such as those of iron near λ 4900, with a very low potential-drop given by direct current, and at the temperatures at which I have regularly observed them with the furnace excited in the usual manner. That Dr. Hemsalech did not observe these lines in his tube furnace resulted, I believe, simply from the faintness which must be expected in the case of lines of Class III. Visual observations cannot be expected to show them, especially with low dispersion, until they have attained the brightness associated with a higher temperature. They may also be lost on a photographic plate having decided contrast, unless it be given long exposure, though the low-temperature lines may be quite distinct.

With a softer plate, and exposure sufficient to produce a strong general intensity, however, the lines of Class III appear distinctly without over-exposure of the rest of the spectrum.

2. *The furnace with insulated inner tube.*—This method and the one following were employed for the purpose of reducing or excluding any action on the vapor by the potential-drop usually present between the ends of the furnace tube. A double tube was arranged as in Figure 1, consisting of a tube of 6.25-mm bore, inside of the regular 12.5-mm tube which carried the current. The inner tube was turned down to give a clearance of about 1 mm between it and the outer tube, and was insulated from the latter by short pieces of quartz tubing at the ends, which were kept cool by the contact blocks. The inner tube, which contained the iron vapor, should have conducted much of the current which otherwise would have passed through the vapor, thus largely avoiding the conditions of a low-tension arc. The ammeter gave no indication of an increase of current resulting from the low-resistance inner tube, and when alternating current was used on the tube at temperatures of 1700° and 2000° C. the spectra were quite the same as for the single tube at the same temperatures. The experiments were carried out both in a partial vacuum and at atmospheric pressure.

FIG. 1.—Arrangement of insulated inner tube

3. *Spectrum photographed with no current in tube.*—The furnace tube, when well protected by an inclosing jacket, cools so slowly that its spectrum fades only gradually when the current is broken. This persistence of the stronger low-temperature lines, which frequently remain visible for several minutes, has often been noted. The photography of this spectrum after the current had ceased was now undertaken.

A jacket was used about the tube similar to that described in the experiments with direct current, and the furnace was excited to a temperature of 2350° C., the window toward the spectrograph being covered by a shutter. The transformer switch was opened and the same hand was then used to open the shutter, thus insuring an interval of at least half a second after the current was broken before the exposure was started. In fifteen seconds the temperature fell below 1500°; after which the tube was heated as before and again exposed with no current. A total exposure of 30 minutes by this method served to build up a spectrogram of sufficient strength. Without opening the furnace, the spectrum was then photographed with a continuous run at reduced voltage, giving a temperature of about 2100° C. The two spectra were the same with respect to lines present and relative intensities; the test iron lines of Class III were distinct, as were also the lines of titanium and vanadium and the cyanogen bands.

This experiment would seem conclusive as to the possibility of producing, without a potential difference, the lines which Dr. Hemsalech considers require the presence of a low-tension arc. Dr. Hemsalech, has, however, also observed a persistence of the group at λ 4900 after the current had been broken and has compared it with the residual luminescence which he observed in spark spectra[1] when the metallic vapor was blown out of the electric field by an air blast. It seems scarcely permissible to compare this phenomenon of the spark with the present experiment, as the time intervals are of quite a different order. The duration of visibility of iron lines in the spark vapor was about 0.0002 sec. Even a line so easily produced as λ 4227 of calcium lasted but 0.0003 sec. The reader must judge whether the radiation of iron lines of Class III and other test lines during several seconds can be reasonably ascribed to the better protection of the vapor afforded by the furnace tube.

4. *Furnace tube heated by an external arc.*—In this experiment, the furnace tube was in effect a horizontal crucible in which iron was vaporized by a heavy-current arc between horizontal carbon electrodes which were brought together beneath the tube. The arrangement is shown in Figure 2. A is a short graphite tube of 6.25-mm bore and 12.5-mm outside diameter. An alternating-current arc carrying 200–300 amperes was formed between the carbon rods B. These were insulated by carborundum plates C

---

[1] *Comptes Rendus*, **150**, 1743, 1910; **151**, 220, 1910.

from the graphite blocks D which inclosed the tube and the arc. The ends of the furnace tube A were fitted into sections of graphite tube of 19-mm outside diameter which passed through holes in the graphite housing and permitted a view of the interior of the tube. A screen at the end toward the spectrograph excluded from the slit all light except that from the vapor within the tube. After each run the tube was carefully examined to see that no hole had been formed which would permit contamination by vapor from the arc.

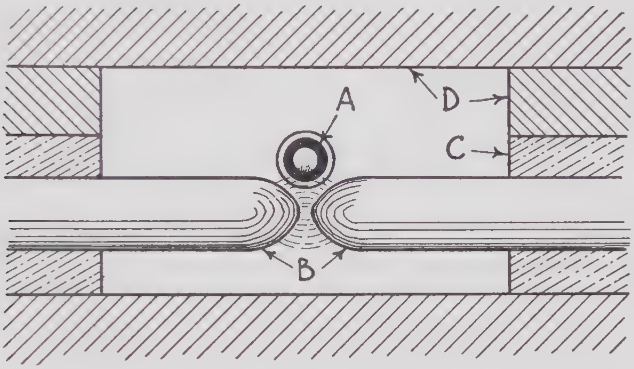

FIG. 2.—Furnace tube (A) heated by external arc (B)

This furnace is not to be recommended for regular work as a substitute for the tube heated by a current, for the shifting of the arc about the ends of the electrodes caused much variation in the heating of the tube. At intervals, however, the tube became hot enough to emit a rich spectrum, which was photographed in the first order of a 1-meter concave grating. The spectra thus obtained showed no essential difference from the numerous spectrograms made with the regular tube furnace at about 2000°. The test lines of interest in this investigation, consisting of the iron lines of Class III near λ 4900, the titanium and vanadium lines given by impurities in the graphite, and the "cyanogen" flutings were all present. The latter were of the strength usual with the tube resistance furnace at atmospheric pressure, and the relative intensities of the metallic lines showed no differences from those given by the resistance furnace.

An interesting feature was the production in the tube of the "red fringe" noted by Dr. Hemsalech near his graphite plate heated by a current. This red glow appeared at the bottom of the tube, next the arc, and occasionally, for short intervals, filled the tube; but usually it extended across about half the diameter, with a sharp boundary above. Above the red glow a yellowish vapor often appeared. The grating photographs, which in the first order show incomplete astigmatism, correspond closely with those taken by Dr. Hemsalech near the hot plate. The low-temperature lines of iron and such impurity lines as λ 4227 of calcium and λ 4607 of strontium, maintain nearly the same intensity across the diameter of the tube; while the iron lines of Class III, the titanium and vanadium lines, and the cyanogen bands are strongest in the portion occupied by the red glow, fading rapidly at its limit. The whole effect seems to me to indicate a chemical condition adjacent to the heated carbon, regulated by the temperature and without any dependence on the passage of a current through the vapor.

It seems a fair conclusion from these experiments that the temperature classification used by the writer for furnace spectra is a sound one, and that any conduction of current by the vapor which may take place at the temperatures on which the classification depends is quite without effect in modifying the spectrum. Instead of accepting Dr. Hemsalech's view that the low-temperature lines are due to a thermo-chemical excitation, and that the high-temperature lines, including those of Class III, require a passage of the current equivalent to a low-tension arc, I believe the experimental evidence indicates that the rôle of chemical action is uncertain, but that it probably acts mainly by affecting the general intensity; and that the effect of such current as may be conducted by the vapor at moderate furnace temperatures is negligible. I have laid stress, as does Dr. Hemsalech, on the lines of Class III, since these are the chief indicators of changing temperature in the furnace; and the object of this investigation has been to show that these lines, which, with the low-temperature lines of Classes I and II, make up the bulk of the furnace spectrum, do not require the passage of a current through the vapor. The lines of Classes IV and V, which are absent or faint at high furnace temperatures, include several varieties between which the furnace does not distinguish. Such lines may be of the diffuse type for which the electrical sources are especially favorable; they may partake of the nature of enhanced lines; or they may be lost in the furnace spectrum through extreme faintness. The question is for the present left open as to how far the effects of higher furnace temperatures, say above 2400° C., may be complicated by conduction of current. For present purposes this is not vital, but would become important if the temperature-range were transferred to a higher level, such as would be needed for the spectrum of tungsten, this metal melting at about 2700° C. when in contact with carbon. An indication is given, however, of the weakness of electrical excitation even at the higher furnace temperatures by the fact that of the enhanced lines of titanium, given in the arc of about the same intensity as the stronger arc lines, only a few are shown as traces in the furnace at 2600° C. The question remains in this case as to whether the high temperature begins to excite these radiations, or whether a weak electrical action causes their emission.

SUMMARY

The material in this paper may be summed up by saying that we have no evidence that so small a potential-drop per cm as that existing in the tube furnace can excite the test lines and bands observed, and that, for the temperatures required to classify the lines of most metallic spectra, the experiments here reported show a definite spectrum for a given temperature when the potential acting on the vapor is reduced, or as far as possible eliminated.

The writer was assisted in this work by Mr. Sinclair Smith, especially in the handling of the arc-heated furnace.

Mount Wilson Observatory
July 1920

Contributions from the Mount Wilson Observatory, No. 194
Reprinted from the *Astrophysical Journal*, Vol. LIII, pp. 161–164, 1921

INTENSITY DIFFERENCES IN FURNACE AND ARC AMONG THE COMPONENT SERIES IN BAND SPECTRA

By ARTHUR S. KING

ABSTRACT

Intensity differences between band spectra emitted by electric furnace and by arc.—Large-scale photographs of the "*cyanogen*" *band at* λ *3883*, made in the third order of a 30-foot spectrograph, showed that the A_1 series of lines is enhanced over the A_2 series so as to become the dominant series (Plate XX). Also some new faint doublets appeared. The two series, then, seem not to belong to the same temperature class, and may be expected to be differently affected by pressure, etc. The "*cyanogen*" *band at* λ *4216* also showed similar changes. In the *Swan band* λ *5165* the triplet series is enhanced in the furnace spectrum with reference to the adjacent doublet series.

In spectrograms of moderate dispersion in which the spectrum of the electric furnace was photographed with comparison arc spectra, it was noted that the "cyanogen" band λ 3883, which frequently appeared, showed an apparent difference in structure, the component lines seeming to be more numerous in the furnace when the general intensity was about the same for both sources. Closer examination showed this to be due to an intensification in the furnace of band lines which are present but relatively faint in the arc.

Since the phenomenon indicated a variability among band lines similar to that generally observed for line spectra given by arc and furnace, the nature of the difference was investigated with higher dispersion, the third order of the 30-foot plane-grating spectrograph being used. As this band is emitted more strongly at atmospheric pressure than in the vacuum furnace, and as it was desirable furthermore to avoid differences of pressure, a new furnace built to stand long exposures at high temperatures was employed. In this, the graphite tube is supported in large bronze holders, cast hollow for water-cooling, with graphite bushings around the ends of the tube. The heated portion of the tube is protected merely by a cast-iron water jacket which retards the wasting away of the tube by preventing active circulation of air. Large-scale photographs were thus secured for tube temperatures of approximately 2700°, 2500°, and 2350° C., a spectrum of the carbon arc being taken in each case adjacent to that of the furnace.

The portion of the band between the first and second heads, being free from the overlapping which occurs beyond the second head, was most suitable for comparison. It was clear that the different appearance in furnace and arc is due to an enhancement in the furnace of the series of lines designated by Uhler and Patterson[1] as "A_1." This is weaker in the arc than the "A_2" series, composed of doublets, up to a point not far from the head of λ3883, some lines of the A_1 series being very faint in a normally exposed arc spectrum. In the furnace, A_1 is the dominant series. At 2350°, the A_1 lines are nearly twice as strong as those of the A_2 series. At 2500°, reversals begin for both series, but a much larger proportion of the A_1 lines is reversed. At 2700°, almost all members of both series are reversed, the reversals of A_1 lines being decidedly wider.

Plate XX shows the section of the band most favorable for examination, with the furnace spectrum at 2500° between two arc spectra of different exposures.

In the following table a comparison is given of the band lines of arc and furnace for a portion of this region. The wave-lengths are those of Uhler and Patterson, and the series symbols and intensities for the arc lines are also taken from their paper. *F* and *f* indicate degrees of faintness, while *w*, *m*, and *i* signify weak, medium, and strong, respectively. The same gradation is adopted for the furnace spectrum and degrees of reversal are indicated by *r* and *R*. The intensity relations for the remaining lines up to the head at λ3883 are similar to those of the last three lines in the table.

In addition to strengthening the A_1 series (and perhaps others beyond the second head), a series of faint doublets, not quite strong enough to measure, appears in the furnace band between λλ 3871 and 3875. These do not show in the arc band even when this is very strong. The furnace thus appears to be especially effective in bringing out the full structure of a band.

---

[1] *Astrophysical Journal*, **42**, 434, 1915.

PLATE XX

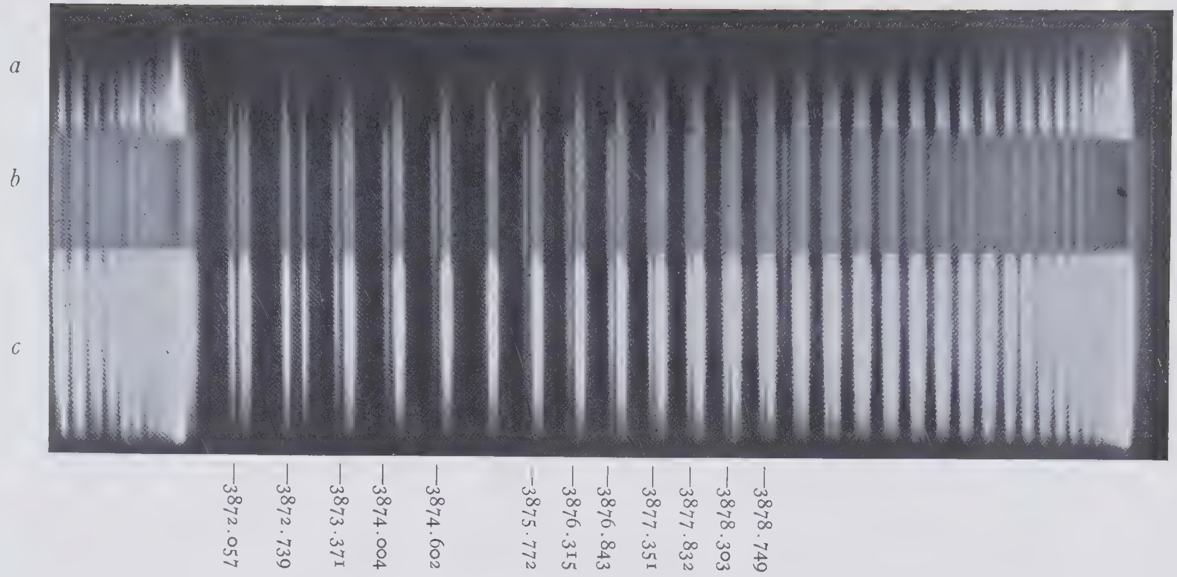

Section of λ 3883 band in furnace (*b*) and arc (*a*, *c*), showing high intensity of A_1 series of single lines (marked) in furnace as compared with A_2 series of doublets.

An examination of the "cyanogen" band at λ4216 and that at λ 5165 belonging to the Swan spectrum, the latter being photographed in furnace and arc under high dispersion, showed in each case a strengthening of certain series by the furnace. The triplet series proceeding from the head at λ5165 is enhanced in the furnace to about the intensity of the strongest line of the adjacent doublet series, thus doing away with the contrast which the arc shows on account of the predominance of the doublet series.

TABLE I

Intensities of Band Lines in Arc and Furnace

λ	Series	Arc (U and P)	Furnace
3872.057	A_1	m	i r
.180	A_2	i	m
.252	A_2	i	m
.739	A_1	i	i r*
.965	A_2	m	m
3873.371	A_1	w	i r
.501	A_2	i	m
.567	A_2	i	m
3874.004	A_1	f	i
.123	A_2	i	m
.190	A_2	i	m
.602	A_1	F	i
.727	A_2	i	m
.791	A_2	i	m
3875.310	A_2	i	m
.375	A_2	i	m
.772	A_1	F	i
.873	A_2	i	i
.939	A_2	i	i
3876.315	A_1	f	i
.415	A_2	i	i
.481	A_2	i	i
.843	A_1	w	i r
.938	A_2	i	i
3877.005	A_2	i	i
.351	A_1	w	i r
.446	A_2	i	i
.506	A_2	i	i
.832	A_1	m	i R
.925	A_2	i	i r
.989	A_2	i	i r
3878.303	A_1	m	i R
.389	A_2	i	i r
.448	A_2	i	i r
.749	A_1	i	i R
.828	A_2	i	i r
.891	A_2	i	i r

* Double, violet component reversed in furnace.

The question as to whether temperature produces the difference between furnace and arc cannot well be tested at present, on account of the great increase in vapor density, with resulting reversals, when the graphite tube is heated to high temperature. A considerable difference in temperature, such as between 2300° and 2700°, involves the uncertainty of comparing sharp and reversed lines. The difference between furnace and arc indicates, however, that the contrasted series belong in different temperature classes. If so, there should be a difference in their response to displacing agencies such as pressure or those electrical actions which affect wave-length, since, for the line-spectra of metals, lines relatively strong in the furnace are less subject to displacements.

A further feature resulting from the fact that the lines composing a band do not behave as a unit is that this dissimilarity must be taken into account in atomic models designed to explain the radiation of band spectra. A considerable degree of independence evidently exists between the centers emitting the component series of a band which itself is a member of a family of bands.

Mount Wilson Observatory
September 1920

Contributions from the Mount Wilson Observatory, No. 195
Reprinted from the *Astrophysical Journal*, Vol. LII, pp. 232–247

STUDIES BASED ON THE COLORS AND MAGNITUDES IN STELLAR CLUSTERS

EIGHTEENTH PAPER: THE PERIODS AND LIGHT-CURVES OF 26 CEPHEID VARIABLES IN MESSIER 72

By HARLOW SHAPLEY and MARY RITCHIE

ABSTRACT

Periods and light-curves of 26 Cepheid variables in Messier 72 have been determined from eighteen plates taken with the 60-inch reflector. The variables are found to be much alike. The periods range from 0.33 to 0.66 day, and the median photographic magnitudes from 16.4 to 16.9, the mean value for all being 16.8. The difference of magnitude between these variables and the 25 brightest stars is unusually small, only 0.94.

Globular cluster Messier 72.—The *photographic magnitudes of twenty-nine comparison stars* were determined by the polar-comparison method. From the median magnitude of the variables the *parallax* of the cluster is computed to be 0.″000039.

1. *Introduction.*—Exploration of the extent of the sidereal universe requires particular knowledge of the most distant objects on record—of the positions in space of faint globular clusters, galactic clouds, and spiral nebulae. For a remote cluster, the Cepheid variables appear to afford the most definite quantitative measure of the position in space, the distances of such stars being uniquely defined by the period-luminosity curve.[1]

The precise determination of the distance of a remote cluster aids also in the correlation between its distance and apparent diameter; and in any cluster the determination of the mean median magnitude of the cluster[2] variables serves in correlating the magnitudes of its brightest stars with the magnitudes of its variables. Thus in two ways the investigation of variables, whenever they can be found, bears on the problem of the distances of all clusters.

---

[1] *Mt. Wilson Contr.*, No. 151; *Astrophysical Journal*, **48**, 89, 1918.

[2] The name "cluster variable" is used exclusively for those variables of the so-called Cepheid type whose periods are shorter than one day.

In view of the significance of these general problems, the discovery and study of Cepheid and cluster variables in the faint globular clusters has been undertaken at Mount Wilson as a feature of the work on the structure of sidereal systems.[1]

Systematic investigations of the periods and light-curves of the variable stars in four bright globular clusters have been published by Professor Bailey in the *Harvard Annals*,[2] affording results that have been of much importance in our work on Cepheid variables and stellar clusters. Bailey's work is based upon long series of plates, some made throughout an interval of more than twenty years—a circumstance that in many cases permits high precision in determining the period and range of light variation and also yields some information as to secular changes in these quantities.

Researches on variations in period and light-curve are necessarily based on extensive material and can be most advantageously made in the case of the brighter clusters, for which observations are easily obtained and analyzed; accordingly, the study at Mount Wilson has included neither this problem of secular variations nor the derivation of precise light-curves, but rather has been specifically concerned with the following points: (1) the average median magnitude of the cluster variables; (2) the bearing of the new material on the period-luminosity relation whenever both long and short period Cepheids are found; (3) the relation of the median magnitude to the brightest stars in the cluster; (4) the correlation of length of period with type of variation, magnitude, range, and distribution in the cluster.

None of these problems requires high accuracy in periods or light-curves if the variables are numerous, and therefore short series of plates are sufficient, provided the observations are properly arranged. In the following discussion of Messier 72 three of the points enumerated above are satisfactorily treated on the basis of twenty photographs with the 60-inch reflector. The variables studied are by far the faintest and most distant for which periods and light-curves are known.

---

[1] Compare section 1, *Mt. Wilson Contr.*, No. 190; *Astrophysical Journal*, **52**, 73; 1920.

[2] Vol. **38**, 1902; **78**, 1913–1919.

2. *Earlier work.*—Messier 72 (N.G.C. 6981 = B.D. − 13°5783) is a faint globular cluster in Capricornus with the equatorial and galactic co-ordinates, for 1900:

Right ascension $= 20^{\mathrm{h}}48^{\mathrm{m}}.0$ Declination $= -12°55'$
Galactic longitude $= 3°$ Galactic latitude $= -34°$

The photographic magnitudes of its brightest stars were determined three years ago (*Mount Wilson Contributions*, No. 152), and the mean of the twenty-five brightest was found to be 15.86.[1]

TABLE I

List of Plates

Plate Number	Date	J.D. and G.M.T (Heliocentric)	Length of Exposure	Quality	Average Deviation (Pg. mag.)
		2420000+			
3874*......	1917, Aug. 13	1454.825	2^{m}, 2^{m}, 2^{m}	Good	....
3949*......	Sept. 9	1481.819	3 , 3 , 3	Good	....
4063.......	Oct. 12	1514.693	10	Fair	±0.06
4163.......	Nov. 10	1543.662	10	Fair	0.06
4975.......	1919, July 21	2161.882	10	Good	0.05
4977.......	July 21	2161.907	10	Very good	0.02
4979.......	July 21	2161.968	10	Fair	0.05
4985.......	July 22	2162.746	15	Fair	0.05
4990†......	July 22	2162.830	10	Very good	0.05
4992.......	July 22	2162.892	12	Very good	0.03
5005.......	July 22	2162.975	15	Poor	0.07
5015.......	July 23	2163.738	12	Good	0.04
5022.......	July 23	2163.828	10	Good	0.05
5024.......	July 23	2163.903	10	Fair	0.07
5032.......	July 24	2164.766	15	Good	0.05
5034.......	July 24	2164.880	12	Very good	0.04
5039.......	Aug. 22	2193.788	10	Fair	0.05
5044.......	Aug. 23	2194.708	12	Good	0.06
5051.......	Sept. 21	2223.648	10 , 10, 2	Poor	0.05
5052.......	Sept. 21	2223.687	8, 8, 8	Good	±0.05
				Mean.....	±0.05

* Used only for bright comparison stars. † Used for positions and reproduction.

The diameter of the cluster was estimated as $2'$, $2'.2$, and $2'.4$ by Melotte, Miss Davis, and Shapley, respectively. On the basis of these measures of diameter and magnitude the parallax was placed at $0''.000034$.

3. *Observations.*—The photographs listed in Table I were made at the primary focus of the 60-inch reflector, the first four on

---

[1] Owing to a typographical error the printed value is 15.94.

Seed 27, the remainder on Seed 30 plates. Multiple exposures, indicated in the fourth column, show which plates were compared directly with the polar standards. The estimated quality of the plate, as recorded at the time of observation, is given verbally in the fifth column; in the sixth column the quality is shown numerically for each plate in the form of average deviations from the adopted means for the magnitudes of comparison stars. This average deviation is the mean of the residuals given in Table II, where it is tacitly assumed that the light of the comparison stars is constant.

4. *Comparison stars.*—The photographic magnitudes of the comparison stars were determined as follows: The polar-comparison plates gave preliminary values; these magnitudes were plotted for all plates against the scale readings, after the usual correction had been applied to the latter for distance from the center and for scale irregularities. For each comparison star the deviation from a smooth curve was then tabulated and the systematic deviation for each star (mean of residuals with regard to sign) was applied as a correction to the preliminary magnitude. The new magnitudes of the comparison stars were again plotted against the scale readings. The residuals from the resulting new curves are those appearing in Table II, which serves to show both the degree of constancy of the light for all comparison stars and the numerical quality of each plate. The magnitudes of the variables have been read from this second set of curves.

The foregoing method of reduction is equivalent (1) to determining the zero point and scale of magnitudes by means of the four polar comparisons, (2) reducing the accidental error in the mean magnitude of a comparison star with data from twenty plates, and (3) deriving each magnitude of a variable star through indirect comparison with twenty-nine stars of sensibly constant light.

Table III gives differential positions and adopted magnitudes of the comparison stars, as well as the average deviation from the adopted means and the final systematic deviations. The last, which are in thousandths of a magnitude, have not been applied to the adopted magnitudes. It was noticed, after the magnitudes

TABLE II

RESIDUALS FOR COMPARISON STARS

PLATE NUMBER	COMPARISON STARS																												
	a	*b*	*c*	*d*	*e*	*f*	*g*	*h*	*k*	*l*	*m*	*n*	*o*	*p*	*q*	*r*	*s*	*t*	*u*	*v*	*w*	*x*	*y*	*z*	α	β	γ	δ	ε
4063	−10	+1	−2	0	−10	+10	0	+3	−2	+4	−11	−8	−5	−9	+5	−4	−5	+9	−6	−8	−10	−9	0	+3	+13	+14	−3	+20	0
4163	−3	0	−9	0	+6	−1	+5	−7	+4	+4	−6	+4	−4	−3	−5	0	+9	+7	−5	−14	−12	−8	−12	+6	−5	−2	−4	+17	0
4975	+4	−1	−1	+2	+7	−11	+6	0	+3	+5	+3	+1	−4	0	+11	−2	−2	−9	−2	−14	−7	+6	+13	−7	−7	+9	−10	+5	0
4977	0	−1	0	−3	−4	+3	−2	0	+1	−3	−2	−5	−10	0	−3	+6	+1	−5	−2	0	+1	+3	+3	+2	+3	0	0	−5	0
4979	−10	−3	−4	+4	−2	+2	−3	+11	−1	+4	+10	+5	−17	−7	−10	−6	+5	0	−7	0	+5	+1	+9	+1	−7	−2	−3	+4	+7
4985	0	+2	+1	+1	+3	+5	0	+6	+8	−12	−6	+1	0	−13	+2	+2	−11	+5	−6	−6	−4	−5	−16	+7	+5	−1	+6	−8	0
4990	−1	+4	+3	−3	−9	+9	+6	+2	+2	+1	−2	−8	+2	+1	−14	−9	−5	−3	−2	−15	+14	+2	+2	+7	+5	0	+3	−9	+10
4992	+5	+1	+2	0	+1	−1	−1	−12	+1	−1	+5	0	+3	+2	+6	+1	−3	+3	−6	−2	+8	+5	0	−3	−1	+1	−4	0	−6
5005	−6	−4	+6	+9	+8	−2	+1	−2	−8	−2	−18	+5	+10	+6	+10	+7	−10	−3	+7	−13	+5	−10	−8	+16	−11	+4	−1	+4	−6
5015	+6	+3	−1	0	+2	+1	−12	+3	−6	....	+2	−3	+7	−5	−1	−6	+4	0	+13	0	0	+7	−4	−19	+1	−3	+6	−6	0
5022	+5	−1	0	−9	+10	+10	−10	+3	−1	+2	+3	−1	−3	−2	−5	−7	+7	+6	−15	0	+4	−3	−5	0	+7	−4	0	−6	+5
5024	0	+2	+2	−5	−10	+5	−4	+4	+17	−13	−1	+1	+9	−16	+1	0	+5	−23	−12	0	+12	+13	−3	+1	+8	−6	+12	−14	0
5032	+1	+3	0	+3	+8	−15	−2	+7	+5	−1	+12	+2	−10	−1	−5	+2	+8	−15	+4	0	−3	0	+4	−5	+5	−17	+6	−4	−6
5034	−2	0	−3	+3	−3	+8	−4	+4	0	−9	−2	0	−17	+1	+1	+4	+7	0	−5	+6	0	+6	−5	+1	+1	−6	+11	0	+11
5039	+2	+1	−3	+6	−7	0	+1	+4	−1	+9	+3	+7	+5	−1	+6	0	+5	+2	−7	−5	−7	−3	+13	−8	−18	+15	−2	−4	0
5044	−7	−5	0	+2	+7	+5	+2	+4	−24	+8	−12	−6	+10	+8	−10	−3	+5	0	+9	−8	0	+6	−6	−2	+2	+9	+10	+1	+7
5051	+5	+4	+5	−7	0	−8	−3	−4	+3	−10	+7	0	−6	+10	+2	−3	−8	....	−1	....	+3	+4	+2	−8	+8	+9	−14	+2	−12
5052	+5	−2	+1	0	+3	−6	0	−3	+3	−6	+12	+8	−5	+2	+2	+3	+8	−10	0	+4	−11	−10	−9	+4	−12	0	+8	−3	0

of the variables had been derived, that the final systematic deviations are negative for all comparison stars fainter than 17.2. This indicates a slight systematic error in drawing the curves; to correct for it, in making Table V we have applied +0.02 to the magnitudes derived for the minima from analysis of the observations in Table IV.

TABLE III

COMPARISON STARS IN MESSIER 72

STAR	POSITION		PHOTOGRAPHIC MAGNITUDE	AVERAGE DEVIATION	SYSTEMATIC DEVIATION
	x	*y*			
a............	+0′40″.5	−1′11″.4	16.08	±0$^{\rm M}$.04	−0$^{\rm M}$.003
b............	−1 7.5	+0 9.0	16.09	0.02	+0.002
c............	+0 43.5	+0 14.4	16.16	0.02	−0.002
d............	−0 28.5	+1 14.4	16.13	0.03	+0.002
e............	−0 47.4	−0 51.0	16.67	0.06	+0.006
f............	+2 7.5	+2 15.6	16.65	0.06	+0.008
g............	+1 24.6	+0 43.5	17.31	0.03	−0.011
h............	−0 35.4	+2 3.0	17.01	0.04	+0.013
k............	−1 17.4	+1 12.6	17.18	0.05	+0.002
l............	−2 18.6	+0 2.4	17.40	0.06	−0.012
m............	−1 17.4	−1 14.4	17.14	0.06	−0.002
n............	+1 27.6	−1 17.4	17.18	0.04	+0.002
o............	+1 12.0	−0 19.5	17.51	0.07	−0.019
p............	+0 58.5	−0 15.6	17.31	0.05	−0.015
q............	+1 46.5	−0 3.6	17.27	0.06	−0.004
r............	+0 31.5	+1 10.5	17.31	0.04	−0.008
s............	+0 39.6	+1 20.4	17.00	0.06	+0.011
t............	+0 14.4	+1 36.0	17.56	0.06	−0.021
u............	+1 9.0	+0 8.4	17.38	0.06	−0.024
v............	−1 48.0	−0 52.5	17.80	0.06	−0.044
w............	−1 9.6	+0 47.4	17.20	0.06	−0.001
x............	−1 21.0	+0 21.6	17.03	0.06	+0.003
y............	−0 39.0	+0 51.0	17.09	0.06	−0.012
z............	+0 33.6	+0 49.5	17.31	0.06	−0.002
α............	−0 42.0	+1 42.6	17.27	0.07	−0.002
β............	−0 46.5	+1 21.0	16.81	0.06	+0.011
γ............	+2 4.5	−0 5.4	16.86	0.06	+0.012
δ............	−0 50.4	+0 13.5	16.22	0.06	−0.003
ε............	−1 41.4	+0 35.4	15.77	±0.04	+0.006
A*..........	+4 25.5	−1 54.0	....	....	....
				Mean ±0.05	

* Star A is B.D.−13°5785 (9$^{\rm M}$.1) = A.G. Camb. 7396.

5. *Magnitudes and light-elements of the variable stars.*—A photographic chart and the differential positions of the thirty-four stars in Messier 72, listed as probably variable by Miss Ritchie, are

given in the first section of *Mount Wilson Contributions*, No. 190. The photographic magnitudes from measures by Miss Ritchie, the phases, and the residuals (in hundredths of a magnitude) from smooth mean curves are given in Table IV. Table V contains the elements of light-variation and other data appropriate for statistical discussion, and is followed by notes on special cases. Except for a few instances cited in the notes, the periods are accurate to the fourth place of decimals. Four representative light-curves are shown in Figure 1. The determination of the periods and light-curves has been largely in the hands of Miss Mayberry.

6. *Discussion of results.*—Numbers 6, 19, 22, 26, and 33 do not appear to be conspicuously variable; Nos. 25, 30, and 34 undoubtedly vary, but it has not been possible to obtain uniform periods for them. For Nos. 18, 24, and 28 the periods are unsatisfactory to the extent stated in the notes to Table V. Twenty-two of the periods and light-curves, however, are sufficiently accurate for the summaries in Tables VI, VII, and VIII, which are arranged respectively with the arguments of period, median magnitude, and range.

Variable No. 27 was omitted from the correlation tables because of its deviation in period, distance from the center, range, and median magnitude from all of the twenty-two other variables with well-determined elements. Possibly it is an isolated variable, only by chance in the direction of Messier 72; but in that case it would be much the most distant isolated star on record, and some 15,000 parsecs from the galactic plane. Number 2, which has the second largest range of variation, is the second most distant from the center, a fact which suggests that No. 27 is probably a member of the cluster notwithstanding its somewhat anomalous character.

From Tables VI, VII, and VIII no definite correlations are evident, except that small range is associated with faint median magnitude—probably an indication merely that the maximum is frequently recorded too faint because of the insufficiency of observations near zero phase. The principal conclusion from these tables is that all the stars are much alike, particularly in median and minimum magnitudes.

TABLE IV

PHOTOGRAPHIC OBSERVATIONS OF VARIABLES IN MESSIER 72

J.D. AND G.H.M.T.	MAGNITUDE	PHASE	RESIDUAL	MAGNITUDE	PHASE	RESIDUAL	MAGNITUDE	PHASE	RESIDUAL
	No. 1. Period 0.61974			No. 2. Period 0.46561			No. 3. Period 0.48965		
2420000+									
1514.693	16.61	0.591	0	16.00	0.005	0	16.56	0.022	0
1543.662	17.25	.432	+ 3	16.87	.106	− 1	16.99	.101	0
2161.882	16.90	.152	− 2	16.04	.462	+ 2	17.33	.383	0
.907	16.94	.177	− 2	16.16	.021	+ 7	17.33	.408	0
.968	17.07	.238	+ 2	16.77	.082	+ 4	16.77	.469	0
2162.746	17.26	.396	+ 5	17.29	.395	0	17.23	.268	0
.830	17.22	.480	− 2	15.99	.013	− 3	17.42	.352	+11
.892	17.26	.542	+ 1	16.42	.075	−22	17.35	.414	+ 2
.975	16.50	.005	+ 8	16.88	.158	−22	16.38	.007	+ 5
2163.738	16.93	.148	+ 2	16.09	.455	− 4	17.16	.280	− 8
.828	16.91	.238	−14	16.68	.080	0	17.34	.370	+ 1
.903	17.20	.313	+ 6	17.17	.155	+ 7	17.28	.445	− 4
2164.766	16.60	.557	−50	16.86	.087	+ 9	17.25	.329	− 4
.880	16.58	.051	− 8	17.18	.201	− 2	17.20	.443	−13
2193.788	17.23	.451	0	17.50	.241	+24	17.25	.462	+24
2194.708	16.87	.131	0	17.38	.230	+14	17.31	.402	− 3
2223.648	17.04	.563	0	17.21	.302	− 8	17.21	.453	− 6
.687	16.78	.602	+29	17.24	.341	− 6	16.19	.002	− 7
	No. 4. Period 0.3619			No. 5. Period 0.4991			No. 7. Period 0.52463		
1514.693	17.22	.318	+11	17.32	.284	− 8	17.19	.289	0
1543.662	16.71	.335	+ 4	17.40	.305	− 1	17.14	.403	−11
2161.882	16.75	.068	−14	17.21	.140	0	16.79	.085	− 7
.907	16.87	.093	−11	17.22	.165	− 6	17.06	.110	+ 8
.968	17.11	.154	− 8	17.43	.226	+ 5	17.11	.171	0
2162.746	17.32	.208	+ 4	16.54	.006	+ 4	17.34	.424	+ 8
.830	17.35	.292	+ 3	17.22	.090	+19	16.44	.508	− 7
.892	16.26	.354	+ 7	17.35	.152	+11	16.60	.045	0
.975	16.68	.075	−16	17.43	.235	+ 4	17.02	.128	− 2
2163.738	17.23	.114	+16	16.39	.000	0	17.26	.367	+ 2
.828	17.22	.204	− 5	16.84	.090	−19	17.19	.457	− 8
.903	17.28	.279	− 2	17.28	.165	0	16.24	.007	0
2164.766	17.22	.056	+53	16.77	.030	+ 3	17.25	.345	+ 3
.880	17.18	.170	− 8	17.14	.144	− 8	17.36	.459	+ 9
2193.788	17.00	.126	−12	16.97	.104	−11	16.59	.513	+18
2194.708	17.36	.323	+42	16.71	.026	− 1	17.20	.384	− 4

	No. 8. Period 0.5743			No. 9. Period 0.5902			No. 10. Period 0.5483		
1514.693	16.76	0.391	−55	17.06	0.123	+17	16.99	0.250	−18
1543.662	16.77	.071	0	16.96	.172	− 6	16.87	.159	− 9
2161.882	17.35	.344	+ 9	17.33	.452	+ 3	17.28	.445	+10
.907	17.27	.369	0	17.22	.477	−10	16.80	.470	−14
.968	17.28	.430	− 1	16.85	.538	− 6	16.43	.531	+10
2162.746	16.69	.060	+ 2	17.03	.136	+10	17.00	.213	−10
.830	16.93	.144	−20	17.12	.220	+ 2	17.29	.297	+ 5
.892	17.19	.206	0	17.24	.282	+ 8	17.22	.359	− 6
.975	17.10	.289	−14	17.22	.365	0	17.33	.442	+14
2163.738	17.16	.477	− 8	17.00	.538	+ 7	16.70	.108	− 8
.828	16.39	.567	− 3	16.57	.038	+ 0	17.12	.198	+ 5
.903	16.66	.068	− 8	16.69	.113	−16	17.20	.273	− 1
2164.766	17.18	.357	− 8	17.18	.385	− 6	16.50	.039	+ 3
.880	17.32	.471	+ 5	17.34	.499	+ 2	16.98	.153	+ 4
2193.788	17.22	.089	+29	17.35	.488	+ 3	16.24	.001	0
2194.708	17.38	.435	+10	17.04	.227	− 7	17.22	.175	+21
2223.648	16.99	.086	+ 9	17.09	.237	− 3	17.14	.253	− 7
.687	17.24	.125	+15	17.11	.276	− 5	17.24	.292	+ 1

	No. 11. Period 0.3345			No. 12. Period 0.4111			No. 13. Period 0.54182		
1514.693	17.13	.218	−11	17.06	.331	− 4	16.82	.261	0
1543.662	16.89	.086	+ 3	16.93	.112	0	16.87	.513	+ 2
2161.882	17.24	.150	+11	16.75	.038	+22	16.75	.517	− 2
.907	17.33	.175	+14	16.59	.063	−12	16.00	.000	−10
.968	17.25	.236	− 1	17.11	.124	+14	16.41	.061	+ 3
2162.746	16.41	.010	0	16.72	.079	− 8	16.97	.297	+10
.830	17.09	.094	+19	16.98	.163	− 9	16.89	.381	−13
.892	17.19	.156	+ 5	17.26	.225	+12	17.10	.443	− 2
.975	17.41	.239	+14	17.29	.308	+15	16.56	.526	0
2163.738	16.37	.333	0	16.95	.249	−20	16.70	.206	− 1
.828	16.78	.087	− 8	16.96	.339	− 9	16.76	.296	−11
.903	17.00	.163	−15	16.32	.003	0	16.94	.371	− 5
2164.766	16.54	.023	+ 3	16.63	.044	+ 5	16.54	.150	− 5
.880	16.85	.137	−23	17.09	.158	+ 2	16.90	.264	+ 8
2193.788	17.32	.277	+ 2	16.97	.289	−19	17.22	.455	+ 8
2194.708	17.14	.194	− 7	16.66	.387	0	16.96	.292	+ 9
2223.648	16.51	.033	− 6	16.99	.138	− 2	16.78	.515	− 1
.687	16.82	0.072	+ 2	17.24	0.177	+14	16.19	0.013	+ 2

TABLE IV—*Continued*

J.D. and G.H.M.T.	Magnitude	Phase	Residual	Magnitude	Phase	Residual	Magnitude	Phase	Residual
	No. 14. Period 0.5904			No. 15. Period 0.5499			No. 16. Period 0.5641		
2420000+									
1514.693	17.10	0.233	+ 8	17.10	0.295	− 7	17.13	0.143	+ 5
1543.662	16.96	.272	− 6	16.87	.119	+17	17.35	.320	+ 1
2161.882	17.16	.342	+13	16.97	.252	−13	17.44	.308	+10
.907	17.03	.367	0	17.22	.277	+ 7	17.30	.333	− 5
.968	17.00	.428	− 3	17.36	.338	+13	17.32	.394	− 1
2162.746	16.51	.026	0	16.25	.016	0	16.72	.044	+17
.830	16.68	.110	−18	16.48	.100	−16	16.98	.128	− 5
.892	16.98	.172	0	16.77	.162	− 8	17.26	.190	+ 6
.975	17.04	.255	+ 2	17.12	.245	+ 4	17.35	.273	+ 3
2163.738	16.93	.428	−10	17.13	.458	−15	17.26	.472	− 2
.828	16.86	.518	0	16.16	.548	0	16.33	.562	0
.903	16.40	.003	0	16.32	.073	−15	16.84	.073	+ 6
2164.766	17.07	.276	+ 5	17.22	.386	− 5	17.12	.372	−22
.880	17.06	.390	+ 3	17.04	.500	+ 5	17.28	.486	+ 3
2193.788	16.90	.368	−13	17.13	.263	+ 1	16.88	.061	+18
2194.708	17.04	.107	+18	16.76	.084	+18	17.17	.417	−20
2223.648	16.81	.118	− 8	17.27	.429	0	16.37	.023	− 2
.687	17.06	.157	+10	17.42	.468	+15	16.54	.062	−16
	No. 17. Period 0.56308			No. 18. Period 0.52016			No. 20. Period 0.59555		
1514.693	17.16	.516	− 3	16.28	.453	+12	17.29	.327	+ 3
1543.662	17.19	.205	+ 5	16.40	.293	+12	16.93	.114	0
2161.882	17.04	.163	− 2	16.08	.042	+17	17.12	.153	+ 7
.907	17.15	.188	+ 4	16.04	.067	+ 2	17.00	.178	−12
.968	17.25	.249	+ 4	16.12	.128	− 5	17.25	.239	+ 5
2162.746	17.34	.464	+ 4	16.28	.386	0	17.29	.422	− 4
.830	16.70	.548	+ 1	15.93	.470	−12	17.45	.506	+ 6
.892	16.68	.047	+ 8	15.77	.012	+ 2	17.17	.568	+17
.975	16.78	.130	−18	15.90	.095	−20	16.59	.055	− 6
2163.738	17.20	.330	− 7	16.32	.338	+ 4	17.13	.222	− 5
.828	17.19	.420	−11	16.16	.428	−10	17.24	.312	− 1
.903	17.32	.495	+ 2	15.79	.503	0	17.28	.387	− 2
2164.766	17.15	.232	− 4	16.21	.326	− 7	16.79	.059	+12
.880	17.23	.346	− 5	16.13	.440	−11	16.98	.173	−13
2193.788	17.02	.537	+ 5	16.18	.219	− 7	17.35	.495	− 3
2194.708	17.41	.331	+14	16.37	.098	+27	17.14	.224	− 4
2223.648	16.39	.553	− 3	16.15	.429	−13	16.61	.578	− 5
.687	16.48	0.029	0	16.14	0.468	+ 7	16.48	0.021	+ 1

	No. 21. Period 0.5310			No. 23. Period 0.5969			No. 24. Period 0.4973		
1514.693	17.10	0.461	− 4	17.06	0.220	− 4	16.54	0.258	− 1
1543.662	17.25	.225	− 4	16.66	.538	−10	16.50	.383	+ 8
2161.882	17.30	.361	− 4	17.24	.370	+ 2	16.24	.459	− 4
.907	17.30	.386	− 4	17.16	.395	− 7	16.13	.484	−10
.968	17.36	.447	+ 4	17.22	.456	− 1	16.22	.048	− 7
2162.746	17.11	.163	− 5	16.30	.040	−12	16.54	.329	+ 5
.830	17.32	.247	+ 1	16.76	.124	−14	16.40	.413	+ 2
.892	17.35	.309	+ 2	17.05	.186	0	16.26	.475	+ 1
.975	17.33	.392	− 1	17.17	.269	0	16.26	.060	− 6
2163.738	16.85	.093	− 7	17.26	.435	+ 4	16.41	.326	− 9
.828	17.22	.183	0	17.19	.525	0	16.31	.416	− 6
.903	17.32	.258	0	16.18	.003	− 2	16.21	.491	0
2164.766	16.99	.059	+26	17.18	.269	+ 2	16.24	.360	−22
.880	17.18	.173	− 2	17.20	.383	− 2	16.28	.474	+ 3
2193.788	17.35	.407	+ 1	16.64	.043	+19	16.36	.041	+ 8
2194.708	17.36	.265	+ 4	17.29	.366	+ 7	16.41	.464	+14
2223.648	16.32	.000	0	16.58	.058	0	16.70	.063	+37
.687	16.52	.039	− 9	16.99	.097	+18	16.42	.102	+ 1

	No. 27. Period 0.65885			No. 28. Period 0.3638			No. 29. Period 0.36865		
1514.693	15.88	.020	+ 1	16.76	.045	+14	17.10	.212	−10
1543.662	15.72	.000	0	16.75	.273	−41	16.84	.058	+ 9
2161.882	16.83	.219	+ 7	16.63	.033	+ 8	16.83	.052	+11
.907	16.78	.244	− 4	16.54	.058	−13	16.87	.077	0
.968	16.75	.305	−17	16.82	.119	− 8	17.07	.138	+ 1
2162.746	17.08	.424	0	17.08	.170	+ 2	17.11	.179	− 3
.830	17.22	.508	+ 9	17.19	.254	0	17.28	.263	0
.892	17.05	.570	− 6	16.71	.316	− 1	17.35	.325	0
.975	15.84	.653	0	16.50	.035	− 6	16.50	.039	−11
2163.738	16.37	.098	+ 7	16.85	.070	+13	16.93	.065	+13
.828	16.68	.188	+ 1	17.12	.160	+ 9	17.14	.155	+ 4
.903	16.91	.263	+ 6	17.17	.235	0	17.32	.230	+ 9
2164.766	17.02	.467	−10	16.84	.007	+37	16.77	.355	0
.880	17.12	.581	+ 7	16.85	.121	− 5	16.79	.101	−17
2193.788	17.17	.500	+ 4	17.11	.289	+ 5	17.23	.254	− 4
2194.708	16.26	.102	− 6	16.69	.117	−19	16.79	.068	− 2
2223.648	16.05	.053	− 1	16.70	.317	0	17.29	.253	+ 2
.687	16.26	0.092	− 1	16.52	0.356	+ 3	17.30	0.292	− 2

TABLE IV—*Continued*

J.D. and G.H.M.T.	Magnitude	Phase	Residual	Magnitude	Phase	Residual	Magnitudes	
	No. 31. Period 0.55465			No. 32. Period 0.50544			No. 6	No. 19
2420000+								
1514.693	17.03	0.504	− 2	16.94	0.447	0	16.99	17.26
1543.662	16.89	.077	− 1	16.84	.107	−13	16.87	17.37
2161.882	17.14	.417	− 3	17.18	.174	+ 6	16.97	17.25
.907	17.16	.442	+ 2	17.12	.199	− 2	16.94	17.36
.968	16.98	.503	− 7	17.16	.260	0	17.11	17.28
2162.746	17.13	.171	0	16.60	.027	− 4	17.00	17.23
.830	17.12	.255	− 8	16.93	.111	− 5	16.93	17.35
.892	17.26	.317	+ 6	17.22	.173	+10	17.03	17.27
.975	17.15	.400	− 3	17.04	.256	−12	16.81	17.07
2163.738	16.77	.054	0	16.53	.008	0	16.79	17.16
.828	16.96	.144	−12	16.91	.098	− 3	16.96	17.28
.903	17.32	.219	+13	17.13	.173	+ 1	16.87	17.20
2164.766	16.82	.527	0	16.77	.025	+16	16.94	17.42
.880	16.96	.087	+ 1	16.96	.139	−15	16.98	17.26
2193.788	17.13	.153	+ 3	17.17	.237	+ 1	17.15	17.22
2194.708	16.98	.518	+ 5	17.25	.146	+17	16.98	17.22
2223.648	16.92	.062	+10	17.12	.276	− 5	17.14	17.35
.687	17.06	0.101	+ 6	17.27	0.315	+10	16.80	17.36

	Magnitudes							
	No. 22	No. 25	No. 26	No. 30	No. 33	No. 34		
1514.693	17.19	16.99	17.03	16.79	17.06	16.08	....	....
1543.662	17.04	16.96	16.93	16.81	17.19	16.43	....	....
2161.882	17.16	16.56	17.25	16.66	17.16	16.66	....	....
.907	17.19	16.45	17.10	16.59	17.14	16.37	....	....
.968	17.22	16.52	17.16	16.75	17.25	16.73	....	....
2162.746	17.13	16.91	17.08	16.49	17.13	16.37	....	....
.830	17.02	16.98	17.26	16.53	17.19	16.06	....	....
.892	17.26	16.60	17.17	16.38	17.08	16.38	....	....
.975	16.97	16.56	17.04	16.44	16.97	16.56	....	....
2163.738	17.20	16.63	17.16	16.91	17.23	16.41	....	....
.828	17.12	16.81	17.03	16.44	17.05	16.26	....	....
.903	17.23	17.04	17.04	16.53	17.17	16.63	....	....
2164.766	17.12	16.72	17.15	16.56	17.07	16.21	....	....
.880	17.18	17.01	17.14	16.72	17.14	16.13	....	....
2193.788	17.17	16.85	17.22	16.56	17.23	16.24	....	....
2194.708	17.04	16.69	17.17	16.87	17.06	16.19	....	....
2223.648	17.19	17.04	17.00	16.61	17.25	16.24		

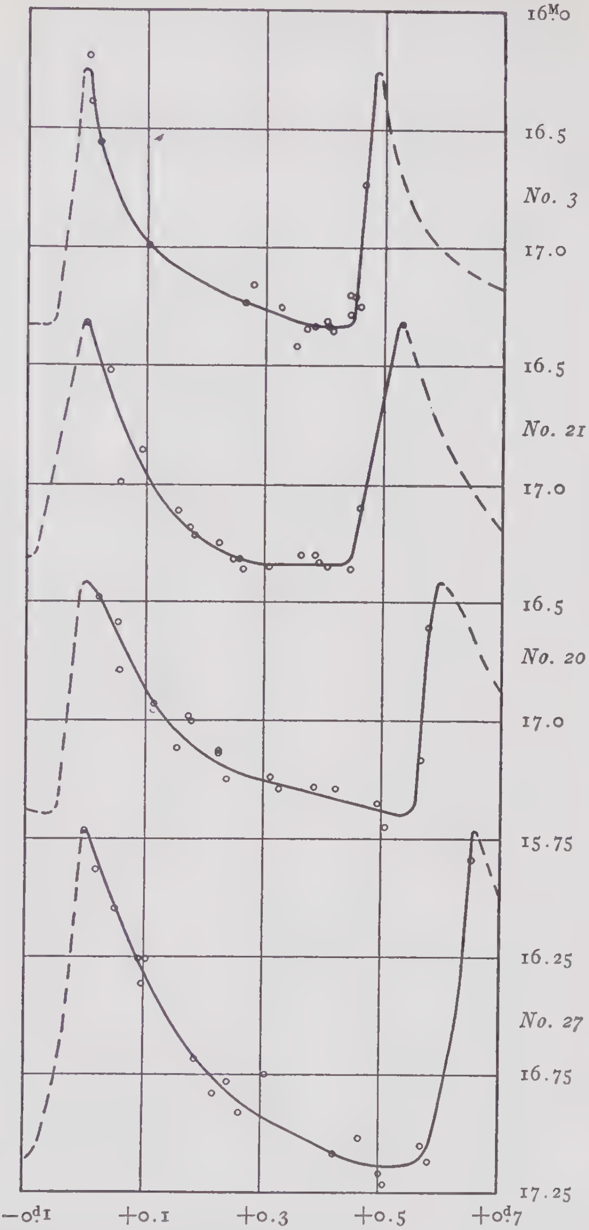

FIG. 1.—Light-curves of cluster variables in Messier 72. Ordinates are photographic magnitudes; abscissae, phases from maximum in days.

TABLE V

ELEMENTS

NUMBER OF VARIABLE	DISTANCE FROM CENTER	EPOCH OF HELIOCENTRIC MAXIMUM	PERIOD	PHOTOGRAPHIC MAGNITUDE			RANGE
				Maximum	Minimum	Median	
		2420000+					
1.......	1$'$.1	2162.97	0^{d}61974	16.40	17.27	16.84	0.87
2.......	3.6	2162.817	.46561	16.00	17.32	16.66	1.32
3.......	1.3	2162.968	.48965	16.25	17.35	16.80	1.10
4.......	1.8	2162.90	.3619	16.16	17.34	16.75	1.18
5.......	0.7	2163.738	.4991	16.40	17.43	16.91	1.03
7.......	0.9	2163.896	.52463	16.20	17.29	16.75	1.09
8.......	1.5	2163.835	.5743	16.40	17.32	16.86	0.92
9.......	0.9	2162.61	.5902	16.30	17.34	16.82	1.04
10.......	1.4	2163.63	.5483	16.23	17.32	16.77	1.09
11.......	1.1	2162.736	.3345	16.35	17.32	16.83	0.97
12.......	0.4	2163.90	.4111	16.31	17.17	16.74	0.86
13.......	0.4	2161.907	.54182	16.10	17.15	16.63	1.05
14.......	0.6	2163.90	.5904	16.40	17.06	16.73	0.66
15.......	1.1	2163.83	.5499	16.15	17.30	16.73	1.15
16.......	0.3	2163.83	.5641	16.30	17.37	16.83	1.07
17.......	0.7	2162.845	.56308	16.35	17.32	16.83	0.97
18.......	0.7	2162.88	.52016	15.70	16.28	15.99	0.58
20.......	0.9	2162.92	.59555	16.42	17.42	16.92	1.00
21.......	1.4	2162.583	.5310	16.32	17.37	16.85	1.05
23.......	2.5	2163.90	.5969	16.20	17.25	16.73	1.05
24.......	0.5	2161.92	.4973:	16.20	16.55	16.38	0.35
25.......	2.5	....	....	16.45	17.06	....	0.61
27.......	4.6	2162.981	.65885	15.72	17.15	16.43	1.43
28.......	1.7	2162.94	.36381	16.48	17.21	16.85	0.73
29.......	1.1	2161.83	.36865	16.40	17.37	16.87	0.97
30.......	2.0	....	....	16.38	16.91	....	0.53
31.......	0.6	2162.02	.55465	16.50	17.22	16.86	0.72
32.......	2.4	2163.73	0.50544	16.50	17.22	16.86	0.72
34.......	0.2	....	....	16.06	16.73	....	0.67

NOTES ON TABLE V

No.

3. The light-curve is shown in Figure 1.
5. The period 0^{d}5072 fits the observations nearly as well as the value in the table.
8. The adopted period is fairly satisfactory except for the unusually large residual for the first observation of the series.
9. The magnitude at maximum is uncertain.
18. This is the brightest variable in the cluster and has one of the smallest ranges of variation. The period is not quite satisfactory because of the large residuals and the gradual rise to maximum; it might be possible to represent the observations as well with a period slightly in excess of one day. If the star is double, as is suspected but not yet proved, the peculiarities of brightness and range are simply accounted for.
20. The light-curve is shown in Figure 1.
21. The light-curve is shown in Figure 1.

No.

24. Although this star is definitely variable, the range is so small that the adopted period cannot be accepted with certainty. The first observation of September 21, 1919, is very discordant.
25. The period appears to be some sub-multiple of one day.
27. The light-curve is shown in Figure 1; this variable has the longest period, the greatest distance, the greatest range, and, excepting No. 18, the brightest median magnitude.
28. The period is very uncertain.
30. The period may be something near $0^{\mathrm{d}}.46$, but apparently the variation is irregular.
31. The magnitude at maximum is uncertain because of the lack of observations within forty minutes of zero phase.
34. The period is some sub-multiple of a day, but no satisfactory value has been found. This variable, which is the nearest of all to the center and was consequently measured with some difficulty, is brighter than the average and has a small range of variation. It may be a multiple star; compare note on No. 18.

TABLE VI

Period	No.	Maximum	Minimum	Median	Range	Distance
$0^{\mathrm{d}}.599$	5	$16^{\mathrm{M}}.34$	$17^{\mathrm{M}}.27$	$16^{\mathrm{M}}.81$	$0^{\mathrm{M}}.92$	$1'.2$
0.559	6	16.32	17.31	16.81	0.99	0.9
0.520	5	16.30	17.29	16.80	0.99	1.2
0.405	6	16.24	17.31	16.78	1.07	1.5

TABLE VII

Median Magnitude	No.	Period	Distance	Range
$16^{\mathrm{M}}.69$	5	$0^{\mathrm{d}}.549$	$1'.6$	$1^{\mathrm{M}}.04$
16.77	6	0.488	1.1	1.06
16.83	5	0.522	0.9	0.99
16.88	6	0.516	1.2	0.89

TABLE VIII

Range	No.	Distance	Period	Median Magnitude
$1^{\mathrm{M}}.17$	5	$1'.8$	$0^{\mathrm{d}}.483$	$16^{\mathrm{M}}.74$
1.06	6	1.1	0.558	16.77
0.99	5	0.9	0.472	16.87
0.79	6	1.1	0.543	16.81

All periods are shorter than a day. They show a considerable dispersion, but are not grouped into distinct classes as in clusters studied by Bailey. Thus we have:

Length of Period in Days	Number of Variables
<0.35	1
0.35–0.4	2
0.4 –0.45	1
0.45–0.5	3
0.5 –0.55	6
0.55–0.6	8
>0.6	1

The mean value of the period is $0^{d}.517$.

The average value of the range in photographic magnitude is 0.99, with extremes, among the well-determined cases, of 1.43 and 0.66. The light-curves, so far as our observations are competent to say, all belong to the type usual in clusters, that is, to Bailey's subclass *a*, except that Nos. 12, 24, 25, and 34 might be assigned to subclass *c*, and 1, 20, and 27 to subclass *b*.

The median magnitude and its probable error is 16.80±0.05, or, if No. 27 is included, 16.78±0.09. The effect on the probable error justifies the exclusion of No. 27.

Using the methods outlined in *Mount Wilson Contributions*, No. 151, we derive for Messier 72 a parallax of $0''.000039$, to which corresponds the space-position

$$R=25.6$$
$$R\cos\beta=21.2$$
$$R\sin\beta=-14.3,$$

where R is the distance in kiloparsecs and β is the galactic latitude. This value of the distance differs about 13 per cent from the value obtained in *Mount Wilson Contributions*, No. 151. The cause of the divergence can be traced to the unusually small difference of magnitude between the twenty-five brightest stars and the median ($m_{25}-med=16.80-15.86=0.94$). For Messier 68, reported in *Mount Wilson Contributions*, No. 175, this same difference was also found to be smaller than the value adopted for earlier computations of the distances of clusters. A revision of the earlier work, based on a new value of $m_{25}-med$, may therefore be necessary, but apparently it would involve only a systematic decrease of the distances by 6 per cent or less.

MOUNT WILSON OBSERVATORY
August 1920

Contributions from the Mount Wilson Observatory, No. 196
Reprinted from the *Astrophysical Journal*, Vol. LIII, pp. 95–98, 1921

THE SPECTROSCOPIC ORBIT OF THE CEPHEID VARIABLE X CYGNI

By JOHN C. DUNCAN

ABSTRACT

Cepheid variable X Cygni.—A brief summary of previous observations relating to this variable is given. From twenty-three spectrograms made at Mount Wilson with the 60-inch reflector and single-prism spectrograph, the *elements of the spectroscopic orbit* have been computed. The values of K (28 km/sec.), of $a \sin i$ (6, 121,000 km), and of the mass-function (0.034) are remarkably large. The probable error for a plate is large in comparison with the deviations in the measures of a single plate made by different observers; but there is no evidence of a secondary oscillation.

The variable star X Cygni ($\alpha = 20^h 39^m\!.5$, $\delta = +35°14'$; 1900.0) was discovered by S. C. Chandler[1] in 1886. Of a number of published determinations of its photometric elements, the best is probably that of M. Luizet,[2] which is based on observations covering 554 periods and made by eight different observers. Luizet gives as the time of maximum brightness

$$\text{J.D. } 2410190.684 \text{ (Paris M.T.)} + 16^d\!.38543\, E,$$

and finds that, though the maxima and minima are repeated with regularity, the amount of the change of light is not constant, the magnitude at maximum ranging from 6.5 to 6.2, and at minimum from 7.4 to 7.2. Secondary oscillations appear in both the rising and the falling branches of the curve. The duration of the increase of light is $6^d\!.1$.

The spectrum as classified at the Harvard Observatory is F5, peculiar. Like other Cepheids, the star is bluer and has stronger hydrogen lines at maximum brilliancy than at minimum. The variation in the radial velocity was discovered by Frost.[3]

Table I gives a list of the spectrograms of X Cygni taken at the Mount Wilson Observatory. They were made by Messrs. Adams, Joy, Strömberg, Sanford, Merrill, and Duncan, with the

---

[1] *Astronomical Journal*, **7**, 32, 1886.

[2] *Astronomische Nachrichten*, **193**, 83, 1912.

[3] *Astrophysical Journal*, **25**, 60, 1907.

60-inch reflector and single-prism spectrograph, using the 18-inch camera. All were measured by Miss Brayton and Mr. Duncan, and some also by Miss Burwell and Messrs. Adams, Joy, Strömberg, and Sanford. No systematic differences in the measures were found, and the column headed "Velocity" gives the mean results, reduced to the sun. The Greenwich mean time given in Table I refers to the middle of the exposure. The phase is the number of days after maximum light according to the elements of Luizet.

TABLE I

Plate Number	Date	G.M.T.	J.D., G.M.T.	Phase	Velocity	O−C	Number of Measures
					km/sec.	km/sec.	
6353..	1917 Nov. 3	16^h03^m	242 1536.669	$7^d.273$	+16.2	−2.2	6
6358..	4	18 05	1537.754	8.358	+24.2	−0.8	5
7213..	1918 Aug. 17	22 31	1823.939	15.991	−14.8	−0.9	4
8261..	1919 June 8	22 05	2118.920	16.034	−17.4	+0.2	2
8329..	July 3	22 01	2143.918	8.261	+26.2	+2.0	2
8336..	5	21 12	2145.884	10.227	+40.4	+6.6	2
8341..	7	22 15	2147.927	12.270	+31.0	−3.0	2
8348..	8	22 49	2148.951	13.294	+27.7	+2.5	2
8357..	10	20 57	2150.858	15.201	− 6.6	−0.4	3
8363..	11	20 39	2151.861	16.302	−23.0	0.0	2
8370..	12	20 10	2152.841	0.798	−17.4	+2.6	2
8375..	13	19 46	2153.824	1.781	−16.6	+0.6	2
8387..	14	22 16	2154.928	2.885	− 7.2	+3.8	2
8400..	15	22 03	2155.919	3.876	− 6.0	−1.5	2
8412..	17	18 50	2157.868	5.825	+ 5.0	−3.9	3
8436..	19	18 13	2159.843	7.800	+20.0	−1.7	2
8478..	Aug. 6	21 14	2177.885	9.457	+34.2	+3.5	2
8482..	7	18 46	2178.782	10.354	+38.6	+4.4	2
8522..	10	19 59	2181.832	13.404	+23.7	−0.1	2
8523..	10	21 11	2181.883	13.455	+19.4	−4.5	2
8545..	11	20 50	2182.868	14.440	+14.4	+7.3	2
8689..	Sept. 10	15 55	2212.663	11.465	+33.6	−2.5	2
8692..	10	20 45	2212.865	11.667	+32.0	−3.6	2

Preliminary elements were derived by the method of Lehmann-Filhés. As no planimeter was available, the necessary areas were determined by tracing the velocity-curve on thin paper, cutting out the areas, and weighing them on a chemical balance. Luizet's photometric period was assumed as the orbital period, and there appeared no good reason for changing it. The preliminary elements are:

$K = 28.0$ km/sec.
$\omega = 110^\circ$
$e = 0.25$
$T = 15^{\mathrm{d}}.0$ after light maximum
$\gamma = +9.5$ km/sec.

A least-squares solution was based on these elements, the observations being given equal weight and grouped to form eighteen normal places. The period was not included in this solution. The following elements were thus obtained:

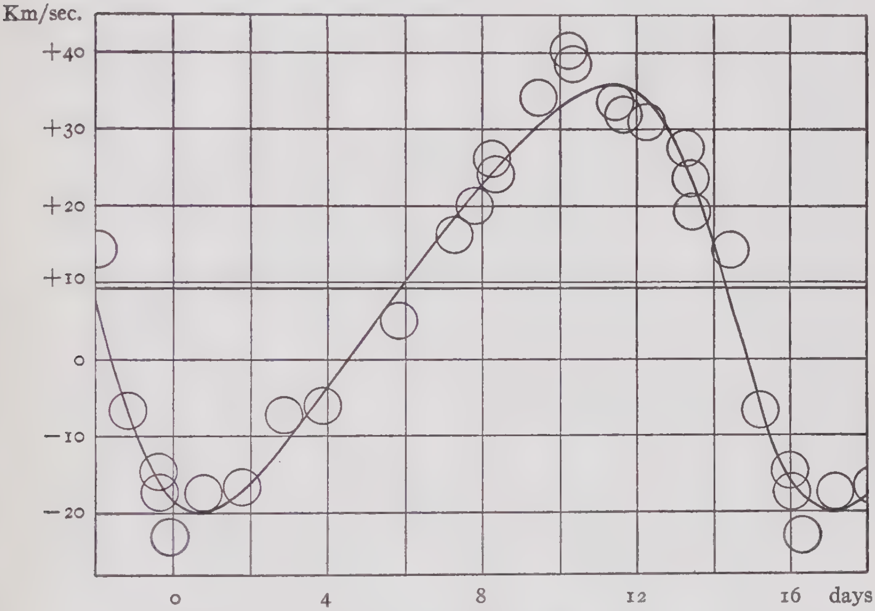

Fig. 1.—Velocity-curve of X Cygni. Abscissae are intervals after maximum light; the radius of the circles representing the observations is equal to the probable error of a single plate.

$K = 28.03 \pm 0.73$ km/sec.
$\omega = 98^\circ.2 \pm 14^\circ.9$
$e = 0.246 \pm 0.027$
$T = 14^{\mathrm{d}}.557 \pm 0^{\mathrm{d}}.523$
$\gamma = +9.32$ km/sec.

By the least-squares adjustment the sum of the squares of the residuals was reduced but slightly, from 78.07 to 76.24.

As ω and T were the only elements greatly changed, and as they showed the greatest probable errors, a second solution was made with these as the only variables. The results were

$$\begin{aligned} \omega &= 101\overset{\circ}{.}1 \pm 4\overset{\circ}{.}3, \\ T &= 14\overset{d}{.}685 \pm 0\overset{d}{.}169. \end{aligned}$$

The sum of the squares of the residuals was again slightly reduced, this time to 75.22. The finally adopted elements, from which the residuals given in Table I and the velocity-curve shown in Figure 1 were computed, are:

$$\begin{aligned} P &= 16\overset{d}{.}38543 \\ K &= 28.03 \text{ km/sec.} \\ \omega &= 101\overset{\circ}{.}1 \\ e &= 0.246 \\ T &= 14\overset{d}{.}685 \text{ after light maximum} \\ \gamma &= +9.32 \text{ km/sec.} \\ a \sin i &= 6{,}121{,}000 \text{ kilometers} \\ \frac{m_1^3 \sin^3 i}{(m+m_1)^2} &= 0.034 \end{aligned}$$

Maximum negative velocity occurs $0\overset{d}{.}7$ after maximum brightness
Maximum positive velocity occurs $1\overset{d}{.}1$ after minimum brightness

The values of K, $a \sin i$, and the mass function are considerably larger than in the case of any other Cepheid which has been spectroscopically investigated. The probable error of a single plate, computed from the residuals in Table I, is ±2.44 km/sec., a value much larger than the good agreement of the different measures on each plate might have led one to expect. There seems, however, to be no good evidence of a secondary oscillation in a period commensurate with that of the principal one.

MOUNT WILSON OBSERVATORY
August 1920

Contributions from the Mount Wilson Observatory, No. 197
Reprinted from *Astrophysical Journal*, Vol. LIII, pp. 121–132, 1921

AN EXAMINATION OF THE INFRA-RED SPECTRUM OF THE SUN, λ 8900–λ 9900

By FREDERICK S. BRACKETT

ABSTRACT

Photography of infra-red spectra to λ 9900.—In previous work scattered light has been a serious obstacle to the extension of observations into the infra-red. By using a monochrometer with the second slit removed the author *eliminated scattered light* and obtained, on plates sensitized with dicyanin, spectrograms of even intensity which show fine structure to λ 9850. This limit seems to be fixed in astronomical work by Langley's broad atmospheric absorption band ϕ. Below λ 9400 a *water solution of malachite green* is recommended as a *screen* since it is almost opaque to wave-lengths shorter than λ 7200.

Infra-red solar spectrum λ 8900 to λ 9900.—Spectrograms made in the first order of a 15-foot concave grating mounted in the constant temperature pit of the Pasadena laboratory gave the *wave-lengths* of 563 lines to about 0.01 A, at least as far as λ 9650 (Table I). To determine the *origin* of the lines, solar-rotation photographs were made with the 13-foot spectrograph of the 60-foot tower telescope, and spectrograms taken under conditions of low and high humidity were compared. It was found that 45 and possibly 70 lines, including one-fifth of the fainter lines observed, are of solar origin, while 60 of the stronger diffuse telluric lines broaden remarkably as the humidity increases and hence undoubtedly form an *absorption band due to water vapor between λ 9300 and λ 9650*. Of the solar lines, 14 are attributed to *iron* and 1 or 2 to *nickel*.

The investigator is naturally attracted to the less refrangible end of the spectrum by the fact that the characteristic displacements due to some of the most interesting spectroscopic phenomena increase with increasing wave-length, among them being the Doppler effect, the Zeeman effect, pressure shift, and the possible Einstein effect. But before work of precision can be done in any region, it is desirable, if not absolutely necessary, to make some preliminary survey of the field. In the case of the infra-red spectrum of the sun the work of Dr. Meggers, which he has been kind enough to furnish the Mount Wilson Observatory in advance of publication, gives identifications and wave-lengths down to 9000 A, and it is the purpose of the present investigation to extend these results as far as can readily be done with dicyanin-bathed plates.

Since Dr. Meggers published his map of the solar spectrum from 6800 A to 9600 A,[1] frequent attempts have been made to extend the limit to still longer wave-lengths by photography with plates bathed in dicyanin, but until recently the attempts have met with little success. In March, 1920, Dr. K. Burns[1] published his photographs showing the more outstanding structure to almost 9900 A. On all of these plates, however, much of the finer structure beyond 9200 A appears to have been lost. That the chief cause of this lack of contrast is scattered light there can now be little doubt. When the present investigation was first undertaken, it was believed that the chief difficulty was the loss of defining power in the lenses, due to a rapid change in the properties of the glass with increasing wave-length. But the appearance of a ghost of the B group between 9600 A and 9700 A on a plate taken with the 13-foot spectrograph of the 60-foot tower telescope seemed to prove that the presence of scattered light was responsible.

---

[1] *Astrophysical Journal*, **47**, 1, 1918.

In order to establish this fact with certainty, a series of tests was made in the laboratory with a one-meter concave grating. Exposures were first tried with a screen opaque to wave-lengths shorter than 6400 A. On these plates the contrast fell off rapidly beyond 9200 A, until even the strongest lines were lost at 9600 A. Exposures were then made through a water solution of malachite green. A screen more than a centimeter in thickness proved almost opaque to all wave-lengths shorter than 7200 A. Photographs taken with this screen were much superior to those previously obtained and showed lines well beyond 9750 A. For infra-red work at wave-lengths shorter than 9400 A this type of screen may be strongly recommended.

As screens opaque to still longer wave-lengths, and at the same time transparent beyond 9000 A, were not available, the only possibility of further progress lay in preliminary analysis. For this purpose a Hilger monochrometer with the second slit removed was set in collimation with the spectrograph. It was found that when the first slit of the monochrometer was open about two millimeters, light extending over several hundred angstroms was admitted to the slit of the spectrograph.

By calibrating the screw of the monochrometer, settings could be made which would admit any desired range of spectrum.

---

[1] *Lick Observatory Bulletins*, 10, 64 (No. 327), 1920.

PLATE XXI

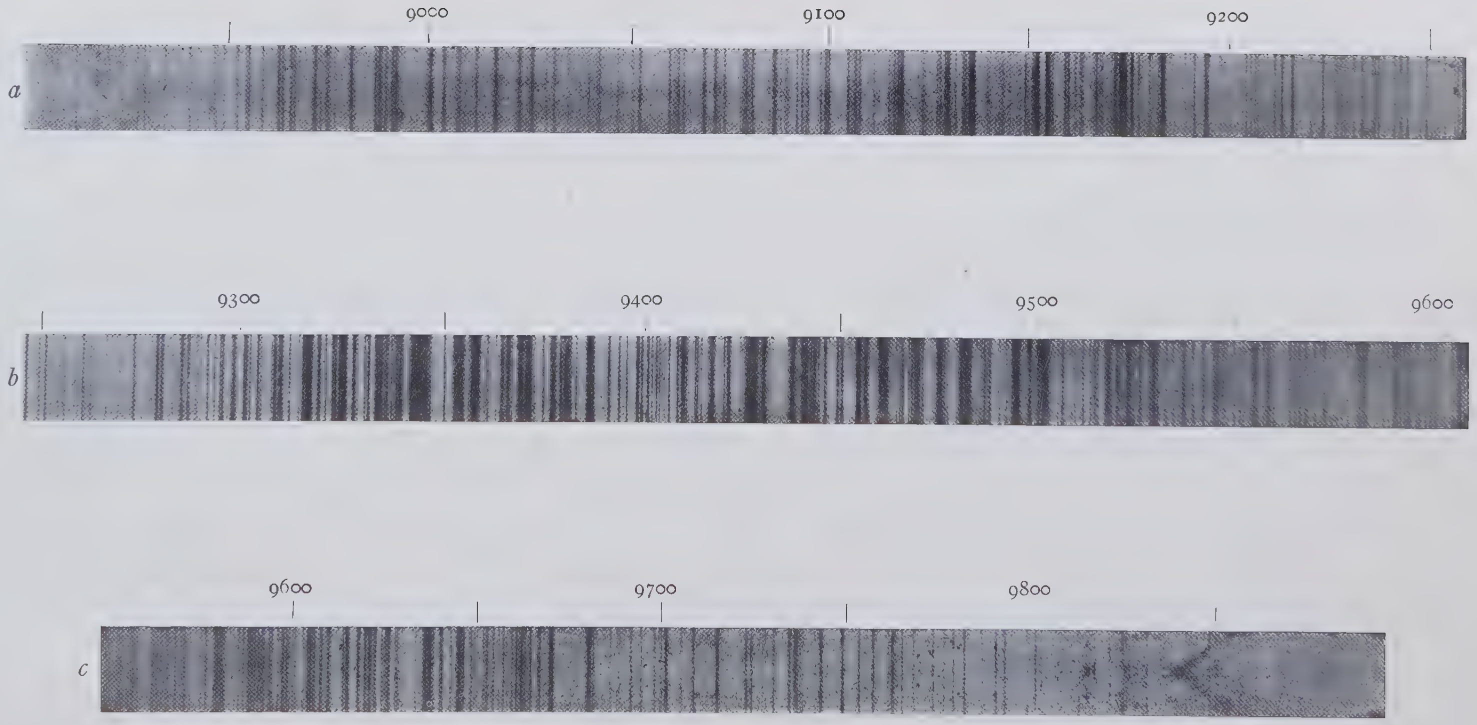

Infra-Red Spectrum of the Sun, λ8900–λ9900

Moreover, this adjustment could be changed during the exposures, so that the intensity could be adapted to the sensitiveness of the plate for a given wave-length. This made it possible, even in the extreme infra-red where the sensitiveness falls off rapidly, to obtain photographs of even density throughout a long range of spectrum. Plates made with this arrangement showed sharply defined lines as far as the slightest trace of continuous background could be detected.

The monochrometer was used with a 15-foot Anderson concave grating in a Rowland mounting placed vertically in a constant temperature pit, and photographs were taken which show the fine structure to 9800 A. The first order of the grating was used, giving a scale of about 3.7 A to the millimeter. Although the grating proved quite fast, the system was optically slow; the aperture ratio was *f*/45 and much of the light was lost because of the astigmatism characteristic of the Rowland mounting, when used at the large angle necessary for the infra-red, even in the first order.

The best dicyanin at hand at the time the investigation was begun was of old German stock, which proved slightly superior to that obtained from the Bureau of Chemistry of the Department of Agriculture. Exposures ranged from seven to twenty-one hours, extending over as many as three days. This is the most rigorous test to which the mounting in the constant temperature pit has been subjected and proves clearly its merit, since even these long exposures show practically no loss of definition. The longest exposure reveals lines to almost 9900 A; the portion of the spectrum between 9600 A and 9900 A shown on this photograph is reproduced in Plate XXI*c*.

In February of this year, however, a shipment of dicyanin labeled A VI–8 was received from the Bureau of Chemistry which proved much faster than anything previously used. Photographs on bathed Seed 23 plates were obtained in seven hours which showed lines beyond 9800 A.

In order to determine the wave-lengths of lines which could be used as a basis for the reduction of the plates, exposures were made on the same plate to the second-order iron arc and to the first-order infra-red solar spectrum. The light from the arc was thrown directly upon the slit by two small prisms on either side of the beam from the monochrometer. Because of astigmatism, however, all the lines extend entirely across the plates. All screening arrangements near the plate were avoided on account of the danger of moving the plate-holder. The arc exposure was made in five parts, distributed symmetrically throughout the solar exposure. The illumination of the grating by both arc and sun was carefully adjusted, so that any possible displacement due to differences in illumination would presumably be small. As the grating used is one of the most perfect, the coincidence of the two orders can be subject to little question. The two plates obtained agreed perfectly. It is to be regretted, however, that lack of time prevented checking them by a different set-up. In measuring these plates all lines were avoided which showed any suggestion of blend.

The rotation plates for the separation of the solar and telluric lines were taken with the 13-foot spectrograph of the 60-foot tower telescope, which projects an image of the sun about 6.7 inches in diameter. Although lenses are used in both collimator and camera of the spectrograph, it was found that a fair focus could be obtained over the whole region. The chief difficulty in the work proved to be the many adjustments necessary for both the monochrometer and the spectrograph. The 13-foot spectrograph is a two-lens system with one reflection, and the grating is set at a considerable angle, so that the dispersion is considerably greater than normal, thus giving a scale in the infra-red of the first order of 3.3 A to the millimeter. Although the aperture ratio of the system is limited by the telescope to *f*/60, being non-astigmatic, it proved over twice as fast as the 15-foot concave grating.

Because of the already complicated optical system, the use of prisms to unite the beams from the limbs of the sun was not attempted. A simple exposing screen in front of the slit was used. The exposure for one limb was made in two parts, one before and one after the exposure for the other limb, so that any mechanical shift would not introduce a displacement.

Photographs of the spectrum of the center of the sun were also taken, in order to determine the wave-lengths of the solar lines. As these plates were taken in the middle of August, a correction of

+0.009 A had to be added because the earth was then approaching the sun. Inasmuch as the period of exposure was longer in the afternoon than in the morning, a slight correction, −0.002 A, had to be subtracted. A total correction of +0.007 A has therefore been applied to all solar wave-lengths.

Fortunately, plates were secured at times of both high and low humidity. An examination of these plates on a comparator showed beyond 9300 A a remarkable broadening of the lines on photographs taken during high humidity, which is entirely independent of exposure time, appearing alike on plates of different densities. As the mean altitude of the sun was about the same for all exposures, there can be little doubt that this effect is due to water-vapor. In the list of wave-lengths only those lines which showed the most marked effect have been attributed to water-vapor, although it is quite likely that others than those so designated are due to this source.

The reduction of the rotation plates showed roughly 10 per cent of the five hundred lines measured to be of solar origin. Of these, fourteen may be attributed to iron and possibly one or two to nickel. In the region between 9300 A and 9650 A over sixty broad diffuse lines appear which are due to water-vapor.

In measuring the plates the chief emphasis has been laid on consistency. The wave-lengths recorded represent measures made on from two to eight plates. In the region from 9000 A to 9650 A the wave-lengths should be reliable to less than ±0.01 A, except where the line is marked with an "a." Beyond 9650 A the wave-lengths are determined by extrapolation, and systematic errors may enter.

On the first plates obtained intensities were estimated between 00 and 10, but on the later plates showing both fainter and broader lines, they were classified between 000 and 12. In the case of the water-vapor lines this classification is not altogether satisfactory, since at times of high humidity some of them extend over several angstroms. These lines also present special difficulty in measurement, not only because of their broad diffuse character, but also because they do not widen symmetrically with increasing humidity. Their wave-lengths are merely approximate.

TABLE I

λ	Intensity	Source Element	λ	Intensity	Source Element
9000.45	7B	....	9100.60	1	*A*, *S*, Fe
9003.81	6	....	9105.47	3	....
9007.02	0	*S*	9106.30	0	*S*, Ni
9007.63	1	....	9107.06	0 U	....
9008.57	000	*S*	9107.42	1	....
9009.09	0	....	9108.41	1V	....
9009.88	00	*S*	9110.57	000	*S*
9010.57	000	*S*	9111.92	0	*S?*
9011.95	4	....	9113.04	00	....
9016.80	5	....	9114.50	000	*S*
9018.12	0	....	9115.73	0	....
9021.68	000	*S*	9117.08	0R	....
9022.71	4	....	9118.09	1	....
9024.53	000	*S*, Fe	9118.98	3	....
9025.97	4	....	9124.37	0	*S*
9029.45	0	....	9124.93	00	....
9031.47	2	....	9127.87	1	....
9034.98	00	....	9128.65	1	....
9040.16	0	....	9129.90	1	....
9041.20	000	....	9130.70	3	....
9042.32	00	....	9132.53	1	....
9042.88	1	....	9134.36	1	....
9047.46	0	....	9134.87	0	*S?*
9048.62	000	....	9136.07	1	....
9051.18	00	....	9136.64	3	....
9053.03	2	....	9137.12	1	....
9060.49	1	....	9139.89	000	....
9061.52	00	*S*	9140.55	0	....
9061.87	00	....	9141.14	00	....
9062.77	1	....	9142.77	00	....
9064.08	1	....	9143.55	00	....
9069.20	4	....	9144.22	0	....
9070.43	000	*S*, Fe	9144.64	00	....
9072.03	5	....	9145.79	000	....
9073.20	00	....	9146.25	0	*S*, Fe
9074.36	3	....	9147.05	000	*S*
9078.33	00	*S*, Ni?	9148.02	00	*S*, Fe
9079.13*a*	00	....	9148.78	00	....
9079.84*a*	1	*A*, *S*, Fe	9150.12	1	....
9080.57	00	....	9150.88	0	....
9081.37	3	....	9151.85	0BR	....
9085.50	00	*S*, Ni?	9152.69	2	....
9086.71	2	....	9153.24	2	....
9087.08	4	....	9154.23	000	*S*
9088.49	0	*S*, Fe	9155.68	6BR	....
9089.55	00	*S*, Fe	9156.93	0	....
9089.94	0	....	9160.15	1	....
9090.42	00	....	9160.97	1	....
9092.58	1	....	9162.69	0V	....
9093.85	1	....	9164.05	0BR	....
9095.01	1	*S*	9167.38	00	....
9095.38	0	....	9168.01	1	....
9098.52	0	....	9168.88	0	*S?*
9099.83	2	....	9169.43	0	....

TABLE I—*Continued*

λ	Intensity	Source Element	λ	Intensity	Source Element
9170.78	00	....	9251.19	2	....
9171.76	00	....	9252.53	00	*S*
9172.58	0	....	9253.23	00	*S*
9172.97	00	....	9253.84	00	*S*
9173.06	0	....	9254.44	0	....
9174.23	3	....	9255.29	00	*S?*
9175.31	2	....	9255.87	1	*S*
9176.97	3	....	9257.01	00	....
9178.62	1	....	9258.36	0	*S*, Fe
9179.39	000	....	9259.17	0	*S?*Fe
9181.30	1	....	9260.45	1	....
9182.15	000	....	9261.06	00	....
9183.59	00	....	9261.67	00	....
9184.48	2	....	9262.35	0	....
9185.06	2	....	9263.16	00	....
9186.56	00	....	9263.97	000	*S*
9190.33	0	....	9266.26	1	....
9191.71	00	....	9267.22*a*	00	....
9192.67	2	....	9269.17	0	....
9195.46	2	....	9270.14	00	*S?*
9196.12	2	....	9270.88	00	*S?*
9199.20	00	....	9272.30	0	....
9205.69	0	....	9273.14	2	....
9206.93	0	....	9274.32	00	....
9207.90	0	....	9275.16	0	....
9208.70	0	....	9275.80	00	....
9210.09	0	*S*, Fe	9276.31	000	....
9212.92	2	....	9276.92	00	....
9214.74	3	....	9277.60	0	....
9215.70	00	....	9278.91	4	....
9217.35	4	....	9279.83	1	....
9218.36	00	*S*	9280.21	0	....
9222.10	0	....	9281.99	0	....
9225.10	2	....	9282.78	0	....
9228.19	00	*S*	9284.22	00	....
9228.76	00	....	9284.98	2	....
9229.70	00	....	9285.70	00	....
9230.58	00	....	9286.53	1	....
9232.84	1	....	9286.90	0	....
9234.85	1	....	9288.09	000	*S*
9235.30	00	....	9288.60	00	*S?*
9235.83	00	....	9288.98	00	*S?*
9237.49	0	*S*	9289.95	0	*S?*
9238.18	1	....	9290.59	00	*S*
9239.07	1	....	9291.43	3	....
9240.03	000	*S*	9292.78	0	....
9240.45	00	....	9293.23	1	....
9242.33	00	*S*, Fe	9294.56	2	....
9243.10	0 U	....	9295.21	3	....
9243.41*a*	00	....	9296.50	00	....
9244.53 44.74	1 2D	....	9297.23	00	....
9244.93	1	....	9297.80	4	....
9246.41	3	....	9298.70	0	....
9249.57	0	....	9300.53	3	....

TABLE I—*Continued*

λ	Intensity	Source Element
9301.14	2	
9301.98	2	
9302.77	00	
9303.92	4	
9304.66	1	
9305.48	00	
9306.34	00	
9307.30	1	
9308.14	4	
9308.97*a*	0	
9309.62	5–9	*w*
9310.91*a*	00	
9311.80	2	
9312.72	000	
9314.08	1	
9315.21	3	
9316.11*a*	4–8 } U	*w*
9319.14*a*	5–9 }	*w*
9320.12	0	
9320.83*a*	4–6	*w*
9321.76	00	
9322.55	3	
9323.20	3	
9324.24	3– }	
9325.06*a*	1 } –9D }	*w*
9325.67*a*	4 } }	*w*
9326.71*a*	00	
9327.82	4	
9328.80	1	
9329.93	00	
9330.53	1	
9331.52	2	
9333.55*a*	5–8 } U	*w*
9334.64*a*	4–7 }	*w*
9335.69	0 }	
9336.13	1 }	
9337.23	3	
9337.88	0	
9338.52	2 } U	
9339.47*a*	5–8 }	*w*
9342.52*a*	6–8 }	*w*
9344.05*a*	9D–12 }	*w*
9345.67*a*	6–8 }	*w*
9346.98	2 }	
9347.70	0	*S?*
9348.46	1	
9349.31	00	
9350.52	3 } U	
9352.01	00 }	
9353.06*a*	3–5 }	*w*
9353.65*a*	3–4 }	*w*
9354.50*a*	5–7 }	*w*
9355.26*a*	1–3 }	*w*
9356.58	1	
9357.55*a*	6–9 } U	*w*
9358.93*a*	5–8 }	*w*
9360.24	000 }	
9360.60	00 }	
9361.28	2	
9361.93	00	
9362.33	0	*S*, Fe
9363.39	1V	
9364.95*a*	4–8 }	*w*
9366.46*a*	5 } 10 }	*w*
9367.41	1B } }	
9369.60*a*	5–9	*w*
9371.58*a*	7B–12B	*w*
9373.14	2	
9374.34	0	
9375.28	3	
9375.74*a*	00	
9377.74*a*	7–11	*w*
9379.74*a*	3–5	*w*
9381.22*a*	7–11 } U	*w*
9382.22	2 }	
9383.63	2	
9385.84*a*	00	
9386.84*a*	7–11 }	*w*
9387.91	3 }	
9390.88	0	
9391.84	3	
9394.43	3	
9396.32	2	
9400.18	2	
9401.68	3BV	
9402.67	1	
9403.31	00	
9404.51	1	
9405.30*a*	00	
9405.78	00B	*A, S?*
9406.96	3	
9408.00	00	
9409.10	3	
9410.44*a*	5–8	*w*
9411.38 } 11.91	1 } 0	*S?*
9412.75 }	1 }	
9413.55	2	*A,S?*
9414.10	2	*A,S?*Fe?
9415.07	1	*S*
9416.08	00	
9416.87	0	*S*
9417.72*a*	4–7	*w*
9420.09	00	
9420.81	0	
9421.90	4	
9424.89	0	
9426.85*a*	7–11 } U	*w*
9428.36*a*	7–10 }	*w*

TABLE I—*Continued*

λ	Intensity	Source Element	λ	Intensity	Source Element
9430.68*a*	5V–8V	*w*	9500.76*a*	6}–12D	*w*
9432.03*a*	000	*S?*	9501.71*a*	4}	*w*
9432.85	00	*S*	9503.30	00B	....
9434.97	00	....	9504.51	1	....
9437.90*a*	7–10 Wings	*w*	9505.68	3B	....
9440.89*a*	10D–14D	*w*	9506.81	00	....
9442.48	1	....	9507.82	0B	....
9443.39*a*	3–5	*w?*	9508.86	0B}	....
9444.47	2	....	9509.38	00}	....
9446.08	4	....	9510.83	2	....
9447.13	00	....	9512.69	1	....
9449.22	2	....	9513.82	1	....
9450.38	3	....	9514.55	1	....
9452.65	00	....	9516.35*a*	1}	....
9454.12*a*	3–5}	*w?*	9517.06*a*	6}–12U	*w*
9454.79*a*	3–5}	*w?*	9518.05	1}	....
9456.22*a*	4–7	*w*	9519.34*a*	3–5}	*w*
9456.98*a*	0–2	*w?*	9520.04*a*	0}	....
9459.96*a*	6–10	*w*	9520.62	00	....
9461.16*a*	7–11	*w*	9522.30*a*	7–12	*w*
9463.03	00	....	9523.62	1	....
9464.05	0	....	9525.16	4	....
9464.88	1	....	9526.91	00	....
9465.52	2	....	9527.60	1	....
9467.12	1	....	9528.53	3BR	....
9467.90	1	....	9529.51	2	....
9468.68	2	....	9531.30	0	....
9469.50	3	....	9531.79	1	....
9470.57	2	....	9533.48	1	....
9471.63	000	*S?*	9535.00	00B	....
9472.51	00	....	9536.12*a*	4–6	*w*
9473.14	00B	....	9538.47	4	....
9474.36	5B}U	....	9540.98	5	....
9475.27	3}	....	9543.93*a*	6–11D	*w*
9476.07	2	....	9544.61	2	....
9476.85	2	....	9545.92	1	....
9478.99	00	....	9546.63	0	....
9480.23*a*	5–7	*w*	9547.15	00	....
9481.97*a*	7 2}–11D	*w*	9548.75	3	....
			9550.05	2R	*A, S*
9484.04	00	....	9550.42	1	....
9485.17	00	....	9551.02	1	....
9486.10	2	....	9553.48*a*	5–7}U	*w*
9486.95	0}	....	9554.51*a*	3–5}	*w*
9487.49	1}	....	9556.11	2	*S*
9489.86	1	....	9557.33*a*	4–6	*w?*
9491.61	1	....	9558.49	3	....
9493.41*a*	4–6}U	*w*	9558.89	3	....
9494.49*a*	6–8}	*w*	9559.70*a*	000	*S*
9496.54	0B}	....	9562.70	4	....
9497.51*a*	5–7}	*w*	9563.91	3	....
9498.88	00	....	9565.11	3	....
9499.60*a*	3–5	*w*	9566.66*a*	4–7	*w*

TABLE I—*Continued*

λ	Intensity	Source Element	λ	Intensity	Source Element
9568.91*a*	3–5	*w*	9640.26	1}	*S?*
9570.42	1B		9640.68	2}	
9571.38*a*	3–5	*w*	9643.17	1	*S?*
9572.85	1		9645.06*a*	2}–8D	*w*
9574.42	0		9645.59*a*	2}	*w*
9575.75	1		9646.50	2	
9577.10	2		9648.68*a*	1–3	*w?*
9579.36*a*	0–2	*w?*	9649.53	0V	
9580.05*a*	3–5	*w?*	9650.28	00	*S*, Fe?
9581.12*a*	3–5}U	*w*	9651.02*a*	00}	
9581.84*a*	2–4}	*w*	9651.33*a*	00}	
9583.66	0		9651.97	1	
9584.82	0		9652.90	2	*A*, *S*
9585.92	2D		9653.64	000	
9587.17	3		9654.68	2	*S*, *A*, Fe?
9588.57	4}		9656.17	1V	
9589.32	5}		9657.37	2	
9590.28	4		9658.47	0	*S?*
9592.00	2}		9659.78	2	
9592.62	3}		9660.92	3	
9594.20	2		9662.36	3V	
9594.86	2		9663.26	0	
9596.46	1B		9664.04	00	
9597.84	4D		9664.68	3R	
9598.91	2		9666.59	1}	
9599.60	0		9667.21	2}	
9600.55	0		9668.27	0	
9601.22	2		9670.04	2V	
9603.43	1V		9670.67	3V	
9604.62	2}	*S?*	9680.41	4	
9605.24	2}		9681.10	0	
9606.22	2		9681.82	1	*S?*
9608.11	4B		9682.70	00	
9610.11	2		9684.25	0B	
9610.69	00		9685.81	00	
9614.13	1		9686.44	2	
9615.26	5D		9688.72	0	
9618.14	3R		9690.21	00	
9620.08	2		9691.93	3	
9621.28	3	*A*, *S?*	9693.99	00	
9622.74	3		9694.74	0B	
9624.56	2		9698.32	2	
9625.32	0}		9699.68	00}	
9625.83	0}		9700.15	0}	*S?*
9626.40	2	*A*, *S?*	9701.47	3	
9628.20	1		9705.53	00B	
9628.74	1		9708.97	1	
9629.32	000		9715.33	4	
9630.06	00		9723.18	2	
9633.58	00		9724.62	2	
9636.16*a*	4–9	*w*	9730.66	1	
9637.58*a*	4–7	*w?*	9735.07	3BV	
9638.45	1	*S*	9736.63	5BDR	

TABLE I—*Continued*

λ	Intensity	Source Element	λ	Intensity	Source Element
9737.83*a*	0	....	9782.35	2	....
9738.54*a*	0	....	9787.19*a*	0	....
9743.53	3B	....	9791.09	2	....
9749.36	3	....	9793.38*a*	1B	....
9753.90	2	....	9795.26*a*	00	....
9757.74	2	....	9799.52	2	....
9761.73*a*	00	....	9801.78	2	....
9762.90	2BR	....	9803.27	1	....
9764.14*a*	00B	....	9813.48*a*	0	....
9765.51	2B	....	9817.70*a*	00	....
9768.71*a*	0B	....	9825.57*a*	00	....
9774.00	2B	....	9831.97*a*	0	....
9776.84	1	....	9848.89*a*	0	....
9779.46	2	....			

The separation of the solar and telluric lines is based chiefly upon two rotation plates. As the Doppler displacement due to solar rotation is of the order of 0.13 A, there is little doubt as to the origin of well-defined lines. But if the lines are diffuse, unsymmetrical, or blended, question arises. If noticeable displacement occurs on one plate but not on the other, a question mark has been placed after the *S*, which is used to indicate lines of solar origin. If the evidence of blending is unmistakable it has been indicated by *A*, *S*. Lines due to water-vapor have been indicated by *w*, and lines showing decided asymmetry by V or R placed after the intensity, according as the line is shaded to the violet or the red, respectively. Where lines were not completely resolved, it has been indicated by joining the intensities by brackets. Where they were practically unresolved, U has been placed after the bracket. Broad lines have been indicated by B.

In conclusion it may be stated that the monochrometer, used instead of a screen, has certain unquestionable advantages over any of the screens at present available: (1) it removes all scattered light from the background and makes it possible, by increasing the exposure sufficiently, to obtain the very faint lines, which are especially important in the region under investigation; (2) it is faster than the battery of screens found necessary to remove even the major portion of the extraneous light in the region beyond

9400 A; (3) it presents for any limited portion of the region a very convenient method of grading the exposure to suit the sensitiveness of the plate.

The results of the investigation show (1) that at least one-fifth of the lines of 0 intensity or less are of solar origin; (2) that one-third of these solar lines are due to iron; (3) that a very strong water-vapor band exists between 9300 A and 9650 A.

The fact that in the present case, as well as in the recent work by Burns and also in the early investigations of Abney, it was found impossible to photograph beyond 9900 A is probably to be explained by the presence of the strong absorption band at about 1 μ, which was designated by Langley[1] by the symbol ϕ. The rapidly falling sensitiveness of the plates renders it impossible to photograph any portion of the spectrum beyond this band.

I am indebted to Mrs. Brackett for the computation and reduction of the measures, and to Dr. St. John and Mr. Babcock for furnishing me with wave-lengths in both sun and iron arc based on the International system. It gives me great pleasure to express my appreciation to these and also to other members of the staff for their interest and help.

Mount Wilson Observatory
September 1920

---

[1] *Annals of Smithsonian Astrophysical Observatory*, 1, 1900.

Contributions from Mount Wilson Observatory, No. 198
Reprinted from *Astrophysical Journal*, Vol. LIII, pp. 133–143, 1921

THE VARIATION WITH TEMPERATURE OF THE ELECTRIC FURNACE SPECTRUM OF MANGANESE

By ARTHUR S. KING

ABSTRACT

Variation of the electric furnace spectrum of manganese with temperature to 2400°.—The spectrum produced in the tube-resistance furnace at 1700°, 2000°, and 2400° C. was examined from λ 2795 to λ 8200: but no lines were found beyond λ 6500. Table I contains the relative intensities of the lines in the arc spectrum and in the furnace spectra for the three temperatures; it also gives the *temperature classification* of these lines according to the method used in previous articles. Some lines observed at 1560° C. are given in Table II; the triplet λ 4031 to λ 4035 was still strong and well reversed at this low temperature. As with other furnace spectra, the ultra-violet wave-length limit is shorter the higher the temperature. In the discussion the interesting behavior of some of the lines is pointed out. None of the enhanced lines given by Lockyer occur in the furnace spectrum.

The following results for the furnace spectrum of manganese were obtained by the methods used in previous studies of metallic spectra.[1] Manganese metal was used in the tube furnace, the inclosing chamber being pumped to a pressure of a few millimeters. Temperatures of approximately 1700°, 2000°, and 2400° C., designated as "low," "medium," and "high," respectively, were employed in studying the range of spectrum from λ 2800 to λ 6600. The peculiarities of the spectral lines as regards the temperature at which they first appear and the rate of increase with rising temperature have been tabulated from these data.

The spectrograms were made for the most part with the first and second orders of a fifteen-foot concave grating, while the very bright spectra given by the second order of a one-meter grating were used for a few photographs.

The operation of the furnace, when the tube was charged with manganese, was without notable features other than the lack of carbide formation, in which this metal contrasted strongly with iron. Instead of sticking to the tube and gradually eating through, the manganese vaporized and then, in diffusing from the tube, condensed in the cooler portions at the ends, leaving but little residue in the hotter region. This necessitated frequent renewal of the charge of metal during the run.

---

[1] *Mt. Wilson Contr.*, Nos. 66, 76, 94, 108, 150, 181; *Astrophysical Journal*, **37**, 239, 1913; **39**, 139, 1914; **41**, 86, 1915; **42**, 344, 1915; **48**, 13, 1918; **51**, 179, 1920.

In order to hold the temperature unchanged during the rather long exposures at low and medium temperatures, direct current from a large generator was frequently used on account of the close adjustment of voltage which can be made. As in the case of the iron spectrum,[1] no difference was observed between the effects of direct and alternating currents at a given temperature.

EXPLANATION OF TABLE I

The first column of Table I gives the arc wave-lengths measured by Exner and Haschek,[2] except in a few cases for which the wave-lengths of close doublets, on the International System, were taken from the measures of Kilby.[3] Frequent references to notes at the end of the table are indicated by asterisks, while a dagger means that the line was found by Kilby to be decidedly stronger in the spark than in the arc.

As in previous papers, the remaining columns give the intensity estimates for lines in the arc and for three furnace temperatures. Nebulous lines are indicated by "n" after the value of the intensity, while "r" and "R" indicate partial and complete self-reversal. Lines of Class I and Class II are strong at low temperature, those of Class II strengthening more rapidly as the temperature rises. Lines of Class III are absent or faint at low temperature, but appear at medium temperature, and are usually considerably stronger at high temperature. Class IV appears at the highest furnace temperatures, while Class V is usually absent in the furnace. "A" after the class number indicates that the line in question is relatively weak in the arc—usually not more than half as strong as in the high-temperature furnace.

---

[1] *Mt. Wilson Contr.*, No. 193; *Astrophysical Journal*, **52**, 187, 1920.

[2] *Spektren der Elemente bei normalem Druck*, Leipzig, 1911.

[3] *Astrophysical Journal*, **30**, 243, 1909.

TABLE I

TEMPERATURE CLASSIFICATION OF MANGANESE LINES

λ (EXNER AND HASCHEK)	ARC INTENSITY	FURNACE INTENSITIES			CLASS
		High Temperature	Medium Temperature	Low Temperature	
2794.92......	500R	500R	....	....	IV
2797.05......	5	1	....	....	IV
2798.37......	400R	400R	....	....	IV
2799.99......	10	2	....	....	IV
2801.20......	400R	400R	....	....	IV
2804.24......	7	3	....	....	IV
2806.25......	6	2	....	....	IV
2808.12......	5	2	....	....	IV
2809.20......	7	2	....	....	IV
2812.99......	7	2	....	....	IV
2813.60......	7	2	....	....	IV
2814.09......	4	....	....	....	V
2818.09......	8	3	....	....	IV
2818.85......	6	1	....	....	IV
2821.58......	5	2	....	....	IV
2822.68......	6	2	....	....	IV
2823.40......	2	1	....	....	IV
2824.5.......	8n	....	....	....	V
2826.8.......	15n	....	....	....	V
2830.92......	6	2	....	....	IV
2836.43......	3	1	....	....	IV
2858.85......	6	1	....	....	IV
2872.68......	5	1	....	....	IV
2892.77†.....	5	....	....	....	V
2907.32......	7	....	....	....	V
2914.71......	50	15	1	....	IV
2925.67*.....	70	8 10	1	....	IV
2928.79......	7	....	....	....	V
2930.35......	5	2	....	....	IV
2933.19†.....	25	tr	....	....	V
2934.13......	6	....	....	....	V
2938.00......	8n	....	....	....	V
2939.40†.....	30	tr	....	....	V
2940.01......	5	....	....	....	V
2940.330*....	10	8	1	....	IV
2940.512*....	10n	5		....	IV
2941.15......	7	1	....	....	IV
2949.31†.....	30	2	....	....	IV
3007.80......	6	1	....	....	IV
3008.35......	4	....	....	....	V
3011.30......	5	tr	....	....	IV
3011.52......	7	1	....	....	IV
3014.82......	5	....	....	....	V
3016.60......	8	1	....	....	IV
3022.90......	10	2	....	....	IV
3040.76......	12	4	....	....	IV
3041.35......	4	....	....	....	V
3042.87......	4	....	....	....	V
3043.46......	9	3	....	....	IV

TABLE I—*Continued*

λ (Exner and Haschek)	Arc Intensity	Furnace Intensities			Class
		High Temperature	Medium Temperature	Low Temperature	
3044.69......	50	7	4	....	III
3045.70......	12	4	....	....	IV
3045.90......	5	....	....	....	V
3047.14......	15	5	1	....	IV
3048.95......	5	1	....	....	IV
3054.53......	40	8	5	....	III
3062.30......	20	5	2	....	III
3066.19......	20	5	2	....	III
3070.46......	20	6	3	....	III
3073.33......	20	7	2	....	III
3079.80......	15	6	1	....	IV
3081.52......	10	5	....	....	IV
3097.18*.....	8	1	....	....	IV
3100.43......	5	2	....	....	IV
3101.67*.....	5	4?	3?	....	III?
3110.86......	6	1	....	....	IV
3115.60......	6	....	....	....	V
3120.54......	4	....	....	....	V
3142.80......	4	....	....	....	V
3148.36......	15	5	1	....	IV
3161.19......	15	6	1	....	IV
3178.61......	15	7	1	....	IV
3207.00......	5	3	....	....	IV
3212.98......	15	9	5	1	III
3217.04*.....	8	?	?	2	II
3224.90*.....	10	?	?	2	II
3226.15......	6	5	1	....	IV
3228.20......	30	20	12	6	II
3230.81......	12	10	7	2	III
3234.0.......	15n	2	....	....	IV
3235.1.......	10n	2	....	....	IV
	15n	3	....	....	IV
3236.90......	20	15	10	5	II
3237.4.......	20n	5	....	....	IV
3240.53......	7	10	2	....	III
3240.75......	5	6	1	....	IV
3243.93......	12	12	6	1	III
3248.64......	15	15	8	3	III
3251.27......	5	6	1	....	IV
3253.09......	12	12	7	2	III
3254.14......	5	4	....	....	IV
3256.25......	12	12	7	2	III
3258.52......	10	12	5	1	III
3260.40......	10	12	3	1	III
3264.83......	10	15	5	1	III
3267.90......	4	....	....	....	V
3268.83......	3	....	....	....	V
3270.49......	3	....	....	....	V
3273.15......	3	....	....	....	V
3278.65......	5	6	....	....	IV
3280.90......	5	6	....	....	IV
3296.16......	4	2	....	....	IV

TABLE I—*Continued*

λ (Exner and Haschek)	Arc Intensity	Furnace Intensities			Class
		High Temperature	Medium Temperature	Low Temperature	
3297.01......	6	8	1	....	IV
3298.35......	5	2	....	....	IV
3303.40......	3	....	....	....	V
3312.05......	6	3	....	....	IV
3313.41......	5n	2	....	....	IV
3313.70......	4	1	....	....	IV
	4	1	....	....	IV
3314.59......	6n	3	....	....	IV
3315.07......	6n	3	....	....	IV
3316.47......	4	2	....	....	IV
3316.61......	5n	1	....	....	IV
3317.47......	10n	5	....	....	IV
3320.82......	6	5	....	....	IV
3330.80......	8	8	1	....	IV
3343.85......	4	2	....	....	IV
3345.47......	4	2	....	....	IV
3420.95......	4	....	....	....	V
3439.13......	6	....	....	....	V
3442.13†.....	30	....	....	....	V
3460.45†.....	25	....	....	....	V
3474.20†.....	12	....	....	....	V
3474.27†.....	10	....	....	....	V
3483.22†.....	20	....	....	....	V
3488.80†.....	20	....	....	....	V
3495.99†.....	10	....	....	....	V
3496.96......	6	....	....	....	V
3497.66†.....	8	....	....	....	V
3531.94†.....	30	10	6	1	III
3532.14†*....	50	15	10	3	III
3532.27†*....	50	15	10	3	III
3547.91†.....	50	20	12	4	III
3548.18†.....	40	20	12	3	III
3548.33†.....	30	10	6	2	III
3569.61†.....	60	30	15	6	III
3569.95†.....	40	20	10	2	III
3570.17†.....	20	8	3	....	III
3577.99*.....	40	?	15	8	II
3586.69*.....	30	?	7	3	II
3595.29......	20	12	4	1	III
3607.69......	20	10	10	4	II
3608.66......	20	10	10	4	II
3610.49......	20	10	8	2	III
3619.42......	15	10	8	1	III
3623.96......	15	8	6	1	III
3629.89......	12	5	4	tr	III
3660.58......	5	....	....	....	V
3670.00......	4	2	1	....	III
3670.67......	5	3	2	....	III
3677.13......	4	....	....	....	V
3682.23......	4	....	....	....	V
3693.83......	6	....	....	....	V
3696.70*.....	8	....	....	....	V

TABLE I—*Continued*

λ (Exner and Haschek)	Arc Intensity	Furnace Intensities			Class
		High Temperature	Medium Temperature	Low Temperature	
3701.88*.....	4	?	2	....	III
3706.23......	5	....	....	....	V
3719.06......	5	....	....	....	V
3732.05......	5	....	....	....	V
3790.38......	10	8	8	2	III
3799.40*.....	4	?	2	....	III
3800.70......	4	....	....	....	V
3802.05......	4	....	....	....	V
3806.90......	20r	15	15	15	I
3809.75*.....	10	?	10	5	II
3816.90......	5	3	3	1	III
3823.64......	20r	15	15	10	II
3824.03*.....	10	?	10	4	II
3829.80*.....	5	?	4	1	III
3834.01*.....	8	?	8	5	II
3834.50......	12	12	12	8	II
3839.90*.....	8	?	6	3	II
3841.23......	10	8	8	4	II
3844.12*.....	7	?	6	3	II
3918.46......	3	....	....	....	V
3921.94*.....	3n	?	tr	....	IV
3924.23*.....	3	?	tr	....	IV
3926.63......	10	....	....	....	V
3929.41......	2	2	....	....	IV
3953.00......	3	....	....	....	V
3985.40......	3	....	....	....	V
3986.98......	3	....	....	....	V
4018.28......	20	20	20	15	I
4026.58......	4	....	....	....	V
4030.92......	200R	200R	200R	200R	I
4033.21......	150R	150R	150R	150R	I
4034.62......	100R	100R	100R	100R	I
4035.88......	15	15	15	12	I
4041.53......	50r	35	30	25	I
4045.31*.....	4	....	....	....	V
4048.90......	15	15	12	10	I
4055.70......	20	20	18	15	I
4058.10......	4	....	....	....	V
4059.09......	10	12	10	8	I
4059.54*.....	5	?	tr	....	IV
4061.90......	5	....	....	....	V
4063.70*.....	8	8?	8?	6?	I
4070.48......	5	6	5	3	II
4079.38......	12	15	12	10	I
4079.61......	10	12	10	8	I
4083.11......	12	15	15	12	I
4083.82......	12	15	15	12	I
4235.125*....	6	2	2	1	II
4235.306*....	8	6	6	4	I
4239.90......	5	2	2	1	II
4257.83......	5	2	2	1	II
4266.10......	6	2	2	1	II

TABLE I—*Continued*

λ (Exner and Haschek)	Arc Intensity	Furnace Intensities			Class
		High Temperature	Medium Temperature	Low Temperature	
4281.30......	6	3	3	2	II
4312.71*.....	3	?	1	tr	II
4412.04......	3	1	....	....	IV
4415.04......	10	6	5	3	II
4436.52......	8	6	4	1	III
4451.78......	15	12	10	6	II
4453.19......	6	5	3	1	III
4455.20......	5	4	2	tr	III
4455.51*.....	6	?	3?	1?	III?
4456.02......	6	5	2	tr	III
4457.22......	5	3	1	tr	III
4457.76*.....	8	?	?	?	?
4458.48......	12	8	4	2	II
4460.59*.....	3	?	?	?	?
4461.30......	8	4	2	tr	III
4462.20......	20	12	6	2	III
4464.88......	8	8	5	3	II
4470.33......	6	6	4	1	III
4472.98......	5	5	3	1	III
4490.27......	5	6	4	1	III
4499.09......	7	8	6	2	III
4502.40......	7	8	6	2	III
4605.52......	4	....	....	....	V
4626.69......	4	3	2	....	III
4671.89......	3	....	....	....	V
4701.31......	3	....	....	....	V
4709.89......	10	6	4	1	III
4727.70*.....	10	?	4	1	III
4739.30......	8	6	3	1	III
4754.24......	50	50	60	40	I
4761.73......	10	10	6	1	III
4762.60......	30	25	20	5	III
4766.08......	10	10	8	2	III
4766.63......	20	20	15	4	III
4783.62......	50	50	60	40	I
4823.71......	50	50	60	40	I
4966.03......	3	3	2	....	III
5005.03......	2	2	1	....	III
5017.77......	2	....	....	....	V
5074.92......	2	....	....	....	V
5118.10......	3	....	....	....	V
5151.10......	3	....	....	....	V
5196.76......	3	3	2	....	III
5197.40......	1	1	....	....	IV
5255.48......	4	4	3	....	III
5341.25*.....	20	50	25	4	IIIA
5377.86......	6	1	tr	....	III
5394.89......	10	30r	30	30	IA
5399.70......	4	2	1	....	III
5407.67......	5	10	8	2	IIIA
5413.90......	2	1	....	....	IV
5420.61......	10	20	15	3	IIIA

TABLE I—*Continued*

λ (Exner and Haschek)	Arc Intensity	Furnace Intensities			Class
		High Temperature	Medium Temperature	Low Temperature	
5432.75	4	35	35	35	IA
5457.64	1	2	2	1	IIA
5470.88	8	20	10	4	IIA
5481.61	4	10	5	2	IIA
5506.10*	2	?	3	1	III
5517.00	7	20	10	2	IIIA
5537.99*	5	?	5	1	III
6013.74	30	30	6	1	III
6016.90	40	40	10	2	III
6022.05	50	50	12	3	III
6384.88	4	....	....	....	V
6413.77	2	4	2	....	IIIA
6441.14	8	2	....	....	IV
6491.92	15	3	....	....	IV
6605.7	6n	....	....	....	V

λ	Remarks
2926	Close doublet, just resolved.
2940.3, 2940.5	Doublet measured by Kilby. Exner and Haschek give 2940.50.
3097	Double. Arc components about equal.
3102	Furnace line may be partly Ni.
3217, 3225	Pure absorption lines at high temperature. Partial absorption at medium temperature.
3532.14, 3532.27	λ's by Hasselberg. Exner and Haschek give 3532.20.
3578–3587	Disturbed by carbon.
3697	Close doublet.
3702	Concealed by continuous ground at high temperature.
3799–3844	Disturbed by carbon.
3922, 3924	Concealed by continuous ground at high temperature.
4045	Close doublet.
4060	Disturbed by carbon.
4064	Blend Fe. Probable intensity of Fe line subtracted.
4235	Doublet measured by Kilby. Exner and Haschek give 4235.41.
4313	Disturbed by carbon.
4455–4457–4460	Blend with impurity lines.
4728	Disturbed by carbon.
5341	Probably double.
5506, 5538	Disturbed by carbon.

DISCUSSION OF RESULTS

Several groups of lines whose behavior is of special interest may be noted. The first is the strong triplet at λλ 2795, 2798, 2801. These lines reverse widely in the high-temperature furnace. The emission wings fill up the space between the lines, but are of low density. The effect is that of three absorption lines on a weak continuous ground. No temperature stage has been found which gives these as narrow emission lines. Presumably they will occur as such at high temperature when a trace of manganese is present, though an examination of some iron spectrograms failed to show them. At reduced temperature the lines are not narrow or indeed visible at all, because the furnace spectrum does not then extend so far into the ultra-violet. This is a peculiarity often met with in furnace spectra; lines in the ultra-violet having the characteristics of low-temperature lines require high temperatures for their production because the low-temperature spectrum ceases before this wave-length is reached. The effect is so general with different elements that there seems to be no reason to ascribe it to absorption by a vapor within the furnace.

At about λ 3000, the medium temperature begins to show some lines distinctly. The prominent lines up to this point, in addition to the λ 2800 triplet, are those of the series triplet λλ 2915, 2926, 2941, of which the last two are clearly complex and probably also the first. The components of λ 2926 are resolved in the furnace spectrum. This triplet is given by Kayser and Runge[1] as belonging to the same series as λλ 3532, 3548, 3570, lines which are also complex; but the two triplets appear in different temperature classes because the member of shorter wave-length occurs at the extreme limit of the medium-temperature spectrum.

λλ 3217 and 3225 show a peculiar behavior. At high temperature they are simple absorption lines, with no sign of emission wings. Their strength at medium temperature is uncertain, the emission being partly neutralized by absorption, while at low temperature they are sharp emission lines. No other lines of this type occur in the spectrum.

The tendency, which prevails throughout the spectrum, for lines of similar type to appear in groups is illustrated by those from λ 3442 to λ 3498. They are absent in the furnace but strong in the arc, and yet stronger in the spark. They are thus enhanced lines of intermediate type. None of the enhanced lines given by Lockyer[2] occur in the furnace spectrum.

---

[1] *Abhandlungen der K. Preuss. Akad. der Wissenschaften*, 1894.

[2] Solar Physics Committee, *Tables of Wave-Lengths of Enhanced Lines*, 1906.

The series triplet λ3532 to λ3570, each member of which has three components, is also strengthened in the spark. In the furnace these lines appear between 1600° and 1700°, but strengthen very rapidly with increasing temperature.

The prominent low-temperature group between λλ4000 and 4100 contains the very sensitive triplet λλ4031, 4033, 4035. These lines are of extreme persistence, occurring very generally as impurity lines in arc spectra. Their intensity in the furnace seems to depend very largely on the vapor density, and with an ordinary charge of manganese present they are always widely reversed. This was the condition at the lowest temperature used, 1560°, when most of the low-temperature lines were barely registered on the plate. The intensities of this triplet given in the table therefore signify little relatively to the general run of the manganese lines. At low temperature, with much vapor present, they can be made much stronger than at high temperature with less vapor. The extreme sensitiveness of these three lines to anomalous dispersion, the degree of which is found to depend on the tendency of a line to reverse, was noted in a former paper.[1]

The group in the blue near λ4450 consists of strong arc lines which are relatively weak in the furnace, being for the most part in Class III. Near λ4800 several prominent furnace lines occur, among them the triplet of Class I, λλ4754, 4784, 4824. These are very strong at low temperature and are placed by Kayser and Runge in the first sub-series, another member of which is the triplet at λλ3148, 3161, 3179. The latter lines are beyond the range of the low-temperature furnace, appearing faintly at medium temperature.

Near λ5400 is another set of prominent lines, which in general are relatively stronger in the furnace than in the arc, a class not noted in other parts of the manganese spectrum. λλ5395 and 5433 are remarkable for their strength at low temperature. λ5341 is stronger than either of these at high temperature, but falls off rapidly below 2000°. The temperature of the furnace, especially in the lower range, may be closely gauged by the relative intensity of λ5341 as compared with λ5395 or λ5433.

---

[1] *Mt. Wilson Contr.*, No. 130; *Astrophysical Journal*, **45**, 254, 1917.

The red end of the manganese furnace spectrum is weak, except for the triplet at λ6014 to λ6022 and this fades rapidly with decreasing temperature. The spectrum was photographed with dicyanin-bathed plates as far as λ8200, but no lines were found in the furnace beyond λ6500.

Table II lists what may be regarded as the residual furnace lines. The intensity estimates were made from a spectrogram of long exposure taken with the one-meter concave grating. The temperature of the furnace read 1560° C. The lines of the triplet λ4031 to λ4035 are strong and well reversed. Evidently they are emitted at a considerably lower temperature than that used here. The other lines in Table II are the most pronounced low-temperature lines and in some cases are just strong enough to be distinctly registered. λλ 5394.89 and 5432.75 would doubtless be listed among these lines if the photograph had included the region.

TABLE II

MANGANESE LINES IN FURNACE AT 1560° C.

λ	Intensity	λ	Intensity
3806.90	2	4055.70	5
3823.64	1	4059.09	1
3834.50	1	4063.70	1
4018.28	3	4079.38 4079.61	3
4030.92	100R		
4033.21	75R	4083.11	2
4034.62	50R	4083.82	2
4035.88	3	4754.24	10
4041.53	10	4783.62	10
4048.90	3	4823.71	10

MOUNT WILSON OBSERVATORY
November 1920

Contributions from Mount Wilson Observatory, No. 199
Reprinted from *Astrophysical Journal*, Vol. LIII, pp. 13–94, 1921

THE PARALLAXES OF 1646 STARS DERIVED BY THE SPECTROSCOPIC METHOD

By W. S. ADAMS, A. H. JOY, G. STRÖMBERG, and
CORA G. BURWELL

ABSTRACT

Spectroscopic method of determining absolute magnitude and parallax.—Some years ago it was discovered that there is a correlation between the relative intensities of certain spectral lines and absolute magnitude for stars of the more advanced spectral types. In the past three years a large number of new trigonometric parallaxes has become available and has enabled this correlation to be established more accurately. For the stars for which trigonometric parallaxes have been determined the absolute magnitudes have been computed directly, but for the Cepheid variables the parallactic motion has been used, and in the case of the giant M stars a combination of results derived from peculiar motion and trigonometric parallaxes. The formulae employed are shown in the text. The absolute magnitudes obtained in this way have been plotted against the relative intensities of certain pairs of lines and from the resulting curves reduction tables have been constructed for each observer. These curves are continuous except in the case of stars of the late K and M types where the division into giants and dwarfs introduces a marked discontinuity. The absolute magnitudes and parallaxes derived by means of these tables are found to have probable errors of ±0.4 magnitude and ±20 per cent, respectively. The method used in classifying the spectra and in estimating the intensities of the spectral lines is described.

Absolute magnitudes and spectroscopic parallaxes of 1646 stars, including revised values for 495 stars contained in the 1917 list.—An extensive table gives the Boss or Cincinnati number, the name and position of each star, the Harvard visual magnitude, total proper motion, spectral type, absolute magnitude, and spectroscopic parallax. The trigonometric parallax is given, if known.

The determination of the absolute magnitudes of stars from the intensities of certain spectral lines has formed a regular part of the stellar spectroscopic work of the Mount Wilson Observatory during the past five years. Photographs of the spectra obtained for measurements of radial velocity have also been utilized for the calculation of absolute magnitudes, and the lists of stars under observation have been selected with both of these purposes in view.

Since the last publication in 1917, of absolute magnitudes and parallaxes for any considerable number of stars, numerous developments and changes have taken place in the methods used for particular groups of stars and in the material upon which the spectroscopic reductions are based. The rapid increase in the number of parallaxes determined trigonometrically by the photographic method has in particular added greatly to the accuracy of the fundamental values used as the basis of the spectroscopic reductions. They have also made it possible to divide the stars into groups of comparatively small range in spectral type, and thus to secure a continuity in the reduction tables which was not possible when the material was more scanty. With the aid of this large amount of valuable trigonometric parallax material, and the results furnished by computations based on the parallactic and peculiar motions in the case of stars having very small parallaxes, we now feel reasonably certain that a reduction scale has been established which will not require very serious modification in the future. Such corrections as may become necessary when our knowledge of systematic errors in trigonometric parallaxes and of mean parallax relationships is more advanced than at present can probably be applied in the form of tabular modifications of the results given here.

The main purpose of this communication is to place in the hands of astronomers the results in the form of absolute magnitudes and parallaxes so far obtained by the use of the spectroscopic method. For this reason no attempt is made in this place to discuss the bearing of the material on a number of stellar problems. We expect, however, at an early date to supplement this article with a consideration of the evidence afforded by the results on such questions as the giant and dwarf divisions among the stars of the several spectral types, the relationship of parallax to proper motion, the probable systematic errors in parallax determinations, and the motion in space of the stars in the list.

DERIVATION OF THE REDUCTION TABLES

The general principle employed in the derivation of the reduction tables has been to group the stars according to spectral type and absolute magnitude, using provisional tables for computing the latter, and then to derive systematic corrections to the provisional absolute magnitudes on the assumption that the corrections are constant for the groups in question.

The relative accuracy of the three methods used in computing mean absolute magnitudes—from trigonometric parallaxes, parallactic motions, and peculiar motions—is quite different for the near and the distant stars. For the nearer stars the trigonometric parallaxes give by far the most reliable results, while for stars among which there are no large parallaxes the parallactic motion gives the best result, provided the peculiar motions are small, no selection based upon proper motion has been made, and the group of stars as a whole is at rest relative to the stars in general. For this reason the parallactic motion has been used to compute the mean absolute magnitudes only for very large groups of stars. The result in such cases has been found to agree closely with that derived from trigonometric parallaxes and hence has been used merely as a check upon the latter. Exceptions are the Cepheids and the stars of similar spectral type for which the parallactic motion has been used exclusively.

A peculiar feature is that the parallactic motion for the dwarf stars gives very much larger mean parallaxes than those derived directly from measured parallaxes, probably indicating that these stars as a whole have a velocity differing from that of the stars in general.

The peculiar motion can give accurate results only if the peculiar velocities are large as compared with the solar motion. The results from the peculiar motion are in good agreement with the results from trigonometric parallaxes for all stars fainter than about absolute magnitude +2. For such stars, however, the measured parallaxes are large enough to provide good determinations of the mean absolute magnitudes, and consequently the only case in which the results from the peculiar velocities have been used is that of the giant M stars, for which a combination of the results from trigonometric parallaxes and from peculiar motions has been employed.

The formulae used for computing mean absolute magnitudes from trigonometric parallaxes, parallactic motions, and peculiar motions will now be deduced.

a) Trigonometric parallaxes.—The following notation has been used:

π = true parallax
π_0 = trigonometric parallax
ϵ_0 = true error of the trigonometric parallax
M_t = true absolute magnitude defined as the apparent magnitude at a distance corresponding to a parallax of 0″1 (10 parsecs)
M = most probable absolute magnitude
M_1 = absolute magnitude as given by the provisional reduction tables
S = systematic correction to M_1 for reducing it to M
T = accidental error of M_1+S
m = apparent magnitude
π_1 = spectroscopic parallax based on M_1 as the absolute magnitude

We then have:

$$M_t = M_1 + S + T = m + 5 + 5 \log (\pi_0 + \epsilon_0)$$

and

$$M_1 = m + 5 + 5 \log \pi_1$$

Hence

$$S + T = 5 \log \frac{\pi_0 + \epsilon_0}{\pi_1}$$

or

$$\left.\begin{aligned} &\pi = \pi_0 + \epsilon_0 = \pi_1 \, 10^{0.2(S+T)} = \pi_1 \sigma \tau \\ \text{where} \quad &\sigma = 10^{0.2S} \text{ and } \tau = 10^{0.2T} \end{aligned}\right\} \qquad (1)$$

Further

$$\left.\begin{aligned} &\tau = 10^{0.2T} = 1 + E + \tfrac{1}{2}E^2 + \ldots \\ \text{where} \quad &E = \frac{0.2\,T}{\text{Mod}} = 0.4605\,T \end{aligned}\right\} \qquad (2)$$

We shall limit ourselves in the following to the second order of the error T.

From equations (1) and (2) we may deduce an expression for the mean of a number of parallaxes. We shall then make use of the well-known approximate formula

$$\overline{ab} = \bar{a}\,\bar{b}$$

which is valid if the two variables a and b vary *independently* of one another. Since π_1 is dependent upon T and thus also upon τ and

E, we must separate π_1 from τ before taking the arithmetical mean. From equation (1) we obtain

$$\pi_1\sigma=\frac{\pi_0+\epsilon_0}{\tau}=(\pi_0+\epsilon_0)(1-E+\tfrac{1}{2}E^2)$$

From this equation we deduce

$$\pi_1\sigma-\pi_0 A=\epsilon_0-\pi E \tag{3}$$

where

$$A=1+\tfrac{1}{2}E^2 \tag{4}$$

In the following we shall assume that the errors ϵ_0 and T, and hence also E, have a normal error-distribution.

Taking the arithmetical mean of a number of equations of form (3) we obtain

$$\overline{\pi_1\sigma}-\overline{\pi}_0\overline{A}=0 \text{ or } \frac{\overline{\pi_1\sigma}}{\overline{A}}=\overline{\pi}_0=\overline{\pi} \tag{5}$$

where

$$\overline{A}=1+\tfrac{1}{2}\overline{E^2}>1 \tag{6}$$

The quantity $\pi_1\sigma$ is the parallax corresponding to the most probable absolute magnitude $M=M_1+S$. The mean of a series of these parallaxes is not exactly equal to the mean of the corresponding trigonometric parallaxes, but is systematically larger. This fact depends upon the unequal effects produced in the spectroscopic parallax by a positive and a negative error of the same size in the estimation of the absolute magnitude.

In order to make the spectroscopic parallaxes directly comparable with the trigonometrical ones, we shall define the quantity $\frac{\pi_1\sigma}{\overline{A}}$ as the spectroscopic parallax π', and in the first instance determine the quantity $\frac{\sigma}{\overline{A}}$. The absolute magnitudes corresponding to these spectroscopic parallaxes have been denoted by M' and are those given in the catalogue.

We then have

$$M'=m+5+5\log\pi_1\sigma-5\log\overline{A}$$

$$M'=m+5+5\log\pi'$$

The most probable absolute magnitude M defined in such a way that a positive and a negative error T have the same probability is related to M' by the equation

$$M = M' + 5 \log \bar{A} \tag{7}$$

and

$$\bar{A} = 1 + \frac{0.02\,\theta^2}{\text{Mod}^2} \tag{8}$$

where θ is the mean error in an estimate of the absolute magnitudes.

In the determination of $\frac{\sigma}{\bar{A}}$ we start from the equations of condition (3)

$$\pi_1\sigma - \pi_0 A = \epsilon_0 - \pi E$$

If the range in the values of π_1 is small, we may find $\frac{\sigma}{\bar{A}}$ by taking arithmetical means of equations (3) multiplied by the relative weights p of the trigonometric parallaxes:

$$\frac{\sigma}{\bar{A}} = \frac{\Sigma p\pi_0}{\Sigma p\pi_1} \tag{9}$$

If the range in π is considerable, we do not utilize to their full extent the higher weights of the larger parallaxes by using equation (9). An ordinary least-squares solution might give erroneous results on account of the effect of large values in the errors E and ϵ_0. For this reason we have in general used a compromise between the direct mean of the equations of condition as given by (9) and the ordinary least-squares solution based upon the weighting of the errors ϵ_0. Dividing the results into three or four groups according to the size of π_1, we have as in (9)

$$\left.\begin{aligned} &\frac{\sigma}{\bar{A}}\Sigma p\pi_1 - \Sigma p\pi_0 = 0 \\ &\text{Weight} = \frac{1}{k^2\Sigma p + \frac{\eta^2(\Sigma p\pi_0)^2}{n}} \end{aligned}\right\} \tag{10}$$

where k is the mean error of the trigonometric parallaxes corresponding to unit weight, n is the number of stars, and

$$\eta^2 = \overline{E^2} = \frac{0.04\,\theta^2}{\text{Mod}^2}$$

If we assume definite values of k and η we can make an ordinary least-squares solution of equations (10). The values of k and η used are

$k = \pm 0''.015$, corresponding to a probable error in π_0 of $\pm 0''.010$
$\eta = \pm 0.205$, corresponding to a probable error in $M_1 + S$ of ± 0.3

In order to secure a grouping independent of the errors in the estimates of the absolute magnitudes, a solution was made using the proper motions reduced to zero apparent magnitude as a basis of the grouping. In this case there is less danger of a systematic effect upon the sums ΣT and ΣE which we have to suppose to be equal to zero.

In the first computation of the systematic correction to the provisional reduction tables all available trigonometric parallaxes for stars in the list were used. The reductions to absolute parallaxes were generally computed from the apparent magnitudes of the comparison stars, using the table given by Kapteyn in *Groningen Publications*, No. 24, page 15. For the parallaxes determined at the Allegheny, McCormick, and Sproul observatories a constant reduction of +0″.005 and for the Mount Wilson parallaxes one of +0″.002 has been applied throughout. The weights of the different determinations based upon the size of the probable errors are as follows:

Mount Wilson	1.5	Vôute	0.5
Greenwich	1.5	Abetti	0.4
Allegheny	1.0	Russell	0.3
McCormick	1.0	Peter	0.3
Sproul	1.0	Jost	0.3
Yerkes	1.0	Kapteyn	0.4
Yale	0.5	Flint I	0.05
Fox	1.0	Flint II	0.2

A second approximation was made using only the parallaxes determined at the Allegheny, McCormick, Yerkes, and Mount Wilson observatories, all being given the same weights. Slight corrections based on this latter computation were then applied to the tables resulting from the first approximation. In the final analysis the reduction tables are thus based almost exclusively on the four series of trigonometric parallaxes mentioned above. The differences between the two solutions are, however, very small.

b) *Parallactic motion.*—The co-ordinates of a star in space relative to the sun and referred to the equatorial system of co-ordinates are

$$\left.\begin{aligned} X&=r\cos\alpha\cos\delta\\ Y&=r\sin\alpha\cos\delta\\ Z&=r\sin\delta \end{aligned}\right\} \qquad (11)$$

where r is the distance from the sun and α and δ are the right ascension and declination of the star. Differentiating these equations with respect to the time, we obtain the velocity components x, y, and z, in km per second relative to the sun.

$$\left.\begin{aligned} x&=V\cos\alpha\cos\delta-\frac{k}{\pi}(\mu_1\sin\alpha+\mu_2\cos\alpha\sin\delta)\\ y&=V\sin\alpha\cos\delta+\frac{k}{\pi}(\mu_1\cos\alpha-\mu_2\sin\alpha\sin\delta)\\ z&=V\sin\delta+\frac{k}{\pi}\mu_2\cos\delta \end{aligned}\right\} \qquad (12)$$

where

V=radial velocity

π=parallax

$\mu_1=\mu_\alpha\cos\delta$

$\mu_2=\mu_\delta$

μ_α and μ_δ=annual proper motion in α and δ in seconds of arc

$$k=\frac{\text{astronomical unit of length in km}}{\text{number of seconds in a year}}=4.737$$

Introducing the velocity components x_0, y_0, and z_0 of the sun relative to the geometrical centroid of a large number of stars, we have

$$x+x_0=\epsilon_1,\qquad y+y_0=\epsilon_2,\qquad z+z_0=\epsilon_3$$

where ϵ_1, ϵ_2, and ϵ_3 are the peculiar velocity components of the star referred to this centroid.

If we use the same co-ordinates for the sun's apex for all spectral types and absolute magnitudes and adopt the values computed for the stars of later type given in *Mount Wilson Contributions*, No. 144, page 14,

$$\alpha_0=270\overset{\circ}{.}9, \qquad \delta_0=+29\overset{\circ}{.}2, \qquad V_0=21.48 \text{ km/sec}$$

we find

$$x_0=+0.28, \quad y_0=-18.75, \quad z_0=+10.48$$

The following auxiliary quantities have been tabulated:

$$\left.\begin{aligned} A_0&=x_0 \sin \alpha-y_0 \cos \alpha \\ B_0&=x_0 \cos \alpha \sin \delta+y_0 \sin \alpha \sin \delta-z_0 \cos \delta \end{aligned}\right\} \tag{13}$$

We can then derive

$$\left.\begin{aligned} \frac{k\mu_1}{\pi}-A_0&=\epsilon' \\ \frac{k\mu_2}{\pi}-B_0&=\epsilon'' \end{aligned}\right\} \tag{14}$$

The quantities ϵ' and ϵ'' are the components of the peculiar velocities of the stars on two axes perpendicular to the line of sight in the direction of increasing right ascension and declination.

In order to obtain the mean absolute magnitude we may proceed in the following way, the notation being the same as in the discussion of the trigonometric parallaxes:

$$\pi=10^{0.2(M_1+S+T-m)-1}=\frac{0.1\,\sigma\tau}{\rho}$$

where

$$\sigma=10^{0.2S}$$
$$\tau=10^{0.2T}$$
$$\rho=10^{0.2\,(m-M_1)}$$

Equations (14) may then be written

$$\frac{10k\mu_1\rho}{\sigma\tau}-A_0=\epsilon', \qquad \frac{10k\mu_2\rho}{\sigma\tau}-B_0=\epsilon'' \tag{15}$$

The components of the proper motions μ_1 and μ_2, however, are affected by systematic and accidental errors. The systematic corrections given by Boss in his *Catalogue*, page xxviii, have been applied.[1] Denoting the accidental errors in μ_1 and μ_2 by η_1 and η_2 we can write equations (15) in the following form:

$$\left.\begin{aligned}\frac{A_0\sigma\tau}{10k}-\mu_1\rho&=\rho\eta_1-\frac{\sigma\tau\epsilon'}{10k}\\ \frac{B_0\sigma\tau}{10k}-\mu_2\rho&=\rho\eta_2-\frac{\sigma\tau\epsilon''}{10k}\end{aligned}\right\}\qquad(16)$$

As in the case of the trigonometric parallaxes, we shall write τ in the form

$$\tau=1+E+\tfrac{1}{2}E^2=A+E$$

The equations of conditions are then

$$\left.\begin{aligned}A_0x-\mu_1\rho&=\rho\eta_1-\frac{\sigma\epsilon'}{10k}-\frac{\sigma A_0E}{10k}\\ B_0x-\mu_2\rho&=\rho\eta_2-\frac{\sigma\epsilon''}{10k}-\frac{\sigma A_0E}{10k}\end{aligned}\right\}\qquad(17)$$

where

$$x=\frac{A\sigma}{10k}=\frac{(1+\frac{1}{2}E^2)\sigma}{10k}$$

The first terms on the right-hand side of these equations increase with the apparent magnitude. The second terms are usually the largest, while the existence of the third terms tends to decrease the weights for stars farthest from the apex and antapex. In order to make the weights more uniform we have in the case of the distant stars limited ourselves to those brighter than apparent magnitude 5.5. At the same time this limitation decreases the effect of a selection among these stars according to proper motion, since nearly all can be assumed to be selected on account of brightness alone. In order to reduce the effect of large peculiar motions and large accidental errors in the absolute magnitudes, we have collected the equations of condition (17) into a few groups according to the size of A_0 and B_0, formed means, and given each of these new equations of condition a weight according to the number of stars.

The new equations of condition are then

$$\left.\begin{aligned}\overline{A_0}x-\overline{\mu_1\rho}&=0\\ \overline{B_0}x-\overline{\mu_2\rho}&=0\end{aligned}\right\}\quad\text{Weight } N\qquad(18)$$

---

[1] The *Catalogue*, however, gives the total proper motion without these corrections.

When x has been found from the solution of equations (18) we have

$$\sigma\bar{A} = 10kx$$

and

$$\frac{\sigma}{\bar{A}} = \frac{10kx}{\bar{A}^2} \tag{19}$$

The mean absolute magnitude M' used for computing the most probable parallaxes can then be obtained by adding the quantity

$$5 \log \frac{\sigma}{\bar{A}} = 5 \log x + 5 \log k + 5 - 10 \log \bar{A}$$

to the mean of the provisional magnitudes $\bar{M}_1$, a provisional value of $\bar{A}$ being used.

This method of deriving mean absolute magnitudes from the components of the parallactic motions requires less computation than that based upon the total parallactic motion. It is similar to that used by Charlier in his study of the B stars.[1] The systematic correction to the absolute magnitudes due to the errors in the estimates of the latter that must be applied in order to obtain the most probable parallaxes ($-10 \log \bar{A}$) has a tendency to make the parallaxes smaller. This would probably account for the difference found in the mean parallax of the B stars when based on the one hand upon the assumption of equality of the absolute magnitudes, and on the other directly upon the proper motions (Kapteyn, Plummer, Bergstrand, and others).

c) *Peculiar motion.*—From equations (16), limiting ourselves to terms of the first order in the errors, we derive

$$\left.\begin{aligned} \xi\mu_1\rho - A_0 &= \epsilon' - \xi\eta_1\rho + A_0E \\ \xi\mu_2\rho - B_0 &= \epsilon'' - \xi\eta_2\rho + B_0E \end{aligned}\right\} \tag{20}$$

where

$$\xi = \frac{10k}{\sigma}$$

From the radial velocities corrected for the sun's motion we can compute for definite groups of stars the average radial velocity

---

[1] *Meddelanden från Lunds Astronomiska Observatorium,* Ser. II, No. 14.

$\frac{\Sigma|V'|}{n}$. This quantity can be supposed to be nearly identical with $\frac{\Sigma|\epsilon'|}{n}$ or $\frac{\Sigma|\epsilon''|}{n}$.

Assuming the dispersion in ϵ' and ϵ'' to be considerably larger than in the other terms on the right-hand sides of equations (20), we derive

$$\left.\begin{aligned}\Sigma|\xi\mu_1\rho-A_0|&=\Sigma|\epsilon'|+\frac{\xi^2\overline{\eta_1^2}\overline{\rho}^2+A_m^2\overline{E^2}}{2\Sigma|\epsilon'|}n^2\\ \Sigma|\xi\mu_2\rho-B_0|&=\Sigma|\epsilon''|+\frac{\xi^2\overline{\eta_2^2}\overline{\rho}^2+B_m^2\overline{E^2}}{2\Sigma|\epsilon''|}n^2\end{aligned}\right\}\qquad(21)$$

where A_m and B_m denote the average numerical values of A_0 and B_0, $\overline{\eta_1^2}$ and $\overline{\eta_2^2}$ are the squares of the mean errors in the measurements of the component of proper motion, $\mu_\alpha \cos\delta$ and μ_δ, and n is the number of stars. Since the results from the peculiar motions were used only for the giant M stars where the peculiar velocities are large, it was found that the second terms in the right-hand members could be neglected. Equations (21) then reduce to the more simple form

$$\left.\begin{aligned}\Sigma|\xi\mu_1\rho-A_0|&=\Sigma|\epsilon'|\\ \Sigma|\xi\mu_2\rho-B_0|&=\Sigma|\epsilon''|\end{aligned}\right\}\qquad(22)$$

The average radial velocities corrected for the solar motion, for the K term, and for the effect of stream motion were then computed and the values of $\Sigma|\epsilon'|$ and $\Sigma|\epsilon''|$ obtained from them. Equations (22) were then solved by assuming approximate values of ξ and computing the corrections to these values. The results thus obtained were nearly the same as those found from computing geometrical mean parallaxes from the τ and υ components according to the method devised in *Mount Wilson Contributions*, No. 144, page 7.

REDUCTION CURVES

The values of $\Delta M_1 = 5 \log \frac{\sigma}{A}$ having been computed for groups of stars of different spectral types and absolute magnitudes, according to formulae (10), (18), and (22), the sums $M_1+\Delta M_1 = M'$ were properly weighted and plotted against the mean intensities of the several spectral lines used in the determination. When the correlation curves were computed, a continuous change of absolute magnitude with line-intensity and with spectral type was found except in the case of stars of the late K and M types, where the division into giants and dwarfs caused a marked discontinuity. The scale used in the estimates of the line-intensities being an arbitrary one, different reduction tables were computed for the three

TABLE I

$\frac{4077}{4072}$	Fo	F8	$\frac{4215}{4250}$	F8	G4	Ko	K4	K8	M
......	......	......	+5.0	−2.9	−2.4	−1.7	−0.6	−2.9	......
+3.0	−0.5	−0.3	+4.0	−1.4	−0.8	+0.4	−0.2	−1.6	......
+2.0	+1.1	+1.5	+3.0	+0.1	+0.6	+2.7	+0.3	−0.4	......
+1.0	+2.3	+2.4	+2.0	+1.7	+2.0	+3.7	+1.2	+0.5	......
0.0	+3.0	+3.3	+1.0	+3.2	+3.8	+4.4	+6.0	......	......
−1.0	+3.8	+4.3	0.0	+4.8	+5.1	+5.2	+6.5	+7.2	......
−2.0	+4.3	+5.0	−1.0	+6.4	+6.1	+6.1	+7.2	+8.2	+ 9.0
......	......	......	−2.0	......	......	+6.9	+7.9	+9.4	+11.4
$\frac{4290}{4271}$	Fo	F8	$\frac{4454}{4461}$	F8	G4	Ko	K4	K8	M
......	......	......	−2.0	......	......	−2.7	0.0	......	......
+2.0	+0.5	+0.3	−1.0	−1.6	−1.1	+2.8	+1.2	......	......
+1.0	+2.0	+1.6	0.0	+3.0	+3.8	+4.9	+5.5	......	......
0.0	+2.9	+2.5	+1.0	+5.5	+5.8	+5.9	+6.2	......	......
−1.0	+4.1	+3.7	+2.0	......	+6.7	+6.5	+6.7	+7.1	+ 7.2
−2.0	+4.3	+4.7	+3.0	......	......	+6.7	+7.3	+7.7	+7.8
−3.0	......	+5.0	+4.0	......	......	......	+7.7	+8.3	+8.4
......	......	......	+5.0	......	......	......	......	+8.8	+9.0
......	......	......	+6.0	......	......	......	......	+9.1	+9.9
......	......	......	+7.0	......	......	......	......	......	+10.8
......	......	......	+8.0	......	......	......	......	......	+11.1
			$\frac{4454}{4494}$	F8	G4	Ko	K4	K8	M
......	......	......	0.0	......	−3.0	−0.4	+0.4	......	......
......	......	......	+1.0	+1.9	+2.4	+4.0	+1.6	......	......
......	......	......	+2.0	+5.1	+5.4	+5.5	+6.0	......	......
......	......	......	+3.0	......	+6.5	+6.2	+6.4	+6.8	......
......	......	......	+4.0	......	......	+6.5	+6.8	+7.3	+ 7.3
......	......	......	+5.0	......	......	......	+7.2	+7.8	+ 7.9
......	......	......	+6.0	......	......	......	......	+8.4	+ 8.5
......	......	......	+7.0	......	......	......	......	+8.8	+ 9.2
......	......	......	+8.0	......	......	......	......	+9.1	+10.0
......	......	......	+9.0	......	......	......	......	+9.5	+10.7
......	......	......	+10.0	......	......	......	......	......	+11.0

observers, Adams, Joy, and Miss Burwell. An abstract of the tables for Mr. Adams' scale is given on page 13. The differences of intensity for the pairs of lines employed are given under their wave-lengths and the corresponding absolute magnitudes under the successive spectral types.

Among the giants the rate of change of absolute magnitude with line-intensity is very large in the case of the line 4454, and for this reason the two estimates of this line whenever made have been given half-weight.

PROBABLE ERRORS OF THE ABSOLUTE MAGNITUDES

A determination of the probable errors of the absolute magnitudes has been made using the trigonometric parallaxes for this purpose.

Equation (3) can be written

$$\pi' - \pi_0 = \epsilon_0 - \pi E = v$$

where π' is the most probable spectroscopic parallax.

Calling the weights of the trigonometric parallaxes p, we find

$$\overline{E^2} = \frac{\Sigma p v^2 - n k^2}{\Sigma p \pi_0^2 - n k^2} \tag{23}$$

where k is the mean error of a parallax of weight unity.

If a star has been measured by several observers, the error in the trigonometric parallax becomes smaller, but the error in the spectroscopic parallax is unaffected. It is, therefore, necessary in some way to equalize the weights of the trigonometric parallaxes, and we have used the method of giving all stars for which the weight is equal to 1 or larger the weight unity, omitting all parallaxes of smaller weights. As before, the unit of weight has been assumed to be such as would correspond to an external probable error of ±0".010. Calling the mean error of the absolute magnitudes θ, we have

$$\theta^2 = 25 \text{ Mod}^2\, \overline{E^2} = 4.715 \overline{E^2}$$

The following table gives the values of the probable errors r computed by this method:

TABLE II

Spectrum	M	Number	r	Spectrum	M	Number	r
A–F4	< 2.0	28	± 0.30	G5–G8	< 1.0	42	± 0.51
	2.1 to 3.0	31	.58		1.1 to 5.0	30	.38
	> 3.0	25	.42		> 5.1	24	.25
F5–F8	< 3.5	38	± 0.34	G9–K4	< 1.0	59	± 0.32
	> 3.6	48	.38		1.1 to 3.0	27	.53
F9–G4	< 4.0	42	± 0.64		3.1 to 6.0	33	.46
	4.1 to 5.0	39	.12		> 6.1	38	.36
	> 5.1	18	.46	K5–K9	< 2.0	23	± 0.00
					> 7.5	25	.24
				M	< 3.0	33	± 0.00
					> 7.0	17	.20

When the probable error is equal to 0.00, the residuals are smaller than those due exclusively to the effect of a probable error $\pm 0''.010$ in the trigonometric parallaxes.

For the sake of convenience we may assume a probable error in the absolute magnitudes of ± 0.40 throughout. The corresponding value of $\bar{A}$ is then

$$\bar{A} = 1 + \frac{\bar{E}^2}{2} = 1 + \frac{0.02r^2}{0.455 \text{ Mod}^2} = 1.0373$$

The correction which must be applied to the absolute magnitudes M' given in the table, in order to convert them into the most probable ones, is therefore (equation 7)

$$5 \log \bar{A} = +0.08$$

The probable errors r' of the spectroscopic parallaxes can be computed from the formula

$$r' = \frac{r}{5 \text{ Mod}} \pi$$

If

$$r = \pm 0.40$$

we find

$$r' = \pm 0.184\,\pi$$

In other words, the probable error of the spectroscopic parallaxes is somewhat below 20 per cent of the parallax itself.

EFFECT OF SYSTEMATIC ERRORS IN THE TRIGONOMETRIC PARALLAXES

Several studies of the systematic difference between various series of trigonometric parallaxes have been made recently. A special solution has been undertaken, applying the systematic corrections derived by van Maanen and Miss Wolfe (*Mt. Wilson Contr.*, No. 189) for reduction to a mean system. The most important of these corrections is that of +0".0027 to the Allegheny parallaxes,[1] which, on account of their large number and high weight, has a tendency to make the spectroscopic parallaxes larger. The effect upon the absolute magnitudes, if these corrections were applied to the measured parallaxes, can be seen from the following table:

TABLE III

Spectrum	A–F8	F9–G8	G8–K4	K5–K9	M
Giants......	+0.03	+0.09	+0.06	0.00	+0.03
Dwarfs......	+0.05	+0.04	+0.03	+0.01	+0.03

The spectroscopic parallaxes would then be increased by a quantity equal to $(10^{0.2\Delta M}-1)$. It thus appears that the systematic effect arising from this source is very small.

COMPARISON WITH TRIGONOMETRIC PARALLAXES

A direct computation of the difference, spectroscopic *minus* trigonometric parallax, has been made for the stars whose parallaxes have been determined at the Allegheny, McCormick, Yerkes, and Mount Wilson observatories. The algebraic mean difference, assigning all the stars the same weight, is given in the third column of the following table, while the weighted mean difference is given in the fourth column. The weights are here based upon the facts that the errors in the spectroscopic parallaxes are proportional to the parallaxes themselves, while the errors in the trigonometric parallaxes are independent of this. The quantity S' is computed from the equations of condition

---

[1] The correction given in the paper cited is +0".0042, which is a mean of two determinations. A mean reduction to absolute parallax of +0".0035 was used, while in the present system we have used +0".005, which accounts for the difference.

$$S'=\pi^{b}-\pi_0, \quad \text{weight } \frac{1}{\overline{\epsilon}_0^2+\overline{E}^2\pi^2}$$

where the errors in the trigonometric parallaxes and the absolute magnitudes are based upon the probable errors ±0″.010 and ±0.4, respectively. We have then

$$\overline{\epsilon}_0^2=0.00022,\ \overline{E}^2=0.0746$$

TABLE IV

	Number	Not Weighted S	Weighted S'
Allegheny	296	+0″.0018	+0″.0031±0″.0007
McCormick	209	−0.0008	+0.0020±0.0010
Yerkes	98	+0.0019	+0.0016±0.0015
Mount Wilson	79	−0.0030	−0.0032±0.0011
	682	+0″.0005	

It is to be noted that in computing the reduction tables the larger parallaxes have the highest weights, so that we cannot expect S and still less S' to become zero when all the stars are taken together.

The weighted means S' can be supposed to represent the systematic corrections to the trigonometric parallaxes, if these corrections can be regarded as constant. They agree well with those found by van Maanen and Miss Wolfe except in the case of the McCormick parallaxes. The difference between the weighted mean S' and the unweighted mean S shows a dependence upon the size of the parallax, which can hardly be due to the spectroscopic parallaxes, since for the other series of results the values of S and S' are very nearly the same. A direct comparison between parallaxes of the same stars measured at the four observatories shows that the correction to the McCormick parallaxes possibly depends upon the apparent magnitude, so that the unweighted mean probably gives a more reliable value for the systematic correction for these stars in general.

THE CEPHEIDS AND PSEUDO-CEPHEIDS

The absolute magnitudes of the Cepheid variables and the stars with similar spectra, which for convenience we may call Pseudo-Cepheids, have been computed from the parallactic motions alone, the trigonometric parallaxes being too small to furnish reliable data for this purpose. These two classes of stars have been reduced with the same tables, as it was found that their mean absolute magnitudes were about the same.

If the absolute magnitudes of the Cepheids are plotted against $0.2m+\log \mu$, a marked correlation between these quantities can be found.

TAURUS GROUP

A comparison of the spectroscopic parallaxes of the stars belonging to the Taurus group with the parallaxes of these stars as measured by Boss[1] and Kapteyn[2] was made and the results are given in the following table:

TABLE V

Spectrum	M	Number*	$\bar{\pi}'$	$\bar{\pi}_0$	ΔM
A8–F2......	1.6 to 2.5	7	0.″017	0.″025	+0.″86
F5–G0......	3.7 to 4.1	7	.020	.024	+0.45
G5–K2......	4.5 to 5.5	4	.022	.023	+0.12
G7–G9......	0.4 to 1.4	4	.025	.025	−0.03

* Several of the stars used here are not given in the main table, as in some cases only one spectrogram has been secured.

The large positive correction to the absolute magnitudes for the F-type stars cannot be reconciled with the great number of large trigonometric parallaxes for the stars of this type in general. Most of the F-type stars belonging to the Taurus group, however, show very hazy lines which are difficult of estimation, and for this reason these stars can probably not be regarded as representative of the F stars in general.

---

[1] *Astronomical Journal*, No. 604, 1908.

[2] *Groningen Publications*, No. 23, 1909.

COMPARISON WITH RESULTS FOR FIVE HUNDRED STARS

The absolute magnitudes of the stars contained in the list of 500 published in 1917[1] were subject to errors due mainly to three causes: (1) the insufficiency of the trigonometric parallax material upon which the reduction curves were based; (2) the resulting necessity for grouping into too large divisions of spectral type; (3) the uncertainty in the reduction of the Cepheid variables.

The discussion of the method of reduction used for the stars contained in this list shows how great an improvement has been effected as regards the first two of these factors. A completely different system of reduction has been used for the Cepheid variables and stars having a similar type of spectrum. These were treated under the normal spectral types in the list of 500 stars, while in the present discussion they have been reduced independently as a special class. This has resulted in a large systematic difference compared with the earlier values, the present absolute magnitudes being considerably brighter.

TABLE VI

DIFFERENCES IN M, 1920 SYSTEM *minus* 500 STARS

	$M<3.0$		$M=3.0-5.0$		$M>5.0$	
	Number	Difference	Number	Difference	Number	Difference
A–F8....	23	−0.46	77	−0.54	1	−0.3
F9–G8...	51	−0.30	51	−0.05	41	−0.20
G9–K4...	78	+0.08	12	+0.83	64	−0.12
K5–K9...	10	−1.01	....	....	29	−0.07
M.......	29	−1.12	....	....	15	−0.10
Cepheids.	14	−2.9	....	....	....	....
All types except Cepheids	191	−0.32	140	−0.24	150	−0.13

The summary above gives the results of a comparison for 495 stars common to the two lists, the differences given being the corrections necessary to apply to the stars in the list of 500 in order to reduce their absolute magnitudes to the present system. As would be expected, the corrections for the fainter stars are considerably smaller than those for the brighter.

---

[1] *Mt. Wilson Contr.*, No. 142; *Astrophysical Journal*, 46, 313, 1917.

METHOD OF ESTIMATION OF INTENSITIES

A brief description of the method of classifying the spectra and of estimating the intensities of the spectral lines used in the determination of the absolute magnitudes will perhaps be of value.

The spectrograms are examined under a Hartmann spectro-comparator and the hydrogen lines are first compared with the neighboring lines λλ 4326, 4352, and 4405 in the case of Hγ, and λλ 4872 and 4957 in the case of Hβ. From the relative intensities of these pairs of lines, with the aid of a reduction table based upon standard spectra, the "measured" type of spectrum is determined. In the case of spectra between F0 and G0 comparisons are also made with λλ 4227 and 4384, while Hβ is omitted.

Estimations of the spectral type are made from direct comparisons with typical spectra selected from the Harvard list. The spectra of three stars having the types F0, F5, and G0 have been photographed upon one standard plate, and those of three other stars with spectra G5, K0, and K5 upon another plate. These spectra are placed under the second microscope of the spectro-comparator and are brought side by side with that of the star to be classified. Values intermediate between those of the typical stars are estimated from comparison with the stars having spectra on either side, especial consideration being given to the calcium line λ 4227 and the chromium lines λλ 4255 and 4275, which vary rapidly with spectral type and form a valuable criterion. It is probable that all three of these lines vary to some extent with absolute magnitude, but the effect seems to be slight except in extreme cases like the Cepheid variables.

The estimations of the relative intensities of the pairs of lines for determinations of absolute magnitude are made in the same way as those of the hydrogen lines. In stars of types A to F7 the lines compared are $\frac{4077}{4072}$ and $\frac{4290}{4271}$. In types F8 to G, the three pairs $\frac{4215}{4250}$, $\frac{4455}{4462}$, and $\frac{4455}{4495}$ have been added, and these have been used exclusively for later types of spectra except the M-type giants. The latter and the Cepheid variables have been treated separately. For the M-type giants the intensities of the lines λλ 4077 and 4215 have been compared directly with those in the spectra of the stars

β Andromedae and μ Geminorum. In the case of the Cepheids the pairs of lines have been $\frac{4077}{4072}$, $\frac{4215}{4250}$, and $\frac{4290}{4271}$, a special table being used for reduction purposes.

DESCRIPTION OF CATALOGUE

In the extensive table which follows, the successive columns contain the following data for each star:

Column 1. Number in Boss *P.G.C.* or in *Cincinnati Publication*, No. 18.
2. Name of star, double stars being assigned the number in Burnham's *General Catalogue* in case they have no Greek letter or Flamsteed number.
3 and 4. Right ascension and declination for 1900.
5. The magnitudes from the revised *Draper Catalogue* are used for stars within the first twelve hours of right ascension. In the case of faint B.D. stars the B.D. magnitude has been corrected in accordance with the values given in *H.A.*, **72**, 214. In the case of double stars and spectroscopic binaries, the magnitude of the brighter component has been calculated from the combined magnitude in accordance with the relative intensities of the two components.
6. Total proper motion taken from Boss's *P.G.C.* or *Cin.* 18 when given.
7. Estimated Mount Wilson spectrum.
8. Spectrum as determined from the intensities of the hydrogen lines.
9. Absolute magnitude M' calculated from the line-intensities.
10. Parallax corresponding to M'.
11. Weighted trigonometric parallax.
12. Authority for the trigonometric parallax. The following are the principal abbreviations used: A, Allegheny; Ab, Abetti; C, Cape; D, Dearborn; F, Flint; G, Greenwich; J, Jewdokimow; Jo, Jost; K, Kapteyn; Kos, Kostinsky; M, McCormick; R, Russell; Ram, Rambaut; S, Sproul; W, Mount Wilson; Y, Yale; Ye, Yerkes.

The significance of the symbols occurring in the catalogue is as follows:

* See note at end of table.
† Magnitude corrected to the brighter component of the double star or spectroscopic binary.
‡ Unpublished proper motion by Kapteyn.
§ Cepheid or Pseudo-Cepheid reduced by special curves.
|| Unpublished proper motion by Roy.

TABLE VII

Boss	Name	α 1900	δ 1900	Harv. Vis. Mag.	μ	Spectrum Est.	Spectrum Meas.	Spect. Abs. Mag.	Spect. π	Trig. π	Auth.
C 2	Bu. 12740 S.	0h 0m.4	+45°16′	8.9	0″.858	K7	......	8.8	0″.096	0″.102	A, Ye, Y, D
3	Bu. 12755 Br.	0 1.0	+57 53	6.4	0.266	G4	G2	5.3	0.060	0.036	S
3	Bu. 12755 Ft.	0 1.0	+57 53	7.5	0.266	G7	G7	5.3	0.036		
6	......	0 1.4	+28 28	6.2	0.419	G9	G7	5.8	0.083	0.150	Y
9	5 Ceti	0 3.1	− 3 0	6.3	0.006	K2	G4	1.2	0.010		
12	β Cassiop.	0 3.8	+58 36	2.4	0.559	F2	F4	1.6	0.069	0.071	A, M, Y, *et al.*
C 9	A.G. Hels. 38	0 4.0	+64 31	7.0	0.30	K0	G9	4.3	0.029		
19	22 Androm.	0 5.1	+45 31	5.1	0.004	F2	F3	1.3	0.017		
......	A.G. Chris. 15	0 5.4	+66 35	9.2	0.138‡	G8	G7	4.1	0.010		
......	A.G. Leiden 33	0 5.4	+32 34	7.2	0.052‡	K5	K0	0.5	0.005		
......	SX Cassiop.*	0 5.5	+54 20	9.1†	......	A6p	......	2.2	0.004		
31	χ Pegasi	0 9.4	+19 39	4.9	0.094	Ma	K2	0.0	0.010	0.015	A
33	7 Ceti	0 9.6	−19 29	4.7	0.068	Ma	K2	1.1	0.019		
41	......	0 11.6	+60 59	5.8	0.002	G3	G2	− 0.9	0.004		
C 25	Groom. 34	0 12.7	+43 27	8.1	2.890	Ma	......	10.4	0.288	0.280	Ye, Y, R, *et al.*
53	ι Ceti	0 14.3	− 9 23	3.8	0.037	K3	K1	0.6	0.023		
56	41 Piscium	0 15.5	+ 7 38	5.6	0.015	K3	K0	0.7	0.010		
62	42 Piscium	0 17.2	+12 56	6.4	0.063	K2	K1	0.9	0.008		
63	9 Ceti	0 17.7	−12 46	6.4	0.396	G2	G2	5.7	0.072		
......	A.G. Leiden 117	0 20.3	+33 34	8.3	0.019‡	K0	G8	1.7	0.005		
......	A.G. Leiden 134	0 22.3	+33 29	8.0	0.075‡	K0	G7	3.3	0.012		
81	47 Piscium	0 22.8	+17 20	5.3	0.117	Mb	G6	0.1	0.009		
84	48 Piscium	0 23.0	+15 54	6.5	0.018	K5	K1	0.5	0.006		
86	......	0 24.5	+76 28	6.4	0.335	K0	G9	3.9	0.032		
89	28 Androm.	0 24.8	+29 12	5.3	0.066	F2	F3	2.5	0.028		

90	12 Ceti	0h24m9	− 4°31′	6.0	0″.011	K4	K2	0.7	0″.008		
96		0 26.2	+52 17	5.7	0.056	K0	G9	0.3	0.008	0″.008	W
106		0 27.5	+27 44	6.4	0.014	G6	G6	− 0.2	0.005	0.005	W
116	13 Ceti	0 30.1	− 4 9	5.7†	0.408	F7	F8	3.8	0.042	0.053	S
121		0 31.3	+43 56	5.4	0.035	K2	G8	1.4	0.016		
125		0 32.0	+34 51	5.6	0.019	G0	F7	− 0.3	0.007		
127	Bu. 335	0 32.2	−25 19	6.4†	1.390	G9	G5	5.5	0.066	0.104	M, F
128		0 32.4	+ 2 35	6.6	0.122	K3	K0	1.1	0.008		
130	ε Androm.	0 33.3	+28 46	4.5	0.336	G3	G3	0.2	0.014	0.063	A, Ye, S
131		0 33.6	+48 48	5.7	0.019	K5	G9	0.5	0.009		
C 80	Lal. 999	0 34.0	+ 2 35	7.4	0.819	G4	G1	5.5	0.042	0.033	Y, J
132	δ Androm.	0 34.0	+30 19	3.5	0.162	K3	K3	0.8	0.029	0.020	A
133	54 Piscium	0 34.2	+20 43	6.1	0.595	K1	K0	6.2	0.105	0.111	A, M, Y
135	α Cassiop.	0 34.8	+55 59	2.5	0.060	G8	G8	− 1.0	0.020	0.023	M, F
C 86	Lal. 1045	0 35.3	+39 39	7.5	0.797	K4	K2	6.3	0.058	0.054	A, Y
C 87	Lal. 1065	0 35.5	−24 21	6.2	0.711	G2	G3	4.7	0.050		
137		0 35.6	− 4 54	6.1	0.023	G8	G6	1.5	0.012		
138	32 Androm.	0 35.7	+38 55	5.4	0.007	G6	G5	1.1	0.013		
	Groom. 127	0 37.8	+70 17	6.9	0.035	G7	G5	1.4	0.008		
147	β Ceti	0 38.6	−18 32	2.2	0.230	G6	G6	0.3	0.042	−0.052	F
C 98	Lal. 1198	0 40.0	+ 1 15	8.1	0.591	K5	K6	6.7	0.052	0.056	M, Y
160		0 41.2	−23 4	5.6	0.189	G7	G6	2.5	0.024		
161	57 Piscium	0 41.3	+14 56	5.6	0.064	Mb	G8	0.4	0.009	0.014	W
164	ζ Androm.	0 42.0	+23 43	4.3	0.129	G7	G4	0.8	0.020	0.031	A
165	60 Piscium	0 42.2	+ 6 12	6.2	0.016	G8	G5	1.4	0.011		
168	η Cassiop. Br.	0 43.0	+57 17	3.7	1.242	F8	G0	4.3	0.132	0.186	A, M, S, *et al.*
168	η Cassiop. Ft.	0 43.0	+57 17	7.4	1.242	K5	K2	8.3	0.151		
171		0 43.1	+ 4 46	5.8	1.366	K3	K1	6.5	0.138	0.170	Y, F
C105	Groom 145	0 43.3	+69 54	8.0	0.415	K3	K2	6.2	0.044	0.028	Y
173	δ Piscium	0 43.5	+ 7 2	4.6	0.093	K5	K1	0.9	0.018	0.017	A

TABLE VII—*Continued*

Boss	Name	α 1900	δ 1900	Harv. Vis. Mag.	μ	Spectrum		Spect. Abs. Mag.	Spect. π	Trig. π	Auth.
						Est.	Meas.				
174	64 Piscium	0h43m.7	+16°24′	5.2	0″.204	F4	F7	3.5	0″.046		
178¹	65¹ Piscium	0 44.5	+27 10	6.3	0.092	F0	F2	0.7	0.008	0″.010	W
178²	65² Piscium	0 44.5	+27 10	6.3	0.092	F0	F1	1.4	0.011		
181	19 Ceti	0 45.1	−11 11	5.2	0.325	F8	F7	3.9	0.055		
189		0 47.1	+60 35	4.9	0.188	F8	F7	3.6	0.055		
191	20 Ceti	0 47.9	− 1 41	4.9	0.017	K6	K0	0.3	0.012		
193	26 Cassiop.	0 49.1	+58 26	5.0	0.053	K2	K1	0.5	0.013		
200	28 Cassiop.	0 50.7	+58 38	4.8	0.100	G5	G6	0.7	0.015	0.073	A
206	η Androm.	0 51.9	+22 53	5.0†	0.060	G6	G8	0.5	0.013	0.011	A
209	68 Piscium	0 52.4	+28 27	5.6	0.017	G7	G6	0.0:	0.008		
210		0 52.7	+13 9	6.4	0.022	G5	G4	0.1	0.005		
217		0 54.6	+ 5 57	6.3	0.023	Mb	G6	1.0	0.009	−0.001	W
218	2 Urs. Min.	0 55.0	+85 43	4.5	0.086	K3	K2	0.5	0.016		
C136	Lal. 1799	0 57.2	+ 4 31	8.4	0.438	K5	K4	7.1	0.055	0.038	M, Y
226	ε Piscium	0 57.8	+ 7 21	4.4	0.085	G6	G6	0.2	0.014	0.027	A, M
233	73 Piscium	0 59.7	+ 5 7	6.2	0.031	K4	K0	0.8	0.008		
C142	A.G. Hels. 914	1 0.3	+63 24	8.7	1.55	K7	K4	8.4	0.087		
243	75 Piscium	1 1.3	+12 25	6.2	0.040	G7	G6	1.8	0.013		
244	μ Cassiop.	1 1.6	+54 26	5.3	3.760	G5	G3	5.6	0.115	0.127	A, Ye, F, *et al.*
C146	Lal. 1964	1 2.2	+22 26	8.6	0.525	K5	K4	7.5	0.060	0.097	Y
252	80 Piscium	1 3.2	+ 5 7	5.7	0.326	F1	F1	2.5	0.023		
C149	Lal. 1966	1 3.3	+61 1	7.8	0.638	F5	F5	3.5	0.014	0.022	Ye, Y
255	η Ceti	1 3.6	−10 43	3.6	0.246	K2	K1	1.2	0.033		
259	β Androm.	1 4.1	+35 5	2.4	0.216	Ma	G8	0.5	0.042	0.049	A, M, F
C150	Lal. 1985	1 4.1	+67 15	6.6	0.236	F7	F8	4.0	0.030	0.023	G

261	81 Piscium	$1^h\ 4^m.5$	+19° 7′	5.6	0″.004	F2	F5	0.4	0″.009		
267	33 Ceti	1 5.4	+ 1 55	6.2	0.004	K4	K0	0.7	0.008		
270	χ Piscium	1 6.1	+20 30	4.9	0.021	G5	G6	0.0	0.010	0″.013	A
271	τ Piscium	1 6.2	+29 34	4.7	0.081	K1	G9	0.5	0.014		
281	φ Piscium	1 8.3	+24 3	4.6	0.047	G7	G7	0.4	0.014		
287	38 Ceti	1 9.7	− 1 31	5.8	0.221	F4	F6	2.8	0.025		
C165	W.B. 1^h161	1 13.5	− 1 23	8.1	0.489	K1	G8	6.1	0.040	−0.011	Y
C167	Lal. 2387	1 14.0	− 9 27	8.9	0.528	G1	G0	4.7	0.014	0.026	Y
C174	W.B. 1^h262	1 15.8	+30 49	8.8	0.50	K2	K2	6.3	0.032		
304	ξ Androm.	1 16.4	+45 0	5.0	0.41	K0	G9	1.0	0.016		
C177	Lal. 2450	1 16.9	+18 10	8.0	0.524	G1	G1	4.7	0.022	0.017	Y
305	43 Ceti	1 17.5	− 0 58	6.5	0.017	K0	G9	0.5	0.006		
310	ψ Cassiop.	1 18.9	+67 36	5.0	0.086	K1	G9	0.8	0.014		
313	θ Ceti	1 19.0	− 8 42	3.8	0.228	K0	G9	0.3	0.020	0.101	F
C185	W.B. 1^h356	1 19.5	+17 59	9.1	0.606	K2	K1	6.3	0.028		
318	ρ Piscium	1 20.9	+18 39	5.3	0.041	F0	F1	2.7	0.030		
321	ω Androm.	1 21.7	+44 53	5.0	0.356	F1	F6	2.6	0.033	0.022	M, Ye, F, J
325	α Urs. Min. §	1 22.6	+88 46	2.1	0.044	F9	F8	− 3.0	0.010	0.041	F *et al.*
C196	Lal. 2682	1 23.6	+21 13	7.9	0.495	K3	K2	6.4	0.050	0.067	Y, D
327	38 Cassiop.	1 23.8	+69 45	6.0	0.158	F4	F6	3.7	0.035	0.039	A
332	μ Piscium	1 24.9	+ 5 38	5.1	0.292	K5	K1	0.5	0.012		
335	η Piscium	1 26.1	+14 50	3.7	0.031	G5	G6	− 0.4	0.015	0.022	A, M
C204	Lal. 2751	1 27.3	+68 26	6.7	0.402	G3	G2	4.7	0.040	0.026	G
338	χ Cassiop.	1 27.4	+58 43	4.9	0.038	G5	G7	−0.1	0.010	0.020	A
....	Groom. 331	1 27.7	+71 56	7.8	0.037	F6	F9	1.5	0.006		
349	40 Cassiop.	1 30.5	+72 32	5.5	0.008	G5	G5	−0.3	0.007		
350	υ Androm.	1 30.9	+40 54	4.2	0.418	F8	F9	3.7	0.079	0.057	M
355	....	1 31.6	+57 28	5.7	0.004	K0	G6	−0.3	0.006		
357	υ Persei	1 31.9	+48 7	3.8	0.127	K4	K1	0.5	0.022	0.034	A
C226	Lal. 2975	1 32.7	+29 4	8.7	0.482	K1	G9	6.1	0.030		

TABLE VII—*Continued*

Boss	Name	α 1900	δ 1900	Harv. Vis. Mag.	μ	Spectrum Est.	Spectrum Meas.	Spect. Abs. Mag.	Spect. π	Trig. π	Auth.
C229	Lal. 3022	$1^{h}33^{m}.9$	+27°36′	7.9	0″.502	G8	G5	5.4	0″.032	0″.047	Y
C231	Lal. 2966	1 34.2	+66 25	7.6	0.753	G4	G1	5.9	0.046	0.036	Y
372	....	1 35.7	+42 7	5.1	0.817	G1	G0	4.8	0.087	0.098	A, M, Y, J
373	....	1 35.7	+25 14	6.3	0.135	F3p	F4	2.6	0.018	0.036	W
375	....	1 36.0	+29 32	6.0	0.013	G7	G7	0.6	0.008		
378	ν Piscium	1 36.2	+ 4 59	4.7	0.021	K4	K1	0.8	0.017	0.055	A
C238	A.Oe. 1867	1 36.8	+63 20	8.2	0.70	K5	K5	7.7	0.079		
381	Bu. 877 Br.	1 36.8	−11 49	6.1†	0.410	F2	F4	2.7	0.021		
382	107 Piscium	1 37.1	+19 47	5.3	0.734	K1	K1	5.8	0.126	0.129	Y
C240	Lal. 3153	1 37.4	−18 24	7.4	0.543	G0	G1	4.7	0.029		
387	....	1 37.7	− 4 12	5.3	0.028	K3	K1	0.5	0.011		
391	τ Ceti	1 39.4	−16 28	3.6	1.922	G7	G5	6.1	0.316	0.317	M, F, Sitt
393	o Piscium	1 40.1	+ 8 39	4.5	0.085	G6	G7	0.0	0.012	0.017	A
394	....	1 40.5	+63 22	5.7	0.634	K0	G9	5.6	0.096	0.089	Y, J
405	....	1 43.0	+32 11	5.8	0.354	F7	F7	3.8	0.040		
410	1 Arietis Br.	1 44.6	+21 47	6.2†	0.018	G9	K0	1.2	0.010		
414	54 Ceti	1 45.6	+10 33	5.9	0.074	F3	......	2.7	0.023		
420	55 Androm.	1 47.3	+40 14	5.6	0.009	K2	K0	0.5	0.010	0.006	W
421	α Trianguli	1 47.4	+29 6	3.6	0.233	F2	F4	1.2	0.033	0.050	A
426	ξ Piscium	1 48.4	+ 2 42	4.8	0.033	G7	G5	0.7	0.015		
430	....	1 50.0	+36 47	6.1	0.005	K3	G9p	1.0	0.009		
432	56 Androm.	1 50.2	+36 46	5.8	0.180	G9	G7	1.7	0.015		
434	7 Arietis	1 50.3	+23 5	6.0	0.011	K0	G8	0.9	0.010		
....	B.D. +32°356	1 52.3	+32 28	8.8	......	F8	F7	2.6	0.006	−0.001	D
....	A.G. Leiden 743	1 53.1	+33 51	7.6	0.033‡	G9	G6	1.9	0.008		

450	112 Piscium	$1^{h}54^{m}9$	+ 2°37′	5.8	0″336	G0	F9	4.0	0″044		
451	57 Ceti	1 55.1	−21 19	5.7	0.014	Ma	G8	0.3	0.008		
453	υ Ceti	1 55.3	−21 34	4.2	0.130	K6	K3	0.7	0.020		
...	Groom. 441	1 56.8	+54 13	7.7	0.026	F6	F6	3.0	0.012		
468	γ^1 Androm.	1 57.8	+41 51	2.3	0.070	K2	G9	−0.1	0.033	0″010	A, S, Y, F
472	...	1 58.2	+17 46	6.4	0.024	K4	K1	0.9	0.008		
477	α Arietis	2 1.5	+22 59	2.2	0.239	K2	K0	0.7	0.050	0.044	A, F, J
C274	Lal. 3922	2 2.5	− 1 5	6.9	0.466	G1	G0	4.1	0.028	−0.042	Y
486	...	2 4.1	+73 33	6.2	0.071	G6	G5	−0.2	0.005		
493	16 Arietis	2 5.5	+25 28	6.2	0.011	K4	K2	0.9	0.008		
498	55 Cassiop.	2 6.6	+66 3	6.2	0.003	F6	F7	3.2	0.025		
500	6 Persei	2 7.0	+50 36	5.4	0.386	G5	G5	0.7	0.012	0.006	A, Ye
C286	Lal. 3987	2 7.5	+67 13	7.8	0.603	K2	K2	6.1	0.046	0.071	S, Y
...	Bu. 1144	2 7.6	+47 1	6.4	0.112‡	F1	F4	3.4	0.025	0.075	S
504	66² Ceti	2 7.7	− 2 52	5.7	0.374	F9	F8	3.3	0.033		
505	65 Ceti	2 7.7	+ 8 23	4.5	0.026	G4	G3	−1.4	0.006		
C288	A.Oe. 2526	2 9.2	+64 30	8.4	0.50	G2	G2	5.8	0.030		
C289	W.B. $2^{h}95$	2 9.5	− 1 40	9.2	1.034	F8	F8	3.9	0.009	0.014	Y
C291	Lal. 4141	2 9.7	+23 49	6.9	0.494	G7	G4	4.7	0.036	0.036	M, Y
513	8 Persei	2 10.9	+57 26	6.1	0.073	K2	K1	0.7	0.008		
514	δ Trianguli	2 10.9	+33 46	5.1	1.182	G0	G0	4.8	0.087	0.101	A, M, Y, *et al.*
515	7 Persei	2 11.0	+57 3	6.2	0.007	G4	G3	−0.3	0.005		
...	Groom. 489	2 11.4	+42 8	7.9	0.022	F1	F3	2.3	0.008		
518	67 Ceti	2 12.0	− 6 53	5.7	0.141	G8	G7	0.9	0.011		
523	...	2 12.8	+ 1 17	5.8	0.527	F7	F8	3.6	0.036	0.024	M
C298	A.Oe. 2618	2 14.0	+70 43	8.5	0.62	K2	K1	6.3	0.036		
532	...	2 14.5	−26 25	6.4	0.505	G7	G6	5.0	0.052		
C300	Lal. 4222	2 14.5	+68 18	7.4	0.13	K0	G9	2.8	0.012		
539	69 Ceti	2 16.8	− 0 4	5.9	0.006	Ma	G7	0.2	0.007		
...	A.G. Leiden 886	2 17.9	+33 24	7.6	0.056‡	K3	K1	0.9	0.005		

TABLE VII—*Continued*

Boss	Name	α 1900	δ 1900	Harv. Vis. Mag.	μ	Spectrum		Spect. Abs. Mag.	Spect. π	Trig. π	Auth.
						Est.	Meas.				
543	κ Fornacis	2h18m.0	−24° 16′	5.4	0″.210	G2	G1	2.4	0″.025		
545	65 Androm.	2 19.0	+49 50	4.9	0.031	K5	K1	0.3	0.012	0″.005	A
556	25 Arietis	2 22.1	+ 9 45	6.5	0.355	F5	F6	3.8	0.029		
572		2 26.3	+ 1 49	5.4	0.013	K3	G9	1.0	0.013		
575	σ Ceti	2 27.3	−15 41	4.8	0.141	F1	F3	2.2	0.030		
577	36 H Cassiop.	2 28.5	+72 23	5.3	0.031	G4	G5	−0.6	0.007		
581		2 29.5	+36 52	5.9	0.010	K3	G9	0.9	0.010		
582	15 Trianguli	2 29.7	+34 15	5.6	0.061	Ma	G7	0.3	0.009	0.015	W
588		2 30.6	+ 6 25	5.9	2.320	K3	K4	6.5	0.132	0.131	A, M, Y, *et al.*
589	ν Ceti	2 30.6	+ 5 9	5.0	0.042	G3	G4	−0.7	0.008		
591	31 Arietis	2 31.2	+12 1	5.7	0.297	F4	F6	3.9	0.044		
592	30¹ Arietis	2 31.2	+24 13	7.4	0.152	F5	F6	3.1	0.014	0.029	W, S
593	30² Arietis	2 31.2	+24 13	6.6	0.140	F3	F4	2.9	0.018		
C340	Lal. 4855	2 32.6	+30 24	7.2	0.625	G0	F8	4.4	0.028	0.026	Y, F
605	ε Ceti	2 34.7	−12 18	5.0	0.280	F4	F4	2.7	0.035		
612	84 Ceti	2 36.1	− 1 7	5.7	0.250	F6	F7	3.5	0.036		
617	θ Persei	2 37.4	+48 48	4.2	0.351	F6	F6	3.9	0.087	0.083	A, Y
619	14 Persei §	2 37.6	+43 52	5.6	0.004	G0p	F7	−2.6	0.003		
622	γ Ceti Ft.	2 38.1	+ 2 49	6.2	0.210	F3	F6	4.1	0.038	0.049	A, M, Ye, Y
631	1 Eridani	2 40.4	−19 0	4.6	0.327	F7	F6	3.6	0.063		
634	39 Arietis	2 42.0	+28 50	4.6	0.196	K1	G9	0.0	0.012	0.027	A
637	SU Cassiop. §	2 43.0	+68 28	6.1	0.016	F4	F4	−1.4	0.003	0.010	W
639	η Persei	2 43.4	+55 29	3.9	0.030	K4	G5	0.4	0.020		
644	16 Persei	2 44.3	+37 54	4.3	0.213	A8	F0:	1.5	0.028	0.022	A
C364	A.G. Bonn 2435	2 44.9	+45 34	9.2	0.63	G4	G3	5.7	0.020		

646	17 Persei	$2^h45^m.4$	+34° 39′	4.7	0″.077	K5	K1	0.7	0″.016	0″.010	A
650	2 Eridani	2 46.5	−21 25	4.8	0.053	G8	G5	1.2	0.019		
653	τ Persei	2 47.2	+52 21	4.1	0.008	G1	G0	−0.2	0.014		
654	20 Persei A	2 47.4	+37 56	5.8†	0.099	F0	F3	2.5	0.022	0.013	Ye, S
660	45 Arietis	2 50.2	+17 56	5.9	0.018	Mc	G8	−0.3	0.006	0.011	W
661	ρ Arietis	2 50.8	+17 37	5.6	0.340	F5	F4	3.5	0.038		
665	η Eridani	2 51.5	− 9 18	4.0	0.229	K0	G9	1.4	0.030		
667	....	2 52.4	+20 16	5.8	0.222	F4	F3	3.3	0.032		
672	....	2 53.0	+46 49	5.6	0.035	G3	G3	0.5	0.009	−0.007	W
C388	W.B. 2^h927	2 55.2	+ 5 36	8.2	0.667	K1	G9	5.7	0.032	0.096	Y
C392	Lal. 5490	2 56.0	+61 20	6.7	1.002	G4	G2	5.2	0.050	0.043	Y, J
691	α Ceti	2 57.1	+ 3 42	2.8	0.078	Ma	G9	−0.1	0.026	0.013	A, M
694	γ Persei	2 57.6	+53 7	3.1	0.010	F9	F9	−0.1	0.023	0.011	A, M
698	ρ Persei	2 58.8	+38 27	3.7	0.173	Mb	G7	−0.8	0.013	0.048	M, R
707	....	3 1.6	− 6 29	5.6	0.002	Ma	G9	0.1	0.008		
710	ι Persei	3 1.8	+49 14	4.2	1.269	G1	G0	4.4	0.110	0.104	Ye, S, Y, *et al.*
712	54 Arietis	3 2.7	+18 25	6.5	0.042	K6	K2	0.5	0.006	0.031	W
713	κ Persei	3 2.7	+44 29	4.0	0.240	K0	G8	0.9	0.024	0.037	A
717	ω Persei	3 4.8	+39 14	4.8	0.022	K1	G9	0.5	0.013		
718	δ Arietis	3 5.9	+19 21	4.5	0.152	K0	G8	0.7	0.017		
721	48 H Cephei	3 7.6	+77 22	5.5	0.083	A7	......	1.6	0.017		
722	94 Ceti	3 7.7	− 1 34	5.1	0.209	F9	F8	4.1	0.063		
723	α Fornacis Br.	3 7.8	−29 23	4.0	0.726	F6	F6	3.6	0.083		
C423	B.D. +71°190	3 8.3	+71 55	9.0	0.43	G7	G8	5.3	0.018	0.015	G
C427	W.B. 3^h113	3 9.4	+ 8 37	7.7	0.578	K1	K1	6.1	0.048	0.079	Y
746	....	3 12.5	+33 51	4.9	0.013	K2	G8	0.2	0.012	0.012	A
752	κ Ceti	3 14.1	+ 3 0	5.0	0.282	G5	G4	4.9	0.096		
755	....	3 14.3	+28 41	4.7	0.027	K4	K0	0.3	0.013		
759	16 Eridani	3 15.1	−22 7	4.0	0.065	Mb	G8	0.0	0.016		
765	....	3 16.0	+64 14	5.6	0.019	K2	G5	1.3	0.013		

TABLE VII—*Continued*

Boss	Name	α 1900	δ 1900	Harv. Vis. Mag.	μ	Spectrum		Spect. Abs. Mag.	Spect. π	Trig. π	Auth.
						Est.	Meas.				
768	62 Arietis	3^h16^m2	+27° 15′	5.6	0″020	G6	G7	0.2	0″008		
770	63 Arietis	3 17.0	+20 23	5.2	0.050	K4	K2	0.4	0.011		
772	α Persei §	3 17.2	+49 30	1.9	0.039	F5	F8	−1.3	0.023	0″017	Ye, M, F
778	ο Tauri	3 19.4	+ 8 41	3.8	0.103	G7	G4	0.1	0.018	0.006	A
C453	Lal. 6320	3 20.1	− 5 42	8.1	0.816	K5	K5	7.2	0.066	0.062	S, Y, J
795	σ Persei	3 23.5	+47 39	4.6	0.023	K4	K0	0.4	0.014	0.013	A
804	5 Tauri	3 25.4	+12 36	4.3	0.018	G6	G5	0.1	0.014		
814	ε Eridani	3 28.2	− 9 48	3.8	0.972	K1	K1	6.0	0.275	0.317	M, Y, F
....	A.G. Berlin 960	3 29.6	+18 34	7.9	0.012‡	Mb	G8	0.1	0.003		
823	Bu. 1787 Br.	3 31.7	+ 0 16	6.2†	0.151	G8p	G9	5.4	0.069	0.012	M
825	10 Tauri	3 31.8	+ 0 5	4.4	0.536	F9	F9	3.6	0.069	0.058	A, M, Y, J
826	....	3 33.5	+62 54	5.3	0.022	Ma	G7	−0.5	0.007		
831	21 Eridani	3 34.1	− 5 57	6.0	0.204	K0	G9	3.6	0.033		
832	....	3 34.5	+59 39	6.0	0.002	K2	G7	2.0	0.016		
C489	W.B. 3^h617	3 35.3	− 3 32	6.7	0.745	F6	F7	3.9	0.028	0.010	M, Y
C499	A.G. Chris. 631	3 38.2	+68 21	9.2	0.30	K8	K3	9.0	0.091	0.074	G
847	ν Persei	3 38.4	+42 16	3.9	0.009	F5	F5	0.6	0.022	0.021	A, M
848	δ Eridani	3 38.5	−10 6	3.7	0.749	G9	G9	3.4	0.087	0.147	M, Y, F
862	Bu. 1854 Br.	3 40.2	+41 9	8.6†	1.372	K0	G6	6.3	0.035	0.030	M, Ye, D, *et al.*
862	Bu. 1854 Ft.	3 40.2	+41 9	9.2	1.372	K2	K0	6.7	0.032		
864	....	3 40.4	+65 13	4.7	0.004	Ma	G5	−0.6	0.009		
....	B.D. +23°535	3 41.4	+23 25	8.0	....	F6	F6	3.6	0.013		
....	B.D. +23°542	3 41.7	+23 18	8.3	....	K1	G9	2.4	0.007	0.065	Y
873	27 Eridani	3 42.5	−23 33	4.3	0.548	F3	F4	2.7	0.048	0.073	M
C513	W.B. 3^h811	3 44.4	+ 1 4	8.6	0.67	K1	K0	5.7	0.026		

C518	B.D. +22°583	3h46m.2	+22°23′	7.8	0″.388	G5	G4	5.2	0″.030	0″.039	Ye
C521	Lal. 7036	3 46.4	+60 53	7.8	0.479	K0	G8	6.1	0.046	0.060	J
889		3 46.4	+48 21	5.9	0.058	K0	G8	0.8	0.009	0.020	W
892		3 47.4	+17 2	6.0	0.147	F1	F0	2.4	0.019		
895		3 48.4	+75 53	8.3	0.646	K6	K5	8.4	0.105	0.060	Ye, Y, K
897	Bu. 1927	3 48.6	+60 49	5.3†	0.016	K4	K0	0.3	0.010		
901	32 Eridani Br.	3 49.3	− 3 15	5.0	0.034	G4	G4	0.2	0.011	0.005	M
	A.G. Albany 1158	3 53.2	+ 1 10	7.9	0.008‡	K1	G9	0.8	0.004		
915	γ Eridani	3 53.4	−13 48	3.2	0.130	K5	K0	0.5	0.029	0.019	M
919		3 55.0	+17 55	5.8	0.141	A8	A9	2.2	0.019		
927		3 56.5	+35 2	8.6	2.200	K0	G8	6.1	0.032	0.040	Ye, S, Y, *et al.*
C542	Bu. 2007	3 57.4	+39 14	7.4†	0.201	G4	G3	4.7	0.029		
933	36 Tauri	3 58.4	+23 50	5.7	0.022	F4p	F7	3.5	0.036	0.014	W
936	37 Tauri	3 58.8	+21 49	4.5	0.113	K0	G9	0.8	0.018	−0.017	A
937		3 58.9	+ 2 33	5.4	0.190	F7	F8	3.2	0.036		
949	49 Persei	4 1.6	+37 28	6.2	0.214	K1	K0	2.4	0.017		
950	50 Persei	4 1.9	+37 47	5.6	0.260	F7	F8	3.9	0.046	0.048	A
C553	Fed. 635	4 2.1	+76 2	8.2	0.25	K0	G9	6.2	0.040	0.025	G
951		4 2.3	+17 4	6.1	0.024	K5	K4	0.4	0.007		
952	43 Tauri	4 3.3	+19 21	5.7	0.114	K1	K0	1.4	0.014	0.024	M
955	44 Tauri	4 4.7	+26 13	5.6	0.046	F1	F2	2.2	0.021		
960	37 Eridani	4 5.5	− 7 11	5.6	0.010	G8	G5	1.5	0.015		
961	45 Tauri	4 6.0	+ 5 16	5.7	0.143	F4	F4	3.1	0.030		
963	o Eridani	4 7.0	− 7 6	4.1	0.081	A8	A9	0.3	0.017		
972	47 Tauri A	4 8.5	+ 9 1	5.1†	0.036	G4	G4	0.2	0.010		
C560	A.G. Berlin 1366	4 8.6	+22 6	9.1	0.54	A8	F2	2.8	0.006		
977		4 9.6	+80 35	5.6	0.020	G8	G7	0.9	0.012		
980	48 Tauri	4 10.1	+15 9	6.4	0.124	F1	F1	1.9	0.013		
984	40 Eridani	4 10.7	− 7 49	4.5	4.085	K1	K0	6.2	0.219	0.196	M, J, F, C
C570		4 11.9	+16 42	8.3	0.110	G7	G6	5.5	0.028		

TABLE VII—*Continued*

Boss	Name	α 1900	δ 1900	Harv. Vis. Mag.	μ	Spectrum		Spect. Abs. Mag.	Spect. π	Trig. π	Auth.
						Est.	Meas.				
1000	γ Tauri	4^h14^m1	+15°23′	3.9	0″.120	G7	G8	0.7	0″.023		
	55 Tauri	4 14.2	+16 17	7.1†	0.107	F7	F7	3.9	0.023		
1002	φ Tauri	4 14.2	+27 7	5.1	0.086	K1	G9	1.4	0.018		
1014	Bu. 2149	4 16.5	+20 35	6.3†	0.011	Ma	G6	0.9	0.008	0″.001	W
	Bu. 2154	4 17.1	+14 49	7.2†	0.096‡	F9	F9	4.1	0.024		
1017	δ Tauri	4 17.2	+17 18	3.9	0.115	G9	G7	0.4	0.020		
	B.D. +16°591	4 18.6	+16 50	7.8	0.102	F5	F5	3.8	0.016		
C 582	Lal. 8256	4 18.7	+16 39	8.0	0.135	G0	F9	4.0	0.016		
1025		4 19.1	+18 49	6.0	0.123	A9	A8	2.0	0.016		
C 585	Lal. 8248	4 20.1	+46 38	6.7	0.317	G4	G3	3.9	0.028	0.002	Jo
C 586	Lal. 8311	4 20.4	+15 18	7.4	0.115	F8	F8	3.9	0.020		
1044	ε Tauri	4 22.8	+18 58	3.6	0.120	G9	G8	1.0	0.030	0.028	A
1045	θ^1 Tauri	4 22.9	+15 44	4.0	0.108	G9	G8	1.4	0.030		
1055	81 Tauri	4 24.9	+15 28	5.5	0.110	F2	F1	1.6	0.017		
1058	85 Tauri	4 26.1	+15 38	6.0	0.109	F0	F0	2.5	0.020		
C 593	Lal. 8610	4 29.2	+16 47	7.4	0.11	K3	K2	1.0	0.005	−0.036	K
1071	47 Eridani	4 29.4	− 8 26	5.4	0.035	Ma	G7	0.7	0.011		
	A.G. Berlin 1228	4 29.6	+19 46	7.2	0.033‡	F8	F7	3.2	0.016		
1074	58 Persei §	4 29.8	+41 4	4.5	0.025	G4p	F8	−4.2:	0.002		
C 594	A.Oe. 4961	4 29.8	+52 42	8.5	0.53	K6	K3	8.5	0.100	0.103	Ye, D
1077	α Tauri	4 30.2	+16 18	1.1	0.203	K4	K2	1.0	0.096	0.055	M, Ye, Y, *et al.*
	SZ Tauri §	4 31.4	+18 20	7.1	0.016‖	F8p	F6	−2.1	0.001		
1086	89 Tauri	4 32.4	+15 50	5.8	0.094	A8	A7	+2.1	0.018		
	B.D. +66°343	4 32.8	+66 32	8.9	0.375‡	G4	G6	5.0	0.017	0.022	G
1091	53 Eridani	4 33.6	−14 30	4.0	0.179	K1	G8	1.9	0.038		

C 602	Groom. 864	4^h34^m5	+41°56′	7.3	0″690	G2	G1	5.6	0″046	0″027	A, Y, Jo, F
1098		4 34.7	−14 33	5.6	0.186	K0	G9	3.1	0.032		
1100		4 35.4	+75 46	6.0	0.138	A8	......	2.0	0.016		
1105	54 Eridani	4 36.1	−19 52	4.5	0.094	Ma	G9	0.1	0.013		
1120		4 40.5	+18 33	6.1	0.091	K3	K3	0.5	0.008		
1128		4 42.7	+63 20	5.8	0.111	Mb	G9	0.5	0.009	0.002	M
1131		4 42.8	+18 33	6.8	0.440	G0	G0	5.0	0.044		
1136	96 Tauri	4 44.0	+15 44	6.3	0.017	K2	G8	0.9	0.008		
C 619	Groom. 884	4 44.4	+45 41	7.1	0.676	F9	F9	5.7	0.052	0.086	S, Y, R, J
1140	π^3 Orionis	4 44.4	+ 6 47	3.3	0.471	F5	F6	3.7	0.120	0.156	M
....	Bu. 2381	4 45.7	+10 54	7.7†	....	G0	F8	4.6	0.024	0.024	A, S, F
....	Bu. 2383	4 46.2	+13 29	6.8†	....	F9	F6	4.0	0.028	0.007	F
1149	4 Orionis	4 46.9	+14 5	5.2	0.059	Ma	G7	0.7	0.012		
1154	5 Orionis	4 48.2	+ 2 21	5.7	0.034	Ma	K0	0.5	0.009	0.009	W
1164		4 49.6	+74 7	6.2	0.050	K3	K1	0.7	0.008		
....	SU Aurigae §	4 49.6	+30 24	8.7	....	F7p	F8	−1.1	0.001		
1167	ι Aurigae	4 50.5	+33 0	2.9	0.028	K3	K0	0.0	0.026	−0.011	F
1168		4 50.6	−16 54	5.8	0.001	G8	G6	1.2:	0.012		
C 634	A.G. Leiden 1812	4 51.3	+34 7	8.0	0.60	G9	G6	6.4	0.048		
1175	99 Tauri	4 51.7	+23 48	6.0	0.025	K0	G8	1.5	0.012		
1176	8 Camelop.	4 51.8	+53 0	6.4	0.012	K3	K0	0.7	0.008		
1179		4 52.7	+66 41	6.3	0.355	F7	F6	3.9	0.033	0.000	Jo
1181	10 Orionis	4 53.4	+ 1 34	4.7	0.006	K2	G9	0.2	0.012		
1182	5 Aurigae	4 53.4	+39 15	6.0	0.013	F0	F3	2.5	0.020	0.002	W
1185	β Camelop. §	4 54.5	+60 18	4.2	0.013	F7p	F8	−2.9	0.004		
....	RX Aurigae §	4 54.5	+39 49	7.6	....	F9p	F7	−1.7	0.001		
1187	ε Aurigae §	4 54.8	+43 41	3.4	0.014	F5p	F9	−2.0	0.008	0.060	J
1190	ζ Aurigae	4 55.5	+40 56	3.9	0.032	G8p	G1	1.6	0.035	−0.007	A, Ab
C 648	W.B. 4^h1189	4 55.9	− 5 52	6.5	1.247	K5	K6	6.9	0.120	0.119	M, S, W, *et al.*
1196	12 Camelop.	4 57.5	+58 53	6.4	0.039	G5	G2	0.2	0.006		

TABLE VII—*Continued*

Boss	Name	α 1900	δ 1900	Harv. Vis. Mag.	μ	Spectrum		Spect. Abs. Mag.	Spect. π	Trig. π	Auth.
						Est.	Meas.				
1202	9 Aurigae	$4^{h}58^{m}.8$	+51°28′	5.0	0″.178	F4	F1	2.3	0″.029		
C 654	Lal. 9428	5 0.0	+64 48	6.4	0.190	F2	F4	2.8	0.019	0″.022	G
1211	ε Leporis	5 1.2	−22 30	3.3	0.072	K4	K1	0.7	0.030	0.022	M
1212	104 Tauri	5 1.5	+18 31	5.0	0.540	G0	G1	4.4	0.076	0.045	A, Y
1217	13 Orionis	5 2.2	+ 9 21	6.3	0.381	G0	G0	5.1	0.058		
1219	14 Orionis	5 2.5	+ 8 22	5.9†	0.066	F2	F2	2.0	0.017	0.022	S
1221	107 Tauri	5 2.9	+19 44	6.6	0.018	G5	G3	0.6	0.006		
1222		5 3.3	+46 50	5.6	0.170	F3	F3	2.3	0.022	0.032	Jo
1234		5 5.9	+15 55	5.4	0.004	K6	K1	0.5	0.010		
1235	19 H Camelop.	5 6.1	+79 7	5.2	0.174	F5	F6	3.0	0.036		
C 674	W.B. $5^{h}87$	5 7.1	− 9 13	8.0	0.57	K0	G9	5.8	0.036	0.049	D
1246	α Aurigae	5 9.3	+45 54	0.7†	0.437	G1	G1	0.1	0.076	0.067	A, Y, Jo, *et al.*
1247		5 9.4	+ 5 2	5.8	0.017	K3	K0	0.7	0.010		
1259	λ Aurigae	5 12.1	+40 1	4.8	0.843	G1	G0	4.3	0.079	0.081	A, M, S, *et al.*
1267		5 13.3	+20 2	6.2	0.048	K0	G7	1.4	0.011	0.021	W
C 683	Lal. 9960	5 14.1	− 3 11	8.6	0.722	K5	K4	7.1	0.050	0.074	Y
1309	17 Camelop.	5 20.7	+62 59	5.8	0.005	Ma	G8	0.7	0.010		
C 698	Bu. 2745 Br.	5 23.3	+54 35	7.6	0.409	G1	G1	5.5	0.038	0.024	Ye
C 699	Lal. 10299	5 23.5	− 3 34	8.6	0.841	K6	K6	8.4	0.091	0.058	Y, D
1323	β Leporis	5 24.0	−20 50	3.0	0.094	G2	G2	−0.7	0.018	0.004	M
1334		5 26.3	+74 59	6.4	0.019	K5	K1	0.4	0.006	0.011	A, Jo
C 705	W.B. $5^{h}592$	5 26.4	− 3 42	8.8	2.222	Ma	......	9.7	0.151	0.165	M, S, Ye, *et al.*
C 706	B.D. −0°981	5 26.6	+ 0 2	8.4	0.507	G6	G6	5.3	0.024		
1347	α Leporis §	5 28.3	−17 54	2.7	0.003	F4p	F4	−0.7	0.021	0.014	M
1348		5 28.4	+54 22	6.0	0.007	K6	K0	0.4	0.008		

1360		$5^h29^m.9$	+85° 9′	6.4	0″.020	K4	K1	0.7	0″.008		
C 709	Groom. 990	5 30.4	+51 23	7.9	0.563	K2	K0	6.3	0.048	0″.036	A, M, Y, Jo
1373	40 Orionis	5 31.4	+ 9 14	4.4	0.321	G7	G6	1.6	0.028	0.029	A, S, Ye
	A.G. Bonn 4626	5 32.3	+42 37	7.4	0.038‡	K4	K1	0.6	0.004		
1380		5 32.4	+65 39	5.8	0.024	K4	K1	0.7	0.010		
1385		5 33.2	+53 26	6.4	0.510	K0	G9	5.7	0.072	0.100	A, Y, Jo, Ab
C 714	Groom. 986	5 33.3	+74 34	7.3	0.240	G4	G3	3.7	0.019	0.021	G
1393	24 Camelop.	5 34.5	+56 32	6.2	0.037	K0	G8	2.3	0.017		
1394	23 Camelop.	5 34.9	+61 26	6.4	0.002	G5	G5	0.2	0.006		
	A.G. Bonn 4686	5 37.0	+43 31	7.7	0.033*	K0	G6	2.8	0.010		
	A.G. Bonn 4698	5 38.4	+42 49	8.0	......	K2	K1	0.0	0.003		
C 725	Lal. 10797	5 39.2	+37 15	7.3	0.706	K1	K0	5.7	0.048	0.086	A, D, Y, J
1419	γ Leporis Ft.	5 40.3	−22 27	6.4	0.461	K5	K3	6.9	0.126	0.149	M
1420	γ Leporis Br.	5 40.3	−22 29	3.8	0.468	F6	F5	3.8	0.100		
1424	130 Tauri	5 41.6	+17 41	5.5	0.010	F4	F2	1.8	0.018		
1429	τ Aurigae	5 42.2	+39 9	4.6	0.035	G5	G7	0.3	0.014	0.014	A
1434	132 Tauri	5 42.9	+24 32	5.0	0.036	K0	G7	2.3	0.029		
1439	υ Aurigae	5 44.2	+37 17	5.0	0.052	Ma	K0	0.0	0.010		
1441		5 44.5	+ 9 50	5.9	0.014	G6	G6	0.8	0.009		
1442	ν Aurigae	5 44.6	+39 7	4.2	0.008	K0	K0	0.2	0.016	0.022	A
1444		5 44.7	+27 56	5.6	0.009	G7	G7	0.1	0.008		
1456	δ Leporis	5 47.0	−20 53	3.9	0.696	G7	G6	1.5	0.033	0.024	M
1461	χ Orionis	5 48.5	+20 15	4.6	0.208	G1	G1	4.4	0.091	0.105	A, M
1468	α Orionis	5 49.8	+ 7 23	0.9	0.029	Ma	G3	−3.8	0.012	0.021	A, Y
C 739	Lal. 11196	5 50.3	+13 55	6.5	0.629	G5	G1	5.7	0.069	0.078	A, Y
1472	δ Aurigae	5 51.3	+54 17	3.9	0.153	G7	G8	0.7	0.023	0.029	A, M, Ye, *et al.*
1476	η Leporis	5 51.9	−14 11	3.8	0.138	F3	F4	2.6	0.058	0.036	M
1479	π Aurigae	5 52.5	+45 56	4.6	0.011	Mb	G6	−0.8	0.008		
1483		5 53.0	+44 35	6.4	0.051	K2	K1	1.1	0.009		
1494		5 55.1	− 3 5	4.7	0.084	K1	G8	2.1	0.030		

TABLE VII—*Continued*

Boss	Name	α 1900	δ 1900	Harv. Vis. Mag.	μ	Spectrum Est.	Spectrum Meas.	Spect. Abs. Mag.	Spect. π	Trig. π	Auth.
C 756	A.G. Berlin 1866	$5^{\mathrm{h}}57^{\mathrm{m}}3$	+19° 23′	9.0	0″93	F9	F9	4.9	0″015		
1508	1 Gemin.	5 58.0	+23 16	4.3	0.108	G4	G3	2.1	0.036	0″025	A
1511		5 59.2	−26 17	5.2	0.104	K2	G8	1.4	0.017		
C 760	Lal. 11471	5 59.5	+35 24	6.1	0.332	G1	G0	4.8	0.055	0.048	A
1513	63 Orionis	5 59.6	+ 5 26	5.8	0.007	G6	G5	0.4	0.008		
1514	66 Orionis	5 59.7	+ 4 10	5.7	0.012	G4	G1	−1.1	0.004		
C 761	B.D. +26°1067	5 59.7	+26 34	8.9	0.42	K4	K2	6.6	0.035	0.021	Ye
	Groom. 1059	6 0.6	+76 31	8.0†	0.004	F5	F7	2.5	0.008		
1549	6 Gemin.	6 6.3	+22 56	6.3	0.027	Ma	G4	0.8	0.008	0.003	W
1560	1 Lyncis	6 8.7	+61 33	5.3	0.005	Mb	G5	0.6	0.011		
1561	η Gemin.	6 8.8	+22 32	3.7	0.065	Ma	G6	−0.5	0.014	0.016	A, M, R
1564	71 Orionis	6 9.0	+19 11	5.2	0.224	F6	F5	2.9	0.035	0.039	A
1565	κ Aurigae	6 9.0	+29 32	4.4	0.274	G8	G7	0.5	0.017	0.026	A, Jo
C 780	W.B. $6^{\mathrm{h}}128$	6 9.6	+44 45	8.6	0.41	G9	G8	6.4	0.036	0.102	Ram
1573	8 Gemin.	6 10.2	+24 0	6.1	0.029	G5	G5	0.7	0.008		
1576	43 Aurigae	6 10.8	+46 24	6.5	0.133	K1	K0	0.7	0.007	0.036	Jo
1577	74 Orionis	6 10.8	+12 18	5.1	0.212	F5	F4	3.4	0.046		
1582		6 12.0	+ 5 8	5.8	0.282	G0	F9	3.8	0.040	0.051	A
1596		6 14.4	+14 42	6.0	0.019	K6	K1	0.6	0.008		
1599		6 15.0	− 2 54	5.2	0.009	Ma	K0	0.0	0.009	−0.004	M
1604	μ Gemin.	6 16.9	+22 34	3.2	0.128	Ma	G6	−0.8	0.016	0.026	A, M
1606	46 Aurigae §	6 17.2	+49 20	5.1	0.014	K2p	G5	−3.6	0.002		
1608	5 Lyncis	6 18.1	+58 28	5.5	0.011	K6	K2	0.6	0.011		
	T Monocer. §	6 19.8	+ 7 8	6.2	0.029‖	G1p	G0	−2.0	0.003		
1622	α Argus*	6 21.7	−52 38	−0.9	0.018			−3:	0.038	0.007	C

1627	6 Lyncis	$6^h22^m.1$	+58° 14′	6.0	0″.330	G8	G7	2.9	0″.024	0″.004	A, Ab, Jo
1629	RT Aurigae §	6 22.1	+30 33	5.3	0.024	F8p	F5	−1.9	0.003	0.031	W, S
1632	47 Aurigae	6 22.6	+46 45	6.0	0.007	K5	K1	0.5	0.008	0.017	M
1643		6 24.9	+78 5	5.9	0.019	K5	K1	0.7	0.009	0.017	W
1646	WW Aurigae	6 25.9	+32 32	6.6†	0.035	A7p	......	1.9	0.012		
1653	12 Monocer.	6 27.0	+ 4 56	6.0	0.027	G8	G7	0.9	0.009		
1665	8 Lyncis	6 28.6	+61 34	6.0	0.341	G8	G6	2.9	0.024	0.035	A, Jo
1673	23 H Camelop.	6 29.2	+79 40	5.6	0.620	F7	F8	4.2	0.052	0.037	Y
	W Gemin. §	6 29.2	+15 24	7.1	0.009‖	Gop	F6	−2.6	0.001		
	Bu. 3474	6 30.2	+27 22	7.0†	0.061*	Go	Go	4.3	0.029	0.040	A, S
1687	51 Aurigae	6 31.7	+39 29	5.7	0.119	K3	K1	1.1	0.012		
	W.B. 6^h886	6 32.0	+12 14	8.3	....	F1	A9	1.8	0.005	−0.021	Ye
1704	25 Gemin.	6 35.0	+28 17	6.5	0.017	G5	Go	−1.2	0.003		
1707	55 Aurigae	6 35.8	+44 37	5.2	0.055	K5	K2	0.8	0.013		
C 824	Lal. 12831	6 37.3	+40 44	6.9	0.171	Mb	G7	0.4	0.005	−0.004	Jo
1717	ε Gemin.	6 37.8	+25 14	3.2	0.020	G8	G2	−1.4	0.012	0.009	A, M
1721	30 Gemin.	6 38.3	+13 20	4.6	0.076	K2	Ko	1.0	0.019		
1724	56 Aurigae	6 39.5	+43 41	5.3	0.158	F9	F9	4.3	0.063	0.077	A, Jo
1725	ξ Gemin.	6 39.7	+13 0	3.4	0.231	F3	F6	2.0	0.052	0.051	A, M
1732	α Can. Maj.	6 40.7	−16 35	−1.58	1.316	A3	......	1.3:	0.376	0.376	F, C
1740	18 Monocer.	6 42.6	+ 2 31	4.7	0.026	Ko	G9	0.2	0.013	0.024	A
1756	35 Gemin.	6 44.8	+13 32	5.9	0.013	K3	Ko	0.8	0.010		
1758	24 H Camelop.	6 45.5	+77 6	4.8	0.085	K5	K5	0.3	0.013		
C 834	Lal. 13284	6 47.4	− 5 3	6.8	0.582	K5	K4	7.1	0.115	0.121	Y
1776	Bu. 3678	6 48.6	+58 33	4.9	0.134	G4	G4	0.1	0.011	0.029	S
1778	38 Gemin.	6 49.0	+13 18	4.7	0.112	A8	A8	2.4	0.035	0.049	A
1783	θ Can. Maj.	6 49.5	−11 55	4.2	0.138	K4	K1	0.8	0.021	0.017	Ye
C 837	A.G. Bonn 5621	6 49.5	+40 13	8.3	0.43	K5	K4	7.3	0.063		
C 841	W.B. 6^h1500	6 51.4	+ 1 18	7.7	0.570	G6	G3	5.6	0.038	0.006	Y
	Groom. 1239	6 51.9	+69 21	7.5	0.005	Ma	G8	0.7	0.004		

TABLE VII—*Continued*

Boss	Name	α 1900	δ 1900	Harv. Vis. Mag.	μ	Spectrum		Spect. Abs. Mag.	Spect. π	Trig. π	Auth.
						Est.	Meas.				
1801	51 H Cephei	6h 53m.7	+87° 12′	5.3	0″.051	Ma	G9	0.4	0″.011		
C 847	Lal. 13427	6 54.0	+48 32	8.2	0.697	K4	K2	6.6	0.048	0″.032	M, Ye, Y
1809		6 57.2	+29 30	6.0	0.838	G2	G1	5.1	0.066	0.061	A, Y, F
1815	ζ Gemin. §	6 58.2	+20 43	4.0	0.009	G0p	F9	−3.4	0.003	0.015	A, S, Ab
1818		6 59.2	− 5 11	5.9	0.006	K2	G6	0.5	0.008		
1822		6 59.6	+34 38	5.6	0.087	G4	G4	0.1	0.008	0.036	W
C 859	Lal. 13792	7 3.5	+25 54	7.0	0.225	G5	G4	4.8	0.036	0.031	A
C 861	Lal. 13849	7 4.2	+21 25	6.5	0.510	G9	G7	4.6	0.042	0.042	A, S, Y
1839	δ Can. Maj. §	7 4.3	−26 14	2.0	0.005	G2p	G0	−2.9	0.010	−0.059	F
1840	τ Gemin.	7 4.8	+30 25	4.5	0.053	K3	K2	0.5	0.016	0.010	A
1841	63 Aurigae	7 4.8	+39 29	5.1	0.048	K3	K1	1.0	0.015		
1846		7 5.6	+51 36	5.7	0.019	Mb	G9	0.1	0.008	0.002	M, W
1854	18 Lyncis	7 7.2	+59 49	5.3	0.272	K2	K0	1.3	0.016	0.036	A
1856	51 Gemin.	7 7.6	+16 20	5.3	0.051	Mb	G7	0.1	0.009		
1860		7 8.4	+47 25	5.6	0.184	F9	F9	5.0	0.076	0.069	Jo
1861	52 Gemin.	7 8.6	+25 4	6.0	0.105	K7	K4	0.4	0.008		
1868	53 Gemin.	7 9.7	+28 4	5.9	0.020	Ma	K2	−0.2	0.006	0.008	W
1873	24 Monocer.	7 10.2	+ 0 1	6.5	0.019	G5	G5	−0.2	0.005		
C 873	Lal. 14146	7 11.3	−12 53	7.7	0.513	F9	F9	3.9	0.017	0.051	M, Y
1898	δ Gemin.	7 14.2	+22 10	3.5	0.025	A7	......	1.1	0.033	0.062	A, M
1909	R Can. Maj.	7 14.9	−16 12	6.0†	0.212	A9	F0	1.7	0.014		
1912	65 Aurigae	7 15.4	+36 57	5.2	0.089	K1	G9	1.2	0.016		
1919	66 Aurigae	7 17.2	+40 52	5.3	0.024	K0	G8	−0.3	0.008	−0.061	Ab
1926	59 Gemin.	7 18.3	+27 50	5.7	0.020	F0	F2	1.3	0.013		
1931	ι Gemin.	7 19.5	+28 0	3.9	0.145	G8	G8	0.5	0.021	0.026	A, M

1937		$7^h20^m.5$	+68°40′	5.8	0″.044	Ko	G7	1.8	0″.016		
1940		7 20.9	+21 44	6.4	0.309	F5	F6	3.9	0.032	0″.040	A
1945	63 Gemin.	7 21.8	+21 39	5.3	0.133	F3	F5	2.8	0.032		
1952	ρ Gemin.	7 22.7	+31 59	4.2	0.236	A9	F1	1.5	0.029	0.055	M, Jo
1962	6 Can. Min.	7 24.2	+12 13	4.8	0.019	K3	Ko	0.4	0.013	0.024	A
1963		7 24.3	− 1 42	5.8	0.011	K3	G8	0.8	0.010		
1971		7 26.0	+17 18	5.6	0.089	K1	Ko	0.7	0.011	0.000	W
	Groom. 1324	7 26.3	+66 41	7.5	0.017	Mb	G9	0.6	0.004		
	Comp. α Gemin.*	7 28.2	+32 8	9.4†	0.203	Mdp	......	9.2	0.091	0.079	A, M, Ye, *et al.*
1987	υ Gemin.	7 29.8	+27 7	4.2	0.119	K6	K2	0.5	0.018	0.015	A
1999	25 Monocer	7 32.3	− 3 53	5.2	0.072	F4	F5	1.3	0.017		
2000	23 Lyncis	7 32.6	+57 19	6.2	0.018	K4	Ko	0.4	0.007		
2001	o Gemin.	7 32.6	+34 49	4.9	0.125	Fo	F1	0.8	0.015	0.023	A, Ab
2005	74 Gemin.	7 33.7	+17 54	5.2	0.004	K8	Ko	−0.3	0.008		
2006		7 33.8	+48 22	5.8	0.144	G7	G8	0.2	0.008	0.011	A
2008	α Can. Min.	7 34.1	+ 5 29	0.5	1.242	F3	F5	3.2	0.347	0.309	M, S, Ye, *et al.*
2020		7 36.4	+14 27	5.8	0.015	Ma	G6	−0.4	0.006	0.006	W
2021	γ Monocer.	7 36.5	− 9 19	4.1	0.079	Ko	G9	0.4	0.018	0.005	M
2023	σ Gemin.	7 37.1	+29 8	4.3	0.247	K1p	G7	2.6	0.046	0.027	A, Ye, Jo
2024	51 Camelop.	7 37.1	+65 42	6.0	0.046	K2	K1	0.8	0.009		
C 922	W.B. 7^h1029	7 38.1	+39 49	6.8	0.68	F6	F8	3.8	0.025	0.025	Ye
2029	κ Gemin.	7 38.4	+24 38	3.7	0.066	G7	G6	0.9	0.028	0.024	A, M
2031	β Gemin.	7 39.2	+28 16	1.2	0.625	G9	G8	1.7	0.126	0.064	Y
2034		7 39.8	+80 31	6.5	0.478	G9	G6	4.8	0.046	0.049	G, Y
2049	π Gemin.	7 41.1	+33 40	5.3	0.040	Ma	Ko	0.3	0.010	0.028	Ab
2051	4 Puppis	7 41.3	−14 19	5.1	0.017	A8	......	1.6	0.020		
2065	ξ Puppis §	7 45.1	−24 37	3.5	0.007	G6p	G1	−4.2:	0.003		
2075	Bu. 4310	7 47.1	−13 38	5.7	0.344	Go	Go	5.2	0.079	0.079	M, S, F
2076	25 Lyncis	7 47.2	+47 39	6.4	0.017	K1	G8	0.4:	0.006		
C 935	Lal. 15290	7 47.2	+30 55	8.2	1.962	F9	F8	4.7	0.020	0.055	A, Y, M, *et al.*

TABLE VII—*Continued*

Boss	Name	α 1900	δ 1900	Harv. Vis. Mag.	μ	Spectrum		Spect. Abs. Mag.	Spect. π	Trig. π	Auth.
						Est.	Meas.				
2079	26 Lyncis	7h47m4	+47° 49′	5.7	0″.043	K4	K1	0.4	0″.009		
	Lal. 15389	7 47.8	−13 36	6.9	0.101*	K0	G9	2.0	0.011		
2084		7 48.2	+74 11	5.6	0.034	K3	K1	0.8	0.011		
C 940	Lal. 15394	7 49.1	+19 31	7.9	0.471	K4	K3	6.5	0.052	0″.075	D
2098	1 Cancri	7 51.3	+16 3	6.0	0.056	K3	K3	0.8	0.009		
C 947	Lal. 15547	7 53.7	+21 8	8.6	0.573	G9	K0	5.6	0.025	0.089	Y
C 949	Lal. 15565	7 54.3	+29 31	6.9	1.170	G7	G4	5.9	0.063	0.066	A, Ye, Y
2117	2 Cancri	7 54.9	+25 40	5.9	0.014	G8	G7	−0.6	0.005		
2118	3 Cancri	7 55.1	+17 35	5.8	0.015	K4	K0	0.4	0.008		
2130		7 57.1	+ 2 37	4.5	0.106	K2	G9	1.1	0.021	0.030	A, S
C 952	Fed. 1221	7 57.2	+72 13	8.0	0.496	G0	G2	5.7	0.035		
2131	χ Gemin.	7 57.4	+28 4	5.0	0.056	K3	K1	0.3	0.012		
C 955	Bu. 4414	7 58.8	+12 35	8.6†	0.141	K0	G9	3.2	0.008	0.088	S
2144	9 Cancri	8 0.4	+22 55	6.2	0.024	Mb	G7	0.4	0.007		
2146	μ Cancri	8 1.9	+21 52	5.4	0.085	G3	G1	3.7	0.046		
2148		8 2.5	+42 43	6.4	0.073	K3	K2	0.8	0.008	−0.030	Ab
2150	55 Camelop.	8 2.9	+68 46	5.5	0.006	G4	G4	−0.7	0.006		
2153	ρ Puppis §	8 3.3	−24 1	2.9	0.100	F7p	F6	−2.1	0.010	0.031	M
2155	29 Monocer. §	8 3.6	− 2 42	4.4	0.025	G3p	F9	−4.2:	0.002		
2157	14 Cancri	8 4.4	+25 49	5.8	0.361	G5	G5	3.2	0.030	0.036	A
2161		8 5.4	+32 46	7.0	0.807	G6	G2	5.8	0.058	0.046	M, Y, Jo
2168	ζ Cancri A	8 6.5	+17 57	5.6	0.155	F9	F9	3.5	0.038	0.038	Ye, S, F
2169	ζ Cancri C	8 6.5	+17 57	6.0	0.155	G0	F9	4.4	0.048		
2174		8 7.0	+76 4	5.7	0.027	G6	G7	0.3	0.008		
2183	20 Puppis	8 8.7	−15 29	5.0	0.015	G3	G1	−2.0	0.004		

2193......	57 Camelop..........	8h 10m.6	+62°49′	5.8	0″.018	G6	G5	0.9	0″.010		
2195......	β Cancri............	8 11.1	+ 9 30	3.8	0.075	K4	K1	0.4	0.021	0″.003	A, M
C 977......	W.B. 8h181..........	8 12.0	+30 56	8.6	0.873	K5	K5	7.2	0.052	0.014	Y, F
2199......	....	8 13.7	−12 18	6.0	1.030	K0	G7	6.2	0.110	0.081	M, S, Y, F
2202......	χ Cancri............	8 14.0	+27 32	5.2	0.388	F7	F7	3.6	0.048	0.066	A, S
2203......	....	8 14.3	+ 60 57	6.5	0.011	K0	G8	2.4	0.015		
2208......	31 Lyncis...........	8 16.0	+43 31	4.4	0.107	K5	K1	0.7	0.018	0.009	A, Ab
C 982......	A.Oe. 8869..........	8 16.3	+66 48	8.9	0.52	K4	K3	6.4	0.032		
2218......	20 Cancri...........	8 17.6	+18 39	5.9	0.064	F1	......	1.9	0.016		
2220......	....	8 17.9	+42 20	6.2	0.011	K6	G8	0.5	0.008		
2223......	21 Cancri...........	8 18.5	+10 57	6.3	0.021	Ma	G8	0.4	0.007		
2224......	298 G Puppis §......	8 18.6	−26 2	5.9	0.017	F5p	F2	−2.0	0.003		
2227......	1 Hydrae............	8 19.6	− 3 26	5.7	0.216	F1	F3	3.6	0.038		
2229......	25 Cancri...........	8 20.2	+17 23	6.2	0.246	F4	F4	2.8	0.021		
2231......	....	8 20.3	+67 38	6.0	0.056	G7	G7	1.4	0.012		
2234......	....	8 20.5	+ 7 53	5.2	0.043	G5	G4	−0.4	0.008		
2236......	....	8 20.6	+45 59	6.3	0.362	G6	G0	4.9	0.052		
2245......	27 Cancri...........	8 21.2	+12 59	5.8	0.116	Mb	G4	0.3	0.008	0.029	W
2247......	o Urs. Maj..........	8 22.0	+61 3	3.5	0.166	G2	G2	−0.8	0.014	0.002	A, F
2268......	....	8 26.4	+38 22	6.0	0.204	K3	K2	0.7	0.009		
2272......	32 Lyncis...........	8 26.9	+36 47	6.1	0.139	F3	F4	3.1:	0.025	0.088	Jo
2275......	32 Cancri...........	8 27.1	+24 25	6.4	0.091	G9	G7	0.7	0.008		
....	A.G. Cam. 3181......	8 28.2	+54 4	8.7	....	G8	G7	2.9	0.007		
2278......	....	8 28.6	+73 59	6.3	0.106	G8	G8	1.6	0.011		
C1000......	W.B. 8h596..........	8 28 8	+42 6	8.6	0.66	K4	K2	6.7	0.042	0.022	Ye
2282......	35 Cancri...........	8 29.6	+19 56	6.6	0.045	F5	F7	1.7	0.011		
2285......	Bu. 4677 Br.........	8 30.5	+ 6 58	6.0	0.195	F8	F7	4.0	0.040	0.024	W
2286......	Bu. 4677 Ft.........	8 30.5	+ 6 58	7.2	0.201	G4	G4	5.5	0.046		
2289......	....	8 30.9	+53 45	5.7	0.072	G4	G4	0.7	0.010		
2290......	π Urs. Maj..........	8 31.5	+64 41	4.8	0.052	K2	G9	1.0	0.017	0.018	A

TABLE VII—*Continued*

Boss	Name	α 1900	δ 1900	Harv. Vis. Mag.	μ	Spectrum		Spect. Abs. Mag.	Spect. π	Trig. π	Auth.
						Est.	Meas.				
2293......	....	$8^h31^m.9$	+53° 4′	6.0	0″.040	K2	K1	1.2	0″.011	−0″.028	A
2294......	....	8 32.1	+33 9	6.1	0.023	K2	G9	0.7	0.008		
C1008......	Lal. 16933...........	8 32.2	+26 24	7.6	0.237	G1	G1	4.5	0.024	0.027	A
C1012......	Lal. 16904...........	8 33.1	+56 2	8.1	0.470	G5	G2	5.4	0.029	−0.042	Y
2302......	σ Hydrae............	8 33.5	+ 3 42	4.5	0.027	K2	K0	−0.1	0.012	0.019	A
C1014......	Lal. 17046...........	8 34.4	+11 53	7.9	0.531	K2	K0	6.3	0.048	0.031	M
2312......	Bu. 4714 Br..........	8 34.8	−22 19	5.4	0.478	G6	G5	3.1	0.035	−0.042	F
....	A.G. Leiden 3622......	8 35.8	+33 44	8.5	....	K2	K1	1.3	0.004		
2321......	9 Hydrae............	8 37.1	−15 35	5.0	0.099	K0	K0	2.4:	0.030		
2333......	....	8 38.6	+42 3	8.2	0.702	K4	K3	7.1	0.060	0.049	S, Y
2335......	31 Monocer...........	8 38.8	− 6 52	4.7	0.007	G2	F7	1.1	0.019		
2336......	δ Cancri.............	8 39.0	+18 31	4.2	0.240	G9	G9	0.8	0.021	0.018	A, M
2338......	46 Cancri............	8 39.2	+31 4	6.1	0.020	G3	G3	−1.0	0.004	0.007	W
....	A.G. Leiden 3648......	8 39.3	+33 36	8.0	0.011‡	K2	G8	1.1	0.004		
2348......	ι Cancri..............	8 40.6	+29 8	4.2	0.054	G5	G5	−1.3	0.008	0.028	A, M
2354 Br....	ε Hydrae AB..........	8 41.5	+ 6 47	3.5†	0.196	F9	G0	2.1	0.052	0.017	A, M, S, Ait
2354 Ft....	ε Hydrae C...........	8 41.5	+ 6 47	7.5	0.196	F5	F7	3.5	0.016		
C1040......	Bu. 4815 S............	8 46.0	+71 11	8.7	1.390	K6	K5	8.7	0.100	0.086	G, F
....	Bu. 4815 N...........	8 46.0	+71 11	9.1	1.390	K9	K5	9.2	0.105		
2378......	53 Cancri............	8 46.5	+28 38	6.3	0.022	Mb	G7	0.8	0.008	0.000	M
2380......	55 Cancri............	8 46.6	+28 43	6.1	0.541	K2	K1	5.7	0.083	0.080	A, M, Y, Jo
2384......	Bu. 4839 Ft..........	8 48.1	+30 57	6.6	0.051	K0	G9	0.9	0.007		
2384......	Bu. 4839 Br..........	8 48.1	+30 57	6.1	0.051	G9	G8	0.0	0.006		
C1050......	W.B. 8^h1147..........	8 49.0	+26 35	6.7	0.44	G1	G1	4.2	0.032	0.018	Ye
2393......	ζ Hydrae............	8 50.1	+ 6 20	3.3	0.104	G5	G7	−0.9	0.014	0.017	A, M

2394	60 Cancri	$8^h50^m.5$	+12° 0′	5.7	0″.021	K4	K0	0.6	0″.010		
2404	ι Urs. Maj.	8 52.4	+48 26	3.1	0.502	A5	......	1.9	0.058	0″.090	Y, Ab, F
2410		8 53.5	+18 31	6.6	0.089	Mc	G9	0.2	0.005		
2411	ρ Urs. Maj.	8 53.5	+68 1	5.0	0.021	Ma	K1	−0.1	0.009		
2412		8 54.0	−15 45	5.9	0.324	F5	F5	3.9	0.040		
2413	10 Urs. Maj.	8 54.2	+42 11	4.1	0.504	F3	F6	3.2	0.066	0.066	A, S, Y, F
2437		9 0.2	+38 51	4.7	0.043	G3	G3	−2.7	0.003	0.007	A
2441	13 Urs. Maj.	9 1.6	+67 32	4.9	0.070	F5	F6	3.8	0.060		
2442	Bu. 4929 Br.	9 1.7	+23 23	7.3	0.161	F3	F5	3.5	0.017 }	0.019	W
2442	Bu. 4929 Ft.	9 1.7	+23 23	7.7	0.161	F4	F4	3.5	0.014 }		
2447	75 Cancri	9 2.9	+27 3	6.0	0.404	G2	G2	4.1	0.042		
2449	ξ Cancri	9 3.6	+22 27	5.2	0.008	K0	G8	0.8	0.013		
2450	κ Pyxidis	9 3.7	−25 27	4.8	0.040	K3	G9	1.1:	0.018		
C1083	Lal. 18067	9 3.8	−14 44	7.3	0.557	G0	G0	4.9	0.033		
2455	79 Cancri	9 4.6	+22 24	6.1	0.010	G8	G6	2.1	0.016		
2464	81 Cancri	9 6.8	+15 24	6.4	0.576	G9	G6	5.5	0.066	0.044	A, Y
....	Bu. 4968 Br.	9 6.9	+47 24	7.8†	0.038	F7	F6	3.3	0.013		
2469	Bu. 4972^1	9 7.6	+53 7	7.9	1.677	K8	K7	8.7	0.145 }	0.152	Ye, F, Ab, *et al.*
2470	Bu. 4972^2	9 7.6	+53 7	8.0	1.686	K6	K5	8.6	0.132 }		
2478		9 9.1	+35 3	6.0	0.149	G1	G1	1.5	0.013		
2490	23 Hydrae	9 11.7	− 5 56	5.4	0.004	K2	K0	0.2	0.009		
C1096	Bu. 5005	9 12.0	+29 0	7.9†	0.517	K3	K3	6.5	0.052	0.067	S, Y, F
2501	83 Cancri	9 13.4	+18 8	6.6	0.180	F6	F7	3.5	0.024		
2507	α Lyncis	9 15.0	+34 49	3.3	0.216	K5	K2	0.6	0.029	−0.057	Jo
2516	θ Pyxidis	9 17.1	−25 32	4.9	0.022	Ma	G9	0.8	0.015		
2524	κ Leonis	9 18.8	+26 37	4.6	0.061	K2	K0	1.3	0.022	−0.004	A
....	A.G. Leiden 3861	9 19.7	+33 12	7.9	0.037‡	G9	G7	2.3	0.008		
2528		9 20.0	+17 1	6.3	0.079	K0	G8	2.2	0.015	0.015	W
2529	28 Hydrae	9 20.4	− 4 41	5.8	0.023	K4	G9	0.6	0.009		
2533	α Hydrae	9 22.7	− 8 14	2.2	0.035	K5	K0	0.1	0.038	0.004	Y, F

TABLE VII—*Continued*

Boss	Name	α 1900	δ 1900	Harv. Vis. Mag.	μ	Spectrum		Spect. Abs. Mag.	Spect. π	Trig. π	Auth.
						Est.	Meas.				
2536......	1 H Draco..........	9h22m9	+81°46′	4.6	0″.027	K4	K1	0.5	0″.015		
2540......	23 Urs. Maj.........	9 23.7	+63 30	3.8	0.117	A6	......	1.3	0.032		
C1126......	Lal. 18672..........	9 24.7	+ 6 5	7.6	0.533	K4	K2	6.6	0.063		
2549......	24 Urs. Maj.........	9 25.6	+70 16	4.6	0.090	G3	G2	2.0	0.030	0″.048	Y
2550......	λ Leonis............	9 26.0	+23 25	4.5	0.056	K6	K2	0.5	0.016	0.039	M
2552......	θ Urs. Maj..........	9 26.2	+52 8	3.3	1.092	F5	F6	3.0	0.087	0.073	A, M, Ab, *et al.*
2555......	ξ Leonis............	9 26.6	+11 45	5.1	0.130	G9	G7	−0.1	0.009		
2556......	6 Leonis............	9 26.6	+10 9	5.3	0.024	K3	K0	0.5	0.011		
C1131......	Lal. 18721..........	9 26.9	+27 26	7.1	0.279	G8	G8	5.2	0.042	0.055	A
....	S Antliae*..........	9 27.9	−28 11	6.5	....	A8p	......	0.7	0.007		
2566......	10 Leo. Min.........	9 28.1	+36 50	4.6	0.030	G4	G4	0.7	0.016		
2573......	11 Leo. Min.........	9 29.7	+36 16	5.5	0.753	K1	G6	5.4	0.096	0.140	A, S, Y, Jo
2580......	8 Leonis............	9 31.5	+16 53	5.9	0.021	K1	G7	0.6	0.009		
C1143......	A.Oe. 10038.........	9 31.5	+72 12	7.8	0.26	F6	F6	3.9	0.017	−0.002	G
2589......	2 Sextantis.........	9 33.2	+ 5 6	4.8	0.176	K2	G9	1.5	0.022		
2595......	ι Hydrae............	9 34.7	− 0 41	4.1	0.085	K3	K1	0.8	0.022		
2602......	o Leonis §..........	9 35.8	+10 21	3.8	0.150	F5p	F6	−1.4	0.009	0.032	A, M
2603......	13 Leonis...........	9 35.9	+26 22	6.4	0.049	K2	G8	0.7	0.008	0.012	W
....	W Urs. Maj.*........	9 36.7	+56 25	8.6†	....	F8p	......	3.5	0.010	0.012	Ye
C1153......	Lal. 19022..........	9 37.1	+43 10	8.1	0.819	K5	K6	7.2	0.066	0.086	Ye, K, F
2609......	....	9 37.7	−23 28	5.0	0.474	F8	F7	4.2	0.069		
2612......	ψ Leonis............	9 38.3	+14 29	5.6	0.014	Ma	G7	0.6	0.010		
2614......	....	9 39.4	+57 35	5.4	0.025	Mb	G6	0.2	0.009		
2618......	ε Leonis............	9 40.2	+24 14	3.1	0.048	G0	G0	−0.9	0.016		
2621......	....	9 40.9	+ 7 10	6.0	0.040	Ma	G8	0.9	0.009		

2622	18 Leonis	9h41m0	+12° 16′	5.9	0″016	K5	G9	0.6	0″008		
2632	υ Urs. Maj.	9 43.9	+59 31	3.9	0.330	A8	A8	1.5	0.033		
2639	23 Leonis.	9 45.6	+13 32	6.7	0.037	K7	K0	0.2	0.005		
2648	μ Leonis	9 47.1	+26 29	4.1	0.227	K3	K2	0.6	0.020	0″025	A
2656		9 49.5	+73 21	6.0	0.079	K2	K1	0.4	0.008	0.001	Ab
2660		9 50.3	+57 54	6.0	0.068	G4	G4	0.3	0.008	0.006	W
2663		9 51.1	+ 9 24	5.9	0.090	K1	G9	0.3	0.008	0.010	W
2671		9 52.8	+ 8 47	6.3	0.035	K4	K1	0.6	0.007		
2680	π Leonis.	9 54.9	+ 8 31	4.9	0.043	Ma	K1	−0.9	0.007		
C1189	Groom. 1596	9 54.9	+56 5	8.3	0.498	G7	G5	5.7	0.030	0.069	Y
2681	20 Leo. Min.	9 55.2	+32 25	5.6	0.681	G7	G3	5.3	0.087	0.064	A, K, Jo, F
C1192	A.Oe. 10427	9 56.1	+71 21	8.3	0.24	G1	G2	3.9	0.013	0.027	G
C1197	Groom. 1603	9 57.9	+38 30	6.8	0.170	F6	F7	3.7	0.024	0.032	A
2696	31 Leonis	10 2.6	+10 29	4.6	0.117	K5	K3	0.4	0.014		
	Comp. α Leonis.	10 2.9	+12 29	7.6	0.247	K2	K0	6.2	0.052	0.033	Y
C1211	Lal. 19780	10 3.6	−19 15	7.2	0.355	G2	G0	5.1	0.038	0.057	F
2701		10 5.0	+41 9	6.5	0.017	K2	G8	0.6	0.007		
C1218	Groom. 1618	10 5.3	+49 58	6.8	1.451	K6	K6	8.3	0.200	0.177	K, F, P
2706	λ Hydrae	10 5.7	−11 52	3.8	0.221	K0	G9	−0.7	0.013		
C1222	Lal. 19821	10 6.3	+24 15	8.6	0.414	G4	G2	5.7	0.026	0.049	Y
C1225	A.Oe. 10640	10 7.5	+53 1	9.2	0.74	K3	K3	7.0	0.036	0.073	Ye
	A.Oe. 10642	10 7.5	+50 48	9.0	...	G6	G4	1.0	0.003		
C1229	Lal. 19896	10 8.9	+ 3 39	7.7	0.464	G1	G0	4.5	0.023	−0.048	Y
2728	35 Leonis.	10 11.0	+24 0	5.9	0.209	G1	G1	3.3	0.030	0.026	A, M
2730	ζ Leonis	10 11.1	+23 55	3.6	0.027	F0	F3	−0.1	0.018	0.010	M
2734	39 Leonis	10 11.7	+23 36	5.8	0.423	F8	F7	3.7	0.038	0.092	Y
2740		10 14.1	+54 43	6.2	0.023	K0	G9	1.3	0.010		
C1244	W.B. 10h234	10 14.2	+20 22	9.2	0.490	Mdp	...	10.5	0.182	0.196	D
2741	40 Leonis	10 14.3	+19 59	5.0	0.329	F5	F5	3.2	0.044	0.052	M
2742	γ Leonis Br.	10 14.5	+20 21	2.6	0.338	G8	G8	0.8	0.044	0.000	M, Y, F
2743	γ Leonis Ft.	10 14.5	+20 21	3.8	0.353	G5	G5	−0.2	0.016		

TABLE VII—*Continued*

Boss	Name	α 1900	δ 1900	Harv. Vis. Mag.	μ	Spectrum Est.	Spectrum Meas.	Spect. Abs. Mag.	Spect. π	Trig. π	Auth.
C1246	Mün. 5178	$10^{h}15^{m}.7$	$-0°58'$	8.9	0".679	K5	K3	7.4	0".050		
2750		10 16.2	+41 44	5.9	0.194	F9	F8	3.5	0.033	0".090	M, Jo
2751	μ Urs. Maj.	10 16.4	+42 0	3.2	0.084	K5	G8	0.7	0.032	0.051	Y
2757	43 Leonis	10 17.8	+ 7 3	6.3	0.108	K2	K0	0.7	0.008		
2762	30 H Camelop.	10 18.9	+83 4	5.3	0.084	F0	F3	2.3	0.025		
2771	μ Hydrae	10 21.3	−16 20	4.1	0.153	K5	K2	0.8	0.022		
2775		10 21.9	+49 19	6.5	0.898	G2	G1	5.6	0.066	0.078	K, R, F
2776	β Leo. Min.	10 22.1	+37 13	4.4	0.161	G6	G7	1.2	0.023	0.013	M, Ab
2780	35 Urs. Maj.	10 22.8	+66 8	6.4	0.045	K2	K1	1.0	0.008		
C1264	W.B. 10^{h} 366	10 23.2	− 6 5	8.1	0.478	G9	G8	5.2	0.026		
2785	36 Urs. Maj.	10 24.2	+56 30	4.8	0.182	F8	F7	3.6	0.058	0.091	A, S
2795		10 25.7	+81 1	6.6	0.016	G6	G7	0.2	0.005		
2799	9 H Draco.	10 26.6	+76 14	5.0	0.030	G7	G7	0.2	0.011		
2800	46 Leonis	10 26.9	+14 39	5.7	0.041	Ma	G7	1.0	0.012	0.005	W
2806		10 27.7	+49 42	7.6	0.292	F8	F6	4.3	0.022	0.045	K
2822		10 31.6	−11 42	5.8	0.734	F7	F6	3.9	0.042	0.007	Y, F
2830	p Velorum*	10 33.1	−47 42	5.1†	0.167	F0p	......	2.2	0.026		
2831	38 Leo. Min.	10 33.4	+38 26	5.8	0.227	F9	F8	2.2	0.019	0.029	Ab
2836	φ Hydrae	10 33.7	−16 21	5.1	0.111	G7	G5	1.0	0.015		
2844	35 H Urs. Maj.	10 35.9	+69 36	5.2	0.023	K4	G9	0.7	0.013		
2846	33 Sextantis	10 36.3	− 1 13	6.4	0.191	K0	G8	3.5	0.026		
	A.G. Albany 4102	10 37.2	+ 1 23	7.6	0.008‡	K0	G8	1.9	0.007		
2853		10 37.7	+46 44	5.3	0.289	A9	A9	1.6	0.018	0.031	Jo
2857		10 38.1	+46 44	8.1	0.280	F9	F9	4.4	0.018	−0.004	K

....	A.G. Leiden 4263	10^{h}38^{m}8	+33° 9′	7.6	0.″033‡	A9	......	2.5:	0.″010		
2865	41 Urs. Maj.	10 40.1	+57 54	6.5	0.081	Ma	K1	1.0	0.008		
2868	37 Sextantis	10 40.9	+ 6 54	6.3	0.039	K1	K0	0.8	0.008		
2881	43 Leo. Min.	10 43.4	+29 57	6.3	0.103	G9	G9	1.3	0.010	0.″036	W
2888	ν Hydrae	10 44.7	−15 40	3.3	0.214	K1	K0	1.0	0.035		
C1307	Lal. 20881	10 46.1	+20 49	8.1	0.502	F1	F0	3.6	0.013	0.007	Y
2897	....	10 46.7	+70 23	6.1	0.403	K0	K1	4.3	0.044	−0.011	Y
....	A.G. Leiden 4299	10 47.1	+33 31	7.6	0.049‡	G9	G8	2.3	0.009		
2899	46 Leo. Min.	10 47.7	+34 45	3.9	0.304	K1	G9	1.4	0.032	0.058	M, Ab
2910	....	10 50.2	+34 2	5.2	0.113	K1	G9	0.7	0.013	0.014	Ab
2912	....	10 50.5	+42 33	6.1	0.101	K1	G9	3.0	0.024		
2915	56 Leonis	10 50.8	+ 6 43	6.0	0.023	Mc	G5	−0.6	0.005	−0.004	W
C1325	Lal. 21008	10 50.9	+28 17	8.6	0.472	G6	G5	5.2	0.021	0.050	Y
2918	....	10 52.0	+78 18	6.3	0.081	G7	G7	0.5	0.007		
2920	47 Urs. Maj.	10 53.9	+40 58	5.1	0.320	G2	G1	4.1	0.063	0.080	A
2921	....	10 54.0	+36 38	6.2	0.095	Ma	G8	1.0	0.009		
2922	....	10 54.5	+46 4	5.7	0.016	K5	K0	0.5	0.009		
2925	α Crateris	10 54.9	−17 46	4.2	0.481	K0	G9	−0.1	0.014		
2927	58 Leonis	10 55.4	+ 4 9	5.0	0.023	K1	G9	0.5	0.013		
2931	61 Leonis	10 56.7	− 1 57	5.0	0.041	K6	K1	0.3	0.012		
2933	α Urs. Maj.	10 57.6	+62 17	2.0	0.139	G8	G8	0.4	0.048	0.037	F
2935	22 H Camelop.	10 57.9	+36 38	7.6	4.779	Ma	......	10.5	0.380	0.411	Ye, S, Y, *et al.*
2938	62 Leonis	10 58.5	+ 0 32	6.2	0.066	K3	K2	0.6	0.008		
2942	χ Leonis	10 59.9	+ 7 53	4.7	0.350	F5	F4	0.8	0.017	0.012	M
2943	51 Leo. Min.	10 59.9	+25 45	7.5	0.409	F7	F7	4.7	0.028	0.039	Y
C1349	Lal. 21258	11 0.5	+44 2	8.9	4.519	Ma	......	10.1	0.174	0.190	M, R, K, *et al.*
2950	65 Leonis	11 1.8	+ 2 30	5.7	0.386	G9	G7	2.6	0.024		
2958	ψ Urs. Maj.	11 4.0	+45 2	3.2	0.069	K0	G9	1.3	0.042		
....	Bu. 5695 B	11 5.5	+31 0	9.8	0.623	Ma	......	8.8	0.063}	0.048	Y
C1361	Bu. 5695 A	11 5.6	+31 0	8.8	0.623	K7	K3	8.4	0.083}		

TABLE VII—*Continued*

Boss	Name	α 1900	δ 1900	Harv. Vis. Mag.	μ	Spectrum		Spect. Abs. Mag.	Spect. π	Trig. π	Auth.
						Est.	Meas.				
....	Bu. 5695 C..........	11^{h} $5^{m}.6$	+31° 2′	9.0	....	G6	G6	3.8	0″.009		
2971......	Bu. 5706 A..........	11 8.6	+74 1	7.8†	0″.405	K5	K4	7.2	0.076	0″.088	F, Bgs
2976......	72 Leonis..........	11 9.9	+23 38	4.9	0.018	Ma	G5	−0.5	0.008		
2978......	73 Leonis..........	11 10.6	+13 51	5.5	0.028	K2	K1	1.0	0.013		
2980......	....	11 11.1	+50 1	6.0	0.092	G6	G9	1.4	0.012	−0.081	Y
2983......	75 Leonis..........	11 12.1	+ 2 34	5.4	0.159	Ma	K2	0.7	0.012		
2984......	ξ Urs. Maj. Br........	11 12.9	+32 6	4.4	0.732	F9	F9	4.9	0.126	0.158	Y, Ab, F
2984......	ξ Urs. Maj. Ft........	11 12.9	+32 6	4.9	0.732	G2	G2	5.3	0.120		
2985......	ν Urs. Maj..........	11 13.1	+33 38	3.7	0.027	K4	G9	0.4	0.022		
2986......	....	11 13.2	− 4 31	7.3	0.808	G8	G6	6.1	0.058	0.034	M, Y
2989......	δ Crateris..........	11 14.3	−14 14	3.8	0.230	G9	G7	0.7	0.024		
C1383......	A.Oe. 11677..........	11 14.8	+66 23	9.2	2.986	Ma	......	10.9	0.219	0.198	F, Bgs
2995......	56 Urs. Maj..........	11 17.3	+44 2	5.1	0.038	G6	G7	−0.1	0.009		
2997......	λ Crateris..........	11 18.4	−18 14	5.2	0.314	F3	F4	1.2	0.016		
2999......	ι Leonis Br..........	11 18.7	+11 5	4.0	0.176	F4	F4	2.8	0.058		
3014......	83 Leonis Br..........	11 21.7	+ 3 33	6.5	0.743	G9	G7	5.3	0.058	0.023	Y, R
3015......	83 Leonis Ft..........	11 21.7	+ 3 33	7.6	0.736	K4	K5	6.4	0.058		
3021......	τ Leonis..........	11 22.8	+ 3 24	5.2	0.028	G7	G6	0.1	0.010		
3022......	....	11 23.4	+62 19	5.9	0.267	F3	F3	3.1	0.028		
3025......	85 Leonis..........	11 24.5	+15 58	6.0	0.066	K3	K2	1.1	0.011		
3029	87 Leonis..........	11 25.2	− 2 27	5.1	0.026	K4	G9	1.1	0.016		
3030......	86 Leonis..........	11 25.3	+18 58	5.7	0.078	K0	G8	1.1	0.012	0.009	W
....	Bu. 5805..........	11 25.4	+41 51	7.6†	0.130‡	F2	F4	2.9	0.012		
3031......	λ Draconis..........	11 25.5	+69 53	4.1	0.045	K5	K0	0.2	0.017	0.018	M
3032......	88 Leonis Br..........	11 26.6	+14 55	6.3†	0.387	F9	F9	3.6	0.029		

3033	Bu. 5811	$11^h26^m.7$	+61°38′	5.8†	0″.079	F4	F6	4.0	0″.044	0″.057	S
C1426	Lal. 21927	11 28.4	+65 48	7.2	0.204	F5	F7	3.7	0.020	0.027	G
3047		11 29.6	−32 18	6.1	1.058	K2	K0	6.2	0.105	0.235	F
3050	2 Draconis	11 30.2	+69 53	5.4	0.176	G5	G7	−0.4	0.007		
3058	υ Leonis	11 31.8	− 0 16	4.5	0.035	G8	G7	1.0	0.020		
	SU Draconis §	11 32.2	+67 53	9.2		A5		0.9:	0.002		
3069	Bu. 5858 Br.	11 33.5	+45 40	6.3	0.583	F8	F9	4.1	0.036	0.038	K
3069	Bu. 5858 Ft.	11 33.5	+45 40	8.6	0.583	K4	K2	6.7	0.042		
3075	61 Urs. Maj.	11 35.8	+34 46	5.5	0.390	G5	G4	4.8	0.072		
3078	62 Urs. Maj.	11 36.4	+32 18	5.7	0.347	F2	F4	3.8	0.042	0.042	W
3081	3 Draconis	11 36.9	+67 18	5.5	0.058	K2	K0	0.6	0.010		
3087	ζ Crateris	11 39.7	−17 48	4.9	0.052	G7	G5	1.1	0.017		
C1452	Groom. 1822	11 40.3	+48 14	8.0	0.644	F9	G0	4.1	0.017	0.024	K
3089	ν Virginis	11 40.7	+ 7 5	4.2	0.188	Ma	G6	0.2	0.016		
3090	χ Urs. Maj.	11 40.8	+48 20	3.8	0.137	K0	G8	1.3	0.032		
3098	93 Leonis	11 42.8	+20 46	4.5	0.155	F4	F7	3.1	0.052	0.029	M
3100		11 43.7	−26 12	5.4	0.028	Mc	G7	0.2	0.009		
3105	β Virginis	11 45.5	+ 2 20	3.8	0.793	F7	F7	3.5	0.087	0.104	A, M, Y
3112	Groom. 1830	11 47.2	+38 26	6.5	7.047	G8	G5	6.0	0.079	0.106	M, Y, K, *et al.*
	A.G. Leip. 4431	11 48.7	+14 35	8.1	0.032‡	F1		2.7	0.008		
C1475	Bu. 5960 S	11 49.4	+19 58	8.4	0.445	G4	G5	5.9	0.032		
C1476	Bu. 5960 N	11 49.5	+19 59	8.4	0.436	G6	G6	5.3	0.024		
3125	66 Urs. Maj.	11 50.8	+57 9	5.9	0.012	K1	G9	0.4	0.008		
C1487	Lac. 4955	11 53.0	−27 8	7.2	1.243	K5	K3	7.0	0.091	0.039	F
3137		11 55.6	− 9 53	5.6	0.491	G9	G7	4.8	0.069	0.101	Y, M
3141		11 56.5	+36 36	5.6	0.136	G9	G8	0.9	0.012	0.036	W
3145		11 57.4	+43 39	6.8	0.629	G7	G5	3.6	0.023	0.017	K, F
3155	ο Virginis	12 0.1	+ 9 17	4.2	0.221	G6	G6	0.4	0.017	0.039	A
C1497	Lal. 22701	12 0.1	− 0 57	8.4	0.531	G8	G6	6.4	0.040	0.110	Y
3157		12 0.6	+63 30	6.2	0.087	K1	K1	2.0	0.014		

TABLE VII—*Continued*

Boss	Name	α 1900	δ 1900	Harv. Vis. Mag.	μ	Spectrum		Spect. Abs. Mag.	Spect. π	Trig. π	Auth.
						Est.	Meas.				
3166	α Corvi	12^h $3^m.3$	−24° 10′	4.2	0″.093	F1	F1	2.8	0″.052		
C1511	Groom. 1855	12 4.6	+40 49	7.4	0.325	K0	G6	5.7	0.046	0″.064	K
3169	10 Virginis	12 4.6	+ 2 28	6.1	0.190	K2	K1	1.6	0.013	0.028	W
3172	ε Corvi	12 5.0	−22 4	3.2	0.065	K3	K1	0.5	0.029	0.026	M
3177	....	12 6.5	+82 16	6.3	0.019	K3	G9	0.8	0.008		
3179	68 Urs. Maj.	12 6.8	+57 37	6.5	0.020	K4	K0	0.8	0.007		
C1522	W.B. 12^h69	12 7.4	− 2 32	7.4	0.732	G6	G2	5.0	0.033	0.011	Y, F
C1523	Lal. 22901	12 7.8	+10 36	8.0	0.430	K0	G9	5.1	0.026		
C1524	Lal. 22908	12 8.1	+11 24	7.9	0.589	G4	G2	5.5	0.033	0.049	A, Y
3186	1 Can. Ven.	12 9.8	+53 59	6.3	0.023	G9	G7	0.5	0.007		
C1533	Lal. 22954	12 10.0	− 9 44	6.1	1.024	F3	F6	3.7	0.033	0.026	Y, F
3193	2 Can. Ven.	12 11.1	+41 13	5.8	0.051	K6	K2	0.6	0.009		
3194	7 Comae	12 11.3	+24 30	5.1	0.028	G8	G7	1.3	0.017		
....	SW Draconis §	12 12.8	+70 4	10.0	....	F4	....	0.6:	0.001		
....	A.G. Berlin 4636	12 13.0	+19 0	7.5	0.026	F6	F6	2.6	0.011		
C1542	Pi. 12^h40	12 14.1	+17 6	7.0	0.237	G2	G2	4.4	0.030	0.024	A
3208	6 B Urs. Min.	12 14.4	+88 15	6.3	0.067	F0	....	2.0	0.014		
3209	9 Comae	12 14.5	+28 43	6.3	0.245	F8	F7	3.4	0.026	0.054	S
3213	16 Virginis	12 15.3	+ 3 52	5.1	0.307	K0	G7	1.6	0.020	−0.006	A
3216	11 Comae	12 15.7	+18 21	4.9	0.139	G6	G6	0.7	0.014		
3217	....	12 15.8	−13 1	5.4	0.002	K1	G9	1.3	0.015		
C1551	W.B. 12^h309	12 16.9	+42 42	9.1	0.57	Ma	....	8.5	0.076		
C1557	A.Oe. 12584	12 17.9	+73 48	8.2	0.49	G6	G6	5.4	0.028		
3230	5 Can. Ven.	12 19.2	+52 7	5.0	0.011	G6	G5	0.1	0.011		
....	Bu. 6158	12 19.4	+26 9	6.6†	....	A8	....	2.1	0.013	−0.022	S

C1563	Lal. 23223	$12^{h}19^{m}.9$	− 3° 40′	8.0	0″.258	G2	G2	5.4	0″.030	0″.055	Ye
C1564	Lal. 23231	12 19.9	+38 52	8.1	0.62	F6	F7	4.3	0.017		
3233	......	12 20.2	+24 29	6.1	0.072	G9	G9	0.6	0.008	0.005	W
3234	71 Urs. Maj.	12 20.3	+57 20	6.0	0.028	Mb	G8	0.5	0.008		
3242	γ Comae.	12 22.0	+28 49	4.6	0.122	K2	K1	0.7	0.017	0.002	A
3248	73 Urs. Maj.	12 22.8	+56 16	5.8	0.031	Ma	K0	0.5	0.009		
3254	18 Comae.	12 24.4	+24 40	5.5	0.025	F2	F3	0.9	0.012		
C1579	Lal. 23361	12 24.6	− 2 46	8.6	0.721	G3	G3	6.1	0.032	0.095	Y
3258	......	12 24.9	−12 50	6.4	0.251	G0	F9	3.9	0.032		
3261	7 Can. Ven.	12 25.3	+52 5	6.2	0.275	F6	F6	3.0	0.023		
3265	4 Draconis.	12 25.7	+69 45	5.2	0.084	Mb	G7	−0.8	0.006		
......	A.G. Berlin 4695	12 26.1	+17 10	7.5	0.025‡	K1	K0	2.0	0.008		
3272	η Corvi.	12 26.9	−15 39	4.4	0.444	F2	......	2.5	0.042		
3274	20 Virginis.	12 28.0	+10 51	6.5	0.063	G8	G8	0.4	0.006		
3279	β Can. Ven.	12 29.0	+41 54	4.3	0.758	G0	G0	4.4	0.105	0.107	A, M, Y, F
3280	β Corvi.	12 29.1	−22 51	2.8	0.061	G5	G4	0.0	0.028		
3285	24² Comae	12 30.1	+18 56	5.2	0.016	K1	K0	0.3	0.011		
3294	......	12 33.3	+ 2 24	6.0	0.090	Mb	G9	0.7	0.009		
3298	χ Virginis.	12 34.1	− 7 27	4.8	0.085	K3	K2	0.6	0.014		
C1604	B.D. +69° 671	12 36.0	+69 21	8.2	0.46	G1	G2	4.9	0.022	0.036	G
3307	γ Virginis S.	12 36.6	− 0 54	3.7	0.564	F0	......	2.2	0.050	0.068	R, F, Bel
3307	γ Virginis N.	12 36.6	− 0 54	3.7	0.564	F1	......	2.4	0.055		
......	Groom. 1923	12 37.8	+84 12	7.2	0.232	F7	F9	3.2	0.016	0.000	G
3321	10 Can. Ven.	12 40.3	+39 49	6.0	0.375	F6	F8	3.9	0.038	0.063	A
3326	33 Virginis.	12 41.3	+10 6	5.9	0.531	K0	G9	4.2	0.046	−0.008	S, Y
3327	27 Comae.	12 41.7	+17 7	5.3	0.008	K3	K1	0.4	0.010		
3336	7 Draconis.	12 43.5	+67 20	5.7	0.008	K3	G8	0.7:	0.010		
C1627	Lal. 23900	12 43.9	+25 23	6.4	0.367	G6	G5	5.3	0.060	0.026	A
C1630	Lal. 23917	12 44.6	+ 1 45	8.1	0.665	G8	G4	6.1	0.040	0.029	A, Y
3344	......	12 46.2	− 9 48	6.5	0.021	G8	G7	0.9	0.008		

TABLE VII—*Continued*

Boss	Name	α 1900	δ 1900	Harv. Vis. Mag.	μ	Spectrum Est.	Spectrum Meas.	Spect. Abs. Mag.	Spect. π	Trig. π	Auth.
3346	37 Virginis	$12^h46^m.5$	+ 3° 36′	6.1	0″.035	K3	K1	0.6	0″.008		
3347	31 Comae	12 46.8	+28 5	5.1	0.031	F6	F7	2.1	0.025		
3348	32 Comae	12 47.2	+17 37	6.5	0.023	K4	G9	0.6	0.007		
C1640	Lal. 23995	12 47.9	−17 57	8.3	0.877	F3	F7	3.4	0.011		
3353	38 Virginis	12 48.1	− 3 1	6.2	0.262	F6	F6	3.3	0.026		
3362	ψ Virginis	12 49.2	− 9 0	4.9	0.032	Ma	G6	−0.3	0.009		
3367	δ Virginis	12 50.6	+ 3 56	3.7	0.479	Mb	G7	0.3	0.021	0″.002	A, Y
C1657	Lal. 24168	12 53.9	− 9 18	7.7	0.850	K2	K0	6.4	0.055	−0.015	Y
3374	36 Comae	12 54.0	+17 57	5.0	0.036	K6	K1	0.9	0.015		
C1664	Pi. 12^h243	12 55.7	+18 55	6.1	0.245	F5	F5	3.4	0.029	0.022	A
C1666	A.Oe. 12585	12 56.1	−26 50	8.2	0.545	F4	F6	3.8	0.013		
C1667	W.B. 12^h920	12 56.2	− 7 54	8.7	0.493	G6	G5	5.7	0.025	0.010	Y
3381	38 Comae	12 56.2	+17 40	6.0	0.033	G8	G7	0.8	0.009		
3383	ε Virginis	12 57.2	+11 30	3.0	0.273	G6	G6	0.0	0.025	0.034	F
3398	40 Comae	13 1.5	+23 9	5.9	0.066	Mc	G8	0.2	0.007	0.043	W
3401	41 Comae	13 2.4	+28 10	4.9	0.089	K4	K2	0.4	0.013		
3402	....	13 2.4	+62 35	6.3	0.045	G8	G7	2.6	0.018		
C1687	Lal. 24414	13 3.8	+ 5 46	6.9	0.682	G4	G2	4.1	0.028	0.029	A, Y
3406	....	13 4.2	+10 33	6.0	0.020	K0	G8	1.2	0.011		
3408	50 Virginis	13 4.5	− 9 48	6.2	0.023	K4	K1	0.5	0.007		
....	B.D. +18° 2696	13 4.6	+18 0	8.1	....	K3	K1	1.0	0.004	−0.002	Ye
3412	α Comae	13 5.1	+18 3	5.2†	0.450	F4	F5	3.9	0.055	0.070	A, Ye, F
C1692	Lal. 24504	13 6.4	+10 9	8.5	0.559	G2	G2	4.7	0.017	0.028	Y
3422	53 Virginis	13 6.7	−15 40	5.1	0.314	F6	F6	3.2	0.042		
C1693	A.Oe. 13407	13 7.0	+68 2	8.8	0.75	K2	K0	5.6	0.023	0.010	G

3424	β Comae	13^{h} $7^{m}.2$	+38° 23′	4.3	1″.184	G1	G0	4.7	0″.120	0″.131	M, Y, F, P
C1695	A.G. Berlin 4855	13 7.5	+18 3	7.8	0.578	F6	F9	4.4	0.021		
3438	57 Virginis	13 10.6	−19 25	5.3	0.322	K1	K0	2.2	0.024		
3442		13 11.5	+81 0	6.3	0.008	G8	G7	0.3:	0.006		
3443	59 Virginis	13 11.8	+ 9 57	5.2	0.382	G0	F9	4.4	0.069	0.075	A
C1712	Bu. 6442 Br.	13 11.9	+17 33	6.6†	0.691	K3	K1	6.4	0.091	0.076	S
3446	σ Virginis	13 12.6	+ 6 0	5.0	0.016	Ma	G6	0.3	0.012		
3447	20 Can. Ven.	13 13.1	+41 6	4.7	0.125	F4	F3	−1.4	0.006		
3448	61 Virginis	13 13.2	−17 45	4.8	1.529	G8	G5	4.9	0.105	0.136	M, F
3449	γ Hydrae	13 13.5	−22 39	3.3	0.083	G7	G5	0.3	0.025	−0.012	M
C1719	W.B. $13^{h}241$	13 14.9	+35 39	9.6	0.884	Ma	K5	9.6	0.100	0.080	Y
C1722	W.B. $13^{h}216$	13 15.7	+ 4 39	8.8	0.575	K3	K3	6.4	0.033	−0.021	Y
C1723	Lal. 24774	13 16.1	+43 38	8.2	0.438	K1	K0	6.1	0.038	0.179	Y
3475	ζ² Urs. Maj.	13 19.9	+55 27	4.0	0.028	A7	......	1.9	0.038	0.022	M
3483		13 22.6	+63 46	6.5	0.444	G7	G5	5.1	0.052		
3485		13 23.2	− 0 19	7.5	0.462	G2	G2	4.2	0.022		
3487	70 Virginis	13 23.5	+14 19	5.2	0.634	G3	G4	3.9	0.055	0.065	A, M, Y
3488		13 23.6	+72 55	6.1	0.030	K4	G9	0.3	0.007		
....	Groom. 2004	13 24.4	+70 50	7.5	0.040	F1	......	2.7	0.011		
....	Groom. 2005	13 25.3	+70 39	7.5	0.039	K0	G8	2.2	0.009		
C1748	Lal. 25012	13 26.6	− 1 49	7.3	0.887	G9	G7	5.9	0.052	0.053	Y
3499	74 Virginis	13 26.8	− 5 44	4.8	0.112	Ma	G8	0.6	0.014		
3500		13 26.9	+42 37	6.2	0.094	K1	K0	1.6	0.012		
3511		13 30.3	+37 42	5.0	0.085	F5	F5	2.4	0.030		
3526	Bu. 6578	13 34.6	+11 15	6.3†	0.112	A9p	......	1.5	0.011	0.015	A, Ye, M, *et al.*
....	B.D. +76° 493	13 34.9	+76 25	8.0	....	G4	G3	4.9	0.024	0.022	G
....	Groom. 2026	13 35.1	+48 24	7.9	0.026	F3	......	2.2	0.007		
....	A.G. Leiden 4974	13 36.0	+33 21	7.8	0.059‡	F8	F7	3.0	0.011		
3534	82 Virginis	13 36.4	− 8 12	5.2	0.108	Ma	G9	0.3	0.011		
3537	84 Virginis	13 38.0	+ 4 3	5.7†	0.302	K3	K1	0.4	0.009		

TABLE VII—*Continued*

Boss	Name	α 1900	δ 1900	Harv. Vis. Mag.	μ	Spectrum		Spect. Abs. Mag.	Spect. π	Trig. π	Auth.
						Est.	Meas.				
3541		13h39m.0	+23°12′	6.4	0″.072	K5	K2	0.7	0″.007		
3542	83 Virginis	13 39.1	−15 41	5.7	0.009	G3p	F7	−0.6	0.006		
C1784	A.G. Berlin 4999	13 40.2	+18 20	9.6	1.86	Ma	......	10.1	0.126	0″.090	D, Ye, R
C1786	Lal. 25372	13 40.7	+15 26	8.5	2.298	Mb	K4	10.2	0.219	0.200	M, Ye, Y, *et al.*
C1789	Pi. 13h200	13 41.5	+56 23	6.4	0.372	F6	F7	3.5	0.026	0.027	A
3551		13 41.9	− 9 13	6.2	0.042	K4	K3	0.6	0.008		
3554		13 42.0	+ 6 51	6.3	0.499	F9	G0	4.3	0.040	0.028	A
3558	τ Boötis	13 42.5	+17 57	4.5	0.487	F7	F6	3.0	0.050	0.046	A, Y
3571	89 Virginis	13 44.4	−17 38	5.1	0.108	K0	G9	1.1	0.016		
C1800	Bu. 6641 Br.	13 44.5	+27 29	7.9	0.455	K6	K4	7.1	0.069		
C1800	Bu. 6641 Ft.	13 44.5	+27 29	8.2	0.455	K6	K4	7.4	0.069		
C1804	Lal. 25484	13 45.8	−23 53	6.5	0.658	G2	G1	5.6	0.066		
3581		13 46.7	+35 10	6.0	0.072	Ma	K0	0.7	0.009	0.012	W
3584		13 47.4	+34 56	5.0	0.044	Ma	G8	0.4	0.012		
3589	10 Draconis	13 48.5	+65 13	4.8	0.004	Mb	G7	−0.5	0.009		
3594	90 Virginis	13 49.6	− 1 1	5.3	0.091	K1	K0	0.4	0.011		
3595	Bu. 6668 Br.	13 49.7	− 7 34	6.5†	0.167	F8	F8	4.1	0.033		
3596	η Boötis	13 49.9	+18 54	2.8	0.373	F9	G0	2.8	0.100		
3605		13 53.8	+15 8	6.0	0.087	K4	K2	0.5	0.008		
3616		13 59.0	−14 29	6.4	0.048	K1	K0	2.1	0.014		
3623	θ Centauri	14 0.8	−35 53	2.3	0.750	K1	G8	1.0	0.055	−0.062	F
3629	96 Virginis	14 3.7	− 9 52	6.5	0.016	G8	G7	−0.1	0.005		
3630		14 3.9	+44 20	5.4	0.037	Mb	G6	−0.8	0.006		
3631	13 Boötis	14 4.6	+49 56	5.4	0.068	Ma	G6	−0.2	0.008		
3635	12 Boötis	14 5.8	+25 34	4.8	0.076	F6	F7	1.9	0.026		

3641......	....	14ʰ 7ᵐ.5	−26° 9′	6.3	0″.004	G8	G6	0.9	0″.008		
3642......	κ Virginis............	14 7.6	− 9 49	4.3	0.130	K2	G9	1.0	0.022		
3644......	....	14 8.5	− 0 22	5.8	0.241	F5	F5	2.6	0.023		
3647......	....	14 9.1	− 5 29	6.3	0.317	F8	F8	3.7	0.030		
3649......	4 Urs. Min...........	14 9.2	+78 1	5.0	0.038	K3	K0	0.7	0.014		
3650......	14 Boötis............	14 9.3	+13 26	5.5	0.267	F7	F6	4.1	0.052	0″.097	W
3656......	....	14 10.2	+69 54	5.4	0.068	Ma	K1	0.3	0.010		
3658......	....	14 10.4	+41 59	6.2	0.122	K3	K2	0.7	0.008	0.025	W
3660......	ι Virginis............	14 10.8	− 5 31	4.2	0.427	F6	F6	2.4	0.044		
3662......	α Boötis.............	14 11.1	+19 42	0.2	2.282	K0	G9	1.2	0.158	0.075	Y, F
3671......	....	14 13.3	−25 22	5.9	0.538	F5	F7	3.7	0.036		
3673......	....	14 13.8	+35 58	4.8	0.016	K0	G9	2.1	0.029		
C1882......	Lal. 26196...........	14 14.4	− 4 41	7.6	0.664	K2	K1	6.3	0.055	0.116	Y, F
C1885......	Lal. 26294...........	14 17.6	+30 6	8.6	0.727	K6	K5	8.4	0.091		
3691......	2 Librae.............	14 18.0	−11 15	6.3	0.066	G8	G7	1.7	0.012		
C1886......	Lal. 26289...........	14 18.1	+ 1 43	6.3	0.525	G2	G2	5.7	0.076	0.070	Y, F
3692......	Bu. 6842 BC..........	14 18.5	+ 8 54	7.4†	0.072	F0	F3	2.2	0.009	0.018	Ye, S
C1894......	A.G. Berlin 5072......	14 21.1	+24 6	9.5	1.39	Ma	K5	9.5	0.100	0.062	Ye, R
3703......	....	14 21.4	+38 51	6.3	0.019	K1	K0	1.0	0.009		
3704......	θ Boötis.............	14 21.8	+52 19	4.1	0.471	F6	F7	3.0	0.060	0.067	A
3715......	24 Boötis............	14 25.2	+50 18	5.6	0.312	G3	G2	1.8	0.017	0.023	A
C1908......	Lal. 26481 Br.........	14 25.8	−15 11	8.2†	0.433	G2	G2	5.3	0.026	0.238	F
3717......	ρ Boötis.............	14 27.5	+30 49	3.8	0.149	K3	K1	0.8	0.025	0.036	A
3718......	5 Urs. Min...........	14 27.7	+76 8	4.4	0.021	K4	K1	0.9	0.020		
3722......	γ Boötis.............	14 28.1	+38 45	3.0	0.182	A7	......	1.8	0.058		
C1913......	B.D. +10° 2703.......	14 28.7	+ 9 47	8.9	0.55	K3	K1	6.2	0.029		
3729......	σ Boötis.............	14 30.3	+30 11	4.5	0.228	F0	......	2.9	0.048		
3734......	....	14 31.7	−11 53	6.2	0.946	F4	F5	3.2	0.025	0.049	Y
3735......	α Centauri Br.*.......	14 32.8	−60 25	0.3	3.680	G6	G5	4.8	0.794	0.759	C, Wr
3735......	α Centauri Ft.*.......	14 32.8	−60 25	1.7	3.680	K4	K3	6.2	0.794		

TABLE VII—*Continued*

Boss	Name	α 1900	δ 1900	Harv. Vis. Mag.	μ	Spectrum		Spect. Abs. Mag.	Spect. π	Trig. π	Auth.
						Est.	Meas.				
3736		$14^h33^m.6$	+18°44′	6.0	0″.096	K0	G9	1.9	0″.015	0″.057	W
3754	32 Boötis	14 36.9	+12 5	5.6	0.205	G5	G5	1.0	0.012		
3758	μ Virginis	14 37.8	− 5 13	4.0	0.339	F1	F3	2.4	0.048	0.048	M
C1939	Bu. 6977	14 38.2	+58 23	7.4†	0.244	K0	G9	4.6	0.028		
3771	ε Boötis Br.	14 40.6	+27 30	2.7	0.049	G8	G7	−0.9	0.019	0.015	A, F
	A.G. Leiden 5276	14 41.1	+34 48	7.8	0.044‡	Ma	G8	0.8	0.004		
C1947	Bu. 6999	14 41.4	+10 4	7.5†	0.272	G3	G2	5.2	0.035		
	Bu. 7001	14 41.7	+42 48	7.8†	0.129*	F5	F7	3.2	0.012	−0.022	S
	A.G. Berlin 5351	14 44.2	+18 37	7.4	0.026‡	K0	G8	2.2	0.009		
3785		14 45.2	+38 13	6.0	0.276	F2	F2	2.4	0.019	0.015	A
	RY Boötis §	14 45.2	+23 27	7.2	0.051‖	F2	F4	0.5:	0.005		
3790	11 Librae	14 45.8	− 1 53	5.0	0.160	G6	G4	0.8	0.014		
C1962	Lal. 27026	14 46.0	−23 53	7.6	1.022	K5	K5	6.9	0.072	0.041	F
3798	ξ Boötis Br.	14 46.8	+19 31	4.8	0.168	G6	G6	5.8	0.158	0.178	A, M
3798	ξ Boötis Ft.	14 46.8	+19 31	6.8	0.168	K4	K3	6.9	0.105		
	Groom. 2165	14 48.6	+66 3	7.2	0.007	Ma	G8	0.4	0.004		
C1972	Lal. 27137	14 48.9	+19 33	6.0	0.485	K1	K0	5.9	0.095	0.086	A
C1973	Lal. 27155	14 49.3	+23 45	8.7	0.817	K4	K3	6.9	0.044		
3809	β Urs. Min.	14 51.0	+74 34	2.2	0.030	K4	K0	0.5	0.046	0.014	F
3810	15 Librae	14 51.3	−11 0	5.6	0.002	K2	K0	1.2	0.013		
3812	Bu. 7060 Ft.	14 51.6	−20 58	8.9	1.916	Ma	......	9.9	0.158	0.194	M, F, Sitt
3813	Bu. 7060 Br.	14 51.6	−20 58	5.8	2.039	K3	K6	6.7	0.151		
C1980	Lal. 27298	14 52.3	+54 4	7.9	1.086	K1	G8	6.3	0.048	0.056	Ye, Y, P, F
3816	1 Serpentis	14 52.4	+ 0 14	5.7	0.069	K1	K1	1.8	0.017	0.044	W
C1986	Pi. 14^h229	14 53.7	− 4 35	6.0	0.384	F8	F8	4.0	0.040		

C1988	Lal. 27274	$14^h54^m.2$	−21°36′	8.5	0″.785	F4	F6	3.3	0″.009		
3827		14 56.0	+66 20	4.9	0.082	Mb	G8	−0.6	0.008		
3833		14 57.1	+82 55	5.7	0.294	F8	F9	3.6	0.038	0″.010	G
3836	β Boötis	14 58.2	+40 47	3.6	0.063	G4	G5	−0.7	0.014	0.030	A, M
3837	σ Librae	14 58.2	−24 53	3.4	0.094	Mb	G7	0.7	0.029		
3842	ψ Boötis	15 0.2	+27 20	4.7	0.178	K2	K0	0.9	0.017		
3843	9 Urs. Min.	15 0.3	+72 9	6.7	0.398	F9	G0	4.3	0.033	0.043	G
3846	44 Boötis Ft.*	15 0.5	+48 3	6.1	....	G2p	G4	5.2	0.066		
3847	44 Boötis Br.	15 0.5	+48 3	5.3	0.387	G0	G0	4.6	0.072		
3855	45 Boötis	15 2.9	+25 16	5.0	0.262	F4	F4	3.3	0.046	0.059	A
C2010	Lal. 27531	15 2.9	− 7 31	8.1	0.484	F9	G0	3.9	0.014		
C2011	Lal. 27558	15 3.0	+ 9 16	8.7	0.534	F6	F9	4.2	0.013		
C2019	A.Oe. 14320	15 4.7	−15 54	9.4	3.680	G9	G5	5.7	0.018	0.039	Ye, R, V
3867		15 7.5	+19 21	6.0	0.004	Mb	G7	0.2	0.007	0.005	W
C2024	Lal. 27742	15 8.3	+19 39	6.8	0.668	G6	G2	4.2	0.030	0.004	Y, R
C2025	Lal. 27743	15 8.3	+19 40	7.6	0.654	G7	G5	5.2	0.033		
C2027	Lal. 27744	15 8.8	− 0 58	7.2†	1.376	K0	G7	5.8	0.052	0.070	Ye, Y, F
3882	3 Serpentis	15 10.2	+ 5 19	5.4	0.023	G9	G7	0.8	0.012		
3887	δ Boötis	15 11.5	+33 41	3.5	0.155	G5	G5	−0.6	0.015	0.031	A
3895	5 Serpentis	15 14.2	+ 2 9	5.2	0.644	F6	F7	3.5	0.046	0.055	A, Y
C2043	Lal. 27922	15 14.6	− 8 18	7.9	0.211	F9	F9	3.5	0.013	−0.005	A
C2044	Lal. 27958	15 14.7	+26 4	8.1	0.568	G9	G5	5.4	0.029	0.031	Y
3900	28 Librae	15 15.2	−17 48	6.2	0.069	G8	G6	0.9	0.009		
3907	6 Serpentis	15 15.9	+ 1 5	5.5	0.125	K2	K2	1.8	0.018	0.133	F
....	A.G. Leiden 5456	15 16.1	+31 3	9.9	....	F5	F6	3.5	0.005		
C2055	W.B. 15^h 268	15 17.7	+ 1 47	8.7	0.507	K4	K3	6.7	0.040	0.118	Y
3923	η Cor. Bor.	15 19.1	+30 39	5.6†	0.237	G0	G0	4.3	0.055	0.084	S, Ye
3926	μ^1 Boötis	15 20.7	+37 44	4.5	0.169	F0	......	2.2	0.035	0.046	M, S, F
3927	μ^2 Boötis	15 20.7	+37 42	7.2†	0.172	G0	G0	4.7	0.032		
3931	9 Serpentis	15 21.2	+15 47	5.5	0.033	K6	K0	0.2	0.009		

TABLE VII—*Continued*

Boss	Name	α 1900	δ 1900	Harv. Vis. Mag.	μ	Spectrum		Spect. Abs. Mag.	Spect. π	Trig. π	Auth.
						Est.	Meas.				
....	A.G. Berlin 5543	15h21m6	+18°31′	8.3†	0″023‡	F7	F7	2.8	0″008		
3936	ι Draconis	15 22.7	+59 19	3.5	0.010	K3	K1	0.1	0.021	0″025	A
C2064	Bu. 7268 Br.	15 22.7	− 8 59	6.8	0.349	G8	G7	5.5	0.055		
....	Bu. 7268 Ft.	15 22.7	− 8 59	8.1	0.349	K2	K2	6.0	0.038		
C2067	B.D. +67° 887	15 23.1	+66 54	9.0	0.28	G8	G7	5.1	0.017	0.017	G
3938	....	15 23.3	+25 27	6.3	0.039	Ma	G9	−0.1	0.005		
3940	β Cor. Bor.	15 23.7	+29 27	3.7	0.190	F2	F4	−0.3	0.016		
3942	34 Librae	15 25.0	−16 16	5.9	0.019	G9	G8	1.2:	0.012		
C2071	Lal. 28358	15 26.6	+57 47	6.9	0.299	F5	F6	4.2	0.029	0.029	F
3952	37 Librae	15 28.7	− 9 43	4.8	0.389	K1	K0	2.9	0.042		
3959	γ Librae	15 29.9	−14 27	4.0	0.065	G9	G8	0.5	0.020		
3960	δ Serpentis Br.	15 30.0	+10 52	4.2	0.068	A7	......	1.4	0.028}	0.013	Ye
3960	δ Serpentis Ft.	15 30.0	+10 52	5.2	0.068	A8	......	1.5	0.018}		
3963	15 Serpentis	15 31.0	+17 59	6.1	0.081	G7	G6	1.0	0.010		
3968	16 Serpentis	15 31.7	+10 21	5.4	0.139	G4	G6	0.1	0.009		
C2086	W.B. 15h716	15 32.4	+40 10	7.9	0.455	K4	K5	6.6	0.055}	0.046	R
C2087	W.B. 15h720	15 32.5	+40 8	7.4†	0.456	K3	K2	6.1	0.055}		
3983	Bu. 7362 Br.	15 35.0	+80 47	6.9	0.246	G3	G3	5.7	0.058	0.022	W
4001	α Serpentis	15 39.3	+ 6 44	2.8	0.139	K2	K1	−0.2	0.025	0.056	A, M, F
4010	λ Serpentis	15 41.6	+ 7 40	4.4	0.244	G0	G0	4.4	0.100	0.086	A
C2112	Groom. 2273	15 41.7	+53 18	7.3	0.261	G2	G3	4.8	0.032	0.015	A
4015	κ Serpentis	15 44.2	+18 27	4.3	0.110	Ma	K0	0.0	0.014		
4024	δ Cor. Bor.	15 45.4	+26 22	4.7	0.110	G4	G3	1.7	0.025	0.013	A
4029	....	15 46.1	−13 50	6.2	0.044	G5	G3	0.3	0.007		
4031	ρ Serpentis	15 46.9	+21 17	4.9	0.049	K5	K2	0.7	0.014		

4032	κ Cor. Bor.	$15^h47^m.5$	+35°58′	4.8	0″.364	K1	K0	1.6	0″.023	0″.030	A
4040	39 Serpentis	15 48.5	+13 31	6.2	0.586	G1	G1	5.1	0.060	0.031	A, Y
4042	χ Herculis	15 49.2	+42 44	4.6	0.760	F7	F9	4.2	0.083	0.099	Y
4048		15 50.2	+20 36	5.8	0.083	K4	G8	0.8	0.010	0.040	W
4054	2 Herculis	15 51.3	+43 26	5.5	0.075	Ma	G8	0.6	0.011		
4055	γ Serpentis	15 51.8	+15 59	3.9	1.332	F5	F6	4.3	0.120	0.063	A, M, Y, *et al.*
4063	ϵ Cor. Bor.	15 53.4	+27 10	4.2	0.109	K2	K1	0.9	0.022		
C2134	W.B. 15^h1323	15 54.5	+28 1	8.1	0.85	G8	G8	6.0	0.038		
4067	49 Librae	15 54.7	−16 14	5.5	0.750	F6	F6	3.6	0.042		
4075	5 Herculis	15 56.7	+18 6	5.3	0.153	G7	G7	0.7	0.012		
4077	ρ Cor. Bor.	15 57.2	+33 36	5.4	0.810	F9	G0	3.6	0.044	0.035	A, M, Y
4082	ξ^1 Scorpii	15 58.9	−11 6	4.8†	0.071	F5	F6	3.0	0.044	0.046	M, Ye
4083	ξ^2 Scorpii	15 58.9	−11 6	7.2	0.080	G7	G6	5.0	0.036		
C2149	Lal. 29307	15 59.9	+25 31	7.1	0.862	K0	G7	5.7	0.052	0.058	Ye
4090	θ Draconis	16 0.0	+58 50	4.1	0.459	F7	F8	3.2	0.066	0.066	Kos
C2152	Lal. 29330	16 1.2	+10 57	8.5	0.491	K0	G9	6.0	0.032		
C2154	Groom. 2305	16 1.5	+39 26	6.8	0.571	G9	G5	6.1	0.072	0.069	Y
4096		16 2.0	−26 4	5.6	0.122	Ma	G8	0.6	0.010		
C2160	Lal. 29439	16 2.9	+38 55	8.6	0.591	K5	K2	7.1	0.050	0.014	Y, K
	Groom. 2312	16 3.3	+70 23	8.2	0.020	Mb	G9	1.0	0.004		
4101	κ Herculis Br.	16 3.6	+17 19	5.3	0.046	G5	G4	−0.2	0.008	−0.011	Ye
4102	κ Herculis Ft.	16 3.6	+17 19	6.5	0.048	K2	K1	1.1	0.008		
4103	47 Serpentis	16 3.6	+ 8 48	5.9	0.024	Mb	G6	0.4	0.008		
C2163	Lal. 29437	16 4.3	+ 6 40	6.0	0.760	K0	K2	4.4	0.048	0.014	A, Y
4106		16 4.6	− 3 12	5.4	0.016	K5	K2	0.3	0.010		
4108	τ Cor. Bor.	16 5.3	+36 45	4.9	0.325	K0	K0	2.8	0.038	0.044	A
4125	10 Herculis	16 7.4	+23 45	6.0	0.028	Mc	G7	0.0	0.006		
4130	9 Herculis	16 8.3	+ 5 17	5.6	0.046	K4	K2	0.8	0.011	0.008	W
4131	χ Scorpii	16 8.3	−11 35	5.5	0.020	K2	K0	1.1	0.013		
4132	Bu. 7551 S.	16 8.6	+13 48	7.6	0.459	G9	G7	5.3	0.035	0.078	M
4132	Bu. 7551 N.	16 8.6	+13 48	7.6	0.459	G9	G8	4.7	0.026		

TABLE VII—*Continued*

Boss	Name	α 1900	δ 1900	Harv. Vis. Mag.	μ	Spectrum		Spect. Abs. Mag.	Spect. π	Trig. π	Auth.
						Est.	Meas.				
....	A.G. Leiden 5723	$16^h\ 9^m.0$	+32°51′	7.9	0″.027‡	K1	K0	1.0	0″.004		
4134	δ Ophiuchi	16 9.1	− 3 26	3.0	0.161	K8	G8	0.3	0.029	0″.045	M
4137	18 Scorpii	16 10.2	− 8 6	5.6	0.563	G2	G1	4.7	0.066	0.039	Y
4138	σ^1 Cor. Bor. Ft.	16 10.9	+34 7	6.7	0.302	F9	F9	4.2	0.032		
4138	σ^2 Cor. Bor. Br.	16 10.9	+34 7	5.8	0.302	F8	G0	3.7	0.038	0.044	A, F
....	A.G. Leiden 5734	16 11.4	+32 24	8.5	0.035‡	K4	G8	1.0	0.003		
....	A.G. Berlin 5827	16 12.5	+19 6	7.6	0.034‡	K2	K0	1.7:	0.006		
4147	ε Ophiuchi	16 13.0	− 4 27	3.3	0.086	G6	G6	0.0	0.022	0.051	M
....	A.G. Lund 6686	16 13.2	+38 53	8.0	0.026‡	K3	G9	0.9	0.004		
4150	....	16 13.3	−19 58	6.4	0.026	G5	G5	0.3	0.006		
4152	....	16 14.0	+66 37	8.2	0.011	K2	G8	1.2	0.004		
4157	20 Urs. Min.	16 15.0	+75 28	6.5	0.041	K2	K1	0.7	0.007		
4159	....	16 15.6	+60 0	5.6	0.022	Mb	G6	−0.3	0.007		
C2184	Lal. 29917	16 16.5	+67 29	8.9	0.505	K6	K4	8.0	0.066	0.117	D, Y
4163	σ Serpentis	16 17.0	+ 1 16	4.8	0.172	A9	......	1.5	0.022	0.031	A
4165	γ Herculis	16 17.5	+19 23	3.8	0.062	A7	......	1.4	0.033	0.017	A
4169	ξ Cor. Bor.	16 18.2	+31 7	4.7	0.132	G9	G9	0.7	0.016	0.014	A
4173	ν^1 Cor. Bor.	16 18.6	+34 2	5.4	0.049	Ma	G9	0.3	0.010		
4175	ν^2 Cor. Bor.	16 18.7	+33 56	5.3	0.055	K6	K2	0.6	0.012		
....	A.G. Leiden 5784	16 19.2	+32 52	7.9	0.011‡	K4	K0	0.7	0.004		
4181	η Urs. Min.	16 20.4	+75 59	5.0	0.261	A8	......	1.7	0.022		
....	A.G. Leiden 5792	16 20.7	+32 42	8.1	0.038‡	K4	K1	0.7	0.003		
....	A.G. Berlin 5877	16 21.0	+17 32	7.9	0.019‡	G0	F9	3.2	0.012		
4188	....	16 22.3	− 7 22	5.4	0.176	Mb	G8	−0.5	0.007		

4192	η Draconis	$16^{h}22^{m}.6$	+61° 44′	2.9	0″.062	G6	G5	0.7	0″.036	0″.019	M, F
4193	α Scorpii	16 23.3	−26 13	1.2	0.034	Ma	G2	−2.7	0.017	0.029	C
4195	......	16 23.5	+ 0 53	5.5	0.076	K5	K3	0.5	0.010	0.016	W
C2199	Bu. 7642	16 24.5	+18 37	7.8†	0.508	K3	K2	6.6	0.058	0.088	Y
4202	φ Ophiuchi	16 25.4	−16 24	4.4	0.066	G5	G6	−0.3	0.012		
C2201	Lal. 30044	16 25.6	+ 4 26	7.4	1.450	F7	F6	4.0	0.021	0.025	A, Y, F
4204	β Herculis	16 25.9	+21 42	2.8	0.107	G5	G6	−1.0	0.017	0.020	F
4206	ω Ophiuchi	16 26.2	−21 15	4.6	0.033	A7	......	1.7	0.026		
C2202	Groom. 2354	16 27.4	+48 11	7.0	0.301	F7	F8	3.8	0.023	0.001	A
4211	31 Herculis	16 27.8	+33 44	6.7	0.039	K4	K1	0.5	0.006		
4212	29 Herculis	16 27.9	+11 42	4.9	0.204	K6	K2	0.5	0.013	−0.012	A
4222	12 Ophiuchi	16 31.1	− 2 7	5.9	0.546	K0	G9	5.6	0.087	0.088	A
C2214	Lal. 30271	16 32.6	+31 9	7.3	0.482	F7	F6	4.1	0.023	0.054	A, D, Y
4228	......	16 33.3	+46 49	6.0	0.020	G6	G6	−0.3	0.007		
......	B.D. +51° 2121	16 34.2	+51 45	9.6	0.119	G3	G2	4.8	0.011	0.017	K
4234	......	16 34.9	+77 39	6.4	0.286	G8	G6	2.4	0.016		
4239	24 Scorpii	16 35.8	−17 33	5.0	0.025	G5	G5	−0.4:	0.008		
4242	42 Herculis	16 36.0	+49 7	5.1	0.044	Ma	G9	−0.3	0.008		
4246	ζ Herculis Br.	16 37.5	+31 47	3.0	0.604	G1	G1	2.4	0.076	0.114	A, Ye, S, *et al.*
4255	η Herculis	16 39.5	+39 7	3.6	0.101	G5	G5	0.9	0.029	0.056	A, M, R, F
4257	41 Herculis	16 40.1	+ 6 17	6.7	0.352	G8	G8	4.7	0.040	0.024	A, Ye
4259	18 Draconis	16 40.2	+64 47	5.0	0.017	K1	G8	1.4	0.019		
4262	......	16 40.8	+15 56	5.8	0.054	Mb	G9	0.8	0.010	0.022	W
4264	43 Herculis	16 41.0	+ 8 46	5.4	0.016	K5	K3	0.8	0.012		
C2238	W.B. $16^{h}1259$	16 41.4	+33 41	8.6	0.37	K8	K5	9.0	0.120	0.199	D
C2242	Lal. 30699	16 42.9	+68 16	7.6	0.509	G9	G6	5.4	0.036	0.047	Y
4270	......	16 43.4	+56 58	4.9	0.062	F0	F1	2.3	0.030		
4273	20 Ophiuchi	16 44.3	−10 36	4.7	0.133	F5	F5	2.7	0.040		
......	Bu. 7778	16 46.4	+ 9 34	7.0†	......	F6	F6	3.1	0.017	0.001	A
......	Bu. 7783	16 47.9	+28 49	6.7†	......	F4	F6	3.4	0.022	0.024	A, Ye, S

TABLE VII—*Continued*

Boss	Name	α 1900	δ 1900	Harv. Vis. Mag.	μ	Spectrum Est.	Spectrum Meas.	Spect. Abs. Mag.	Spect. π	Trig. π	Auth.
C2248	Lal. 30694	16h47m9	+ 0°11′	6.8	1″664	K0	G6	5.8	0″063	0″099	A, Y, F
C2251	W.B. 16h906	16 50.1	− 8 9	9.2	1.234	Md	......	10.1	0.151	0.150	Ye, Y
4303	......	16 50.3	−16 39	6.5	0.089	K0	K0	4.1	0.033		
4305	......	16 50.4	+43 0	6.7	0.349	F9	G0	4.0	0.029	0.031	A
4307	......	16 50.6	+21 7	5.5	0.059	G7	G6	0.9	0.012	0.001	W
4311	54 Herculis	16 51.0	+18 36	5.6	0.106	K6	K3	0.3	0.009	0.008	A
4315	κ Ophiuchi	16 52.9	+ 9 32	3.4	0.295	K2	K0	0.6	0.028		
4316	57 Herculis	16 53.4	+25 30	6.7	0.008	G5	G5	0.8	0.007		
4318	......	16 53.8	−24 56	5.9	0.022	Ma	K1	0.2	0.007		
4322	19 Draconis	16 55.5	+65 17	4.8	0.252	F7	F8	3.6	0.058	0.087	A
4323	30 Ophiuchi	16 55.8	− 4 4	5.0	0.103	K5	K3	0.2	0.011		
4326	29 Ophiuchi	16 56.0	−18 44	6.4	0.052	K0	G8	2.1	0.014		
4327	ε Urs. Min.	16 56.2	+82 12	4.4	0.015	G2	G2	−1.4	0.007		
4336	32 Ophiuchi	16 58.5	+14 14	5.1	0.070	Mb	K0	−0.1	0.009		
C2277	Lal. 31132	16 59.8	+47 12	6.7	0.856	K0	G4	6.0	0.072	0.090	A, Y
4342	......	16 59.8	− 4 54	7.9	1.464	K5	K5	7.9	0.100	0.060	Ye, Y, F
4343	......	16 59.9	+35 33	6.8	0.058	Mb	G7	0.1	0.005	0.009	W
C2279	Lal. 31065	17 0.2	+ 0 51	5.9	0.321	G0	F9	4.1	0.044	0.039	A
4354	μ Draconis S.	17 3.3	+54 36	5.8	0.108	F5	F5	3.0	0.028		
4354	μ Draconis N.	17 3.3	+54 36	5.8	0.108	F5	F6	2.9	0.026		
......	Groom. 2420	17 3.4	+73 27	7.7	0.007	K5	K0	0.7	0.004		
4364	......	17 6.3	+40 54	5.1	0.053	K3	K2	0.8	0.014		
4370	36 Ophiuchi S.	17 9.2	−26 27	5.3	1.235	K1	K1	6.3	0.158		
4371	36 Ophiuchi N.	17 9.2	−26 27	5.3	1.224	K2	K0	6.3	0.158	0.140	F
4372	......	17 10.1	−26 24	6.7	1.223	K4	K3	7.3	0.132		

4373	α^1 Herculis	17h10m.1	+14°30′	3.5	0″.030	Mb	G5	−2.3	0″.007	−0″.004	A, M
4374	α^2 Herculis	17 10.1	+14 30	5.4	0.032	F9	G0	1.7	0.018		
4379	41 Ophiuchi	17 11.5	− 0 20	4.8	0.065	K2	K1	1.2	0.019		
4381	π Herculis	17 11.6	+36 55	3.4	0.025	K4	K1	0.4	0.025	0.017	A
4393		17 14.9	+28 56	5.8	0.045	G8	G8	0.6	0.009	0.015	W
C2310	Lal. 31528	17 15.4	+ 9 34	8.2	0.313	G0	G1	4.3	0.017	−0.017	A
4403	72 Herculis	17 16.9	+32 36	5.4	1.060	F8	G1	5.5	0.105	0.087	A, S, Y, F
4413		17 18.7	−21 21	6.0	0.045	G8	G5	1.7	0.014		
4414		17 19.0	−24 9	6.3	0.004	K1	G8	1.3	0.010		
4420	44 Ophiuchi	17 20.3	−24 5	4.3	0.132	A9	F0	1.6	0.029		
C2322	W.B. 17h322	17 20.8	+ 2 14	7.9	1.315	K5	K6	8.0	0.105	0.132	Ye, R, Y, F
4423		17 21.3	− 5 0	5.0†	0.104	F1	F3	2.1	0.026		
4424		17 21.4	−12 25	6.3	0.075	F6	F6	3.1	0.023		
4425	σ Ophiuchi	17 21.6	+ 4 14	4.4	0.004	K1	G8	0.7	0.018		
4433	Bu. 8038	17 25.2	− 0 59	6.0†	0.215	G6	G5	5.0	0.063	0.065	Ye, S
C2333	Lal. 32047	17 25.3	+67 23	6.3	0.536	K0	G8	5.9	0.083	0.071	A, G, Y
....	Lal. 31905	17 26.5	+ 1 45	7.2	....	K2	K3	2.1	0.010	0.039	Y
4438	λ Herculis	17 26.7	+26 11	4.5	0.021	K2	K1	0.4	0.015		
4443	β Draconis §	17 28.2	+52 23	3.0	0.016	G0p	F8	−3.5	0.005	0.005	A, M
4447		17 29.2	+16 23	5.7	0.058	G9	G8	1.8	0.017		
C2341	Bu. 8068 C	17 29.9	+ 6 4	8.6	0.623	F6	F8	3.8	0.011	−0.004	Y
....	Bu. 8068 A	17 30.0	+ 6 6	7.9	0.070*	F8	F7	3.8	0.015		
4464	27 Draconis	17 32.4	+68 12	5.2	0.138	G9	G9	1.1	0.015		
C2347		17 33.4	+18 37	9.1	1.39	K9	K5	9.7	0.132	0.128	Ye
4470	26 Draconis	17 34.0	+61 57	5.3	0.563	G0	G0	4.0	0.055	0.084	A, Ye, S, Y
....	B.D. +18° 3424	17 34.3	+18 37	9.4	....	K2	K0	6.1	0.022	0.008	Ye
....	7:1917 Serpentis*	17 34.3	−11 53	10.5	....	A8p	......	2.9	0.003		
C2351	A.G. Chris. 2703	17 35.8	+68 52	8.5	0.150	K0	G9	3.3	0.009		
C2353	Lal. 32322	17 36.3	+37 16	8.5	0.945	F7	F9	4.1	0.013		
C2354	A.Oe. 17415	17 37.0	+68 26	9.5	1.334	Mb	......	10.5	0.158	0.254	Ye, G, F, *et al.*

TABLE VII—*Continued*

Boss	Name	α 1900	δ 1900	Harv. Vis. Mag.	μ	Spectrum		Spect. Abs. Mag.	Spect. π	Trig. π	Auth.
						Est.	Meas.				
4480	Bu. 8114 Br.	$17^h37^m.0$	+24°34′	6.5	0″.052	K2	K1	0.8	0″.007	0″.022	W
....	Bu. 8114 Ft.	17 37.0	+24 34	8.6	0.052	F0	F1	2.5	0.006		
....	B.D. +68° 947	17 37.2	+68 27	8.0	....	F2	F4	2.4	0.008	0.011	Ye
4483	ω Draconis	17 37.5	+68 48	4.9	0.327	F2	F3	2.8	0.038	0.045	A
4487	β Ophiuchi	17 38.5	+ 4 37	2.9	0.158	K2	K1	0.6	0.035	0.025	A, M
C2358	Lal. 32390	17 39.0	+21 40	7.4	0.623	G8	G7	5.8	0.048		
4488	84 Herculis	17 39.3	+24 22	5.7	0.132	G2	G2	3.3	0.033	0.006	A
4493	X Sagittarii §	17 41.3	−27 48	4.7	0.023	F9p	F8	−1.3	0.006		
4497	μ Herculis A	17 42.5	+27 47	3.5	0.817	G5	G5	3.7	0.110	0.105	A, M, Y, *et al.*
4504	ψ Draconis Br.	17 43.7	+72 12	4.9	0.267	F3	F6	3.1	0.044	0.030	A
4505	ψ Draconis Ft.	17 43.7	+72 12	6.1	0.279	F7	F9	3.7	0.033		
4508	87 Herculis	17 44.8	+25 39	5.3	0.046	K1	G9	1.6	0.018		
....	Groom. 2485	17 50.9	+42 40	7.6	0.004	K0	G7	2.4	0.009		
4530	....	17 51.6	+22 29	5.7	0.002	K2	K0	0.3	0.008		
4531	ξ Draconis	17 51.8	+56 53	3.9	0.123	K3	K1	0.7	0.023	0.026	A
4535	θ Herculis	17 52.8	+37 16	4.0	0.006	G9	G7	−0.3	0.014	0.000	A
4536	ν Ophiuchi	17 53.5	− 9 46	3.5	0.118	G7	G8	−0.2	0.018	0.029	M
....	Z Herculis	17 53.6	+15 9	7.6	....	F2p	F5	2.7	0.011	0.033	Ye
4538	ξ Herculis	17 53.9	+29 16	3.8	0.090	G7	G5	0.9	0.026	0.025	A
4539	35 Draconis	17 53.9	+76 59	5.0	0.244	F5	F6	3.2	0.044	0.012	A, G
4541	γ Draconis	17 54.3	+51 30	2.4	0.027	K5	K1	0.6	0.044	0.012	A, M, F, *et al.*
4542	ν Herculis §	17 54.7	+30 12	4.5	0.004	F2p	F3	−0.2	0.012		
4544	ρ Serpentis	17 55.2	− 3 41	4.6	0.153	F0	F3	1.9	0.029		
4546	6 Sagittarii	17 55.6	−17 9	6.3	0.012	K1	G7	0.2	0.006		
4547	93 Herculis	17 55.6	+16 45	4.7	0.012	K2	G8	−0.3	0.010		

4554	34 Draconis	$17^{\mathrm{h}}56^{\mathrm{m}}.9$	+72° 1′	5.5	0″.009	F4	F5	1.7	0″.017		
4555		17 57.1	+45 30	5.9	0.044	K6	K3	0.6	0.009	0″.026	W
4556	95^{1} Herculis	17 57.3	+21 36	5.2	0.030	G1	G2	−0.3	0.008		
C2388	W.B. $17^{\mathrm{h}}1805$	17 58.4	+26 20	7.1	0.72	K1	K0	6.0	0.060	0.040	A
4564	W Sagittarii §	17 58.6	−29 35	4.7	0.015	G0p	F5	−2.0	0.004		
4571	70 Ophiuchi Br.	18 0.4	+ 2 31	4.3	1.131	K0	G9	5.8	0.200	0.187	A, M, Ye, *et al.*
4571	70 Ophiuchi Ft.	18 0.4	+ 2 31	6.0	1.131	K4	K7	7.2	0.174		
C2392	W.B. $17^{\mathrm{h}}1236$	18 0.7	+ 4 39	6.8	0.296	G1	G0	5.4	0.052	0.053	A
	Groom. 2506	18 1.4	+42 51	7.5	0.035	K2	G8	1.1	0.005		
C2396	Pi. $17^{\mathrm{h}}368$	18 2.1	+ 8 52	7.7	0.152	F7	F7	3.2	0.013	0.009	A
4580	71 Ophiuchi	18 2.5	+ 8 43	4.7	0.025	G6	G7	−0.1	0.011		
4582	99 Herculis	18 3.2	+30 33	5.2	0.113	F5	F7	4.4	0.069	0.045	M, Ṣ, Ye, *et al.*
	W Serpentis §*	18 4.1	−15 34	9.0	......	F9p	G0	−0.6	0.001		
4593		18 4.6	+36 23	5.7	0.213	K3	K1	0.6	0.010		
4595		18 4.9	+ 3 6	5.7	0.205	F4	F5	2.8	0.026	0.085	A
	Groom. 2521	18 5.9	+43 33	8.1	0.017	K1	G8	1.3	0.004		
C2403	Lal. 33439	18 6.3	+38 27	6.4	0.58	K3	K2	6.5	0.105	0.082	A, Y
4601		18 6.5	+36 27	5.9	0.009	G7	G6	1.0	0.011		
4606	104 Herculis	18 8.1	+31 23	5.0	0.018	Ma	K0	−0.1	0.010		
4609		18 8.5	+54 15	5.9	0.274	G9	G9	2.8	0.024	0.012	A
	A.G. Leiden 6547	18 8.5	+33 16	7.1	0.020‡	K6	K1	0.5	0.005		
4618		18 11.6	− 3 2	6.1	0.274	G2	G2	−0.3	0.005		
4623	36 Draconis	18 13.3	+64 22	5.0	0.346	F2	F4	3.5	0.050		
4629	105 Herculis	18 15.1	+24 24	5.5	0.016	K2	K0	0.2	0.009	0.002	W
4630		18 15.4	−24 58	6.4	0.011	Mc	G5	0.8	0.007		
4632	Y Sagittarii §	18 15.5	−18 54	5.8	0.013	G2p	F8	−1.6	0.003		
4635	74 Ophiuchi	18 15.9	+ 3 20	4.9	0.015	G5	G7	−0.5	0.008		
4636	106 Herculis	18 16.1	+21 55	5.0	0.062	K6	K3	0.2	0.011		
4638	η Serpentis	18 16.1	− 2 55	3.4	0.898	G8	G7	2.5	0.066	0.057	Y, J
4647		18 17.6	+51 18	6.2	0.062	K1	K0	0.7	0.008	0.036	W

TABLE VII—*Continued*

Boss	Name	α 1900	δ 1900	Harv. Vis. Mag.	μ	Spectrum		Spect. Abs. Mag.	Spect. π	Trig. π	Auth.
						Est.	Meas.				
....	A.G. Leip. 8449	$18^h18^m.0$	+ 7° 9′	7.6	0″.012‡	K2	K1	0.8	0″.004		
4650	ζ Scuti	18 18.2	− 8 59	4.8	0.062	G8	G8	0.4	0.013		
4656	109 Herculis	18 19.4	+21 43	3.9	0.324	K1	K0	1.5	0.033	0″.015	A, Jo
....	Groom. 2557	18 19.9	+43 53	8.2	0.001	G8	G7	1.1	0.004		
....	A.G. Leip. 8478	18 20.3	+ 9 41	7.9	0.016‡	K3	G8	0.8	0.004		
4660	....	18 20.8	+ 7 59	5.7	0.004	G0	G0	−0.8	0.005		
C2420	B.D. +8° 3689	18 21.4	+ 8 44	7.9	0.55	G5	G4	5.5	0.033	0.033	A, K
C2421	B.D. +8° 3692	18 21.6	+ 8 34	8.5	0.47	G9	G6	5.2	0.022	0.041	A, K
4665	λ Sagittarii	18 21.8	−25 29	2.9	0.197	K0	G9	3.2	0.115	0.069	F
....	A.G. Leip. 8507	18 22.0	+ 8 3	8.9	0.151	G2	G1	5.7	0.023	0.015	K
4672	χ Draconis	18 22.9	+72 41	3.7	0.638	F5	F6	4.1	0.120	0.105	M, G, Y
C2423	Groom. 2571	18 23.7	+46 1	8.3	0.398	G0	F9	4.5	0.017	0.006	A
4678	60 Serpentis	18 24.5	− 2 3	5.4	0.038	G9	G9	1.7	0.018		
....	Groom. 2577	18 25.3	+44 11	7.7	0.014	K3	K0	1.0	0.005		
4686	42 Draconis	18 25.7	+65 30	5.0	0.104	K1	G9	1.3	0.018		
....	U Sagittarii §	18 26.0	−19 12	6.9	0.012‖	G0p	F7	−1.4	0.002		
....	A.G. Leip. 8585	18 26.1	+ 8 1	7.6	0.029‡	Ma	K0	1.5	0.006		
4688	....	18 26.3	+59 29	6.5	0.061	G8	G7	2.8	0.018		
4701	....	18 28.6	+23 33	6.0	0.011	K4	K1	0.4	0.008		
4705	1 Aquilae	18 29.8	− 8 19	4.1	0.318	K4	K1	0.6	0.020		
....	Groom. 2622	18 31.6	+65 18	8.7	0.023	F0	......	2.4	0.006		
4711	....	18 31.7	+52 16	5.4	0.008	G7	G7	−0.4	0.007		
4713	....	18 31.8	+ 6 36	5.4	0.146	F0	F1	1.6	0.017	0.024	A
....	Bu. 8679	18 33.2	− 3 17	7.1†	......	G0	F8	4.6	0.032	0.035	Ye
4723	....	18 34.5	+63 37	8.1	0.254	F7	F7	4.0	0.015	0.028	A

4724		18h34m6	+77°28′	5.8	0″006	K2	G8	0.6	0″009		
4731	2 Aquilae	18 36.8	− 9 9	4.7	0.014	F5	F3	1.3	0.021		
C2450	W.B. 18h1064	18 37.1	+31 28	8.8	0.82	K3	K2	6.6	0.036	0″033	A
4750		18 41.2	−10 14	5.8	0.005	F6	F3	1.1	0.012		
4753	110 Herculis	18 41.4	+20 27	4.3	0.345	F4	F6	3.3	0.063	0.057	A, M, Jo
C2456	Bu. 8798 Br.	18 41.7	+59 29	8.8	2.307	Mb	......	10.7	0.240	0.289	Ye, D, R, *et al.*
4758		18 42.0	+26 33	4.9	0.029	K1	G9	1.5	0.021		
4763	Bu. 8825	18 43.1	+60 57	6.3†	0.010	K0	G7	1.6	0.012		
....	YZ Sagittarii §	18 43.7	−16 50	7.4	....	G1p	F9	−2.7	0.001		
C2462	Lal. 34986	18 43.8	+10 39	8.0	0.463	K4	K4	6.8	0.058	0.062	A, Y
....	Lal. 34958	18 44.1	−10 29	7.9	....	K2	K1	4.9	0.025		
....	Bu. 8849	18 44.9	+49 20	7.8†	....	F2	F3	1.4	0.005	0.017	Ye
4780	33 Sagittarii	18 48.0	−21 29	5.8	0.012	G9	G5	0.2	0.008		
4787		18 49.3	+52 51	5.6	0.288	G8	G8	3.2	0.033	0.048	A
4790	o Draconis	18 49.7	+59 16	4.8	0.086	G8	G4	−0.5	0.009		
4797	113 Herculis	18 50.5	+22 31	4.6	0.005	F9	G0	1.7	0.026		
4800	12 Lyrae	18 51.0	+36 46	4.5	0.010	Mb	G4	−1.2	0.007		
4805		18 51.7	+41 28	5.6	0.007	G8	G9	0.0	0.008		
4809	37 Sagittarii	18 51.8	−21 14	3.6	0.037	K0	K0	0.7	0.026		
4814	R Lyrae	18 52.3	+43 49	4.3	0.077	Mc	G8	−1.4	0.007	0.028	Ab
C2475	Mün. 18180	18 53.1	+ 5 48	9.8	1.247	Ma	K6	9.7	0.095	0.069	A, R
4815		18 53.3	+32 46	5.2	0.235	G0	F9	4.8	0.083	0.095	A, S, F, J
4817		18 53.8	+17 14	5.4	0.009	F8	F7	0.3	0.010	0.001	W
4823	ε Aquilae	18 55.1	+14 56	4.2	0.100	K1	K0	1.0	0.023		
....	A.G. Berlin 7148	18 56.2	+18 20	8.0	0.017	G7	G4	1.7	0.006		
4834	12 Aquilae	18 56.3	− 5 53	4.2	0.048	K1	K0	2.0	0.036		
4847	o Sagittarii	18 58.7	−21 53	3.9	0.098	G8	G9	1.3	0.030		
4852	15 Aquilae Ft.	18 59.7	− 4 11	7.2	0.037	K5	K4	0.8	0.005		
4860		19 1.2	+31 36	5.8	0.085	K5	K1	0.7	0.010	0.026	W
C2492	B.D. +7° 3967	19 2.2	+ 7 29	9.5	0.812	K5	K3	7.8	0.046	0.040	Ye

TABLE VII—*Continued*

Boss	Name	α 1900	δ 1900	Harv. Vis. Mag.	μ	Spectrum		Spect. Abs. Mag.	Spect. π	Trig. π	Auth.
						Est.	Meas.				
....	TT Aquilae §.........	19h 3m.2	+ 1° 9′	7.6	....	G2p	F9	−1.4	0″.002		
C2495......	Lal. 35851............	19 3.5	+16 42	6.0	0″.308	G4	G4	3.7	0.035	0″.063	A
4874......	π Sagittarii §..........	19 3.8	−21 11	3.0	0.040	F4p	F3	−0.8	0.017	0.017	M
4880......	....	19 6.5	−21 49	6.4	0.032	K0	K0	1.4	0.010		
C2507......	Bu. 9114 A...........	19 7.7	+38 37	8.2	0.267	G4	G6	5.5	0.029	0.023	M, S
C2507......	Bu. 9114 BC..........	19 7.7	+38 37	8.7†	0.267	K0	G9	5.8	0.026		
C2508......	Bu. 9116 C...........	19 8.0	+16 41	7.6	0.243	G6	G7	5.0	0.030	0.021	M
4892......	Bu. 9137 Ft...........	19 9.5	+49 40	6.8	0.630	G4	G2	5.5	0.055	0.045	M, W, R, *et al.*
4893......	Bu. 9137 Br...........	19 9.5	+49 40	6.6	0.654	G6	G3	5.7	0.066		
....	Bu. 9136..............	19 10.0	+18 54	7.7†	0.031‡	F7	F7	3.3	0.013		
4898......	....	19 10.8	+14 55	5.7	0.020	G8	G7	−1.4	0.004		
4903......	43 Sagittarii..........	19 11.8	−19 8	5.0	0.023	G7	G6	0.5	0.013		
4909......	δ Draconis...........	19 12.5	+67 29	3.2	0.133	G8	G7	0.8	0.033	0.035	A
4910......	....	19 12.7	+49 54	6.3	0.014	G8	G6	1.5	0.011		
4912......	θ Lyrae...............	19 12.9	+37 57	4.5	0.010	K0	G7	0.2	0.014		
4915......	....	19 13.3	−15 43	6.3	0.285	K3	G9	0.9	0.008		
4919......	24 Aquilae...........	19 13.7	+ 0 9	6.5	0.009	G9	G7	1.2	0.009		
4920......	....	19 14.0	+46 49	6.0	0.285	F4	F6	2.8	0.023	0.018	A
4923......	κ Cygni...............	19 14.8	+53 11	4.0	0.133	G7	G7	1.1	0.026	0.040	A, Ab
4926......	26 Aquilae...........	19 15.2	− 5 36	5.1	0.110	G7	G7	2.6	0.032		
4932......	44 Sagittarii..........	19 15.9	−18 2	4.0	0.031	A8	......	1.7	0.035	0.049	M
4940......	τ Draconis...........	19 17.5	+73 10	4.6	0.176	K4	K3	0.5	0.015		
4950......	31 Aquilae...........	19 20.2	+11 44	5.2	0.961	G8	G6	5.1	0.095	0.067	A, M, Ye, *et al.*
4953......	δ Aquilae............	19 20.5	+ 2 55	3.4	0.265	A9	......	1.8	0.048	0.057	A, M
4961......	....	19 21.3	+24 44	6.2	0.658	F6	F4	3.9	0.035	0.060	Y, Jo, F

	RR Lyrae §	19^h22^m3	+42°35′	7.3	0.″221‖	Fop	F3	0.3	0.″004		
	U Aquilae §	19 24.0	− 7 15	6.6	0.017‖	Gop	F7	−2.3	0.002		
4976	α Vulpeculae	19 24.5	+24 28	4.6	0.170	Ma	K0	0.1	0.013		
4978	8 Vulpeculae	19 24.8	+24 34	6.0	0.012	G9	G8	0.7	0.009		
4985		19 26.4	−28 13	7.0	0.741	G6	G4	5.8	0.058		
4986	β^1 Cygni	19 26.7	+27 45	3.2	0.009	K0	G6	0.8	0.033	0.″000	A, M, Y
	Bu. 9401 Br.	19 29.0	+20 11	7.4†	0.057*	A7	......	1.1	0.006	−0.018	A
4995	μ Aquilae	19 29.2	+ 7 10	4.6	0.262	K3	K2	0.7	0.017	0.021	A
C2554	Groom. 2875	19 29.5	+58 23	6.7	0.664	K4	K2	6.7	0.100	0.030	A, Y
C2558	Lal. 37120	19 29.7	+32 59	6.6	0.517	G1	F9	4.4	0.036	0.043	A, M, Y
5005		19 31.7	+51 1	5.8	0.205	F6	F6	3.3	0.032		
	U Vulpeculae §	19 32.3	+20 7	7.0	0.031‖	Gop	F9	−2.0	0.002		
5009	σ Draconis	19 32.6	+69 29	4.8	1.840	G9	G7	5.8	0.158	0.192	M, Y, P, *et al.*
5014	θ Cygni	19 33.8	+49 59	4.6	0.249	F2	F5	3.4	0.058	0.070	A, M, Y, *et al.*
5019	54 Sagittarii	19 35.0	−16 31	5.4	0.085	K1	K0	1.7	0.018		
5021	φ Cygni	19 35.4	+29 55	4.8	0.035	G8	G8	0.9	0.017		
5023	α Sagittae	19 35.6	+17 47	4.4	0.036	F9	F8	−0.9	0.009	−0.004	M
5027	β Sagittae	19 36.6	+17 15	4.4	0.038	G8	G7	0.0	0.013		
5031		19 37.8	+45 17	5.0	0.142	F4	F4	1.5	0.020	−0.003	Y
5033	χ Aquilae	19 37.9	+11 35	5.6†	0.013	F5	F7	2.4	0.023		
5037	16^1 Cygni	19 39.2	+50 18	6.3	0.217	G2	G1	5.1	0.058	0.038	A, M, S, Ye
5038	16^2 Cygni	19 39.2	+50 17	6.4	0.204	G3	G3	4.6	0.044		
	Bu. 9569	19 39.8	+26 53	6.6	0.062	G0	F9	1.8	0.011	−0.010	A
5043		19 40.4	+41 32	6.0	0.017*	K6	K2	0.4	0.008	0.006	W
5044	56 Sagittarii	19 40.5	−20 0	5.1	0.165	K0	G9	1.7	0.021		
5045	15 Cygni	19 40.7	+37 7	5.0	0.076	G7	G7	0.1	0.011	0.020	A
	SU Cygni §	19 40.8	+29 1	6.6	....	F7p	F5	−1.1	0.003		
5047	γ Aquilae	19 41.5	+10 22	2.8	0.014	K3	G9	0.3	0.032	0.034	M
C2579	Bu. 9602	19 41.8	+33 22	9.2†	0.433	K4	K2	6.7	0.032	0.041	M
5051	17 Cygni Br.	19 42.6	+33 30	5.0	0.452	F6	F5	2.9	0.038	0.045	A, M, Y
5051	17 Cygni Ft.	19 42.6	+33 30	8.1	0.452	K4	K2	6.5	0.048		

TABLE VII—*Continued*

Boss	Name	α 1900	δ 1900	Harv. Vis. Mag.	μ	Spectrum		Spect. Abs. Mag.	Spect. π	Trig. π	Auth.
						Est.	Meas.				
5052	δ Sagittae	19h42m.9	+18°17′	3.8	0″.009	Ma	G1	0.2	0″.019		
C2585	Bu. 9650	19 45.0	+35 4	6.9†	0.119	F4	F4	3.1	0.017	0″.021	S
5063		19 45.9	+38 27	6.2	0.016	G3	G3	−0.5	0.005		
5071	η Aquilae §	19 47.4	+ 0 45	4.1	0.012	F9p	F9	−2.7	0.004	0.004	M
5075	20 Cygni	19 48.1	+52 44	5.2	0.072	K5	K3	0.2	0.010	0.020	Ab
5079	ε Draconis	19 48.5	+70 1	4.0	0.087	G2	G5	0.7	0.022		
5082	56 Aquilae	19 48.7	− 8 50	6.0	0.022	K4	K2	0.9	0.010		
5089	ξ Aquilae	19 49.4	+ 8 12	4.9	0.126	G9	G9	0.8	0.015	0.039	M
5093	β Aquilae	19 50.4	+ 6 9	3.9	0.484	G8	G7	3.9	0.100	0.076	A, M, S
5096		19 51.2	+36 44	5.8	0.008	F6	F6	0.9	0.011		
5098	S Sagittae §	19 51.5	+16 22	5.8	0.004	G1p	F8	−2.5	0.002		
5103	η Cygni	19 52.6	+34 49	4.0	0.052	K0	G9	1.8	0.036		
5116		19 54.0	+58 35	5.1	0.025	K5	K1	0.4	0.012		
5118	γ Sagittae	19 54.3	+19 13	3.7	0.062	K6	K2	0.5	0.023	0.005	A
5119		19 54.4	−10 13	5.9	0.488	F8	F8	4.2	0.046	−0.004	Y
C2607	Lal. 38139	19 55.5	−12 31	7.6	0.504	F6	F6	4.5	0.024		
5125	13 Sagittae	19 55.6	+17 15	5.6	0.015	Mc	G6	0.5	0.010		
5129	62 Sagittarii	19 56.5	−27 59	4.6	0.037	Mb	G7	0.3	0.014		
C2616	Lal. 38287	19 58.0	+15 20	7.2	0.608	G8	G5	5.6	0.048	0.085	M, Y
5142	62 Aquilae	19 59.2	− 0 59	5.8	0.119	K1	G7	1.7	0.015		
5143	τ Aquilae	19 59.3	+ 7 0	5.6	0.025	G8	G7	0.0	0.008		
5144		19 59.5	+29 38	5.7	0.853	G7	G7	4.8	0.066	0.049	A, Y, F
5146	15 Sagittae	19 59.6	+16 48	5.9	0.578	G1	G0	5.0	0.066	0.104	Y, Jo
C2620	Lal. 38383	19 59.7	+23 5	7.2	1.369	K2	K0	6.6	0.076	0.059	A, M, Y, *et al.*

5149	64 Draconis	20^{h}	$0^{\mathrm{m}}.4$	$+64^{\circ}32'$	5.4	0".015	Ma	G8	−0.1	0".008		
5153	ρ Draconis	20	2.4	+67 35	4.7	0.051	K2	K1	0.7	0.016		
5157	27 Cygni	20	2.6	+35 42	5.5	0.496	G8	G6	4.1	0.052	0".050	Ye
5163		20	3.6	+52 52	5.7	0.334	F4	F4	3.9	0.044	0.066	Ab, Y
	B.D. +36° 3883	20	3.7	+36 17	7.1		Ma	G7	1.0	0.006	−0.004	M
5166		20	4.6	−36 21	5.3	1.626	K3	K0	6.7	0.190		
5167	17 Sagittae C	20	5.5	+20 36	7.3	0.011	K1	K0	2.9	0.013	0.028	S
5169	17 Sagittae A	20	5.5	+20 37	6.3	0.111	F2	F2	3.0	0.022	0.019	S
C2634	Pi. $20^{\mathrm{h}}23$	20	6.6	+15 53	7.3	0.578	K2	K1	6.0	0.055	0.065	Y, M
5176	2 Capricorni	20	6.9	−12 55	5.9	0.269	F4	F4	3.8	0.038		
	Bu. 9979	20	7.1	+43 39	7.7†		G5	G3	5.1	0.030	0.049	S
5177	19 Vulpeculae	20	7.6	+26 31	5.8	0.020	K3	G8	0.5	0.009		
	A.G. Berlin 8022	20	8.2	+15 47	7.6	0.016	F6	F7	3.4	0.014		
5180		20	9.1	−27 20	5.7	1.256	K2	K2	5.9	0.110	0.042	F, V
5184	68 Draconis	20	9.9	+61 47	5.7	0.155	F6	F5	3.0	0.029	0.037	W
5187	o² Cygni	20	10.5	+46 26	4.0	0.002	G9p	G1	−2.0	0.006	−0.002	A, M
C2645	Bu. 10044 A	20	11.0	+52 49	7.2†	0.179	F5	F7	3.4	0.017	0.016	A
5197	α¹ Capricorni §	20	12.1	−12 49	4.6	0.015	G0p	F7	−3.9	0.002	−0.012	M
5201	24 Vulpeculae	20	12.5	+24 22	5.4	0.027	G7	G5	0.5	0.011	−0.027	A
5202	α² Capricorni	20	12.5	−12 51	3.8	0.058	G8	G6	1.2	0.030	−0.012	M
5206	σ Capricorni	20	13.6	−19 26	5.5	0.011	K2	K0	1.3	0.014		
5216	β Capricorni	20	15.4	−15 6	3.2	0.035	F8	F7	0.3	0.026	0.007	M
	Bu. 10135 Ft.	20	15.9	+55 5	7.4	0.021	F3	F3	2.8	0.012		
5219		20	16.5	+66 32	6.1	0.557	G2	G1	5.2	0.066	0.120	Y, J
C2654	A.Oe. 20452	20	17.7	−21 40	8.2	1.182	F6	F7	3.7	0.013	0.044	F, V
5229	γ Cygni §	20	18.6	+39 56	2.3	0.003	G0p	G0	−3.0	0.009	0.014	A, M, Y, F
5231		20	19.2	+40 42	6.1	0.054	K6	K0	0.2	0.007		
5235	39 Cygni	20	19.9	+31 52	4.6	0.041	K5	K2	0.5	0.015		
5244	ρ Capricorni A §	20	23.2	−18 9	5.1	0.026	A9	F0	−1.0	0.010	0.024	M
5255	41 Cygni §	20	25.3	+30 2	4.1	0.010	F6	F4	−1.1	0.009	−0.018	M

TABLE VII—*Continued*

Boss	Name	α 1900	δ 1900	Harv. Vis. Mag.	μ	Spectrum		Spect. Abs. Mag.	Spect. π	Trig. π	Auth.
						Est.	Meas.				
5256		20h25m.5	−15°23′	6.2	0″.073	G2	G2	−0.2	0″.005		
5263		20 26.9	−10 12	5.8	0.317	G3	G2	4.9	0.066		
5267	44 Cygni	20 27.2	+36 36	6.3	0.013	F6	F6	0.8	0.008	0″.035	F
5276		20 29.5	+56 26	6.3	0.021	K4	K0	0.8	0.008		
C2667	Groom. 3215	20 29.3	+41 33	7.0	0.475	K0	G7	6.0	0.063	0.017	A, Y, Jo
5280		20 30.4	+72 12	6.4	0.025	K4	K2	0.8	0.008		
5284	70 Aquilae	20 31.5	− 2 54	5.2	0.011	K4	G8	1.0	0.014		
	V Vulpeculae §	20 32.3	+26 11	8.6	......	G7p	G9	−0.8	0.001		
5291	β Delphini	20 32.9	+14 15	4.0†	0.113	F3	F5	2.3	0.046	0.027	M, S, Ye, F
C2672	Lal. 39816	20 34.2	−24 8	6.3	0.658	G8	G7	6.2	0.095		
5304	κ Delphini	20 34.3	+ 9 44	5.2	0.315	G2	G1	3.4	0.044		
5305	1 Aquarii	20 34.3	+ 0 8	5.4	0.094	G9	G9	1.6	0.017		
C2673	Groom. 3243	20 34.4	+42 29	7.1	0.197	F6	F6	3.2	0.017	0.000	A
5306	υ Capricorni	20 34.4	−18 29	5.3	0.035	Ma	G7	0.2	0.010		
C2676	Lal. 39866	20 34.6	+ 4 37	8.4	0.844	K5	K4	8.0	0.083	0.061	A, Ye, Y
5317	10 Delphini	20 36.6	+14 14	6.2	0.012	K3	K0	1.0	0.009		
5319	49 Cygni	20 37.0	+31 57	5.9†	0.018	G8	G4	0.0	0.007		
	A.G. Berlin 8332	20 37.6	+19 30	7.5	0.009	K1	G8	2.0	0.008		
5321		20 38.2	+60 9	6.0	0.186	F5	F6	3.6	0.033	0.049	Y, Ab
	X Cygni §	20 39.5	+35 14	6.5	0.018	G3p	G0	−2.1	0.002	0.006	S
	A.G. Leiden 8454	20 41.1	+31 25	8.0	0.015	K1	G9	1.5	0.005		
5331	52 Cygni	20 41.5	+30 21	4.3	0.027	G8	G7	1.2	0.024	0.014	M
	Bu. 10504 Br.	20 41.5	+15 32	7.5	0.121*	G8	G6	5.5	0.040	0.016	A
	Bu. 10504 Ft.	20 41.5	+15 32	8.2	0.100*	G6	G7	5.3	0.026		
5334	γ¹ Delphini Ft.	20 42.0	+15 46	5.5	0.195	F6	F7	3.0	0.032	0.026	M, S
5335	γ² Delphini Br.	20 42.0	+15 46	4.5	0.207	K1	K1	1.1	0.021		

5336	ε Cygni	$20^h42^m.2$	+33°36′	2.6	0″.483	G7	G7	0.8	0″.044	0″.036	A, M, F, J
5338	3 Aquarii	20 42.5	− 5 24	4.6	0.039	Ma	K0	0.4	0.014		
5344		20 42.9	+57 13	4.6	0.241	F8	F8	3.5	0.060	0.032	A, Y
5346	η Cephei	20 43.3	+61 27	3.6	0.826	G8	G8	3.2	0.083	0.092	A, M, Ye, *et al.*
5370	T Vulpeculae §	20 47.2	+27 53	5.8	0.015	F9	F7	−1.7	0.003		
5373	31 Vulpeculae	20 47.8	+26 43	4.8	0.103	G2	G3	−1.6	0.005		
5379	32 Vulpeculae	20 50.3	+27 41	5.2	0.009	K5	K3	0.5	0.012		
5385	17 Delphini	20 50.9	+13 20	5.4	0.023	K0	G7	0.4	0.010		
C2707	A.Oe. 21338	20 51.3	+61 48	8.6	0.77	Ma	K5	9.4	0.144	0.139	A
5388		20 52.1	+80 11	5.6	0.040	K0	G9	1.6	0.016		
C2709	Fed. 3638	20 52.4	+74 23	7.9	0.691	G6	G4	5.3	0.030	0.015	A, Y, F
	Groom. 3359	20 53.6	+69 34	7.8	0.020	G9	G5	1.7	0.006		
5397	33 Vulpeculae	20 53.8	+21 56	5.6	0.005	K4	K0	1.0	0.012		
5399	ε Equulei AB	20 54.1	+ 3 55	6.0†	0.191	F1	F4	2.4	0.019	0.019	M, S
5399	ε Equulei C	20 54.1	+ 3 55	7.4	......	F2	F2	3.3	0.015		
5409	Bu. 10659	20 55.9	+18 56	6.2†	0.075	Ma	K1	0.5	0.007	0.009	W
C2718	Groom. 3357	20 56.1	+39 52	6.6	0.314	F7	F8	3.9	0.039	0.040	Ye, Jo
	A.G. Leiden 8661	20 58.8	+31 57	7.2	0.014‡	K4	G9	0.5	0.005		
C2728	W.B. 20^h1454	20 59.1	+ 2 36	8.1	0.485	F6	F7	3.9	0.014	−0.015	M, Y
5420		20 59.2	+38 16	6.2	0.012	G8	G6	1.5	0.012		
5422	3 Equulei	20 59.6	+ 5 6	5.9	0.019	K3	K0	1.0	0.011		
C2732	Lal. 40844	21 0.4	+ 6 41	8.9	0.553	K7	K5	8.7	0.091	0.081	Ye, Y
5430	24 Capricorni	21 1.3	−25 24	4.6	0.059	K4	K1	0.7	0.017		
5431	ξ Cygni §	21 1.3	+43 32	3.9	0.007	K2p	G5	−2.9	0.004	−0.003	A
5432		21 2.3	+30 47	5.9	0.010	F7	F6	0.7	0.009		
5433	61^1 Cygni	21 2.4	+38 15	5.6	5.267	K7	K7	8.3	0.347	0.307	A, M, W, *et al.*
5434	61^2 Cygni	21 2.4	+38 15	6.3	5.153	K8	K7	8.7	0.302		
5441	ν Aquarii	21 4.1	−11 47	4.5	0.094	G8	G8	2.0	0.032		
	A.G. Leiden 8741	21 4.9	+32 22	8.1	0.023‡	K0	G6	2.4	0.007		

TABLE VII—*Continued*

Boss	Name	α 1900	δ 1900	Harv. Vis. Mag.	μ	Spectrum		Spect. Abs. Mag.	Spect. π	Trig. π	Auth.
						Est.	Meas.				
....	B.D. +38° 4362.......	$21^{h}\ 5^{m}.2$	+38° 19′	7.8	....	K2	G9	1.7	0″.006	−0″.031	R
5443......	γ Equulei............	21 5.5	+ 9 44	4.8	0″.169	F0	F0	−0.4	0.009		
C2749......	W.B. $21^{h}97$...........	21 7.4	+17 21	7.3	0.915	F4	F3	4.0	0.022	0.032	A, Y, F, J
5452......	ζ Cygni..............	21 8.7	+29 49	3.4	0.059	G6	G7	−1.1	0.013	0.026	A, M
C2753......	Fed. 3738............	21 8.8	+73 18	8.6	0.518	K0	K1	6.1	0.032		
5455......	δ Equulei AB..........	21 9.6	+ 9 36	5.1†	0.306	F6	F7	4.0	0.060	0.053	M, F, Hus
5456......	φ Capricorni..........	21 9.9	−21 4	5.4	0.007	K2	G8	1.1	0.014		
5457......	29 Capricorni.........	21 10.2	−15 35	5.5	0.019	Mb	G9	0.4	0.010		
5460......	τ Cygni..............	21 10.8	+37 37	3.8	0.455	F1	F3	1.9	0.042	0.042	A, M, S, *et al.*
5461......	α Equulei............	21 10.8	+ 4 50	4.1	0.104	F6	F7	1.9	0.036	0.034	A
C2763......	Lal. 41348............	21 12.9	− 0 15	8.6	0.476	K5	K3	7.0	0.048		
....	A.G. Berlin 8683......	21 13.8	+17 18	7.6	0.022‡	K1	G9	1.5	0.006		
....	A.G. Berlin 8684......	21 13.9	+17 34	7.2	0.016‡	F4	F3	3.5	0.018		
C2769......	Bu. 10881 Br..........	21 14.0	−26 46	6.6†	0.665	G8	G5	5.6	0.063	−0.100	F
5476......	16 Aquarii............	21 15.8	− 4 59	6.0	0.026	G7	G6	1.6	0.013		
5481......	....	21 16.5	+58 12	5.8	0.014	F3	F7	1.7	0.015		
5482......	34 Vulpeculae.........	21 16.6	+23 26	5.8	0.253	G9	G9	0.6	0.009		
5486......	....	21 16.8	+76 35	6.2	0.020	K4	K1	0.5	0.007		
5489......	1 Pegasi..............	21 17.5	+19 23	4.2	0.118	K0	K0	1.4	0.028	0.020	A, Ye
5490......	17 Aquarii............	21 17.6	− 9 45	6.2	0.050	K4	K2	0.8	0.008		
....	A.G. Berlin 8723......	21 18.4	+16 4	7.6	0.022‡	K4	K0	1.1	0.005		
....	A.G. Bonn 15400......	21 18.6	+41 26	9.1	....	K3	K1	1.2	0.003		
5507......	ζ Capricorni §.........	21 21.0	−22 51	3.9	0.023	G1p	F9	−3.9	0.003		
5519......	....	21 23.9	+31 47	5.7	0.134	F0	F1	2.9	0.028	0.032	W
C2790......	W.B. $21^{h}502$..........	21 24.5	−12 56	9.4	1.052	K6	K6	8.5	0.066		

5522......	2 Pegasi.............	$21^h25^m.4$	+23°12′	4.8	0″.017	K4	K2	0.6	0″.014		
5523......	71 Cygni............	21 25.8	+46 6	5.3	0.114	G9	G8	1.5	0.017	0″.036	A, S, Ye, Ab
C2797......	W.B. 21^h594.........	21 26.0	+45 27	7.9	0.56	G8	G7	5.6	0.035	0.025	A
5527......	β Aquarii §..........	21 26.3	− 6 1	3.1	0.017	F9	F8	−2.1	0.009	−0.016	M, F
....	B.D. +45° 3566.......	21 26.8	+46 6	8.3	....	F0	F0	2.0	0.006		
....	Groom. 3502.........	21 30.0	+67 56	8.7	0.027	K2	K0	2.1	0.005		
5542......	....	21 30.1	− 4 26	5.8	0.021	K0	G8	−0.1:	0.007		
5543......	ρ Cygni.............	21 30.2	+45 9	4.2	0.099	G5	G4	1.3	0.026	0.013	A, Ab, Y
5546......	72 Cygni............	21 30.7	+38 5	5.0	0.148	G9	K0	0.6	0.013	0.003	A, Y
....	A.G. Leiden 9045......	21 33.8	+32 41	7.6	0.045‡	G8	G7	1.2	0.005		
5559......	24 Aquarii...........	21 34.4	− 0 30	7.4†	0.236	F8	F7	4.0	0.021	0.017	F, J
5560......	25 Aquarii...........	21 34.5	+ 1 48	5.3	0.088	K0	G9	1.9	0.021		
5562......	γ Capricorni §........	21 34.6	−17 7	3.8	0.188	F4	F4	−0.7	0.013	0.018	M
....	A.G. Leiden 9056......	21 35.1	+31 5	8.2	0.047	F8	F8	3.0	0.009		
5566......	42 Capricorni.........	21 36.1	−14 30	5.3	0.331	G0	G1	3.8	0.050		
5569......	26 Aquarii...........	21 37.1	+ 0 50	5.8	0.015	K2	G9	1.0	0.011		
5570......	κ Capricorni..........	21 37.1	−19 19	4.8	0.142	G2	G3	−1.4	0.006		
5583......	....	21 39.1	+40 42	5.5	0.026	Ma	G9	0.3	0.009		
5584......	ε Pegasi..............	21 39.3	+ 9 25	2.5	0.025	K0	G4	−0.3	0.028	0.006	A, M, F
5587......	μ^1 Cygni A...........	21 39.7	+28 18	4.7	0.370	F5	F6	3.5	0.058	0.046	M
5589......	46 Capricorni.........	21 39.7	− 9 33	5.3	0.010	G7	G6	−0.1	0.008		
C2823......	A.G. Berlin 8366......	21 39.7	+24 53	9.1	0.65	K0	G7	6.1	0.025		
5590......	9 Pegasi.............	21 39.8	+16 53	4.5	0.029	G5	G0	−0.6	0.010		
5591......	....	21 39.9	+28 19	7.6†	0.061	A9	......	2.3	0.009		
5592......	κ Pegasi.............	21 40.1	+25 11	5.3†	0.033	F2	F5	2.7	0.030	0.038	A, M, S, *et al.*
5593......	μ Cephei.............	21 40.4	+58 19	4.5	0.002	Ma	G8	0.3	0.014	0.010	A
5594......	11 Cephei............	21 40.5	+70 51	4.8	0.153	K1	K1	0.6	0.014		
5595......	47 Capricorni.........	21 40.9	− 9 44	6.2	0.016	Mb	G7	0.1	0.006		
5599......	12 Pegasi............	21 41.5	+22 29	5.4	0.016	K0	G2	1.5	0.017		
5602......	....	21 41.8	+25 6	6.5	0.148	K1	K2	1.9	0.012	0.005	W

TABLE VII—*Continued*

Boss	Name	α 1900	δ 1900	Harv. Vis. Mag.	μ	Spectrum Est.	Spectrum Meas.	Spect. Abs. Mag.	Spect. π	Trig. π	Auth
5614	12 Cephei	21ʰ44ᵐ.5	+60°14′	5.6	0″.006	K5	K3	0.5	0″.010		
5616	13 Pegasi	21 45.4	+16 49	5.3	0.096	A 8	......	1.4	0.015		
....	A.G. Leiden 9158	21 46.5	+32 12	8.6	....	K0	G6	3.3	0.009		
....	Groom. 3594	21 47.2	+64 46	7.9	0.010‡	Mb	G6	0.8	0.004		
....	A.G. Leiden 9164	21 47.3	+31 27	7.5	0.029‡	K4	K2	0.9	0.005		
5623	μ Capricorni	21 47.8	−14 1	5.2	0.308	A9	F2	1.9	0.022		
....	Groom. 3604	21 48.7	+66 22	8.2	0.014	F2	F3	3.3	0.011		
5638	....	21 51.4	+53 28	6.9	0.172	F6	F7	3.2	0.018	0″.014	A
5645	....	21 53.2	−21 40	6.2	0.015	Mb	G7	0.7	0.008		
5650	....	21 53.8	+63 9	5.4	0.012	Mdp	......	−0.3	0.007		
5651	....	21 54.3	+29 21	6.8	0.540	F6	F4	4.1	0.029	0.040	S, Y, F, J
5655	28 Aquarii	21 56.0	+ 0 7	5.8	0.006	K4	K2	1.2	0.012		
5657	19 Pegasi	21 56.2	+ 7 47	5.8	0.022	K4	K1	1.0	0.011		
5658	20 Pegasi	21 56.2	+12 38	5.7	0.077	F3	F3	2.3	0.021		
5661	16 Cephei	21 57.8	+72 42	5.2	0.174	F3	F3	2.6	0.030	0.038	A
5671	32 Aquarii	21 59.6	− 1 23	5.2	0.045	A9	......	1.0	0.014		
5674	ν Pegasi	22 0.6	+ 4 34	4.9	0.144	K6	K3	0.3	0.012	0.016	A, M
5676	α Aquarii §	22 0.6	− 0 48	3.2	0.015	G0	F8	−2.8	0.006	0.010	M
5677	ξ¹ Cephei Ft.	22 0.9	+64 8	6.5	0.226	F7	F7	3.9	0.030	0.029	A
5682	Bu. 11514 Br.	22 1.8	+82 23	7.1	0.141	F6	F6	3.5	0.019	0.006	W
5683	Bu. 11514 Ft.	22 1.9	+82 23	7.8†	0.142	G3	G4	4.8	0.025		
5688	ι Pegasi	22 2.4	+24 51	4.0	0.299	F4	F6	3.6	0.083	0.079	A, M, S
5691	....	22 2.7	+18 59	5.8	0.126	F1	F5	2.4	0.021	0.013	W
C2885	Groom. 3689	22 3.1	+52 39	7.9	0.629	K1	G7	4.8	0.024	0.051	Ye, Y, F, J
5694	....	22 3.8	+58 21	6.3	0.030	G6	G5	1.0	0.009		

5707		22^h $5^m.3$	−4°46′	6.1	0″.063	G9	G7	1.1	0″.010		
5709	π Pegasi	22 5.5	+32 41	4.4	0.026	A9	......	0.3	0.015	0″.005	A
5714	ζ Cephei	22 7.4	+57 42	3.6	0.012	K2	G4	0.5	0.024	0.026	A, M
5716	24 Cephei	22 7.9	+71 51	5.0	0.028	G2	G3	−2.0	0.004		
5721		22 8.2	+56 21	5.4	0.270	F6	F7	3.4	0.040	0.027	A
5723		22 8.4	+69 38	5.5	0.058	F2	F2	2.6	0.026	0.084	S
5724		22 8.4	+34 7	5.4	0.047	K2	K1	0.8	0.012		
5744	θ Aquarii	22 11.6	− 8 17	4.3	0.112	G5	G7	−0.7	0.010		
5745		22 11.6	− 9 32	6.1	0.053	K3	K1	0.8	0.009		
5746	1 Lacertae	22 11.6	+37 15	4.2	0.020	K3	K1	0.4	0.017	0.005	A
5749	44 Aquarii	22 11.9	− 5 53	5.8	0.020	G5	G4	−0.4	0.006		
C2903	Lal. 43492	22 12.3	+12 24	7.0	0.853	G1	G0	5.7	0.055	0.038	A, M, Y, *et al.*
5752	45 Aquarii	22 13.6	−13 48	6.1	0.074	G9	G9	1.7	0.013		
5769		22 18.3	− 7 42	6.1	0.006	G6	G6	0.6	0.008		
5772	33 Pegasi	22 18.8	+20 21	6.1	0.338	F4	F5	4.1	0.040	0.060	W
5776	β Lacertae	22 19.6	+51 44	4.6	0.190	G8	G8	2.1	0.032	0.017	A
5782	53^2 Aquarii A	22 21.1	−17 15	6.4	0.225	G1	G1	4.3	0.038		
5786	34 Pegasi	22 21.5	+ 3 53	5.8	0.295	F7	F7	3.9	0.042	0.067	F, J
5790	35 Pegasi	22 22.8	+ 4 12	4.9	0.325	K0	G9	1.8	0.024	0.033	A
....	Groom. 3781	22 23.1	+69 23	8.0	0.019	G7	G5	2.3	0.007		
....	A. G. Berlin 9185	22 23.4	+16 45	7.5	0.017‡	K0	G8	2.2	0.009		
5793	ζ^1 Aquarii	22 23.7	− 0 32	4.6	0.173	F2	F2	1.6	0.025	0.036	M
5794	ζ^2 Aquarii	22 23.7	− 0 32	4.4	0.212	F2	F4	1.6	0.028		
C2922	Krüger 60 A	22 24.4	+57 11	9.3†	0.87	Mb	......	10.8	0.200	0.261	M, Ye, R, Bar
5800	37 Pegasi	22 24.9	+ 3 55	5.7†	0.141	F1	F2	0.9	0.011		
5804	5 Lacertae §	22 25.4	+47 12	4.6	0.021	K2p	G4	−2.8	0.003	0.005	A
5807	δ Cephei §	22 25.5	+57 54	4.1	0.012	G0	F9	−2.7	0.004	0.011	A
....	Groom. 3813	22 27.1	+75 43	7.9	0.009‡	K1	G8	1.7	0.006		
5822		22 30.1	−24 30	6.0	0.016	K0	G7	1.1	0.011		
C2937	A.G. Albany 7817	22 30.5	+ 4 52	8.4	0.45	G1	G2	4.1	0.014		

TABLE VII—*Continued*

Boss	Name	α 1900	δ 1900	Harv. Vis. Mag.	μ	Spectrum Est.	Spectrum Meas.	Spect. Abs. Mag.	Spect. π	Trig. π	Auth.
5835	κ Aquarii	$22^h32^m.6$	− 4°45′	5.3	0″.138	K2	K1	0.8	0″.013		
5838	31 Cephei	22 33.3	+73 7	5.2	0.171	F2	F3	0.2	0.010	−0″.034	Y
5851	Bu. 11895	22 35.9	+14 1	6.6†	0.302	G4	G5	4.5	0.038		
5852	11 Lacertae	22 36.1	+43 45	4.6	0.097	K2	K0	0.7	0.017		
5865	η Pegasi	22 38.3	+29 42	3.1	0.036	G1	G3	−0.2	0.022	−0.003	A, M, S, F
5868	Bu. 11936 A	22 39.6	+38 56	6.2†	0.016	K4	K2	0.4	0.007	0.006	W
5868	Bu. 11936 B	22 39.6	+38 56	8.3	0.016	G8	G8	1.5	0.004		
C2968	Pi. 22^h214	22 40.9	+29 56	6.5	0.461	K0	G8	4.8	0.046	0.015	Ye, Y
5874	ξ Pegasi	22 41.7	+11 40	4.3	0.545	F5	F6	3.8	0.079	0.058	A, M, Y
5875	λ Pegasi	22 41.7	+23 2	4.1	0.060	G7	G6	−0.3	0.013	0.037	A
5878	68 Aquarii	22 42.2	−20 8	5.4	0.237	G6	G6	1.4	0.016		
5884	τ Aquarii	22 44.3	−14 7	4.2	0.039	K5	K2	0.5	0.018		
5885	μ Pegasi	22 45.2	+24 4	3.7	0.154	G7	G6	1.1	0.030	0.024	A, M
5891	ι Cephei	22 46.1	+65 40	3.7	0.139	K0	G9	1.1	0.030	0.042	A, M
5892		22 46.4	+13 26	8.0	0.474	K2	K1	6.3	0.046	0.150	J
5894	σ Pegasi	22 47.3	+ 9 18	5.3	0.516	F4	F6	3.2	0.038	0.042	Ye, Y, F
5895	λ Aquarii	22 47.4	− 8 7	3.8	0.036	Ma	G9	0.3	0.020		
5899	34 H Cephei	22 47.9	+82 37	5.0	0.064	K2	K0	1.6	0.021		
5909	Bu. 12046	22 50.0	− 5 31	6.0†	0.018	G8	G6	1.7	0.014		
5914		22 52.0	+49 12	5.1	0.012	K2	K5	0.8	0.014		
5915		22 52.1	− 5 21	6.4	0.023	G6	G7	1.5	0.011		
5917	51 Pegasi	22 52.6	+20 14	5.6	0.210	G4	G3	4.6	0.063		
5920	Bu. 12090	22 53.5	+ 8 50	7.0†	0.420	G0	F9	4.2	0.028		
5923		22 54.3	−13 36	6.3	0.014	K3	K0	0.4	0.007		
C3001	Lal. 44964	22 55.0	−23 4	7.7	0.899	K4	K1	7.2	0.079		

C3002	A.G. Chris. 3703	$22^h55^m.1$	+68°29′	8.4	0″.066	K0	G8	5.6	0″.028		
5927	36 H Cephei	22 55.2	+83 49	5.0	0.106	K5	K2	0.4	0.012		
5931	B.D. +56° 2923 §	22 55.9	+56 25	5.5	0.009	G2p	G2	−2.6	0.002		
C3007	Lal. 45028	22 56.7	− 4 23	7.6	0.478	K3	K3	6.1	0.050	0″.053	M, Y
5940	β Pegasi	22 58.9	+27 32	2.6	0.234	Mb	G7	0.0	0.030	0.000	A, M, J, F
5942	3 Androm.	22 59.7	+49 30	4.9	0.230	G9	G8	1.3	0.019	−0.004	A
C3019	Fed. 4371	23 1.2	+67 52	7.5	0.615	G6	G1	5.7	0.044	0.056	Y
5950	86 Aquarii	23 1.3	−24 17	4.8	0.068	G5	G6	1.2	0.019		
5952	55 Pegasi	23 2.0	+ 8 52	4.7	0.016	Ma	K4	0.3	0.013	0.005	A
5954	56 Pegasi	23 2.2	+24 56	5.0	0.038	Kop	G2	1.9	0.025		
5958	5 Androm.	23 3.2	+48 45	5.8	0.194	F6	F5	3.4	0.033		
C3028	Lal. 45292	23 4.0	− 2 48	8.3	0.587	K4	K3	6.5	0.044	0.035	Y
5962	57 Pegasi	23 4.5	+ 8 8	5.4	0.004	Mb	G3	0.2	0.009		
5963	89 Aquarii §	23 4.6	−23 0	4.9	0.013	F8	F9	−0.7	0.008		
5966	π Cephei	23 4.7	+74 51	4.7†	0.028	G2	G1	−0.2	0.011	−0.014	S
5972	6 Androm.	23 5.8	+43 0	5.8	0.275	F5	F4	3.7	0.038		
5975	7 Androm.	23 8.0	+48 52	4.6	0.134	F0	F0	2.3	0.035	0.048	A, M
5976		23 8.5	+56 37	5.6	2.102	K5	K5	7.2	0.209	0.172	S, J, P, F
5977	Bu. 12234 Br.	23 8.9	− 9 28	8.3	0.557	F5	F7	3.9	0.013	0.019	Y
	Bu. 12234 Ft.	23 8.9	− 9 28	9.4	0.557	G2	G3	5.6	0.017		
5978	φ Aquarii	23 9.1	− 6 35	4.4	0.193	K9	K2	0.6	0.017		
5981	91 Aquarii	23 10.7	− 9 38	4.5	0.367	K0	G9	1.4	0.024		
5982	61 Pegasi	23 10.9	+27 42	6.5	0.015	G3	F9	0.0	0.005		
5988	γ Piscium	23 12.0	+ 2 44	3.8	0.753	G5	G4	0.5	0.022	0.021	A, M, Y
5989		23 12.1	+52 40	5.6	0.270	F8	F8	3.9	0.046	0.049	W
5993	8 Androm.	23 13.1	+48 28	5.0	0.038	Ma	G9	0.2	0.011		
C3053	Bu. 12290	23 13.8	+ 4 52	9.0†	0.492	K2	G9	6.4	0.030	0.011	M, Ye, Y, J
5998	94 Aquarii	23 13.9	−14 0	5.3	0.314	G5	G5	2.1	0.023		
5999	96 Aquarii	23 14.2	− 5 40	5.7	0.193	F1	F2	2.7	0.025		
6000	o Cephei	23 14.5	+67 34	5.0†	0.066	G7	G7	0.7	0.014	0.032	A

TABLE VII—*Continued*

Boss	Name	α 1900	δ 1900	Harv. Vis. Mag.	μ	Spectrum		Spect. Abs. Mag.	Spect. π	Trig. π	Auth.
						Est.	Meas.				
C3054	W.B. $23^{h}257$	$23^{h}15^{m}.0$	+28°19′	8.8	0″.66	K1	K0	6.2	0″.030	0″.061	Ye
6002		23 15.0	+47 50	6.4	0.206	K1	K0	1.0	0.008		
C3059	Lal. 45755	23 16.8	+43 33	7.6	0.671	K0	G7	6.0	0.048	0.039	Y, R
6012	98 Aquarii	23 17.7	−20 39	4.2	0.153	K0	G8	1.6	0.030		
6016		23 18.1	+59 35	5.9	0.003	K4	G8	0.5	0.008		
6020		23 18.9	+31 59	6.5	0.233	A9	F3	2.3	0.014		
6024	υ Pegasi	23 20.4	+22 51	4.6	0.191	F6	F7	1.3	0.022	0.025	A, M
	A.G. Cam. 8232	23 21.0	+52 26	6.9	....	Mb	G9	0.5	0.005		
	A.G. Bonn 17799	23 22.6	+43 19	8.0	....	K2	K1	1.5	0.005		
6040	70 Pegasi	23 24.1	+12 13	4.7	0.062	G6	G5	0.5	0.014		
6042		23 24.4	− 5 5	6.4	0.283	K5	K4	0.6	0.007		
	Groom. 4079	23 25.8	+43 25	8.1	0.009	K0	G7	2.8	0.009		
6048	d'Agelet 6348	23 26.4	− 4 38	6.5	0.247	F8	F9	3.6	0.026		
6049	14 Androm.	23 26.4	+38 41	5.3	0.294	G9	G7	1.5	0.017		
C3081	A.Oe. 25685	23 26.5	+58 37	6.8	1.06	K0	K0	5.6	0.058	0.075	Y
C3085	A.Oe. 25734	23 28.2	+62 36	7.4	0.42	G4	G3	4.0	0.021	−0.012	Y
6059	72 Pegasi	23 29.0	+30 46	6.0†	0.053	K4	K2	0.7	0.009		
	Groom. 4094	23 29.3	+73 40	8.0	0.013	G8	G5	2.0	0.006		
C3096	d'Agelet 6348	23 31.0	+17 53	8.0	0.702	G5	G5	5.7	0.035		
6071	λ Androm.	23 32.7	+45 55	4.0	0.449	G8	G5	2.5	0.050	0.028	A, Y
6077	ι Piscium	23 34.8	+ 5 5	4.3	0.574	F4	F7	3.9	0.083	0.098	M, Y, J
6078	γ Cephei	23 35.2	+77 4	3.4	0.169	K1	K1	2.3	0.060	0.070	Ye
	Groom. 4129	23 36.9	+75 2	8.0	0.028	G9	G7	2.5	0.008		
6089	77 Pegasi	23 38.3	+ 9 47	5.4	0.007	Ma	G6	−0.1	0.008		
C3115	Pi. $23^{h}164$	23 38.5	+57 31	7.0	0.610	G2	F9	4.7	0.035	−0.062	Y, F

6094......	78 Pegasi............	23h39m.0	+28°48′	5.0	0″.080	G7	G7	1.1	0″.017		
6097......	....	23 39.9	+55 15	6.6	0.029	G6	G6	0.3	0.006	0″.008	W
C3117......	W.B. 23h819..........	23 40.0	+29 0	8.9	0.91	K1	K1	6.2	0.029		
6101......	ψ Androm............	23 41.1	+45 52	5.1	0.022	G5p	G0	−3.8	0.002		
6105......	Lal. 46607...........	23 42.1	+56 54	5.8	0.021	K3	G8	0.3	0.008		
6106......	τ Cassiop............	23 42.2	+58 6	5.1	0.087	K0	G9	0.4	0.012		
6109......	....	23 43.4	− 6 56	6.3	0.026	K1	G9	1.6	0.012		
C3124......	Lal. 46650...........	23 44.0	+ 1 52	8.7	1.393	Ma	K4	10.1	0.190	0.182	Ye, Y, R, *et al.*
C3126......	A.G. Albany 8170.....	23 44.9	+ 2 19	8.4	0.499	G8	G5	4.6	0.017	0.027	Ye, R
6123......	22 Piscium...........	23 46.8	+ 2 22	5.8	0.020	K4	K0	0.7	0.010		
6124......	....	23 47.2	+77 3	6.5	0.278	F2	F4	3.4	0.024		
6127......	φ Pegasi.............	23 47.4	+18 34	5.2	0.047	Ma	K0	0.4	0.011	0.014	A
6129......	....	23 47.5	+74 59	6.6	0.332	K3	K3	6.7	0.105	0.097	A, M, W
6135......	ρ Cassiop. §..........	23 49.4	+56 57	4.8	0.007	G5p	G4	−3.3	0.002	0.032	A, M.
C3131......	Lal. 46867...........	23 49.9	+28 5	7.3	0.573	K2	K3	6.0	0.055		
....	Groom. 4170..........	23 51.4	+73 35	8.2	0.020	K2	K1	1.4	0.004		
6145......	....	23 52.0	+42 6	6.0	0.012	F6	F4	1.7	0.014		
6150......	ψ Pegasi..............	23 52.7	+24 35	4.8	0.056	Ma	G8	0.1	0.012		
6151......	....	23 53.0	+49 53	6.8	0.245	G4	G4	5.0	0.044		
6156......	ω Piscium............	23 54.2	+ 6 19	4.0	0.186	F3	F4	2.3	0.046	0.013	A, M
....	B.D. +26° 4721.......	23 54.2	+26 43	8.3	....	G9	G6	2.1	0.006	0.006	F
C3146......	A.Oe. 23166..........	23 54.3	−20 35	7.4	0.608	G5	G4	5.7	0.046		
6171......	30 Piscium...........	23 56.8	− 6 34	4.7	0.053	Mb	G7	0.0	0.012		
6172......	85 Pegasi A..........	23 56.9	+26 33	5.8	1.291	G3	G2	5.6	0.091	0.096	A, S, Ye, *et al.*
6176......	Bu. 12704 Br..........	23 57.5	+65 33	5.8	0.018	G8	G7	0.8	0.010		
C3162....	Pi. 23h267...........	23 59.7	+34 6	6.2	0.766	G1	G0	4.3	0.042	0.033	A, Y

NOTES

SX Cassiopeiae. Period 36.5 days. Enhanced line spectrum similar to α Cygni Hydrogen lines $H\beta$ and $H\gamma$ have bright edges.

A.G. Bonn 4686. Proper motion from Groombridge.

Boss 1622. Estimates made from plates lent by the Lick Observatory.

Bu. 3474. Proper motion by Batterman.

Comp. α Geminorum. Bu. 4122C, distant 72″. A spectroscopic binary having bright hydrogen lines.

Lal. 15389. Proper motion by Bossert.

S Antliae. Short-period variable. Period $=0\overset{\mathrm{d}}{.}32$. Spectrum lines extremely poor, probably indicating rapid rotation. Secondary component suspected.

W Ursae Majoris. Algol variable. Period 8 hours. Both spectral components show. Lines very wide due to rapid rotation of the two stars.

Boss 2830. A close visual and spectroscopic binary. Estimates made from plates taken by Sanford at the Mills Station of the Lick Observatory.

Boss 3735. Estimates from plates lent by the Lick Observatory.

Bu. 7001. Proper motion from Greenwich.

Boss 3846. Spectrum lines very poor, resembling those of W Ursae Majoris.

Bu. 8068A. Proper motion from Porter.

7:1917 Serpentis. Peculiar variable discovered by Wolf and Barnard. $H\beta$ bright.

W Serpentis. Spectrum shows doubly reversed bright hydrogen lines.

Bu. 9401 Br. Proper motion from A.G. Berlin.

Bu. 9569. Proper motion from Auwers.

Bu. 10504 Br. and Ft. Proper motion from A.G. Berlin.

Mount Wilson Observatory
October 1920

END OF VOL. IX

INDEX TO VOLUME IX

Nos. 169 to 199

AUTHORS

PAGE

Abetti, Giorgio. *See* Joy, Alfred H.

Adams, Walter S., and Cora G. Burwell—
  The Spectrum of Nova Ophiuchi 1919 147

Adams, Walter S., Alfred H. Joy, Gustaf Strömberg, and Cora G. Burwell—
  The Parallaxes of 1646 Stars Derived by the Spectroscopic Method 423

Anderson, J. A.—
  Application of Michelson's Interferometer Method to the Measurement of Close Double Stars 225
  Spectrum of Electrically Exploded Wires 135

Babcock, Harold D.—
  Note on the Polarization of the Night Sky 33

Brackett, Frederick S.—
  An Examination of the Infra-Red Spectrum of the Sun, λ 8900–λ 9900 399

Burwell, Cora G. *See* Adams, Walter S.

Davis, Helen N. *See* Shapley, Harlow

Duncan, John C.—
  Bright Nebulae and Star Clusters in Sagittarius and Scutum . . 125
  The Spectroscopic Orbit of the Cepheid Variable X Cygni . . 395

Hubble, Edwin P. *See* Seares, Frederick H.

Joy, Alfred H., and Giorgio Abetti—
  The Orbit of the Spectroscopic Binary Boss 2285 37

Joy, Alfred H. *See also* Adams, Walter S.

Kapteyn, J. C., and P. J. van Rhijn—
  On the Distribution of the Stars in Space, Especially in the High Galactic Latitudes 289

PAGE

KING, ARTHUR S.—
The Characteristics of Absorption Spectra Produced by the Electric Furnace 41
Experiments on the Possible Influence of Potential Differences on the Radiation of the Tube Resistance Furnace 363
Intensity Differences in Furnace and Arc among the Component Series in Band Spectra 375
Observations of the Electric Furnace Spectra of Cobalt, Nickel, Barium, Strontium, and Calcium in the Region of Greater Wave-Length 167
Preliminary Observations of the Zeeman Effect for Electric Furnace Spectra 153
The Variation with Temperature of the Electric Furnace Spectrum of Manganese 411

MERRILL, PAUL W.—
Note on the Air Lines in Spark Spectra from λ 5927 to λ 8719 . 211

MICHELSON, A. A.—
On the Application of Interference Methods to Astronomical Measurements 219

PEASE, FRANCIS G.—
Photographs of Nebulae with the 60-Inch Reflector, 1917–1919 . 239

RITCHIE, MARY. *See* Shapley, Harlow

SEARES, FREDERICK H.
Magnitudes of Faint Comparison Stars for Nova Persei, No. 2 . 359
The Surface Brightness of the Galactic System as Seen from a Distant External Point and a Comparison with Spiral Nebulae 337

SEARES, FREDERICK H., AND EDWIN P. HUBBLE—
The Color of the Nebulous Stars 273

SHAPLEY, HARLOW—
Studies Based on the Colors and Magnitudes in Stellar Clusters.
Fifteenth Paper: A Photometric Analysis of the Globular System Messier 68 71
Seventeenth Paper: Miscellaneous Results 323

SHAPLEY, HARLOW, AND HELEN N. DAVIS—
Studies Based on the Colors and Magnitudes in Stellar Clusters.
Sixteenth Paper: Photometric Catalogue of 848 Stars in Messier 3 85

PAGE

Shapley, Harlow, and Mary Ritchie—
  Studies Based on the Colors and Magnitudes in Stellar Clusters. Eighteenth Paper: The Periods and Light-Curves of 26 Cepheid Variables in Messier 72 379

Strömberg, Gustaf—
  Note on the Relationship of Mean Parallax to Mean Proper Motion 21

Strömberg, Gustaf. *See also* Adams, Walter S.

Takamine, Toshio—
  The Stark Effect for Metals 1

van Maanen, Adriaan—
  The Photographic Determination of Stellar Parallaxes with the 60-Inch Reflector. Fourth Series 175

van Maanen, Adriaan, and Coral Wolfe—
  On the Systematic Differences in Trigonometrically Determined Parallaxes 305

van Rhijn, P. J.—
  On the Brightness of the Sky at Night and the Total Amount of Starlight 41

van Rhijn, P. J. *See also* Kapteyn, J. C.

Wolfe, Coral. *See* van Maanen, Adriaan

SUBJECTS

Absorption spectra produced by electric furnace, characteristics, 61
Air lines in spark spectra, 211
Barium, electric furnace spectra, in region of greater wave-length, 167
Binaries, spectroscopic, orbit of Boss 2285; 37
Boss 2285, orbit, 37
Calcium, electric furnace spectra, in region of greater wave-length, 167
Capella, interferometer measurement, 225
Cepheid variables, periods and light-curves, 379
——, spectroscopic orbit of X Cygni, 395
Clusters, globular, photometric analysis of Messier 68; 71
——, in Sagittarius and Scutum, 125
——, photometric catalogue of 848 stars in Messier 3; 85
——, studies based on their colors and magnitudes, 71, 85, 323, 379
Cobalt, electric furnace spectra, in region of greater wave-length, 167
Color of the nebulous stars, 273
Colors and magnitudes in stellar clusters, 71, 85, 323, 379
Distribution of stars in space, 289
Double stars, application of interferometer to their measurement, 225
Electric furnace absorption spectra, characteristics, 61
Electric furnace spectra, observations of Zeeman effect, 153
——, of cobalt, nickel, barium, strontium, and calcium in the region of greater wave-length, 167
Electric furnace spectrum of manganese, variation with temperature, 411
Furnace. *See* Electric furnace and Tube resistance furnace
Galactic system, surface brightness as seen from distant external point, 337
Globular clusters. *See* Clusters, globular
Interferometer, application to astronomical measurements, 219
——, application to measurement of close double stars, 225
Magnitudes in stellar clusters, 71, 85, 323, 379
——, of faint comparison stars for Nova Persei, No. 2, 359
Manganese, electric furnace spectrum, 411
Messier 3, photometric catalogue of 848 stars, 85
Messier 8, 16, 17, and 22; 125
Messier 68, photometric analysis, 71
Messier 72; 379
Nebulae in Sagittarius and Scutum, 125
——, photographed with the 60-inch reflector, 239
——, spiral, compared with galactic system as to surface brightness, 337
Nebulous stars, color, 273

N.G.C. 6523, 6530, 6611, 6618, and 6656; 125
Nickel, electric furnace spectra, in region of greater wave-length, 167
Nova Ophiuchi 1919, spectrum, 147
Nova Persei, No. 2, magnitudes of faint comparison stars, 359
Parallax, mean, relationship to mean proper motion, 21
Parallaxes, of 1646 stars, derived by spectroscopic method, 423
———, trigonometric, determination with 60-inch reflector, 175
———, trigonometrically determined, systematic difference, 305
Polarization of the night sky, 33
Proper motion, mean, relationship to mean parallax, 21
Radiation of the tube resistance furnace, influenced by potential difference, 363
Sagittarius, bright nebulae and star clusters, 125
Scutum, bright nebulae and star clusters, 125
Sky at night, brightness, 41
———, polarization, 33
Spark spectra. *See* Spectra
Spectra, absorption, produced by electric furnace, 61
———, band, intensity differences in furnace and arc among their component series, 375
———, electric furnace, observations of Zeeman effect, 153
———, spark, air lines from λ 5927 to λ 8719, 211
Spectroscopic binary Boss 2285, orbit, 37
Spectroscopic parallaxes of 1646 stars, 423
Spectrum, infra-red, of sun, 399
———, of electrically exploded wires, 135
———, of manganese, electric furnace, variation with temperature, 411
———, of Nova Ophiuchi 1919, 147
Stark effect for metals, 1
Starlight, total amount, and brightness of sky at night, 41
Stars, distribution in space, 289
———, double, measured by interferometer, 225
———, nebulous, color, 273
———, parallaxes derived by spectroscopic method, 423
Strontium, electric furnace spectra, in region of greater wave-length, 167
Sun, infra-red spectrum, 399
Swan nebula, 125
Systematic differences in trigonometric parallaxes, 305
Tube resistance furnace, influence of potential difference on its radiation, 363
Variable stars, periods and light-curves of 26 Cepheid variables in Messier 72; 379
———, spectroscopic orbit of the Cepheid variable X Cygni, 395
Wires, electrically exploded, spectrum, 135
Zeeman effect for electric furnace spectra, 153

a39001 006937216b

522 19 C28 V09
MOUNT WILSON OBSERVATORY CONTRIBUTION

INSERT BOOK
MASTER CARD
FACE UP IN
FRONT SLOT
OF S.R PUNCH

MASTER CARD

GLOBE 901144-0

UNIVERSITY OF ARIZO
LIBRARY

72-1